Case No. 84739

IN THE SUPREME COURT OF THE STATE OF NEVADA

ADAM SULLIVAN, P.E., NEVADA STATE ENGINEER, et al.

Appellants,

vs.

LINCOLN COUNTY WATER DISTRICT, et al.

<u>JOINT APPENDIX</u>

VOLUME 29 OF 49

Ground-Water Conditions in the Vicinity of Lake Mead Base Las Vegas Valley, Nevada

By OMAR J. LOELTZ

CONTRIBUTIONS TO THE HYDROLOGY OF THE UNITED STATES

GEOLOGICAL SURVEY WATER-SUPPLY PAPER 1669-Q

Prepared on behalf of the U.S. Department of Defense

UNITED STATES GOVERNMENT PRINTING OFFICE, WASHINGTON : 1963

UNITED STATES DEPARTMENT OF THE INTERIOR

STEWART L. UDALL, *Secretary*

GEOLOGICAL SURVEY

Thomas B. Nolan, *Director*

For sale by the Superintendent of Documents, U.S. Government Printing Office
Washington, D.C., 20402

CONTENTS

ILLUSTRATIONS

CONTRIBUTIONS TO THE HYDROLOGY OF THE UNITED STATES

GROUND-WATER CONDITIONS IN THE VICINITY OF LAKE MEAD BASE, LAS VEGAS VALLEY, NEVADA

By Omar J. Loeltz

ABSTRACT

The principal source of ground water for the Lake Mead Base well field is precipitation in the Las Vegas drainage basin northwest of the well field. The amount of water moving through the area is small. Locally, the chemical quality of the water is unsatisfactory for most uses. The present supply of water of satisfactory chemical quality from two of four wells probably can be maintained, if pumpage from these wells is not increased significantly.

Additional ground-water supplies of satisfactory chemical quality probably can be developed west of the present well field.

INTRODUCTION

In April 1955, at the request of the Department of Defense, the U.S. Geological Survey began an investigation of ground-water conditions in the vicinity of Lake Mead Base, Las Vegas Valley, Nev. The chemical quality of the water from two of four wells supplying the base had deteriorated to the point where it was wholly unsatisfactory for use. The study was made to determine the cause of the deterioration and to provide data that might be helpful in maintaining a satisfactory supply for the base.

As part of the study, all known pertinent geologic and hydrologic data for the area were assembled and studied. During the investigation, considerable additional data were collected and studied. These data were obtained from pumping tests in the area, current-meter and conductivity surveys, and chemical analyses of water samples from wells.

The results of the investigation were made available to the Department of Defense upon completion of the study. On the basis of the 1955 study, a well was drilled in the summer of 1961 to augment the water supply of Lake Mead Base (R. J. Houghton, oral communication, 1962). The well is 2,000 feet west of well 4 and is pumped at the rate of 130 gpm (gallons per minute). The chemical quality of the water is more suitable for use on the base than the chemical quality of the water from any of the other wells. No significant change in chemical quality or yield of the water from wells 2, 3, and 4 has been noted.

Data on file at Lake Mead Base were used extensively in the present study of the wells and water supply. Useful data also were obtained from a study by Maxey and Jameson (1948) and from a guidebook to the geology of Utah (Intermountain Association of Petroleum Geologists, 1952). In this report wells are given the same numbers used by the defense agencies for designating wells on their respective bases.

GEOGRAPHY

LOCATION

The area described in this report is in the eastern part of Las Vegas Valley (see fig. 1). The area studied most intensively is near the eastern edge of the valley between Nellis Air Force Base and Lake Mead Base, about 10 miles northeast of Las Vegas, where the well field for Lake Mead Base is located.

TOPOGRAPHIC FEATURES

Las Vegas Valley trends northwestward about 50 miles and is as much as 20 miles wide. The Spring Mountains, which have a maximum altitude of 11,910 feet, border the west side of the valley. The southern parts of the Pintwater, Desert, Sheep, and Las Vegas Ranges form the northeastern boundary. Frenchman and Sunrise Mountains and a group of unnamed low hills border the east side of the valley. The River Mountains and the McCullough Range form the southeastern boundary.

The relief of the mountains ranges from a few thousand feet to about 10,000 feet. The mountains are rugged and commonly rise abruptly above the alluvial apron that separates them from the basin lowlands. Large alluvial fans extend far out from the Spring Mountains. The alluvial fans on the east side of the valley are small. The fans merge into the basin lowlands, which are nearly flat and slope southeastward.

Drainage is southeastward to the Colorado River (east of the area shown in fig. 1) through Las Vegas Wash. There are no perennial streams in the area. Runoff ordinarily infiltrates into the ground high on the alluvial fans. After intense summer storms, however, the runoff may be sufficient for short periods of time to flow onto the floor of the valley. Occasionally the runoff causes extensive damage to railroads, roads, and urban areas.

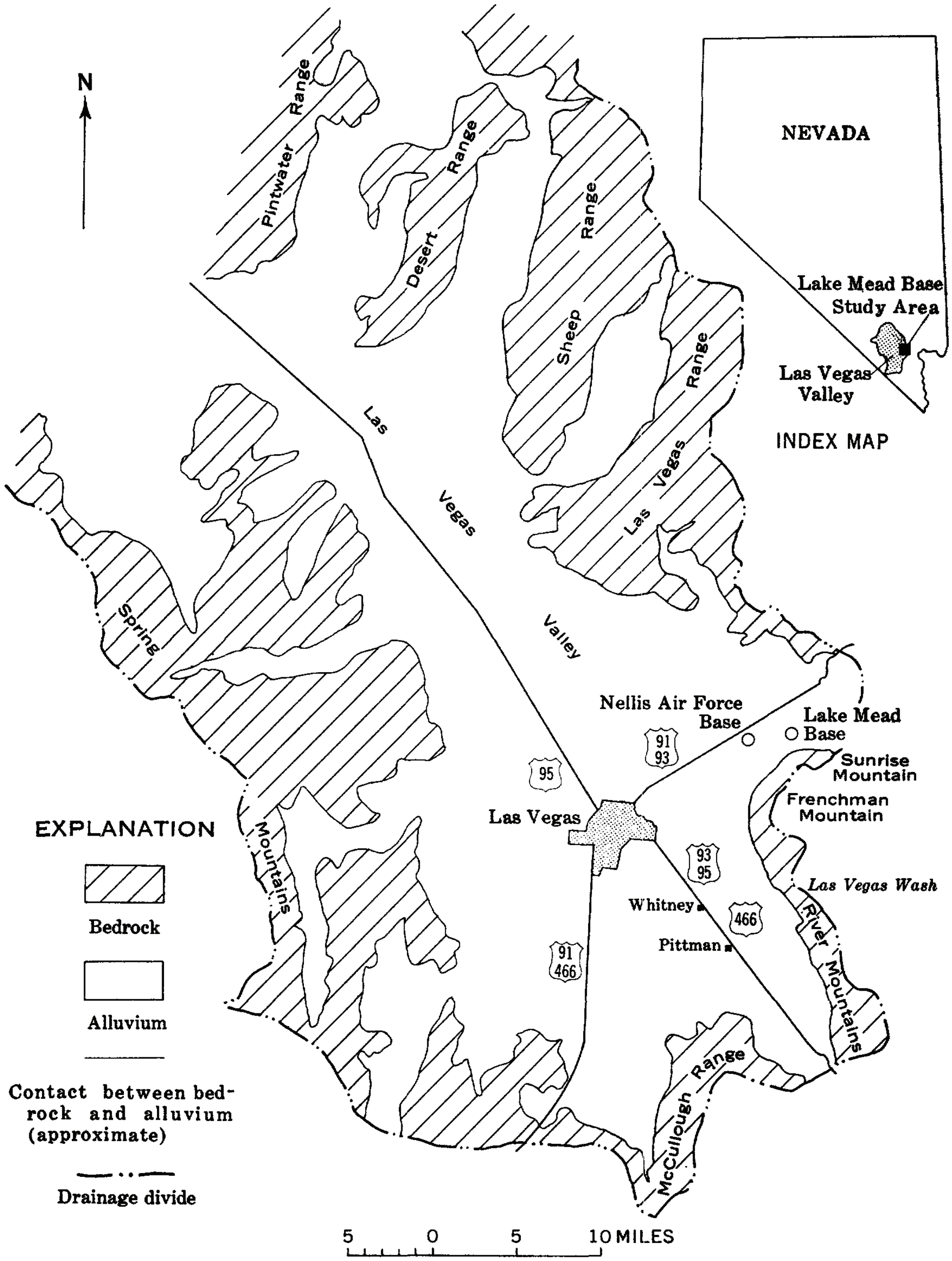

FIGURE 1.—Sketch map of Las Vegas Valley, Clark County, Nev.

CLIMATE

The climate is arid. Relative humidity is low, the percentage of sunshine is high, and the daily and seasonal range in temperature is large. Strong winds are common throughout the year.

GEOLOGY

The mountains generally are composed of consolidated sedimentary and igneous rocks of Precambrian, Paleozoic, Mesozoic, and early Tertiary age. Rocks of Precambrian age are exposed only at the base of Frenchman Mountain. The structure of the consolidated rocks is exceedingly complex because of numerous thrust, lateral, and normal faults. The alluvial apron and the valley fill are composed mostly of unconsolidated deposits of Miocene(?), Pliocene, Pleistocene, and Recent age.

Except for the Sultan and the Monte Cristo Limestones of middle Paleozoic age, the older rocks of the mountains generally are barriers to the movement of ground water. The Sultan and the Monte Cristo Limestones locally transmit large quantities of water through solution channels formed mainly along faults and joints. These rocks are exposed in Frenchman Mountain, and they probably are in contact with saturated alluvium east of Nellis Air Force Base.

The alluvial apron is composed largely of poorly sorted gravel, sand, silt, and clay. However, some of the alluvial fans that extend far out from the mountains contain clean gravel strata on their higher slopes. Most of these fans emerge from canyons in the Spring Mountains and are the principal areas of recharge to the ground-water reservoir of Las Vegas Valley.

The valley fill consists, to an unknown depth, of deposits of gravel, sand, silt, and clay. Most of the water developed to date has been from strata less than 700 feet deep. At greater depths the deposits tend to be finer grained and may be consolidated.

GROUND WATER

RECHARGE

The source of recharge to the ground-water reservoir of Las Vegas Valley is within the drainage basin. Precipitation in the Spring Mountains is the major source of the recharge, although some recharge results from the infiltration of precipitation and resulting runoff on the lower ranges.

The aquifers in the Nellis Air Force Base area are recharged principally from precipitation on the alluvial fans at the south end of the Las Vegas Range, although part of the recharge may be derived from precipitation in the Spring Mountains.

Probably the only significant source of recharge to the aquifers in the Lake Mead Base area is precipitation on the southern part of the Las Vegas Range. Thus, most of the ground-water recharge to the respective well fields is from a common source, precipitation on the southern part of the Las Vegas Range and the alluvial fans that border it.

MOVEMENT AND DISCHARGE

Ground water in Las Vegas Valley moves from the Spring Mountains and other recharge areas toward pumped and flowing wells and toward springs and areas of evapotranspiration, principally near and east of Las Vegas.

In the vicinity of Las Vegas, artesian water moves generally eastward toward Frenchman Mountain and then southward along the east side of the valley toward Las Vegas Wash.

Data for the area near Lake Mead Base and Nellis Air Force Base are insufficient for accurate mapping of the direction of ground-water movement, but it is inferred to be southeastward beneath the military bases toward Frenchman Mountain. (See fig. 2.)

Whether some or all of the ground water in the Lake Mead Base area moves southeastward into Frenchman Mountain is not known. The possibility of movement into the mountain is recognized because the contours on the piezometric surface, although insufficiently controlled, infer such movement, and the nature and structure of the rocks do not preclude movement of water through them. As was pointed out in the discussion on the geology of the valley, the Sultan and Monte Cristo Limestones, both exceptions to the general rule that the rocks of the mountains are barriers to the movement of ground water, are probably in the zone of saturation in the Lake Mead Base area. Furthermore, the rocks into which the water may be moving have been extensively faulted, a condition that might allow the transmission of water in otherwise nearly impermeable rocks. The fact that no large springs or large areas of evapotranspiration are known to result from the southeastward movement of water through Frenchman Mountain does not preclude such movement, because the amount of water involved (see p. Q10) probably is very small.

CHEMICAL QUALITY OF THE WATER

Much of Las Vegas Valley yields water suitable for most domestic uses and for irrigation. In general, ground water in the northern and central parts of the valley has a low dissolved-solids content. For example, near Las Vegas the dissolved-solids content generally is about 300 ppm (parts per million). In the southern part of Las Vegas Valley, however, much of the ground water is so highly mineralized that it is unsatisfactory for domestic and irrigation use. For example, in the vicinity of Whitney and Pittman the concentration of dissolved solids commonly is several thousand parts per million.

690-209—63——2

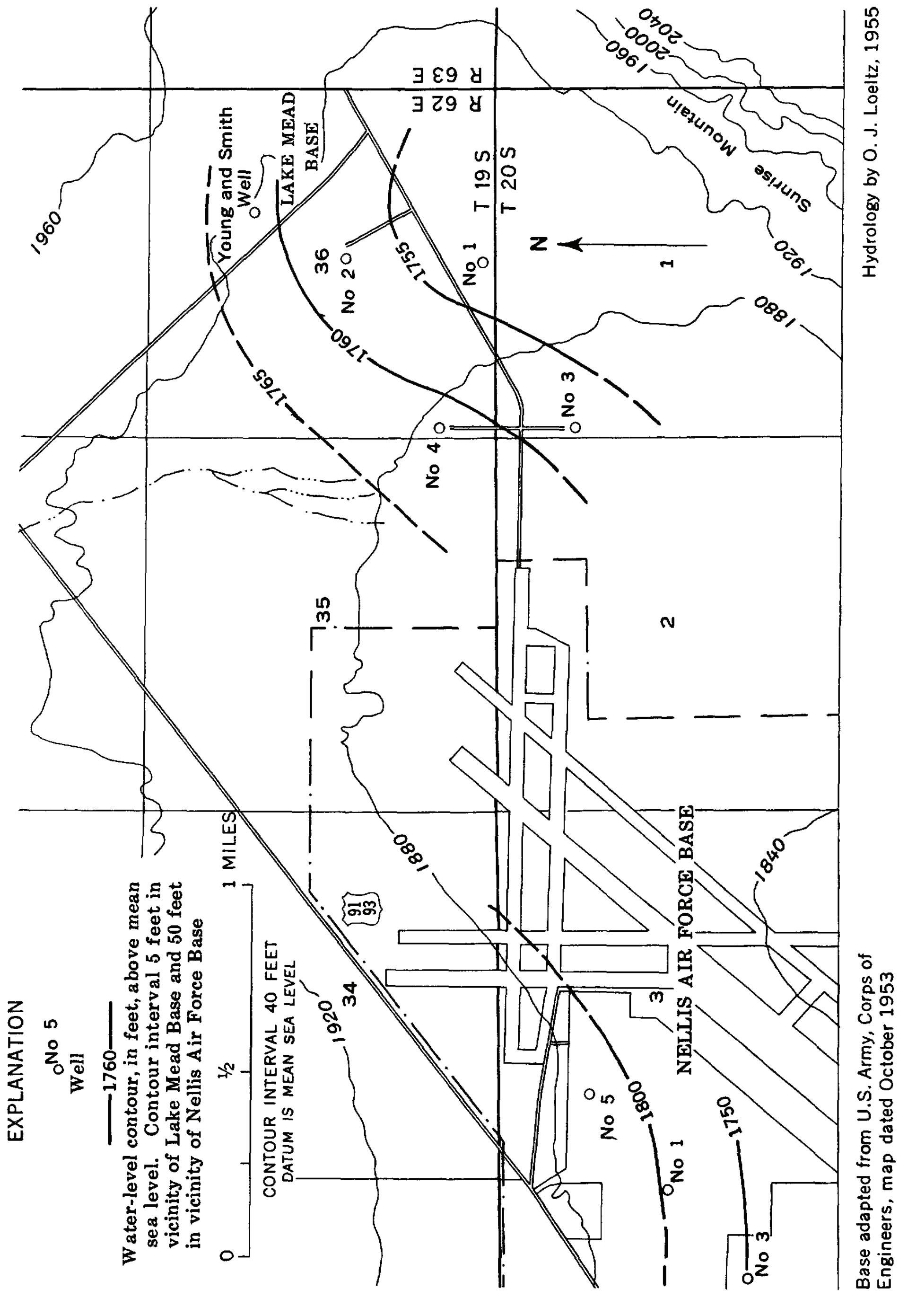

FIGURE 2.—Map of Lake Mead Base area, Las Vegas Valley, Nev., showing water-table contours and location of wells.

SE ROA 42923

A notable exception to the rule that water in the central part of the valley commonly has a low dissolved-solids content is the water in wells 1 and 2 at Lake Mead Base. The dissolved-solids content of the water of well 1, on Mar. 2, 1955, after the well had not been used for months, was 1,810 ppm. The dissolved-solids content of the water of well 2, on the same date, was 1,170 ppm. These values are in marked contrast to those of the water of the other two wells on the base (about 500 ppm) and to those of the water of the wells supplying Nellis Air Force Base (250 to 500 ppm). The water from wells 1 and 2 was used during 1953 and 1954 to supply the needs of Lake Mead Base. It is reported that the water was unsatisfactory in many respects, especially for evaporative coolers and for the hot-water system. In 1955, wells 3 and 4 supplied water for the base, and wells 1 and 2 were virtually unused.

INVESTIGATIONAL PROCEDURES AND CONCLUSIONS

PIEZOMETRIC SURFACE

In an effort to determine the direction of ground-water movement in the vicinity of Lake Mead Base, contour lines of the piezometric surface in that area were drawn (fig. 2). (Meinzer (1923) defined the piezometric surface as an imaginary surface that everywhere coincides with the static level of the water in the aquifer.) In this study, the nonpumping levels of water in the wells in the spring of 1955 were considered to be points on the piezometric surface. The position and shape of the surface at other points were inferred from these few known points, and contour lines were drawn to show the position and shape of the piezometric surface as of that time.

The position of the contour lines on figure 2 is considered tentative because of inadequate and conflicting water-level data. If some of the data collected previous to the investigation had been used, the contour lines in the vicinity of the well field of Lake Mead Base would have been almost at right angles to those shown in figure 2. The altitude of the water level in well 1 in March 1952 reportedly was 1,768 feet. At the time of the investigation, April 1955, the altitude of the water level was 1,754 feet. The altitude of the water level in well 2 in March 1952, according to the same source, was 1,765 feet. During the present study, the altitude was 1,762 feet. The altitude of the water level in the Young and Smith well, which is about half a mile northeast of well 2, was 1,794 feet in January 1953, if the depth to water as given in the driller's log is correct. In April 1955, the altitude of the water level was 1,762 feet.

In contrast to these declines, the available data indicate a substantial rise in water levels in wells 3 and 4 since the date of their completion in late 1953. Reportedly, the altitude of the water level in well 3 in December 1953 was 1,734 feet. During the present study, the altitude of the water level was 1,758 feet. The same source indicates that the altitude of the water level in well 4 in December 1953 was 1,739 feet. During the present study the altitude of the water level was 1,761 feet.

Because the methods used to collect data prior to the present study and the circumstances under which those data were collected are not fully known, the following statements are based largely on data obtained and verified during the present study in which depths to water were measured with a steel tape.

The contour lines (fig. 2) suggest that the main source of the ground water beneath the Lake Mead Base well field is the precipitation and runoff that infiltrates into the alluvial fans at the southern end of the Las Vegas Range (fig. 1). A negligible amount also may be derived from precipitation on the hills and mountains north and east of the base. Because of the gypsiferous nature of some of the rocks comprising these hills and mountains, such water may be highly mineralized. Whether the water passing beneath the well field moves southeastward into Frenchman Mountain or is deflected southward along the base of the mountain is not known. In any event, the source of the water of low dissolved-solids content appears to be northwest of the well field.

ATTITUDE OF PRINCIPAL AQUIFERS

Electric logs are available for wells 1 to 4. The logs indicate that the principal aquifers dip eastward 500 feet per mile and more. At well 3, the principal aquifers are about 150 feet lower than at well 4; at well 2 they are more than 500 feet lower; at well 1 they are about 300 feet lower. Because the alluvium slopes southwestward in the vicinity of the well field, the depth to the principal aquifers increases rapidly eastward. The main aquifers, which to date have been tapped by the Lake Mead Base wells, therefore, probably lie at shallower depths westward from wells 3 and 4.

PUMPING TESTS

To obtain estimates of the coefficients of transmissibility and storage, wells 2 and 4 were pumped at constant rates at different times, and the effects of such pumping on the water levels in the pumped wells and the other wells in the well field were noted.

Beginning at 9:23 a.m. on April 18, 1955, well 4 was pumped at a nearly constant rate of 130 gpm for 30 hours. Although none of the wells had been pumped for 24 hours before the test, the wells were recovering from the effects of earlier pumping. The rate of recovery in well 4 was considerably less than 0.1 foot per hour at the time the pumping test began. Based on the drawdown and subsequent recovery data, the coefficient of transmissibility was computed to be somewhat less than 1,500 gpd (gallons per day) per ft. Periodic measurements were made in wells 1, 2, and 3 to the nearest hundredth of a foot, and the Young and Smith well was equipped with a recording gage. Effects of the pumping could be identified only in well 3, and these effects, a marked change in the previously established pattern of recovery of water levels in well 3, were noted about 7 hours after beginning of pumping of well 4. By extrapolating the recovery curve for well 3, it is estimated that pumping well 4 for 30 hours retarded the normal rate of recovery of well 3 by more than 1 foot.

That interference effects were noted in well 3 indicates that some of the strata common to both wells contain confined (artesian) water, because under unconfined (water-table) conditions the effects of the pumping would have been too small to be measurable. The coefficient of storage, 3.6×10^{-5}, computed on the basis of interference effects in well 3, also indicates artesian conditions. However, the value obtained may be considerably in error, because the coefficient of transmissibility for aquifers tapped by well 3, computed from the intereference data, is about 20,000 gpd per ft, or about 20 times larger than a much more reliable determination of the coefficient of transmissibility made from data obtained when well 3 itself was pumped. (See p. Q10.) The coefficient of transmissibility computed from interference data will exceed the true value if either well taps aquifers that are not common to both or if, because of the duration of this particular pumping test and the distance between wells, either well taps strata containing unconfined water. One of these conditions, perhaps both, probably exists, hence, the value of the coefficient of transmissibility as determined by interference effects very likely is too high.

The lack of measurable interference effects in wells 1 and 2 and in the Young and Smith well indicates that these wells have little, if any, artesian hydraulic connection with well 4. The test does not eliminate the possibility that the wells are connected hydraulically with well 4 by a water-table aquifer. Under water-table conditions, pumping at 100 gpm might be continued for 30 days or more before interference effects of 0.01 foot or more between wells 2,000 feet apart would occur.

Well 2 was pumped at a constant rate of about 140 gpm for 20 hours, beginning at 12:08 p.m. on April 20, 1955. The computed coefficient of transmissibility was about 800 gpd per ft. Because no interference with other wells could be detected as a result of the pumping, a value for the coefficient of storage could not be obtained.

The hydraulic continuity under artesian conditions, if any, is evidently poorer between wells 1 and 2 than it is between wells 3 and 4. However, as noted earlier, all the wells still may be hydraulically connected under unconfined conditions. The foregoing tests show that interference effects between wells spaced 2,000 feet apart are negligible for the rates of pumping and the pumping schedules that have been used on the base in the past.

Well 3 was pumped for 1 hour at 195 gpm, beginning at 10:06 a.m. on April 21, 1955. The coefficient of transmissibility was computed to be about 1,000 gpd per ft.

The low coefficients of transmissibility of the aquifers tapped by the Lake Mead Base wells indicate that it is not possible to obtain yields of more than a few gallons per minute per foot of drawdown from these wells.

To estimate the amount of water moving through the area under natural conditions, pumping tests also were made on all the Nellis Air Force Base wells for which the required data could be obtained. In the Lake Mead Base well field, the coefficient of transmissibility was estimated to be 1,000 gpd per ft. In the vicinity of Nellis Air Force Base, the coefficient of transmissibility was estimated to be 5,000 gpd per ft. The general hydraulic gradient toward Lake Mead Base is about 30 feet per mile, and that toward Nellis Air Force Base is about 40 feet per mile. Thus, in the vicinity of the Lake Mead Base well field, only about 30,000 gpd moves across each mile-wide section normal to the direction of ground-water movement, and in the Nellis Air Force Base area the quantity is about 200,000 gpd. Although these estimates show only the general order of magnitude of the quantity of water that is moving through the saturated deposits beneath the two bases, they indicate that the quantity is small and that the demand for water can easily equal or exceed the amount of water naturally passing through a given area.

The peak demand at Lake Mead Base in 1961 exceeded 100,000 gpd. The yearly demand averaged about 85,000 gpd, and a substantial increase in demand is anticipated. The natural movement of water through that part of the well field from which ground-water withdrawals were being made, a strip about half a mile wide, was only about 10,000 gpd. To continue to meet the demands of the base indefinitely, water will have to be diverted to the well field. This diversion can be accomplished by continuing withdrawals to meet the demands of the base, provided the demands do not greatly exceed several hundred thousand gallons per day. Under this practice, water will be taken from ground water in storage and water levels will continue to decline. As the practice is continued, however, more of the water that is diverted to the well field from storage will be derived from an ever increasing volume of sedimentary deposits, probably principally from deposits of Las Vegas Valley lying west of the well field, and consequently water levels will decline at a slower rate for a given withdrawal. Although the total decline, including the general decline of water levels anticipated for Las Vegas Valley, may be substantial, it will hardly in the forseeable future reach the several hundred feet that would be required to deplete the supply to the well field to the point where the field would be incapable of meeting demands of the base.

CHEMICAL ANALYSES

The records to date indicate that, except for wells 1 and 2, the water from wells in the Lake Mead Base and Nellis Air Force Base well fields is only moderately mineralized.

The hardness (as $CaCO_3$) of the water from well 3 is about 300 ppm, about 100 ppm higher than the hardness of the water from well 4 and from the wells supplying Nellis Air Force Base. The dissolved-solids content of water from wells 3 and 4 is about 500 ppm, or several hundreds parts per million higher than that of most of the water used at Nellis Air Force Base. The higher dissolved-solids content in the ground water of the Lake Mead Base well field probably is due partly to the slower movement of water in the vicinity of Lake Mead Base and partly to the mineralogy of the sedimentary strata. The valley fill in the vicinity of the Lake Mead Base well field probably contains a large amount of gypsum because the hills and mountains north and east of the well field from which at least part of the fill was derived contain gypsum. Ground water moving through the valley fill dissolves some of the gypsum and becomes highly mineralized.

There is no evidence that withdrawals have caused a significant deterioration of the quality of the water yielded by most of the wells of Lake Mead Base and Nellis Air Force Base. Water from Nellis Air Force Base well 1 in the SE¼SE¼NE¼ sec. 4, T. 20 S., R. 62 E., probably has been analyzed over the longest period of time. On May 5, 1941, the hardness was 220 ppm, and the dissolved-solids content was 255 ppm. On November 28, 1954, the hardness was 105 ppm, and the dissolved-solids content was 263 ppm. Other analyses between these dates likewise indicate no significant change.

Water from well 1 of Lake Mead Base, however, not only is highly mineralized, but the degree of mineralization changes with the amount of water pumped from the well. For example, the dissolved-solids content reportedly decreased from 1,310 to 861 ppm in a 1-week period in March 1952. A later analysis on November 30, 1953, after the well had been pumped for almost 6 months, showed that the dissolved-solids content had decreased only slightly, from 861 to 851 ppm, but that the hardness of the water had increased from 357 to 422 ppm.

On March 2, 1955, after well 1 had been idle for several months, a sample of water collected from it at the end of a 1-hour period of pumping at about 225 gpm had a hardness of 1,210 ppm and dissolved-solids content of almost 1,900 ppm. Even higher concentrations were noted at the beginning of the pumping period. A sample, collected 6 minutes after pumping began, had a hardness of 1,590 ppm, and; the specific conductance indicated a dissolved-solids content of more than 2,300 ppm. Measurements of the conductivity of samples collected during the period of pumping indicated that the conductivity, and hence the dissolved-solids content, decreased only slightly during the last 30 minutes of pumping. How much more the mineralization might have been reduced by continued pumping is not known, but it seems unlikely that the dissolved-solids content could have been lowered to the point where it approached that of the water from wells 3 and 4. The constituents principally responsible for increase in the dissolved-solids content are calcium, magnesium, and sulfate.

The results of chemical analyses of typical samples of water obtained during this investigation are shown in the following table.

Chemical analyses of water samples from Lake Mead Base wells, Las Vegas Valley, Clark County, Nev.

[Analyses by U.S. Geol. Survey. Chemical constituents in parts per million]

Well No.	1	2	3	4
Salt Lake City laboratory No.	13958	14220	13960	14219
Date of collection	3-2-55	4-21-55	3-2-55	4-19-55
Pumping period ... hours	1	19	1	30
Pumping rate ... gpm	250	140	220	130
Temperature ... °F	80	84	77	82
Silica (SiO_2)	77	81	70	40
Iron (Fe) [total]	.14	.32	.06	.1
Manganese (Mn)	.03	.04	.02	.0
Calcium (Ca)	190	106	47	41
Magnesium (Mg)	172	75	43	23
Sodium (Na)	102	86	46	90
Potassium (K)	9.5	11	4.5	8.1
Bicarbonate (HCO_3)	134	142	198	187
Carbonate (CO_3)	0	0	0	0
Sulfate (SO_4)	1,150	549	171	172
Chloride (Cl)	55	43	39	48
Fluoride (F)	1.8	1.9	1.3	1.5
Nitrate (NO_3)	1.6	9.9	2	1.9
Dissolved solids:				
Total ... ppm	1,810	1,030	522	518
Residue on evaporation at 180° C ... do	1,990	1,050	544	510
Hardness:				
As $CaCO_3$ ... do	1,180	573	294	197
Noncarbonate ... do	1,070	456	132	44
Specific conductance ... micromhos at 25° C	2,180	1,330	748	786
pH	7.6	7.4	7.6	7.4
Color	5	5	5	5

EXPLORATION OF WELL 1

In addition to the 1-hour pumping test on March 2, 1955, during which changes in temperature and chemical constituents of water from well 1 were observed, two other tests were made to obtain additional information as to the quality and quantity of the water yielded by different strata.

On June 30, 1955, after the well had been idle for months, the conductivity of the water in the well versus depth was determined by a conductivity apparatus lowered into the well. The survey showed an increase in the conductivity of the water to a depth of about 300 feet below the top of the casing, after which little change in conductivity was noted. (See fig. 3.) A survey by means of a deep-well current meter indicated that, if there was movement from strata below a depth of 680 feet to higher strata, such movement was too slow to be detected by the current meter. The meter probably would have detected movements as small as a gallon or two per minute, because a gasket of rubber belting attached to the meter tube presumably forced virtually all the water in the casing to pass through the 3-inch-diameter tube in which the meter was housed. The sensitivity of the meter to vertical movement was lessened considerably at depths above 600 feet, because the casing diameter changed from 10 to 14 inches at 600 feet. Nevertheless, any substantial movement in the 14-inch casing probably would have been detected.

On July 1, 1955, from 7:30 a.m. to 9:20 a.m., water from wells 3 and 4 was introduced into well 1 at a rate of about 210 gpm. At 9:10 a.m., a conductivity survey showed a rather uniform low conductivity at all depths above 1,040 feet, and indicated that all the water in the well above that point had been displaced by the mixture of water from wells 3 and 4. At 9:22 a.m., a survey was started from the bottom of the well to the top of the water. Four other surveys were made shortly thereafter. The results of all the surveys are shown in figure 3. From the surveys one can infer that water in strata at depths of 300, 350, 850, and 910 feet probably has a higher head than water in other strata, because the strata having higher heads more likely would be the first to redischarge the highly mineralized water into the wells after recharge operations were stopped. The additional downward movement shown from strata in the region of 350 feet to strata at least 450 feet deep indicates that aquifers containing water under less head are at or below that depth. One might also infer that strata below a depth of 920 feet contain water whose head is lower than the head immediately above a depth of 920 feet.

On September 9, 1955, well 1, which had been idle since the surveys in July, was started and a conductivity survey was made while the

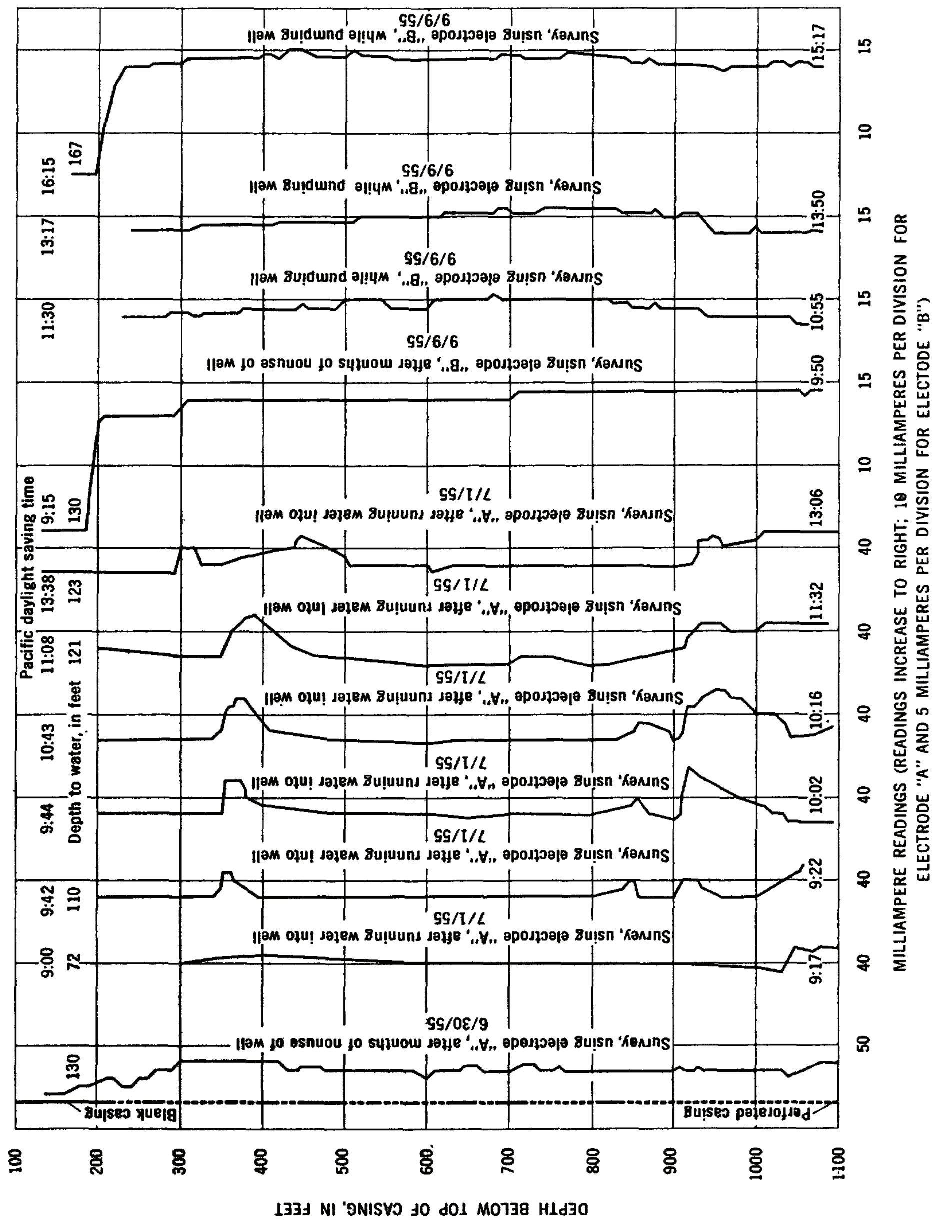

FIGURE 3.—Conductivity curves for well 1, Lake Mead Base, Las Vegas Valley, Nev.

well was being pumped. The bottom of the suction pipe was 220 feet below the top of the casing, or about 90 feet below the nonpumping level. The well was pumped at about 80 gpm from 9:57 a.m. to 12:45 p.m., then at about 150 gpm to 12:53 p.m., at which time the water level had lowered to the bottom of the suction pipe, and then at about 110 gpm until the completion of the survey at 5 p.m. At 10:15 a.m., the conductivity of the water being pumped was 3,200 micromhos at 25° C., the temperature of the water was 72° F. At 10:42 a.m., these characteristics were 3,080 and 73°, respectively; at 12:40 p.m., they were 2,990 and 77°; at 2 p.m., 2,970 and 77.5°; and at 3:17 p.m., 2,850 and 78°. The readings of the milliammeter at various depths below the top of the casing are shown in figure 3.

The data obtained on September 9, 1955, indicate that the dissolved-solids content above 200 feet was only about half the dissolved-solids content below that depth. The data indicate also that strata at about 920 feet are contributing water that is more highly mineralized than that from the lower strata. The concentration of dissolved solids does not appear to decrease significantly at any point between the depths of 500 and 920 feet, the region in which the highest concentrations occur; hence, it seems unlikely that water of satisfactory chemical quality can be obtained at reasonable rates from this section.

Although the water in the casing below 920 feet is of somewhat better chemical quality, the dissolved-solids content is not sufficiently less to offer any encouragement for obtaining a satisfactory supply from that section of the well either.

On the basis of milliampere readings, the dissolved-solids content of the best quality of water in the well is about half that of the water pumped from depths in excess of 250 feet. However, the fact that a sample of the water that was being used on the base at the time of the survey showed a reading of only about 4 milliamperes, or slightly more than half the reading obtained from the best quality of water in well 1, indicates that even this lower concentration may still be high.

The relative volumes of water from aquifers above 220 feet (the depth of the bottom of the suction pipe) and from aquifers below this depth, based on a milliampere reading of 7 for the water above 220 feet, 14 for the water below 220 feet, and 11 for the water discharged by the pump, are two-sevenths for the water above 220 feet and five-sevenths for the water below 220 feet.

As a result of the exploratory work done on well 1, it cannot be stated positively that water of satisfactory chemical quality cannot be developed at the site, though it almost certainly would be impractical to do so.

Because the chemical quality of the water deteriorates with nonuse of the well, it is inferred that one or more strata contain highly mineralized water at heads higher than the heads in strata containing water having a lower dissolved-solids content. When the well is not used, the highly mineralized water flows into the well and out again into the strata containing the water of lower mineralization under lesser head and thus contaminates these strata. When the well is pumped, the strata that received the highly mineralized water will, of course, yield the highly mineralized water back to the well before yielding the water of lower mineralization.

The length of pumping time and rate of pumping that will be necessary to cause aquifers to yield the true quality of the water they contain are dependent on the preceding length of nonpumping time and the rate of leakage under nonpumping conditions. The opportune time to determine the true chemical quality of the water in the various strata in a well in which leakage from one strata to another is taking place is immediately upon its completion.

In well 1, months of continuous pumping to waste at a rate of 100 gpm or so may be required to flush the aquifers that have been contaminated as a result of nonuse of the well. Whether this would be a justifiable procedure is questionable, because of a lack of evidence that strata penetrated by the well contain a sufficient quantity of water of satisfactory chemical quality or that they contain any satisfactory water at all.

SUMMARY

The findings of the study may be summarized as follows:

1. The principal source of the water in the Lake Mead Base well field is precipitation in the Las Vegas Valley drainage basin northwest of the well field.
2. The ground water is moving southeastward.
3. The amount of water passing through the area under natural conditions is small.
4. The principal aquifers in the well field probably dip eastward 500 feet per mile or more.
5. There is no conclusive evidence that withdrawals to date have caused a marked lowering of water levels.
6. By lowering the water levels, sufficient additional water can be diverted to the area from the main supply of Las Vegas Valley or obtained from storage to take care of the foreseeable needs of the base.

7. Wells having specific capacities in excess of a few gallons per minute per foot of drawdown are not likely to be developed in the immediate area of the base.
8. Interference effects between existing wells are too small to be measured or are insignificant under the present pumping schedules.
9. There is a good probability that all the wells are hydraulically connected; therefore, continued pumping from wells 3 and 4 at sufficiently high rates eventually may cause the more highly mineralized water in wells 1 and 2 to enter wells 3 and 4.
10. As yet, there has been no significant deterioration in the chemical quality of the water from wells 3 and 4.
11. The mineralization of the water from wells 1 and 2 increases during periods of nonuse.
12. Calcium, magnesium, and sulfate are the principal constituents of the highly mineralized water.
13. It does not appear practical to attempt to obtain a satisfactory supply of water from well 1.
14. Additional data relative to pumpage, water levels, and changes in chemical quality of the water are needed for more accurate future evaluation of the geologic and hydrologic factors that control the occurrence, movement, and chemical quality of the ground water.

REFERENCES CITED

Intermountain Association of Petroleum Geologists, 1952, Guidebook to the geology of Utah, no. 7, Cedar City, Utah, to Las Vegas, Nevada, 3d Ann. Field Conf., 1952: Salt Lake City, Utah, 165 p.

Maxey, G. B., and Jameson, C. H., 1948, Geology and water resources of Las Vegas, Pahrump, and Indian Spring Valleys, Clark and Nye Counties, Nev.: Nevada Water Resources Bull. 5, 121 p. app. 2, 43 p.

Meinzer, O. E., 1923, Outline of ground-water hydrology, with definitions: U.S. Geol. Survey Water-Supply Paper 494, 71 p.

Text and references to accompany Nevada Bureau of Mines and Geology Map 150

GEOLOGIC MAP OF PARTS OF THE COLORADO, WHITE RIVER, AND DEATH VALLEY GROUNDWATER FLOW SYSTEMS

NEVADA, UTAH, AND ARIZONA

by

William R. Page[1], Gary L. Dixon[2], Peter D. Rowley[3], and David W. Brickey[4]

[1] U.S. Geological Survey, Denver, CO
[2] Southwest Geology Inc., Blackfoot, ID
[3] Geologic Mapping Inc., New Harmony, UT
[4] TerraSpectra Geomatics, Las Vegas, NV

INTRODUCTION

The mapped area is greater than 20,000 km^2, and is largely within the Basin and Range physiographic province and its transition with the Colorado Plateau. The area is a desert, with little precipitation except in the mountains and few perennial streams and rivers besides the Colorado River and two tributaries, the Virgin and Muddy Rivers. The Colorado River is impounded by Hoover Dam, in the southwestern corner of the map area, to create Lake Mead, which volumetrically is the largest reservoir in the country. Lake Mead provides most of the culinary and agricultural water to southern California, southern Nevada, and southern Arizona, all among the fastest growing parts of the United States.

The geologic map provides a basis for understanding the complex geology and groundwater hydrology of a vast area whose population is experiencing increasingly significant water shortages (Page and others, 2003). Specifically, rapid urbanization and commercial development is taking place in the I-15 transportation corridor, from Las Vegas, Nevada, through Mesquite, Nevada, and the Arizona Strip to St. George, Utah. This growth has caused increased demand for water from surface sources and from local and regional aquifers. As a result, the geologic framework in the area needs to be described.

The main purpose of the geologic map is to provide our sponsors (National Park Service, U.S. Fish and Wildlife Service, Southern Nevada Water Authority, and Virgin Valley Water District) with digital geologic framework data used as important parameters in developing numerical groundwater flow models. These data describe the distribution, geometry, thickness, composition, and physical properties of geologic units. This information is required to define hydrogeologic units and potential aquifers and confining units. These data also describe the distribution, geometry, and characteristics of faults. Faults act as both conduits and barriers to groundwater flow depending on a variety of factors. When combined with geologic cross sections, well data, and geophysical subsurface information, these data provide a 3-dimensional geologic model characterizing the configuration of hydrogeologic units and faults in the map area that can be integrated with groundwater models using GIS analyses. The map is a printed version of an ARC/Info GIS data base. Geologic cross sections in the map area are being prepared in a separate report.

The southern half of Nevada and its adjacent states contain several huge groundwater basins, known as regional groundwater flow systems that may encompass a dozen or more of the closed topographic basins because they are interconnected in the subsurface. These regional flow systems are defined by hydrologic and geochemical evidence that indicate their groundwater flow paths pass beneath topographic barriers and continue beneath adjacent basins and ranges, referred to as interbasin flow (Eakin, 1966; Eakin and Winograd, 1965). Thomas and others (1986, 1996), Harrill and others (1988), Prudic and others (1995), and Harrill and Prudic (1998) summarized these flow systems for the Great Basin.

The main regional groundwater flow systems covered by this geologic map include parts of the Colorado flow system (Harrill and Prudic, 1998), the White River groundwater flow system (Eakin, 1964, 1966; Thomas and

Welch, 1984; and Kirk, 1987), and the Death Valley groundwater flow system (e.g., Winograd and Thordarson, 1975; Laczniak and others, 1996; Harrill and Prudic, 1998; D'Agnese and others, 2002; Workman and others, 2002, 2003). The White River flow system is contained within the much larger Colorado flow system; our map covers only the southern part of these flow systems and the eastern part of the Death Valley system (see figure on map sheet).

The primary source (recharge area) of the water in the flow systems is precipitation in the mountains surrounding basins in the map area and the numerous basins farther north and northeast. The principal discharge area for the White River flow system is Muddy River springs (Dettinger and others, 1995) (fig. 1), a series of about eight major springs (Schmidt and Dixon, 1995) that discharge 36,000 ac-ft/yr (44 hm^3/yr) to form the Muddy River. Movement of groundwater in the map area is primarily by fracture flow, that is along fractures (mostly joints; the "damage zone" of Caine and others, 1996) formed by faulting (e.g., Haneberg and others, 1999). The flow paths are generally southward, as indicated by potentiometric maps based on water levels in wells (Thomas and others, 1986; Wilson, 2001). They thus follow the general slope of the topography, from high areas in central Nevada to the low canyons of the Colorado River in southern Nevada. The flow is driven by the hydraulic head parallel to the southward topographic gradient.

Aquifers in the flow systems consist of Paleozoic carbonate rocks and subordinate volcanic rocks and basin-fill sediments (e.g., Plume and Carlton, 1988; Dettinger and others, 1995; Prudic and others, 1995; Burbey, 1997; Harrill and Prudic, 1998). In fact, the importance of the Paleozoic carbonate-rock aquifer to the flow systems that cover much of southern Nevada and adjacent states is so significant that many regional hydrologic reports have focused on the distribution and features of this aquifer (e.g., Dettinger and others, 1995; Burbey, 1997; Wilson, 2001).

METHODS AND DATA SOURCES

The geologic map contains greater detail and more recent compilations than existing regional geologic maps in the study area and provides stratigraphic and structural continuity across county and state boundaries. It was assembled by compiling all available regional and detailed geologic maps in the area. These maps were modified by the authors, as required to apply new information and concepts about the geology. The sources of geologic mapping are shown in figures 2 and 3. Figure 2 lists detailed map sources at 1:24,000-scale and figure 3 includes regional map sources from 1:50,000 to 1:250,000 scale. In a few remote areas not covered by existing geologic maps, we compiled the geology using reconnaissance scale county geologic maps (Longwell and others, 1965; Tschanz and Pampeyan, 1970) in combination with Landsat and aerial photo interpretation.

Geophysical studies have been completed in many of the major basins of the map area in order to understand the subsurface geology. These studies mainly applied gravity and magnetic methods in combination with analyses of seismic reflection data. Subsurface studies are especially significant in locating buried faults that may control groundwater flow and in modeling basins to better understand interbasinal groundwater flow. Bohannon and others (1993) interpreted subsurface faults and stratigraphic units in the Virgin Valley area based mostly on seismic reflection and well data. Jachens and others (1998) interpreted subsurface faults and other geologic features in the Virgin Valley and Tule Springs Hills areas based on high-resolution aeromagnetic studies. Langenheim and others (2000, 2001a, b, c) modeled the Virgin Valley, Las Vegas Valley, and California Wash basins using seismic reflection and gravity data. Phelps and others (2000) interpreted subsurface faults in the Coyote Spring Valley area based on gravity data.

ACKNOWLEDGMENTS

Funding for this geologic map was provided by the Southern Nevada Water Authority, U.S. Fish and Wildlife Service, National Park Service, and Virgin Valley Water District. We are grateful to Ernie Anderson, Bob Scott, and Van Williams of the USGS for their unpublished map data. Vicky Langenheim, Geoff Phelps, Bob Morin, Bob Jachens, and Tom Hildenbrand conducted geophysical surveys in the map area. We also thank Mel Kuntz of the USGS, Jim Faulds of the Nevada Bureau of Mines and Geology, Grant Willis of the Utah Geological Survey, and an anonymous reviewer for their technical reviews of the manuscript. Terry Katzer and David Donovan of the Southern Nevada Water Authority provided helpful suggestions to improve the manuscript.

STRATIGRAPHY

Proterozoic and Paleozoic Rocks

The oldest rocks in the map area are Early Proterozoic metamorphic and intrusive rocks consisting of gneiss, granite, and schist that are about 1.7 Ga (Quigley and others, 2002); their surface distribution is shown in figure 4. These crystalline rocks form both geologic and hydrologic basement and are considered barriers to groundwater flow because of their low permeability. The crystalline rocks may be locally permeable where highly fractured, but fractures in these rocks are generally poorly connected (D'Agnese and others, 1997). Early Proterozoic rocks exposed in the Beaver Dam and Virgin Mountains form the eastern boundary of the flow systems. Early Proterozoic rocks also form the core of the Mormon Mountains in the central part of the map area (fig. 4), where they act as a local barrier to groundwater flow (Burbey, 1997), although through-going, north-striking faults in the eastern Mormon Mountains may provide conduits for some component of southward groundwater flow through the mountain range.

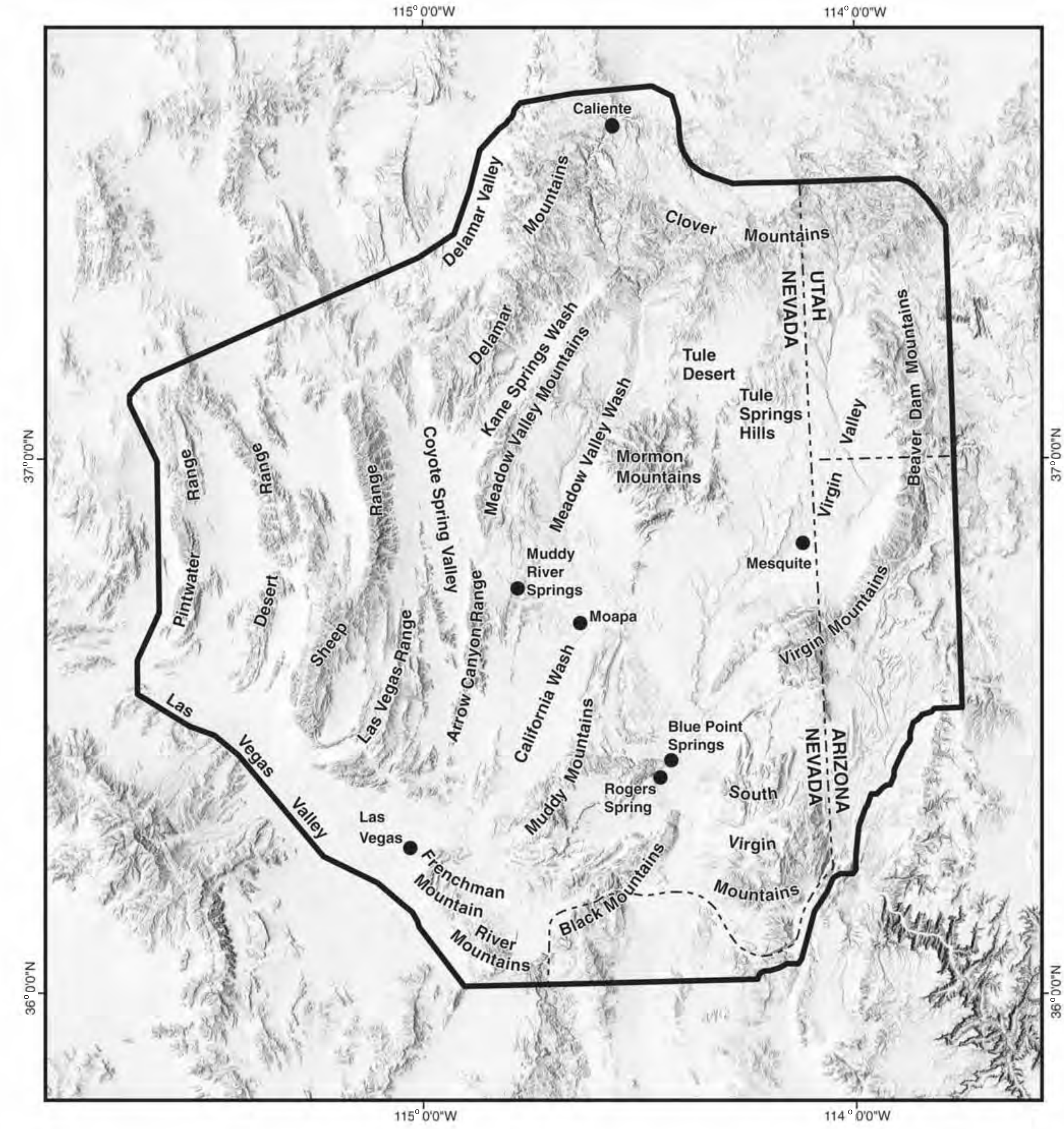

Figure 1. Index map showing major physiographic features in the map area.

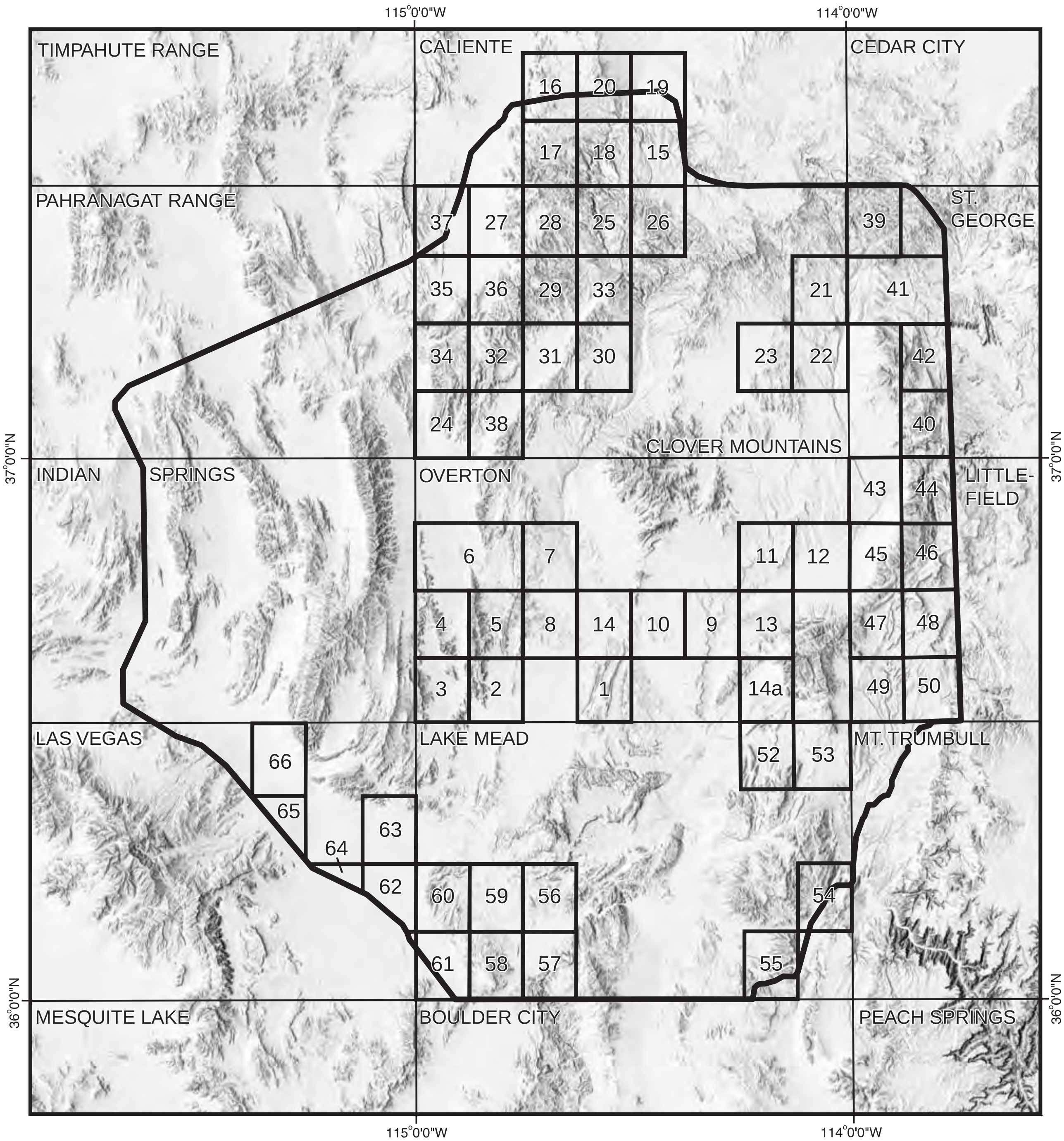

Figure 2. Index to 1:24,000-scale geologic mapping sources. See table 1 for quadrangle names and references.

Table 1. Geologic mapping sources for the study area. Locations of the 1:24,000-scale geologic maps are shown in figure 3.

Overton 30 x 60 Quadrangle

1. Weiser Ridge (Bohannon, 1992a)
2. Arrow Canyon SE (W.R. Page, unpub. mapping, 1999)
3. Arrow Canyon SW (W.R. Page, unpub. mapping, 1999)
4. Arrow Canyon NW (Page, 1998)
5. Arrow Canyon (Page, 1992)
6. Wildcat Wash SE and Wildcat SW (Page and Pempeyan, 1996)
7. Farrier (Schmidt, 1994)
8. Moapa West (Schmidt and others, 1996)
9. Overton NE (V.S. Williams, unpub. mapping, 1999)
10. Overton NW (V.S. Williams, unpub. mapping, 1999)
11. Flattop Mesa (V.S. Williams, unpub. mapping, 2000)
12. Mesquite (Williams, 1996)
13. Riverside (Williams and others, 1997a)
14. Moapa East (Williams and others, 1997b)

14a. Whitney Pocket (Beard, 1993)

Caliente 30 x 60 Quadrangle

15. Eccles (P.D. Rowley, unpub. mapping,1993)
16. Caliente NW (P.D. Rowley, unpub. mapping,1993)
17. Chokecherry Mtn. (P.D. Rowley, unpub. mapping,1993)
18. Caliente (P.D. Rowley and others, unpub. mapping,1993)
19. Indian Cove (Rowley and Shoba, 1991)
20. Chief Mountain (Rowley and others, 1994)

Clover Mountains 30 x 60 Quadrangle

21. Dodge Spring (Anderson and Hintze, 1993)
22. Scarecrow Peak (Hintze and Axen, 1995)
23. Lime Mountain (Hintze and Axen, 2001)
24. Delamar 3 SW (Page and others, 1990)
25. Elgin NE (P.D. Rowley, unpub. mapping, 1994)
26. Ella Mountain (P.D. Rowley, unpub. mapping, 1994)
27. Delamar (P.D. Rowley, unpub. mapping, 1995)
28. Slidy Mountain (P.D. Rowley and R.B. Scott, unpub. mapping, 1994)
29. Elgin SW (R.B. Scott, unpub. mapping, 1994)
30. Vigo NE (R.B. Scott and A. Harding, unpub. mapping, 2003)
31. Vigo NW (Scott and others, 1991a)
32. Delamar 3 NE (Scott and others, 1990a)
33. Elgin (R.B. Scott and P.D. Rowley, unpub. mapping, 1993)
34. Delamar 3 NE (Scott and others, 1990b)
35. Delamar Lake (Scott and others, 1993)
36. Gregerson Basin (Scott and others, 1991b)
37. Delamar NW (Swadley and Scott, 1990)
38. Delamar 3 SE (Swadley and others, 1994)

St. George 30 x 60 Quadrangle

39. Goldstrike (R.E. Anderson, unpub. mapping, 1993)
40. Jarvis Peak (Hammond, 1991)
41. Motoqua and Gunlock (Hintze and others, 1994)
42. Shivwits (Hintze and Hammond, 1994)

Littlefield 30 x 60 Quadrangle

43. Littlefield (Billingsley, 1995)
44. Mountain Sheep Spring (Bohannon and others, 1991)
45. Elbow Canyon (Billingsley and Bohannon, 1995)
46. Mount Bangs (Bohannon and Lucchitta, 1991)
47. Jacobs Well and southern part of the Elbow Canyon (Bohannon, 1991)
48. Cane Springs (Lucchitta and others, 1995a)
49. Red Pockets (Bohannon, 1992b)
50. Cane Springs Southeast (Lucchitta and others, 1995b)

Lake Mead 30 x 60 Quadrangle

52. Devils Throat (Beard, 1991)
53. St. Thomas Gap (Beard, 1992)
54. Iceberg Canyon (Brady and others, 2002)
55. Hiller Mountains (Howard and others, 2003)
56. Callville Bay (Anderson, 2003)
57. Hoover Dam (Mills, 1994)
58. Boulder Beach (Smith, 1984)
59. Government Wash (Duebendorfer, 2003)
60. Frenchman Mountain (Castor and others, 2000)
61. Henderson (Bell and Smith, 1980)

Las Vegas 30 x 60 Quadrangle

62. Las Vegas NE (Matti and others, 1993)
63. Valley (Lundstrom and others, 1998)
64. Las Vegas NW (Matti and others, 1987)
65. Tule Springs Park (Bell and others, 1998)
66. Corn Creek Springs (Bell and others, 1999)

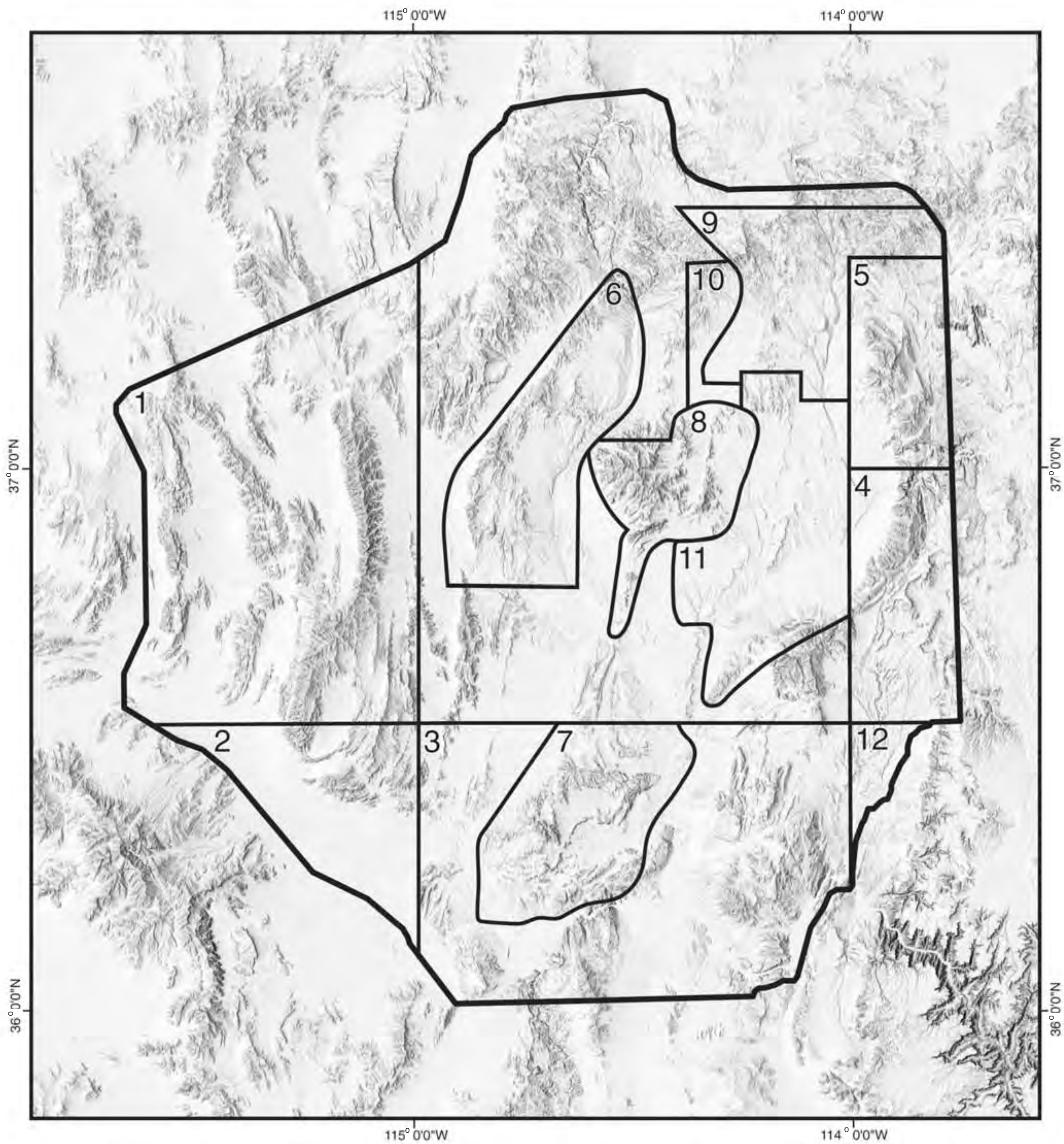

1. Workman and others (2003)
2. Page and others (2005)
3. Beard and others (in press)
4. Billingsley and Workman (1998)
5. Hintze (1986)
6. Pampeyan (1993)
7. Bohannon (1983)
8. Axen and others (1990), Skelly (1987), Olmore (1971), and Wernicke and others (1985)
9. R.E. Anderson (unpub. mapping, Clover Mountains and Bull Valley Mountains, 1990)
10. Ekren and others (1977)
11. Dixon and Katzer (2002)
12. Billingsley and Wellmeyer (2003)

Figure 3. Index to geologic mapping sources, 1:50,000 to 1:250,000-scale maps.

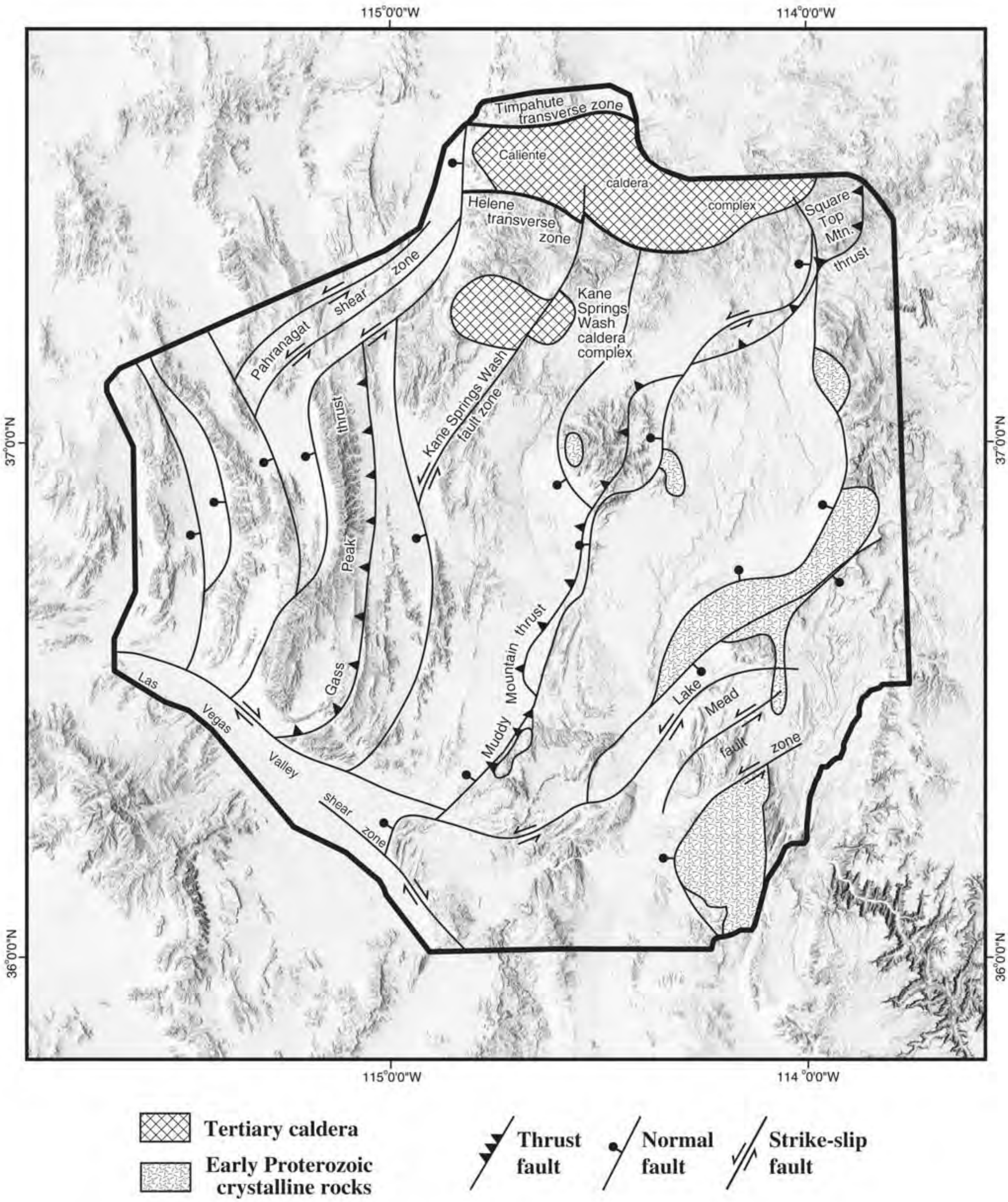

Figure 4. Generalized map of the principal structural features in the map area.

Late Proterozoic sedimentary rocks are exposed in the Desert and Sheep Ranges and northern Delamar Mountains. These are mostly clastic rocks and consist of quartzite, conglomerate, sandstone, siltstone, and shale, but they contain subordinate amounts of limestone and dolostone. The Late Proterozoic sedimentary rocks are well-cemented, contain few or no pore spaces, and have low permeability. They were deposited in shallow marine waters along a passive continental margin of what is now western North America (Stewart, 1976; Stewart and Poole, 1972). Late Proterozoic rocks are interpreted to represent initial deposits of the Cordilleran miogeocline (Stewart and Poole, 1972; Stewart, 1972, 1976).

Like the Late Proterozoic sedimentary rocks, Lower Cambrian rocks are also predominantly well-cemented, clastic units containing mainly quartzite, conglomerate, siltstone, and shale. Together, the Lower Cambrian and Late Proterozoic sedimentary rocks in the western part of the map area form a confining unit. In the Desert Range, these rocks attain their maximum thickness in the map area and may form a potential barrier to westward groundwater flow. In the Death Valley groundwater flow system, these same rocks are referred to as the lower clastic aquitard (Winograd and Thordarson, 1975), or the lower clastic confining unit (Belcher and others, 2002). Late Proterozoic clastic units pinch out in the eastern part of the map area and are absent in the Mormon, Virgin, and Beaver Dam Mountains. Here, the lower clastic confining rocks include the Lower Cambrian Tapeats Sandstone and the Lower and Middle Cambrian Bright Angel Shale that have a combined thickness ranging from 125 to 445 m.

Middle Cambrian through Lower Permian rocks are widely distributed in the map area and record a significant shift in deposition to predominantly carbonate sedimentation, from mostly clastic sedimentation in pre-Bonanza King Late Proterozoic and Cambrian units. The carbonate rocks are predominantly limestone and dolostone and form the regional aquifer in the map area (Dettinger and others, 1995). The Middle and Upper Cambrian Bonanza King Formation (and equivalent Highland Peak and Muav Formations) forms the basal part of the regional carbonate aquifer in the White River and Colorado flow systems, and in the Death Valley groundwater flow system (Winograd and Thordarson, 1975; Laczniak and others, 1996; Belcher and others, 2002; D'Agnese and others, 2002). Groundwater flow through the carbonate rocks is mostly through fractures and faults. Because the rocks are soluble in groundwater, dissolution features are also important in the development of secondary porosity and permeability. Zones of high transmissivity in the carbonate rock aquifer are indicated by large spring discharge (36,000 ac-ft/yr [44 hm^3/yr] at Muddy River Springs) in areas of low potentiometric gradient, and by water wells exhibiting extremely high hydraulic conductivity (900 ft^2/d [84 m^2/d] at MX-5 in Coyote Spring Valley) (Dettinger and others, 1995).

Middle Cambrian through Lower Permian rocks are dominantly carbonate rocks with the exception of several units that have greater proportions of clastic material: these units include the Upper Cambrian Dunderberg Shale Member of the Nopah Formation, Middle Ordovician Eureka Quartzite, Upper Mississippian Chainman Shale, Upper Mississippian Indian Springs Formation, and the Lower Permian redbeds. These clastic units are generally not thick enough to form regional confining units in the map area, but they may act as confining units locally within the region, especially the Lower Permian redbeds which have a maximum thickness of 600 m.

The upper part of the carbonate aquifer in the map area includes the Bird Spring Formation and partly equivalent Callville Limestone. Lower Permian redbeds overlie these formations and represent a shift from dominantly carbonate marine to mostly continental and marginal marine sedimentation. Continental sedimentation predominated through the Mesozoic and into the lower Tertiary.

Late Proterozoic-Paleozoic facies belts

Late Proterozoic-Paleozoic rocks in the map area can be broadly subdivided into western, central, and eastern facies belts (see correlation of map units). Rocks in the western belt include Late Proterozoic through Devonian units deposited as part of the Cordilleran miogeocline in offshore carbonate shelf and intertidal depositional settings, and an overlying Mississippian to Permian sequence deposited mostly in a carbonate platform depositional setting. Units of the western belt are exposed as far east as the Las Vegas Range, Arrow Canyon Range, Meadow Valley Mountains, and Delamar Mountains (fig. 1).

The eastern facies belt includes cratonic platform rocks of the Colorado Plateau region exposed in the Beaver Dam and Virgin Mountains, and in the Lake Mead area including Frenchman Mountain. The rocks are mostly shallow marine sediments deposited in near-shore, intertidal, and continental settings. The facies belt is characterized by a large magnitude unconformity separating Middle Devonian from Upper Cambrian rocks (see correlation of map units). Rock units in the belt also include significant amounts of evaporite deposits, especially in the Permian formations. The central facies belt includes rocks that are transitional between the eastern and western belts; these rocks are exposed in the Muddy Mountains, Mormon Mountains, and Tule Springs Hills (fig. 1).

Thickness of Middle Cambrian to Lower Permian carbonate rocks, which define the regional aquifer, decrease dramatically across the belts from west to east over a distance of about 100 km—from about 4 to 6 km thick in the western belt to less than 2 km thick in the eastern belt. The carbonate rocks average about 2.5 km thick in the central belt. The thinning resulted from erosion of individual units along major unconformities and stratigraphic thinning of individual units toward the craton, but the large thickness variation across the belts is primarily due to southeast-vergent Mesozoic thrusting (see section on Structural Geology below).

Mesozoic Rocks

Mesozoic rocks are predominantly continental clastic units consisting of conglomerate, sandstone, siltstone, mudstone, shale, gypsum, but they also include minor limestone and dolostone. These rocks were deposited in fluvial, lacustrine, eolian, and marginal marine environments, and include Triassic, Jurassic, and Cretaceous units that are about 3 to 4 km thick (Bohannon, 1983). These rocks have low permeability compared with the Paleozoic carbonate rocks because of their high proportion of clastic material. They are generally considered confining units, but they may be permeable where highly fractured. Units containing large amounts of shale and mudstone, such as in the Triassic formations, generally have low permeability. The Jurassic Navajo Sandstone in the Utah part of the map area is an aquifer (Heilweil and others, 2002), but in other parts of southern Nevada, such as in Las Vegas Valley, the Aztec Sandstone has low permeability. This example illustrates the variability in hydrologic properties of the Mesozoic rocks in the map area. The distribution of Mesozoic rocks is limited to the eastern half of the map area, although some units extend into the Basin and Range province and westward into the Jurassic arc terrane of southeastern California (Marzolf, 1990). East-vergent thrusting related to the Sevier orogeny affected the map area from Early Cretaceous into early Tertiary time (see structure section below).

Tertiary Rocks

Tertiary rocks in the map area belong to three sequences based on age. The oldest is the basal Tertiary unit of fluvial and lacustrine origin, partly derived from erosion of highlands resulting from Sevier deformation to the west. The best-known unit is the Eocene and Oligocene Claron Formation (Anderson and Rowley, 1975) that makes up the colorful rocks of Bryce Canyon National Park, but these rocks are confined to the northeastern part of the map area.

The second sequence consists of voluminous calc-alkaline volcanic rocks of rhyolite to andesite composition, as well as their source plutons. Most of these igneous rocks were deposited between about 35 to 20 Ma, but in the northern Colorado River extensional corridor near and south of Lake Mead, calc-alkaline magmatism began at about 20 Ma and continued until about 12 Ma (Faulds and others, 2001). Many volcanic rocks are ash-flow tuffs erupted from calderas, but stratovolcanoes were locally present. Ash-flow tuffs are potential aquifers where broken by faults. The largest caldera in the map area is the east-elongated (80 km east-west versus 35 km north-south) Caliente caldera complex (at least 24 Ma to 13.5 Ma, representing eruptions of calc-alkaline rocks, then bimodal rocks) in the northeastern part of the area (fig. 4). The caldera is broken by numerous north-striking fault zones that may provide important conduits for north-south groundwater flow in the region.

The third sequence of Tertiary rocks evolved during the major episode of east-west basin-range extension. North of Lake Mead, this extension took place from about 20 Ma to present (e.g., Rowley and Dixon, 2001). Over most of the map area, volcanic rocks of bimodal composition (high-silica rhyolite and basalt) and of generally low volume intertongue with basin-fill deposits. In the northern Colorado River extensional corridor, however, major extension followed and accompanied later calc-alkaline volcanism, whereas basalts generally accompanied only the waning stages of extension (Faulds and others, 2001). The basin-fill deposits are mostly fluvial sediments deposited in grabens that resulted from the basin-range faults. In some places, as in the Virgin Valley, the basin-fill sediments are at least 8 km thick (Langenheim and others, 2000, 2001a); they constitute the dominant aquifer in the Virgin Valley basin (Dixon and Katzer, 2002; Johnson and others, 2002). Langenheim and others (2001c) reported Tertiary basin-fill deposits in the California Wash basin (fig. 1) to be from 2 to 3 km thick based on seismic reflection and gravity data. The geometry of basins in the map area is generally complex, and geophysical investigations have demonstrated that many of the basins, such as Virgin Valley, Las Vegas Valley, and Meadow Valley Wash, consist of a series of sub basins (Langenheim and others, 2000, 2001a, b).

During basin-range extension, the map area was broken by mostly north-striking normal faults. Northeast-striking left lateral faults, northwest-striking right-lateral faults, and low angle normal (detachment) faults occur locally. In addition, the map area includes a series of east-striking transverse faults, which started to form in the late Mesozoic and early Tertiary (Ekren and others, 1976; Brothers and others, 1996; Rowley, 1998; Rowley and Dixon, 2001) and continued to deform the area.

Structural Geology

Major thrust faults in the map area include the Muddy Mountain thrust in the Muddy Mountains and its equivalent thrusts that extend northward to the Beaver Dam Mountains (Square Top Mountain thrust), and the Gass Peak thrust in the eastern Sheep Range (fig. 4). The faults strike north to northeast and are part of the Sevier orogenic belt (Armstrong, 1968; Fleck, 1970). The Muddy Mountains thrust is the frontal thrust of the Sevier orogenic belt in southern Nevada. The thrust is reported to be late Albian to Cenomanian(?) in age (Bohannon, 1983; Carpenter and Carpenter, 1994; Fleck and Carr, 1990).

The thrust faults partly control the thickness of the Paleozoic carbonate aquifer from west to east across the map area. The Gass Peak thrust transported thick western facies rocks about 30 km eastward (Guth, 1980, 1981) above thin transitional central facies rocks. The Muddy Mountain thrust juxtaposes transition rocks above even thinner eastern facies cratonic platform rocks. Therefore, a large thickness variation exists in the Paleozoic rocks from west to east (from 6 km to less than 2 km) across the map area, because the rocks were telescoped into a narrower zone by Mesozoic thrusting.

The control of groundwater flow by thrust faults in the map area is poorly understood. Burbey (1997) suggested that Late Proterozoic-Lower Cambrian clastic confining units in the upper plate of the Gass Peak thrust may restrict eastward groundwater flow from the Sheep Range and areas to the west. The Muddy Mountain thrust in the Muddy Mountains juxtaposes Paleozoic carbonate rocks in the upper plate against less permeable Mesozoic rocks in the lower plate; such relationships suggest that the thrust acts as a flow barrier. Although the thrust may act as a barrier in localized zones along strike, we believe that overprinting of the thrust by Tertiary normal faults (California Wash fault zone; Langenheim and others, 2002) provides linkage between rocks in the upper and lower plates allowing for some component of groundwater flow across the thrust. This example may apply to other pre-Tertiary thrust faults in the map area, especially where the thrusts are highly modified by younger Tertiary extensional faults.

During Sevier thrusting and following its termination in the Paleocene, erosion of highlands created by these thrusts contributed clastic material that was shed largely to the east. The early Tertiary was a time of deep dissection of these highlands, with deposition of the resulting detritus in the northeastern part of the area and in areas farther east.

East-striking transverse fault zones began to form in the late Mesozoic and transected the Great Basin (Ekren and others, 1976; Rowley, 1998; Rowley and Dixon, 2001). Like transform zones in the ocean basins, they allowed the bounding crustal blocks to deform in different ways and at different rates. The transverse zones also partly controlled emplacement of plutons and caldera complexes, beginning with the start of calc-alkaline magmatism at about 35 Ma. The most notable of these zones in the map area is the Timpahute transverse zone (fig. 4), which defined the northern side of the Caliente caldera complex. Another zone, the Helene transverse zone (fig. 4), controlled not only the southern side of the Caliente caldera complex but also gold mineralization in Delamar and other mining districts on the southern side of the caldera complex. The Caliente caldera complex is elongated east-west because it was extended in that direction by north-striking normal faults and synchronous intracaldera eruptions were focused by bounding transverse faults.

In the northern part of the map area, east-west extension took place during calc-alkaline magmatism. Extension was accompanied by north-directed lateral compression, resulting in north-northeast- and north-northwest-striking strike-slip and oblique-slip faults (Rowley and Dixon, 2001). The oblique left-lateral, north-northeast-striking Kane Springs Wash fault zone (fig. 4) likely began to form during the time of calc-alkaline magmatism, as did the many unnamed right-lateral, northwest-striking faults in the northeastern part of the mapped area.

At about 20 Ma, with increased east-west extension, bimodal magmatism began in the Great Basin in the northern part of the map area (Rowley and Dixon, 2001). To the south, calc-alkaline intermediate magmatism began about 20 Ma and continued to about 12 Ma (Faulds and others, 2001). Locally before 10 Ma, basin-range faulting blocked out north-trending ranges and intervening basins. These faults, which define the Desert, Sheep, Arrow Canyon, and Delamar Ranges, are especially prominent in the western part of the map area. Locally, during east-west extension, east-northeast-striking faults formed, including the Pahranagat shear zone (fig. 4). The east-northeast-striking fault zones accommodate left-lateral oblique-slip movement and merge laterally with north-striking basin-range faults. The northwest-striking Las Vegas Valley shear zone (fig. 4) is a large magnitude right-lateral strike-slip transverse fault zone (Rowley, 1998) with about 50 km lateral offset. Major movement on the shear zone is constrained between 14 and 8.5 Ma (Duebendorfer and Black, 1992). The shear zone truncates the southern Las Vegas, Sheep, Desert, and Pintwater Ranges in the area and extends for nearly 150 km from the Lake Mead area to Mercury, Nevada.

Description of Map Units

Surficial Units

Relative age assignments for surficial deposits are estimated chiefly on the basis of their height above present streams, degree of post-depositional modification of original surface morphology, and degree of soil development—especially the morphology and thickness of calcium-carbonate-enriched horizons.

Qa **Channel alluvium (Holocene)** Unconsolidated silt, sand, and gravel in active channels and flood plains of rivers and streams. As thick as 10 m.

Qay **Young alluvium (Holocene to latest Pleistocene)** Unconsolidated fine- to coarse-grained gravel and sand and less common silt and clay deposited in alluvial fans and piedmont slopes. Deposits exhibit minor to no dissection. From 1 to 20 m thick.

Qayf **Young fine-grained alluvium (Holocene to late Pleistocene)** Unconsolidated silt, sand, and minor pebble gravel. Deposits form low relief surfaces and exhibit little or no dissection. Exposed in axial parts of valleys in distal portions of alluvial fans and adjacent to playa deposits (Qp). As thick as 10 m.

Qp **Playa deposits (Holocene to late Pleistocene)** Clay, silt, sand, and minor secondary carbonate and evaporite minerals. Playa surfaces are smooth and flat. As thick as 10 m.

Qe **Eolian deposits (Holocene)** Unconsolidated to slightly consolidated silt and sand deposited as dunes, sand ramps, and sand sheets. Deposits include buried paleosols. As thick as 10 m.

Qsa **Spring-apron deposits (Holocene to middle Pleistocene)** Mostly consolidated limestone and travertine deposited near fault-controlled springs. Limestone and travertine deposits contain organic debris (root casts and other plant material) and form spring mounds and aprons. Deposits exposed at southern end of Meadow Valley Mountains and California Wash areas, Nevada, and Virgin Valley area of Utah and Nevada. Generally less than 10 m thick.

Qds **Modern and past groundwater discharge deposits (Holocene to late Pleistocene)** Mostly unconsolidated to consolidated mud, silt, and sand, that locally form small bluffs in the axial parts of major basins. These sediments locally contain organic zones (black mats) and fossils such as fresh-water mollusks and late Pleistocene bone fragments of mammoth, horse, camel, and bison (Quade and others, 1995, 1998). Thickness 1 to 10 m.

Qayo **Intermediate alluvium (late to middle Pleistocene)** Partially consolidated sand and medium- to coarse-grained gravel deposited in alluvial fans and piedmont slopes. Deposit surfaces have low to moderate relief and dissection and may stand as high as 10 m above active channels. From 0 to 10 m thick.

Qao **Old alluvium (middle to early Pleistocene)** Partly consolidated silt, sand, and medium- to coarse-grained gravel deposited in alluvial fans and piedmont slopes. Deposits have well-developed calcareous soils and are moderately to highly dissected. From 0 to 30 m thick.

QTa **Oldest alluvium (early Pleistocene to Pliocene)** Consolidated sand and medium- to coarse-grained gravel deposited in alluvial fans and piedmont slopes; includes well developed soil horizons. Deposit surfaces form ballena topography and are highly dissected. Unit mostly exposed in the proximal parts of major drainages flowing into the Colorado River, including Beaver Dam and Meadow Valley Washes. Unit may be 100 m thick or greater.

QTls **Landslide and megabreccia deposits (Pleistocene to Miocene?)** Unit includes highly brecciated rock-avalanche deposits and kilometer-size coherent landslide blocks. Base of unit may be bound by shear slip surface. Unit is composed mostly of Paleozoic bedrock units exposed along mountain range margins, as along the west side of the Sheep Range and west flank of the Beaver Dam Mountains. Maximum thickness about 100 m.

QTc **Calcrete (Pleistocene and Pliocene)** Well consolidated caliche containing embedded pebbles, cobbles, boulders, sand and silt. Caliche beds contain laminar and thin bedded to massive carbonate nodules and pisolites. Deposit surfaces have low relief and represent soil and/or groundwater deposition. Unit best exposed at Mormon Mesa (Machette, 1985). Unit is 1 to 20 m thick.

Bedrock Units

Within much of the Tertiary section, we have followed the mapping strategy of Ekren and others (1977), in which sedimentary and volcanic units are subdivided based upon rock type and age range. The age range follows five main stages in the evolution of this part of the Basin and Range province. Unit 1 consists of sedimentary rocks that predate the oldest Tertiary volcanic units in the area. Unit 2 consists of the oldest Tertiary volcanic rocks of calc-alkaline composition, about 32 to 26 Ma; no sedimentary rocks are associated with this age range. Unit 3 consists of younger calc-alkaline volcanic rocks and related sedimentary rocks ranging in age from 26 to 18 Ma. Unit 4 consists of the older bimodal sequence (locally calc-alkaline) of volcanic rocks and related sedimentary rocks, associated in most areas with the early phases of major regional basin-range extension and ranging in age from 17 to 11 Ma. Unit 5 consists of the younger bimodal sequence of volcanic rocks and related sedimentary rocks associated with both the main episode of regional extension and waning extension, and ranges in age from about 11 to 2 Ma; volcanic rocks of this age are included within the older basaltic flows (Tb). Within the pre-Tertiary regional sedimentary section, some regional sedimentary units are separated geographically, into Proterozoic-Paleozoic facies belts, even though they may be partly or entirely correlative (see correlation of map units). This is because facies changes prevent exact correlations between areas and thus different names have been applied to rocks of the same age.

Qb **Younger basaltic lava flows (Pleistocene)** Exposed only in the northeastern Beaver Dam Mountains. Resistant, dark-gray and black, mostly crystal-poor olivine basalt lava flows and cinder cones. Maximum thickness of individual flow sequences about 100 m.

Tb **Older basaltic lava flows (Pliocene and Miocene)** Resistant, dark-gray and black, mostly crystal-poor olivine basalt lava flows and cinder cones. Includes flows in and near Kane Springs Valley of about 8.0 to 5.6 Ma (Scott and others, 1995b), and in the Lake Mead area of about 11 to 4.4 Ma (Faulds and others, 2001). Maximum thickness of individual flow sequences about 200 m.

Ts5 **Sedimentary rocks, unit 5 (Pliocene and Miocene)** The primary unit is the Muddy Creek Formation (11 to 5 Ma). Muddy Creek Formation is soft to moderately consolidated, tan, gray, and pink, fluvial and lacustrine, tuffaceous sandstone, mudstone, gypsum, halite, and conglomerate that fills fault-block basins. Other named and unnamed units of the same general age fill many other basins: these include the Panaca Formation in the Panaca basin (Rowley and Shroba, 1991), and several unnamed units in northern Kane Spring Valley. The unit also includes age-equivalent basin-fill deposits in the Lake Mead area consisting of conglomerate, sandstone, siltstone, mudstone, limestone, and gypsum. Maximum thickness at least 1,000 m, but may be 3,000 m or more in deeper basins.

Ts4 **Sedimentary rocks, unit 4 (Miocene and Oligocene)** Moderately to well consolidated, mostly gray and tan, fluvial and lacustrine, locally tuffaceous sandstone, tuff, conglomerate, limestone, siltstone, mudstone, and gypsum that fill the lower parts of fault-block basins. The primary unit is the Horse Spring Formation (20 to 12 Ma; Bohannon, 1984). Also included is the red sandstone unit (12 to 11 Ma) that unconformably overlies the Horse Spring Formation (Bohannon, 1984). Total maximum thickness of the Horse Spring at least 2,600 m in Muddy Mountains (Bohannon, 1984), but may be 3,000 m or more in deeper basins.

Ts1 **Sedimentary rocks, unit 1 (Oligocene and Eocene)** Moderately to well consolidated, white, pink, red, and tan, fluvial and lacustrine limestone, sandstone, mudstone, and conglomerate that pinch out westward. Includes the Claron Formation (Oligocene and Eocene) in the northeast part of the map area; roughly correlative rocks extend as far west as the Dodge Spring Quadrangle (Anderson and Hintze, 1993), although they are only 70 m thick at that locality. Unit also includes age-equivalent basin-fill conglomerate and tuff as much as 100 m thick in the Pintwater Range area (Guth, 1980). Maximum thickness about 500 m.

Tt4 **Ash-flow tuffs and interbedded airfall tuffs, unit 4 (Miocene)** Poorly to densely welded, crystal-poor, bimodal high-silica rhyolite and peralkaline ash-flow tuff and related airfall tuffs; gray, red, tan, and brown. Includes Ox Valley Tuff (13.5 Ma), tuff of Etna (14.0 Ma), tuff of Rainbow Canyon (15.6 Ma), tuff of Acklin Canyon (17.1 Ma), and tuff of Dow Mountain (17.4 Ma), derived from the Caliente caldera complex (Rowley and others, 1995; Snee and Rowley, 2000). Also includes the tuff of Narrow Canyon (15.8 Ma), tuff of Boulder Canyon (15.1 Ma), and Kane Wash Tuff (14.7 to 14.4 Ma), derived from the Kane Springs Wash caldera complex (Scott and others, 1995a, b). Maximum thickness of outflow sheets generally less than 200 m, but intracaldera tuffs at least 500 m thick.

Tt3 **Ash-flow tuffs and interbedded airfall tuffs, unit 3 (Miocene and Oligocene)** Poorly to densely welded, crystal-poor and crystal-rich, calc-alkaline, low-silica rhyolite and dacite ash-flow tuff and related airfall tuffs; gray, brown, tan, and pink. Includes the tuff of Teepee Rocks (17.8 Ma), Hiko Tuff (18.3 Ma), Racer Canyon Tuff (18.7 Ma), and both Bauers Tuff Member (22.8 Ma) and Swett Tuff Member (23.7 Ma) of the Condor Canyon Formation, all derived from the Caliente caldera complex (Rowley and others, 1995; Snee and Rowley, 2000); the Harmony Hills Tuff (22.0 Ma), probably derived from the eastern Bull Valley Mountains (Williams, 1967; Anderson and Rowley, 1975); the Leach Canyon Formation (23.8 Ma), probably derived from the Caliente caldera complex (Williams, 1967; Anderson and Rowley, 1975); and the Pahranagat Formation (22.6 Ma) and Shingle Pass Tuff (26.4 Ma), derived from the central Nevada caldera complex (Best and others, 1993) 50 km north of the map area. Thickness of individual outflow sheets generally less than 300–450 m, but thickness of intracaldera tuffs at least 1,000 m.

Tt2 **Ash-flow tuffs and interbedded airfall tuffs, unit 2 (Oligocene)** Moderately to densely welded, crystal-poor and crystal-rich, calc-alkaline, low-silica rhyolite, dacite, and trachydacite ash-flow tuff and related airfall tuffs; gray, brown, reddish-brown, and pink. Includes the Isom Formation (about 27 Ma), probably derived from the Indian Peak caldera complex (Best and others, 1993) 20 km north of the map area; the Monotony Tuff (27.3 Ma), derived from the central Nevada caldera complex (Best and others, 1993); and the Needles Range Group (32 to 28 Ma), derived from the Indian Peak caldera complex (Best and others, 1989). Thickness of individual outflow sheets generally less than 500 m.

Tr4 **Rhyolite lava flows, unit 4 (Miocene)** High-silica rhyolite. Includes thick sequences in the Caliente caldera complex, some related to emplacement of the Ox Valley Tuff. Maximum thickness about 300 m.

Tr3 **Rhyolite lava flows, unit 3 (Miocene and Oligocene)** Low-silica rhyolite. Includes an east-striking string of domes and dikes along the south side of the Caliente caldera complex that have the same age as the Hiko Tuff. Maximum thickness about 300 m.

Ta4 **Intermediate-composition lava flows, unit 4 (Miocene)** Andesitic and locally dacitic lava flows, flow breccia, and mudflow breccia; red, reddish-brown, brown, and gray. Andesite of the Hamblin-Cleopatra volcano (14.2 to 11.5 Ma) in the southern Lake Mead area (Anderson, 1973). Maximum thickness about 300 m.

SE ROA 42949

JA_12829

Ta3 **Intermediate-composition lava flows, unit 3 (Miocene and Oligocene)** Andesitic and locally dacitic lava flows, flow breccia, and mudflow breccia; red, reddish-brown, brown, and gray. In the northeast part of the map area, includes the crystal-rich andesite of Maple Ridge underlying the Racer Canyon Tuff, and the andesite of Little Creek that lies between the Harmony Hills Tuff and the Condor Canyon Formation (Blank, 1959, 1993; Rowley and others, in press). Includes thick stratovolcano deposits, derived from an adjacent pluton, between the Caliente and Kane Springs Wash caldera complexes. Maximum thickness about 1,000 m.

Tg **Granitic intrusive rocks (Miocene)** Granite or other silicic intrusive rock; gray, tan, and locally pink. On the north side of the Kane Spring Wash caldera complex, includes the trachyte stock of Sawmill Spring (14.4 Ma), which postdates volcanic units from the complex. On the west side of the Kane Springs Wash caldera complex, includes the stock of Jumbo Wash, which predates volcanic units from the complex, but is probably less than 15.6 Ma (Scott and others, 1995b).

Tai **Intermediate-composition intrusive rocks (Miocene and Oligocene)** Gray quartz monzonite, granodiorite, diorite, and other intermediate-composition intrusive rocks. In the Lake Mead area, includes diorite and granodiorite source plutons for the Hamblin-Cleopatra volcano and the volcanic rocks of the Black Mountains. In the south Clover Mountains and southwest Bull Valley Mountains, includes 22 to 20 Ma quartz monzonite porphyry plutons of the northeast-striking Iron Axis, such as the Mineral Mountain pluton (Hacker and others, 2002; Rowley and others, in press); includes small dioritic breccia pipes and a nearby large, although fault-fragmented, diorite and granodiorite pluton that was the source of an andesitic stratovolcano complex along the south side of the Caliente caldera complex. Includes the 25-Ma Cobalt Canyon stock of quartz monzonite at the northern edge of the map area (Rowley and others, 1994).

TKg **Grapevine Wash Formation (Tertiary? and Cretaceous?)** Mostly tan conglomerate and sandstone derived from erosion of Sevier thrust sheets. Exposed northwest of Gunlock, Utah, where its maximum thickness is about 600 m.

Kmg **Granite of Walker Wash (Upper Cretaceous)** Muscovite-biotite granite exposed in Walker Wash of the Lake Mead area; intrudes Early Proterozoic gneiss.

Ku **Cretaceous rocks, undivided (Upper and Lower Cretaceous)** Sevier-age synorogenic deposits, including the Baseline Sandstone and Willow Tank Formation, and the Iron Springs Formation and Cedar Mountain Formation. The Baseline Sandstone consists of red, white, and brown sandstone and conglomerate. The Willow Tank Formation consists of conglomerate, sandstone, siltstone, and mudstone; also includes tuff beds with a K-Ar date of about 98 Ma (Fleck, 1970). The Baseline Sandstone and Willow Tank Formation, which overlie Jurassic sandstone along an angular unconformity, are exposed mostly in the Muddy Mountains and are from 1,000 to more than 1,600 m thick. In the northeast part of the map area, unit consists of the Iron Springs Formation, which is tan mudstone, shale, sandstone, and conglomerate about 1,000 m thick. The Iron Springs Formation is underlain by a 7-m-thick bentonite bed which has a fission-track date of 101.7 Ma; beneath the bentonite bed is the Cedar Mountain Formation which is gray conglomerate about 20 m thick (Biek, 2003; Hintze and others, 1994).

Jct **Carmel and Temple Cap Formations, undivided (Middle Jurassic)** The Carmel Formation consists of red and gray siltstone, limestone, dolostone, and mudstone about 160 m thick and containing a tuff bed dated at 165 Ma (Hintze and others, 1994). The underlying Temple Cap Formation consists of red mudstone, sandstone, and gypsum as much as 150 m thick.

Jam **Aztec Sandstone, Navajo Sandstone, Kayenta Formation, and Moenave Formation, undivided (Lower Jurassic)** Includes the Aztec Sandstone in most of southern Nevada (Basin and Range province), and the correlative Navajo Sandstone in southwest Utah and northwest Arizona (Colorado Plateau province). Unit also includes the Kayenta and Moenave formations which underlie both the Aztec Sandstone and Navajo Sandstone. Aztec, Navajo, and Kayenta Formations are red, yellow, and light gray, fine-grained, cliff-forming, cross-bedded quartzose sandstone; the Moenave Formation consists of resistant red siltstone, shale, and sandstone. Gradational contact between map unit and underlying Triassic rocks. Aztec is from 850 to 1,200 m thick in the Muddy and Virgin Mountains and about 200 m thick at Frenchman Mountain; Navajo is 600–700 m thick; combined thickness of Kayenta and Moenave Formations ranges from 170 to 800 m.

Ŧu **Triassic rocks, undivided (Triassic)** Includes Chinle and Moenkopi Formations. The Chinle Formation (Upper Triassic) consists of the Petrified

SE ROA 42950

JA_12830

Forest and Shinarump Members; the Petrified Forest Member is variegated red, purple, gray, and yellow, bentonitic mudstone, siltstone, and sandstone. The underlying Shinarump Member is orange, brown and gray, massive-bedded, trough-crossbedded conglomeratic sandstone and conglomerate; includes some petrified wood fragments. The Chinle Formation unconformably overlies the Moenkopi Formation (Middle? and Lower Triassic) which consists, from top to base, of the upper red member, Shnabkaib Member, Virgin Limestone Member, lower red member, and Timpoweap Member. The upper red member is red sandstone, siltstone, mudstone, conglomerate, and gypsum. The Shnabkaib Member is white, light gray, and pink to red slope-forming dolostone, mudstone, siltstone, sandstone, and gypsum. The Virgin Limestone Member is thin bedded to laminated limestone and dolostone, and gypsiferous siltstone and mudstone. The Timpoweap Member is gray, sandy limestone and gypsiferous siltstone, yellow and red conglomeratic sandstone, and gray to brown conglomerate. Moenkopi Formation unconformably overlies the Kaibab Limestone. Map unit is about 1,000 m thick.

Pkt **Kaibab and Toroweap Formations undivided (Lower Permian)** The Kaibab Formation consists of the Harrisburg and Fossil Mountain Members. The Harrisburg Member consists of gray and yellow cherty dolostone and limestone, and red and gray siltstone, sandstone, and gypsum. The Fossil Mountain Member is yellowish-gray sandy and cherty limestone. The Toroweap Formation consists of the Woods Ranch, Brady Canyon, and Seligman Members. The Woods Ranch Member is gray, orange, and red siltstone, sandstone, gypsum, and minor dolostone and limestone. The Brady Canyon Member is gray cherty limestone and dolostone. The Seligman Member is gray and red sandy limestone, dolostone, gypsiferous sandstone, siltstone, and minor shale. The Toroweap Formation unconformably overlies the Lower Permian redbeds unit. Combined, the Kaibab and Toroweap Formations are about 300 to 550 m thick.

Pr **Lower Permian redbeds** Red and tan cross-bedded sandstone, siltstone, and sandy shale. Unit defined by Longwell and others (1965) and correlated with parts of the Queantoweap and Esplanade Sandstones and the Hermit Formation. Unit is 400 to 600 m thick.

PIPc **Callville Limestone and related rocks (Lower Permian and Pennsylvanian)** Mapped in the Virgin and Beaver Dam Mountains. Map unit partly equivalent to the Bird Spring Formation. The Callville Limestone (Pennsylvanian) consists of gray fossiliferous limestone and dolostone. Also includes layers and nodules of brown chert; brown sandstone beds common in upper half. Map unit includes the Pakoon Dolostone (Lower Permian). The Pakoon is light-gray dolostone with minor limestone, sandstone, and gypsum. Unit is from 460 to 880 m thick.

PMb **Bird Spring Formation and related rocks (Lower Permian to Upper Mississippian)** Gray and yellowish-gray bioclastic limestone, dolostone, siltstone, silty limestone, brown sandstone, and gray and red shale. Forms stair-step ledges. Contains abundant discontinuous layers and nodules of gray to brown-weathering chert; chert makes up more than 50 percent of rock volume in some beds. Upper part is mostly gray cherty bioclastic limestone and brown sandstone of Leonardian age (Page and others, 2005). Middle part is a distinctive red, silty limestone marker unit (Page, 1992, 1993, and 1998); marker unit contains submarine debris flow conglomerate and turbidite beds and represents a slope to basin sequence in contrast to the carbonate shelf sequence that typifies most of the Bird Spring Formation in the region. The basal 20 to 60 m of the map unit in west and south-central parts of map area consists of the Upper Mississippian Indian Springs Formation of Webster and Lane (1967) and Webster (1969). The Indian Springs Formation is yellowish-gray bioclastic limestone, black to red shale, and tan sandstone. The map unit attains a maximum thickness in the Las Vegas Range area, where it is about 2,500 m thick; top of unit not exposed in most of map area.

Msc **Scotty Wash Quartzite and Chainman Shale (Upper Mississippian)** Mapped in northern Meadow Valley Mountains near the margin of Kane Springs Wash. Scotty Wash Quartzite is tan, red and brown crossbedded quartzite. The Chainman Shale is black, olive-gray, and brown, fissile shale, red siltstone, and gray limestone. The siltstone is exposed mostly in the lower part of the unit and is interbedded with thin, crinoidal limestone. Map unit is partly correlative with Indian Springs Formation of Webster and Lane (1967). Unit is 200 to 320 m thick.

Mm **Monte Cristo Group of Langenheim and others (1962) (Upper and Lower Mississippian)** Carbonate platform rocks consisting of Yellowpine, Bullion, Anchor, and Dawn Limestones. The Yellowpine Limestone is gray limestone containing sparse nodules of gray to brown chert. The Bullion Limestone is gray encrinitic limestone and some beds of brown chert. The Anchor Limestone is gray limestone and brown chert. The Dawn Limestone is gray bioclastic, oolitic limestone and brown chert. The Monte Cristo Group is about 300 m thick in the Muddy Mountains and Tule Springs Hills, 280 m thick in the Mormon Mountains, 460 m thick in the southern Meadow Valley Mountains, and about 500 m thick in the Arrow Canyon and south Las Vegas Ranges.

Mr **Redwall Limestone (Upper and Lower Mississippian)** Consists of the Horseshoe Mesa, Mooney Falls, Thunder Springs, and Whitmore Wash Members. Unit is mostly equivalent to the Monte Cristo Group of Langenheim and others (1962) but is thinner and represents cratonic platform sequence of the Colorado Plateau province. Members of the Redwall are correlative and lithologically similar to the Yellowpine, Bullion, Anchor, and Dawn Limestones of the Monte Cristo Group, respectively. The Horseshoe Mesa Member consists of cliff-forming limestone containing nodules and layers of chert. The Mooney Falls Member is cliff-forming bioclastic limestone. The Thunder Springs Member consists of bioclastic limestone and chert. The Whitmore Wash Member is gray, bioclastic limestone and dolostone. Mapped in the Virgin and Beaver Dam Mountains and Lake Mead area. The Redwall Limestone is about 200 to 260 m thick.

MDu **Lower Mississippian to Middle Devonian rocks, undivided** In western part of the map area unit consists of the Upper and Middle Devonian Guilmette Formation and either the overlying Lower Mississippian and Upper Devonian Crystal Pass Limestone (in the Arrow Canyon Range and south Meadow Valley Mountains) or the Lower Mississippian and Upper Devonian Pilot Shale and Lower Mississippian Joana Limestone (in the north Meadow Valley Mountains, Delamar Mountains, and Sheep Range). The Crystal Pass Limestone is micritic limestone containing sparse gastropods and intraclasts and is about 60 to 70 m thick. The Joana Limestone is gray, cherty, bioclastic limestone about 250 m thick. The Pilot Shale is gray and red platy limestone and is about 215 m thick in the Meadow Valley Mountains. The Guilmette Formation is gray burrow-mottled dolostone and limestone and minor dolomitic quartzite. The Guilmette Formation is 440 to 480 m thick. In eastern part of map area (Muddy Mountains, Tule Springs Hills, and Mormon Mountains), map unit includes Sultan Limestone of Hewett (1931). The Sultan Limestone is mostly equivalent to, but thinner than the Guilmette Formation, and includes the Crystal Pass, Valentine, and Ironside Members. The Valentine and Ironside Members consist of dark-gray limestone and light-gray dolostone. The Sultan is 200 to 400 m thick in the map area.

Dtb **Temple Butte Formation (Upper and Middle? Devonian)** Gray dolostone with subordinate beds of purple and gray siltstone and sandstone. Unit represents a cratonic platform sequence of the Colorado Plateau province and is partly equivalent to the Sultan Limestone and Guilmette Formation but is restricted to a Devonian age. Also partly equivalent to the Muddy Peak Limestone of Longwell (1921). Unit mapped in the Virgin and Beaver Dam Mountains and the Lake Mead area. Unit is 150 to 220 m thick in the Beaver Dam Mountains and 60 to 120 m thick in the Virgin Mountains.

DSu **Middle Devonian to Silurian rocks, undivided** Miogeoclinal sequence exposed in western part of map area, includes rocks equivalent to parts of the Middle Devonian Simonson Dolomite, the Lower Devonian Sevy Dolomite, and the Silurian Laketown Dolomite. The Simonson Dolomite consists of light to dark gray dolostone, 250 m thick in the Sheep Range and southern Delamar Mountains, 170 m thick in the Meadow Valley Mountains, and 100 m thick in the Arrow Canyon Range. The Sevy Dolomite consists of gray, aphanic dolostone to dolomudstone that includes cherty argillaceous unit of Johnson and others (1989) at top. The Sevy Dolomite is 235 m thick in the southern Delamar Mountains, and 100 to 150 m thick in the Meadow Valley Mountains and Arrow Canyon Range. The Laketown Dolomite displays a tri-part character that is widely recognized in the Great Basin: upper dark, middle light, and lower dark dolostone parts; the upper dark dolostone is medium dark gray, fossiliferous dolostone. The middle part is light-gray, fossiliferous dolostone. The lower part is medium-gray, vuggy and burrowed dolostone containing some layers and nodules of brown chert. The Laketown Dolomite is Early Silurian age based on conodonts collected in the Sheep Range (Page and others, 2005). The Laketown Dolomite is about 300 m thick in the Sheep Range and southern Delamar Mountains, 150 m thick in the Meadow Valley Mountains, about 160 m thick in the Lime Mountain area, and about 100 m thick in the Arrow Canyon Range. In the latter two areas, typical tri-part character is absent and the rocks are mostly light-gray dolostone.

SOu **Silurian and Ordovician rocks, undivided** Unit mapped only in Mormon Mountains and Tule Springs Hills and includes rocks equivalent to parts of the Silurian Laketown Dolomite, Upper Ordovician Ely Springs Dolomite, Middle Ordovician Eureka Quartzite, and Middle and Lower Ordovician Pogonip Group. Unit is about 260 m thick in the Mormon Mountains and 730 m thick in Tule Springs Hills.

Oes **Ely Springs Dolomite (Upper Ordovician)** In the western part of map area, uppermost part of unit is composed of light-olive-gray, burrow-mottled, finely saccharoidal dolostone to dolomudstone. Middle and lower parts of the formation consist of medium-dark-gray dolostone containing planar laminations and some scattered chert. In the Arrow Canyon Range, basal beds include pale-red shale and siltstone. Unit unconformably overlies Eureka Quartzite. Unit is from 120 to 140 m thick in the western part of the map area, and 100 m thick in the Tule Springs Hills and Mormon Mountains, and is absent in the Virgin, Beaver Dam, and Muddy Mountains, as well as at Frenchman Mountain and in the Lake Mead area.

Oep **Eureka Quartzite (Middle Ordovician) and Pogonip Group (Middle Ordovician to Upper Cambrian), undivided** Unit mapped in the Meadow Valley Mountains (460 m thick), southern Delamar Mountains (610 m thick), and the Arrow Canyon Range (650 m thick). Rocks are lithologically similar to, but thinner than those described for the Eureka Quartzite (Oe) and Pogonip Group (O€p) below.

Oe **Eureka Quartzite (Middle Ordovician)** Light- to moderate-brown and white to light-brown, fine to medium grained quartzite, friable sandstone, and minor sandy carbonate beds. Contains tabular-planar crossbeds and *skolithus* burrows. Map unit is 50 to 120 m thick in the Sheep and Desert Ranges, 40 to 50 m thick in the southern Delamar Mountains and Arrow Canyon Range, 10 m thick in the Dry Lake Range, and 3 to 8 m thick in the Mormon Mountains and Tule Springs Hills. Unit is absent in cratonic platform (Frenchman Mountain, Lake Mead area, and the Muddy, Virgin, and Beaver Dam Mountains).

Op **Pogonip Group (Lower Ordovician)** Unit exposed only in the Muddy Mountains and consists of cherty gray dolostone equivalent to Lower Ordovician part of the Pogonip Group; these rocks were called the Monocline Valley Formation by Longwell and Mound (1967) and Bohannon (1983). Map unit is 220 m thick. Ordovician rocks are absent in cratonic platform (Frenchman Mountain, Lake Mead area, and Virgin and Beaver Dam Mountains).

O€p **Pogonip Group (Middle Ordovician to Upper Cambrian)** Miogeoclinal section of the Pogonip Group exposed in western part of map area. Consists of the Antelope Valley and Goodwin Limestones. The Antelope Valley Limestone consists of gray to orange and yellowish-gray bioclastic and arenaceous limestone and dolostone. Beds are burrow-mottled and have abundant ooids, oncoids, and intraclasts, and contain scattered brown chert nodules and layers. Lower part of unit is equivalent to the Goodwin Limestone which consists of orange and gray limestone and abundant brown chert layers, intraclasts, and ooids. Samples from the lower beds of the Goodwin Limestone in the Sheep Range and in ranges to the west have produced Late Cambrian conodonts (Page and others, 2005). Pogonip Group is 600 to 900 m thick.

€nb **Nopah (Upper Cambrian) and Bonanza King (Upper and Middle Cambrian) Formations, undivided** Mapped only in the Mormon Mountains and Tule Springs Hills.

€n **Nopah Formation (Upper Cambrian)** Light- to dark-gray burrow-mottled dolostone, minor gray to orange silty limestone, and scattered chert layers and nodules. Alternating light and dark gray beds form several distinctive color bands. At base of unit, includes the Dunderberg Shale Member, which consists of brown silty limestone and siltstone and olive green shale. Map unit is 300 to 380 m thick in the Sheep Range, 560 m in the southern Delamar Mountains, about 400 m thick in the Meadow Valley Mountains, 115 m thick in the Mormon Mountains, about 200 m thick in the Tule Springs Hills and Muddy Mountains, and 400 m thick in the Beaver Dam Mountains.

€bk **Bonanza King Formation (Upper and Middle Cambrian)** Light- to dark-gray and olive-gray dolostone and subordinate light-brown to orange, silty dolostone. Partly equivalent to the Highland Peak Formation as used by Tschanz and Pampeyan (1970) in Lincoln County, and to the Muav Formation of the Colorado Plateau province. Unit is 900 m thick in the Sheep Range, 700 m thick in the Meadow Valley Mountains, 770 m thick in the Mormon Mountains and Tule Springs Hills, and 1,800 m thick in the Desert Range.

€hp **Highland Peak Formation (Upper and Middle Cambrian)** Light- and dark-gray limestone and dolostone. Unit is restricted to Delamar Mountains in the northern part of the map; well exposed in the Pioche mining district where it was first named (Westgate and Knopf, 1932) and described (Merriam, 1964). Unit has a maximum thickness of 1,500 m.

Ꞓm **Muav Limestone (Middle Cambrian)** Light to dark gray and brown limestone, dolostone, and mudstone. Cratonic platform facies exposed in the eastern part of the map area (Beaver Dam and Virgin Mountains, Lake Mead area, and Frenchman Mountain). Unit as much as 410 m thick in the northern Virgin Mountains.

Ꞓc **Carrara Formation (Middle and Lower Cambrian)** Gray, yellow, and red limestone, siltstone, sandstone, and shale. Exposed in the western part of the map area. About 300 m thick in the Desert Range area, and about 265 m thick in the Sheep Range.

Ꞓcp **Chisholm Shale and Lyndon Limestone (Middle Cambrian) and Pioche Shale (Middle and Lower Cambrian), undivided** Unit exposed only in the Delamar Mountains in northern part of map area. Chisholm Shale is brown shale (Walcott, 1916; Westgate and Knopf, 1932) about 35 m thick. The Lyndon Limestone is gray limestone and sandstone (Westgate and Knopf, 1932) about 50 m thick. The Pioche Shale is green shale (Walcott, 1908) as much as 275 m thick.

Ꞓbt **Bright Angel Shale (Middle and Lower Cambrian) and Tapeats Sandstone (Lower Cambrian), undivided** Cratonic platform facies mapped in the Mormon Mountains, Tule Springs Hills, Frenchman Mountain, Lake Mead area, and Virgin and Beaver Dam Mountains. The Bright Angel Shale is greenish gray and gray micaceous siltstone, sandstone, quartzite, and minor limestone and dolostone. Equivalent to the Pioche Shale, Lyndon Limestone, and Chisolm Shale defined in the Pioche, Nevada area, and to the Carrara Formation in the western part of the map area. The Bright Angel Shale is about 140 m thick in the Mormon Mountains, 80 to 100 m thick in the Beaver Dam and Virgin Mountains, and 180 m thick at Frenchman Mountain. The Tapeats Sandstone is orange quartzite, conglomerate, and sandstone. Equivalent in part to the Prospect Mountain Quartzite as used in parts of Lincoln and Clark County, Nevada (Tschanz and Pampeyan, 1970; Longwell and others, 1965). About 145 m thick in the Mormon Mountains, 365 m thick in the Beaver Dam Mountains, 80 m thick in the Virgin Mountains, and 50 m thick at Frenchman Mountain.

ꞒZw **Wood Canyon Formation (Lower Cambrian and Late Proterozoic)** Brown quartzite, sandstone, siltstone, shale, and sandy shale. Lower contact with the Stirling Quartzite is transitional. Unit is about 600 to 700 m thick in the Desert Range, and an incomplete section in the Sheep Range is about 450 m thick. Unit is exposed in the northern part of the map area in Delamar Mountains, and is as much as 480 m thick (Stewart, 1984).

Zs **Stirling Quartzite (Late Proterozoic)** Purple, pink, maroon, gray, and white conglomeratic quartzite, quartzite, and sandstone, and minor beds of sandy shale and siltstone. Lower contact with the Johnnie Formation is transitional. Unit is 945 m thick in the Desert Range, but only the uppermost 100 m is exposed in Las Vegas Range (Maldonado and Schmidt, 1991). In the north part of the map area (Delamar Mountains), upper contact is transitional with the Wood Canyon Formation, and formation is as much as 600 m thick, with the base not exposed (Stewart, 1984).

Zj **Johnnie Formation (Late Proterozoic)** Brown, gray, and green quartzite, sandstone, siltstone, and dolostone. Upper part contains greater proportion of shale compared to lower part and several brown to tan oolitic dolostone beds. Lower part is predominantly fine-grained quartzite and thin beds of shale. Unit is about 1,580 m thick in the Desert Range.

Xu **Early Proterozoic crystalline rocks** Gneiss, schist, and granite exposed at Frenchman Mountain, Lake Mead area, Virgin Mountains, Beaver Dam Mountains, and Mormon Mountains. Rocks are dated at 1.7 Ga (Quigley and others, 2002).

REFERENCES

Anderson, J.J., and Rowley, P.D., 1975, Cenozoic stratigraphy of the southwestern High Plateaus of Utah, *in* Anderson, J.J., Rowley, P.D., Fleck, R.J., and Nairn, A.E.M., eds., Cenozoic geology of southwestern High Plateaus of Utah: Geological Society of America Special Paper 160, p. 1–52.

Anderson, R.E., 1973, Large magnitude late Tertiary strike-slip faulting north of Lake Mead, Nevada: U.S. Geological Survey Professional Paper 794, 18 p.

Anderson, R.E., 2003, Geologic map of the Callville Bay Quadrangle, Clark County, Nevada, and Mohave County, Arizona: Nevada Bureau of Mines and Geology Map 139, 1:24,000.

Anderson, R.E., and Hintze, L.F., 1993, Geologic map of the Dodge Spring Quadrangle, Washington County, Utah, and Lincoln County, Nevada: U.S. Geological Survey Geologic Quadrangle Map GQ-1721, scale 1:24,000.

Armstrong, R.L., 1968, Sevier orogenic belt in Nevada and Utah: Geological Society of America Bulletin v. 79, p. 429–458.

Axen, G.J., Wernicke, B.P., Skelly, M.F., and Taylor, W.J., 1990, Mesozoic and Cenozoic tectonics of the Sevier thrust belt in the Virgin River Valley area, southern Nevada, *in* Wernicke, B.P., ed., Basin and Range extensional tectonics near the latitude of Las Vegas, Nevada: Geological Society of America Memoir 176, p. 123–154.

Beard, Sue, 1991, Preliminary geologic map of the Devils Throat quadrangle, Clark County, Nevada: U.S. Geological Survey Open-File Report 91-132, scale 1:24,000.

Beard, Sue, 1992, Preliminary geologic map of the St. Thomas Gap quadrangle, Clark County, Nevada, and Mohave County, Arizona: U.S. Geological Survey Open- File Report 92-326, scale 1:24,000.

Beard, Sue, 1993, Preliminary geologic map of the Whitney Pocket quadrangle, Clark County, Nevada: U.S. Geological Survey Open-File Report 93-716, scale 1:24,000.

Beard, Sue, Anderson, R.E., Block, D.L., Bohannon, R.G., Brady, R.J., Castor, S.B., Duebendorfer, E.M., Faulds, J.E., Howard, K.A., Kuntz, M.A., Rowland, S.M., Wallace, M.A., and Williams, V.S., in press, Geologic map of the Lake Mead 30’ x 60’ Quadrangle, Nevada, U.S. Geological Survey Scientific Investigation Map Series, scale 1:100,000.

Belcher, W.R., Faunt, C.C., and D’Agnese, F.A., 2002, Three-dimensional hydrogeologic framework model for use with a steady-state numerical ground-water flow model of the Death Valley regional flow system, Nevada and California: U.S. Geological Survey Water-Resources Investigations Report 01-4254.

Bell, J.W., and Smith, E.I., 1980, Geologic map of the Henderson Quadrangle, Clark County, Nevada: Nevada Bureau of Mines and Geology Map 67, scale 1:24,000.

Bell, J.W., Ramelli, A.R., and Caskey, S.J., 1998, Geologic map of the Tule Springs Park Quadrangle, Clark County, Nevada: Nevada Bureau of Mines and Geology Map 113, scale 1:24,000.

Bell, J.W., Ramelli, A.R., dePolo, C.M., Maldonado, F., and Schmidt, D.L., 1999, Geologic map of the Corn Creek Springs Quadrangle, Clark County, Nevada: Nevada Bureau of Mines and Geology Map 121, scale 1:24,000.

Best, M.G., Christiansen, E.H., and Blank, R.H., Jr., 1989, Oligocene caldera complex and calc-alkaline tuffs and lavas of the Indian Peak volcanic field, Nevada and Utah: Geological Society of America Bulletin, v. 101, p. 1076–1090.

Best, M.G., Scott, R.B., Rowley, P.D., Swadley, W C, Anderson, R.E., Gromme, C.S., Harding, A.E., Deino, A.L., Christiansen, E.H., Tingey, D.G., and Sullivan, K.R., 1993, Oligocene-Miocene caldera complexes, ash-flow sheets, and tectonism in the central and southeastern Great Basin, *in* Lahren, M.M., Texler, J.H., Jr., and Spinosa, C., eds., Crustal evolution of the Great Basin and Sierra Nevada: Field Trip Guide, Geological Society of America, Cordilleran and Rocky Mountain Sections Meeting, p. 285–311.

Biek, R.F., 2003, Geologic map of the Harrisburg Junction Quadrangle, Washington County, Utah: Utah Geological Survey Map 191, 1:24,000.

Billingsley, G.H., 1995, Geologic map of the Littlefield quadrangle, northern Mohave County, Arizona: U.S. Geological Survey Open-File Report 95-559, scale 1:24,000, 15 p.

Billingsley, G.H., and Bohannon, R.G., 1995, Geologic map of the Elbow Canyon quadrangle, northern Mohave County, Arizona: U.S. Geological Survey Open-File Report 95-560, scale 1:24,000, 16 p.

Billingsley, G.H., and Wellmeyer, J.L., 2003, Geologic map of the Mount Trumbull 30' X 60' Quadrangle, Mohave and Coconino Counties, Arizona: U.S. Geological Survey Geological Investigations Series Map I-2766, scale 1:100,000.

Billingsley, G.H., and Workman, J.B., 1998, Geologic map of the Littlefield 30' x 60' Quadrangle, Mohave County, northwestern Arizona: U.S. Geological Survey Miscellaneous Field Investigations Map I-2628, scale 1:100,000.

Blank, H.R., Jr., 1959, Geology of the Bull Valley district, Washington County, Utah [Ph.D. dissertation]: University of Washington, 177 p.

Blank, H.R., 1993, Preliminary geologic map of the Enterprise Quadrangle, Washington and Iron Counties, Utah: U.S. Geological Survey Open-File Report 93-203, scale 1:24,000.

Bohannon, R.G., 1983, Geologic map, tectonic map, and structure sections of the Muddy and northern Black Mountains, Clark County, Nevada: U.S. Geological Survey Miscellaneous Investigations Map I-1406, scale 1:62,500.

Bohannon, R.G., 1984, Nonmarine sedimentary rocks of Tertiary age in the Lake Mead region, southeastern Nevada and northwestern Arizona: U.S. Geological Survey Professional Paper 1259, 72 p.

Bohannon, R.G., 1991, Geologic map of the Jacobs Well and southern part of the Elbow Canyon quadrangles, Mohave County, Arizona: U.S. Geological Survey Miscellaneous Investigations Series Map I-2288, scale 1:24,000.

Bohannon, R.G., 1992a, Geologic map of the Weiser Ridge Quadrangle, Clark County, Nevada: U.S. Geological Survey Geologic Quadrangle Map GQ-1714, scale 1:24,000.

Bohannon, R.G., 1992b, Geologic map of the Red Pockets quadrangle, Mohave County, Arizona: U.S. Geological Survey Miscellaneous Investigations Series Map I-2288, scale 1:24,000.

Bohannon, R.G., Grow, J.A., Miller, J.J., and Blank, R.H., Jr., 1993, Seismic stratigraphy and tectonic development of Virgin River depression and associated basins, southeastern Nevada and northwestern Arizona: Geological Society of America Bulletin, v. 105, p. 501–520.

Bohannon, R.G., and Lucchitta, Ivo, 1991, Geologic map of the Mount Bangs quadrangle, Mohave County, Arizona: U.S. Geological Survey Miscellaneous Investigations Series Map I-2166, scale 1:24,000.

Bohannon, R.G., Lucchitta, Ivo, and Anderson, R.E., 1991, Geologic map of the Mountain Sheep Spring quadrangle, Mohave County, Arizona: U.S. Geological Survey Miscellaneous Investigations Map I-2265, scale 1:24,000.

Brady, R.J., Fryxell, J.E., and Wernicke, B.P., 2002, Preliminary geologic map of the Iceberg Canyon Quadrangle, Clark County, Nevada and Mohave County, Arizona: Nevada Bureau of Mines and Geology Open-File Report 03-18, 1:24,000.

Brothers, K., Katzer, T., and Johnson, M., 1996, Hydrology and steady state ground-water model of Dry Lake and Delamar Valleys, Lincoln County, Nevada: Las Vegas Valley Water District, Cooperative Water Project, Water for Nevada's Future, Report no. 16, Hydrographic basins 181 & 182, 47 p.

Burbey, T.J., 1997, Hydrogeology and potential for ground-water development, carbonate-rock aquifers, southern Nevada and southeastern California: U.S. Geological Survey Water-Resources Investigations Report 95-4168, 65 p.

Caine, J.S., Evans, J.P., and Forster, C.B., 1996, Fault zone architecture and permeability structure: Geology, v. 24, p. 1025–1028.

Carpenter, J.A., and Carpenter, D.G., 1994, Structural and stratigraphic relations in a critical part of the Mormon Mountains, Nevada, *in* Dobbs, S.W., and Taylor, W.J., eds.: Nevada Petroleum Society 1994 Conference Volume II, (Book 1), p. 95–126.

Castor, S.B., Faulds, J.E., Rowland, S.M., and dePolo, C.M., 2000, Geology of the Frenchman Mountain Quadrangle, Clark County, Nevada: Nevada Bureau of Mines and Geology Map 127, scale 1:24,000.

D'Agnese, F.A., Faunt, C.C., Turner, K., and Hill, M.C., 1997, Hydrogeologic evaluation and numerical simulation of Death Valley regional ground-water flow system, Nevada and California: Water-Resources Investigations Report 96-4300, 124 p.

D'Agnese, F.A., O'Brien, G.M., Faunt, C.C., Belcher, W.R., and San Juan, Carma, 2002, A three-dimensional numerical model of predevelopment conditions in the Death Valley regional ground-water flow system, Nevada and California: U.S. Geological Survey Water-Resources Investigations Report 02-4102, 114 p.

Dettinger, M.D, Harrill, J.R., Schmidt, D.L., and Hess, J.W., 1995, Distribution of carbonate-rock aquifers and the potential for their development, southern Nevada and adjacent parts of California, Arizona, and Utah: U.S. Geological Survey Water Resources Investigations Report 91-4146, 100 p.

Dixon, G.L., and Katzer, T.C., 2002, Geology and hydrology of the lower Virgin River Valley in Nevada, Arizona, and Utah: Virgin Valley Water District, Mesquite, Nevada, Report no. VVWD-01, 126 p.

Duebendorfer, E.M., 2003, Geologic map of the Government Wash Quadrangle, Clark County, Nevada: Nevada Bureau of Mines and Geology Map 140, scale 1:24,000.

Duebendorfer, E.M., and Black, R.A., 1992, Kinematic role of transverse structures in continental extension: an example from the Las Vegas Valley shear zone, Nevada: Geology, v. 20, p. 1107–1110.

Eakin, T.E., 1964, Ground-water appraisal of Coyote Spring and Kane Springs valleys and Muddy River Springs area, Lincoln and Clark Counties, Nevada: Nevada Department of Conservation and Natural Resources, Ground-water Resources Reconnaissance Series, Report 25, 40 p.

Eakin, T.E., 1966, A regional interbasin groundwater system in the White River area, southeastern Nevada: Water Resources Research, v. 2, p. 251–271.

Eakin, T.E., and Winograd, I.J., 1965, Interbasin movement of ground water in south central Nevada-Some implications: Geological Society of America Special Paper 82, 52 p.

Ekren, E.B., Bucknam, R.C., Carr, W.J., Dixon, G.L., and Quinlivan, W.D., 1976, East-trending structural lineaments in central Nevada: U.S. Geological Survey Professional Paper 986, 16 p.

Ekren, E.B., Orkild, P.P., Sargent, K.A., and Dixon, G.L., 1977, Geologic map of Tertiary rocks, Lincoln County, Nevada: U.S. Geological Survey Miscellaneous Investigations Series Map I-1041, scale 1:250,000.

Faulds, J.E., Feuerbach, D.L., Miller, C.F., and Smith, E.I., 2001, Cenozoic evolution of the northern Colorado River extensional corridor, southern Nevada and northwest Arizona, *in* Erskine, M.C., Faulds, J.E., Bartley, J.M., and Rowley, P.D., eds., The geologic transition, High Plateaus to Great Basin-A symposium and field guide (The Mackin Volume): Utah Geological Association and Pacific Section of the American Association of Petroleum Geologists: Utah Geological Association Publication 30, p. 239–272.

Fleck, R.J., 1970, Tectonic style, magnitude, and age of deformation in the Sevier orogenic belt in southern Nevada and eastern California: Geological Society of America Bulletin, v. 81, p. 1705–1720.

Fleck, R.J., and Carr, M.D., 1990, The age of the Keystone thrust: Laser-fusion $^{40}Ar/^{39}Ar$ dating of foreland basin deposits, southern Spring Mountains, Nevada: Tectonics, v. 9, p. 467–476.

Guth, P.L., 1980, Geology of the Sheep Range, Clark County, Nevada [Ph.D. thesis]: Massachusetts Institute of Technology, 189 p.

Guth, P.L., 1981, Tertiary extension north of the Las Vegas Valley shear zone, Sheep and Desert Ranges, Clark County, Nevada: Geological Society of America Bulletin, v. 92, p. 763–771.

Hacker, D.B., Holm, D.K., Rowley, P.D., and Blank, H.R., 2002, Associated Miocene laccoliths, gravity slides, and

SE ROA 42956

JA_12836

volcanic rocks, Pine Valley Mountains and Iron Axis region, southwestern Utah, *in* Lund, W.R., ed., Field guide to geologic excursions in southwestern Utah and adjacent areas of Arizona and Nevada, Field trip guide, Geological Society of America, Rocky Mountain section meeting, Cedar City, Utah: U.S. Geological Survey Open-File Report 02-172, p. 236–283.

Hammond, B.J., 1991, Geologic map of the Jarvis Peak Quadrangle, Washington County, Utah: Utah Geological Survey Open-File Report 212, scale 1:24,000.

Haneberg, W.C., Mozley, P.S., Moore, J.C., and Goodwin, L.B., eds., 1999, Faults and subsurface fluid flow in the shallow crust: American Geophysical Union Geophysical Monograph 113, 222 p.

Harrill, J.R., Gates, J.S., and Thomas, J.M., 1988, Major ground-water flow systems in the Great Basin region of Nevada, Utah, and adjacent states: U.S. Geological Survey Hydrologic Investigations Atlas HA-694-C, scale 1:1,000,000.

Harrill, J.R., and Prudic, D.E., 1998, Aquifer systems in the Great Basin region of Nevada, Utah and adjacent states-Summary report: U.S. Geological Survey Professional Paper 1409A, 61 p.

Heilweil, V.M., Watt, D.E., Solomon, D.K., and Goddard, K.E., 2002, The Navajo aquifer system of southwestern Utah, *in* Lund, W.R., ed., Field Guide to Geologic Excursions in Southwestern Utah and Adjacent areas of Arizona and Nevada, Geological Society of America Rocky Mountain Section Meeting, Cedar City, Utah, May 7th-9th, 2002; U.S. Geological Survey Open-File Report 02-172, p. 105–130.

Hewett, D.G., 1931, Geology and ore deposits of the Goodsprings Quadrangle, Nevada: U.S. Geological Survey Professional Paper 162, 172 p.

Hintze, L.F., 1986, Stratigraphy and structure of the Beaver Dam Mountains, Southwestern Utah, *in* Griffen, D.T., and Phillips, R.J., eds., Thrusting and Extensional Structures and Mineralization in the Beaver Dam Mountains, Southwestern Utah: Utah Geological Association Publication 15, p. 1–36.

Hintze, L.F., Anderson, R.E., and Embree, G.F., 1994, Geologic map of the Motoqua and Gunlock Quadrangles, Washington County, Utah: U.S. Geological Survey Miscellaneous Investigations Series Map I-2427, scale 1:24,000.

Hintze, L.F., and Axen, G.J., 1995, Geologic map of the Scarecrow Peak Quadrangle, Washington County, Utah, and Lincoln County, Nevada: U.S. Geological Survey Geologic Quadrangle Map GQ-1759, scale 1:24,000.

Hintze, L.F., and Axen, G.J., 2001, Geologic map of the Lime Mountain Quadrangle, Lincoln County, Nevada: Nevada Bureau of Mines and Geology Map 129, scale 1:24,000.

Hintze, L.F., and Hammond, B.J., 1994, Geologic map of the Shivwits Quadrangle, Washington County, Utah: Utah Geological Survey Map 153, 21 p., scale 1:24,000.

Howard, K.A., Hook, S.J., Phelps, G.A., and Block, D.L., 2003, Geologic map of the Hiller Mountains Quadrangle, Clark County, Nevada, and Mohave County, Arizona: Nevada Bureau of Mines and Geology Map 137, 1:24,000.

Jachens, R.C., Dixon, G.L., Langenheim, V.E., and Morin, R., 1998, Interpretation of an aeromagnetic survey over part of Virgin Valley, Tule Desert, and the valley surrounding Meadow Valley Wash, southeastern Nevada: U.S. Geological Survey Open-File Report 98-804, 16 p.

Johnson, J.G., Sandberg, C.A., and Poole, F.G., 1989, Early and Middle Devonian paleogeography of western United States, *in* McMillan, N.J., Embry, A.F., and Glass, D.J., eds., Devonian of the World: Calgary, Canadian Society of Petroleum Geologists, Memoir 14, v. 1, Regional synthesis, p. 161–182.

Johnson, Michael, Dixon, G.L., Rowley, P.D., Katzer, T.C., and Winters, Michael, 2002, Hydrology and ground-water conditions of the Tertiary Muddy Creek Formation in the lower Virgin River basin of southeastern Nevada and adjacent Arizona and Utah, *in* Lund, W.R., ed., Field guide to geologic excursions in southwestern Utah and adjacent areas of Arizona and Nevada, Field trip guide, Geological Society of America, Rocky Mountain section meeting, Cedar City, Utah: U.S. Geological Survey Open-File Report 02-172, p. 284–315.

Kirk, S.T., 1987, Analysis of the White River groundwater flow system using a deuterium-calibrated discrete-state compartment model [M.S. thesis]: University of Nevada, Reno, 81 p.

Laczniak, R.J., Cole, J.C., Sawyer, D.A., and Trudeau, D.A., 1996, Summary of hydrogeologic controls on ground-water flow at the Nevada Test Site, Nye County, Nevada: U.S. Geological Survey Water-Resources Investigations Report 96-4109, 60 p.

Langenheim, R.L., Jr., Carss, B.W., Kennerly, J.B., McCutcheon, V.A., and Waines, R.H., 1962, Paleozoic section in Arrow Canyon Range, Clark County, Nevada: American Association of Petroleum Geologists Bulletin vol. 46, no. 5, p. 592–609.

Langenheim, V.E., Glen, J.M., Jachens, R.C., Dixon, G.L., Katzer, T.C., and Morin, R.L., 2000, Geophysical constraints on the Virgin River depression, Nevada, Utah, and Arizona: U.S. Geological Survey Open-File Report 00-407, 26 p.

Langenheim, V.E., Bohannon, R.G., Glen, J.M., Jachens, R.C., Grow, J.A., Miller, J.J., Dixon, G.L., and Katzer, T.C., 2001a, Basin configuration of the Virgin River depression, Nevada, Utah, and Arizona-A geophysical view of deformation along the Colorado Plateau-Basin and Range transition, *in* Erskine, M.C., Faulds, J.E., Bartley, J.M., and Rowley, P.D., eds., The geologic transition, High Plateaus to Great Basin-A symposium and field guide (The Mackin Volume): Utah Geological Association and Pacific Section of the American Association of Petroleum Geologists: Utah Geological Association Publication 30, p. 205–226.

Langenheim, V.E., Grow, J.A., Jachens, R.C., Dixon, G.L., and Miller, J.J., 2001b, Geophysical constraints on the location and geometry of the Las Vegas valley shear zone, Nevada: Tectonics, v. 20, no. 2, p. 189–209.

Langenheim, V.E., Miller, J.J., Page, W.R., and Grow, J.A., 2001c, Thickness and geometry of Cenozoic deposits in California Wash area, Nevada, based on gravity and seismic reflection data: U.S. Geological Survey Open-File Report 01-393, 24 p.

Langenheim, V.E., Page, W.R., Miller, J.J., and Grow, J.A., 2002, Geophysical and geological constraints on the hydrogeologic framework of the California Wash region, southern Nevada: Geological Society of America Abstracts with Programs, v. 34, no. 4, p. A-16.

Longwell, C.R., 1921, Geology of the Muddy Mountains, Nevada, with a section to the Grand Wash Cliffs in Arizona: American Journal of Science. 5th Series, v. 1, p. 39-62.

Longwell, C.R., and Mound, M.C., 1967, A new Ordovician formation in Nevada dated by conodonts: Geological Society of America Bulletin, v. 78, p. 405-412.

Longwell, C.R., Pampeyan, E.H., Bowyer, B., and Roberts, R.J., 1965, Geology and mineral deposits of Clark County, Nevada: Nevada Bureau of Mines and Geology Bulletin 62, 177 p.

Lucchitta, Ivo, Basdekas, P.G., Bohannon, R.G., and Reick, H.J., and Dehler, C.M., 1995a, Geologic map of the Cane Springs quadrangle, Mohave County, Arizona: U.S. Geological Survey Open-File Report 95-86, scale 1:24,000.

Lucchitta, Ivo, Dehler, C.M., and Basdekas, P.G., 1995b, Geologic map of the Cane Springs Southeast quadrangle, northern Mohave County, Arizona: U.S. Geological Survey Open-File Report 95-48, scale 1:24,000.

Lundstrom, S.C., Page, W.R., Langenheim, V.E., Young, O.D., Mahan, S.A., and Dixon, G.L., 1998, Preliminary geologic map of the Valley quadrangle, Clark County, Nevada: U.S. Geological Survey Open-File Report 98-508, scale 1:24,000.

Machette, M.N., 1985, Calcic soils of the southwestern United States: Geological Society of America Special Paper 203, p. 1-21.

Maldonado, F., and Schmidt, D.L., 1990, Geologic map of the southern Sheep Range, Fossil Ridge, and Castle Rock area, Clark County, Nevada: U.S. Geological Survey Miscellaneous Investigations Series Map I-2086, scale 1:24,000.

Marzolf, J.E., 1990, Reconstruction of extensionally dismembered early Mesozoic sedimentary basins; southwestern Colorado Plateau to the eastern Mojave Desert, *in* Wernicke, B.P., ed., Basin and Range extensional tectonics near the latitude of Las Vegas, Nevada, Geological Society of America Memoir 176, p. 477-500.

Matti, J.C., Castor, S.B., Bell, J.W., and Rowland, S.M., 1987, Geologic map of the Las Vegas NW Quadrangle, Clark County, Nevada: Nevada Bureau of Mines and Geology Map 3Dg, scale 1:24,000.

Matti, J.C., Castor, S.B., Bell, J.W., and Rowland, S.M., 1993, Las Vegas NE Quadrangle geologic map: Nevada Bureau of Mines and Geology Map 3Cg, scale 1:24,000.

Merriam, C.W., 1964, Cambrian rocks of the Pioche mining district, Nevada: U.S. Geological Survey Professional Paper 469, 55 p.

Mills, J.G., Jr., 1994, Geologic map of the Hoover Dam Quadrangle, Arizona and Nevada: Nevada Bureau of Mines and Geology Map 102, scale 1:24,000.

Olmore, S.D., 1971, Style and evolution of thrusts in the region of the Mormon Mountains, Nevada [Ph.D. dissertation]: University of Utah, 211 p.

Page, W.R., 1992, Preliminary geologic map of the Arrow Canyon Quadrangle, Clark County, Nevada: U.S. Geological Survey Open-File Report 92-681, 1:24,000-scale.

Page, W.R., 1993, A regional marker unit within the Upper Paleozoic Bird Spring Formation, southern Nevada-Evidence for slope facies [abs.]: Geological Society of America Abstracts with Programs, v. 25, no. 5, p. 131.

Page, W.R., 1998, Geologic map of the Arrow Canyon NW Quadrangle, Clark County, Nevada: U.S. Geological Survey Geologic Quadrangle Map GQ-1776, scale 1:24,000.

Page, W.R., and Pampeyan, E.H., 1996, Preliminary geologic map of the Paleozoic rocks in the Wildcat Wash SE and Wildcat Wash SW Quadrangles, Lincoln and Clark Counties, Nevada: U.S. Geological Survey Open-File Report 96-26, 18 p., scale 1:24,000.

Page, W.R., Lundstrom, S.C., Harris, A.G., Langenheim, V.E., Workman, J.B., Mahan, S.A., Paces, J.B., Rowley, P.D., Dixon, G.L., Burchfiel, B.C., Bell, J.W., and Smith, E.I., 2005, Geologic and geophysical maps of the Las Vegas 30' x 60' Quadrangle, Clark and Nye Counties, Nevada, and Inyo County, California: U.S. Geological Survey Scientific Investigations Map 2814, 1:100,000-scale.

Page, W.R., Rowley, P.D., Dixon, G.L., and Brickey, D.W., 2003, Geologic map of the lower Colorado regional ground-water flow system, Nevada, Arizona, and Utah [abs.]: Nevada Water Resources Association Annual Conference, Sparks, Nevada, p. 57

Page, W.R., Swadley, W.C., and Scott, R.B., 1990, Preliminary geologic map of the Delamar 3 SW Quadrangle, Lincoln County, Nevada: U.S. Geological Survey Open-File Report 90-366, scale 1:24,000.

Pampeyan, E.H., 1993, Geologic map of the Meadow Valley Mountains, Lincoln and Clark Counties, Nevada: U.S. Geological Survey Miscellaneous Investigations Series Map I-2173, scale 1:50,000.

Phelps, G.A., Jewel, E.B., Langenheim, V.E., and Jachens, R.C., 2000, Principal facts for gravity stations in the vicinity of Coyote Spring Valley, Nevada, with initial gravity modeling results: U.S. Geological Survey Open-File Report 00-420, 18 p.

Plume, R.W., and Carlton, S.M., 1988, Hydrogeology of the Great Basin region of Nevada, Utah, and adjacent states: U.S. Geological Survey Hydrologic Investigations Atlas HA-694-A, scale 1:1,000,000.

Prudic, D.E., Harrill, J.R., and Burbey, T.J., 1995, Conceptual evaluation of regional ground-water flow in the carbonate-rock province of the Great Basin, Nevada, Utah, and adjacent states: U.S. Geological Survey Professional Paper 1409-D, 102 p.

Quade, J., Mifflin, M.D., Pratt, W.L., McCoy, W., and Burckle, L., 1995, Fossil spring deposits in the southern Great Basin and their implications for changes in water-table levels near Yucca Mountain, Nevada, during Quaternary time: Geological Society of America Bulletin, v. 107, p. 213–230.

Quade, J., Forester, R.M., Pratt, W.L., and Carter, C., 1998, Black mats, spring-fed streams, and late-glacial-age recharge in the southern Great Basin: Quaternary Research, v. 49, p. 129–148.

Quigley, M.C., Karlstrom, K., Beard, S., and Bohannon, R.G., 2002, Influence of Proterozoic and Laramide structures on the Miocene extensional strain field, north Virgin Mountains, Nevada/Arizona, *in* Lund, W.R., ed., Field Guide to Geologic Excursions in Southwestern Utah and Adjacent areas of Arizona and Nevada, Geological Society of America Rocky Mountain Section Meeting, Cedar City, Utah, May 7th-9th, 2002; U.S. Geological Survey Open-File Report 02-172, p. 86–104.

Rowley, P.D., 1998, Cenozoic transverse zones and igneous belts in the Great Basin, western United States—their tectonic and economic implications, *in* Faulds, J.E., and Stewart, J.H., eds., Accommodation zones and transfer zones—the regional segmentation of the Basin and Range province: Geological Society of America Special Paper 323, p. 195–228.

Rowley, P.D., and Dixon, G.L., 2001, The Cenozoic evolution of the Great Basin area, U.S.A.—New interpretations based on regional geologic mapping, *in* Erskine, M.C., Faulds, J.E., Bartley, J.M., and Rowley, P.D., eds., The geologic transition, High Plateaus to Great Basin-A symposium and field guide (The Mackin Volume): Utah Geological Association and Pacific Section of the American Association of Petroleum Geologists: Utah Geological Association Publication 30, p. 169–188.

Rowley, P.D., and Shroba, R.R., 1991, Geologic map of the Indian Cove Quadrangle, Lincoln County, Nevada: U.S. Geological Survey Geologic Quadrangle Map GQ-1701, scale 1:24,000.

Rowley, P.D., Nealey, L.D., Unruh, D.M., Snee, L.W., Mehnert, H.H., Anderson, R.E., and Gromme, C.S., 1995, Stratigraphy of Miocene ash-flow tuffs in and near the Caliente caldera complex, southeastern Nevada and southwestern Utah, *in* Scott, R.B., and Swadley, W C, eds., Geologic studies in the Basin and Range-Colorado Plateau transition in southeastern Nevada, southwestern Utah, and northwestern Arizona, 1992: U.S. Geological Survey Bulletin 2056, p. 43–88.

Rowley, P.D., Shroba, R.R., Simonds, F.W., Burke, K.J., Axen, G.J., and Olmore, S.D., 1994, Geologic map of the Chief Mountain Quadrangle, Lincoln County, Nevada: U.S. Geological Survey Geologic Quadrangle Map GQ-1731, scale 1:24,000.

Rowley, P.D., Williams, V.S., Vice, G.S., Maxwell, D.J., Hacker, D.B., Snee, L.W., and Mackin, J.H., in press, Geologic map of the Cedar City 30′ x 60′ Quadrangle, Iron and Washington Counties, Utah: Utah Geological Survey Map, scale 1:100,000.

Schmidt, D.L., 1994, Preliminary geologic map of the Farrier Quadrangle, Lincoln and Clark Counties, Nevada: U.S. Geological Survey Open File Report 94-625, scale 1:24,000.

Schmidt, D.L., and Dixon, G.L., 1995, Geology and aquifer system of the Coyote Spring Valley area, southeastern Nevada: U.S. Geological Survey Open-File Report 95-579, 47 p.

Schmidt, D.L., Page, W.R., and Workman, J.B., 1996, Preliminary geologic map of the Moapa West Quadrangle, Clark County, Nevada: U.S. Geological Survey Open-File Report 96-521, scale 1:24,000.

Scott, R.B., Grommé, C.S., Best, M.G., Rosenbaum, J.G., and Hudson, M.R., 1995a, Stratigraphic relationships of Tertiary volcanic rocks in central Lincoln County, southeastern Nevada, *in* Scott, R.B., and Swadley, W.C., eds., Geologic studies in the Basin and Range-Colorado Plateau transition in southeastern Nevada, southwestern Utah, and northwestern Arizona, 1992: U.S. Geological Survey Bulletin 2056, p. 5–42.

Scott, R.B., Harding, A.E., Swadley, W.C., and Pampeyan, E.H., 1991a, Preliminary geologic map of the Vigo NW Quadrangle, Lincoln County, Nevada: U.S. Geological Survey Open-File Report 91-389, scale 1:24,000.

Scott, R.B., Novak, S.W., and Swadley, W.C., 1990a, Preliminary geologic map of the Delamar 3 NE Quadrangle, Lincoln County, Nevada: U.S. Geological Survey Open-File Report 90-33, scale 1:24,000.

Scott, R.B., Page, W.R., and Swadley, W.C., 1990b, Preliminary geologic map of the Delamar 3 NW Quadrangle, Lincoln County, Nevada: U.S. Geological Survey Open-File Report 90-405, scale 1:24,000.

Scott, R.B., Swadley, W.C., and Novak, S.W., 1993, Geologic map of the Delamar Lake Quadrangle, Lincoln County, Nevada: U.S. Geological Survey Geologic Quadrangle Map GQ-1730, scale 1:24,000.

Scott, R.B., Swadley, W.C., and Page, W.R., 1991b, Preliminary geologic map of the Gregerson Basin Quadrangle, Lincoln County, Nevada: U.S. Geological Survey Open-File Report 90-646, scale 1:24,000.

Scott, R.B., Unruh, D.M., Snee, L.W., Harding, A.E., Nealey, L.D., Blank, H.R., Jr., Budahn, J.R., and Mehnert, H.H., 1995b, Relations of peralkaline magmatism to heterogeneous extension during the middle Miocene, southeastern Nevada: Journal of Geophysical Research, v. 100, no. B6, p. 10,381–10,401.

Skelly, M.F., 1987, The geology of the Moapa Peak area, southern Mormon Mountains, Clark and Lincoln Counties, Nevada [M.S. thesis]: University of Northern Arizona, 150 p.

Smith, E.I., 1984, Geologic map of the Boulder Beach Quadrangle, Clark County, Nevada: Nevada Bureau of Mines and Geology Map 81, scale 1:24,000.

Snee, L.W., and Rowley, P.D., 2000, New 40Ar/39Ar dates from the Caliente caldera complex, Nevada-Utah-at least 10 million years of Tertiary volcanism in one of the World's largest caldera complexes: Geological Society of America Abstracts with Programs, v. 32, no. 7, p. A461.

Stewart, J.H., 1972, Initial deposits in the Cordilleran geosyncline: evidence of a late Precambrian (<850 m.y.) continental separation: Geological Society of America Bulletin, v. 83, p. 1345–1360.

Stewart, J.H., 1976, Late Precambrian evolution of North America: plate tectonics implication: Geology, v. 4, p. 11–15.

Stewart, J.H., 1984, Stratigraphic sections of Lower Cambrian and upper Proterozoic rocks in Nye, Lander, and Lincoln Counties, Nevada, and Sonora, Mexico: U.S. Geological Survey Open-File Report 84-691, 53 p.

Stewart, J.H., and Poole, F.G., 1972, Lower Paleozoic and uppermost Precambrian Cordilleran Miogeocline, Great Basin, western United States, *in* Dickinson, W.R., ed., Tectonics and Sedimentation, Society of Economic Paleontologists and Mineralogists Special Publication 22, p. 28–57.

Swadley, W.C., Page, W.R., Scott, R.B., and Pampeyan, E.H., 1994, Geologic map of the Delamar 3 SE Quadrangle, Lincoln County, Nevada: U.S. Geological Survey Geologic Quadrangle Map-GQ-1754, scale 1:24,000.

Swadley, W.C., and Scott, R.B., 1990, Preliminary geologic map of the Delamar NW Quadrangle, Lincoln County, Nevada: U.S. Geological Survey Open-File Report 90-622, scale 1:24,000.

Thomas, J.M., Mason, J.L., and Crabtree, J.D., 1986, Groundwater levels in the Great Basin region of Nevada, Utah, and adjacent states: U.S. Geological Survey Hydrologic Investigations Atlas HA-694-B, scale 1:1,000,000.

Thomas, J.M., and Welch, A.H., 1984, Isotope hydrology and aqueous geochemistry of the White River groundwater basin, a regional carbonate aquifer in eastern Nevada [abs.]: Geological Society of America Abstracts with Programs, v. 16, no. 6, p. 689.

Thomas, J.M., Welch, A.H., and Dettinger, M.D., 1996, Geohemistry and isotope hydrology of representative aquifers in the Great Basin region of Nevada, Utah, and adjacent states: U.S. Geological Survey Professional Paper 1409-C, 100 p.

Tschanz, C.M., and Pampeyan, E.H., 1970, Geology and Mineral deposits of Lincoln County, Nevada: Nevada Bureau of Mines and Geology Bulletin 73, 188 p.

Walcott, C.D., 1908, Nomenclature of some Cambrian Cordilleran formations: Smithsonian Miscellaneous Collections, v. 53, no. 1, p. 1–12.

Walcott, C.D., 1916, Cambrian trilobites: Smithsonian Miscellaneous Collections, v. 64, no. 5, p. 302-456.

Webster, G.D., 1969, Chester through Derry conodonts and stratigraphy of northern Clark and southern Lincoln Counties, Nevada: University of California Publications in Geological Sciences, v. 79, 121 p.

Webster, G.D., and Lane, N.R., 1967, The Mississippian-Pennsylvanian boundary in southern Nevada, *in* Teichert, C., and Yochelson, E.L., eds., Essays in paleontology and stratigraphy, R.C. Moore Commemorative Volume: Lawrence, Kansas, Kansas University Press, Department of Geology Special Publication 2, p. 503–522.

Wernicke, B., Walker, J.D., and Beaufait, M.S., 1985, Structural discordance between Neogene detachments and frontal Sevier thrusts, central Mormon Mountains, southern Nevada: Tectonics, v. 4, no. 2, p. 213–246.

Westgate, L.G., and Knopf, A., 1932, Geology and ore deposits of the Pioche district, Nevada: U.S. Geological Survey Professional Paper 171, 79 p.

Williams, P.L., 1967, Stratigraphy and petrography of the Quichapa Group, southwestern Utah and southeastern Nevada [Ph.D. dissertation]: University of Washington, 182 p.

Williams, V.S., 1996, Preliminary geologic map of the Mesquite Quadrangle, Clark County, Nevada: U.S. Geological Survey Open-File Report 96-676, scale 1:24,000.

Williams, V.S., Bohannon, R.G., and Hoover, D.L., 1997a, Geologic map of the Riverside Quadrangle, Clark County, Nevada: U.S. Geological Survey Geologic Quadrangle Map GQ-1770, scale 1:24,000.

Williams, V.S., Schmidt, D.L., and Bohannon, R.G., 1997b, Preliminary geologic map of the Moapa East Quadrangle, Clark County, Nevada: U.S. Geological Survey Open-File Report 97-449, scale 1:24,000.

Wilson, J.W., 2001, Potentiometric surface, carbonate-rock province, southern Nevada and southeastern California, 1998-2000: U.S. Geological Survey Open-File Report 01-335, 15 p.

Winograd, I.J., and Thordarson, W., 1975, Hydrologic and hydrochemical framework, south-central Great Basin, Nevada-California, with special reference to the Nevada Test Site: U.S. Geological Survey Professional Paper 712C, p. C1–C126.

Workman, J.B., Menges, C.M., Page, W.R., Ekren, E.B., Rowley, P.D., and Dixon, G.L., 2002, Tectonic map of the Death Valley ground-water model area, Nevada and California: U.S. Geological Survey Miscellaneous Field Studies Map MF-2381-B, 58 p.

Workman, J.B., Menges, C.M., Page, W.R., Taylor, E.M., Ekren, E.B., Rowley, P.D., Dixon, G.L., Thompson, R.A., and Wright, L.A., 2003, Geologic map of the Death Valley ground water model area, Nevada and California: U.S. Geological Survey Miscellaneous Field Studies MF-2381-A, 1:250,000 scale.

MAP I-2173

U.S. DEPARTMENT OF THE INTERIOR
U.S. GEOLOGICAL SURVEY

GEOLOGIC MAP OF THE MEADOW VALLEY MOUNTAINS, LINCOLN AND CLARK COUNTIES, NEVADA

By E.H. Pampeyan

PAMPEYAN—GEOLOGIC MAP OF THE MEADOW VALLEY MOUNTAINS, LINCOLN AND CLARK COUNTIES, NEVADA 1:50,000 MAP I-2173

MISCELLANEOUS INVESTIGATIONS SERIES
Published by the U.S. Geological Survey, 1993

GEOLOGIC MAP OF THE MEADOW VALLEY MOUNTAINS,

LINCOLN AND CLARK COUNTIES, NEVADA

by
Earl H. Pampeyan

INTRODUCTION

The Meadow Valley Mountains are located in Lincoln and Clark Counties, southern Nevada, in the southern part of the Basin and Range province. They lie east of the interior drainage of the Great Basin and are in the Colorado River drainage system. The center of the range is about 103 km north-northeast of Las Vegas (fig. 1). The range is separated from the Mormon Mountains on the east and Clover Mountains on the north by Meadow Valley Wash, from the Delamar Mountains to the northwest by Kane Springs Wash, from the Sheep Range to the west by Pahranagat Wash and Coyote Spring Valley, and from Arrow Canyon Range to the south by Nevada Highway 168. The map area is bounded on the northwest by Nevada Highway 317 in Kane Springs Valley (a narrow alluviated drainage area commonly referred to as Kane Springs Wash), on the east by Meadow Valley Wash, and on the north by a dirt road connecting Nevada Highway 317 with Lyman Crossing in Meadow Valley Wash. The terrain is hilly to rugged with steep bedrock scarps on the west side and sharply incised gentle to moderately inclined alluviated slopes on the east side. The highest point is an unnamed ridge near the center of the range that stands 1,759 m above sea level, 853 m above the adjacent floor of Kane Springs Wash.

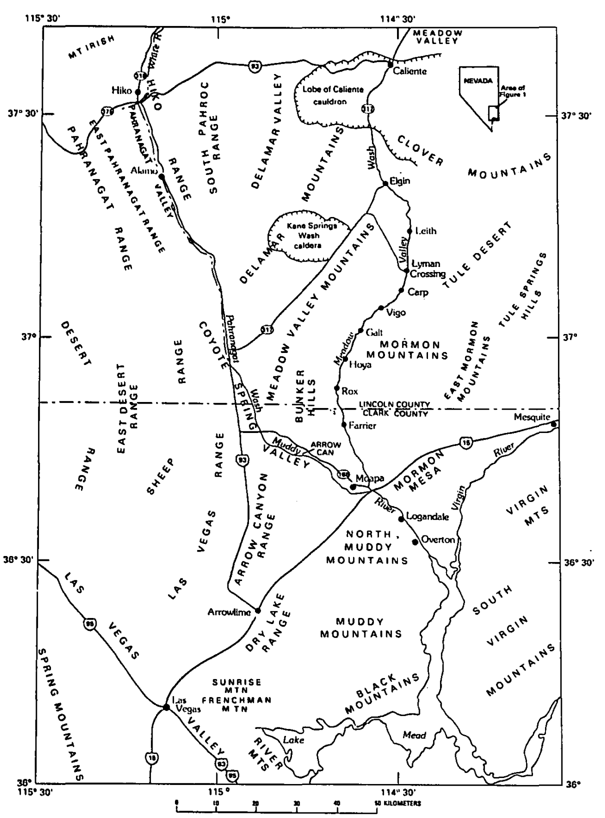

Figure 1. Index map of southeastern Nevada showing location of Meadow Valley Mountains.

The names Farrier, Rox, Hoya, Galt, Vigo, Carp, Leith, and Elgin formerly marked sites of small railroad maintainence stations spaced about 8 km apart along the Union Pacific Railroad in Meadow Valley Wash. These names now apply to railroad sidings at those sites. Sunflower Mountain, Grapevine Spring, Bunker Hills, Farrier Wash, and Hackberry Canyon are the principal formally named geographic or topographic features in the map area and for lack of other formally named features these are used as reference points. The names "Two Flats" and "Anticline" are informally applied to canyons along the west edge of the range (map sheet 2) where the range front changes direction from north-south to northeast.

PREVIOUS AND PRESENT INVESTIGATIONS

The pre-Tertiary sedimentary rocks of the Meadow Valley Mountains were mapped in a rapid reconnaissance fashion in the late 1950's as part of geologic studies of Clark (Bowyer and others, 1958; Longwell and others, 1965) and Lincoln (Tschanz and Pampeyan, 1961, 1970) Counties, Nev. These early studies include descriptions of the geology and mineral deposits of this map area and the surrounding region (fig. 2). Detailed geologic mapping of small areas in the Meadow Valley Mountains was done by Duley (1957), Webster and Lane (1967), and Webster (1969) as part of stratigraphic studies of Mississippian rocks, and by Heston (1982) who studied the distribution of trace elements in the Chainman Shale near Grapevine Spring. The Tertiary volcanic rocks were examined by Cook (1965; unpub. data, 1955-1968), who measured stratigraphic sections in and near the Meadow Valley Mountains, and by Ekren and others (1977) as part of

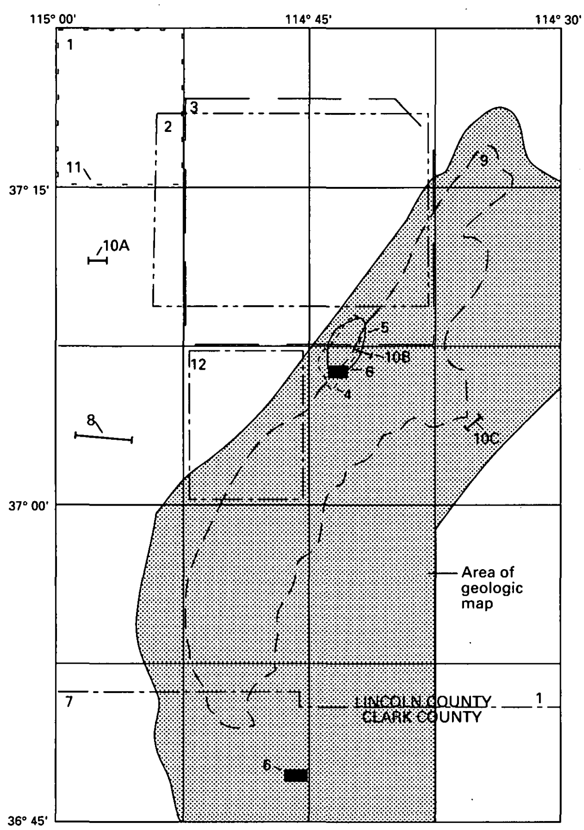

1. Tschanz and Pampeyan (1961, 1970); Ekren and others (1977)
2. Noble (1968)
3. Novak (1984, 1985)
4. Duley (1957)
5. Heston (1982)
6. Webster (1969)
7. Longwell and others (1965); Bowyer and others (1958)
8. P.H. Heckel and A. Reso, south Delamar section (unpub. data, 1960)
9. Pampeyan and others (1988); Campbell (1987)1
10. A, Cook (1965); B, E.F. Cook, Kane Wash section (unpub. data, 1955); C, E.F. Cook, Meadow Valley section (unpub. data, 1956)
11. Scott and others (1988)
12. Swadley and others (1990)

Figure 2. Sources of geologic data used in this report.

regional study that refined the volcanic stratigraphy of Lincoln County. Studies of the Kane Springs Wash caldera in the adjacent southern Delamar Mountains (fig. 1) were made by Noble (1968) and Novak (1984, 1985), and the Paleozoic section there was measured by P.H. Heckel and Anthony Reso (unpub. data, 1960). Detailed mapping in the southern Delamar Mountains (Scott and others, 1988, 1990; Swadley and others, 1990; Page and others, 1990) and northern Meadow Valley Mountains (Anne Harding, written commun., 1987; Harding and others, 1991), some of which overlaps this map area, commenced after this study was completed. The studies by Cook, Novak, Heckel and Reso, Scott and others, and Swadley and others provided stratigraphic information useful in this report.

Mineral resources of the region have been studied by several investigators. Gypsum deposits of the region were described by Jones and Stone (1920) and perlite deposits in and near Meadow Valley Wash were evaluated by K.L. Cochran (written commun., 1951). The oil and gas potential of a region including the Meadow Valley Mountains was evaluated by Sandberg (1983). A reconnaissance geochemical assessment of the map area was made by Hoffman and Day (1984), and the mineral resources of the map area were described by Campbell (1987).

This map was prepared from data gathered during eight weeks of reconnaissance geologic mapping between April 1985 and September 1987 supplemented with photogeologic interpretation of 1:31,680-scale natural-color aerial photographs of the map area. This work was an integral part of a study requested by the U.S. Bureau of Land Management to evaluate the mineral resource potential of the Meadow Valley Range Wilderness Study Area, a cooperative effort by the U.S. Geological Survey and the U.S. Bureau of Mines (Pampeyan and others, 1988). The Meadow Valley Range Wilderness Study Area covers about 393 km^2 (97,180 acres) or about 30 percent of the area included in this map.

ACKNOWLEDGMENTS

The author was assisted in the field at various times by Jacqueline C. Shulters, David A. Plume, John C. Monroe, and Kari N. Bassett. Paul Henri, James and Donald Bradshaw of Caliente, Nev., and Henry Rice of Logandale, Nev., supplied information on the history of, and access to, the map area. Randy Wilson of the U.S. Department of Agriculture Soil Conservation Service, Caliente District Office, provided information on soil surveys in and near the map area, and oil companies provided some generalized stratigraphic information on the Paleozoic rocks.

GEOLOGIC SETTING

The Meadow Valley Mountains are underlain by a sequence of folded and faulted sedimentary rocks of Cambrian through Triassic age that are well exposed in the south half of the range. The sedimentary rocks are unconformably overlain in the north half of the range by a sequence of interlayered volcanic tuffs and flows of Miocene age, some of which originated just west of the study area in the Kane Springs Wash caldera (fig. 1; Noble, 1968; Novak, 1984). The remainder of the volcanic rocks are thought to have originated to the north in the Caliente cauldron complex (fig. 1; Ekren and others, 1977).

The volcanic sequence consists mainly of welded ash-flow tuffs, with minor rhyolitic and basaltic flows, and rhyolite dikes that cut the tuffs and flows. Correlation of volcanic units in the map area is based on field megascopic examination of rocks and comparison with written descriptions by E.F. Cook (1965; unpub. data, 1955-1968), Williams (1967), Ekren and others (1977), and Novak (1984). For details on the mineralogy and chemistry of the welded tuffs see Cook (1965), Williams (1967), Noble (1968), Ekren and others (1977), and Novak (1984, 1985). The volcanic rocks in the northern part of the volcanic terrane, whose stratigraphic relations are complex and largely unknown, consist of interlayered welded tuffs and flows cut by dikes. Detailed mapping in that area (Harding and others, 1991) has begun to uncover the key to relations between the Kane Springs Wash caldera to the west (Noble, 1968; Novak, 1984), the volcanic rocks in northernmost part of the Meadow Valley Mountains, and the Caliente cauldron complex to the north (Ekren and others, 1977). The volcanic sequence in the south half of the volcanic terrane can be divided into upper and lower halves. The upper half of the volcanic sequence consists largely of rhyolitic ash-flow tuffs and flows of the Kane Wash Tuff, related rocks, and some basalt flows (Cook, 1965; Ekren and others, 1977; Novak, 1984), most of which erupted from in or near the Kane Springs Wash caldera whose east end is in the Meadow Valley Mountains. The rhyolitic flows are locally perlitic, and some of the interlayered tuffs are zeolitized. The lower half of the volcanic sequence consists of four dacitic to rhyolitic welded ash-flow tuff formations which are from youngest to oldest the Hiko Tuff, Harmony Hills Tuff, Bauers Tuff Member of the Condor Canyon Formation, and Leach Canyon Formation, and a basalt flow-breccia that is present only in the southeast corner of the volcanic terrane underlying the Harmony Hills Tuff. The ash-flow tuff formations in the lower half of the volcanic sequence probably erupted from the Caliente cauldron north of the study area (Noble and McKee, 1972; Ekren and others, 1977); the basalt breccia may have originated from a vent a few kilometers west of Vigo, where the thickest section of breccia is exposed.

The total volcanic sequence is about 720 m thick in the escarpment along Kane Springs Wash and thins to about 651 m west of Vigo (fig. 3). The volcanic sequence is of Miocene age, the upper half 15.4 to 11.4 Ma (Novak, 1984), and the lower half 24.6 to 18 Ma (Armstrong, 1970; Noble and McKee, 1972; Marvin and others, 1973; Rowley and others, 1975). Patches of welded tuff are present throughout the southern part of the map area. All but one of these patches appears to be Kane Wash Tuff, and the exception appears to be Hiko Tuff. For convenience, Novak's (1984) nomenclature for the Kane Wash Tuff, where applicable, has been used in this map.

The northwest-facing escarpment along Kane Springs Wash provides an excellent stratigraphic section of the welded ash-flow tuff formations from the Leach Canyon through Kane Wash units. The volcanic section exposed in Hackberry Canyon is somewhat similar but contains other interlayered volcanic units, for example, the thick unit of basalt breccia, a thin amygdaloidal basalt flow, and some thin welded tuff that was not recognized elsewhere in the map area.

Basalt flows (Tb_1, Tb_2, Tb_3) represent separate pulses of activity from different(?) but related sources, some of which were along Kane Springs Wash (Novak, 1984) and others near Hackberry Canyon. Unit Tb_3, the youngest flow in the map area, rests unconformably on units 2 (Tku_2) and 3 (Tku_3) of the Kane Wash Tuff and has a K-Ar age of 11.4 Ma (Novak, 1984); unit Tb_2 consists of thin flows interlayered with rhyolitic flows and tuffs in the upper(?) part of the Kane Wash Tuff (Tk) and rhyolite (Tr) units; unit Tb_1, an amygdaloidal basalt, rests unconformably on Hiko Tuff (Th) and is overlain by undivided strata of the Kane Wash Tuff (unit Tku). The oldest basalt in the map area is exposed at one locality near the mouth of Hackberry Canyon where it rests on red-bed strata at the base of the volcanic section. This flow and a thin overlying ash-fall(?) tuff pinch out laterally and a lens of conglomerate (Tc) is found at the next exposure of this stratigraphic interval. The old basalt, tuff, and conglomerate, however, are too thin to show at the map scale of 1:50,000. Basalts younger than 11.4 Ma are present outside of the map area, for example, at Leith siding, about 3 km east of the map area (fig. 1), a basalt flow resting on Kane Wash Tuff has a K-Ar age of 8.7 Ma (Ekren and others, 1977).

The Kane Wash Formation, as defined by Cook (1965) in the southern Delamar Mountains, included a basalt flow as the basal unit. Noble (1968) stratigraphically restricted the flow rocks (and unrelated sedimentary rocks) from the formation and applied the name Kane Wash tuff to the remaining units described by Cook (1965) and considered them to have been erupted from the Kane Springs Wash caldera. Novak (1984) refined the stratigraphy of the Kane Wash Tuff and applied letter-symbol names to mappable cooling units, some of which are used in this report. Novak (1984) also determined that the lower two units of the Kane Wash Tuff (Tko and Tkw) had an eruptive source west of the Kane Springs Wash caldera. Subsequently, workers in the southern Delamar Mountains (Scott and others, 1988), in the process of formalizing the member status of the cooling units, have substituted geographic names for Novak's letter-symbol names. In the Meadow Valley Mountains the upper part of the Kane Wash Tuff consists of at least three welded ash-flow tuffs, in ascending order units 1, 2, and 3 (Tku_1, Tku_2, and Tku_3, respectively); the lower part consists of a thick lithic tuff, unit W (Tkw) overlying a densely welded tuff, unit O (Tko). On this map the upper three units are mapped separately near the center of the volcanic terrane but are left undivided (Tku) throughout most of the map area.

In this study, no biotite or plagioclase was recognized in tuff above the Hiko near Cook's Meadow Valley and Kane Wash measured sections, and this agrees with the findings of Noble (1968) and Novak (1984) that plagioclase and biotite are rare or absent in true Kane Wash tuffs. However, R.B. Scott (written commun., 1988) reports xenocrystic plagioclase and biotite in some samples from Cook's (1965) type section of the Kane Wash Formation in the southern Delamar Mountains. It is possible, therefore, that Cook either misidentified altered mafic minerals and sanidine in his modal analyses (fig. 3) or did not recognize the xenocrystic origin of the plagioclase and biotite he reported in his samples.

Occurrences of carbonate-rich Kane Wash lithic-crystal tuff are present 5.6 km northeast of Grapevine Springs in unit 1 (Tku_1) where calcite has replaced the groundmass leaving the crystals suspended in a calcite matrix. This calcification appears to have selectively affected certain layers of tuff, for the lateral extent of the bodies is significantly greater than the vertical extent, and

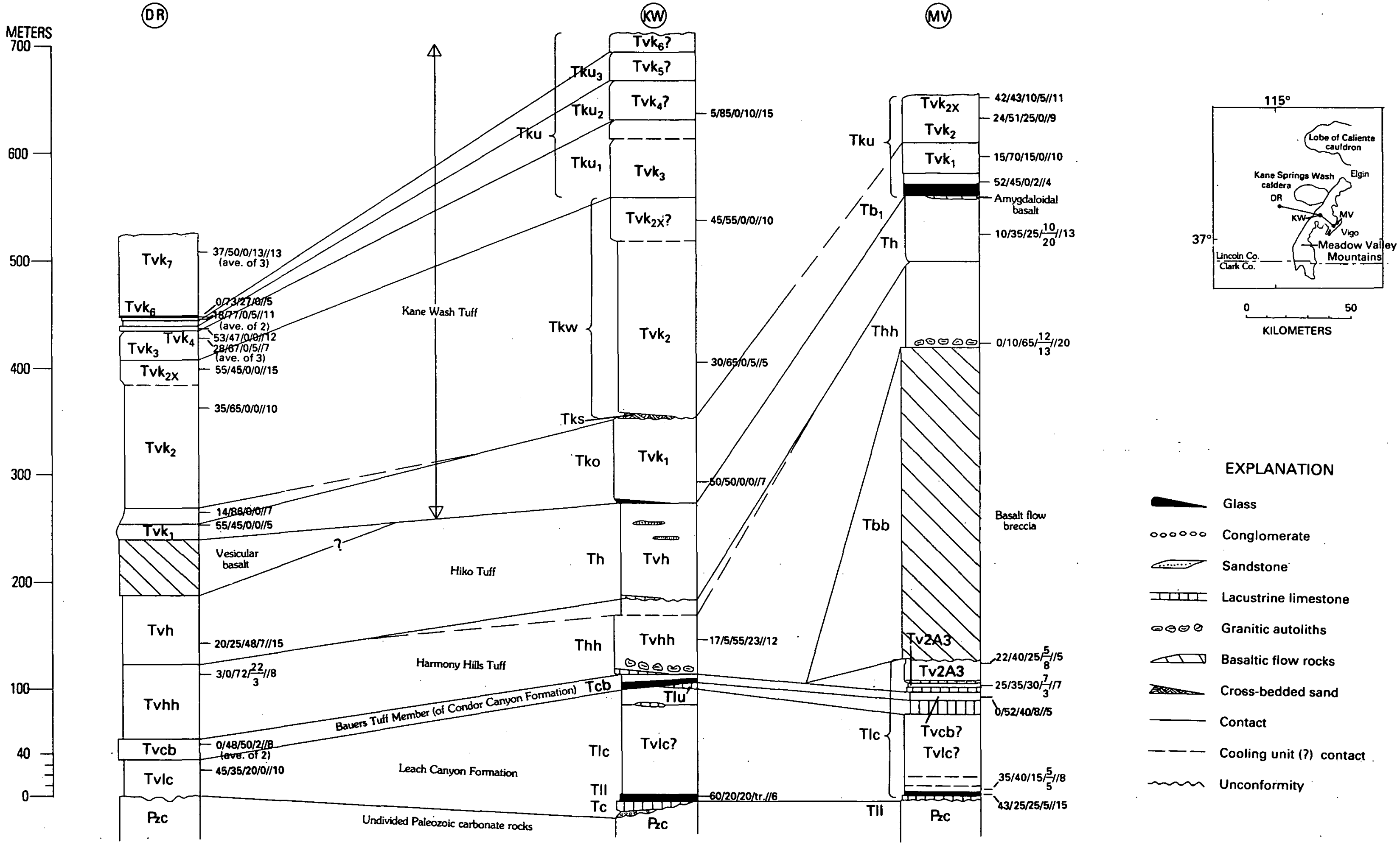

Figure 3. Stratigraphic sections of volcanic rocks in the Meadow Valley Mountains (localities KW and MV) compared with the type section of the Kane Wash Tuff in the southern Delamar Mountains (locality DR), modified from Cook (1965) and E.F. Cook, unpublished data, 1955, 1956 (see also Noble, 1968. Novak, 1984). The exact locations of sections KW (Kane Wash) and MV (Meadow Valley) are unknown. KW appears to be a composite section from the escarpment east of Grapevine Spring. MV probably is along a north trending line 2.4 km west of Vigo siding. Unit symbols inside section columns are from Cook (1965); E.F. Cook, unpub. data, 1955, 1956); unit symbols to outside columns are those used in this report. Numbers to right of columns (for example 45/25/20/$\frac{7}{3}$//10) represent phenocryst composition, in percent, as percentage of total crystals in specimens collected at these sites—that is: quartz/sanidine, plagioclase/$\frac{\text{biotite}}{\text{hornblende}}$//crystal content in percent of entire rock (Williams, 1960; Cook, 1965); tr, trace; ave., average of more than one sample. Cook's inclusion of plagioclase and biotite as primary constituents in his modal analyses of the Kane Wash Tuff samples is questionable. The Kane Wash Tuff contains biotite-rich lithic fragments and plagioclase xenocrysts from underlying formations (R.B. Scott, written commun., 1988) but lacks primary biotite or plagioclase (Novak, 1984). Tuffs overlying the Hiko Tuff (unit **Th**), and shown as the uppermost part of the Kane Wash Tuff (unit **Tku**) in the vicinity of Hackberry Canyon, near the location of Cook's section MV, do not closely resemble corresponding tuffs near Kane Springs Wash but do contain adularescent (sodic) sanidine, which most commonly occurs in units of the Kane Wash Tuff. See Description of Map Units (map sheet 1) for complete explanation of map unit symbols used in this report.

SE ROA 42965

JA_12845

no crosscutting relations were seen. Carbonate-rich float identical to the above described rock was found downslope from a locality at the crest of the volcanic escarpment, 3.6 km northeast of Sunflower Mountain. This locality was described by Tieh and Cook (1971) as an occurrence of carbonate-rich dikes in the Kane Wash Tuff where the carbonate probably originated through melting of limestone by a rhyolite magma.

A thin feldspathic sandstone (Tks) lies between units O (Tko) and W (Tkw) of the Kane Wash Tuff. In one area 1.6 km west of Sunflower Mountain the sandstone is about 12 m thick and consists of an upper half of grayish-yellow, well-sorted and crossbedded sandstone with interlayered ash beds and a lower half of light- to moderate-red, poorly sorted sandstone in graded and cross-stratified beds. Crossbedding in this sandstone is large scale trough type with wavelengths of several meters. The sandstone was not seen north of the vicinity of Grapevine Spring or in the volcanic scarp west of Vigo; its northeastern-most exposure is 9.5 km northwest of Vigo. At a few localities a thin, poorly exposed, partly welded lithic tuff separates the sandstone (Tks) or overlying unit W from an underlying erosion surface developed on densely welded unit O. In most exposures unit O is densely welded—slabs emitting a metallic ring when struck with a hammer—and is easily recognized by its unique eutaxitic texture. Near its northernmost exposure the upper part of unit O appears to be altered to a depth of about 4 m, possibly the result of its proximity to the eastward projection of the Kane Springs Wash caldera boundary.

Volcanic rocks in the northernmost part of the map area consist of rhyolitic flows and ash-flow tuff of the undivided rhyolite and Kane Wash Tuff unit (Trk). Locally some of the tuff appears to have melted and flowed during welding and superficially resembles a rhyolite flow.

Numerous rhyolite dikes, some of which form resistant ridges in the host rocks and others which blend into the host rocks, are present in the volcanic terrane. The dikes commonly have thin, black or dark-green, vitreous margins and yellowish-gray to pale-yellowish-brown, flow-banded cores and do not appear to have significantly altered the enclosing rocks. The dikes average a few meters in thickness and the most prominent ones form a north-trending swarm about 3 km long. Stream-sediment samples from the area cut by dikes contain anomalous amounts of beryllium, tin, thorium, and yttrium (Hoffman and Day, 1984), but subsequent samples of stream sediment and dike rock from the same area were not enriched in those elements (Pampeyan and others, 1988). A dike containing flow-banded rhyolite breccia cemented by color-banded carbonate minerals cuts the Harmony Hills Tuff 1.6 km northeast of Grapevine Spring. This latter dike bears no resemblance to the rhyolite dikes farther north or to the carbonate-rich Kane Wash Tuff noted above.

The Hiko and Harmony Hills Tuffs are easily recognized over most of the volcanic terrane, but the underlying Bauers Tuff Member of the Condor Canyon Formation is thin and mostly concealed by slope wash. About 4 km south of Sunflower Mountain, however, the Bauers is well exposed and appears to be as thick as 80 m. The Leach Canyon Formation is poorly exposed and commonly appears as a light-gray amorphous blanket of poorly welded tuff particles resting on a ledge of lacustrine limestone and overlain by Harmony Hills Tuff.

In Hackberry Canyon and the volcanic escarpment to the south, a distinctive unit of basalt breccia and related rocks (Tbb) underlies the Harmony Hills Tuff. This unit is thickest about 2.4 km west of Vigo and thins away from there suggesting its source was somewhere in the vicinity of the thickest exposure. The source, however, if exposed, was not recognized.

In the south-facing volcanic escarpment west of Vigo, the Leach Canyon Formation is overlain by a sequence of three lacustrine limestones separating three ash-flow tuff units (fig. 3), all of which are too thin to show at this map scale. The lowest tuff unit is mineralogically equivalent to the Bauers. E.F. Cook (unpub. data, 1956) designated the upper two tuff units Tv2A3, a symbol he used for pumice sillars and pumiceous tuffs with interlayered volcanic and lacustrine sediments lying between the Leach Canyon Formation and Harmony Hills or Hiko Tuffs in his draft stratigraphic sections of the Delamar, Pahroc, and Tempiute ranges, Tower Spring, and Black and Condor Canyons, in addition to the Meadow Valley Mountains. These tuff units in all sections except for the Meadow Valley Mountains have no megascopic mafic component; the average phenocryst content is 10 percent, which consists of 46 percent quartz, 42 percent alkali feldspar, and 12 percent plagioclase (Cook, 1965). In Cook's Meadow Valley section (MV, fig. 3) both biotite and hornblende, and a greater amount of plagioclase, are present in tuff he designated Tv2A3.

Lacustrine limestone is present locally at several horizons in the volcanic section but is almost everywhere present at the base of the section, resting on folded and faulted Paleozoic and Mesozoic strata, typically as a single unit about 20 m thick. Locally, a reddish-orange-weathering cobble conglomerate (Tc) underlies the lower lacustrine limestone (Tll), appearing to fill depressions in an erosion surface developed on deformed pre-Tertiary sedimentary strata. In a few places, for example, 3 km northeast of Sunflower Mountain, the lower lacustrine limestone appears to interfinger with the cobble conglomerate. Lacustrine limestone higher in the volcanic section occurs only locally and in places is interlayered with very thin tuff units, for example, as noted above, west of Vigo (MV, fig. 3). Only one occurrence of limestone within the volcanic sequence (unit Tlu 3 km north of Sunflower Mountain) was large enough to be shown on the geologic map. The lacustrine limestone in Lincoln County was considered to be Miocene or younger in age, on the basis of fossil pollen and pre-1960 K-Ar ages of 24 to 28 Ma, and the conglomerate probably Cretaceous to Oligocene (Tschanz, 1960; Tschanz and Pampeyan, 1970). Use of more recent radiometric age data from the volcanic sequence in adjacent areas indicates the lower lacustrine limestone (Tll) of the map area is more likely late Oligocene instead of Miocene; the lower limestone appears to be a partial time-equivalent of the Claron Formation of southwest Utah (Ekren and others, 1977). The age of the conglomerate is less certain, but it may be as old as Late Cretaceous or as young as Oligocene and in this report is considered to be early Tertiary.

The Muddy Creek Formation ("Muddy Creek beds" of Stock, 1921a; "Muddy Valley beds" of Stock 1921b) was named for exposures along Muddy Valley near Overton (fig. 1), where Stock (1921a, b) believed mammalian remains represented an age earlier than Pliocene, possibly Miocene. Potassium-Argon and fission-track ages indicate the Muddy Creek Formation near Lake Mead, about 35 km southeast of the map area, is no older than 10.6 Ma and no younger than 6 Ma (Bohannon, 1984, p. 14). In the vicinity of Rox and Galt, beds here tentatively assigned to the Muddy Creek Formation contain interbedded welded and nonwelded tuff and a thin white horizon that may be a volcanic ash. The welded tuff (Tku) resembles some Kane Wash tuff but the origin of the white nonwelded tuff (Tk) and ash(?) is unknown. In this report, the Muddy Creek Formation is considered to be Miocene and Pliocene(?) in age.

A high cliff exposure of Muddy Creek strata along the east side of Meadow Valley Wash 1.2 km southeast of Rox has a noticeably coarser texture and may be a near-source facies of the Muddy Creek Formation. Olmore (1971, p. 63), however, describes a section of his Rox conglomerate unit in the same area which he believes may correlate with a conglomerate member of the Horse Spring Formation as mapped by Rubey and Callaghan (1936, pl. 8). In this report the Rox section is included within the Muddy Creek Formation because the lithologic characteristics of the two appear to match.

Meadow Valley Wash marks the approximate boundary between thin Paleozoic shelf deposits on the east and thickening miogeosynclinal deposits on the west (Tschanz and Pampeyan, 1970, p. 105; Wernicke and others, 1984). About 8,200 m of pre-Tertiary sedimentary rocks are present in the map area, but no single location displays a continuous section; the sedimentary section here is almost twice as thick as the age-equivalent section in the nearby Mormon Mountains (fig. 3). The apparent rapid change in thickness and lithology has been emphasized by eastward thrusting of the miogeosynclinal section onto the stable shelf section (Wernicke and others, 1984).

Permian and Triassic red-bed and carbonate deposits are present near the center of the Meadow Valley Mountains but—if present—are not exposed in ranges to the north, west, or south. In the Meadow Valley Mountains the Permian and Triassic rocks are assumed to lie under a thrust plate composed of Bird Spring Formation. In the ridge 5 km west of Vigo, an unbroken section consisting of Moenkopi Formation—716 m of Virgin Limestone Member underlain by 30 m of Timpoweap Member—is exposed, and its Shnabkaib Shale Member is assumed to exist under the covered interval to the west (Olmore, 1971). Map measurements indicate the total thickness of Moenkopi strata between the red beds on the east and Shinarump Member of the Chinle Formation on the west is about 825 m, assuming no repetition or reduction by faulting in the covered interval. Olmore (1971) describes the Timpoweap Member, made up of siltstone and sedimentary chert breccia lenses, as being conformable with his overlying Virgin Member (of the Moenkopi Formation), and describes an unconformity about 163 m below the top of the Virgin Member indicating uplift and erosion during, as well as before, deposition of the Moenkopi. In addition to Olmore's two unconformities, however, at some places the chert breccia is bounded above as well as below by an angular discordance.

Exposures of cherty limestone in Hackberry Canyon and in the outlier to the north were assigned to the lower part of the undivided Kaibab Limestone and Toroweap Formation (Pkt) on the basis of lithology. At these localities, however, there is no chert breccia or chert-rich conglomerate between the cherty strata and underlying red-weathering sandy carbonate beds assigned to the Permian red beds (Prb). An outlier of cherty limestone exposed at Rox was previously mapped as Kaibab Limestone (Tschanz and Pampeyan, 1961, 1970; Wernicke and others, 1984).

The Bird Spring Formation is widely exposed in the Bunker Hills where an incomplete folded section is estimated to be about 1,650 m thick. A prominent pinkish-weathering silty dolomite interval (d) 106 to 150 m thick, is present about 900 m above the base of the formation. Fossils collected from strata immediately below this interval in Farrier Wash include a primitive *Schwagerina* species of probable early Wolfcampian age (C.H. Stevens, oral commun., 1987) and suggest that the Pennsylvanian-Permian boundary lies a short distance below the silty dolomite interval. The silty dolomite interval loses its characteristic appearance south of Farrier Wash. Near Arrow Canyon, in the Arrow Canyon Range, the Pennsylvanian-Permian boundary is about 25 m below a silty dolomite and limestone interval, unit BSe of Langenheim (1964), which is possibly the same as the silty dolomite interval (d) of this report. This boundary occurs about 732 m above the base of the Bird Spring Formation as used herein.

About 305 m of the uppermost part of the Bird Spring is exposed along Meadow Valley Wash between Vigo and Galt, conformably underlying the section of Permian red beds. The relation of this partial section to the Bunker Hills section is unknown, but at least the uppermost 150 m of this section was not recognized in the Bunker Hills.

The undivided Scotty Wash Quartzite and Chainman Shale unit (Msc) is based on stratigraphic nomenclature previously used for rocks widely exposed to the north and west of the map area (see Tschanz and Pampeyan, 1961, 1970). The individual formations are recognizable along Kane Springs Wash in the vicinity of Grapevine Spring (Duley, 1957), and a similar but much thinner interval of shaley rocks is present in the south half of the range. This interval is lithologically equivalent to the Chainman Shale and Indian Springs Formation of Webster and Lane (1967) and Webster (1969) in the Meadow Valley Mountains and to the Indian Springs Member of Longwell and Dunbar (1936) of the Bird Spring Formation in its type section. According to Duley (1957, p. 41) the

Chainman Shale at Kane Springs Wash is, at least in part, correlative with the upper part of the Monte Cristo Limestone at Arrow Canyon, the result of a facies change between clastic rocks of eastern Nevada and carbonate rocks of southern Nevada, an opinion also shared by Webster and Lane (1967). Duley (1957) tentatively placed the Mississippian-Pennsylvanian boundary within the upper part of the Scotty Wash Quartzite and reported no faunal change between the Scotty Wash and lowermost beds of the Bird Spring Formation. Webster and Lane (1967) and Webster (1969), however, place the Mississippian-Pennsylvanian boundary in the Meadow Valley Mountains and at Arrow Canyon in the lower part of the Bird Spring Formation at the top of the *Rhipidomella nevadensis* zone, 15 m above the top of their Indian Springs Formation. Unit Msc, as mapped, consists of a predominantly weak, yellow-, red-, red-brown-, and black-weathering shaley interval with thin interbeds of fossiliferous limestone, siltstone, and quartzite, lying between thick-bedded dark Mississippian limestone and medium-bedded cherty Pennsylvanian limestones of the Bird Spring Formation.

Mississippian limestone (Mmc) exposed in the southern Meadow Valley Mountains appears to be a geographic extension of the Arrow Canyon Range Mississippian section, which was divided into Dawn, Anchor, Bullion, and Yellowpine Limestones of the Monte Cristo Group of Langenheim and others (1962). In Bunker Hills, however, the Yellowpine Limestone appears to be absent, and at the north end of the outcrop area some silty to sandy limestones and fragmental limestones are present in the Dawn and Anchor Limestones. These clastic intervals may have good petroleum reservoir characteristics (Pampeyan, 1988). Mississippian limestone north of Sunflower Mountain is correlated with the Joana Limestone (Tschanz and Pampeyan, 1970).

In the Bunker Hills area the Pilot Shale, which was previously shown on maps by Tschanz and Pampeyan (1961, 1970), does not exist. Instead, the dark Devonian and Mississippian limestones are separated by a light-gray- to white-weathering Upper Devonian limestone that is here mapped as the uppermost part of the Guilmette Formation. Only a partial section of Pilot Shale is exposed in the Meadow Valley Mountains, along the Meadow Valley thrust east of Sunflower Mountain, where it is representative of a different facies of Upper Devonian and Mississippian strata described in a later section.

Devonian strata in the Meadow Valley Mountains are represented by the Sevy Dolomite, Simonson Dolomite, and Guilmette Formation. The Guilmette and Simonson are readily recognizable, but the Sevy is not as distinctive here as it is across Kane Springs Wash in the southern Delamar Mountains and farther north. The Guilmette Formation, as used in this report, consists of a thin, upper, light-gray, white-weathering limestone unit, a thick, middle limestone unit with some interbedded dolomite and sandstone layers, and a thin, basal yellowish-gray-weathering dolomite unit, the so-called yellow bed. These three units are correlated with, in descending order, the Crystal Pass Limestone, Arrow Canyon Formation, and Moapa Formation of Langenheim and others (1962) in the Arrow Canyon Range. North of the Bunker Hills, the Guilmette Formation is overlain by a platy limestone unit that most closely resembles the Upper Devonian and Lower Mississippian Pilot Shale.

The Simonson Dolomite occurs in both halves of the map area, but more detailed studies will be required to identify specific lithologic differences between its northern and southern exposures. The Sevy Dolomite also is present from the vicinity of Sunflower Mountain southward, and its outcrop color and thickness change southward, becoming darker and thinner until in the southern part of the range it is difficult to distinguish from the underlying Laketown and overlying Simonson Dolomites. The Simonson and Sevy Dolomites are correlated with the Piute Formation of Langenheim and others (1962) in the Arrow Canyon Range. One area 9 km southwest of Sunflower Mountain, herein mapped as undivided Devonian and Silurian carbonate rocks (DSc), has subsequently had its complex structural and stratigraphic details resolved by Swadley and others (1990).

Ordovician and Devonian strata of the map area are separated by Middle and Upper Silurian strata of the Laketown Dolomite. Across Kane Springs Wash in the southern Delamar Mountains the Laketown is easily recognized as a three-part section consisting of an upper thin, black dolomite, a middle, light-gray cherty dolomite, and a lower, dark-gray cherty dolomite (Heckel and Reso, 1962), all of which are fossiliferous. In the map area the upper interval and part(?) of the middle interval appear to be absent, as they are in the Arrow Canyon Range (Heckel and Reso, 1962), and the dolomites are more medium to dark gray. Thicknesses reported are 296 m in the southern Delamar Mountains (Heckel and Reso, 1962) and 78 to 101 m in the Arrow Canyon Range (Langenheim and others, 1962). In the Meadow Valley Mountains the Laketown ranges in thickness from about 70 to 150 m.

In the map area as well as in adjacent ranges to the north, west, and south, Upper Ordovician strata are represented by the Ely Springs Dolomite. This formation is a distinctive black-weathering, cliff-forming unit lying between medium- to dark-gray dolomite above and slope-forming, medium- to brownish-gray limestone below. In much of the Great Basin the Ely Springs is underlain by the Eureka Quartzite, another distinctive marker formation. In the map area, however, the Eureka ranges from a maximum thickness of 4.5 m on the west side of the range to less than 1 m on the east side—too thin to portray on the map—and therefore is included with the underlying Pogonip Group (Oep). The Pogonip has not been subdivided into its component formations in this report even though a three-part breakdown is evident in much of its outcrop area. In the map area the Pogonip Group is about 460 m thick and appears to thin gradually eastward from 545 m in the southern Delamar Mountains (P.H. Heckel and Anthony Reso, unpub. data, 1960) to 260 m in the Mormon Mountains (Wernicke and others, 1984). The Pogonip section in the Arrow Canyon Range is 741 m thick (Langenheim and others, 1962).

Conformably underlying Pogonip limestone is a section of Upper Cambrian carbonate rocks here assigned to the upper part of the Nopah Formation (€nc); these rocks were previously referred to as Upper Cambrian limestone and dolomite by Tschanz and Pampeyan (1961, unit eld; 1970, upper part of unit €ld). The upper half is a distinctive black-white-black interval which contrasts with the overlying brownish-gray Pogonip limestone and the underlying lower half of yellowish-gray and light-olive-gray color-banded carbonate rocks. A continuous section is not exposed in the map area but the total thickness is estimated to be about 365 m. A section equivalent to the carbonate member of the Nopah Formation exposed in the southern Delamar Mountains (fig. 4) was measured by P.H. Heckel and Anthony Reso (unpub. data, 1960) and correlated with the Desert Valley Formation of Reso (1963) exposed in the Pahranagat Range, about 50 km to the northwest. In the southern Delamar Mountains section the Cambrian-Ordovician boundary was placed about 120 m below the Pogonip-Desert Valley contact; in the Meadow Valley Mountains no fossil control on which to locate the Cambrian-Ordovician boundary was found. The carbonate member of the Nopah Formation, like the Pogonip Group, thins eastward (fig. 4) from 679 m for equivalent rocks in the southern Delamar Mountains to 190 m in the Mormon Mountains (Wernicke and others, 1984). The Dunderberg Shale Member of the Nopah Formation is exposed at several localities as the basal part of the Nopah, but it typically is distorted by faulting and folding so its true thickness is uncertain. In the southern Delamar Mountains the Dunderberg is 105 m thick (P.H. Heckel and Anthony Reso, unpub. data, 1960) and it appears to be absent in the Mormon Mountains (Wernicke and others, 1984).

The lowest stratigraphic unit in the map area is the Highland Peak Formation, which is best exposed in a faulted anticline between the Two Flats canyon and Anticline canyon faults along the west side of the Meadow Valley Mountains (map sheet 2). Possibly as much as 700 m of Middle and Upper Cambrian section is exposed here, and correlative strata in the Mormon Mountains (Bonanza King Formation of Wernicke and others, 1984) are about 580 m thick. A composite section of Highland Peak in the Delamar Mountains 55 km north, is more than 1,000 m thick (Callaghan, 1937; Wheeler, 1948).

STRUCTURAL SETTING

The Meadow Valley Mountains are in the Sevier orogenic belt (Armstrong, 1968), a south-southwest-trending zone of large-scale overthrusting and folding extending from western Utah through southern Nevada to southeastern California. Within the orogenic belt overthrusting was from west to east juxtaposing thick miogeosynclinal and thin shelf stratigraphic sequences (Fleck, 1970; Stewart, 1980) along the east edge of the Basin and Range province. This episode of crustal compression took place in Cretaceous time (Armstrong, 1968) and was followed by a period of erosion during which coarse clastic deposits accumulated on the erosion surface. Time of cessation of thrusting is unknown, but coarse clastic deposits (Tc) unconformably overlie folded and thrust Paleozoic and Mesozoic strata in the Meadow Valley, Delamar, and Clover Mountains. The coarse clastic rocks are, in turn, overlain by upper Oligocene lacustrine limestone and a thick sequence of lower to middle Miocene welded tuff formations. In general the volcanic formations are conformable, with local lenses of limestone or sandstone between formations or members of formations. The sedimentary units indicate quiescent intervals during early Miocene volcanic activity. The hiatus between units O and W of the Kane Wash Tuff marked by up to 12 m of crossbedded sandstone (Tks), is recognized over a wider area than are the intravolcanic limestones. No similar sandstone or limestone units were seen in the Kane Wash Tuff above unit W. During middle to late Miocene time an episode of crustal extension began that resulted in the present-day landscape of deformed sedimentary strata unconformably overlain by gently dipping, broadly warped volcanic rocks cut by high-angle normal faults. Continuing tectonic activity is indicated by northeast-trending normal faults parallel to the range front cutting alluvial fan deposits and by the ongoing seismic activity of the region (Smith and Sbar, 1974; Rogers and others, 1987).

Regional structural interpretations indicate that the Meadow Valley Mountains are part of the Keystone-Muddy Mountain-Glendale thrust plate of the Mormon Peak allochthon and are characterized by a structural style of local tight folding and minor thrust faulting (Wernicke and others, 1984). The structural style and Paleozoic sections of the Meadow Valley, Arrow Canyon, and Las Vegas ranges are reported to be extremely similar to the part of the Spring Mountains between the Keystone and Wheeler Pass thrust faults (about 100 km to the southwest) (Wernicke and others, 1984, p. 482).

Most of the west edge of the Meadow Valley Mountains is bounded by the northeast-trending Kane Springs Wash fault, a narrow zone of faults subparallel to the Pahranagat shear system of Tschanz and Pampeyan (1970, p. 84). The southwest boundary is along north-trending faults that appear to be related to the Kane Springs Wash fault in the same sense as the Maynard Lake fault and Delamar Mountains and Sheep Range breakaway faults are related (Liggett and Ehrenspeck, 1974; Wernicke and others, 1984, figs. 9, 10), that is, the Kane Springs Wash fault may be an oblique-slip fault that connects with a breakaway fault zone towards the south. In general, the range is a gently east dipping block with the dip steepening eastward and reversing to form a major syncline and anticline in the Bunker Hills and a faulted syncline in the hills west of Vigo. The Paleozoic and Mesozoic sedimentary strata locally are tightly folded and overturned, commonly in proximity to thrust faults, and are cut by numerous high-angle faults. The sedimentary rocks were folded, faulted, and eroded prior to eruption of the Miocene volcanic rocks, for flat-lying to gently dipping welded tuffs are found both capping the folded and thrusted strata and prevolcanic conglomerate and in canyons eroded along steeply dipping faults. Near the center of the map area, parts of the sedimentary section are missing and are

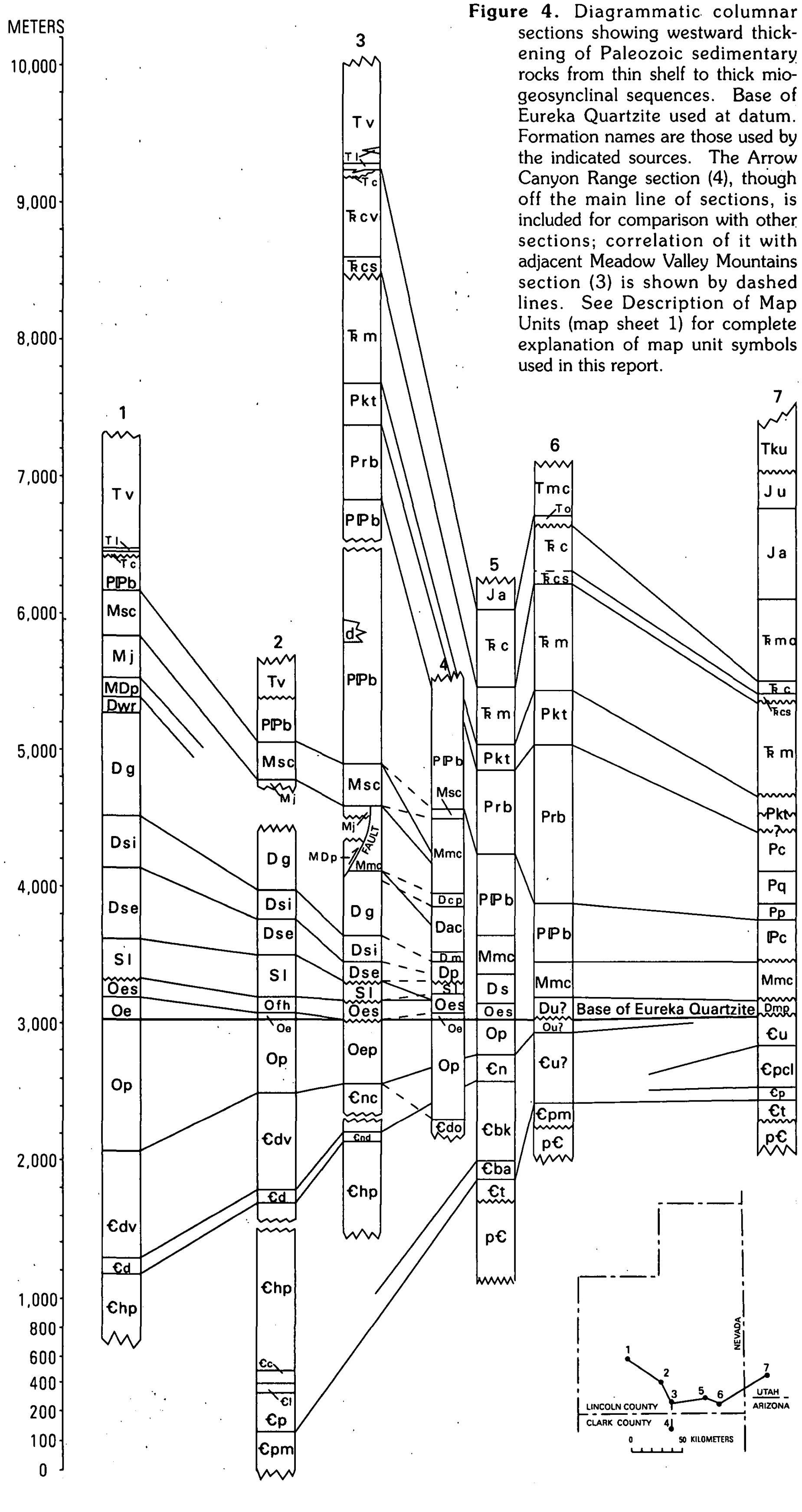

Figure 4. Diagrammatic columnar sections showing westward thickening of Paleozoic sedimentary rocks from thin shelf to thick miogeosynclinal sequences. Base of Eureka Quartzite used at datum. Formation names are those used by the indicated sources. The Arrow Canyon Range section (4), though off the main line of sections, is included for comparison with other sections; correlation of it with adjacent Meadow Valley Mountains section (3) is shown by dashed lines. See Description of Map Units (map sheet 1) for complete explanation of map unit symbols used in this report.

Figure 4. continuation

GEOLOGIC UNIT SYMBOLS

Tmc	Tertiary Muddy Creek Formation
To	Tertiary Overton(?) Fanglomerate
Tv	Tertiary volcanic rocks
Tl	Tertiary limestone
Tc	Tertiary conglomerate
Tku	Tertiary and Cretaceous rocks, undivided
Ju	Jurassic rocks, undivided
Jn	Jurassic Navajo Sandstone
₹mo	Triassic Moenave Formation
₹cv	Triassic upper sandstone member (of Chinle Formation)[3]
₹c	Triassic Chinle Formation
₹cs	Triassic Shinarump Member (of Chinle Formation)
₹cs	Triassic Shinarump Conglomerate (of Chinle Formation)[6,7]
₹m	Triassic Moenkopi Formation
Pkt	Permian Kaibab Limestone and Toroweap Formation, undivided
	Permian Kaibab LimestoneFormation and Toroweap Formation, undivided[6,7]
Prb	Permian red beds
Pc	Permian Coconino Sandstone
Pq	Permian Queantoweap Sandstone
Pp	Permian Pakoon Formation
PIPb	Permian and Pennsylvanian Bird Spring Formation—Includes silty dolomitic interval (d) present in the Bunker Hills
	Permian and Pennsylvanian Bird Spring Group[4]
IPc	Pennsylvanian Callville Limestone
Msc	Mississippian Scotty Wash Quartzite and Chainman Shale, undivided
	Mississippian Scotty Wash Quartzite and Chainman Shale, undivided[1]
Mmc	Mississippian Monte Cristo Limestone
	Mississippian Monte Cristo Group[4,7]
	Mississippian Monte Cristo Group[5]
Mj	Mississippian Joana Limestone
MDp	Mississippian and Devonian Pilot Shale
	Mississippian and Devonian Pilot Formation[1]
Du	Devonian(?) rocks, undivided
Dwr	Devonian West Range Limestone
Dcp	Devonian Crystal Pass Limestone
Dg	Devonian Guilmette Formation
Dac	Devonian Arrow Canyon Formation
Dm	Devonian Moapa Formation
Dp	Devonian Piute Formation
Dsi	Devonian Simonson Dolomite
	Devonian Simonson Formation[1]
Dse	Devonian Sevy Dolomite
Ds	Devonian Sultan Formation
Dmp	Devonian Muddy Peak Limestone
Sl	Silurian Laketown Dolomite
Ou	Ordovician(?) rocks, undivided
Oes	Ordovician Ely Springs Dolomite
Ofh	Ordovician Fish Haven Dolomite
Oe	Ordovician Eureka Quartzite
Oep	Ordovician Eureka Quartzite and Pogonip Group, undivided
Op	Ordovician Pogonip Group
Єu	Cambrian rocks, undivided
Єdv	Cambrian Desert Valley Formation
Єn	Cambrian Nopah Formation
Єnc	Cambrian carbonate unit (of Nopah Formation)[3]
Єdo	Cambrian dolomite—Correlative with Nopah Formation
Єnd	Cambiran Dunderberg Shale Member (of Nopah Formation)
Єd	Cambrian Dunderberg Formation[1]
	Cambrian Dunderberg Shale[2]
Єbk	Cambrian Bonanza King Formation
Єhp	Cambrian Highland Peak Formation
	Cambrian Highland Peak Limestone[2]
Єpcl	Cambrian Peasley Limestone, Chisholm Shale, and Lyndon Limestone, undivided
Єc	Cambrian Chisholm Shale
Єl	Cambrian Lyndon Limestone
Єp	Cambrian Pioche Shale
Єpm	Cambrian Prospect Mountain Quartzite
Єba	Cambrian Bright Angel Shale
Єt	Cambrian Tapeats Sandstone
PЄc	Precambrian crystalline rocks

——— Contact

~~~~~~ Unconformity

Superscripts indicate columnar sections in which informal names or stratigraphic terminology not presently accepted by the U.S. Gological Survey appear.

EXPLANATION

1	**Pahranagat Range**—Modified from Reso, 1963
2	**Delamar Mountains**—Bird Spring Formation to Joana Limestone, Tschanz and Pampeyan, 1970; Joana Limestone to Dunderberg Shale, P.H. Heckel and A. Reso, unpub. data, 1960; Highland Peak Limestone to Prospect Mountain Quartzite, Wheeler, 1943, and Callaghan, 1937. With minor modifications
3	**Meadow Valley Mountains**—Scotty Wash Quartzite and Chainman Shale, Duley, 1957
4	**Arrow Canyon Range**—Bird Spring Group to Upper Cambrian dolomite, Langenheim and others, 1962; Scotty Wash Quartzite through Monte Cristo Limestone, Duley, 1957
5	**Mormon Mountains**—Modified from Wernicke and others, 1984
6	**East Mormon Mountains**—Modified from Olmore, 1971
7	**Beaver Dam Mountains**—Modified from Langenheim and Larson, 1973
~~~~~~

believed to have been cut out along thrust faults. On the basis of abrupt changes in thickness and lithology across faults, the Paleozoic rocks present in the Meadow Valley Mountains appear to represent more than one facies (as described below) that have been juxtaposed by faulting.

For convenience of description, the area underlain by sedimentary rocks is divided into three fault-bounded blocks (fig. 5): (1) the Bunker Hills block includes most of the south half of the map area bounded on the north by a concealed northwest-trending fault, referred to as the Bunker Hills fault, and a vertical, northeast-striking fault, referred to as the Two Flats canyon fault; (2) the Sunflower Mountain block north of the Bunker Hills block bounded by the Kane Springs Wash fault and a thrust fault, referred to as the Vigo West thrust, juxtaposing Bird Spring and Moenkopi strata; and (3) the Vigo block lying east of the Vigo West thrust fault and west of the Mormon Mountains. As noted above, the major structural relations exposed are pre-Miocene in age.

The west-facing part of the Bunker Hills block is bounded and cut by several high-angle, west-dipping normal faults with relatively small offsets, similar to those in the west face of the Arrow Canyon Range to the south. There is, however, a significant structural break between the two ranges, concealed by flat-lying Muddy Creek deposits, that separates northward-plunging Monte Cristo strata at the north end of the Arrow Canyon Range from Pogonip strata at the south end of the Meadow Valley Mountains. This break may possibly be the northward continuation of the Dry Lake thrust (Longwell and others, 1965) or a breakaway boundary of the Meadow Valley Mountains. In this area a swarm of small-offset high-angle faults cuts both Muddy Creek and alluvial fan deposits. Most of the offsets are down to the west but a few appear to have formed east-facing scarps. Geomorphic features along the range front indicate that the faults are young, and exposures of alluvial fan deposits faulted against Pogonip strata confirm that observation.

The northeast end of the Bunker Hills terminates abruptly in a northwest-trending front that is aligned with an exposed fault. The linear aspect of this edge of the Bunker Hills strongly suggests fault control, and the name Bunker Hills is applied to this lineament and short segments of fault actually exposed. The Two Flats canyon and Bunker Hills faults separate Ordovician to Permian strata of one facies from Cambrian to Pennsylvanian strata that appear to represent another facies, the differences being most noticeable in the Upper Devonian through Upper Mississippian part of the section. The Two Flats canyon and Bunker Hills faults come together in a complex of fault blocks where the Two Flats canyon fault appears to split. The west branch steps left and continues north-northeast beyond Sunflower Mountain to the Kane Springs Wash fault; the east branch continues northeast, but major offset appears to end at the intersection with the Bunker Hills fault. The Two Flats canyon fault separates gently dipping Ordovician to Mississippian strata in the Bunker Hills block to the southeast from folded Cambrian strata on the northwest, indicating a stratigraphic throw of about 2,500 m. Where exposed, the Two Flats canyon fault dips vertically but no evidence indicating sense of movement was seen. The linear trace and offset of the range front suggest strike-slip movement, but the movement may be largely normal, placing folded strata of one thrust plate against undeformed strata of another thrust plate. At the intersection of Two Flats canyon and Bunker Hills faults the stratigraphic throw between Bunker Hills and Sunflower Mountains blocks is about 1,600 to 2,000 m, but north of the intersection the throw on the Two Flats canyon fault is only about 150 m, suggesting that the northeast continuing fault is unrelated to the large-offset fault.

The east half of the Bunker Hills block is underlain by Bird Spring strata folded into a syncline and anticline, and locally along the east edge the dips are steep to the east or overturned to the west suggesting eastward transport of the block. This block also is cut by many east-trending faults with small offsets, only a small number of which are shown on the map. The adjacent bedrock exposures to the east are the Kaibab Limestone in Meadow Valley Wash at Rox, strata that should be structurally and stratigraphically higher than the Bird Spring strata. According to Wernicke and others (1984) the Kaibab outliers and Meadow Valley Mountains are part of the Glendale thrust plate (Mormon Peak allochton) that is characterized by local tight folding and minor thrusting. The east edge of the Bunker Hills block may be bounded by a minor thrust within the Glendale plate. It is possible that the Meadow Valley Mountains are part of a breakup zone at the edge of the Glendale plate, and the various fault-bounded blocks described here resulted from the breakup. A well drilled on the axis of the Bunker Hills anticline bottomed in the lower part of the Monte Cristo Formation at a depth of 2,143 m without crossing any major fault (Texaco Inc., log of Texaco Federal No. 1), so any major surface of large-scale displacement probably lies below that depth.

The Sunflower Mountain block lies north of the Bunker Hills block forming the main scarp of the range along Kane Springs Wash. The Kane Springs Wash fault, a narrow zone of northeast-striking high-angle faults along the southeast edge of Kane Springs Wash, was originally described as a normal fault (Tschanz and Pampeyan, 1970) but later Ekren and others (1977) considered it to have left-lateral strike-slip or oblique-slip displacement of at least 8 km on the basis of an abundance of horizontal slickensides near the head of Kane Springs Wash, offset post-Kane Wash Tuff rhyolitic lavas, and apparent offset of Bird Spring strata and thrust and fold belts (Delamar Mountains thrust and fold belt and Meadow Valley thrust of Tschanz and Pampeyan, 1970). One other line of evidence suggestive of left slip is found in the aeromagnetic map of this region which shows the east end of an anomaly over intrusive rocks of the Kane Springs Wash caldera curving northward as though in response to left-lateral offset of the source (Pampeyan and others, 1988), an interpretation confirmed by recognition of the east end of the Kane Springs Wash caldera in the northern Meadow Valley Mountains (Harding and others, 1991). The Paleozoic strata in the Meadow Valley and Delamar Mountains, on opposite sides of the fault, cannot

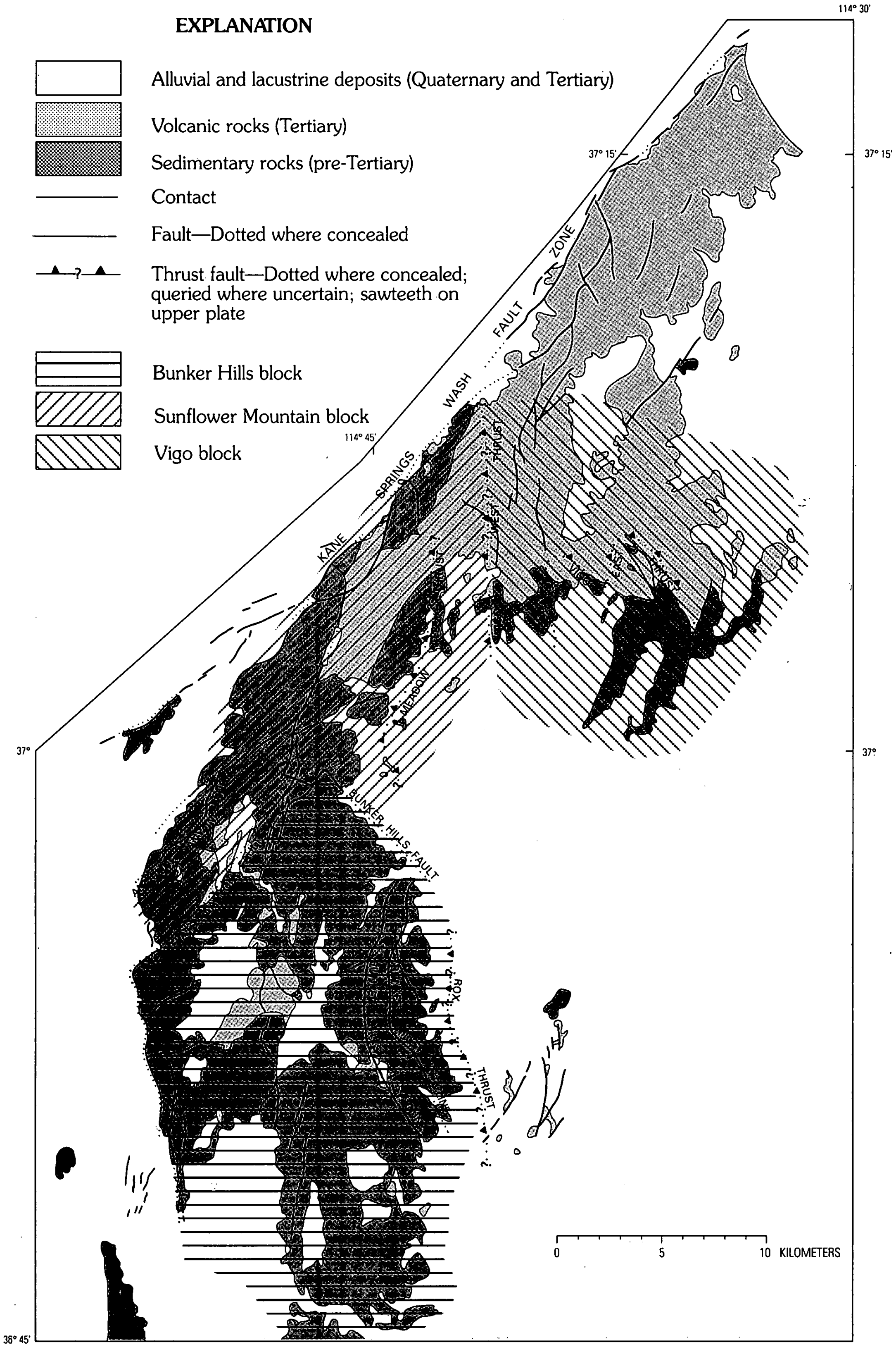

Figure 5. Sketch map of Meadow Valley Mountains showing subdivision into structural blocks based on stratigraphy and style of deformation. See text for discussion.

SE ROA 42973

JA_12853

be used with any certainty to determine displacement across the Kane Springs Wash fault largely because the Upper Cambrian, Silurian, and Lower Devonian formations in the southern Delamar Mountains are considerably thicker and may represent a different facies. The Kane Springs Wash caldera appears to be offset about 4.5 km in a left-lateral sense, but a significant component of dip slip is suggested by the high scarp along the south edge of the wash. As noted above, the Kane Springs Wash fault zone may be an oblique-slip or transfer fault or it may mark a breakaway zone rotating the southern Delamar Mountains away from the Meadow Valley Mountains.

Splays of the Kane Springs Wash fault cut alluvial fan deposits and mark the north edge of an isolated block of Devonian strata near the mouth of Kane Springs Wash. This block is made up of light- and dark-gray limestone and dolomite and brown-weathering sandy limestone and sandstone, a lithology resembling the sandy limestone facies of the Guilmette Formation (Tschanz and Pampeyan, 1970, p. 37) in contrast with limestone-facies Guilmette strata present in the adjacent Delamar and Meadow Valley Mountains. This block better resembles the Guilmette Formation of the Pahranagat Range to the northwest; Swadley and others (1990), however, consider it to consist of the Sevy and Simonson Dolomites. South of this block the range front is controlled by north-trending faults. The change in direction occurs in an area where three northeast-striking vertical faults emerge from the range, the Two Flats canyon or southernmost fault juxtaposing gently eastward-dipping Ordovician to Mississippian and folded Cambrian formations in a canyon informally referred to as Two Flats canyon. The second fault emerges about 4 km north and is referred to as the Anticline canyon fault after an anticline developed in Highland Peak and Nopah strata. The anticline's east limb dips moderately to steeply east with some minor overturning in the Dunderberg Shale Member; the west limb has been thrust over the main fold axis and contains minor folds cut by low-angle normal faults. The third fault, about 1.2 km farther north, also is formed in Cambrian and Ordovician strata and consists of several en echelon right-stepping segments suggesting a component of left slip. Strata of the Pogonip Group are tightly folded between the Anticline canyon fault and unnamed third fault as are strata in the upper part of the Nopah where the Anticline canyon fault branches and steps left. The three faults merge northward, the Two Flats canyon fault being the main trace, and continue north-northeast. The northern part of this fault juxtaposes relatively undeformed Upper Cambrian to Lower Ordovician and Middle Devonian strata indicating a stratigraphic throw of about 1,100 m, somewhat more than the 793 m estimated by Tschanz and Pampeyan (1970, p. 107). The Kane Springs Wash fault, the three sub-parallel faults described above, and the faults cutting Cenozoic deposits in Kane Springs Wash appear to be part of a system of northeast-trending faults that occupy a narrow zone at the head of Kane Springs Wash and widen to the southwest by branching (fig. 5). A second system of north-trending faults is exposed along the west edge of the Bunker Hills block, as well as the west edge of the Arrow Canyon Range, and the shape and development of the Meadow Valley Mountains has been controlled by interaction of these two systems.

About 40 m of Joana Limestone, in fault contact with Guilmette strata, is present on the northwest side of the Sunflower Mountain block, but all of the Joana and part of the Chainman Shale are cut out on the southeast side along a fault which juxtaposes platey limestones of the Pilot Shale and shaley beds of the undivided Scotty Wash Quartzite and Chainman Shale unit. The fault on the southeast side was named the Meadow Valley thrust and was interpreted to extend north under the volcanic cover and join at depth with the fault on the northwest side (Tschanz and Pampeyan, 1970, fig. 3). The Meadow Valley thrust is projected south between the continuous Devonian exposures and an outlier of Bird Spring strata. The Middle Devonian to Lower Pennsylvanian sections (Guilmette Formation, Pilot Shale, Joana Limestone, Chainman Shale, Scotty Wash Quartzite, and Bird Spring Formation) on opposite sides of the Sunflower Mountain block appear to belong to the same facies but have been telescoped by thrusting.

The east boundary of the Sunflower Mountain block is drawn along the Vigo West thrust. The Vigo West thrust has at least 2,400 m of stratigraphic throw, the amount of displacement required to account for the juxtaposition of strata of the lower part of the Bird Spring and Moenkopi, and an amount considerably larger than the 1,372 m estimated by Tschanz and Pampeyan (1970, p. 106). The actual Bird Spring-Moenkopi contact is overlain by Tertiary conglomerate (**Tc**) at the head of a linear arroyo separating the two formations, but deformation in the Bird Spring near the contact and low-angle, west-dipping structures in the Moenkopi strata in the ridge east of the Bird Spring contact strongly suggest the Bird Spring is thrust over the Moenkopi. In addition, the contact is the west edge of a Permian and Triassic red-bed and limestone sequence in southern Nevada, and the abrupt disappearance of more than 3,400 m of section composed of these rocks is more easily explained by an overriding thrust than by normal faulting. The Vigo West thrust may consist of at least two imbricate faults, and the thrust contact is inferred to extend north under the volcanic terrane east of Grapevine Spring and to be truncated by the Kane Springs Wash fault zone. East of the Vigo West thrust Paleozoic and Mesozoic strata of the Vigo block, namely the red-beds unit and Moenkopi Formation, are increasingly deformed northward towards the volcanic cover. Within the Vigo block the Moenkopi is thrust over the Moenkopi(?), Chinle Formation, and red beds with large angular discordances between the units visible at three localities along the Vigo East thrust. In addition, it is possible that the basal contact of the Moenkopi in the linear ridge 4.2 km west of Vigo may be part of the Vigo East thrust owing to angular discordances of up to 20° between the Moenkopi and the underlying undivided Kaibab Limestone and Toroweap Formation (**Pkt**) and folded Permian red beds.

In the north half of the map area (sheet 1) the volcanic section appears to rest on an erosion surface of low relief, while in the south half (sheet 2), patches of Kane Wash Tuff (Tku) are present at various levels on an irregularly eroded surface, for example, in the vicinity of Two Flats canyon welded ash-flow tuff of the same(?) cooling unit caps the highlands and coats the canyon walls over a vertical range of more than 200 m. In general the tuff dips eastward 10°-35°, but in a few places the dip is as steep as 65°. Some of the steep dips, for example in and near Two Flats canyon, appear to be due to compaction during welding and elsewhere are due to post-volcanic extensional faulting. In the vicinity of Sunflower Mountain the tuff is warped into open folds, either in response to compaction over buried topography or to post-volcanic deformation. In the Kane Springs Wash escarpment, dips decrease upwards in the volcanic section from about 35° to less than 10°. Numerous steeply dipping, north-trending normal faults cut the volcanic sequence, but the offsets on these faults are less than a few tens of meters. In the vicinity of Sunflower Mountain, however, the volcanic section is offset a minimum of 250 m along a branch of the Two Flats canyon fault. Structural and stratigraphic relations of the volcanic sequence near Vigo are less evident than they are to the west, and in the northernmost part of the map area the relations are even more complex. Detailed mapping will be required to unravel the problems left unanswered in this report. According to R.B. Scott (written commun., 1988) the northern part of the volcanic area may contain outflow from an older buried caldera to the north.

The linear escarpment along Kane Springs Wash displays the complete stratigraphic section of welded ash-flow tuffs and strongly resembles a fault scarp. However, no evidence of faulting was seen along the Paleozoic rocks-volcanic rocks contact so the escarpment probably is a fault-line scarp along the Kane Springs Wash fault zone. The conspicuous hill composed of Bird Spring strata located between Sunflower Mountain and Grapevine Spring and the outliers of Permian strata in the volcanic terrane appear to be erosional remnants on the low-relief surface subsequently indundated by ash-flow tuffs.

Along the west bank of Meadow Valley Wash opposite Hoya siding, strata of the Muddy Creek Formation have collapsed into the drainage channel forming an area of jumbled slump blocks 0.2 to 0.4 km wide by 3.5 km long in response to undercutting of the bank. The linear drainage and headwall scarp may have been controlled by faults or fractures similar to the subparallel linear feature, less than 1 km to the west, visible on aerial photographs. Similar but smaller slumps are present just north of Hoya. Other landslide deposits of sedimentary and volcanic rocks are present in the north-central map area.

Along the range front near Grapevine Spring patches of the Hiko and Kane Wash Tuffs rest directly on Paleozoic strata. Ekren and others (1977) show the tuffs in normal contact on Paleozoic rocks but assign them tentatively to their unit Tt3 which includes the Hiko Tuff through the Leach Canyon Formation. Stewart and Carlson (1978) show these tuffs as one northwest-dipping low-angle fault block. These volcanic rocks are cut by many faults and may be remnants of old landslide blocks shed from a retreating volcanic scarp.

GEOPHYSICAL SETTING

The gravity of the region surrounding the Meadow Valley Mountains is dominated by a strong down-to-the-north gradient of more than 50 mGals north of the south edge of the volcanic terrane (fig. 6). Eaton and others (1978) analyzed this gradient and pointed out that it roughly coincides with the south edge of a vast field of predominantly rhyolitic rocks and concluded that it mainly reflects a density contrast resulting from emplacement at shallow depth of large volumes of silicic magma in middle Tertiary time. Precambrian crystalline basement rock exposed in the Mormon Mountains is neither exposed nor does it have magnetic expression north of the gravity gradient. A down-to-the-north step of Precambrian basement in the vicinity of latitude 37° N. may account for part but not all of the gradient (Eaton and others, 1978). Other gravity lows that appear as perturbations of the regional gradient in Kane Springs and Meadow Valley Washes and Coyote Spring Valley reflect thick deposits of Miocene and younger unconsolidated sedimentary deposits (Pampeyan and others, 1988).

An aeromagnetic map of the region (fig. 7) shows positive anomalies centered over the Mormon, Clover, and Delamar Mountains. The anomaly over the Mormon Mountains is thought to represent a domoform uplift of strongly magnetic Precambrian crystalline basement and a possible Tertiary granitic intrusive body (Shawe and others, 1988), whereas the Clover and Delamar anomalies most likely are due to middle Tertiary intrusive bodies in eruptive centers. One of these anomalies in the Delamar Mountains coincides roughly with the Kane Springs Wash caldera (fig. 7) and extends eastward over the northern Meadow Valley Mountains where the east end of the anomaly curves northward, either in response to left-lateral displacement of the causative source along the Kane Springs Wash fault, or structural control of the source by a north-curving arcuate fracture (Pampeyan and others, 1988). According to Harding and others (1991) the Kane Springs Wash caldera does extend east into the Meadow Valley Mountains and is offset 4.5 km in a left-lateral sense along the Kane Springs Wash fault. The anomaly low north of the volcanic center coincides with a deep gravity low and suggests that an older buried collapse caldera is present north of the Kane Springs Wash volcanic center (Moring and others, 1988).

ECONOMIC GEOLOGY

Much of the Permian clastic rocks are red-bed deposits, some of which contain bedded evaporite deposits of gypsum (Jones and Stone, 1920). These deposits have been prospected but, to date, none have been developed. Locally the Chainman Shale contains phosphatic beds that have been explored for vanadium (Heston, 1982) and siltstone beds that have been quarried for ornamental stone. In addition, the Mississippian carbonate rocks of a region including the Meadow Valley

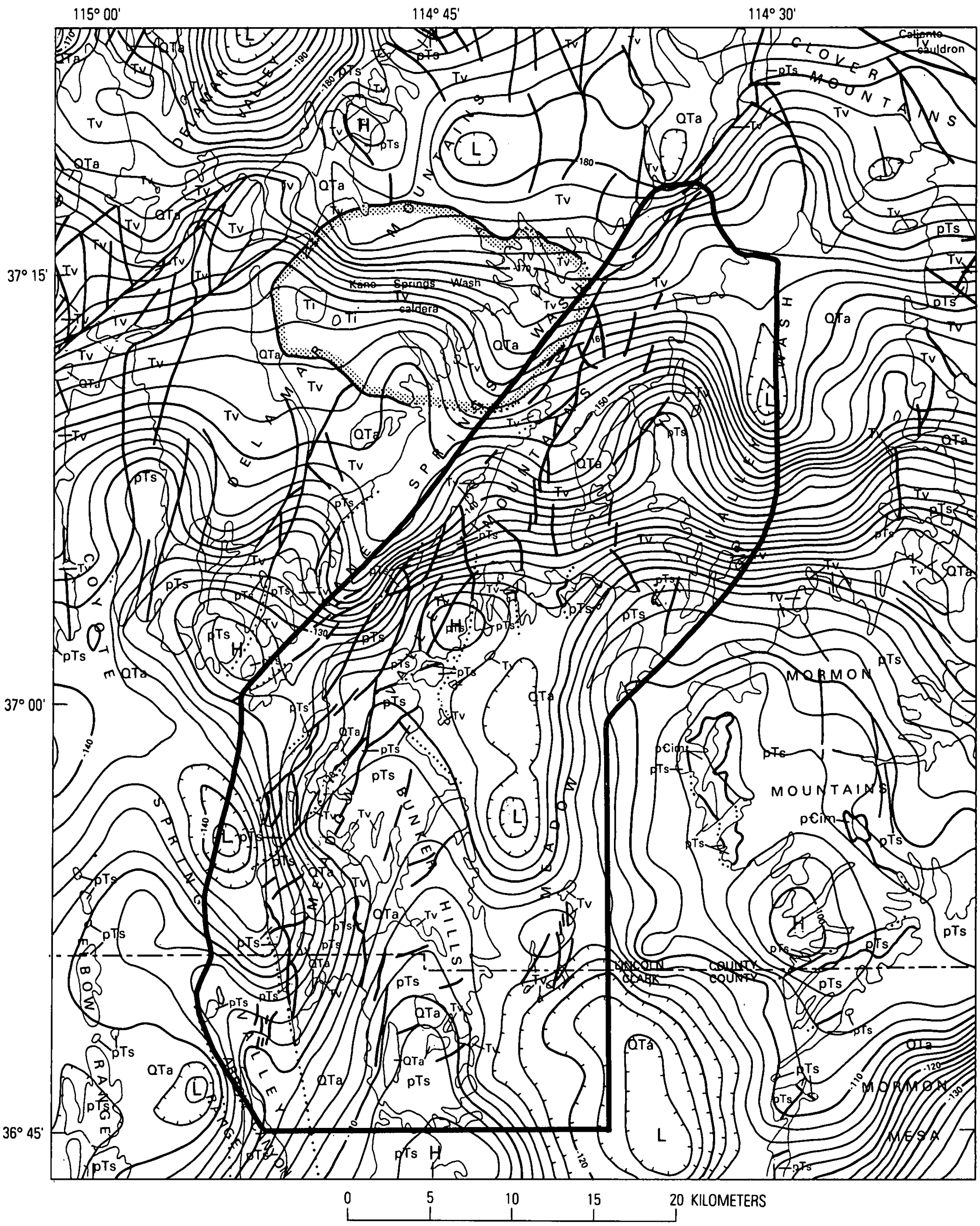

EXPLANATION

QTa, Alluvial and lacustrine deposits (Quaternary and Tertiary); Ti, Intrusive rocks (Tertiary); Tv, Volcanic rocks (Tertiary); pTs, Sedimentary rocks (pre-Tertiary); p€im, Igneous and metamorphic rocks (Precambrian); ——— Contact; ——— Fault; ░░░░ Edge of collapse caldera; ▬▬ Approximate boundary of geologic map area. x, gravity station.

Figure 6. Complete Bouguer gravity-anomaly map of the Meadow Valley Mountians and vicinity, Lincoln and Clark Counties, Nev. Contour interval, 2 mGals; reduction density, 2.67 f/cm^3; H, gravity high; L, gravity low. Adapted from Pampeyan and others (1988).

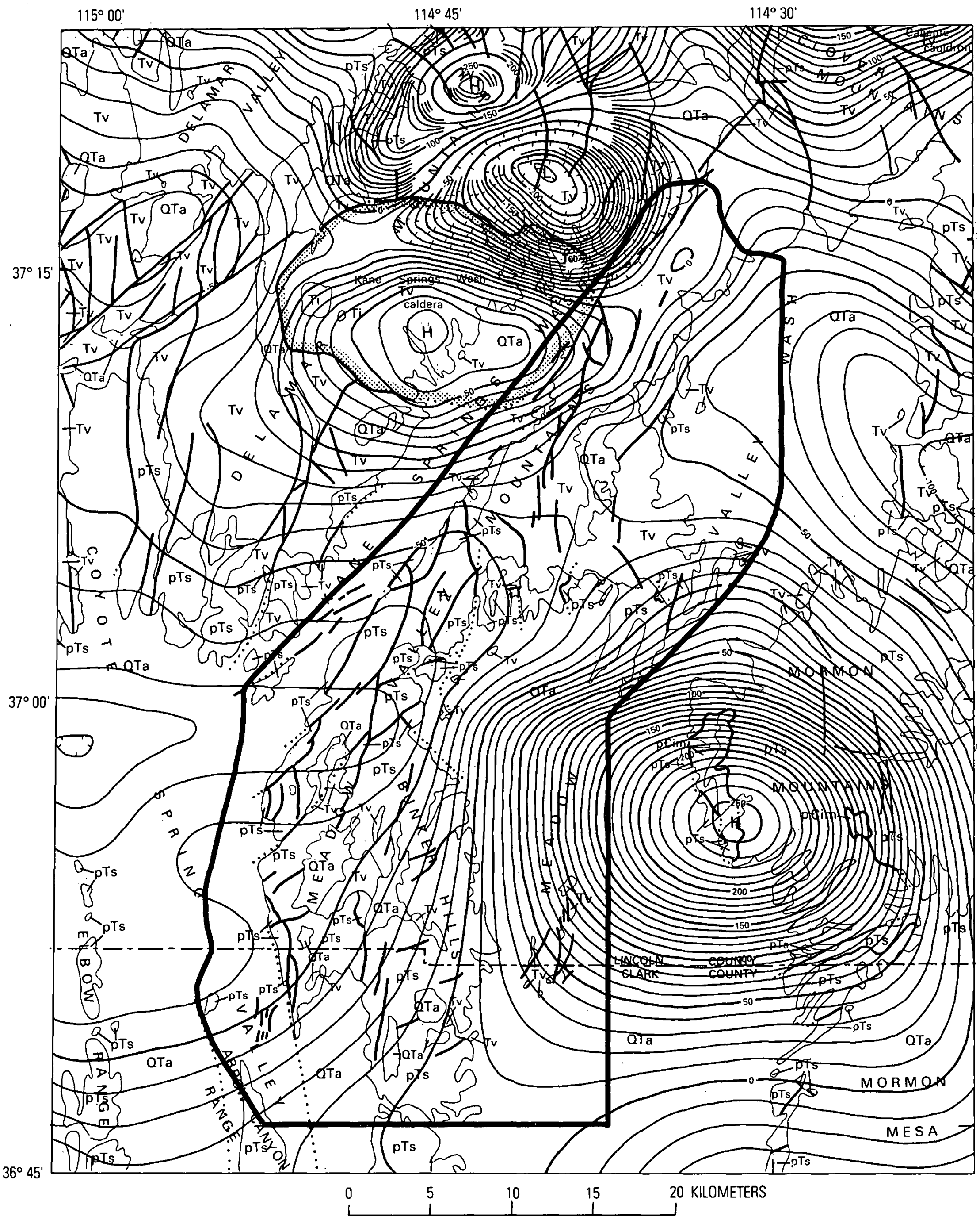

EXPLANATION

QTa, Alluvial and lacustrine deposits (Quaternary and Tertiary); Ti, Intrusive rocks (Tertiary); Tv, Volcanic rocks (Tertiary); pTs, Sedimentary rocks (pre-Tertiary); p€im, Igneous and metamorphic rocks (Precambrian); ——— Contact; ——— Fault; ░░░ Edge of collapse caldera; ▬▬ Approximate boundary of geologic map area. x, gravity station.

Figure 7. Residual and total-intensity aeromagnetic map of the Meadow Valley Mountains and vicinity, Lincoln and Clark Counties, Nev. Contour interval, 10 nT; altitude of observation, 12,500 ft above sea level; H, magnetic high; L, magnetic low. Adapted from Pampeyan and others (1988)..

Mountains have been classified as having a medium potential for occurrence of oil and gas on the basis of Conodont Alteration Index and other lithologic and stratigraphic characteristics (Sandberg, 1983; Pampeyan, 1988). In 1972 a well was drilled to test the Mississippian rocks in the Bunker Hills anticline, but no shows of oil or gas were reported (Garside and others, 1977). The uppermost part of the Guilmette Formation in the Bunker Hills block is composed of light-gray limestone occupying the same stratigraphic position as the Crystal Pass Member of the Sultan Limestone (Crystal Pass Limestone of Langenheim and others, 1962) which is mined as high-calcium limestone at Arrowlime, 62 km south of the map area (Longwell and others, 1965). Purity of the limestone here is unknown.

The rhyolitic lavas in the northernmost part of the Meadow Valley Mountains contain large tonnages of perlite and much of the interlayered lithic tuff contains zeolites, but neither commodity has been produced commercially from this area. Near the north end of the map area, the Sunshine prospect was staked on rhyolite dikes cutting rhyolitic volcanic rocks. Samples from this prospect contained no silver or gold. In Two Flats canyon Devonian carbonate rock in contact with rhyolitic welded tuff is silicified and cut by quartz veinlets, and samples of silicified rock from the D and D prospect on this contact contained trace amounts of silver but no gold (Pampeyan and others, 1988). For additional information on actual and potential mineral resources of the Meadow Valley Mountains the reader is referred to reports by Campbell (1987) and Pampeyan and others (1988).

REFERENCES CITED

Armstrong, R.L., 1968, Sevier orogenic belt in Nevada and Utah: Geological Society of America Bulletin, v. 79, no. 4, p. 429-458.

_____ 1970, Geochronology of Tertiary igneous rocks, eastern Basin and Range province, western Utah, eastern Nevada, and vicinity, USA: Geochimica et Cosmochimica Acta, v. 34, p. 203-232.

Bohannon, R.G., 1984, Nonmarine sedimentary rocks of Tertiary age in the Lake Mead region, southeastern Nevada and northwestern Arizona: U.S. Geological Survey Professional Paper 1259, 72 p.

Bowyer, Ben, Pampeyan, E.H., and Longwell, C.R., 1958, Geologic map of Clark County, Nevada: U.S. Geological Survey Mineral Investigations Field Studies Map MF-138, scale 1:200,000.

Callaghan, Eugene, 1937, Geology of the Delamar district, Lincoln County, Nevada: University of Nevada Bulletin, v. 31, no. 5, Geology and Mining Series no. 30A, 72 p.

Campbell, H.W., 1987, Mineral resources of the Meadow Valley Range Study Area, Clark and Lincoln Counties, Nevada: U.S. Bureau of Mines Mineral Land Assessment Open-File Report 27-87, 27 p.

Cook, E.F., 1965, Stratigraphy of Tertiary volcanic rocks in eastern Nevada: Nevada Bureau of Mines Report 11, 61 p.

Dolgoff, Abraham, 1963, Volcanic stratigraphy of the Pahranagat area, Lincoln County, southeastern Nevada: Geological Society of America Bulletin, v. 74, no. 7, p. 875-899.

Duley, D.H., 1957, Mississippian stratigraphy in the Meadow Valley and Arrow Canyon Ranges, southeastern Nevada: Berkeley, Calif., University of California, M.A. thesis, 103 p.

Eaton, G.P., Wahl, R.R., Prostka, H.J., Mabey, D.R., and Kleinkopf, M.D., 1978, Regional gravity and tectonic patterns: their relations to late Cenozoic epirogeny and lateral spreading in the western Cordillera, *in* Smith, R.B., and Eaton, G.P., eds., Cenozoic tectonics and regional geophysics of the western Cordillera: Geological Society of America Memoir 152, p. 51-92.

Ekren, E.B., Orkild, P.P., Sargent, K.A., and Dixon, G.L., 1977, Geologic map of Tertiary rocks, Lincoln County, Nevada: U.S. Geological Survey Miscellaneous Investigations Series Map I-1041, scale 1:250,000.

Fleck, R.J., 1970, Tectonic style, magnitude, and age of deformation in the Sevier orogenic belt in southern Nevada and eastern California: Geological Society of America Bulletin, v. 81, p. 1705-1720.

Garside, L.J., Weimer, B.S., and Lutsey, I.A., 1977, Oil and gas developments in Nevada, 1968-1976: Nevada Bureau of Mines and Geology Report 29, 32 p.

Goddard, E.N., chm., 1948, Rock-color chart: prepared by the Rock-color Chart Committee, National Research Council, Washington, D.C.

Harding, A.E., Scott, R.B., Mehnert, H.H., and Pampeyan, E.H., 1991, Kane Springs Wash caldera, southeast Nevada—the other half of the story (abs.): Geological Society of America Abstracts with Programs, v. 23, no. 4, p. 30.

Heckel, P.H., and Reso, Anthony, 1962, Silurian and Lower Devonian section in the southwestern part of the Delamar Range, Lincoln County, Nevada (abs.): Geological Society of America Abstracts for 1961, p. 32.

Heston, D.A., 1982, Geology of the Bradshaw vanadium prospect, Meadow Valley Mountains, Lincoln County, Nevada: Fort Collins, Colo., Colorado State University, M.S. thesis, 106 p.

Hewett, D.F., 1931, Geology and ore deposits of the Goodsprings quadrangle, Nevada: U.S. Geological Survey Professional Paper 162, 172 p.

Hoffman, J.D., and Day, G.W., 1984, Reconnaissance geochemical assessment of the Meadow Valley Mountains Bureau of Land Management Wilderness Study Area (NV-050-0156), Lincoln and Clark Counties, Nevada: U.S. Geological Survey Open-File Report 84-0655, 63 p., scale 1:100,000.

Jones, J.C., and Stone, R.W., 1920, (Deposits in) Southern Nevada, *in* Stone, R.W., and others, Gypsum deposits of the United States: U.S. Geological Survey Bulletin 697, p. 155-160.

Langenheim, R.L., Jr., and Larson, E.R., 1973, Correlations of Great Basin stratigraphic units: Nevada Bureau of Mines and Geology, Bulletin 72, 36 p., 3 plates.

SE ROA 42978

JA_12858

Langenheim, R.L., Jr., Carss, W.B., Kennerly, J.B., McCutcheon, V.A., and Waines, R.H., 1962, Paleozoic section in Arrow Canyon Range, Clark County, Nevada: American Association of Petroleum Geologists Bulletin, v. 46, no. 5, p. 592-609.

Langenheim, V.A.M., 1964, Pennsylvanian and Permian paleontology and stratigraphy of Arrow Canyon, Arrow Canyon Range, Clark County, Nevada: Berkeley, Calif., University of California, M.A. thesis, 194 p.

Liggett, M.A., and Ehrenspeck, H.E., 1974, Pahranagat shear system, Lincoln County Nevada: U.S. National Aeronautics and Space Administration, NASA contractor report CR-136388 (prepared for Goddard Space Flight Center by Argus Exploration Company, 555 S. Flower Street, Los Angeles, CA 90071), 6 p.

Longwell, C.R., and Dunbar, C.O., 1936, Problems of Pennsylvanian-Permian boundary in southern Nevada: American Association Petroleum Geologists Bulletin, v. 20, no. 9, p. 1198-1207.

Longwell, C.R., Pampeyan, E.H., Bowyer, Ben, and Roberts, R.J., 1965, Geology and mineral deposits of Clark County, Nevada: Nevada Bureau of Mines Bulletin 62, 218 p., map scale 1:250,000.

Marvin, R.F., Mehnert, H.H., and McKee, E.H., 1973, A summary of radiometric ages of Tertiary volcanic rocks in Nevada and eastern California—Part III, Southeastern Nevada: Isochron/West, no. 6, p. 1-30.

McNair, A.H., 1951, Paleozoic stratigraphy of part of northwestern Arizona: American Association of Petroleum Geologists Bulletin, v. 35, no. 3, p. 503-541.

Moring, Barry, Blank, H.R., Jr., Hoffman, J.D., and McHugh, E.L., 1988, Mineral resources of the Clover Mountains Wilderness Study Area, Lincoln County, Nevada: U.S. Geological Survey Bulletin 1729-D, 18 p.

Noble, D.C., 1968, Kane Springs Wash volcanic center, Lincoln County, Nevada, *in* Eckel, E.C., ed., Nevada Test Site: Geological Society of America Memoir 110, p. 109-116.

Noble, D.C., and McKee, E.H., 1972, Description and K-Ar ages of volcanic units of the Caliente volcanic field, Lincoln County, Nevada, and Washington County, Utah: Isochron/West, no. 5, p. 17-24.

Novak, S.W., 1984, History of the rhyolitic Kane Springs Wash volcanic center, Nevada: Journal of Geophysical Research, v. 89, no. B10, p. 8603-8615.

_____ 1985, Geology and geochemical evolution of the Kane Springs Wash volcanic center, Lincoln County, Nevada: Stanford, Calif., Stanford University, Ph.D. dissertation, 173 p.

Olmore, S.D., 1971, Style and evolution of thrusts in the region of the Mormon Mountains, Nevada: Salt Lake City, Utah, University of Utah, Ph.D. dissertation, 213 p.

Osmond, J.C., 1954, Dolomites in Silurian and Devonian of east-central Nevada: American Association of Petroleum Geologists Bulletin, v. 38, no. 9, p. 1911-1956.

_____ 1962, Stratigraphy of Devonian Sevy Dolomite in Utah and Nevada: American Association of Petroleum Geologists Bulletin, v. 46, p. 2033-2056.

Page, W.R., Swadley, W C, and Scott, R.B., 1990, Preliminary geologic map of the Delamar 3 SW quadrangle, Lincoln County, Nevada: U.S. Geological Survey Open-File Report 90-336, 17 p., scale 1:24,000.

Pampeyan, E.H., Blank, H.R., Jr., and Campbell, H.W., 1988, Mineral resources of the Meadow Valley Range Wilderness Study Area, Lincoln and Clark Counties, Nevada: U.S. Geological Survey Bulletin 1729-C, 24 p.

Reber, S.J., 1952, Stratigraphy and structure of the south-central and northern Beaver Dam Mountains, Utah; Cedar City, Utah to Las Vegas, Nevada: Utah Geological Society Guidebook, no. 7, p. 101-108.

Reso, Anthony, 1963, Composite columnar section of exposed Paleozoic and Cenozoic rocks in the Pahranagat Range, Lincoln County, Nevada: Geological Society of America Bulletin, v. 74, no. 7, p. 901-918.

Rogers, A.M., Harmsen, S.C., and Meremonte, M.E., 1987, Evaluation of the seismicity of the southern Great Basin and its relationship to the tectonic framework region: U.S. Geological Survey Open-file Report 87-408, 196 p.

Rowley, P.D., Anderson, J.J., and Williams, P.L., 1975, A summary of Tertiary volcanic stratigraphy of southwestern High Plateaus and adjacent Great Basin, Utah: U.S. Geological Survey Bulletin 1405-B, 20 p.

Rubey, W.W., and Callaghan, Eugene, 1936, Magnesite and brucite, *in* Hewett, D.F., and Schaller, W.T., eds., Mineral resources of the region around Boulder Dam: U.S. Geological Survey Bulletin 871, p. 113-144.

Sandberg, C.A, 1983, Petroleum potential of wilderness lands in Nevada, *in* Miller, B.M., ed., Petroleum potential of wilderness lands in the western United States: U.S. Geological Survey Circular 902, p. H1-H11.

Scott, R.B., Page, W.R., and Swadley, W C, 1990, Preliminary geologic map of the Delamar 3 NW quadrangle, Lincoln County, Nevada: U.S. Geological Survey Open-File Report 90-405, 14 p., scale 1:24,000.

Scott, R.B., Swadley, W C, and Novak, S.W., 1988, Preliminary geologic map of the Delamar Lake quadrangle, Lincoln County, Nevada: U.S. Geological Survey Open-File Report 88-576, 11 p., scale 1:24,000.

Shawe, D.R., Blank, H.R., Jr., Wernicke, B.P., Axen, G.J., Barton, H.N., Day, G.W., and Rains, R.L., 1988, Mineral resources of the Mormon Mountains Wilderness Study Area, Lincoln and Clark Counties, Nevada: U.S. Geological Survey Bulletin 1729-B, 22 p.

Smith, R.B., and Sbar, M.L., 1974, Contemporary tectonics and seismicity of the western United States with emphasis on the Intermountain seismic belt: Geological Society of America Bulletin, v. 85, p. 1205-1218.

Steiger, R.H., and Jager, E., 1977, Sub-commission on geochronology: Convention on the use of decay constants in geo- and cosmochronology: Earth and Planetary Science Letters, v. 36, p. 359-362.

Stewart, J.H., 1980, Geology of Nevada: Nevada Bureau of Mines and Geology Special Pub. 4, 156 p.

Stewart, J.H., and Carlson, J.E., 1978 (1979), Geologic map of Nevada: U.S. Geological Survey, State Geologic Map, scale 1:500,000.

Stock, Chester, 1921a, Late Cenozoic mammalian remains from the Meadow Valley region, southeastern Nevada [abs.]: Geological Society of America Bulletin, v. 32, p. 146-147.

____ 1921b, Later Cenozoic mammalian remains from the Meadow Valley region, southeastern Nevada: American Journal of Science, 5th Series, v. 2, p. 250-264.

Swadley, WC, Page, W.R., Scott, R.B., and Pampeyan, E.H., 1990, Preliminary geologic map of the Delamar 3 SE quadrangle, Lincoln County, Nevada: U.S. Geological Survey Open-File Report 90-221, 16 p., scale 1:24,000.

Taylor, W.J., and Bartley, J.M., 1988, Stratigraphy and structure of the North Pahroc and eastern Seaman Ranges, *in* Weide, D.L., and Faber, M.L., eds., This extended land, Geological journeys in the southern Basin and Range: Geological Society of America, Cordilleran Section, Field Trip Guidebook, p. 5-7.

Tieh, T.T., and Cook, E.F., 1971, Carbonate-rich dikes in ignimbrites of southeastern Nevada: Geological Society of America Bulletin, v. 82, no. 5, p. 1293-1304.

Tschanz, C.M., 1960, Regional significance of some lacustrine limestones in Lincoln County, Nevada, recently dated as Miocene: U.S. Geological Survey Professional Paper 400-B, p. B293-B295.

Tschanz, C.M., and Pampeyan, E.H., 1961, Preliminary geologic map of Lincoln County, Nevada: U.S. Geological Survey Mineral Investigations Field Studies Map MF-206, scale 1:200,000.

____ 1970, Geology and Mineral deposits of Lincoln County, Nevada: Nevada Bureau of Mines Bulletin 73, 187 p., scale 1:250,000.

Webster, G.D., 1969, Chester through Derry conodonts and stratigraphy of northern Clark and southern Lincoln Counties, Nevada: California University Publications in the Geological Sciences, v. 79, 121 p.

Webster, G.D., and Lane, N.G., 1967, Mississippian-Pennsylvanian boundary in southern Nevada, *in* Essays in Paleontology and Stratigraphy, Teichert, Curt, and Yochelson, E.L., eds.: University of Kansas Press, Lawrence, p. 503-522.

Wernicke, Brian, Guth, P.L., and Axen, G.J., 1984, Tertiary extensional tectonics in the Sevier belt of southern Nevada, *in* Lintz, Joseph, Jr., ed., Western geological excursions, v. 4, p. 473-510, prepared for the 1984 Annual Meetings of the Geological Society of America and affiliated societies at Reno.

Wheeler, H.E., 1943, Lower and Middle Cambrian stratigraphy in the Great Basin area: Geological Society of America Bulletin, v. 54, p. 1781-1822.

Williams, P.L., 1960, A stained slice method for rapid determination of the phenocryst composition of volcanic rocks: American Journal of Science, v. 258, p. 148-152.

____ 1967, Stratigraphy and petrology of the Quichipa Group, southwestern Utah and southeastern Nevada: Seattle, Washington Univ. Ph.D. thesis, 139 p.

University and Community
College System of Nevada

desert research institute

Water Resources Center

Investigation of the Origin of Springs in the Lake Mead National Recreation Area

Karl F. Pohlmann
David J. Campagna
Jenny B. Chapman
Sam Earman

March 1998

Publication No. 41161

prepared by
Water Resources Center
Desert Research Institute
University and Community College System of Nevada

prepared for
National Park Service, Water Resources Division

Investigation of the Origin of Springs in the Lake Mead National Recreation Area

Karl F. Pohlmann
David J. Campagna
Jenny B. Chapman
Sam Earman

March 1998

Publication No. 41161

prepared by
Water Resources Center
Desert Research Institute
University and Community College System of Nevada

prepared for
National Park Service, Water Resources Division

Investigation of the Origin of Springs in the Lake Mead National Recreation Area

Karl F. Pohlmann[1]
David J. Campagna[2]
Jenny B. Chapman[1]
Sam Earman[1]

March 1998

Publication No. 41161

prepared by
Water Resources Center
Desert Research Institute
University and Community College System of Nevada

prepared for
National Park Service, Water Resources Division

[1]Water Resources Center, Desert Research Institute
[2]College of William and Mary, Williamsburg, Virginia

ABSTRACT

Increasing demands for water supply have accompanied rapid population growth in the Las Vegas Valley and portions of surrounding southern Nevada. Exploration and development of groundwater resources to meet these demands increases the potential for impact on groundwater systems to the north and west of the Lake Mead National Recreation Area. Because the park is located down-hydraulic-gradient from these areas, large-scale changes in groundwater use may affect groundwater resources and, ultimately, discharge from natural springs within the park. This study was conducted for the National Park Service to investigate the hydrology and hydrogeochemistry of selected springs in the Lake Mead and Black Canyon areas, and to determine the source areas associated with these springs.

Thirty six springs were visited and described. Historic geochemical data were compiled and supplemented by new stable and radioactive isotopic data. Three classifications of source area were defined, primarily based on hydrogeologic setting and stable isotopic data. Almost one third of the springs were found to discharge from local groundwater systems, many of which are entirely contained within the park boundaries. These springs are generally not related to major structural features and their stable isotopic values indicate that they receive most or all of their recharge locally and at low elevations, despite the minimal groundwater recharge generally assumed for low elevations in southern Nevada. A second set of springs was found to discharge groundwater that originates outside local flow systems, and therefore outside the park boundaries. Many of these springs are related to major, regional structural features, and their stable isotopic values are indicative of recharge at elevations higher than most of the region surrounding Lake Mead, although they do not appear to be directly related to regional groundwater flow from the White River Flow System or the Virgin River basin. Data obtained from a third set of springs, located below Hoover Dam in Black Canyon, suggests that these springs are strongly influenced by recirculated Lake Mead water, confirming earlier work.

SE ROA 42984

JA_12864

CONTENTS

TABLES

SE ROA 42985

FIGURES

SE ROA 42986

JA_12866

INTRODUCTION

Springs on the western edge of Lake Mead and in the Black Canyon of the Colorado River are important natural hydrologic features of the Lake Mead National Recreation Area. Although many springs are little more than seeps, their discharge represents the only available perennial surface flow in large portions of this arid region. These springs appear to originate from a variety of sources ranging from precipitation in local drainage basins to regional interbasin groundwater flow systems.

Rapid population growth in portions of southern Nevada, particularly in the Las Vegas Valley, has increased the need for additional water supplies in the area, including groundwater. As a result, there has been a dramatic increase in the potential for additional large-scale development of groundwater resources to the west and north of Lake Mead, areas which are hydraulically upgradient of many of the springs. If large-scale development of groundwater resources occurs in source areas or along flow paths leading to springs, the discharge of these springs could be impacted.

To address concerns regarding potential impacts on spring resources, and to plan for their management and protection, the National Park Service (NPS) requires scientific information on the hydrology and hydrogeochemistry of springs near Lake Mead, and particularly whether the waters are of local or regional origin. This investigation was undertaken to: 1) provide a comprehensive database of spring chemical and isotopic composition; and 2) determine the source areas of and flow paths to selected springs.

Geography and Climate

The waters of the Colorado River impounded by Hoover Dam form Lake Mead and divide southeastern Nevada from northwestern Arizona (Figure 1). The lake is located near the transition between the Great Basin and Colorado Plateau physiographic provinces. Elevations in the region adjacent to the lake are generally less than 1000 m (all elevations given in this report are referenced to mean sea level), and range from about 200 m at the Colorado River below Hoover Dam to over 1600 m in the Muddy Mountains. The highest mountain ranges in southern Nevada are the Spring Mountains (3630 m) and the Sheep Range (3020 m) which rise 60 km to the west and northwest, respectively, of Lake Mead.

The climate is one of extremes, ranging from arid in the low elevation basins, where the highest temperatures and lowest precipitation amounts in the Great Basin occur, to sub-humid in the higher mountains. In the Las Vegas Valley, the mean summer temperature at an elevation of 640 m is 30.8°C and the mean annual precipitation is 10.4 cm (Western Regional Climate Center, 1997). Orographic effects cause precipitation amounts to increase with elevation such that the upper elevations of the Spring Mountains receive up to 70 cm of precipitation annually (Malmberg, 1961).

Annual precipitation trends show a pronounced seasonality, with maximum amounts typically received in December and August. Winter precipitation generally falls as long-duration, low-intensity frontal storms derived from moisture moving eastward from the Pacific Ocean, while summer precipitation originates to the south in the Gulf of California and the Gulf of Mexico and is often delivered as short-duration, intense thunderstorms (Quiring, 1965; French, 1983). The rainshadow effect of the Sierra Nevada Mountains in the winter and the incomplete flow of moisture

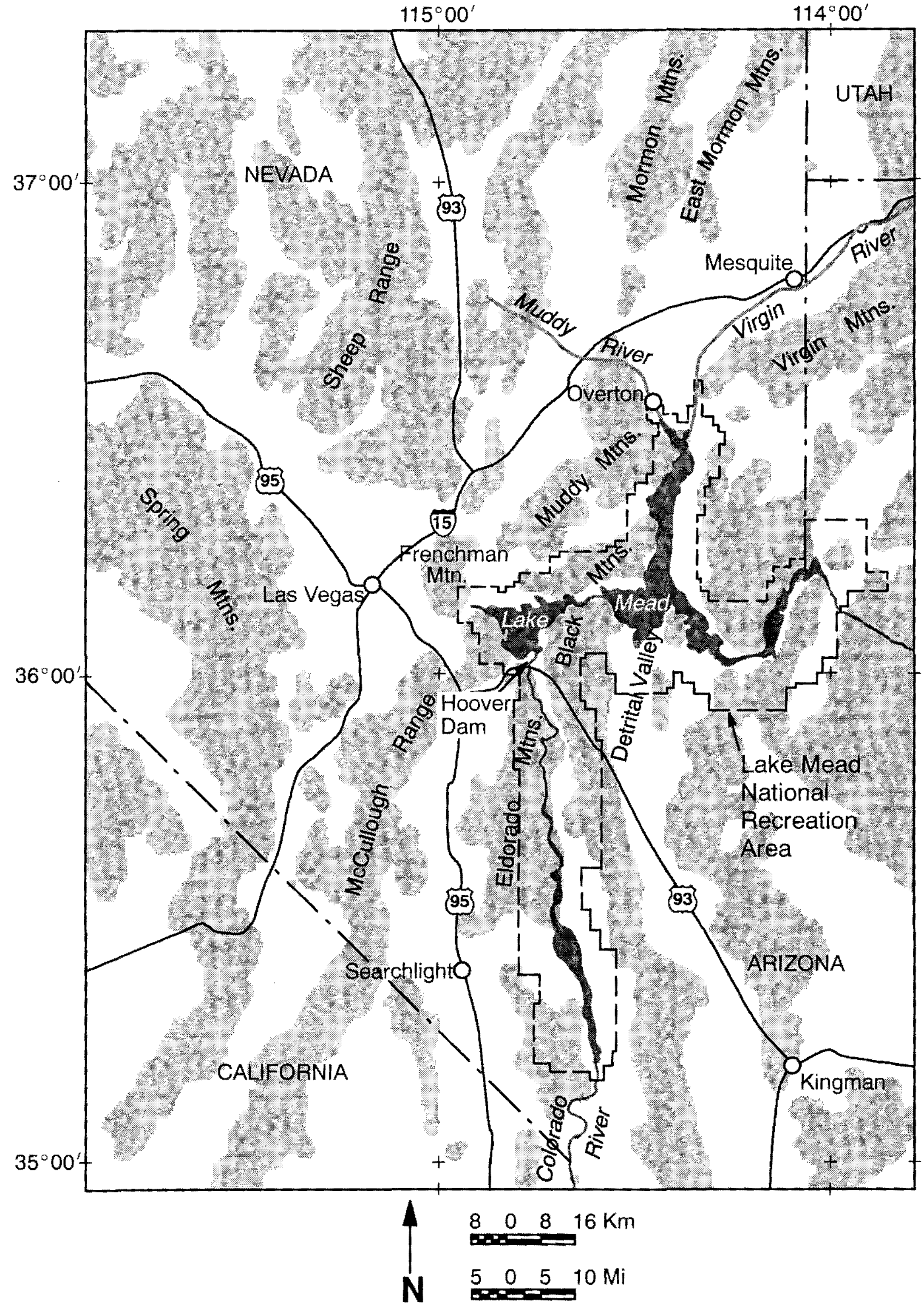

Figure 1. Location of the study area in southeastern Nevada and northwestern Arizona.

SE ROA 42988

from the south in the summer forms a zone of precipitation deficit in the western portion of southern Nevada (Quiring, 1965). The eastern portion is less affected by the Sierra Nevada rainshadow and is open to the flow of moisture from the south in the summer, thus causing a zone of precipitation excess.

Estimates of groundwater recharge from precipitation in Nevada are commonly developed using the Maxey-Eakin method (Maxey and Robinson, 1947; Maxey and Eakin, 1949), which is based on empirically-derived relationships between precipitation and recharge in several groundwater basins in the state. In the Las Vegas Valley, the Maxey-Eakin method predicts that groundwater recharge is negligible where annual precipitation is less than 25.4 cm, corresponding to elevations below approximately 1800 m (Maxey and Robinson, 1947). Below this elevation, the estimated annual precipitation volume is calculated to be lost to evapotranspiration (due to high air temperatures and low humidity) and surface runoff (due to sparse vegetation and low-permeability soils). Thus, on the scale of groundwater basins, recharge is considered to be minimal in much of southern Nevada.

Previous Studies of Springs in the Region

Chemical and isotopic data are available for numerous springs in southeastern Nevada, primarily as a result of the Nevada Carbonate Aquifer Program studies. Lyles *et al.* (1987) compiled chemistry data for wells and springs in Nevada within a 160 km radius of Las Vegas. Thomas *et al.* (1991) compile a similar database, but include isotopic data collected from wells, springs, and streams. Thomas *et al.* (1997) supplement the earlier database with data from additional sampling sites, describe chemical and isotopic processes and composition of groundwater in basin-fill and carbonate aquifers, and delineate flow systems in the carbonate rocks of southern Nevada. Studies of hydrogeologic resources pertinent to the present study have been conducted by Laney (1981) and Laney and Bales (1996) as part of an ongoing series of reconnaissance studies of the Lake Mead National Recreation Area. These reports provide physical descriptions, geologic setting, and chemical data for many of the springs. In the only detailed interpretive study of springs within the recreation area, McKay and Zimmerman (1983) investigated springs in Black Canyon using hydrogeochemical, stable isotope, and tritium data. Finally, the Southern Nevada Water Authority (SNWA) has initiated an investigation of the origins of groundwater issuing from springs on the Nevada side of Black Canyon, collecting extensive chemical and isotopic data.

Acknowledgements

The authors wish to thank Paul Christensen of the National Park Service, Water Resources Division, for facilitating this research and providing guidance in the early going. Bill Burke and the Resource Management staff at the Lake Mead National Recreation Area are thanked for providing background information on the history and locations of the springs. Alan McKay of the Desert Research Institute and James Thomas of the U.S. Geological Survey are thanked for invaluable insights into the hydrogeology of the region. The majority of this work was funded by the National Park Service.

METHODOLOGY

The chemistry of groundwater is a result of the type and amount of minerals present in the rocks through which the groundwater moves, and the conditions of recharge and discharge. Generally, groundwater chemistry evolves along flow paths from recharge areas to discharge areas as geochemical reactions occur between the water and rock. At the local scale, however, local geologic complexity can lead to large variations in groundwater chemistry.

Although flow paths that supply groundwater to springs can be described using the geochemistry of spring discharge, delineation of recharge sources is often more effectively approached using the spring's isotopic composition. Because the principal objective was to delineate groundwater source areas, this study focused on several stable and radioactive isotopes in groundwater. Ratios of the stable isotopes in water molecules, oxygen-18 (^{18}O) to oxygen-16 (^{16}O) and deuterium (D) to hydrogen (^{1}H), often provide more definitive identification of source areas for groundwater than water chemistry. In addition, the radioactive isotopes tritium (^{3}H) and carbon-14 (^{14}C) can be used to determine relative ages of groundwater. A relatively young age reflects the dominance of local recharge and short residence times, while an older age reflects a longer residence time and often indicates lengthy travel times in regional flow systems. Finally, radioactive isotopes of uranium (^{234}U and ^{238}U) can be used for tracing groundwater masses from recharge areas to discharge areas. Background information on these techniques is provided below for ease of reference.

The stable isotopes D and ^{18}O are useful tools for tracing groundwater because, unlike major ion geochemistry, stable isotopic composition is essentially unchanged by the rocks through which groundwater travels (under non-geothermal conditions). The stable isotopic composition of groundwater recharge is related to the temperature, amount, distance from the ocean, and altitude of precipitation (Mazor, 1997), therefore, groundwaters originating in a common source area often share similar stable isotopic composition. Stable isotopes are particularly useful in this study because the pervasive gypsum deposits and other evaporites in the region cause dramatic changes in groundwater geochemistry near spring discharge areas, effectively masking the original geochemical composition of the groundwater.

The stable isotope ratio $^{13}C/^{12}C$ (expressed in a delta notation as $\delta^{13}C$) is very sensitive to biologic processes and thus there can be large differences in $\delta^{13}C$ of carbon subjected to differing photosynthetic, bacterial and other processes. Recharge water, percolating through soils, dissolves CO_2 gas that has a $\delta^{13}C$ signature characteristic of the local plant cover. Reactions with carbonate rocks impart enriched $\delta^{13}C$ values, sensitive to the carbonate origin in pedogenic and marine deposits. In addition to this tracing function of $\delta^{13}C$, the isotope is also used to correct ^{14}C groundwater ages for dilution by dissolved rock carbon. ^{14}C is a radioactive isotope present in dissolved inorganic carbon in groundwater. As such, ^{14}C does not provide a direct age measurement of the water, as tritium does, but requires an understanding of the source of the dissolved inorganic carbon for correct interpretation (Mook, 1980). The long half-life of ^{14}C (5730 years) makes it useful for dating groundwaters with residence times in excess of several decades.

The radioactive isotope tritium provides a semi-quantitative means for dating groundwater with residence times of several decades or less (Mazor, 1997). Groundwaters having tritium concentrations below 5 pCi/L are considered to be derived primarily from recharge prior to the onset of atmospheric testing of nuclear bombs in 1952, while groundwaters having concentrations greater than 5 pCi/L are considered to have at least some component recharged after 1952. Due to its short half life (12.3 years), tritium concentrations in atmospheric precipitation have declined since the period of maximum testing in 1962. In 1994 through 1996, tritium concentrations in southern Nevada precipitation ranged between 10 and 20 pCi/L in the winter and between 20 to 60 pCi/L in the summer (Dennis Farmer, U.S. EPA, personal communication). This cycle between winter lows and summer highs is observed worldwide and is related to the circulation of moisture in the upper atmosphere (Roether, 1967).

The radioactive isotopes of uranium can be useful groundwater tracers because of their high solubility, insensitivity to chemical reactions, and long half-lives (Osmond and Cowart, 1976; Cowart, 1979). They are especially useful in southern Nevada because of the wide range of natural uranium concentrations in the groundwaters of the region (Farmer, 1996). Since uranium is presently less widely-used for tracing groundwater than the isotopes described above, a more detailed description of the method follows. Uranium is a naturally-occurring element which dissolves in groundwater when dilute recharge waters interact with uranium-bearing minerals in the subsurface. The vast majority (99.725 percent) of natural uranium occurs as the isotope ^{238}U, which has a half-life of 4.46×10^9 years. The radioactive decay of ^{238}U produces ^{234}U, which comprises about 0.005 percent of naturally-occurring uranium, and has a half-life of 2.45×10^5 years.

The activity of a radionuclide is defined by the equation $A = N\lambda$, where A is the activity of any radionuclide, N is the number of atoms of that nuclide present in the system being examined, and λ is the decay constant for that nuclide (Osmond and Cowart, 1976). The value of λ indicates the number of disintegrations an isotope undergoes per unit time, and is thus inversely proportional to the half-life of an isotope. The activity equation shows that two radionuclides that have significantly different numbers of atoms present in a system can have the same activities if their half-lives are sufficiently different. This proves to be the case with ^{234}U and ^{238}U, which, in closed geologic systems (such as unweathered rocks), tend to achieve a state known as secular equilibrium, where the activity of ^{234}U (low number of atoms, but relatively short half-life causing a high number of decays per unit time) and that of ^{238}U (high number of atoms, but relatively long half-life causing a low number of decays per unit time) become equal. It takes approximately 10^6 years from the time of formation for a system to achieve this secular equilibrium (Osmond *et al.*, 1968).

^{234}U and ^{238}U tend to achieve secular equilibrium in closed geologic systems. However, in natural rock-groundwater systems, disequilibrium between ^{234}U and ^{238}U is quite common (Thurber, 1962) and thought to be present due to side effects resulting from the radioactive decay process (Gascoyne, 1992). Disequilibrium is typically quantified via the $^{234}U/^{238}U$ activity ratio (AR). A system in secular equilibrium would have an AR equal to one; a system with "excess" ^{234}U activity would have AR greater than one, and a system with "excess" ^{238}U would have an AR less

SE ROA 42991

than one. The majority of groundwaters exhibiting disequilibrium show AR greater than one, indicating an excess of ^{234}U (Osmond and Cowart, 1976).

Uranium has two naturally occurring valence states (+4 and +6). U^{6+}, which is present in oxidizing conditions, is soluble, while U^{4+}, which predominates in reducing conditions, has an extremely low solubility, and is thus considered immobile. The presence of reducing conditions can greatly complicate the analysis of uranium, but the waters sampled for this study consistently showed dissolved oxygen content indicative of oxic waters (Table A-1). Although deep groundwater is typically thought to be anoxic, deep waters in Nevada and other parts of the Basin and Range physiographic province are commonly found to be oxic (Winograd and Robertson, 1982).

Most of the springs in the present investigation have been visited and described during the studies described above, and discharge measurements, chemical indicator measurements, and water chemistry analyses are available. However, few of the springs have been sampled for stable and radioactive isotope analysis. The historic inventories and previous studies provided a basis for identifying the locations of springs and for the building of the present database of physical, chemical, and isotopic data. Data collection for the present study focused on isotopic constituents.

All of the springs were visited at least once during the course of this study. Spring coordinates were determined using a Magellan 9500 Pro hand-held GPS unit in autonomous mode. Low discharge rates were measured using a beaker and stopwatch and high discharge rates were measured using a Marsh-McBirney Flo-Mate 2000 flow meter. Field measurements were made of temperature, pH, electrical conductivity (EC), dissolved oxygen (DO), and alkalinity (HCO_3) using standard field analytical equipment. The physical, chemical, and isotopic data derived from previous studies, and data collected for the present study, are compiled in Appendix A. Geologic descriptions and sketch maps were developed for each spring area and are included in Appendix B. Isotopic data for selected southern Nevada groundwaters are compiled in Appendix C.

This report describes thirty-six springs which are located in two general areas (Table 1). One is the Lake Mead basin, including the area west of the Overton Arm and the area north of Lake Mead (Figure 2). The other is the area of the Black Canyon of the Colorado River, downstream of Hoover Dam (Figure 3).

GEOLOGIC SETTING

The Lake Mead National Recreation Area is located near the eastern margin of the Basin and Range geologic province, a region comprised of broad, flat-lying valleys underlain by thick alluvial deposits and bordered by narrow, nearly parallel mountain ranges. Situated between mountain ranges composed of Paleozoic to Mesozoic sedimentary rocks and a Precambrian terrain intruded by Cenozoic igneous rocks (Figure 4), the recreation area lies near the southeastern end of the regional carbonate-rock aquifer system. This large aquifer system is defined as the area where 80 percent of the measured section is over 50 percent carbonate rock (Mifflin, 1968), and underlies 260,000 km^2 of eastern Nevada, western Utah, southeastern Idaho, and extreme southeastern California (Dettinger, 1989). Table 2 presents a simplified stratigraphic column used in the present study.

SE ROA 42992

Table 1. Identification Numbers and Names of Springs Included in this Study. Names in the Lake Mead basin are official names. Names in Black Canyon are unofficial names given by McKay and Zimmerman (1983), with the exception of springs given unofficial names by the National Park Service.

ID	Name	Comments
		Lake Mead Basin
1	Kelsey Spring	
2	Unnamed	Located in Magnesite Wash
3	Unnamed	Located in Kaolin Wash
4	Getchel Spring	
5	Unnamed	Uppermost Spring in Valley of Fire Wash
6	Unnamed	Upper Spring in Valley of Fire Wash
7	Unnamed	Lower Spring in Valley of Fire Wash
8	Blue Point Spring	
9	Unnamed	Located 0.8 km south of Spring 8
10	Unnamed	Located 0.8 km southeast of Spring 9
11	Rogers Spring	
12	Scirpus Spring	
13	Corral Spring	
14	Unnamed	Located northwest of Rogers Bay
15	Bitter Spring	
16	Sandstone Spring	
17	Cottonwood Spring	
18	Gypsum Spring	
19	Unnamed	South of Rainbow Gardens
		Black Canyon
20	Pupfish Spring	
21	Arizona Hot Spot	
22	Sauna Cave	
23	Nevada Hot Spring	NPS name, "Fort Lucinda" of McKay and Zimmerman (1983)
24	Nevada Hot Spot	
25	Palm Tree, Hot	
26	Palm Tree, Cold	
27	Unnamed Spring	Located in Horsethief Canyon
28	Boy Scout Canyon, Hot Spring	NPS name, "Rifle Range" of McKay and Zimmerman (1983)
29	Boy Scout Canyon, Cold Spring	
30	Arizona Hot Spring	NPS name, "Ringbolt Rapids" of McKay and Zimmerman (1983)
31	Unnamed	Cold Spring located near Arizona Hot Spring
32	Nevada Falls	
33	Bighorn Sheep Spring	
34	Arizona Seep	
35	Latos Pool	
36	Unnamed	Located in Aztec Wash

SE ROA 42993

JA_12873

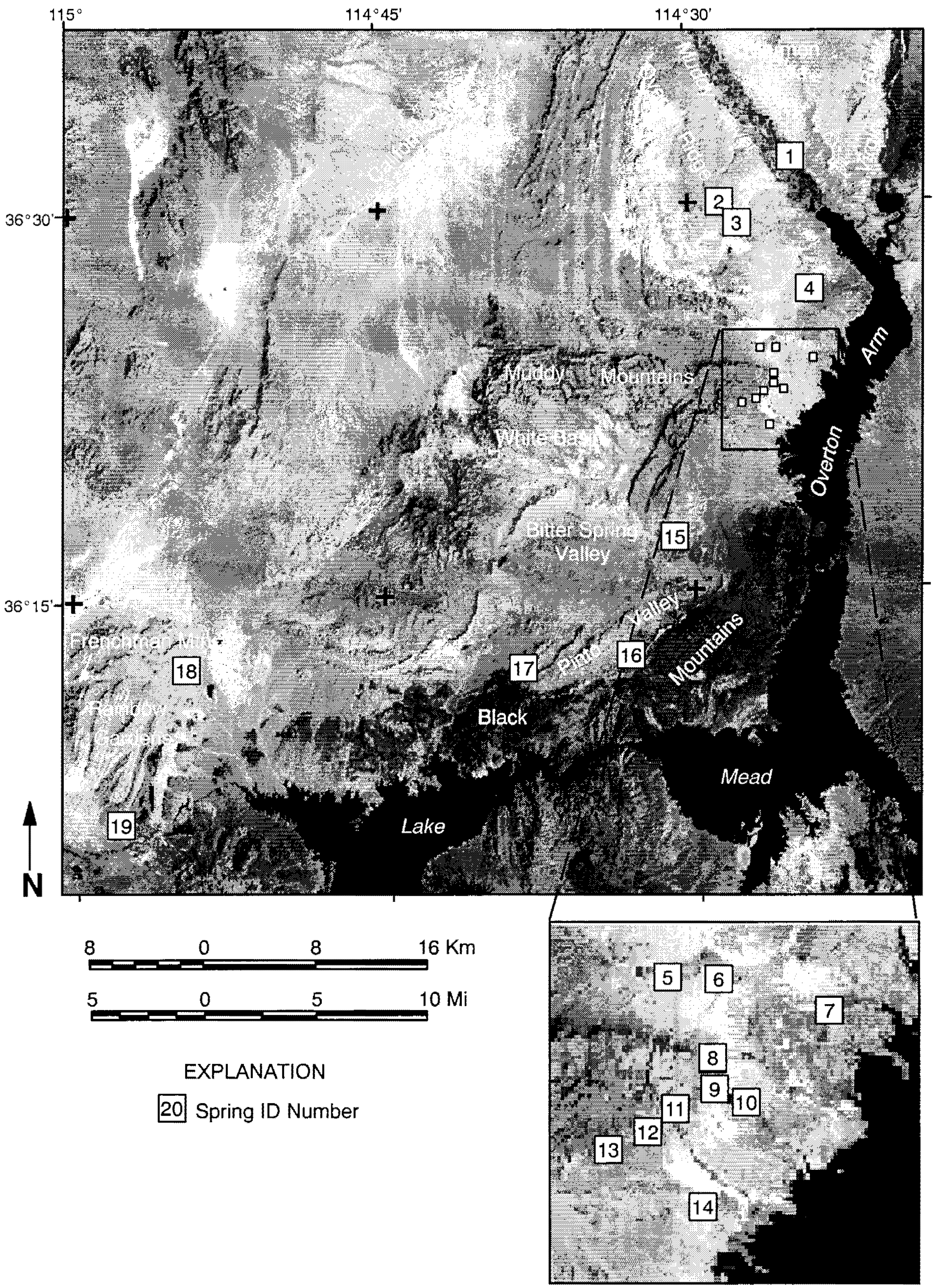

Figure 2. Locations of springs in the Lake Mead basin. Detail shows springs in the North Shore complex.

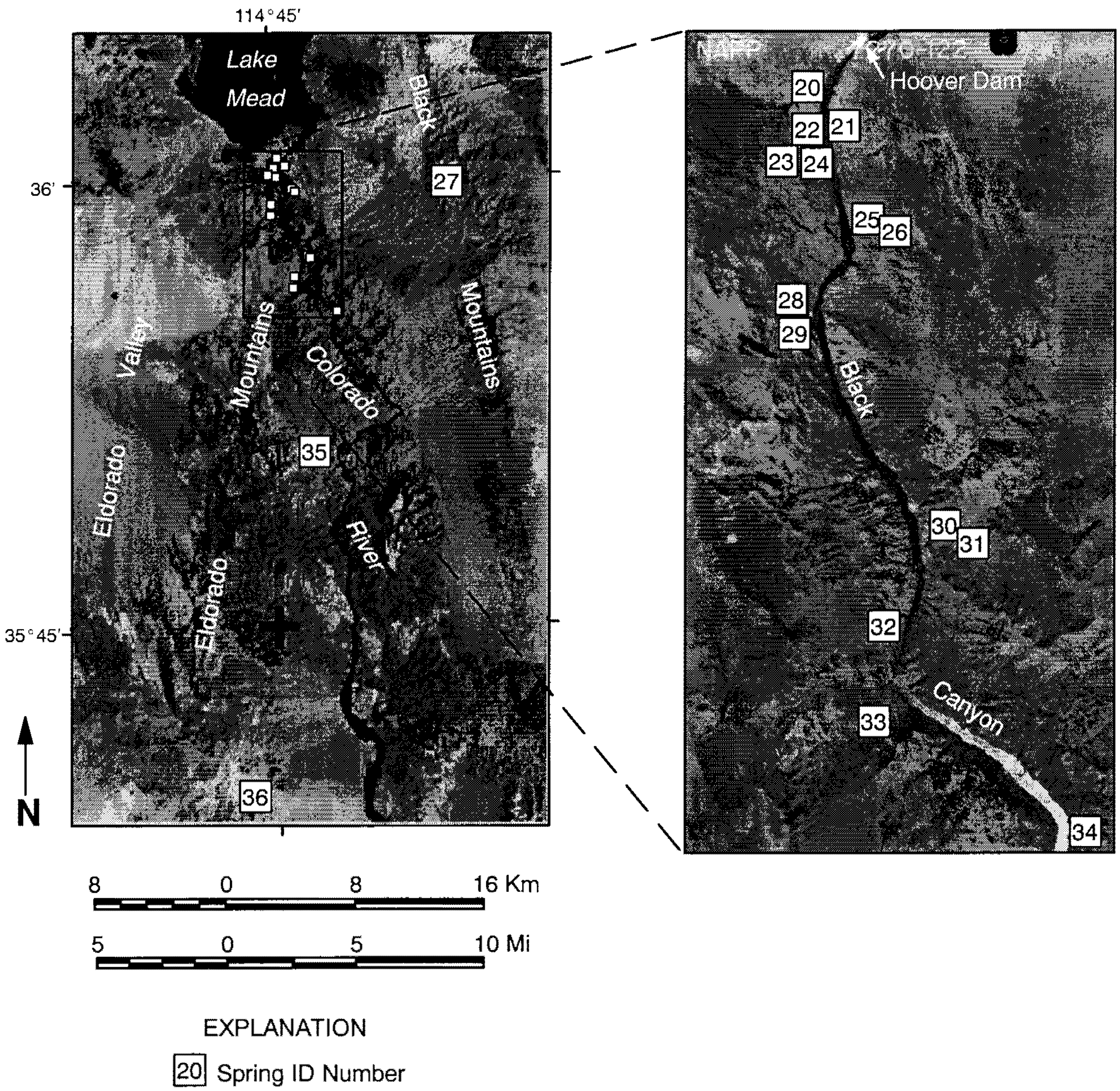

Figure 3. Locations of springs in the Black Canyon area. Detail shows springs in Black Canyon proper.

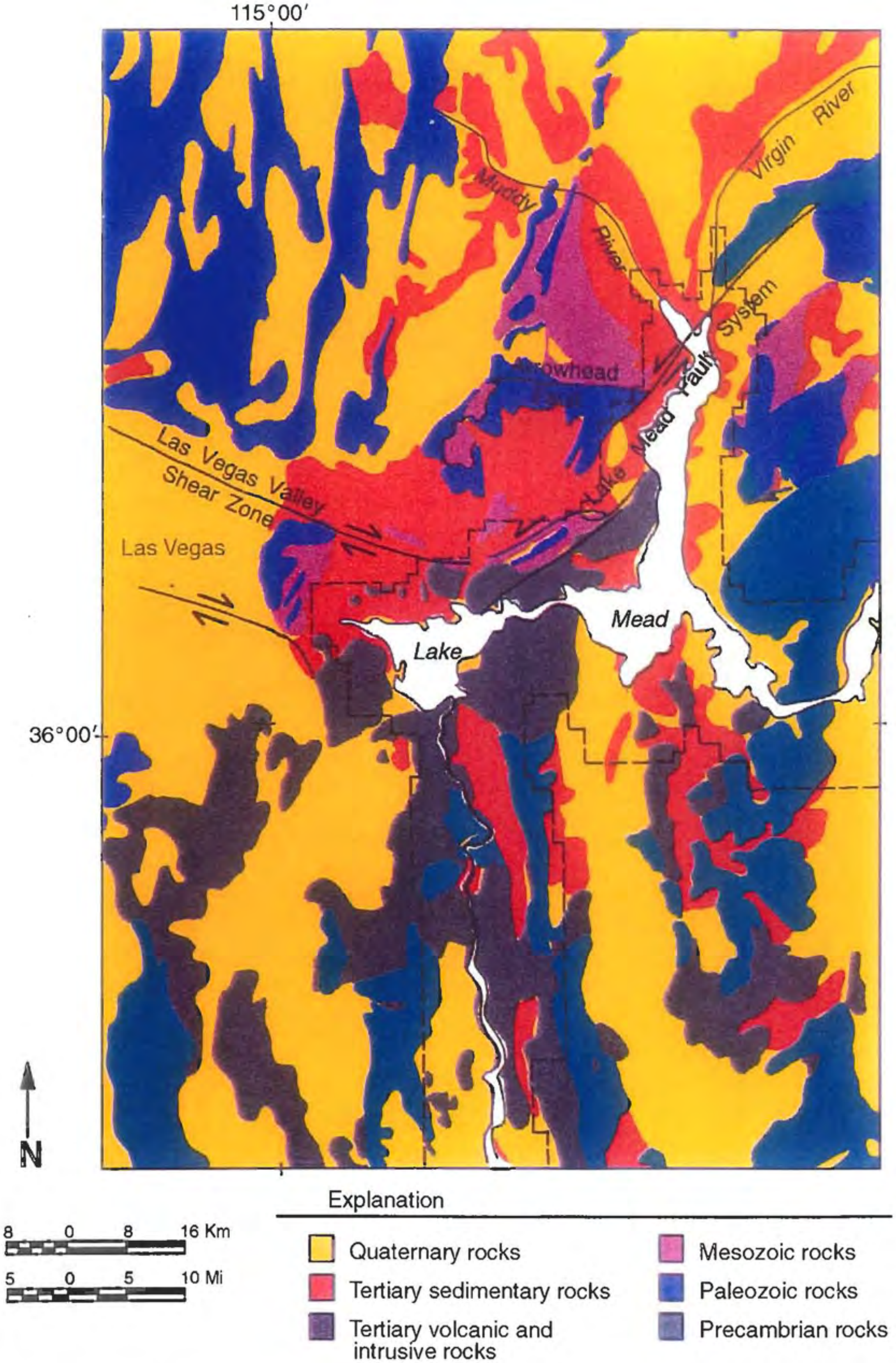

Figure 4. Generalized geologic map of southeastern Nevada and northwestern Arizona. Modified from Longwell *et al.* (1965), Reynolds (1988), and Campagna and Aydin (1994).

Table 2. Generalized Stratigraphic Column for the Study Area.

Time		Unit	Symbol	Description and Reference
Cenozoic	Quaternary	Alluvium (Holocene to Pleistoncene?)	Qal	Silts, sands, pebbles, cobbles, and boulders in modern drainages. Angular to subrounded particles. Unconsolidated, locally derived. (Bohannon, 1984).
		Older Alluvium (Pleistocene)	Qoa	Silt, sand, pebbles, cobbles, and boulders in alluvial fans, thick colluvial deposits, alluvial flood plains, and channels. Poorly sorted, angular to subround unconsolidated particles. Locally derived. (Bohannon, 1984).
		Terrace Deposits (Pleistocene?)	Qt	Silt, sand, pebbles, cobbles, and boulders. Compacted and/or cemented. Locally derived. (Bohannon, 1984).
	Tertiary	Miocene Volcanics (undifferentiated)	Tmv	Lava flows of Callville Mesa and Overton Arm and intrusive rocks north of Callville Mesa, western Bitter Spring Valley, and northeastern Muddy Mountains. (Bohannon, 1984).
		Muddy Creek Formation	Tm	Bedded siltstone, sandstone, gypsum, gypsiferous siltstone, and conglomerate near basin margins. (Bohannon, 1984).
		Horse Spring Formation	Th	Limestone, dolomite, conglomerate, sandstone, volcanic tuff, gypsum and breccia. Includes clastic and gypsum facies of the Thumb Member. (Bohannon, 1984).
		Rainbow Gardens Basal Conglomerate	Thrc	Conglomerate consisting of sandstone, siltstone, gypsum, gypsiferous siltstone, carbonates, and magnesite. Lowest unit in the Horse Spring Fm, and marks the Tertiary unconformity. (Bohannon, 1984).
		Mount Davis Volcanics (undifferentiated)	Td	Miocene lava and flow breccias. (Anderson, 1978).
		Intrusive Rocks (undifferentiated)	Ti	Miocene intrusive rocks. Includes the Boulder City pluton, a mixture of medium-grained granodiorite and andesitic border facies (Anderson, 1969), and the Wilson Ridge pluton, a biotite granite through horneblende-biotite granodiorite to pyroxene-biotite diorite. (Anderson, 1978).
		Patsy Mine Volcanics (undifferentiated)	Tpv	Miocene. In the study areas andesitic lava and breccia. (Anderson, 1978).
Mesozoic	Jurassic-Cretaceous	Autochthonous Jurassic and Cretaceous Formations	JKau	Baseline Sandstone (K): sandstone and conglomerate. Willow Tank Formation (K): Conglomerate, claystone, sandstone, tuff, and mudstone. Aztec sandstone (J, K?): red quartz arenite w/hematite cement. (Bohannon, 1984).
	Triassic	Autochthonous Triassic Formations	₹au	Moenave and Kayenta Formations: gypsiferous sandstone and siltstone. Chinle Formation: sandstone, siltstone, claystone, conglomerate, minor limestone. Moenkopi Formation: siltstone, sandstone, gypsum, gypsiferous siltstone, limestone, conglomerate. (Bohannon, 1984).

SE ROA 42997

Table 2. Generalized Stratigraphic Column for the Study Area (Continued).

Paleozoic	Permian	Autochthonous Permian Red Beds and Kaibab-Toroweap Formations	Pau	Permian Red Beds (lower P): sandstone, siltstone, gypsum. Kaibab-Toroweap Fms (P): limestone, chert, siltstone, gypsum. (Bohannon, 1984).
	Cambrian-Pennsylvanian	Allochthonous Paleozoic Rocks (undifferentiated)	OIPal	Bonanza King Fm. (Є) through Bird Spring Fm (P IP): limestone, dolomite, sandstone, quartzite, shale. (After Bohannon, 1984).
Proterozoic	Precambrian	Variegated Metamorphic Rocks	pЄ	Predominantly biotite-almandine gneiss and schist and garnetiferous granite pegmatite. (Anderson, 1978).

The Precambrian/Cenozoic terrain in the southern portion of the study area includes the Black Mountains, the Eldorado Mountains, and Black Canyon. The Precambrian section is comprised of variegated metamorphic rocks consisting of biotite-almandine gneiss and schist and garnetiferous granite pegmatite (Anderson, 1978). These rocks are exposed in the Lake Mead area where structural highs formed during the late Cretaceous to early Tertiary Sevier orogeny resulted in erosion of the overlying Paleozoic and Mesozoic sedimentary rocks (Bohannon, 1984). Tertiary volcanic and intrusive rocks (described below) extensively intrude the Precambrian rocks.

Paleozoic rocks are exposed in the northern portion of the study area in the Muddy Mountains, North Muddy Mountains, and the western portion of Frenchman Mountain. The Paleozoic rocks are predominantly limestone and dolomite (carbonate rocks), with lesser amounts of sandstone, quartzite, and shale. To the northwest, the Paleozoic section reaches a thickness of 5,000 m near the Sheep Range (Longwell *et al.*, 1965) and 7600 m near the Nevada Test Site (Tschanz and Pampeyan, 1970). However, the section thins dramatically eastward in the area west of the Overton Arm, reflecting a hinge line between deep-water and shelf deposits (Stewart, 1970). At the Muddy Mountains, the Paleozoic section is reduced to a thickness of 1200 m (Longwell *et al.*, 1965).

Mesozoic rocks are exposed in the Valley of Fire area, the northern edge of the Black Mountains bordering Pinto Valley, and the eastern portion of Frenchman Mountain. Mesozoic rocks are predominantly sandstones, siltstones, and conglomerates, with varying amounts of gypsum. The Formations exposed in the study area are shown in the stratigraphic column (Table 2).

Tertiary volcanic and intrusive rocks are found within the Precambrian terrain in the southern portion of the study area. The oldest Tertiary rocks are andesitic lava and breccia of the Miocene Patsy Mine volcanic rocks (Anderson, 1971) and are well exposed along the cliffs of Black Canyon. The intrusive rocks include the Miocene-aged Hoover Dam and Wilson Ridge plutons, and numerous dikes of rhyolitic to basaltic composition (Anderson, 1978).

Tertiary sedimentary rocks are exposed throughout the study area, yet predominate in the north. These rocks were initially deposited in a broad shallow basin unconformably covering the autochthonous rocks (Bohannon, 1984). The Rainbow Gardens Member of the Horse Spring Formation represents the lower Tertiary section. The Rainbow Gardens includes clastic rocks ranging in grain size from conglomerate to claystone, several types of carbonates, evaporites, and cherts. Later faulting disrupted this broad basin, and sedimentation of the upper Horse Spring Formation (the Thumb Member and above) occurred within smaller, fault-controlled basins (Bohannon, 1984). The upper Horse Spring includes clastic, carbonate, and tuffaceous rocks. The nearly unconsolidated Tertiary Muddy Creek Formation and Quaternary fanglomerates filled most of the fault-controlled basins, reaching thicknesses of at least 215 m in the Muddy and Virgin river valleys, and 425 m in Detrital Valley (Bohannon, 1984). The Muddy Creek Formation consists of siltstone, sandstone, gypsum, gypsiferous siltstone, and conglomerate. Tertiary and later sediments are thin or absent in the Black Canyon area, having been scoured away by the Colorado River (Anderson and Laney, 1975).

Unconsolidated Pleistocene or Recent alluvial deposits are composed of alluvial fan, fluvial, fanglomerate, lakebed, and aeolian deposits (Longwell *et al.*, 1965). Locally, coarse-grained Quaternary deposits are cemented with calcium carbonate. Older, moderately-well-cemented, fluvial deposits are exposed in the walls of Mormon Mesa, between the Virgin and Muddy Rivers.

One of the earlier periods of deformation that strongly affected the study area was the Sevier orogeny during late Cretaceous to early Tertiary. This event of eastward-directed thrust faulting disrupted the stratigraphic section, placing Paleozoic carbonates over Jurassic sandstones. One of the easternmost thrust systems is the Muddy Mountain thrust system which formed the Muddy Mountains located in the northern portions of the study area (Longwell, 1922).

During late Tertiary, major strike-slip and normal faulting associated with Basin and Range extension disrupted the Lake Mead area. Strike-slip faulting dominates the study area north of the lake and these late Miocene faults are known collectively as the Lake Mead fault system (Anderson, 1971). Comprised of numerous discontinuous left-lateral strike-slip faults, the Lake Mead fault system has an estimated total displacement of 60 km distributed along its entire length and fault segments (Bohannon, 1984). Two of these fault segments, the Bitter Spring Valley and the Rogers Spring faults, bound the Overton Arm pull-apart basin (Campagna and Aydin, 1994). Several large springs in the study area are located along the Rogers Spring fault near its southwestern terminus. There, the Rogers Spring fault separates the younger Tertiary through Quaternary sediments of the Overton Arm basin on the east from the allochthonous Paleozoic section of the Muddy Mountains on the west. In this area, the fault strikes N50°E, is vertical to 75°SE dipping, and has a gouge zone up to 5 m thick (Campagna and Aydin, 1994). Northeast of the Muddy Mountains, the Rogers Spring fault lies entirely within the Muddy Creek Formation, strikes N60°E, and is nearly vertical. The thickness of the zone of low-permeability fault gouge and the transition from transmissive carbonate rocks to low-permeability basin-fill sediments creates a barrier to further eastward flow of groundwater.

The extreme western portions of the study area include Frenchman Mountain, which is bounded by northwest trending right-lateral strike-slip faults of the Las Vegas Valley shear zone. Longwell (1960) first identified the Las Vegas Valley shear zone as a northwest-trending right-lateral strike-slip fault beneath the alluvial fill of Las Vegas Valley. One of the faults passes

SE ROA 42999

north of Frenchman Mountain and terminates at or near the southwestern extension of the Lake Mead fault system (Cakir, 1990; Duebendorfer and Wallin, 1991). Other faults within the system continue southeast past Frenchman Mountain (Campagna and Aydin, 1994), presumably terminating at the River Mountains and McCullough Range.

Normal faults, characteristic of Basin and Range extensional deformation, are most common south of the lake. In the Black Canyon area, normal faults are associated with magmatism, strike North-South, and dip at high angles to the west and east (Anderson *et al.*, 1994). These high-angle faults may become listric at depth (Anderson, 1971), providing horizontal pathways for groundwater flow in the volcanic terrain (McKay and Zimmerman, 1983). In addition, numerous small faults in this area strike N50°W and are oblique right-lateral strike-slip faults (Anderson, 1971).

In summary, the most important stratigraphic units that shape the hydrogeologic setting are the thick Paleozoic carbonates in the northwest, the thick Tertiary sediments that fill structural basins in the north, and the Precambrian and Tertiary igneous and metamorphic rocks in the south. The most important structural features are the Lake Mead strike-slip fault system in the north, and the normal faulting in the south.

GROUNDWATER FLOW SYSTEMS

Regional Flow Patterns

Groundwater flow systems in the Basin and Range province range in size from small local systems to regional systems that extend over hundreds of kilometers. Local systems usually occupy a single topographic or hydrographic basin and have short flow paths relative to regional systems. Regional systems incorporate multiple topographic basins and therefore interbasin flow is important. While local systems may receive the majority of their recharge in the local topographic basin, regional systems typically receive recharge from multiple basins, and local recharge in any particular basin may be minimal.

Southeastern Nevada comprises the ultimate groundwater discharge location for much of the eastern portion of the regional carbonate aquifer (Dettinger *et al.*, 1995). Major groundwater flow systems comprised of thick carbonate rocks enter the area from the north and meet hydrogeologic barriers to flow, formed by thick, low-permeability Tertiary basin-fill deposits and a Precambrain terrain intruded by Cenozoic igneous rocks. Near these barriers, groundwater is discharged directly at regional springs, or by upward flow into basin-fill aquifers and subsequently discharged by evapotranspiration, spring flow, and streams. Groundwater flow in northwestern Arizona is less well-defined, but generally occurs as northward flow in the basin-fill deposits of Detrital Valley, with ultimate discharge to Lake Mead, and westward flow in basin-fill deposits, and perhaps igneous rocks, toward the Colorado River (Bedinger *et al.*, 1984). The generalized directions of groundwater flow in southeastern Nevada and northwestern Arizona are shown in Figure 5.

Most groundwater in the Basin and Range geologic province flows through carbonate-rock aquifers interconnected with unconsolidated basin-fill aquifers. In southern Nevada, basin-fill aquifers tend to be isolated by topographic divides and contribute to multi-basin groundwater flow

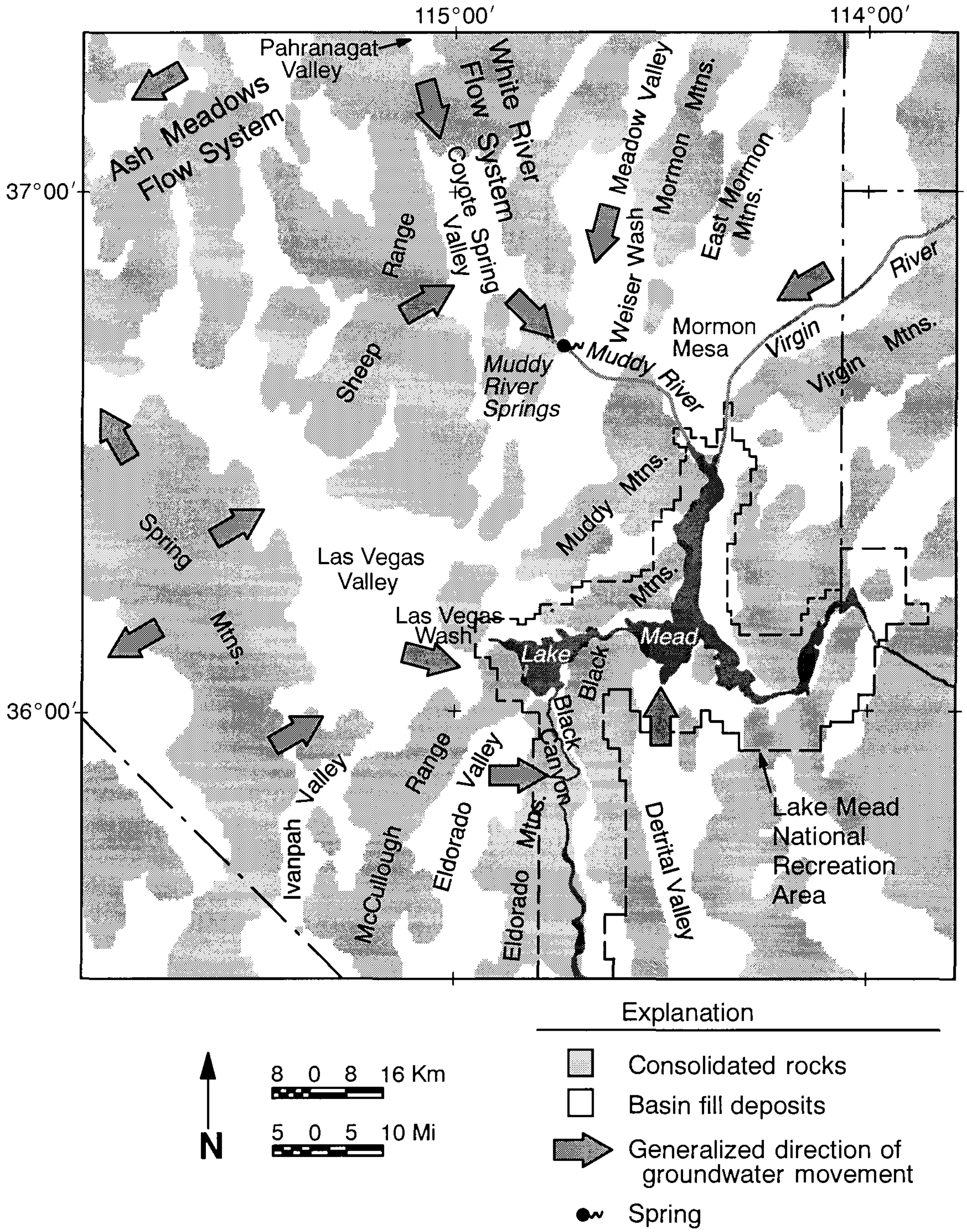

Figure 5. Regional groundwater flow patterns in southeastern Nevada and extreme northwestern Arizona. Modified from Harrill *et al.* (1988) and Bedinger *et al.* (1984).

systems only when they are in close hydraulic connection with underlying carbonate rocks. The most permeable basin-fill sediments were deposited as alluvial-fan, lake-bed, or fluvial deposits in basins formed by late Tertiary and Quaternary normal faulting. The earlier Tertiary basin-fill sediments of the Horse Spring and Muddy Creek Formations are generally less permeable due to finer grain size.

SE ROA 43001

High transmissivities in carbonate rocks result from their great thickness, numerous faults and fractures caused by extensional deformation of the brittle carbonate rock, and to a lesser degree, solution enlargement of fractures and joints (Dettinger *et al.*, 1995). The high transmissivity of these rocks has been demonstrated during pumping tests in several wells, including the MX wells in Coyote Spring Valley (Bunch and Harrill, 1984) and the Arrow Canyon well in the Moapa Valley (Buqo, 1993), and by the high discharge rates from regional springs in the carbonate-rock province (Eakin, 1964). The carbonate rocks do not form a continuous unit, but rather are composed of many discrete structural blocks bounded by faults (Plume and Carlson, 1988). This pattern is manifested at land surface as distinct, often closed, topographic basins surrounded by mountain ranges. The transmissive carbonate rocks often provide a mechanism for deep groundwater flow between basins where topographic divides prevent shallow flow between adjacent basin-fill aquifers (Eakin, 1966).

Orographic effects cause most recharge within the carbonate rock province to be derived from precipitation in the higher elevations of east-central Nevada (Eakin, 1966). Groundwater recharge is minimal in low-elevation basins because potential recharge from precipitation is quickly lost to evapotranspiration (Maxey *et al.*, 1966). The carbonate aquifers of southern Nevada are recharged primarily from precipitation at high altitudes in the nearby Sheep and Spring Mountains (Winograd and Riggs, 1984), and from flow that enters the region from carbonate aquifers to the north.

Two major flow systems have been delineated within the southern part of the carbonate terrain. One discharges approximately 130 km west of the study area at Ash Meadows and Death Valley (Winograd and Thordardson, 1975) and the other, the White River flow system, discharges at the Muddy River Springs in the Moapa Valley (Eakin, 1966). The latter flow system is pertinent to any study of groundwater resources in southeastern Nevada because it supplies the vast majority of groundwater flow into the region. It comprises thirteen interconnected groundwater basins that extend over 370 km north to Long Valley (Eakin, 1968). The Muddy River springs are believed to be the primary regional discharge point of the White River System (Eakin, 1968), although groundwater from other basins, namely Meadow Valley, may contribute some discharge to the springs (Schroth, 1987; Kirk and Campana, 1988; Thomas *et al.*, 1997). In addition, Thomas *et al.* (1997) suggest that most groundwater recharge in the Sheep Range, which is located directly west, may be discharged at the Muddy River Springs. The Muddy River spring area represents the single greatest groundwater discharge point in southern Nevada, with estimated annual discharge of approximately 36,000 acre-ft/year (AFY) (Eakin, 1964; Prudic *et al.*, 1993; Thomas *et al.*, 1997).

Dettinger *et al.* (1995) summarize the evidence for the discharge at the Muddy River Springs and the related upward flow into overlying basin-fill aquifers in the area as being the terminus of the White River flow system. First, geologic constraints to the east and southeast of the Muddy River Springs suggest further flow in those directions and toward Lake Mead is unlikely. These constraints include the thinning of carbonate rocks and exposure of Precambrian crystalline basement rocks on the western edge of the Mormon Mountains; thick (over 1200 m), low-permeability basin-fill sediments just east of the springs below California Wash; and, except for isolated areas, few carbonate rocks extending below Lake Mead (Longwell, 1936). Second, Longwell's mapping of the floor of present-day Lake Mead revealed no evidence of spring discharge. Finally, spring

SE ROA 43002

temperatures and stable isotopic data (to be discussed in more detail in a later section of this report) suggest that large down-gradient springs (Rogers and Blue Point springs near the Overton Arm of Lake Mead) are not directly related to discharge at the Muddy River Springs.

There is, however, evidence of groundwater discharge to the Muddy River about 20 km downstream of the Muddy River springs. Here, the Muddy River passes through "The Narrows" formed by the North Muddy Mountains and the Mormon Mountains. Rush (1968) reports gains in Muddy River discharge of 170 L/s in this reach and suggests that the most probable source for the flow is consolidated rocks underlying the thin alluvium. Although not discussed by Rush (1968), this discharge might represent the last point of discharge for flow from the White River flow system, or might represent flow from the Weiser Wash and Mormon Mountain regions directly north.

Another source of groundwater flow into southeastern Nevada is the Virgin River Valley to the northeast of the Overton Arm, although there is disagreement as to the amounts and locations of discharge. Glancy and Van Denburgh (1969) estimate groundwater discharge to Lake Mead through the valley fill and underlying consolidated rocks to be as much as 40,000 AFY. Most of this discharge was thought to be seepage from the Virgin River, which is a losing stream through much of the lower Virgin River Valley. However, Prudic *et al.* (1993) include no subsurface discharge from the Virgin River Valley to Lake Mead in their numerical model of regional groundwater flow. Instead, all groundwater in the near-surface aquifer is simulated as discharge by evapotranspiration (8000 AFY) or baseflow to the Virgin River (5000 AFY), while all discharge in the lower layer of the model (presumably consolidated rocks) is simulated as discharge at Rogers and Blue Point Springs (1200 AFY). The remainder of the discharge is considered surface flow in the Virgin River, and is not included in the model.

In the Las Vegas Valley, numerical modeling (Harrill, 1976; Morgan and Dettinger, 1994) and stable isotopic data (Thomas *et al.*, 1997) indicate that the majority of groundwater originates in the Spring Mountains to the west, with only minor amounts of recharge received from the Sheep Range. Thomas *et al.* (1997) suggest that structural constraints to the west, south, and southeast of the Sheep Range prevent groundwater flow in those directions, thus forcing flow toward Coyote Spring Valley to the northeast. Based on hydraulic head data, Thomas *et al.* (1997) suggest that a small amount of groundwater flow may also originate from Ivanpah Valley to the southwest, although, based on stable isotopic data, the southern portion of the Spring Mountains is the most important source of recharge to the southwestern portion of the Las Vegas Valley.

Hydraulic head relationships indicate that discharge from the Las Vegas Valley is to the east toward Lake Mead, although the amounts are likely to be small (Rush, 1968). Significant subsurface flow beneath Las Vegas Wash is unlikely because the basin fill below the channel is comprised of deposits of the low-permeability Muddy Creek Formation (Rush, 1968). Elsewhere, subsurface flow must pass through low permeability consolidated rocks and is therefore considered minimal. Calibration of numerical models (Harrill, 1976; Morgan and Dettinger, 1994) suggests less than 2000 AFY is discharged from the Las Vegas Valley toward Lake Mead in the area of Frenchman

Mountain. There exists little evidence for significant groundwater flow in the Tertiary volcanic rocks near Lake Mead (Laney and Bales, 1996).

The termini of groundwater flow systems in southern Nevada are located in areas where geologic constraints prevent further subsurface flow, causing discharge at the surface via springs and evapotranspiration; or where land surface elevations are sufficiently low to intersect groundwater flow paths. As previously described, the Muddy River Springs area is representative of the first mechanism, forming the terminus of the White River flow system and discharging approximately 36,000 AFY. The locations of Rogers and Blue Point springs, which have a combined discharge of approximately 1200 AFY (Laney and Bales, 1996), and other nearby springs, are also related to geologic constraints; that is, the transition from transmissive carbonate rocks to low-permeability basin-fill formed by the Rogers Spring Fault. Until recently however, the origin of groundwater discharged at these springs has been uncertain. Similarities between the geologic setting west of the Overton Arm and in the Moapa Valley lead early workers to group them with the Muddy River springs, making Rogers and Blue Point springs the terminal end of the White River flow system. Additional information about the physical, chemical, and isotopic nature of groundwater flow systems in southern Nevada has lead to new interpretations, including probable flow from the Virgin Valley to the north (Prudic *et al.*, 1993) and from recharge areas in the Sheep Range to the west and/or Mormon Mountains to the northwest (Dettinger *et al.*, 1995; Thomas *et al.*, 1997).

The Black Canyon of the Colorado River is suggested by Rush and Huxel (1966) and Mifflin (1968) as another discharge area within southern Nevada, primarily for the McCullough Range and Eldorado Valley. Evidence includes the presence of several springs and seeps at the base of Black Canyon near the present location of Hoover Dam that were noted during investigations for, and construction of, the dam (U.S. Bureau of Reclamation, 1950). The adjacent Black Mountains and Eldorado Mountains are suggested by McKay and Zimmerman (1983) as possible sources for several springs in Black Canyon, based on stable isotopic data that indicate low-elevation recharge. However, stable isotopic data for local precipitation and groundwater recharge were not available at the time of their study, and McKay and Zimmerman conclude that insufficient evidence existed for significant groundwater recharge at the low elevations in these areas. In addition, McKay and Zimmerman (1983) suggest that the permeability of faults and fractures in the volcanic rocks of Black Canyon is sufficient to provide important pathways for groundwater flow. Finally, McKay and Zimmerman (1983) provide strong evidence for the influence of recirculated Lake Mead water on several springs in Black Canyon.

Chemical Composition of Groundwaters

The limestone and dolomite that form carbonate aquifers are dominated by the soluble minerals calcite and dolomite, resulting in a calcium and magnesium-bicarbonate water composition that is fairly homogeneous throughout the carbonate-rock province of eastern and southern Nevada (Hess and Mifflin, 1978). Other minerals, such as gypsum and halite, are present in carbonate rocks in minute amounts but are more soluble than the carbonate minerals. Maxey and Mifflin (1966) show that solution of these minerals causes characteristic increases in the concentrations of the ions sodium, potassium, chloride, and sulfate as groundwater moves along regional flow paths. Overall, the water quality in carbonate rocks in southern Nevada is generally good, with TDS concentrations less than 600 mg/L (Lyles *et al.*, 1987).

Hershey and Mizell (1995) demonstrate the evolution of groundwater chemistry in the carbonate flow system of southern Nevada using a trilinear plot of major dissolved ions in regional carbonate springs (Figure 6). The groundwater flow paths implied on this plot are based on regional flow patterns proposed by Harrill *et al.* (1988). Groundwater intermediate in the flow system is represented by springs in Pahranagat Valley and White River Valley (the next valley north and upgradient of Pahranagat Valley) which show the calcium, sodium-bicarbonate and sulfate composition typical of carbonate waters. One evolutionary trend follows the flow path toward the regional discharge point at the Muddy River Springs. Groundwater flow along this path is

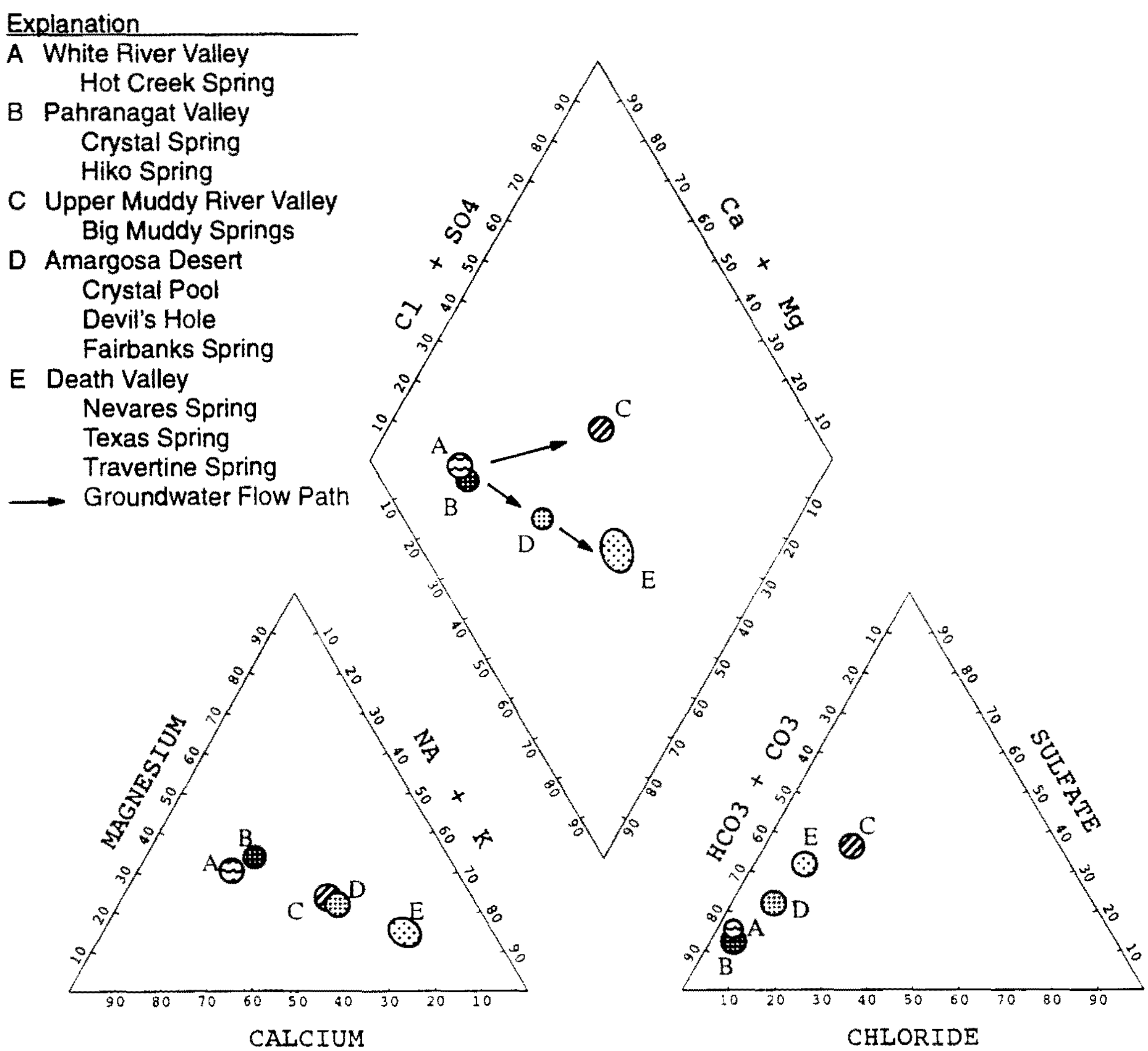

Figure 6. Trilinear diagram showing major dissolved ions of regional springs in the carbonate-rock province of eastern Nevada, showing evolution of groundwater chemistry along two flow paths. Modified from Hershey and Mizell (1995).

SE ROA 43005

accompanied by increases in the concentrations of sodium, potassium, sulfate, and chloride ions attributed to solution of evaporite minerals in the Horse Spring and Muddy Creek Formations near the discharge point. Calcium and magnesium also increase, but to a lesser degree. The other evolutionary trend follows a flow path through Ash Meadows to the regional discharge point in Death Valley. Increases in the concentrations of all major ions except calcium and magnesium along this flow path to Ash Meadows are attributed to solution of Tertiary silicic volcanic rocks (Winograd and Thordardson, 1975). From Ash Meadows to Death Valley, concentrations of all major ions except calcium and magnesium increase as a result of solution of Tertiary and Quaternary lacustrine and alluvial deposits. Declines in the concentrations of calcium and magnesium are attributed to cation-exchange with clays and precipitation of travertine deposits at the springs.

Groundwater in volcanic rocks northwest of Las Vegas is generally of sodium and potassium-bicarbonate composition, reflecting dissolution of feldspar and mafic minerals along relatively long flow paths (Winograd and Thordardson, 1975; Lyles *et al.*, 1987). Locally, waters collected from springs south of Las Vegas in the McCullough Range and a well and springs in the Eldorado Mountains have a mixed cation-sulfate or a mixed cation-bicarbonate composition (Lyles *et al.*, 1987; SNWA, unpublished data) (Figure 7), similar to springs that represent early-stage recharge chemistry in volcanic rocks of central Nevada (Raker and Jacobson, 1987). TDS concentrations of the McCullough Range samples range from 414 mg/L to 664 mg/L while the Eldorado Mountains samples range from 957 mg/L to 1390 mg/L.

Groundwater in basin-fill deposits is categorized as calcium and magnesium-bicarbonate, mixed cation-sulfate, and sodium and potassium-bicarbonate composition (Figure 7) (data from Lyles *et al.*, 1987). Composition varies considerably across the region, depending on lithology, residence time, and origin. Groundwater quality is poorest in the eastern portion of the region, and is characterized by TDS concentrations that range from about 1000 mg/L to well over 2000 mg/L, and mixed cation-sulfate composition (Lyles *et al.*, 1987). The sulfate is derived from solution of evaporite minerals, including gypsum and thenardite (Lyles *et al.*, 1987), in sedimentary rocks of Tertiary age (Muddy Creek and Horse Springs Formations), Triassic age (Moenave, Kayenta, and Moenkopi Formations), and Permian age (Permian Red Beds and Kaibab-Toroweap Formations) (Bohannon, 1984). These rocks are abundant at the surface and in the near surface from Frenchman Mountain northeast to the Overton Arm, and commonly overlie, or are structurally adjacent to, Paleozoic carbonate rocks. Thus, groundwater in this area is likely to pass through evaporite deposits at some point along flow paths, greatly increasing TDS and sulfate concentrations.

Isotopic Composition of Groundwaters

Groundwater in southern Nevada is derived from two principal sources: recharge from local precipitation, and groundwater flowing into the area from regional and subregional aquifer systems described above. Groundwater recharge can be further divided into recharge at altitudes less than 1500 m, which includes most of the region; and recharge at altitudes above 1500 m, which in southern Nevada is limited primarily to the Spring Mountains and Sheep Range. Although smaller in area and lower in altitude than these ranges, the Mormon Mountains also receive precipitation

SE ROA 43006

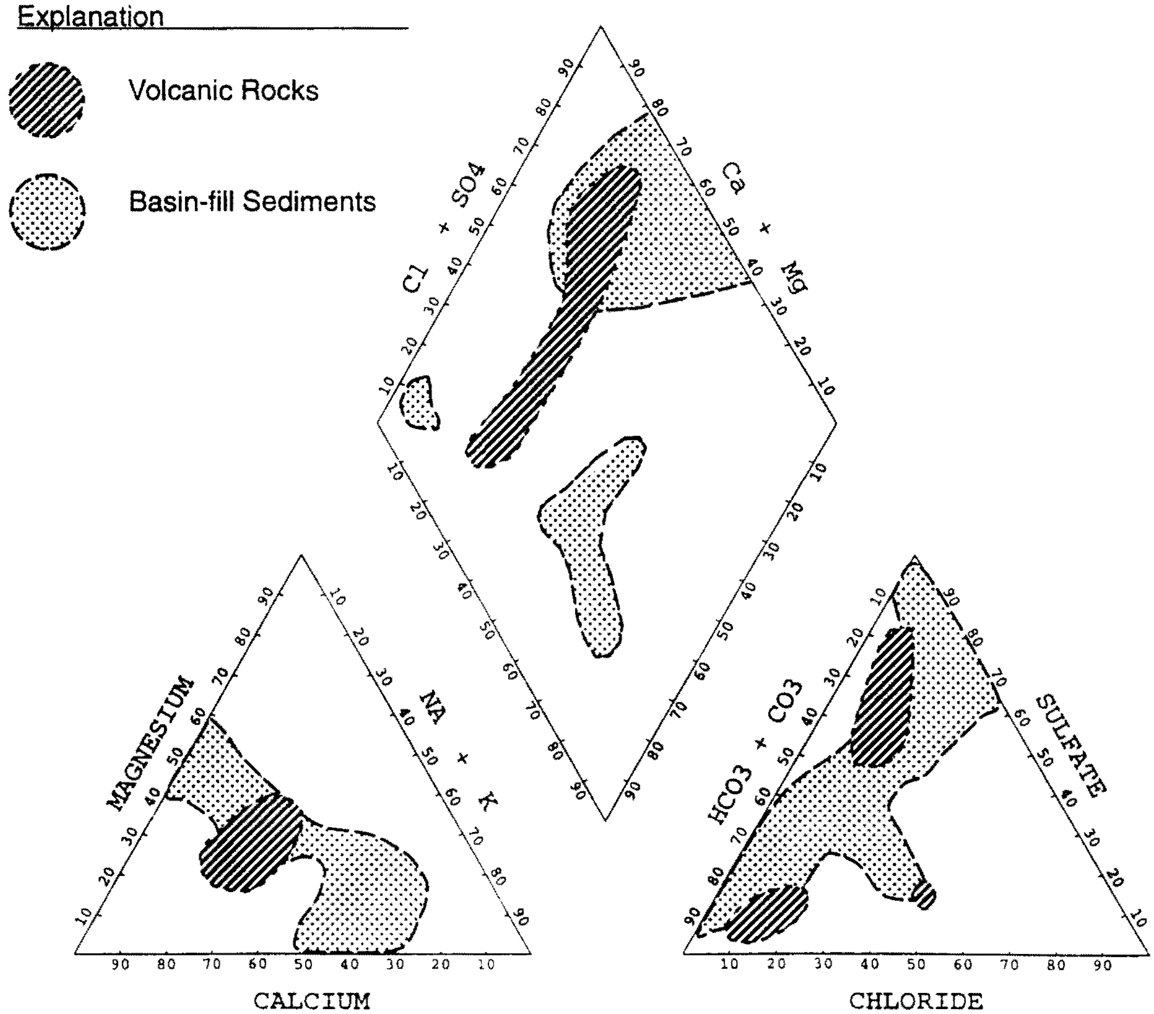

Figure 7. Trilinear diagram showing major dissolved ions in groundwaters collected from volcanic rocks and basin-fill sediments in southern Nevada. Modified from Lyles *et al.* (1987), with additional data from SNWA (unpublished data).

at altitudes above 1500 m and are located much closer to Lake Mead. Although precipitation is the ultimate source of groundwater recharge, evaporation and associated isotope fractionation during recharge under arid conditions causes recharge waters to have a different isotopic composition than the original precipitation. Therefore, selected spring data are used in the present study to represent the stable isotopic composition of groundwater recharge. In addition, local precipitation data were not available at the time of the present study and the timeframe of the study did not allow for long-term precipitation collection.

The stable isotopic values of springs in selected groundwater recharge areas are shown in Figure 8. Also shown is the global Meteoric Water Line (MWL) that represents the linear relationship between $\delta^{18}O$ and δD described by Craig (1961) using data from over 400 rivers, lakes, and precipitation. The local MWL shown represents precipitation (falling as rain) at 32 sites in

SE ROA 43007

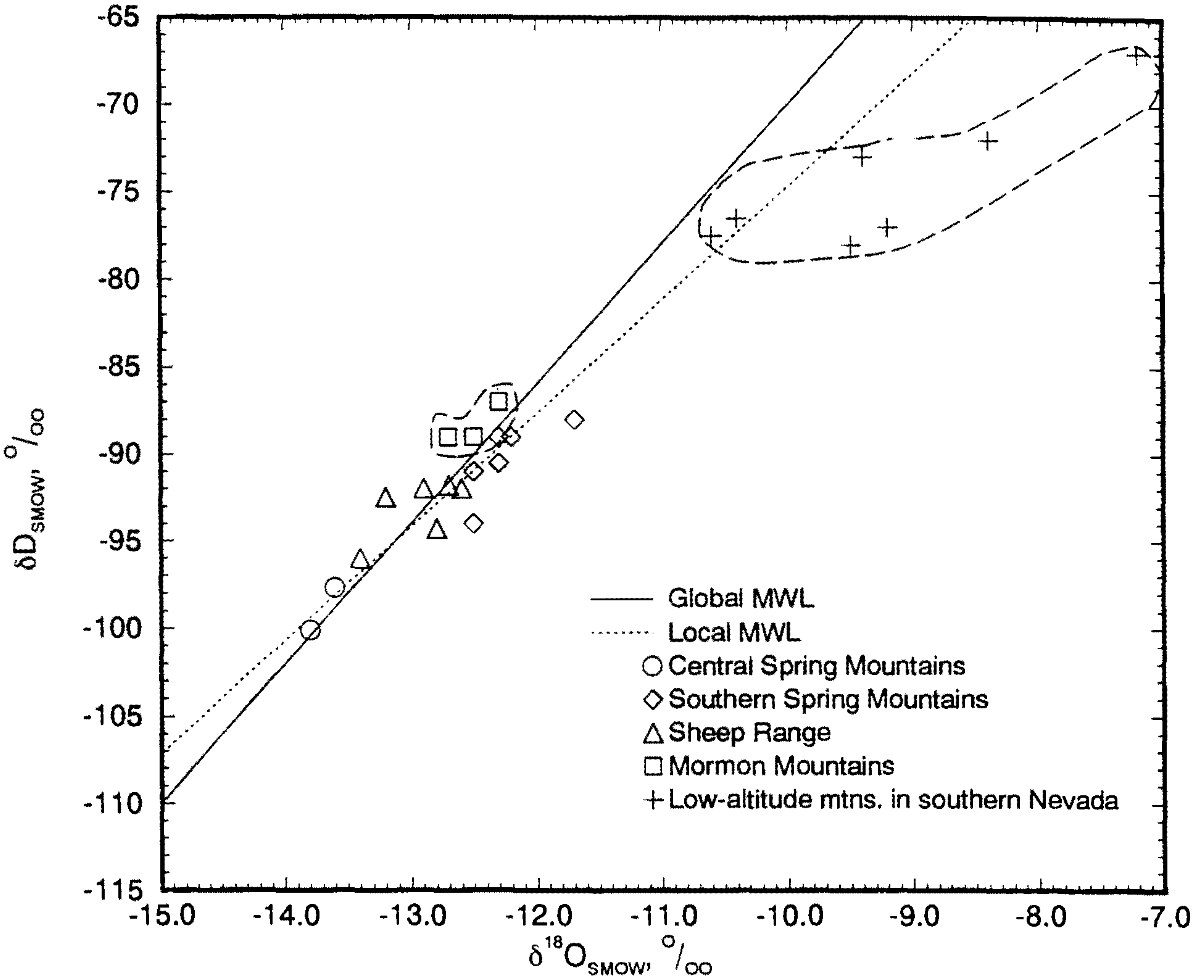

Figure 8. Stable isotopic composition of springs in groundwater recharge areas in southern Nevada, the global meteoric water line (after Craig, 1961), and a local meteoric water line (see text for description). Groundwater recharged at high altitudes in the Spring Mountains, Sheep Range, and Mormon Mountains is isotopically lighter than groundwater recharged in low-altitude mountain ranges. Data are compiled in Table C-1.

southeastern California between April 1986 and October 1987 (Friedman *et al.*, 1992). The equation for the least squares line for this data set is $\delta D=6.5\delta^{18}O-9.7$. Springs located at altitudes above 1100 m in the Spring Mountains, Sheep Range, and Mormon Mountains plot as the isotopically lightest points on Figure 8 (data from Thomas *et al.*, 1997). As atmospheric moisture rises up the mountain fronts, the heavier isotopes of hydrogen and oxygen are selectively removed with precipitation and the residual moisture becomes isotopically lighter. Thus, groundwater recharged at high altitudes in these mountains is isotopically lighter than groundwater recharged at lower altitudes. Thomas *et al.* (1997) also note that the higher altitudes of the central Spring Mountains result in more depleted stable isotopic compositions compared to the southern Spring Mountains. Springs in both portions of the Spring Mountains also contain tritium concentrations of up to 257 pCi/L (analyzed in 1976), indicating a major component of post-1952 recharge. The $\delta^{13}C$ concentrations range from -7.9 to -11.2 per mil, reflecting the enrichment of $\delta^{13}C$ by dissolution of carbonate rocks.

SE ROA 43008

The isotopically heavier, low altitude points shown on Figure 8 represent springs that are derived from recharge that occurs at altitudes less than 1500 m in the McCullough Range and Eldorado Mountains adjacent to Black Canyon, the Highland Range and New York Mountains south of Eldorado Valley, and the East Mormon Mountains northwest of Lake Mead (Thomas *et al.*, 1997; SNWA, unpublished data). These springs are located in ranges, or in portions of ranges, that receive most of their recharge at altitudes lower than about 1500 m. Because they are located at altitudes above the adjacent valleys, and therefore are unrelated to regional groundwater flow systems, groundwater discharged from these springs represents local, low-elevation recharge rather than regional groundwater flow. The existence of these springs indicates that local recharge can be more significant than basin-wide predictions developed using the Maxey-Eakin method.

The greater spread of the low altitude data points on Figure 8 likely results from local differences in conditions and seasons of recharge in each individual spring catchment area. The isotopic composition of these springs is reasonably consistent with precipitation data collected at Searchlight, Nevada between the years of 1982 to 1989 (average annual δD of -73 per mil) (Friedman *et al.*, 1992) and at the Nevada Test Site (average annual δD of -80 per mil) (Ingraham *et al.*, 1991). Therefore, the stable isotopic composition of local, low-elevation recharge in the area of study is assumed to be that of these low-elevation mountain springs. It should be noted that these springs plot close to the estimated composition of present-day groundwater recharge near Searchlight, Nevada (δD of -80 per mil) (Smith *et al.*, 1992).

Tritium data for the low-elevation springs are sparse. However, tritium values have been measured at two springs in the Eldorado Mountains. These concentrations (19 and 24 pCi/L – analyzed in 1995; SNWA, unpublished data) indicate that post-1952 recharge contributes to flow at these springs. The only ^{14}C data available for low-elevation springs is for a single spring in the McCullough Range. This spring contains 68.1 percent modern carbon (PMC), for an uncorrected age of 3,175 years, which further distinguishes it from older, regional groundwater flow.

The stable isotopic composition of groundwater in regional and subregional flow systems is shown in Figure 9. Data from the White River flow system of the regional carbonate aquifer (Thomas *et al.*, 1991; DRI, unpublished data) show a trend toward heavier composition along the flow path from Pahranagat Valley (white triangles), through Coyote Spring Valley and other nearby valleys (light shaded triangles), to the Muddy River Springs (dark triangles). Groundwater is isotopically lightest at the recharge areas in east-central Nevada, where recharge occurs at higher elevations and under different climatic conditions, and becomes isotopically heavier as local, lower-elevation precipitation recharges the system. Between Pahranagat Valley and the Muddy River Springs, the addition of isotopically heavier groundwater originating from the Meadow Valley flow system to the northeast, and recharge in the Sheep Range to the west is thought to cause the composition observed at the Muddy River Springs (Kirk and Campana, 1988; Thomas *et al.*, 1997).

Tritium is below detection levels in the southern part of the regional carbonate aquifer (Hershey and Mizell, 1995), reflecting long travel times from recharge areas and/or the dilution of local recharge with regional flow. In addition, the carbonate system shows trends of decreasing PMC and

SE ROA 43009

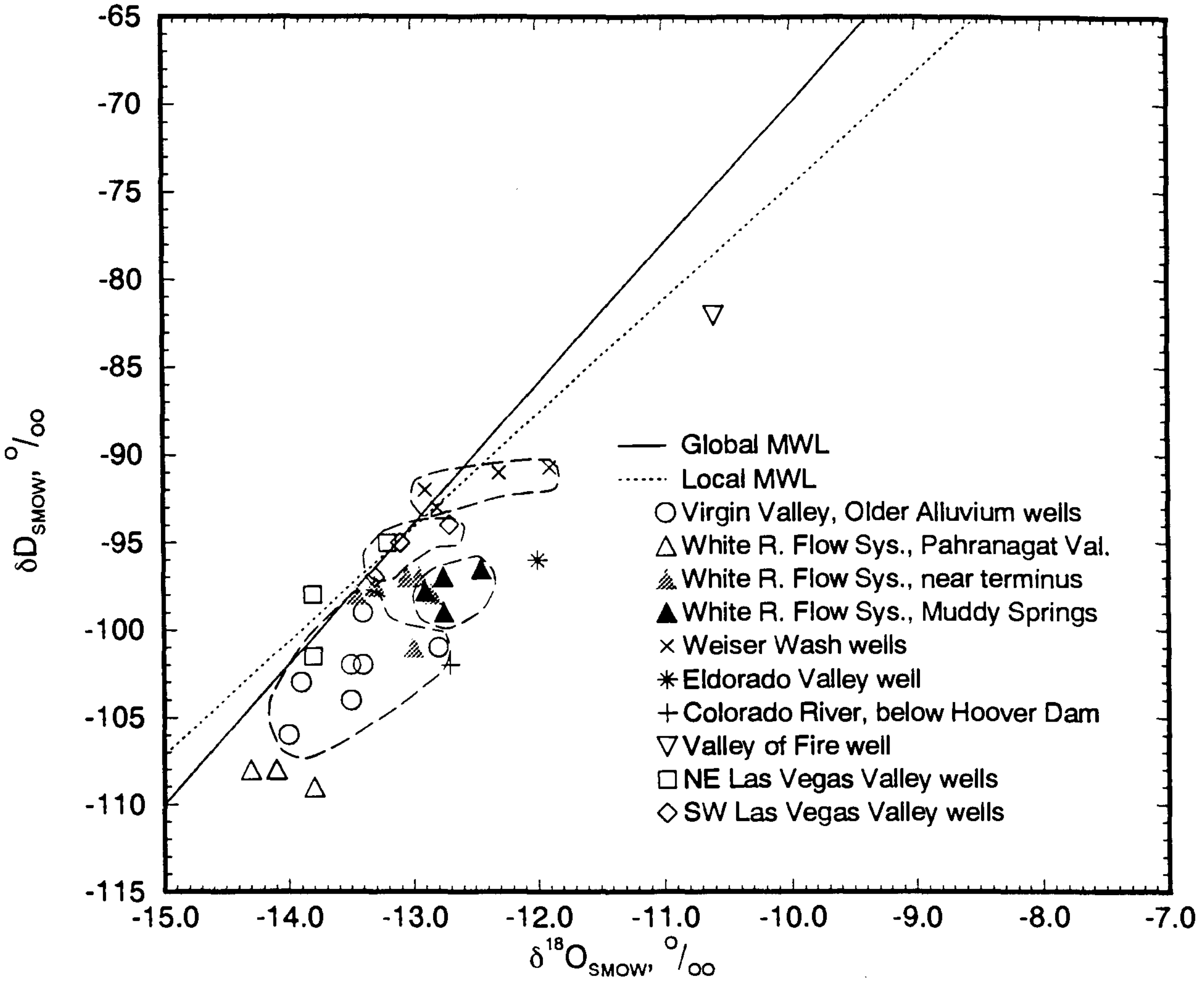

Figure 9. Stable isotopic composition of selected groundwaters of southern Nevada. Data are compiled in Table C-1.

increasing $\delta^{13}C$ values along regional flow paths, reflecting the increasing age of groundwater and dissolution of carbonate minerals with the addition of dead carbon and enrichment of $\delta^{13}C$ (Hershey and Mizell, 1995). Known regional springs in the carbonate aquifer system have PMC values of 2.8 to 11.2 and $\delta^{13}C$ values of -5.8 to -3.9 per mil (Hershey and Mizell, 1995).

In the Virgin Valley, groundwater obtained from wells in the Older Alluvium (which includes the Tertiary Muddy Creek Formation) is isotopically lighter than groundwater in the near surface aquifers and the Virgin River, suggesting a different origin (Metcalf, 1995). The composition is similar to that of groundwater at the southern end of the White River flow system, which may reflect a similar recharge source for Older Alluvium waters, such as carbonate aquifers to the north of the Virgin Valley (Glancy and Van Denburgh, 1969).

Isotopic similarities between groundwater in the basin-fill of Eldorado Valley and of southwest Las Vegas Valley, suggest a common origin. In addition to their similar δD values (Figure 9), groundwater in these two areas share $\delta^{13}C$ values between -6.8 and -7.8 which suggests flow in

SE ROA 43010

carbonate rocks (or possible reactions with pedogenic carbonates or carbonate dust). Furthermore, PMC values of 7.75 and below are similar to the older, regional groundwaters noted above. Finally, the lack of detectable tritium in the Eldorado Valley sample suggests a pre-1952 age. Thomas *et al.* (1997) propose that groundwater in southwest Las Vegas Valley originates from low elevation recharge in the southern Spring Mountains. Although only a single data point is available in Eldorado Valley, the similarity to groundwater in southwest Las Vegas Valley is consistent with the idea of interbasin groundwater flow into and through Eldorado Valley, as proposed by McKay and Zimmerman (1983) and Harrill *et al.* (1988).

Groundwater of a more local, low-elevation origin is found in the Weiser Wash area, between the Mormon Mountains and the Muddy River. Here, water in the Muddy Creek Formation and underlying rocks is isotopically heavier (DRI, unpublished data) than groundwater in the Older Alluvium of Virgin Valley and groundwater discharged at the Muddy River Springs. This groundwater may represent a mixture of groundwater from the Meadow Valley Wash flow system (described by Thomas *et al.*, 1997) and isotopically heavier recharge (average δD of -88 per mil) in the Mormon Mountains. Tritium and carbon data are not available for this area.

Groundwater that appears to have a major component of locally-derived recharge occurs at Valley of Fire State Park, where a sample collected from the headquarters well has a heavier isotopic composition than most other groundwater in the region. Although the hydraulic head measured in this well conforms to the regional hydraulic head gradient between the Muddy River springs and Lake Mead, this area may represent a groundwater cell receiving local recharge through the Mesozoic sandstone terrain that covers the area. The $\delta^{13}C$ value of -8.5 per mil might represent reactions with pedogenic carbonates or carbonate dust, or might suggest a portion of the groundwater flows through carbonate rocks. The PMC value of 18.7, which is at least twice that of the upgradient Muddy River springs, indicates the presence another source of modern carbon.

Colorado River water (collected just below Hoover Dam) is isotopically lighter than most groundwater in the region, reflecting the isotopically-depleted composition of precipitation at higher elevations and cooler climates in the upper Colorado River drainage basin. The tritium concentration was 51 pCi/L in a water sample collected in 1997.

A selected set of uranium data for groundwaters in the region, including Rogers and Blue Point springs, is shown in Figure 10. This plot displays the $^{234}U/^{238}U$ activity ratio (AR) as a function of the inverse of total uranium concentration (µg/L). This plot reveals that there is an inverse relationship between uranium concentration (note that the x-axis is the reciprocal of concentration, so high concentrations plot to the left, and low concentrations plot to the right) and $^{234}U/^{238}U$ AR. This relationship has been widely observed, and has often been attributed to a trend line which shows evolution along a flowpath. According to this scenario, AR increases with the time that water has in contact with the aquifer matrix, and the concentration decreases as groundwater moves deeper along a flowpath, because it encounters reducing zones which causes uranium to precipitate from solution (Osmond and Cowart, 1992). Obviously, this scenario does not apply to waters of the region examined during this study, as no reducing zone is known to exist, even at great depths below ground

SE ROA 43011

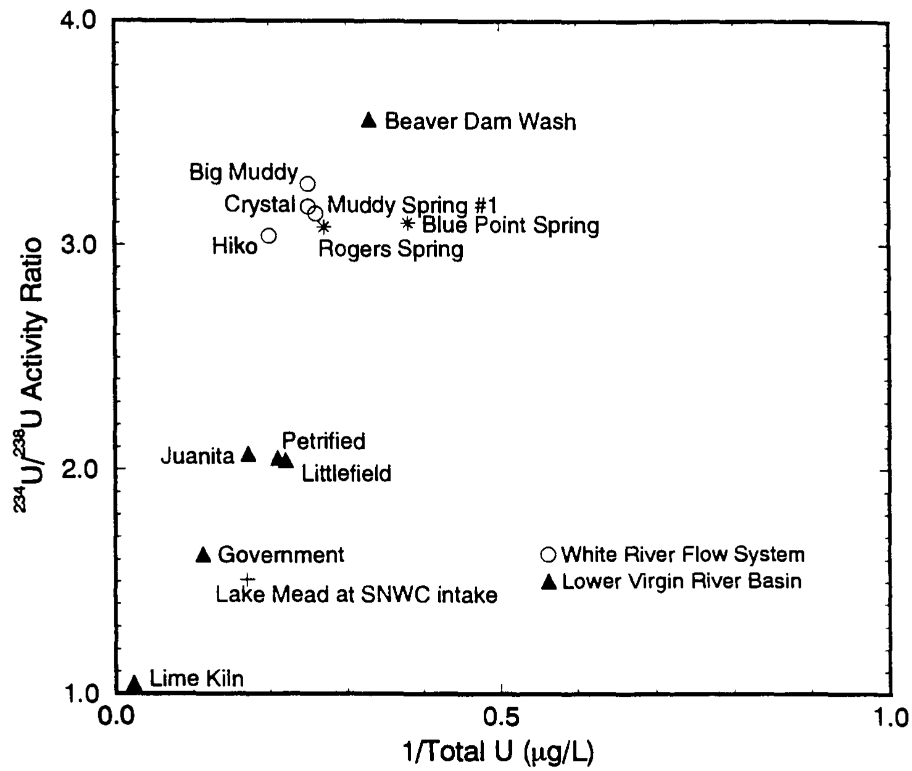

Figure 10. Uranium data for selected groundwaters of southern Nevada and southwestern Utah. Data compiled from Yelken (1996) and Farmer (1996).

surface. Kronfeld *et al.* (1994) present a scenario applicable to the deep oxygenated waters of the Basin and Range province, based on their study of an oxygenated carbonate aquifer in South Africa. The aquifer was found to exhibit a similar trend line to that seen in the present study, with the AR inversely related to concentration. Using ^{3}H and ^{14}C to date waters collected along the flowpath of the aquifer, the AR was shown to increase with the age of the water, indicating that a water moving along a flowpath would evolve from a low AR-high concentration signature to a high AR-low concentration signature with increasing residence time in the aquifer. Rainwater, which is typically very dilute, will begin to leach uranium from the soil and rock materials it encounters while recharging and flowing through an aquifer. As water flows through the aquifer, its AR increases, because ^{234}U, which is produced by alpha decay, is preferentially introduced due to a process called "alpha-recoil". Alpha-recoil enrichment is the result of the alpha decay process, which damages mineral crystal lattices in which decay occurs, making decayed mineral grains more susceptible to leaching than undamaged crystal sites; in other cases, the product of a decay can be injected directly into the liquid phase (Osmond and Cowart, 1994). Kronfeld *et al.* (1994) show that the uranium concentration in an oxygenated carbonate aquifer declines as water moves along the flowpath as a result of extensive ion exchange and/or sorption reactions with the aquifer matrix, with the ion exchange scenario appearing more likely. Based on these results, uranium data from this study may be interpreted such that waters with low ARs and high concentrations have had relatively short

SE ROA 43012

periods of interaction with aquifer materials, and waters with high ARs and low concentrations have experienced relatively long periods in contact with aquifer materials.

The data shown in Figure 10 are derived from two primary areas – the lower Virgin River basin (Yelken, 1996) and the White River flow system (Farmer, 1996). Rogers and Blue Point Springs plot near members of the White River flow system, suggesting that waters from these two systems flow through rocks of similar type, and may have similar residence times. Waters in the Lower Virgin River Basin exhibit a wide rage of values, with outlier values suggesting both short and long residence times. The majority of these values are positioned so as to indicate intermediate travel times, suggesting that the springs in this region discharge waters having relatively short to intermediate residence times. These data support the classification of springs in the Virgin Mountains (Lime Kiln, Government, and Juanita Springs) as locally-derived, based on geographic considerations and stable isotope composition (Metcalf, 1995). Intermediate residence times for Petrified and Littlefield Springs (adjacent to the Virgin River, northeast of Mesquite, Nevada) support Metcalf's (1995) conclusion, based on stable isotope data, that these springs are not entirely locally-derived. The high AR of the sample from Beaver Dam Wash indicates a long residence time, suggesting that regional groundwater flow may form a significant component of baseflow to the wash.

RESULTS AND DISCUSSION

The physical, chemical, and isotopic data derived from previous studies, and collected for the present study, are compiled in Appendix A.

Spring Classification

For the purpose of the following discussion, the thirty-one springs in the Lake Mead National Recreation Area and the five nearby springs are divided into three sets based on the geographic nature of their source areas: local springs, subregional springs, and springs derived from Lake Mead water. Local springs discharge groundwater from small flow systems that receive most or all of their recharge locally and at low altitudes. Many of these local flow systems are contained entirely within the park boundaries. Subregional springs are dominated by groundwater that originates outside local topographic basins and flow systems, and may include groundwater recharged at higher altitudes. Most of the groundwater systems supplying the subregional springs extend beyond the park boundaries. In southern Nevada, a "regional" groundwater system generally denotes one that is part of the multi-basin carbonate aquifer system that extends over hundreds of kilometers. The term "subregional" is used here to avoid confusion. A third set of springs is derived from recirculated Lake Mead water.

Springs within each of the three sets share similar hydrogeologic settings and stable isotopic compositions, while discharge rates, temperatures, and tritium concentrations generally show considerable overlap. The distinct D and ^{18}O compositions of groundwater source areas and flow systems in southern Nevada makes the use of stable isotopes ideal for relating springs to their associated recharge sources. The following discussion will therefore focus on the hydrogeologic settings and the isotopic compositions of springs as they relate to spring source areas. Discussion of the uranium data, which are available only for springs in the Lake Mead basin, follows in a separate section.

Local Springs

Lake Mead Basin

Six springs in the Lake Mead basin are considered local springs (Springs 1, 15, 16, 17, 18, and 19). Other than Spring 15, these springs have the lowest discharge rates in the Lake Mead basin, and their temperatures are strongly influenced by fluctuations in ambient air temperature (Table A-1 shows the pronounced differences between temperatures measured in October and February at these springs). These springs are not related to major structural features in the region, instead issuing from stratigraphic contacts, small faults or fractures, or simply at the intersection of the water table with land surface. With the exception of Spring 1, which issues from Quaternary terrace deposits at the base of Mormon Mesa, these springs discharge from alluvium or consolidated rocks in wash channels, and all support varying degrees of vegetation at their orifices. Evapotranspiration is a major controlling factor on the flow rate from these low-discharge springs, as evidenced by the variation in discharge observed at several springs between the seasons and time of day. Although a systematic study was not possible during the present investigation, flow rates at several low-discharge springs were highest during the winter months, and in the early morning hours during the summer months, when evapotranspiration rates of the vegetation surrounding the orifice are low. Discharge rates at these same springs was observed to be lower in the middle of the day in the summer months, when evapotranspiration rates are high.

Local springs in the Lake Mead basin exhibit a mixed cation-sulfate composition (Figure 11). Despite relatively short groundwater flow paths, these springs all have TDS values that exceed 1,200 mg/L. The high sulfate and TDS concentrations both originate from solution of the evaporite minerals so ubiquitous to the Permian, Triassic, and Tertiary rocks of the Lake Mead region.

The stable isotopic compositions of Springs 1, 15, 16, 17, 18, and 19 support their geographic and geologic designations as local springs. The stable isotopic compositions resemble local, low-elevation precipitation, especially if more depleted winter precipitation (Ingraham *et al.*, 1991) is considered (Figure 12). Springs 16 and 17 are located at altitudes above regional hydraulic heads, thus they may extend our definition of local recharge to more depleted δD values of -80 per mil. Additionally, these springs are significantly enriched in heavy isotopes compared to regional groundwater, indicating no relation to groundwater flow systems outside the study area.

The recharge areas for Springs 16 and 17 lie entirely within the park boundaries, in the Black Mountains area. The other local springs in the Lake Mead basin are recharged at least in part outside the park boundaries. Springs 1 and 15 lie on or near the eastern boundary, and their recharge areas extend outside the park. Recharge to Spring 15 originates within Bitter Spring Valley and White Basin, with possible contributions from the surrounding Muddy Mountains and other nearby, low-elevation areas. The δD composition of Spring 1 (-81 per mil) falls midway between the average

SE ROA 43014

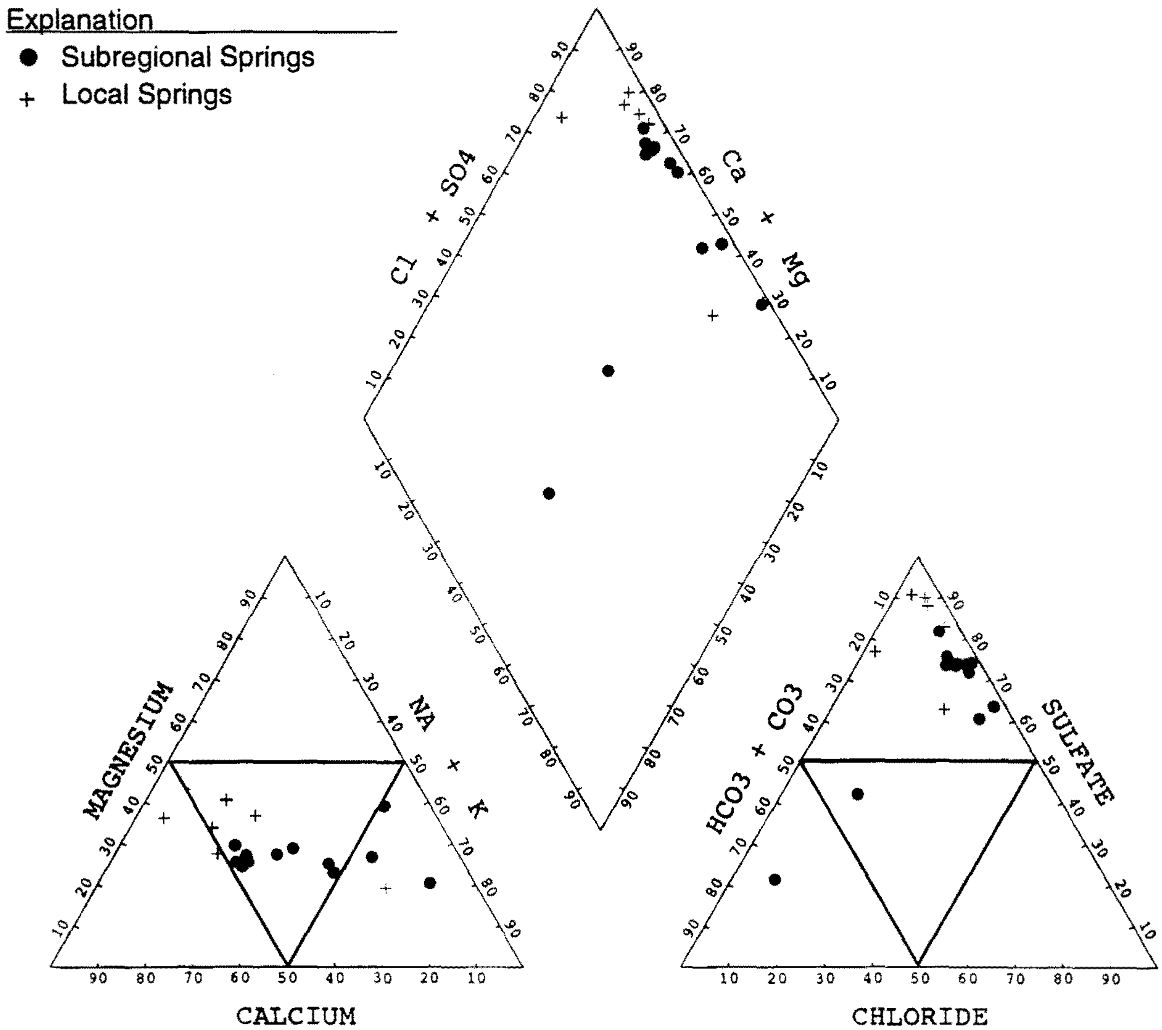

Figure 11. Trilinear diagram showing major dissolved ions of springs in the Lake Mead basin.

δD compositions of springs in the Mormon Mountains and springs in the East Mormon Mountains. Thus, it appears likely that flow from Spring 1 originates in the Mormon and East Mormon Mountains to the north, and travels through the alluvium that forms the upper portion of Mormon Mesa.

With the exception of Spring 1, local springs in the Lake Mead basin issue from alluvium or consolidated rocks in wash channels. However, the absence of atmospheric tritium indicates that groundwater travel times are long and that spring flow does not simply represent discharge of groundwater recharged during recent precipitation events.

Spring 18 appears to be controlled by the intersection of the water-bearing unit with land surface; as no structural control is evident. This spring plots in the region of low-elevation recharge which indicates that its flow originates locally. Although the elevation of the spring is lower than water levels in the carbonate aquifer to the north in Dry Lake Valley and to the west in the Las Vegas

SE ROA 43015

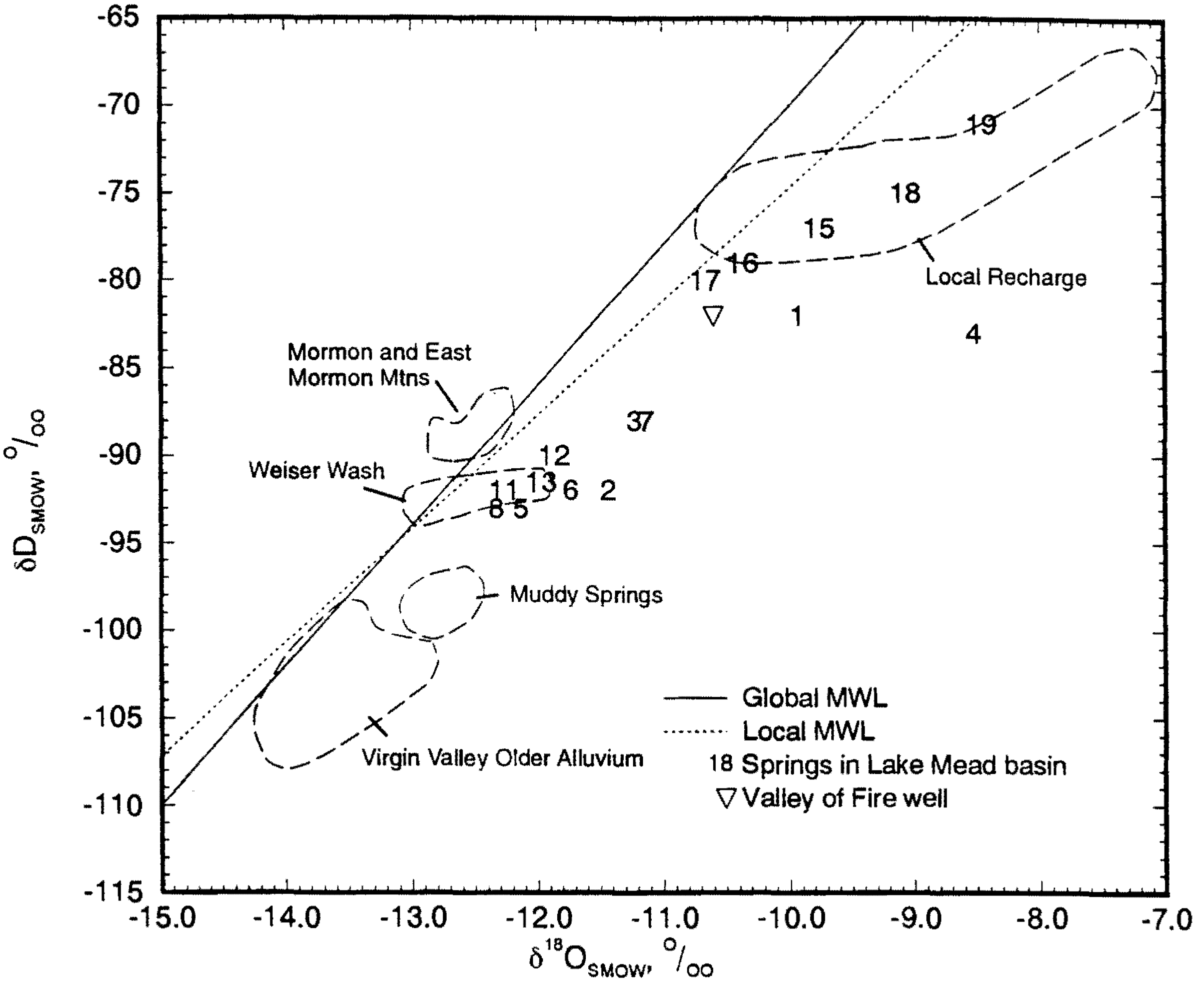

Figure 12. Stable isotopic composition of springs in the Lake Mead basin, as compared to other waters in the region.

Valley, the much more enriched δD composition of -75 per mil indicates that neither the carbonate aquifer nor Las Vegas Valley aquifers are the source.

Black Canyon

Three springs (Springs 27, 35, and 36) in the Black Canyon area are considered to be entirely of local origin. Discharge rates from these springs are less than 2 L/min, temperatures are less than 25°C, and though these springs issue from alluvium in wash channels, their flow appears to originate from small faults or fractures in the underlying rock. Springs 27 and 36 are located at altitudes above regional hydraulic head in the Black Mountains and Eldorado Mountains, respectively, and their stable isotopic compositions fall within the region of low-elevation recharge on a plot of δD as a function of $\delta^{18}O$ (Figure 13). Spring 35 is located at a much lower altitude (960 m) and might be thought to be related to subregional flow; however, the stable isotopic composition clearly indicates local origin.

SE ROA 43016

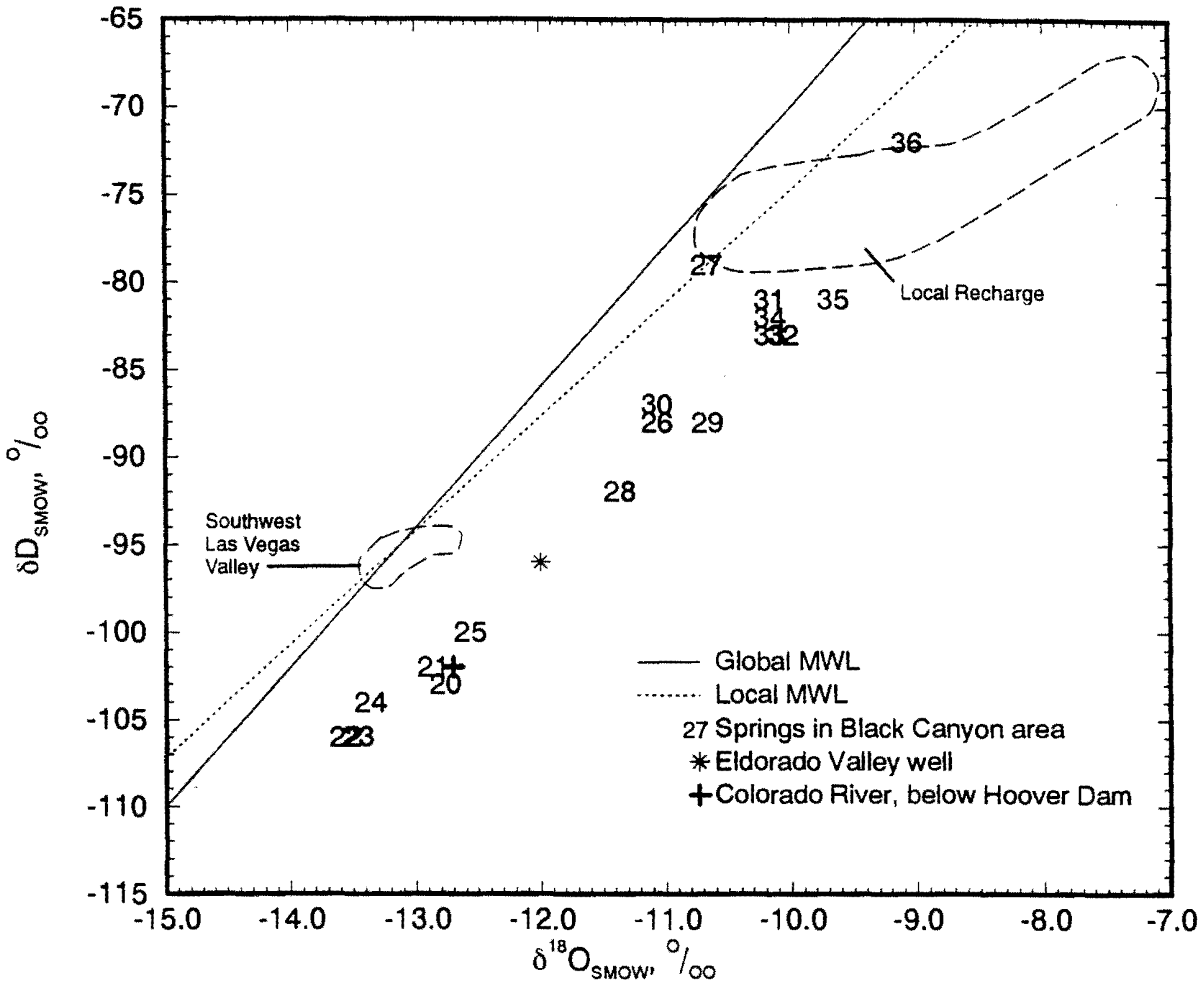

Figure 13. Stable isotopic composition of springs in the Black Canyon area, as compared to other waters in the region.

Unlike other locally-derived springs in the study area, Springs 27, 35 and 36 contain small quantities of detectable atmospheric ^3H (8.0, 8.2, and 18 pCi/L, respectively), indicating part of their discharge was recharged from precipitation after 1952. The fact that these springs contain atmospheric ^3H, while springs in the Lake Mead basin do not, may result from differences in the morphology of recharge catchment areas, and/or reflect infiltration of more recent precipitation in the alluvium upgradient of the springs. (Springs 27, 35, and 36 were sampled approximately one year after the others).

Four other springs in the Black Canyon area (Springs 31, 32, 33, and 34) are considered to be locally derived, but unlike Springs 27, 35, and 36, these springs are located in or near the bottom of Black Canyon. These springs range in distance from 6 to 11 kilometers south of Hoover Dam, and with the exception of Spring 31, issue directly from small faults in volcanic rock. Spring 31 issues from alluvium in the base of a wash channel, immediately upstream of where the channel becomes incised in volcanic bedrock. The discharge rates of these springs are higher than most of

SE ROA 43017

the other locally-derived springs in the study area, ranging from less than 1 L/min to 10.2 L/min. Temperatures also tend to be higher, ranging from 19° to 32°C, reflecting the geothermal influence of intrusive rocks in the region (McKay and Zimmerman, 1983).

Springs 31, 32, 33, and 34 have virtually identical stable isotopic compositions (Figure 13), suggesting very similar conditions of groundwater recharge, despite the fact that two of the springs are located on the east side of the Colorado River and two are located on the west. The location of these springs at low altitudes near the groundwater discharge zone of the Colorado River suggests a potential relation to subregional flow, represented on the Nevada side by Eldorado Valley groundwater, and on the Arizona side by Detrital Valley groundwater. However, their stable isotopic compositions are very similar to local, low-elevation recharge, and are much more enriched in heavy isotopes than the Eldorado Valley well sample (δD composition of -96 per mil). These springs are slightly isotopically lighter than most of the other locally-derived springs, although the δD difference between them and locally-derived Spring 27 is only 3.3 per mil. Though this could result from different conditions of recharge, mixing of local precipitation with isotopically light subregional groundwater could also account for the isotopic composition and would be consistent with these springs' elevation, temperature, and flow rates. Due to their proximity, the Eldorado Mountains and Black Mountains represent the most likely sources of local, low-elevation recharge for these springs. Recharge from the McCullough Range, or other more distance ranges appears less likely due to the absence of any evidence of mixing with subregional groundwater (e.g., Eldorado Valley).

Though Spring 34 has a $\delta^{13}C$ composition similar to that of many other springs (-7.0 per mil, indicating a dissolved carbonate mineral contribution), Springs 31 and 33 are more unique, with their lighter carbon compositions (-13.2 and -24.9 per mil, respectively) indicating less contact between the groundwater and solid carbonate phases. For Springs 31 and 33, this suggests recharge through poorly developed soil and flow through strictly igneous terrain. A $\delta^{13}C$ value is not available for Spring 32. Considering the similar geologic settings of Springs 31, 33, and 34, the differences between their $\delta^{13}C$ values are not well understood at this time.

The absence of detectable atmospheric tritium in Springs 31, 32, 33, and 34 indicate that groundwater travel times are long and that these springs do not simply represent discharge of groundwater recharged during recent precipitation events. Limited ^{14}C data confirm this, but indicate widely varying apparent ages from 1660 to 15,500 years. Groundwater travel times from recharge areas to the springs of several thousands of years are consistent with their "local" designation and the arid environment. However, the age of 15,000 years obtained for Spring 33 seems inconsistent with other evidence of local origin, and indicates a more complex hydrochemical history than assumed here.

Subregional Springs

Lake Mead Basin

The majority of the springs studied in the Lake Mead basin are considered to be subregional springs. Most of these springs are located along North Shore Road, and as a group are termed the

SE ROA 43018

North Shore Complex. These springs can be geographically divided into three areas: the Rogers/Blue Point group (consisting of Springs 8 through 14 and numerous small springs and seeps); the Valley of Fire Wash group (Springs 5, 6, and 7); and Springs 2, 3, and 4 located further to the north. Many of these springs are related to regional structural features and generally have higher discharge rates and temperatures than locally-derived springs. Furthermore, these springs have similar isotopic compositions that are distinct from the compositions of the local springs.

Springs comprising the Rogers/Blue Point group are directly related to the Rogers Spring Fault, a major strike-slip fault in the Lake Mead area. The fault separates lower Paleozoic carbonate rocks of the Muddy Mountains on the northwest from Quaternary and Tertiary basin-fill deposits on the southeast. The low permeability basin-fill deposits form a barrier to eastward groundwater flow and cause the Rogers Spring Fault to act as a conduit for upward flow from the carbonates. Springs 8, 11, 12, and 13 issue directly from the fault, and Springs 9, 10, and 14 issue from the basin fill between the fault and Lake Mead. In addition, Spring 8 is located at the point of intersection of the Rogers Spring Fault and the Arrowhead Fault. Discharge rates of 1040 and 2750 L/min from Springs 8 and 11 (respectively) are the highest in the Lake Mead basin, reflecting the role of the Rogers Spring fault as an important conduit for groundwater flow in the region.

The regional nature of these springs is also reflected in the absence of a relation between discharge and precipitation patterns. Continuous measurements of the discharge rate at Spring 11 have been collected by the U.S. Geological Survey since October 1985. A comparison of the monthly discharge at Spring 11 (U.S. Geological Survey Water-Data Reports, Water Years 1984 through 1996) and the monthly precipitation in southern Nevada (based on data from 16 low elevation stations) (National Climatic Data Center, 1997) is shown in Figure 14. There is no consistent relationship between

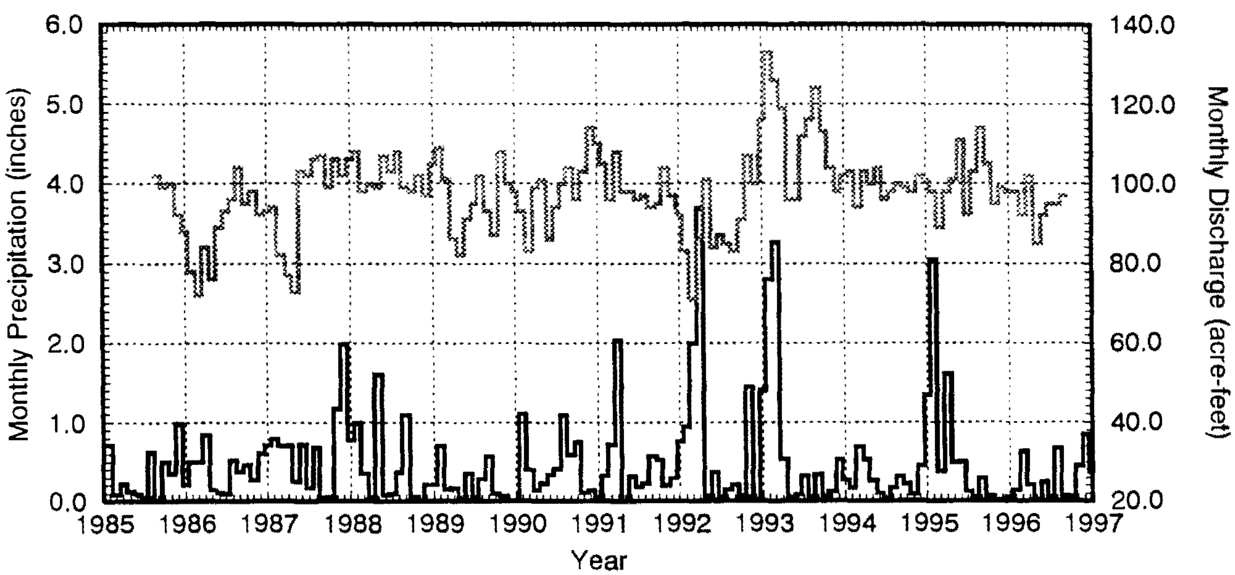

Figure 14. Comparison of monthly discharge at Spring 11 — with monthly precipitation — in southern Nevada.

SE ROA 43019

precipitation and discharge, and although precipitation is generally greatest in the winter months when groundwater recharge is expected to be greatest, there is no consistent seasonal variation in discharge rate. This evidence suggests that discharge patterns at the North Shore Springs are more strongly related to regional flow than to local groundwater recharge.

In addition to the direct discharge represented by the North Shore springs, diffuse groundwater discharge occurs by evaporation and transpiration in several areas between the Muddy Mountains and the Overton Arm. Salt crusts on the soil surface indicate that evaporation from the water table is occurring near spring orifices and along drainage channels. Transpiration is indicated by thick stands of tamarisk, mesquite, acacia, various grasses, and other vegetation surrounding spring orifices and lining drainage channels. The amount of groundwater discharged by evapotranspiration (ET) may be significant relative to surface discharge at the spring orifice. Investigation of the amount of ET in the area of each spring was beyond the scope of the present study, though there is literature that can provide insight into the magnitude of groundwater discharge by this mechanism (Ball *et al.*, 1994; Smith *et al.*, 1996).

Springs of the Valley of Fire Wash group (Springs 5, 6, and 7) do not issue directly from the Rogers Spring Fault. Instead, Springs 5 and 6 are located in the area of an unconformable contact of Jurassic and Triassic clastic rocks on the west with the Tertiary Muddy Creek Formation on the east, near the Rogers Spring Fault. The mechanism of discharge is similar in that the springs occur where eastward flowing groundwater meets a low-permeability barrier formed by the Muddy Creek Formation and is forced upward, possibly along fault planes, to discharge points at ground surface. Spring 7 issues from Quaternary Older Alluvium near an exposure of the Muddy Creek formation.

The other subregional springs (Springs 2 and 3) in the Lake Mead basin are also unrelated to major structural features. Springs 2 and 3 are located near the unconformable contact of the Tertiary Horse Spring Formation on the west with the Tertiary Muddy Springs Formation on the east. Both springs are located in wash channels that cut through Overton Ridge, at the lowest land-surface elevations just upgradient from the low-permeability barrier of the Muddy Creek Formation. Thus, if groundwater in the area is assumed to be moving generally northeast or east toward the Muddy River and Colorado River, then these springs discharge at the intersection of the water table with land surface. Spring 4 issues from a gypsum unit within the Muddy Creek Formation.

Most subregional springs in the Lake Mead basin are of the mixed cation-sulfate composition (as shown in Figure 11), which is typical of the regional groundwaters in southern Nevada discussed earlier. Exceptions are the mixed cation-bicarbonate compositions of Springs 2 and 3, which will be discussed below. The generally higher Na and K concentrations of the subregional springs distinguish them from the local springs. Despite this relationship, this pattern does not represent an evolutionary trend from local springs to subregional springs in the Lake Mead basin because groundwater flow paths do not exist between the areas of local and subregional springs.

Despite differences in major ion chemistries, subregional springs in the Lake Mead basin show remarkably similar stable isotopic compositions (Figure 12); with the exception of Spring 4, their δD compositions range from -93.5 to -88 per mil. The stable isotope values of Spring 4 are indicative

SE ROA 43020

JA_12900

of evaporation. The loose and open structure of the gypsiferous soil in the vadose zone near the spring and the high potential for evaporation from the slow moving water at the orifice suggest that significant evaporation occurs at the spring discharge point. A line extending from the subregional group to the composition of Spring 4 has a slope of about 2.6, which is consistent with kinetic isotopic enrichment during evaporation under conditions of low humidity. However, because Spring 4 issues from gypsum deposits, there is the possibility of altering the groundwater's isotopic composition by exchange and/or mixing with gypsum hydration water. Under dry conditions, gypsum can conserve its primary isotopic composition, but the exchange process is relatively rapid under wet conditions (Sofer, 1978). The effect of hydration water on groundwater composition would be a shift toward a heavier isotopic composition, reflective of the evaporated condition of the water that precipitated the gypsum. Thus, mixing with hydration water could account for the enriched composition of Spring 4, but without data on the gypsum composition, this cannot be proved. Despite their enrichment, the general coincidence of the isotopic composition of Spring 4 with other area groundwaters suggests the influence of hydration water, if any, is minimal, and that Spring 4 is subregionally-derived rather than local.

The stable isotopic compositions of the North Shore springs are isotopically lighter than locally-derived springs sampled in the Lake Mead basin, but are heavier than the regional carbonate aquifer at the terminal end of the White River Flow System (Figure 12). It is unlikely that the composition at the North Shore springs results from mixing isotopically lighter groundwater from the White River system with local, isotopically heavier groundwater because the volume of local recharge appears to be insufficient to cause the observed shift. A mixture of 75 percent groundwater having the composition of the Muddy River springs (average δD of -97.5 per mil) and 25 percent local recharge (average δD of -76 per mil) would be required to reach the composition of the North Shore springs. Twenty-five percent of the discharge of the North Shore springs is approximately 418 AFY (this value is a minimum since it does not include discharge by evapotranspiration), which is over 2.5 times larger than the amount of groundwater recharge estimated by Rush (1968) to originate from precipitation in the lower Moapa Valley, Black Mountains area (including the Muddy Mountains), and California Wash. In addition, extensive geologic evidence suggests that the Muddy River Springs form the terminus of the White River flow system (Dettinger *et al.*, 1995).

It is also unlikely that groundwater in the lower Virgin Valley is a major contributor to spring flow at the North Shore springs. Heads at the North Shore springs are higher than most of the heads measured by Metcalf (1995) in wells in the Older Alluvium in the Virgin River Valley, and higher than the altitude of the pre-Lake Mead confluence of the Muddy River and Virgin River, which lies between the Virgin Valley and the North Shore springs. Although limited to a single data point, the pre-Lake Mead hydraulic head near the confluence of the Muddy and Virgin Rivers appears to be approximately 265 m above mean sea level (Carpenter, 1915), which is 223 m below the Rogers Spring orifice. Furthermore, the Muddy Creek Formation may be more than 800 m thick below the Overton Arm and includes at least 300 m of very low permeability salt (Anderson and Laney, 1975). Finally, the limited volume of local, isotopically heavy groundwater is insufficient to cause the shift from the very light groundwater in the Older Alluvium to the composition of the North Shore Springs.

The isotopic composition of the North Shore springs is in fact very similar to basin-fill aquifers in Weiser Wash, which appear to represent a mixture of groundwater moving south from Meadow Valley with groundwater recharged in the Mormon Mountains. This groundwater is isotopically heavier than the regional carbonate aquifer because these aquifers receive recharge from precipitation at lower elevations. Not surprisingly, the range of $\delta^{13}C$ values at Springs 8 and 11 (-3.9 to -6.2 per mil; Thomas *et al.*, 1991; Hershey and Mizell, 1995) indicate interaction with carbonate rocks, since these springs issue from carbonates. The ^{14}C values range from 3.0 to 7.2 PMC, indicating a long residence time in the groundwater system and the contribution of dead carbon from rock dissolution (uncorrected ages of approximately 20,000 to 30,000 years). The absence of atmospheric tritium in any North Shore springs indicates that all the groundwater is of a pre-1952 age.

Further discussion of the springs in Magnesite Wash and Kaolin Wash (Springs 2 and 3, respectively) is necessary here. These springs are located in wash channels that cut through Overton Ridge, down-gradient from a basin in Valley of Fire State Park that is comprised of Mesozoic sandstones and covered by thick, sandy soils. The lack of vegetation in this basin suggests that precipitation may infiltrate rapidly and is not available to support plant growth. The relatively low TDS contents of these springs (462 and 626 mg/L, respectively) suggest that they may originate from local recharge with minimal chemical interaction with the aquifer matrix in the basin, which is typical of groundwater flow in quartz arenites. However, the stable isotopic composition of these springs is much lighter than local, low-elevation recharge, instead plotting with the springs in the North Shore Complex. The $\delta^{13}C$ composition of these springs (-5.0 and -6.5) falls within the range of the North Shore Complex and indicates a contribution from dissolved carbonate minerals. Furthermore, the lack of atmospheric tritium indicates the groundwater residence time is relatively long. The apparent disagreement between the local origin suggested by the geographic and geochemical evidence and the subregional origin suggested by the isotopic evidence illustrates the complex hydrogeologic setting of these springs and indicates that their origin remains uncertain. However, one possible explanation is that these springs represent discharge from a subregional system that originates in the Mormon Mountains, as discussed below.

Taken as a whole, the isotopic data suggest that groundwater discharged at the North Shore Spring Complex is recharged in the region surrounding Lake Mead and is not directly related to flow in the regional carbonate aquifer of the White River Flow System. The most likely possibilities include the Muddy Mountains and the Mormon Mountains. Recharge in the Muddy Mountains alone is insufficient to provide the volume of discharge at the North Shore Springs. Evidence indicates that recharge in the Mormon Mountains represents the most likely source for the subregional flow system that discharges at the North Shore Spring Complex. Autochthonous Paleozoic carbonate rocks, well exposed throughout the mountains, provide the point of infiltration and recharge to the carbonate aquifer system. These autochthonous carbonate rocks continue southwest and plunge below ground surface at the Muddy Mountains. The autochthonous carbonate rocks are also exposed in the North

Muddy Mountains, though at lower elevations than at the Mormon Mountains. Not until crossing the Arrowhead fault do the autochthonous carbonate rocks descend completely into the subsurface, covered by the Mesozoic clastic formations and the allochthonous Paleozoic carbonate rocks of the Muddy Mountain thrust system. The autochthonous carbonate section is exposed again south of White Basin in the ridges just north of the Black Mountains. Here, the units are topographically much higher than at the major spring discharge of the subregional system at the Rogers/Blue Point complex.

The only structural obstruction in this flow path might occur near Glendale, just north of the North Muddy Mountains. It has been postulated that a strike-slip fault, the Moapa shear zone, separates the Mormon Mountains from the Virgin River depression to the south (Wernicke *et al.*, 1988). Whereas a major fault does separate the Mormon Mountains from the Tertiary sediments of the Virgin River depression, Anderson and Bernhard (1993) argue against a major through-going fault separating the North Muddy Mountains from the Mormon Mountains. The existence of this flow path is supported by evidence of groundwater discharge to the Muddy River reported by Rush (1968) in the reach passing through The Narrows at the northern edge of the North Muddy Mountains. This discharge indicates the presence of significant flow through the carbonate rocks between the Mormon and North Muddy Mountains, with upward flow occurring at favorable locations where overlying rocks are thin. Further evidence of this flow path may be provided by springs in Overton Ridge (Springs 2 and 3), that are located between The Narrows and the North Shore springs, are slightly lower in elevation than The Narrows, and have stable isotopic compositions indicative of subregional flow. Finally, the consistency of stable isotopic signatures of groundwater in the Mormon Mountains, Weiser Wash, Overton Ridge, and the North Shore Spring Complex indicate no major structural obstruction of the groundwater system's flow path until its primary discharge at the Rogers Spring Fault.

Black Canyon

In Black Canyon, Springs 26, 28, 29, and 30 are classified as subregional springs. Though these springs have widely varying temperatures (13° to 55°C) and discharge rates (13.2 to 960 L/min), their stable isotopic compositions are similar (as shown in Figure 13) and indicative of a common origin. In addition, these springs all possess a similar sodium and potassium-chloride composition (Figure 15), suggesting that their flow passes through rocks of similar minerology. Springs 26 and 30 issue from Tertiary volcanic rocks near northwest trending, right lateral strike-slip faults. Springs 28 and 29 issue from the Miocene Boulder City pluton at points where near vertical, north-south-trending faults intersect from below an unconformable barrier. This unconformity appears to act as a "ceiling", preventing further upward flow within the plutonic rocks.

The stable isotopic composition of Springs 26, 28, 29, and 30 is approximately midway between the end member compositions of subregional groundwater in Eldorado Valley, and local, low-elevation recharge. Note that using the Eldorado Valley water as an end-member is highly uncertain for the following reasons: only one sample is available from this basin; there are few data available from other, nearby deep basins; and there are no data from Arizona. Though Lake Mead

SE ROA 43023

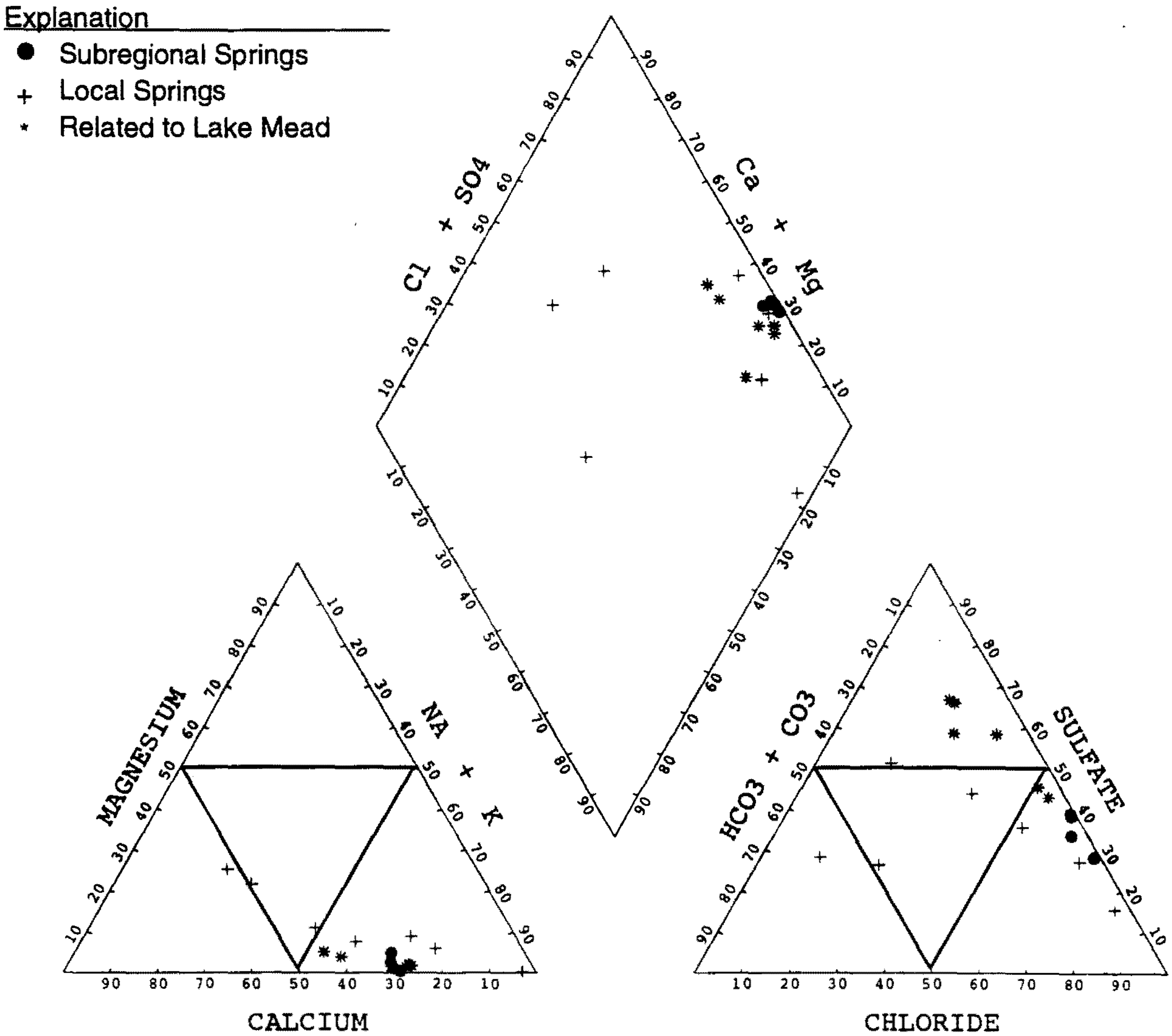

Figure 15. Trilinear diagram showing major dissolved ions of springs in the Black Canyon area.

water also represents a possible stable isotope end-member, Springs 26, 28, 29, and 30 can be distinguished from the springs affected by Lake Mead water by the following: with the exception of Spring 26, they contain no atmospheric tritium (the tritium content of Spring 26 is 21 pCi/L); they have TDS concentrations over 2000 mg/L; and they are at least 10 per mil enriched in δD with respect to springs located near the dam. Therefore, it appears unlikely that these springs are influenced by groundwater originating from Lake Mead.

Springs Influenced by Lake Mead Water

McKay and Zimmerman (1983) use environmental isotopes and water chemistry to demonstrate the hydraulic connection between Lake Mead and thermal springs in Black Canyon. Additional data collected for the present study confirm many of those results, and provide for some further refinement. Springs near Hoover Dam (Springs 20, 21, 22, 23, 24, and 25) share several

SE ROA 43024

physical, geochemical, and isotopic properties: They tend to have the highest discharge rates and the highest temperatures (32° to 58°C) of springs in Black Canyon. Additionally, the TDS contents more closely resemble Colorado River water than other high discharge, subregional springs. The high discharge rates of many of the Black Canyon springs appear to result from the large hydraulic gradient imposed on the system by the altitude of the surface of Lake Mead, which is approximately 166 m above the river. The high temperatures reflect circulation near the Boulder City pluton. The temperature of Spring 20 is significantly lower than the others. This spring is closest to the dam, and the lower temperature may reflect less contact with the pluton than the other springs.

Springs near Hoover Dam also have the highest tritium activities (72 to 148 pCi/L) and the lightest $\delta^{18}O$ and δD values (δD of -106 to -100 per mil) (Figure 13). The high tritium activities indicate post-1952 groundwater recharge (a sample from the Colorado River on February 11, 1997 had a tritium activity of 51 pCi/L). The stable isotopes reflect the influence of Lake Mead water (a sample from the Colorado River on February 11, 1997 water had a δD content of -102 per mil). McKay and Zimmerman postulate a decreasing influence of the lake downstream, although they state that it is likely that all the springs in Black Canyon are influenced to some degree by Lake Mead. However, the tritium and stable isotope data collected during the present study suggest that the influence of Lake Mead water appears to end at a distance beyond Spring 25, which is 2.4 km downstream from the dam (Figure 16). Lake Mead water does not appear to impact Spring 26, which is within several hundred meters of Spring 25, is 35°C cooler, and is much more isotopically enriched. This suggests very different flow paths and/or origins for these two springs. Spring 26 is considered a subregional spring, as discussed above.

Uranium Signatures

The uranium data gathered for this study are shown, along with pertinent data from other sources, in Figure 17. The springs shown in this plot can be divided into two major groups – one with high uranium concentrations and low activity ratios (Springs 4, 15, 16, 17, 18, 19, and 36), the other with higher ARs, but generally lower uranium concentrations than the first group (Springs 1, 2, 3, 6, 7, and 11). The uranium signature of the first group suggests residence times which are relatively short, as relatively little leaching has taken place. The second group appears to have had a longer residence time, as increased leaching has caused a shift in the U signatures to a higher AR, with lower concentration. One obvious explanation for the different uranium signatures relates to the source area for any given spring – water discharging from springs which have a local source would have relatively short flowpaths, while water discharging from springs which have source areas outside local basins would typically require a longer transport time from recharge to discharge. Thus, locally-derived springs would display low activity ratios and high concentrations, and regional springs would display high ARs and low concentrations.

The springs that exhibit high concentrations and low ARs share similar uranium isotope signatures with locally-derived springs in the Virgin Mountains (the lower most triangles in Figure 17). With the exception of Spring 4, the uranium isotope signature of these springs supports their geographic and stable isotope designation as local springs. The stable isotope data suggests Spring 4

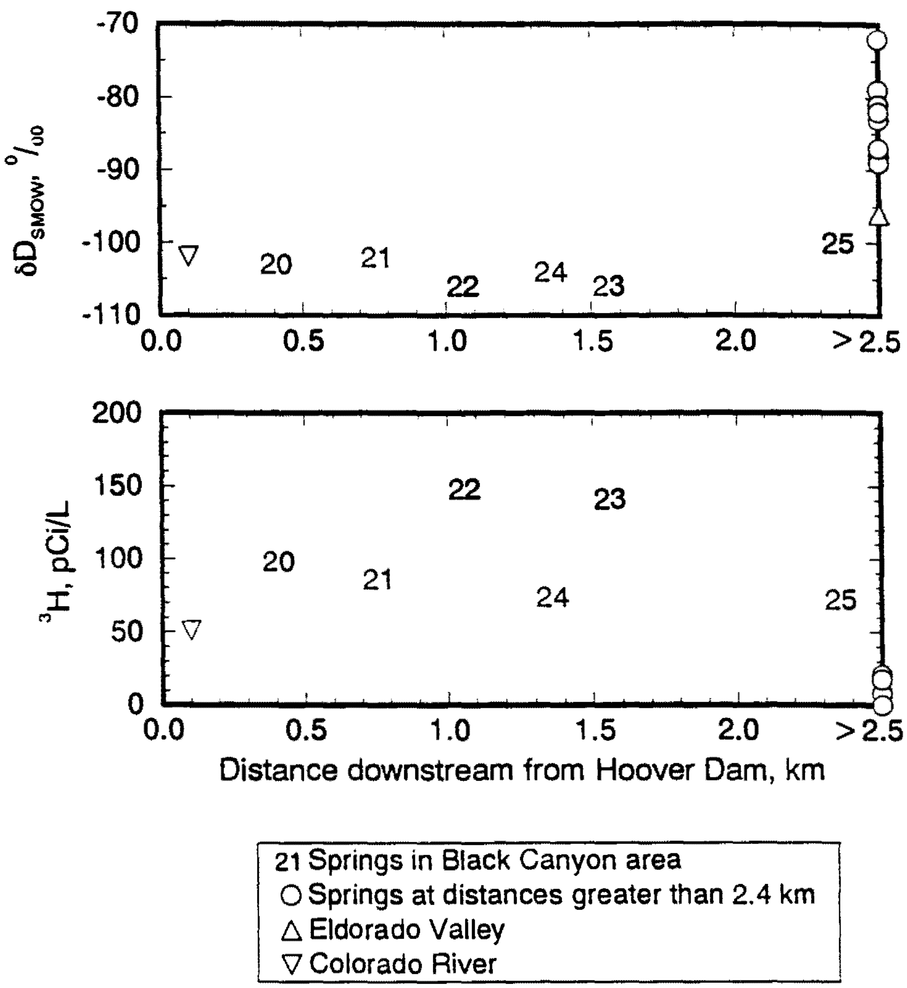

Figure 16. Plot of δD and ^3H as a function of distance downstream from Hoover Dam.

is derived from flow outside the local basin and that the discharge has been subjected to evaporation, as discussed above. The uranium isotope signature of the other group of springs is indicative of longer residence times, and supports their designation as subregional springs based on geographic and geologic settings and the stable isotopic data. For the most part, these springs have lower ARs than other regional springs in southern Nevada and southwestern Utah for which data are available. Although regional data for uranium are not as abundant as data for stable isotopes, the recent studies by Farmer (1996) and Yelken (1996) may be indicative of broader awareness and acceptance of uranium-series disequilibrium as an interpretive tool for investigating groundwater flow in southern Nevada. If this is the case, further interpretation of spring sources and water evolution along flowpaths will be possible as the regional uranium database grows.

For springs in the Valley of Fire Wash group, the uranium data may provide additional insight into flow patterns delineated using stable isotope data. Stable isotope data in non-geothermal systems provides information on initial recharge conditions and any subsequent

SE ROA 43026

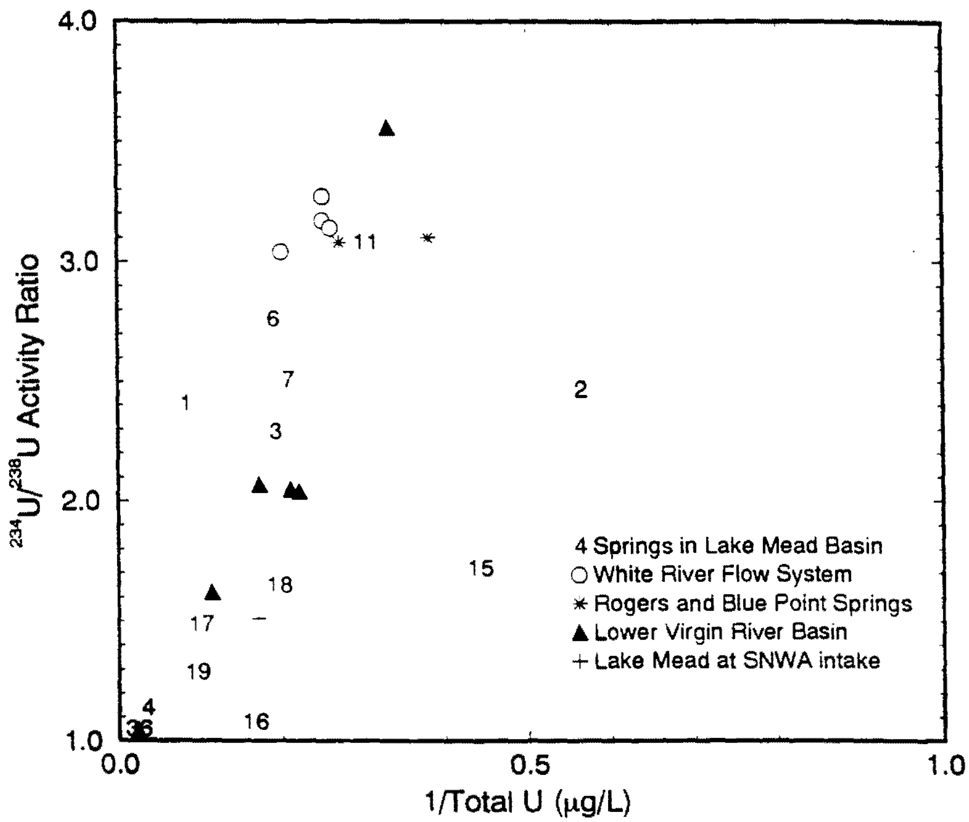

Figure 17. Uranium composition of springs in the Lake Mead basin, as compared to other waters in the region.

evaporation, but typically are not affected by water-rock interaction. Uranium isotope values can change as water moves along a flowpath and evolves due to interaction with aquifer materials.

Springs 6 and 7, which plot together with the Rogers/Blue Point group on the stable isotope graph, exhibit lower activity ratios and slightly higher concentrations than do Rogers and Blue Point springs. This may be suggestive of mixing between a lower-concentration, higher-AR water (discharge at Rogers and Blue Point springs) and a water which is leaching a "fresher" source of uranium. Water flowing through a rock body which has had less leaching take place would tend to provide a higher uranium concentration, but a lower AR than a water interacting with a more highly leached rock body (Osmond and Cowart, 1992). Perhaps, then, the springs in Valley of Fire Wash share a common water source with Rogers and Blue Point Springs, but are more recent in origin.

The uranium signature for Spring 2 indicates a significantly lower concentration than the North Shore Complex springs, to which it is related by location and stable isotope signature. Since evaporation is not apparent in the stable isotope data, the two most likely explanations for the uranium signature are either dilution at some point along the flowpath for this spring, or flow toward other springs in the group passing through a localized area of anomalously high uranium concentration.

SE ROA 43027

JA_12907

CONCLUSIONS

Thirty-six springs in and around the Overton Arm, Boulder Basin, and Black Canyon areas of the Lake Mead National Recreation Area were visited and described. Historical data, which generally included discharge measurements, chemical indicator measurements, and water chemistry analyses, were compiled and supplemented by stable and radioactive isotopic data collected during the present study.

Three classifications of source area have been defined for the springs, primarily based on hydrogeologic setting and the stable isotopic data. Distinguishing characteristics of these three classifications, and the springs included in each, are listed in Table 3.

Table 3. Characteristics of the Three Spring Classifications Defined by this Study, and the Springs Included in Each.

	Local	Subregional	Lake Mead
Geologic Setting	Generally not related to regional structural features.	Often related to regional structural features such as faults.	Related to normal faulting around Boulder City pluton.
Discharge Rate	Less than 20 L/min, most less than 3 L/min	1 to 2750 L/min	10 to 1540 L/min
Temperature	10 to 25°C	15 to 30°C	32 to 58°C
δD	-67 to -80 per mil	-88 to -93 per mil	-106 to -100 per mil
^3H	Less than 5 to 18 pCi/L	Less than 5 pCi/L	74 to 141 pCi/L
Uranium Activity Ratio	Less than 2.0	Greater than 2.0	—
Spring Name and ID	Kelsey (1) Bitter (15) Sandstone (16) Cottonwood (17) Gypsum (18) Unnamed, in Rainbow Gardens (19) Unnamed, in Horsethief Canyon (27) Unnamed, near Spring 30 (31) Nevada Falls (32) Bighorn Sheep (33) Arizona Seep (34) Latos Pool (35) Unnamed, in Aztec Wash (36)	Unnamed, in Magnesite Wash (2) Unnamed, in Kaolin Wash (3) Getchel (4) Unnamed, in Valley of Fire Wash (5) Unnamed, in Valley of Fire Wash (6) Unnamed, in Valley of Fire Wash (7) Blue Point (8) Unnamed (9) Unnamed (10) Rogers (11) Scirpus (12) Corral (13) Unnamed (14) Palm Tree, Cold (26) Boy Scout Canyon, Hot (28) Boy Scout Canyon, Cold (29) Arizona Hot Spring (30)	Pupfish (20) Arizona Hot Spot (21) Sauna Cave (22) Nevada Hot Spring (23) Nevada Hot Spot (24) Palm Tree, Hot (25)

Almost one third of the springs studied are considered to be of local origin. Locally-derived springs discharge groundwater from small flow systems that receive most or all of their recharge

SE ROA 43028

locally and at low altitudes. These springs are generally not related to major structural features, instead discharging from small fractures or joints, or the bottoms of wash channels. The low discharge rates of local springs result from the limited groundwater recharge that occurs at low elevations in this arid region. Temperatures are lower than the other springs because of rapid equilibration of the low volume discharge with ambient land surface and air temperatures, and because groundwater does not circulate to great depths. The stable isotopic values are indicative of low-elevation recharge in southern Nevada. Low uranium activity ratios and relatively higher uranium concentrations are indicative of relatively short residence times, which generally result from shorter flow paths, and support the designation of these springs as locally derived. Despite their local origin, however, non-detectable to very low tritium concentrations suggest travel times longer than several decades and very limited recharge by recent precipitation events.

Local springs are unrelated to regional groundwater flow systems such as the carbonate aquifer system. For springs in the Lake Mead basin, recharge occurs in the Black Mountains, Bitter Spring Valley (and possibly the slopes of surrounding ridges), and the area surrounding Rainbow Gardens. Local springs in Black Canyon originate from recharge in the Black Mountains and Eldorado Mountains. Most of the local springs in the recreation area discharge from localized groundwater flow systems that are contained within the park boundaries. Although the Maxey-Eakin method predicts that groundwater recharge is neglibible at low elevations in southern Nevada, the existence of these springs indicates that certain geologic, topographic, climatic, and hydrologic conditions can combine to produce local flow systems that are capable of supplying perennial springs. The small sizes of these flow systems, which suggests that their groundwater storage potential is small, means that locally-derived springs are more sensitive to local climate and recharge conditions than the larger, subregional springs, and therefore may require special management and protection.

Subregional springs are dominated by groundwater that originates outside local flow systems, and therefore outside the recreation area, and may include groundwater recharged at higher elevations. The locations of subregional springs are often related to major, regional structural features. Most of the subregional springs in the Lake Mead basin (the Rogers/Blue Point and Valley of Fire Wash groups) are related to the Lake Mead strike/slip fault system, while most of the subregional springs in the Black Canyon area are related to a system of north-south-trending normal faults. Most of these springs represent the ultimate discharge of subregional groundwater flow systems and therefore have higher discharge rates than the local springs. Their higher temperatures result from deeper circulation and less equilibrium with ambient land surface and air temperatures. The stable isotopic values are indicative of higher elevation recharge sources than most of the region surrounding Lake Mead. Non-detectable tritium concentrations and low percentages of modern carbon indicate that these waters have long residence times. Higher uranium activity ratios are indicative of longer residence times, and generally longer groundwater flow paths, where the water has more time in contact with the rock.

Subregional springs in the Lake Mead basin appear to be most strongly related to groundwater systems that extend north to the Weiser Wash and Mormon Mountains area, rather than to the regional White River Flow System or Virgin River basin. Subregional springs in the Black Canyon area appear to originate from a mixture of subregional flow (e.g., Eldorado Valley in Nevada, possibly Detrital Valley in Arizona) and local, low-elevation recharge in the Black Mountains and Eldorado Mountains. The subregional origin of these springs suggests that they may be more sensitive than previously thought to groundwater impacts in the areas adjacent to the park.

A third set of springs is derived from recirculated Lake Mead water, as first described by McKay and Zimmerman (1983). These springs are related to normal faulting around the Boulder City pluton, which provides the heat source for their high temperatures. The high discharge rates exhibited by several of these springs probably relate to the very high gradient of hydraulic head that results from the impoundment of Lake Mead by Hoover Dam. The stable isotope values form a range around the present composition of the Colorado River, implicating it as the most probable source. In addition, the tritium contents of these springs indicates that at least a portion of these waters were recharged after 1952.

REFERENCES

Anderson, R.E., T.P. Barnhard and L.W. Snee, 1994. Roles of plutonism, midcrustal flow, tectonic rafting, and horizontal collapse in shaping the Miocene strain field of the Lake Mead area, Nevada and Arizona. *Tectonics*, vol. 13, no. 6, pp. 1381-1410.

Anderson, R.E. and T.P. Bernhard, 1993. Heterogeneous strain and its bearing on horizontal extension and horizontal and vertical contraction at the margin of the extensional orogen, Mormon Mountains area, Nevada and Utah. U.S. Geological Survey Bull. 2001, 43 p.

Anderson, R.E., T.P. Barnhard and L.W. Snee, 1984. Roles of plutonism, midcrustal flow, tectonic rafting, and horizontal collapse in shaping the Miocene strain field of the Lake Mead area, Nevada and Arizona. *Tectonics*, vol. 13, no. 6, pp.1381-1410.

Anderson, R.E., 1978. Geologic Map of the Black Canyon 15 Minute Quadrangle, Mohave County, Arizona, and Clark County, Nevada. U.S. Geological Survey GQ-1394.

Anderson, R.E. and R.L. Laney, 1975. The Influence of Late Cenozoic Stratigraphy on Distribution of Impoundment-Related Seismicity at Lake Mead, Nevada-Arizona. *Journal of Research*, U.S. Geological Survey, 3(3), pp. 337-343.

Anderson, R.E., 1973. Large-Magnitude Late Tertiary Strike-Slip Faulting North of Lake Mead, Nevada. U.S. Geological Survey Professional Paper 794, 18 p.

Anderson, R.E., 1971. Thin skin distention in Tertiary rocks of southeastern Nevada. *Geol. Soc. of America Bulletin*, vol. 82, pp. 43-58.

Anderson, RE., 1969. Notes on the Geology and Paleohydrology of the Boulder City Pluton, Southern Nevada. U.S. Geological Survey Professional Paper 650-B, pp. B35-B40.

Ball, J.T., J.B. Picone and P. Ross, 1994. Evapotranspiration by Riparian Vegetation along the Lower Colorado River. Desert Research Institute, Biological Sciences Center, prepared for the U.S. Bureau of Reclamation, Contract No. 1-CP-30-08910, 188 p.

Bedinger, M.S., T.W. Anderson and W.H. Langer, 1984. Maps Showing Ground-Water Units and Withdrawal, Basin and Range Province, Arizona. U.S. Geological Survey Water-Resources Investigation Report 83-4114-A.

Bell, J.W., 1980. Geologic Map of the Henderson Quadrangle, Nevada. Nevada Bureau Mines and Geology Map 67.

Bohannon, R.G., 1984. Nonmarine Sedimentary Rocks of Tertiary Age in the Lake Mead Region, Southeastern Nevada and Northwestern Arizona. U.S. Geological Survey Professional Paper 1259.

Bohannon, R.G., 1983. Geologic map, tectonic map and structure sections of the Muddy and northern Black Mountains, Clark County, Nevada. U.S. Geological Survey Misc. Investigations Series, Map I-1406.

Bohannon, R.G., 1978. Preliminary geologic map of the Las Vegas 1° x 2° quadrangle, Nevada, Arizona, and California. U.S. Geological Survey Open-File Report 78-670.

Bunch, R.L. and J.R. Harrill, 1984. Compilation of Selected Hydrologic Data from the MX Missile-Siting Investigation, East-Central Nevada and Western Utah. U.S. Geological Survey Open-File Report, 84-702, 123 p.

Buqo, T.S., 1993. Results of Phase One Testing of the Arrow Canyon Well. Thomas S. Buqo, Consulting Hydrogeologist, prepared for Moapa Valley Water District, 25 p.

Cakir, M., 1990. Deformation Around the Intersection of the Las Vegas Shear Zone and the Lake Mead Fault System, SE Nevada. M.S. thesis, Purdue University, West Lafayette, Ind.

Campagna, D.J. and A. Aydin, 1994. Basin genesis associated with strike-slip faulting in the Basin and Range, southeastern Nevada. *Tectonics*, vol. 13, no. 2, pp. 327-341.

Carpenter, E., 1915. Ground water in southeastern Nevada. U.S. Geological Survey Water Supply Paper 365, 86 p.

Cowart, J.B., 1979. Uranium isotopes in the Paleozoic carbonate aquifer of south central Nevada and adjacent California. Geological Society of America, Abstracts with Program, vol. 11, no.7, 405 p.

Craig, H., 1961. Isotopic Variations in Meteoric Waters. *Science*, vol. 133, pp. 1702-1703.

Dettinger, M.D., J.R. Harrill, D.L. Schmidt and J.W. Hess, 1995. Distribution of Carbonate-Rock Aquifers and the Potential for their Development, Southern Nevada and Adjacent Parts of California, Arizona, and Utah. U.S. Geological Survey Water-Resources Investigations Report 91-4146.

Dettinger, M.D., 1989. Distribution of Carbonate-Rock Aquifers in Southern Nevada and the Potential for Their Development – Summary of Findings, 1985-88. Carson City, Nevada, Program for the Study and Testing of Carbonate-Rock Aquifers in Eastern and Southern Nevada, Summary Report no. 1, 37 p.

Duebendorfer, E.M. and E.T. Wallin, 1991. Basin development and syntectonic sedimentation associated with kinematically coupled strike-slip and detachment faulting, southern Nevada. *Geology*, 19, pp. 87-90.

Eakin, T.E., 1968. A Regional Interbasin Groundwater System in the White River Area, Southeastern Nevada. *Water Resources Research*, vol. 2, pp. 251-271.

Eakin, T.E., 1966. A Regional Interbasin Groundwater System in the White River Area, Southeastern Nevada. Nevada Department of Conservation and Natural Resources. Water Resources Bulletin no. 33, pp. 251-271.

Eakin, T.E., 1964. Ground-Water Appraisal of Coyote Spring and Kane Spring Valleys and Muddy River Springs Area, Lincoln and Clark Counties, Nevada. Ground-Water Resources – Reconnaissance Series Report 25, 40 p.

Farmer, D.E., 1996. Investigation of Regional Flow Patterns in the Ash Meadows Ground-water Basin of Southern Nevada Using Uranium Isotope Ratios. Unpublished M.S. Thesis, Department of Geoscience, University of Nevada, Las Vegas, 142 p.

French, R.H., 1983. A Preliminary Analysis of Precipitation in Southern Nevada. Desert Research Institute, Water Resources Center, Publication #45031, 39 p.

Friedman, I., G.I. Smith, J.D. Gleason, A. Warden and J.M. Harris, 1992. Stable isotope composition of waters in southeastern California: Part 1, Modern precipitation. *J. Geophys. Res.*, vol. 97, no. D5.

Gascoyne, M., 1992. *Geochemistry of the Actinides and their Daughters, in Uranium Series Disequilibrium: Applications to Earth, Marine, and Environmental Sciences*. 2nd ed. Eds. M. Ivanoritch and R.S. Harmon, Oxford University Press, New York.

Glancy, P.A. and A.S. Van Denburgh, 1969. Water-Resources Appraisal of the Lower Virgin River Valley Area, Nevada, Arizona, and Utah. Nevada Division of Water Resources, Reconnaissance Report 51, 87 p.

Harrill, J.R., J.S. Gates and J.M. Thomas, 1988. Major Ground-Water Flow Systems in the Great Basin Region of Nevada, Utah, and Adjacent States. U.S. Geological Survey Hydrologic Investigations Atlas HA-694-C.

Harrill, J.R., 1976. Pumping and ground-water storage depletion in Las Vegas Valley, Nevada, 1955-74. Nevada Division of Water Resources, Bulletin 44, 70 p.

Hershey, R.L. and S.A. Mizell, 1995. Water Chemistry of Spring Discharge from the Carbonate-Rock Province of Nevada and California – Volume 1. Desert Research Institute, Water Resources Center, Publication #41040, 119 p.

Hess, J.W. and M.D. Mifflin, 1978. A Feasibility Study of Water Production from Deep Carbonate Aquifers in Nevada. Desert Research Institute, Water Resources Center, Publication #41054, 125 p.

Ingraham, N.L., B.F. Lyles, R.L. Jacobson and J.W. Hess, 1991. Stable isotope study of precipitation and spring discharge in southern Nevada, *J. Hydrol.*, 125, pp. 243-258.

Kirk, S.T. and M.E. Campana, 1988. Simulation of Groundwater Flow in a Regional Carbonate-Alluvial System with Sparse Data: The White River Flow System, Southeastern Nevada. Desert Research Institute, Water Resources Center, DRI-41115, 76 p.

Kronfeld, J., J.C. Vogel and A.S. Talma, 1994. A new explanation for extreme $^{234}U/^{238}U$ disequilibria in a dolomitic aquifer. *Earth and Planetary Science Letters*, vol. 123, pp. 81-93.

Laney, R.L. and J.T. Bales, 1996. Geohydrologic Reconnaissance of Lake Mead National Recreation Area – Las Vegas Wash to Virgin River, Nevada. U.S. Geological Survey, Water-Resources Investigations Report 96-4033, 44 p.

Laney, R.L., 1981. Geohydrologic Reconnaissance of the Lake Mead National Recreation Area – Las Vegas, Wash to Opal Mountain. U.S. Geological Survey Open-File Report 82-115.

Longwell, C.R., E.H. Pampeyan, B. Bowyer and R.J. Roberts, 1965. Geology and Mineral Deposits of Clark County, Nevada. Nevada Bureau of Mines, Bulletin 62, 218 p.

Longwell, C.R., 1963. Reconnaissance geology between Lake Mead and Davis Dam, Arizona-Nevada. U.S. Geological Survey Professional Paper 374-E, 51 p.

Longwell, C.R., 1960. Possible explanation of diverse structural patterns in southern Nevada. *Am. J. Sci*, 258-A, pp. 192-203.

Longwell, C.R., 1936. Geology of the Boulder Reservoir floor. *Geol. Soc. of America Bulletin*, vol. 47, pp. 1393-1476.

Longwell, C.R., 1922. Muddy Mountain overthrust in southeastern Nevada. *J. Geol.*, 30, pp. 63-72.

Lyles, B.F., R.L. Jacobson and J.W. Hess, 1987. Reconnaissance of Groundwater Quality in Trace Element Analysis of Selected Springs in the Virgin River Basin Southern Nevada. Desert Research Institute, Water Resources Center, Publication #41101, 83 p.

Malmberg, G.T., 1961. A Summary of the Hydrology of the Las Vegas Valley Ground-Water Basin, with special reference to the available supply. State of Nevada, Office of the State Engineer, Water Resources Bulletin 18, 23 p.

Maxey, G.B., A.L. Mindling and P.A. Domenico, 1966. Ground Water in the Upper Muddy River Basin. Desert Research Institute, Water Resources Center, DRI-44003, 24 p.

Maxey, G.B. and M.D. Mifflin, 1966. Occurrence and movement of ground water in carbonate rocks of Nevada. *National Speleological Society Bulletin*, vol. 28, pp. 141-157.

Maxey, G.B. and T.E. Eakin, 1949. Ground Water in White River Valley, White Pine, Nye, and Lincoln Counties, Nevada. State of Nevada, Office of the State Engineer, Water Resources Bulletin 8, 59 p.

Maxey, G.B. and T.W. Robinson, 1947. Ground Water in Las Vegas, Pahrump, and Indian Spring Valleys, Nevada – A Summary. State of Nevada, Office of the State Engineer, Water Resources Bulletin 6, 23 p.

Mazor, E., 1997. *Chemical and Isotopic Groundwater Hydrology.* 2nd ed. Marcel Dekker, Inc., New York, 413 p.

McKay, W.A. and D.E. Zimmerman, 1983. Hydrogeochemical Investigation of Thermal Springs in the Black Canyon – Hoover Dam Area, Nevada and Arizona. Desert Research Institute, Water Resources Center, Publication #41092, 40 p.

Metcalf, L., 1995. Ground Water – Surface Water Interactions in the Lower Virgin River Area. Unpublished M.S. Thesis, Department of Geoscience. University of Nevada. Las Vegas, 181 p.

Mifflin, M.D., 1968. Delineation of Ground-Water Flow Systems in Nevada. Desert Research Institute, Water Resources Center, Technical Report Series H-W, Publication #4, 110 p.

Mills, J.G., Jr., 1994. Geologic map of the Hoover Dam Quadrangle, Arizona and Nevada. Nevada Bureau of Mines and Geology, Map 102.

Mook, W.G., 1980. Carbon-14 in hydrogeological studies. *In* Handbook of Environmental Isotopes Geochemistry: Vol. 1., Eds. P. Fritz and J.Ch. Fontes, Elsevier Pub. Co., Amsterdam, pp. 49-71.

Morgan, D.S. and M.D. Dettinger, 1994. Ground-Water Conditions in Las Vegas Valley, Clark County, Nevada – Part II, Geohydrology and Simulation of Ground-Water Flow. U.S. Geological Survey Open-File Report 90-179, 151 p.

National Climatic Data Center, 1997. CLIMVIS Information [Online]. Available: www.ncdc.noaa.gov/onlineprod/drought/xmgrgl.html.

Osmond, J.K. and J.B. Cowart, 1992. Ground Water. *In* Uranium Series Disequilibrium: Applications to Earth, Marine, and Environmental Sciences. 2nd ed. Eds. M. Ivanovitch and R.S. Harmon, Oxford University Press, New York.

Osmond, J.K. and J.B. Cowart, 1976. The theory and uses of natural uranium isotopic variations in hydrology. *Atomic Energy Review*, 14(4), pp. 621-679.

Osmond, J.K., H.S. Rydell and M.I. Kaufman, 1968. Uranium Disequilibrium in Groundwater: An Isotope Dilution Approach in Hydrologic Investigations. *Science*, vol. 162, pp. 997-999.

Plume, R.W. and S.M. Carlson, 1988. Hydrogeology of the Great Basin region of Nevada, Utah, and adjacent states. U.S. Geological Survey Hydrologic Investigations Atlas HA-694-A.

Prudic, D.E., J.R. Harrill and T.J. Burbey, 1993. Conceptual Evaluation of Regional Ground-Water Flow in the Carbonate Rock Province of the Great Basin, Nevada, Utah, and Adjacent States. U.S. Geological Survey Open-File Report 93-17D, 103 p.

Quiring, R.F., 1965. Annual Precipitation as a Function of Elevation in Nevada South of 38 1/2 Degrees Latitude. U.S. Weather Bureau Research Station, Las Vegas, Nevada. Prepared for U.S. Geological Survey, 14 p.

Raker, S.L. and R.L. Jacobson, 1987. Chemistry of Groundwater in Tuffaceous Rocks, Central Nevada. Desert Research Institute, Water Resources Center, Prepared for Nevada Nuclear Waste Project Office, NWPO-TR-006-87, 111 p.

Reynolds, S.J., 1988. Geologic map of Arizona. Arizona Geological Survey Map 26.

Roether, W., 1967. Estimating Tritium Input to Groundwater from Wine Samples: Groundwater and Direct Run-Off Contribution to Central European Surface Waters. *In* Isotopes in Hydrology: Proceedings of a Symposium, Vienna, 14-18 November, 1966, International Atomic Energy Agency, Vienna.

Rush, F.E., 1968. Water-Resources Appraisal of the Lower Moapa-Lake Mead Area, Clark County, Nevada. State of Nevada, Department of Conservation and Natural Resources, Water Resources –Reconnaissance Series, Report 50.

Rush, F.E. and C.J. Huxel, 1966. Groundwater Appraisal of the Eldorado-Piute Valley Area, Nevada and California. State of Nevada, Department of Conservation and Natural Resources, Water Resources – Reconnaissance Series, Report 36.

Schroth, B.K., 1987. Water Chemistry Reconnaissance and Geochemical Modeling in the Meadow Valley Wash Area, Southern Nevada. Unpublished M.S. Thesis, University of Nevada, Reno, 97 p.

Smith, G.I., I. Friedman, J.D. Gleason and A. Warden, 1992. Stable isotope composition of waters in southeastern California: Part 2, Groundwaters and their relation to modern precipitation. *J. Geophys. Res.*, vol. 97, no. D5, pp. 5813-5823.

Smith, S.D., A. Sala, D.A. Devitt and J.R. Cleverly, 1996. Evapotranspiration from a saltcedar-dominated desert floodplain: A scaling approach. *In* Proceedings of the Symposium on Shrubland Ecosystem Dynmaics in a Changing Climate, May 1995, Eds. N.M. Las Cruces, J.R. Barrow, E.D. McArthur, R.E. Sosebee and R.J. Tausch, U.S. Department of Agriculture, Forest Service, Intermountain Research Station.

Sofer, Z., 1978. Isotopic composition of hydration water in gypsum. *Geochimica et Cosmochemica Acta*, vol. 42, pp. 1141-1149.

Stewart, J.H., 1970. Upper Precambrian and Lower Cambrian strata in the southern Great Basin, California and Nevada, U.S. Geological Survey Professional Paper 620, 206 p.

SE ROA 43035

Thomas, J.M., A.H. Welch and M.D. Dettinger, 1997. Geochemistry and Isotope Hydrology of Representative Aquifers in the Great Basin Region of Nevada, Utah, and Adjacent States. U.S. Geological Survey Professional Paper 1409-C, 100 p.

Thomas, J.M., B.F. Lyles and L.A. Carpenter, 1991. Chemical and Isotopic Data for Water from Wells, Springs, and Streams in Carbonate-Rock Terrane of Southern and Eastern Nevada and Southeastern California, 1985-88. U.S. Geological Survey Open-File Report 89-422, 24 p.

Thurber, D.L., 1962. Anomalous $^{234}U/^{238}U$ in Nature. *Journal of Geophysical Research*, 67(11), pp. 4518-4520.

Tschanz, C.M. and E.H. Pampeyan, 1970. Geology and Mineral Deposits of Lincoln County, Nevada. Nevada Bureau of Mines and Geology, Bulletin 73, 188 p.

U.S. Bureau of Reclamation, 1950. Bulletin 1, Geological Investigations. *In* Boulder Canyon Project Final Reports, Part III – Preparatory Examinations.

U.S. Geological Survey, 1997. Water Resources Data, Nevada, Water Year 1996. Compiled by R.E. Bostic, R.L. Kane, K.M. Kipfer and A.W. Johnson, Water-Data Report NV-96-1, 611 p.

U.S. Geological Survey, 1996. Water Resources Data, Nevada, Water Year 1995. Compiled by D.J. Bauer, B.J. Foster, J.D. Joyner and R.A. Swanson, Water-Data Report NV-95-1, 734 p.

U.S. Geological Survey, 1995. Water Resources Data, Nevada, Water Year 1994. Compiled by S.L. Clary, D.R. McClary, R. Whitney and D. Reeves, Water-Data Report NV-94-1, 768 p.

U.S. Geological Survey, 1994. Water Resources Data, Nevada, Water Year 1993. Compiled by D.C. Emett, D.D. Hutchinson, N.A. Jonson and K.L. O'Hair, Water-Data Report NV-93-1, 596 p.

U.S. Geological Survey, 1993. Water Resources Data, Nevada, Water Year 1992. Compiled by D.L. Hess, K.A. Mello, R.J. Sexton and R.L. Young, Water-Data Report NV-92-1, 511 p.

U.S. Geological Survey, 1992. Water Resources Data, Nevada, Water Year 1991. Compiled by K.T. Garcia, G.C. Gortsema, R.N. Pennington and A.M. Preissler, Water-Data Report NV-91-1, 481 p.

U.S. Geological Survey, 1991. Water Resources Data, Nevada, Water Year 1990. Compiled by R. Bostic, D. Hitch, L.C. Van Gordon and R. Swanson, Water-Data Report NV-90-1, 358 p.

U.S. Geological Survey, 1990. Water Resources Data, Nevada, Water Year 1989. Compiled by A. Pupacko, L.C. Van Gordon, J.R. Swartwood and R.P. Collins, Water-Data Report NV-89-1, 332 p.

U.S. Geological Survey, 1989. Water Resources Data, Nevada, Water Year 1988. Compiled by A. Pupacko, R.J. LaCamera, M.M. Riek and J.R. Swartwood, Water-Data Report NV-88-1, 265 p.

U.S. Geological Survey, 1989. Water Resources Data, Nevada, Water Year 1987. Compiled by A. Pupacko, R.J. LaCamera, M.M. Riek and J.R. Swartwood, Water-Data Report NV-87-1, 250 p.

U.S. Geological Survey, 1988. Water Resources Data, Nevada, Water Year 1986. Compiled by A. Pupacko, R.J. LaCamera, M.M. Riek and D.B. Wood, Water-Data Report NV-86-1, 263 p.

Wernike, B.P., G.J. Axen and J.K. Snow, 1988. Basin and Range tectonics at the latitude of Las Vegas. *Geol. Soc. Amer. Bull.*, 100, no. 11, pp. 1738-1757.

Western Regional Climate Center, 1997. Las Vegas WSO Airport, Nevada-Climate Summary [Online]. Available: www.wrcc.sage.dri.edu/cgi-bin/cliMAIN.pl?nvlasv.

Winograd, I.J. and A.C. Riggs, 1984. Recharge to the Spring Mountains; isotopic evidence. Geological Society of America, Abstracts with Program, 97th Annual Meeting, vol. 16, no. 6, 698 p.

Winograd, I.J. and F.N. Robertson, 1982. Deep Oxygenated Ground Water: Anomaly or Common Occurrence?. *Science*, vol. 216, pp. 1227-1230.

Winograd, I.J. and F.J. Pearson Jr., 1976. Major carbon-14 anomaly in a regional carbonate aquifer–possible evidence for megascale channeling, south-central Great Basin. *Water Resources Research*, vol. 12, no. 6, pp. 1125-1143.

Winograd, I.J. and W. Thordardson, 1975. Hydrogeologic and Hydrogeochemical Framework of the Southcentral Great Basin, Nevada, California, with Special Reference to the Nevada Test Site. U.S. Geological Survey Professional Paper 712-C, 126 p.

Yelken, M.A., 1996. Trace Element Analysis of Selected Springs in the Virgin River Basin. Unpublished M.S. Thesis, Dep. of Geoscience, University of Nevada, Las Vegas, 156 p.

APPENDIX A

PHYSICAL, CHEMICAL, AND ISOTOPIC DATA

Table A-1. Field Measurements.

ID	Latitude (d m s)	Longitude (d m s)	Altitude (m)	Discharge Rate (L/min)	Temp (°C)	EC (µS/cm)	pH (Std. Units)	DO (mg/L)	HCO_3 (mg/L)	Date
1	36 31 38	114 24 51	375	<1	22	3561	7.05	3.8	147	03/07/96
2	36 29 59	114 28 35	427	<1	16	470	7.85	8.1	—	10/04/95
2	36 29 59	114 28 35	427	<1	11.1	552	8.25	8.8	200	02/09/96
3	36 29 14	114 28 00	439	<1	19	545	8.13	7.6	—	10/04/95
3	36 29 14	114 28 00	439	<1	14.1	770	8.46	6	180	02/09/96
4	36 26 36	114 24 17	424	<1	10.8	23905	7.88	8.8	—	02/09/96
5	36 24 21	114 26 38	450	~1	15	3590	7.61	5.25	156	03/07/06
6	36 24 19	114 25 50	450	13.1	13.5	8024	7.76	3.9	118	03/07/96
7	36 24 05	114 24 07	381	~40	23	5520	7.1	5	—	02/09/96
8	36 23 24	114 25 59	470	—	30	4535	7.03	2.1	—	10/04/95
8	36 23 24	114 25 59	470	1040	29.6	4270	7.05	2.65	—	02/08/96
9	36 22 59	114 26 00	494	<1	17	4235	8.02	7	—	02/08/96
10	36 22 45	114 25 30	430	>40	15	8100	7.55	7.5	—	02/08/96
11	36 22 37	114 26 40	488	2750[2]	30	4190	7.22	4.6	—	10/03/95
11	36 22 37	114 26 40	488	—	30	3860	7.03	2.6	—	02/08/96
12	36 22 37	114 26 57	480	<1	17	4935	7.13	0.7	—	02/07/96
13	36 22 14	114 27 36	485	<1	17	4315	7.31	6.2	152	02/07/96
14	36 21 28	114 26 14	396	30	17	5590	8.04	8.6	—	02/08/96
15	36 17 06	114 30 51	506	12	25	4090	7.43	3.15	—	10/03/95
15	36 17 06	114 30 51	506	—	17.2	4021	7.58	4.75	104	02/06/96
16	36 12 40	114 33 24	601	<1	19	1265	7.06	1.25	—	10/03/95
16	36 12 40	114 33 24	601	<1	11	1450	7.03	1.95	146	02/07/96
17	36 12 12	114 38 37	661	<1	18	3690	7.63	2.4	—	10/03/95
17	36 12 12	114 38 37	661	0.07	12.6	3625	7.81	6.5	173	02/06/96
18	36 12 29	114 54 44	530	<1	22	4860	7.56	7.2	—	10/02/95
18	36 12 29	114 54 44	530	<1	15.8	4230	7.38	4.2	114	02/06/96
19	36 06 26	114 58 10	500	<1	25	4900	7.05	2.5	—	10/02/95
19	36 06 26	114 58 10	500	<1	15.5	4785	7.81	3.8	129	02/05/96
20	36 00 40	114 44 35	240	636	36	1204	7.79	3.3	—	02/11/97
21	36 00 05	114 44 30	210	60	55.1	2775	7.62	3.1	—	01/31/97
22	36 00 11	114 44 36	220	22.2	45	1893	7.66	4	—	02/01/97
23	36 00 10	114 44 58	280	1536	46	1788	7.36	1.6	—	01/31/97
24	36 00 04	114 44 36	210	18	58	2323	8	3	—	01/31/97
25	35 59 43	114 44 19	230	10.2	48	3599	7.55	2.5	—	02/01/97
26	35 59 41	114 44 15	235	13.2	13	7059	7.95	10.0	—	02/01/97
27	35 59 56	114 37 58	988	2	12	1069	7.66	—	—	02/03/97
28	35 58 59	114 44 49	260	960[1]	55	4601	7.43	1.9	—	02/02/97
29	35 58 59	114 44 49	263	—	24	4313	7.10	8.0	—	02/02/97
30	35 57 39	114 43 32	245	126	44	4991	7.70	2.4	—	02/01/97
31	35 57 39	114 43 32	249	4.2	19	3368	7.78	6.8	—	02/01/97
32	35 56 43	114 43 55	211	8.4	19	1022	7.34	—	—	02/02/97
33	35 56 21	114 44 03	245	10.2	32	816	7.92	4.2	—	02/02/97
34	35 55 35	114 42 24	220	<1	24	7171	7.47	—	—	02/03/97
35	35 50 55	114 43 33	293	2	25	750	8.08	4.5	—	05/06/97
36	35 39 36	114 46 20	605	<1	18	1505	7.34	1.7	—	02/05/96
36	35 39 36	114 46 20	605	2	15	1874	7.54	3.45	—	02/11/97
ES[3]	35 48 13	115 00 14	550	—	23	891	8.68	3.6	96	05/02/97
CR[3]	36 00 35	114 44 40	200	—	14	927	8.18	8.4	—	02/11/97

[1] Combined discharge of hot and cold springs
[2] Annual mean based on water years 1985 to 1994 in U.S.G.S. Water-Data Reports
[3] ES Eldorado Substation Well
CR Colorado River, below Hoover Dam

SE ROA 43039

JA_12919

Table A-2. Major Ion and Trace Metal Chemistry.

ID	EC (lab) (µS/cm)	pH (lab) Std. Units	TDS mg/L	HCO_3 (lab, mg/L)	CO_3 mg/L	Cl mg/L	SO_4 mg/L	NO_3 mg/L	Na mg/L	K mg/L	Ca mg/L	Mg mg/L	SiO_2 mg/L	Li mg/L	F mg/L	Fe mg/L	N mg/L	B mg/L	Mn mg/L	Date	Source[1]
1	3640	7.5	2721	319	—	332	1180	—	547	25.4	156	92.9	46.8	—	—	—	0.84	—	—	03/07/96	f
2	574	8.27	462	249	0	18.9	60	—	52	25.6	34.7	16.8	5	—	—	—	0.04	—	—	02/09/96	f
3	819	8.35	626	213	2.2	46.5	168	—	77.6	21.3	48.9	25.9	19.1	—	—	—	3.32	—	—	02/09/96	f
4	17500	8.1	16300	270	0	2100	8800	—	3800	300	470	610	54	—	2.6	0.2	—	17	0.3	05/17/78	g
5	4350	7.62	3841	169	—	278	2290	—	295	51.1	537	208	12.4	—	—	—	—	—	—	03/07/06	f
6	—	7.9	9970	240	0	1900	4800	—	1900	130	590	510	16	1.1	2	0.01	0.05	7.3	0.02	05/05/77	g
7	—	—	4710	140	0	600	2600	—	600	45	510	260	24	—	1.6	0	—	2.2	0.03	05/19/78	g
8	4100	7.8	—	160	—	400	1900	—	330	23	470	160	16	0.68	1.5	<0.009	0.2	—	<0.003	07/01/85	a
9	4190	7.5	3710	220	0	370	2100	—	340	27	560	180	21	—	1.5	0.01	—	1.4	0.01	05/19/78	g
10	—	7.7	9270	650	0	1700	4300	—	1700	130	300	720	89	—	4.5	0.02	—	6.2	0.04	05/19/78	g
11	—	7.48	—	161	0	327	1620	—	291	22.7	423	143	16.8	—	1.4	—	0.27	—	—	03/19/92	e
12	4440	7.6	3787	266	0	386	2040	—	350	25.3	513	186	20.4	—	—	—	<0.04	—	—	02/07/96	f
13	—	—	3440	180	0	400	1900	—	340	23	510	160	16	0.7	1.6	0.01	0.1	1.3	0.01	05/04/77	g
14	5600	—	4930	170	0	680	2700	—	580	18	580	250	33	0.96	2	0.03	0	1.8	0.02	05/19/77	g
15	4200	8.1	3730	140	0	160	2400	—	270	22	580	190	33	0.83	2.8	0.01	0.02	1.5	0.01	05/03/77	g
16	1550	7.58	1215	249	0	16.9	725	—	21.9	4.96	209	79.2	13.8	—	—	—	1.15	—	—	02/07/96	f
17	3890	7.99	3660	205	0	63.6	2410	—	209	10.7	524	220	17.4	—	—	—	<0.04	—	—	02/06/96	f
18	4450	7.79	4253	146	0	151	2840	—	231	21.5	532	308	23.6	—	—	—	<0.04	—	—	02/06/96	f
19	5280	7.62	4931	144	0	379	3040	—	405	38.8	569	332	13.9	—	—	—	9.26	—	—	02/05/96	f
20	1250	—	757	116	—	108	335	1.77	188	4.5	59.9	2.9	29.6	—	—	—	0.4	—	—	05/02/95	b
21	—	—	1749	77.5	—	476	589	<0.4	451	9.48	140	5.9	34.3	—	—	—	—	—	—	01/31/97	f
22	1780	—	1280	141	—	134	584	0.27	210	8.27	150	11	50.1	—	—	—	0.06	—	—	05/02/95	b
23	1780	—	1260	135	—	145	584	0.31	226	7.53	138	8.4	48	—	—	—	0.07	—	—	05/02/95	f
24	2340	—	1580	98.1	—	283	644	<0.04	343	8.24	133	4.1	48.7	—	—	—	<0.01	—	—	05/02/95	b
25	—	—	2017	70.7	—	591	644	0.09	522	11	172	6.11	36.8	—	—	—	—	—	—	02/01/97	f
26	—	—	4235	151	—	1514	1100	0.31	1030	16.9	382	40.7	53.6	—	—	—	—	—	—	02/01/97	f
27	—	—	784	324	—	101	140	<0.04	51.8	11.9	120	34.8	62	—	—	—	—	—	—	02/03/97	f
28	4500	—	2920	28.5	—	956	843	0.09	695	14.4	247	2.3	44.7	—	—	—	0.02	—	—	05/03/95	b
29	4500	—	2490	33.2	—	962	827	<0.04	680	15.8	257	6	51.7	—	—	—	<0.01	—	—	05/03/95	b
30	—	—	2635	37.3	—	1078	587	4.92	650	15.2	249	13.5	39.4	—	—	—	—	—	—	02/01/97	f

Table A-2. Major Ion and Trace Metal Chemistry (Continued).

ID	EC (lab) (μS/cm)	pH (lab) Std. Units	TDS mg/L	HCO_3 (lab, mg/L)	CO_3 mg/L	Cl mg/L	SO_4 mg/L	NO_3 mg/L	Na mg/L	K mg/L	Ca mg/L	Mg mg/L	SiO_2 mg/L	Li mg/L	F mg/L	Fe mg/L	N mg/L	B mg/L	Mn mg/L	Date	Source[1]
31	—	—	1933	97.9	—	755	410	11	407	11	212	28.6	33.2	—	—	—	—	—	—	02/01/97	f
32	1210	—	691	83.8	—	194	182	6.91	178	3.14	38.2	7.5	29	—	—	—	1.56	—	—	05/03/95	b
33	820	—	493	81.5	14.6	89.7	145	12.5	164	0.89	4.26	0.3	24.4	—	—	—	2.82	—	—	05/04/95	b
34	—	—	4228	148	—	2019	525	18.5	1103	25.4	313	76.4	40.6	—	—	—	—	—	—	02/03/97	f
35	347	—	215	112	6.7	13.5	42	8.95	34.3	6.46	28.5	4.6	11.1	—	—	—	2.02	—	—	04/20/95	b
36	—	—	1298	363	—	102	445	<0.04	118	5.89	178	47.6	38.9	—	—	—	—	—	—	0[illegible]/05/96	f
ES[2]	795	—	498	124	10.6	119	60.9	14.4	154	4.01	6.84	0.5	64.9	—	—	—	3.24	—	—	09/26/95	b
CR[2]	—	—	689	160	—	80	245	1.51	94.6	4.87	74.4	28.3	8.7	—	—	—	—	—	—	02/11/97	f

[1] Sources of data:
a Thomas *et al.*, 1991
b SNWA, unpublished data
e Hershey and Mizell, 1995
f This study
g Lancy and Bales, 1996

[2] ES Eldorado Substation Well
CR Colorado River, below Hoover Dam

SE ROA 43041

JA_12921

Table A-3. Isotopic Compositions.

ID	^{3}H (pCi/L)	$\delta^{18}O$ (per mil)	δD (per mil)	$\delta^{13}C$ (per mil)	14 PMC	$^{234}U/^{238}U$ (act. ratio)	Total U (µg/L)	Date	Source[1]
1	—	−10	−82	−7.6	—	2.41	13.3	03/07/96	f
2	<10	−11.5	−92	−5.0	—	2.47	1.8	02/09/96	f
3	<10	−11.3	−88	−6.5	—	2.29	5.45	02/09/96	f
4	<10	−8.6	−83	—	—	1.14	37.9	02/09/96	f
5	—	−12.2	−93	—	—	—	—	03/07/96	f
6	—	−11.8	−92	—	—	2.76	5.50	03/07/96	f
7	—	−11.2	−88	−6.8	—	2.51	5.0	02/09/96	f
8	—	−12.4	−93	−6.2	3.5	3.07	—	06/24/85	a
8	—	−12.5	−93.5	−5.3	7.2	—	—	07/01/85	a
8	<10	−12.3	−91	—	—	—	—	02/08/96	f
11	<10	−12.4	−92	−3.9	3	~4.0	~2.9	03/19/92	e
11	—	−12.4	−91	—	—	3.08	3.49	02/08/96	f
12	—	−12	−90	—	—	—	—	02/07/96	f
13	—	−12.1	−91.5	—	—	—	—	02/07/96	f
15	<10	−9.9	−77	−4.3	—	1.72	2.35	02/06/96	f
16	—	−10.5	−79	—	—	1.08	6.69	02/07/96	f
17	<10	−10.8	−80	—	—	1.49	12.0	02/06/96	f
18	<10	−9.2	−75	—	—	1.65	5.59	02/06/96	f
19	<10	−8.6	−71	—	—	1.29	12.8	02/05/96	f
20	—	—	—	−6.6	—	—	—	02/11/97	f
20	98	−12.9	−103	—	—	—	—	05/02/95	b
21	86	−13	−102	−7.4	—	—	—	01/31/97	f
22	148	−13.7	−106	—	—	—	—	05/02/95	b
23	141	−13.6	−106	−28.65	62.9	—	—	05/02/95	b
24	74	−13.5	−104	—	—	—	—	05/02/95	b
25	72	−12.7	−100	−8.0	—	—	—	02/01/97	f
26	21	−11.2	−88	−11.8	—	—	—	02/01/97	f
27	8	−10.8	−79	—	—	—	—	02/03/97	f
28	<10	−11.5	−92	−27.64	26.98	—	—	05/03/95	b
29	<10	−10.8	−88	—	—	—	—	05/03/95	b
30	<5	−11.2	−87	−11.5	50.71	—	—	02/01/97	f
31	<5	−10.3	−81	−13.2	81.82	—	—	02/01/97	f
32	<10	−10.2	−83	—	—	—	—	05/03/95	b
33	<10	−10.3	−83	−24.91	15.34	—	—	05/04/95	b
34	<5	−10.3	−82	−7.0	—	—	—	02/03/97	f
35	8.2	−9.8	−81	−11.9	—	—	—	05/06/95	f
36	18	−9.2	−72	—	—	1.05	134	02/05/96	f
36	—	—	—	−13.2	—	—	—	02/11/97	f

[1] Sources of data:
a Thomas *et al.*, 1991
b SNWA, unpublished data
e Hershey and Mizell, 1995
f This study

SE ROA 43042

JA_12922

APPENDIX B

GEOLOGIC DESCRIPTIONS

Spring 1 – Kelsey Spring

Topographic base: 7.5' Overton Quadrangle
Geology references: This study

Kelsey Spring is located at the northeast edge of the Overton Wildlife Management area at the base of Mormon Mesa. The orifice is covered by a concrete vault (having dimensions 1.5 by 2 m wide and 1.5 m high) with an access door in the top. There was approximately 0.75 m of standing water in the vault when this spring was visited on 3-7-96. Seepage from the vault occurs in cracks in the concrete near its base. Samples were collected from this seepage. In addition, a 10-cm-diameter steel pipe extends south about 20 m from the vault and discharges at ground surface within a stand of very dense vegetation. A large area of reeds extends north and slightly uphill from the vault, suggesting that groundwater is near ground surface and that additional discharge may be occurring in that area.

Kelsey Spring discharges near the base of Quaternary terrace deposits at the edge of Mormon Mesa. Other seeps are located at the base of the terrace, as indicated by several stands of palm trees to the northwest.

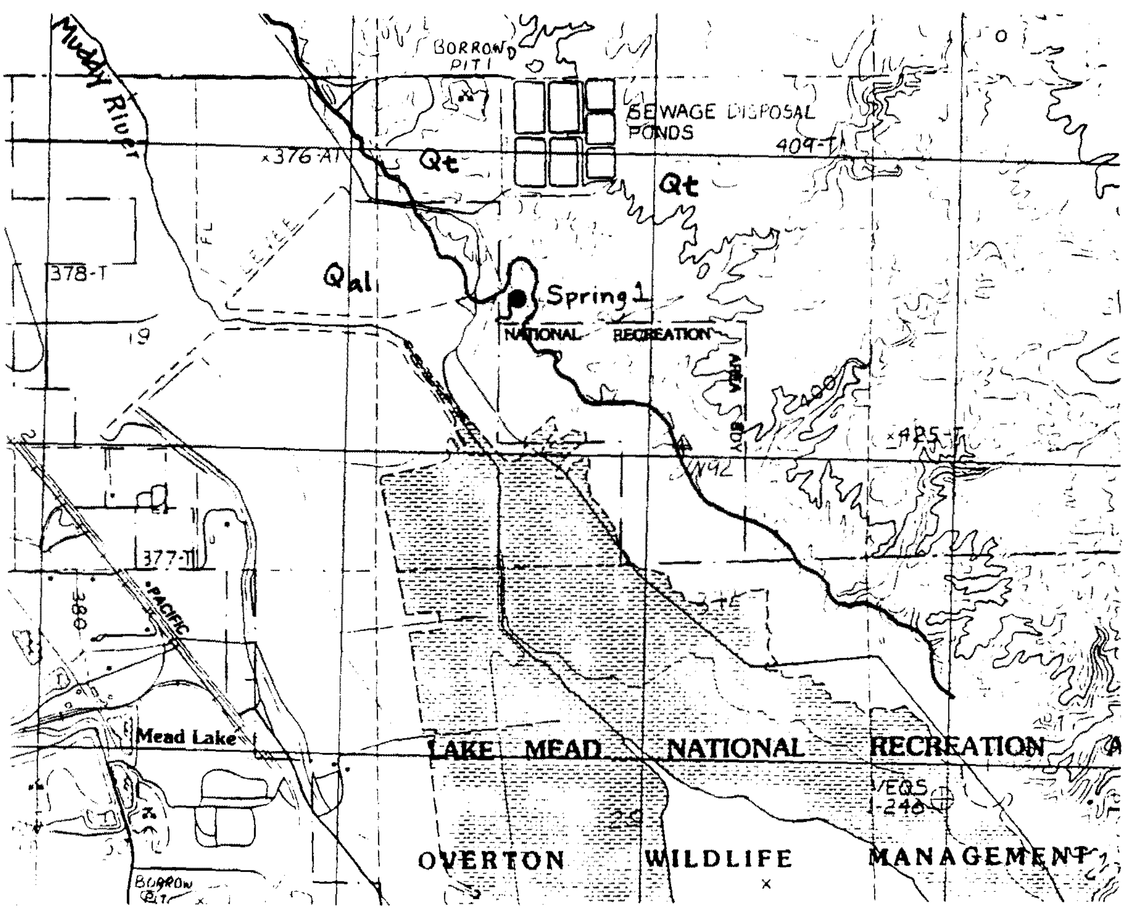

SE ROA 43044

Spring 2 – Unnamed spring in Magnesite Wash

Topographic base: 7.5' Overton Quadrangle
Geology references: Bohannon (1983)

The spring is located in a gap in Overton Ridge though which the Magnesite Wash channel passes. The spring issues as subsurface discharge into a 10-m-diameter pool. Additionally, minor seepage can be observed up to 5 m above the pool from fractures in the Tertiary Basal Conglomerate. Surface flow occurs for only a few 10s of meters downstream from the pool, which is surrounded by reeds, willows, and grape vines.

The spring is located at the contact of the Basal Conglomerate with the upper Rainbow Gardens Member (both of the Tertiary Horse Spring Formation), and about 200 m west of the unconformable boundary with the Tertiary Muddy Springs Formation. The spring is not associated with any major structural features. Rather, if groundwater is assumed to be moving generally west or northwest toward the Muddy River and Colorado River, then the spring is located at the lowest elevation just upgradient from the low-permeability barrier of the Muddy Creek Formation. Upstream of the spring, Magnesite Wash passes through a basin comprised of Mesozoic sandstones and covered by thick, sandy soils.

Spring 3 – Unnamed spring in Kaolin Wash

Topographic base: 7.5' Valley of Fire, East Quadrangle
Geology references: Bohannon (1983)

The setting for this spring is similar to the Magnesite Wash spring; a gap in Overton Ridge through which Kaolin Wash passes, although the gap at Kaolin Wash is much narrower. At Kaolin wash, the spring issues as subsurface discharge into a 5-m-diameter pool. Additionally, minor seepage can be observed from fractures in the Thumb Member. Surface flow occurs for approximately 400 m downstream from the pool, which is surrounded by reeds.

The spring issues from the Thumb Member of the Teriary Horse Spring Formation, and about 1 km upstream (southwest) of the contact between the the Thumb Member and the Muddy Creek Formation. And, similar to the Magnesite Wash spring, the Kaolin Wash spring is located near the lowest elevation just upgradient from the low-permeability barrier of the Muddy Creek Formation.

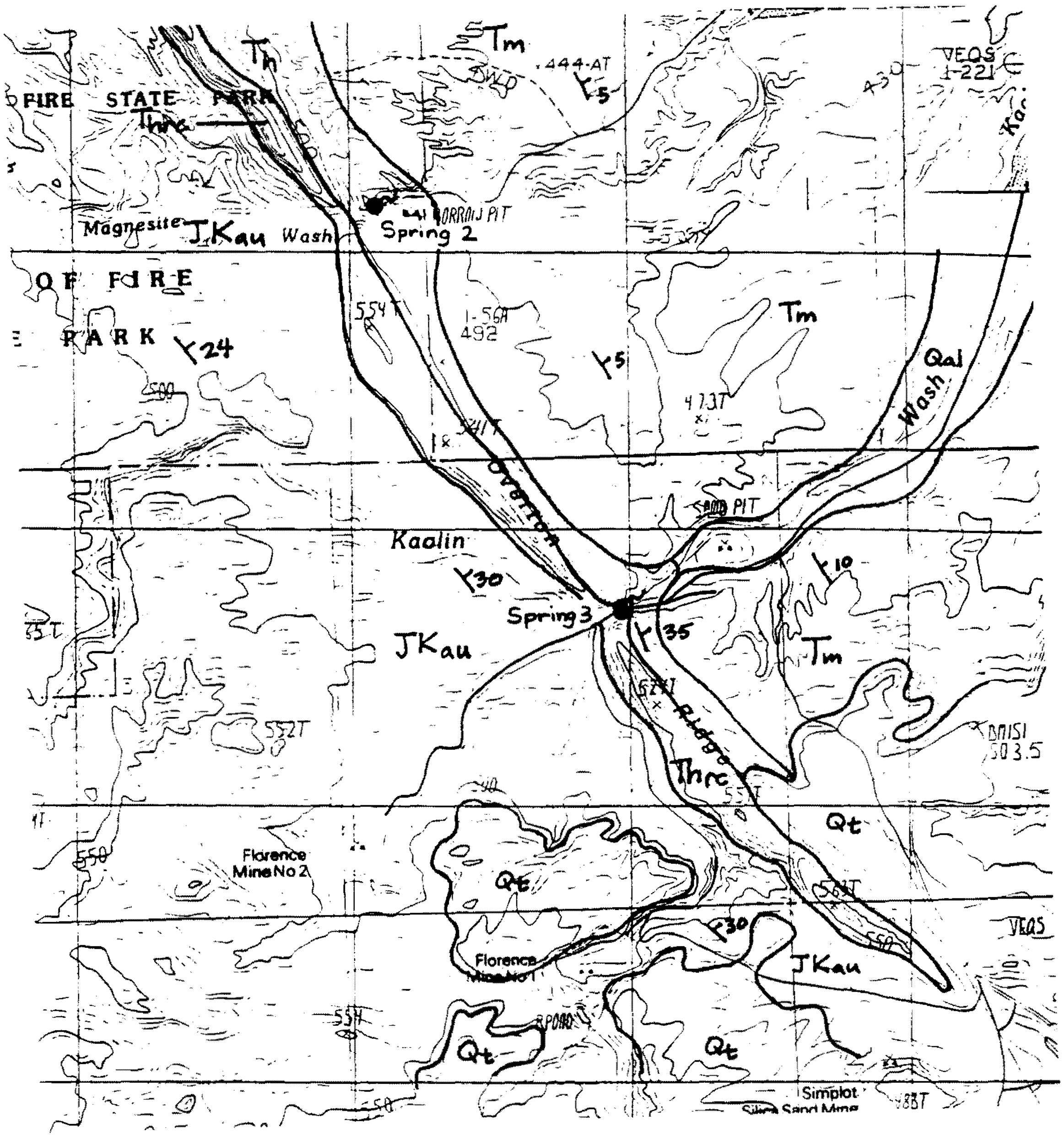

FIRE STATE PARK
Th
Tm
Thrc
Magnesite
JKau
Wash
Spring 2
BORROW PIT
OF FIRE
PARK
Kaolin
Spring 3
Overton
Ridge
Qal
Wash
Qt
Florence Mine No 2
Florence Mine No 1
Simplot
Silica Sand Mine
SAND PIT

SE ROA 43046

Spring 4 – Getchel Spring

Topographic base: 7.5' Valley of Fire, East Quadrangle
Geology references: Bohannon (1983)

Getchell Spring is located approximately 0.75 km northeast of the intersection of Northshore Road with the Overton Beach Road. Discharge occurs in the bottom of a 4-m-deep ravine cut into unconsolidated sands and silts of the Muddy Creek Formation. Many gypsum beds are evident within the Muddy Creek Formation near the spring. Surface flow was observed for an approximate 50 m length of the ravine on 2-9-96, although the flow was very slow to stagnant. Small amounts of vegetation were present at the orifice but very little vegetation was observed downstream.

Much of the area surrounding the spring is capped by a gyspum unit which could be in place or colluvium from above. There are no major structural features evident at ground surface, but Bohannon (1983) maps a strike-slip fault through the area, possibly related to the Lake Mead Fault System. The Rogers Spring Fault lies about 1.5 km to the southeast.

There is a dug well to the northwest of Getchel spring which contained standing water at both visits to the area (10-4-95 and 2-9-96). The well is about 2 m in diameter, 2 m deep, and filled with reeds. There is also a brick-lined cavity (cistern?) about 50 m south of the dug well and 100 m west northwest of Getchel Spring. This feature is 3 m deep and 2 m in diameter at the surface, and though it contained no water at either of our visits, it appears to be the feature labeled as Getchel Spring on the "Valley of Fire, East" 7.5' quadrangle map.

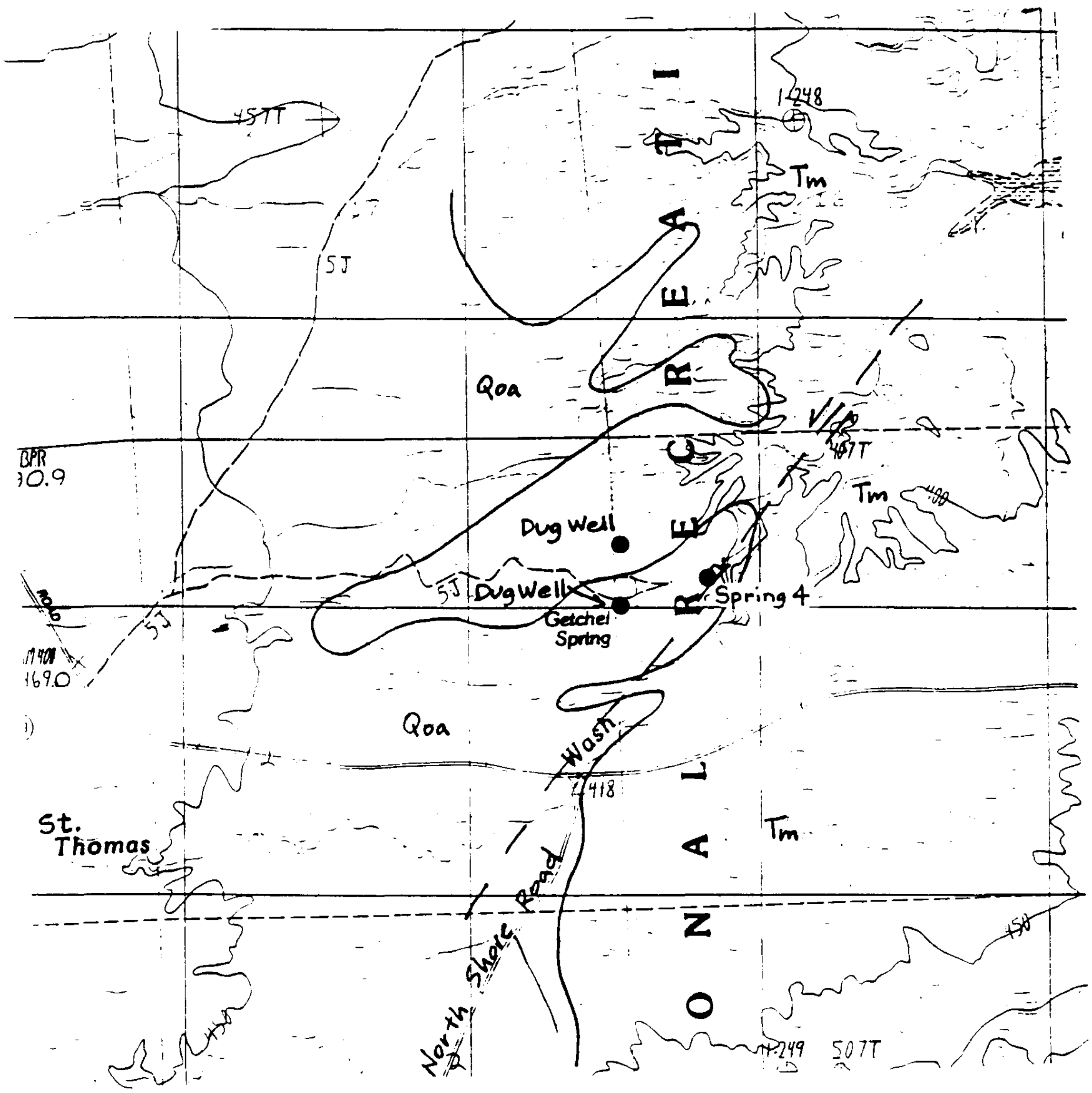

457T
1248
Tm
5J
Qoa
R E C R E A T I O N A L
BPR
30.9
Dug Well
Dug Well
Getchel Spring
Spring 4
Tm
407T
Qoa
Wash
418
1690
St. Thomas
Tm
North Shore Road
450
1249
507T

SE ROA 43048

Spring 5 – Unnamed uppermost spring in Valley of Fire Wash

Topographic base: 7.5' Valley of Fire, East Quadrangle
Geology references: Campagna (1990) unpublished mapping

This spring issues from several seeps at the base of the northern bank of Valley of Fire Wash, at the boundary of the recreation area. Surface flow in the wash was observed for a distance of 200 to 300 m on 3-7-96.

The spring is located on a fault contact between JKau on the west and TRau on the east, but is probably a result of the proximity of the contact between the Jurassic and Triassic clastic rocks with the Tertiary Muddy Creek Formation (see description of Spring 6).

Spring 6 – Unnamed upper spring in Valley of Fire Wash

Topographic base: 7.5' Valley of Fire, East Quadrangle
Geology references: Campagna (1990) unpublished mapping

Several orifices and seeps are located along the banks of the Valley of Fire Wash near the power line crossing. Surface flow from this spring area extended to within a few hundred m of North Shore Road at our 3-7-96 visit. The spring area supports a great deal of vegetation along the banks of the wash. Most of the springs and seeps are on the south side of the wash and within 5 m of the wash bottom; however, one small channel extends to the south out of the wash, originating at a spring just southwest of the power line road. Our samples were collected at this orifice, which issues from a thin veneer of Quaternary gravels on top of the Triassic Moenavi and Kayenta Formations. There appears to be considerable subsurface flow within these gravels because flow at the orifice is much lower than flow from the same channel downstream at the Valley of Fire Wash.

The spring area is located at an unconformable contact of Jurassic and Triassic clastic rocks on the west with the Tertiary Muddy Creek Formation on the east, and near the Rogers Spring Fault. The springs occur where eastward flowing groundwater meets the low-permeability barrier formed by the Muddy Creek Formation and is forced upward, possible along fault planes, to discharge points at ground surface.

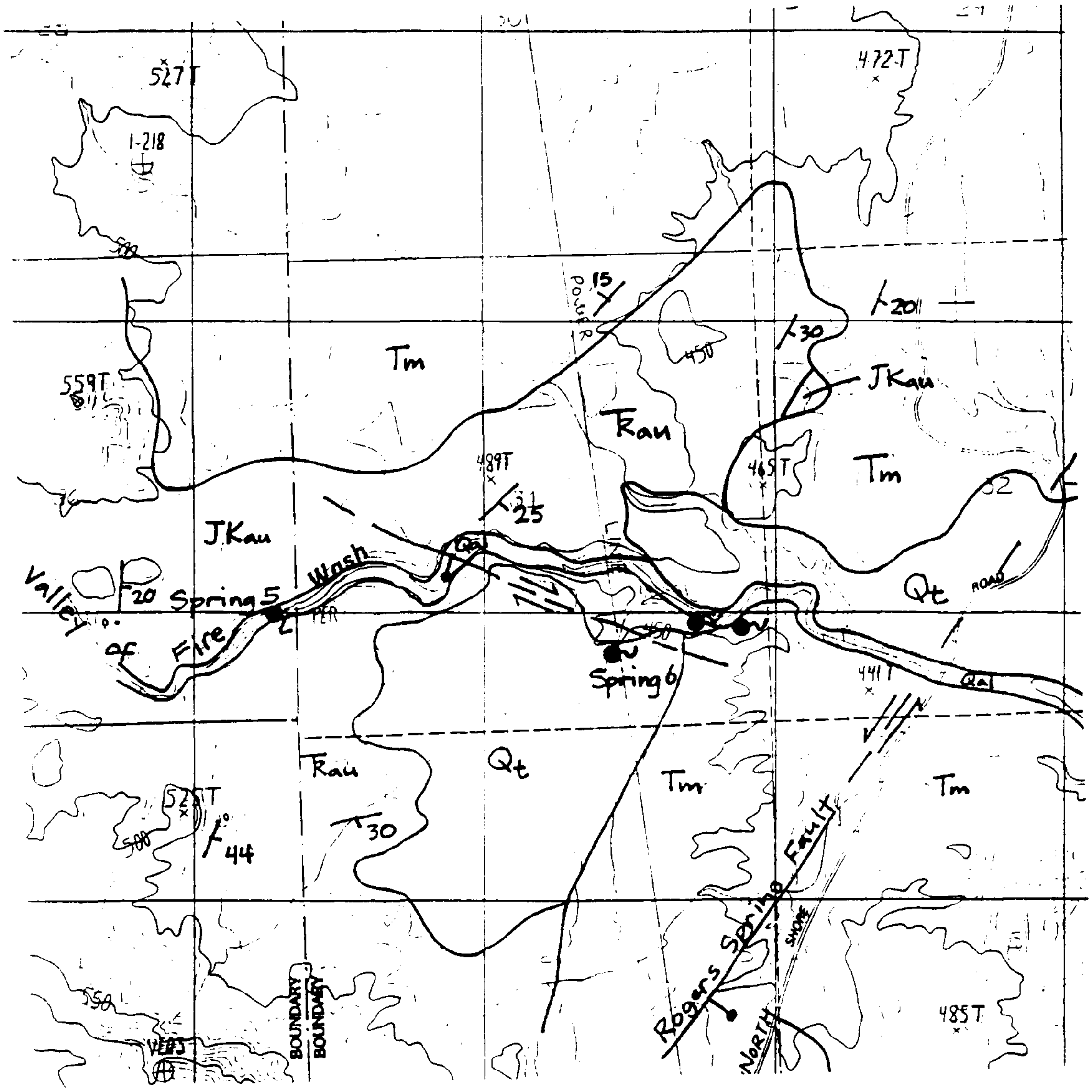
527T
1-218
559T
Tm
Ŧau
JKau
489T
25
15
POWER
450
465T
Tm
32
20
30
JKau
Qt
ROAD
Valley of Fire Wash
Spring 5
20
Qal
450
Spring 6
441T
Qal
Ŧau
Qt
Tm
Tm
525T
44
30
500
Rogers Spring Fault
SHORE
NORTH
550
485T
BOUNDARY
BOUNDARY

SE ROA 43050

Spring 7 – Unnamed lower spring in Valley of Fire Wash

Topographic base: 7.5' Valley of Fire, East Quadrangle
Geology references: Bohannon (1983)

The spring is located on the north bank of the Valley of Fire Wash and about 5 m above the base of the wash. Surface flow was evident in the wash from the spring to Lake Mead on our 2-9-96 visit, a distance of about 1 km. Seepage into the wash may be occurring along this stretch. The banks of the wash are covered by thick stands of tamarisk and other vegetation, but the main spring is in a small clearing. Several orifices and seeps are distributed along the bank. Samples were collected from the largest.

The spring issues from Quaternary Older Alluvium near an exposure of the Muddy Creek formation.

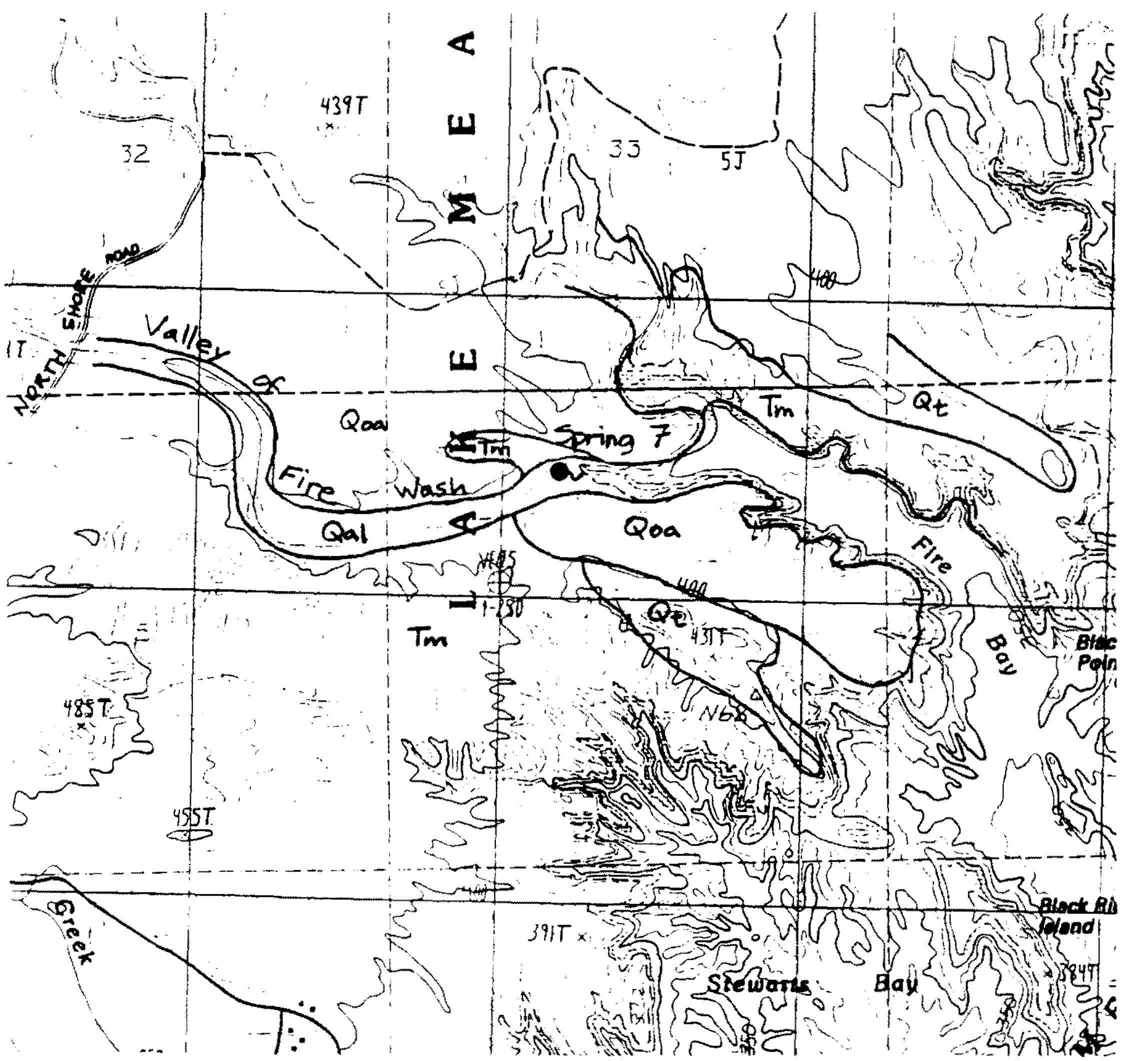

SE ROA 43051

Spring 8 – Blue Point Spring

Topographic base: 7.5' Valley of Fire, East Quadrangle
Geology references: Bohannon (1983), Campagna and Aydin (1994)

Blue Point Spring is at the base of the Muddy Mountains, 350 m west of North Shore Road. The spring issues from colluvium about 10 m horizontally from the nearest limestone exposure, and into a 3-m-deep ravine. The surface flow forms Slim Creek, which flows southeast toward Stewarts Point and Lake Mead. Parts of Slim Creek flow underground in locations where the gypsum–rich soils have been dissolved. The spring orifice is surrounded by thick acacia and other vegetation. Samples were collected at the orifice.

The spring is located at the point of intersection of the Rogers Spring Fault and the older west-northwest-trending Arrowhead Fault.

Spring 9 – Unnamed spring 0.8 km south of Spring 8

Topographic base: 7.5' Valley of Fire, East Quadrangle
Geology references: Bohannon (1983), Campagna and Aydin (1994)

Spring is located approximately 50 m east of a culvert under North Shore Road. No surface flow was evident although saturated soils support a dense stand of cat tails and other vegetation, including several cottonwood trees, in an area about 20 m wide.

Spring issues from unconsolidated and partially consolidated red and tan silts, with interbedded sand, pebbles, and gypsum.

Spring 10 – Unnamed spring 0.8 km southeast of spring 9

Topographic base: 7.5' Valley of Fire, East Quadrangle
Geology references: Bohannon (1983), Campagna and Aydin (1994)

Spring is located about 0.8 km southeast and in the same wash channel as Spring 9. Discharge is diffuse and widely-distributed across the base of the wash channel (25 to 30 m wide), although several small (less than 1 m across and 0.1 m deep) channels have been developed. Dense vegetation throughout seep area, including mesquite, tamarisk, and reeds. Our discharge measurement was made upstream of the most diffuse flow and therefore does not account for the diffuse discharge, which is the majority of the discharge from this spring.

Spring issues from Quaternary terrace deposits.

Spring 11 – Rogers Spring

Topographic base: 7.5' Valley of Fire, East Quadrangle
Geology references: Bohannon (1983), Campagna and Aydin (1994)

Rogers Spring is 300 m west of the North Shore Road at the base of the Muddy Mountains. The spring issues from brecciated limestone into a manmade pool having a diameter of about 25 m. The orifice is below the surface of the pool. Overflow from the pool enters Rogers Wash and flows southeast across basin-fill deposits about 3 km to where it enters Lake Mead. Rogers Spring is the largest spring in the study area, with a relatively constant discharge of 2,550 L/min measured since 1985 (USGS, 1996). Samples were collected by submerging and opening the sample bottles below the pool surface at the spring orifice.

The spring is located on the Rogers Spring Fault, a major strike-slip fault in the Lake Mead area. The fault separates lower Paleozoic carbonate rocks of the Muddy Mountains on the west from Quaternary and Tertiary basin-fill deposits to the east. The low permeability basin fill is a barrier to groundwater flow that causes the Rogers Spring Fault to act as a conduit for flow from depth within the carbonates. Four springs issue directly from the fault and several more issue from the basin fill between the fault and Lake Mead.

Rogers Spring is at a step-over in the main Rogers Spring Fault. Fracture density increases near step-over zones in extensional terrains, increasing the potential for groundwater flow paths.

Spring 12 – Scirpus Spring

Topographic base: 7.5' Echo Bay Quadrangle
Geology references: Bohannon (1983), Campagna and Aydin (1994)

Scirpus Spring is 550 m southwest of Rogers Spring. The spring consists of a primary pool 3 m long and 0.5 m wide that is surrounded by very thick reeds, shrubs, and grape vines. No surface flow was evident when this spring was visited (2-7-96). However, abundunt phreatophytes grow in the ravine below the spring indicating evapotranspiration is a major component of spring discharge. Samples were collected from the pool.

The spring is located along the Rogers Spring fault and issues from brecciated limestone about 25 m downslope from bedded limestone of the Muddy Mountain front.

Spring 13 – Corral Spring

Topographic base: 7.5' Echo Bay Quadrangle
Geology references: Bohannon (1983), Campagna and Aydin (1994)

Corral Spring is the southernmost spring on the Rogers Spring Fault and is located about 1.7 km southwest of Rogers Spring. The spring issues from colluvium in a steep canyon that extends into the limestone of the Muddy Mountain front. The spring consists of several isolated seeps and small pools distributed along a 100 m length of the base of the canyon. Little surface flow was evident, however. This area supports a great deal of vegetation, suggesting that evapotranspiration is a major component of spring discharge. Samples were collected from the highest pool, which was about 4 m long and 2 m wide, and half filled with reeds, at our 2-7-96 visit.

SE ROA 43053

Spring 14 – Unnamed spring northwest of Rogers Bay

Topographic base: 7.5' Echo Bay Quadrangle
Geology references: Bohannon (1983)

Spring issues from wash bottom as seeps. Discharge measurement made approximately 20 m downstream from highest seep. Grasses and mesquite surround the spring area, but there is considerably less vegetation than at other springs in the North Shore Spring Complex. Spring issues from Quaternary terrace deposits.

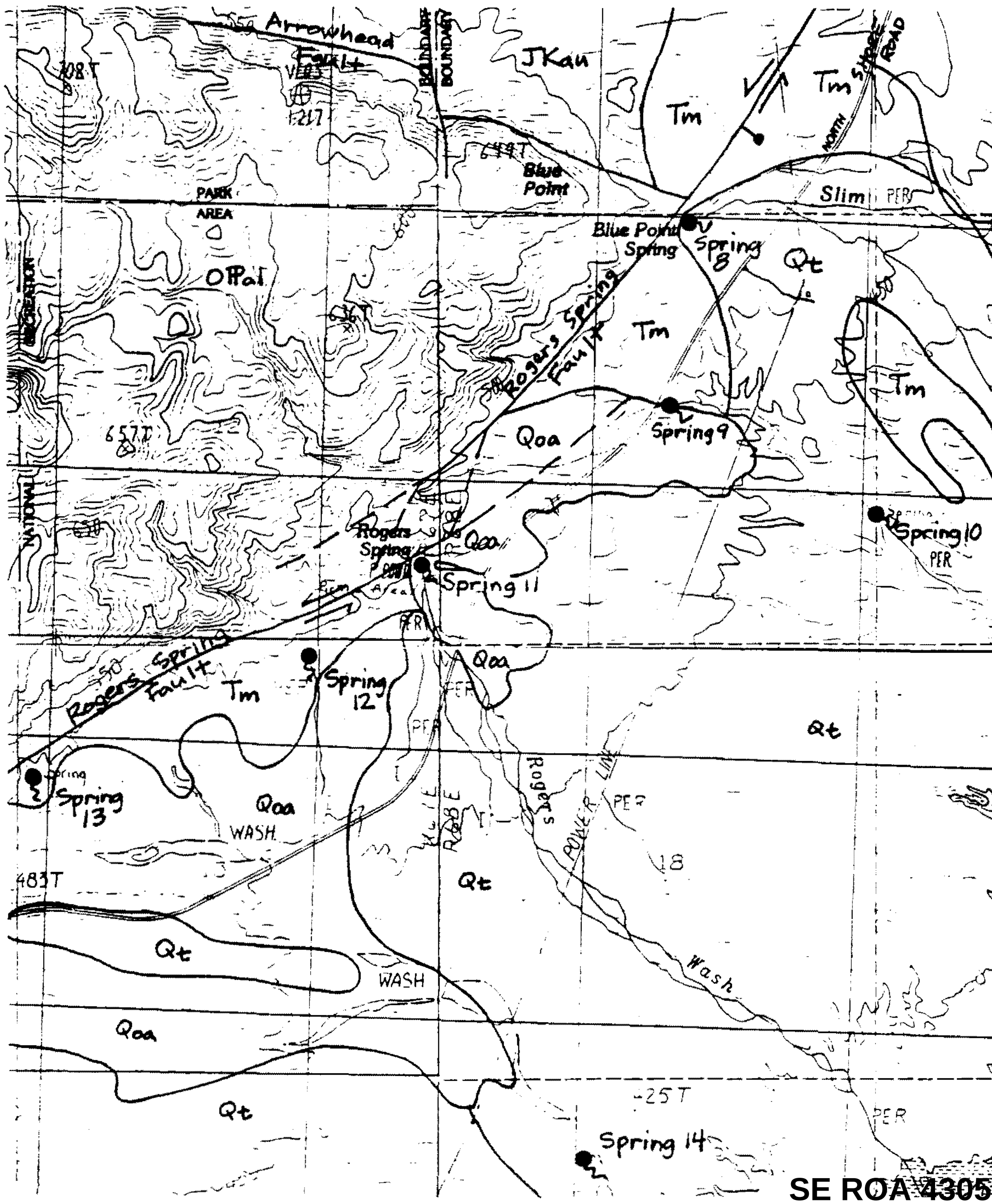

Spring 15 – Bitter Spring

Topographic base: 7.4' Bitter Spring Quadrangle
Geology references: Bohannon (1983)

Bitter Spring is located in Echo Wash at the eastern margin of Bitter Spring Valley. The spring consists of relatively diffuse flow issuing from coarse sand and gravel alluvium in the center of the wash, approximately 0.5 km east and downstream of the channel knick point, which is composed of consolidated Older Alluvium. At the spring, the wash channel is incised in clastic and associated chemical and tuffaceous rocks of the Thumb member of the Tertiary Horse Springs Formation, which dips 25 to 35 degrees east.

Surface drainage to Bitter Spring originates in Bitter Spring Valley directly to the west, and White Basin to the northwest of that. Bitter Spring Valley is composed of approximately 1,500 m of Horse Spring Formation and is covered by Pleistocene alluvium, Pleistocene terrace deposits, and Thumb Member. Bohannon (1983) hypothesizes a section of Paleozoic carbonate rocks below the Thumb. The Bitter Spring Valley margins are composed of Horse Spring Formation to the north and west (Bitter Ridge), and autochthonous Triassic and Permian formations to the south (Razorback Ridge and Pinto Ridge). The subsurface geology of White Basin is similar, but the surface geology differs in that Thumb Member is not exposed and large deposits of Miocene Red Sandstone are present. On the west, White Basin is bordered by Autochthonous Jurassic, Cretaceous, and Triassic rocks; and on the north by Allochthinous lower Paleozoic rocks (Muddy Mountains).

Bitter Spring is located near the eastern terminus of the Borax Fault, and the southern end of East Longwell Ridge; however, the spring does not appear to be directly related to any major structural feature.

Surface flow from the spring is evident, but discontinuous, over a 300 m distance below the orifice, and is accompanied by dense stands of phreatophytes (primarily tamarisk). It is likely that our measurement of discharge at Bitter Spring represents only a small portion of the total spring flow when compared to underflow in the wash sediments, evaporation from the surface channels, and transpiration from plants. Samples were collected from the highest discharge point.

SE ROA 43055

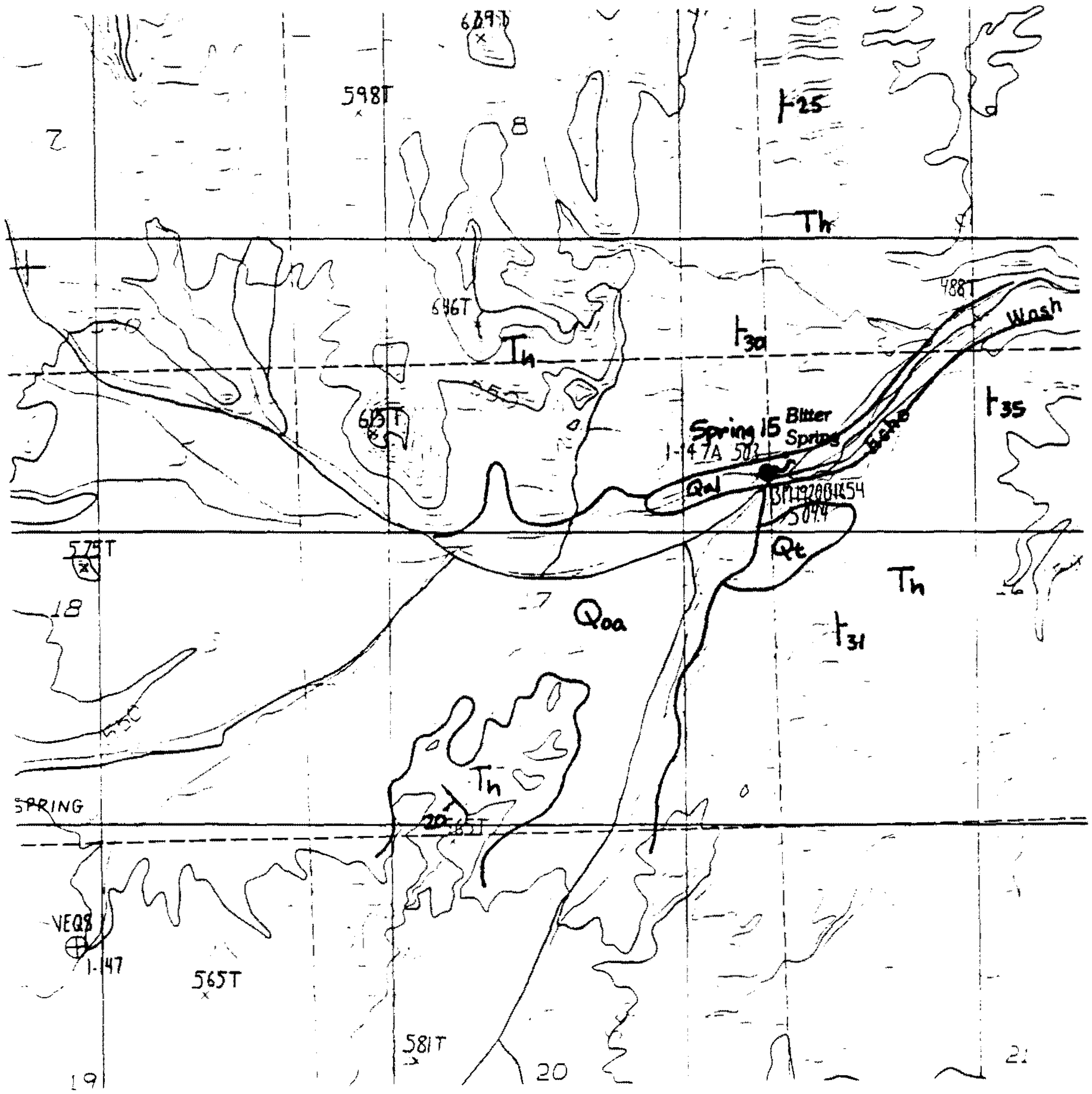

598T
8
7
Th
646T
613T
Spring 15
Bitter Spring
1-147A 503
Qal
488T
Wash
Echo
Qt
Th
Qoa
18
579T
SPRING
VEQ8
1-147
565T
581T
19
20

SE ROA 43056

Spring 16 – Sandstone Spring

Topographic base: 7.5' Boulder Canyon Quadrangle
Geology references: Bohannon (1983)

Sandstone Spring is located at the southeast margin of Pinto Valley, and northwest of the Black Mountains. The spring issues at the base of a cliff composed of Aztec Sandstone, which is several hundred meters in height, and into a single pool having a diameter of approximately 2 m. A steel pipe leads from the pool to a steel tank about 20 m downhill from the spring, but the tank contained no water at either of our visits (10-3-95 and 2-7-96). Samples were collected from seepage into the pool. Longwell noted the existence of this spring in his (date?) report and described its quality and quantity as sufficient for watering horses.

Large surface runoff events are evident through the spring area as indicated by the wash channel that cuts into the alluvial fan deposits northwest of the spring and then extends downstream from the spring, and the eroded surface of the sandstone on the cliff face above the spring. Surface flow of this type may serve to recharge shallow sediments and provide temporary "spring discharge" during wet periods; however, atmospheric tritium was not detected in a sample collected 2-7-96 indicating that flow paths are long and that recent recharge was not a major component of spring discharge at that time.

Sandstone Spring is located at a contact of the Jurassic Aztec Sandstone with the underlying Triassic Moenave and Kayente Formations (clastic, nearshore marine and nonmarine rocks). The contact trends N 60 E and dips 60 degrees to the southeast. Discharge at Sandstone Spring may be related to nearly vertical fractures in the Aztec that trend north-south.

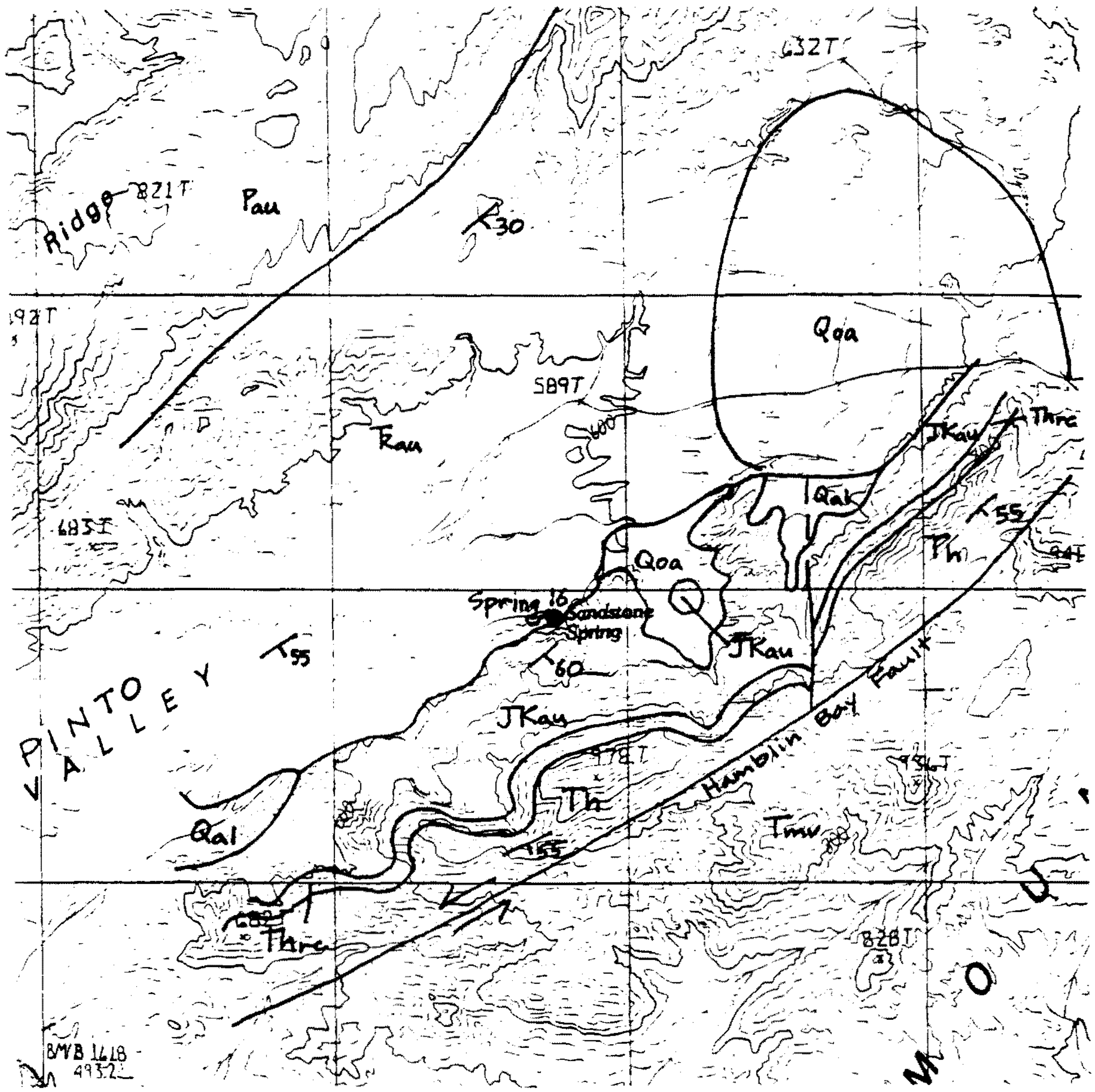

Ridge
821T
Pau
30
Qoa
632T
589T
Rau
683T
JKau
Thrc
Qal
55
Th
Qoa
Spring 16
Sandstone Spring
60
JKau
55
PINTO VALLEY
JKau
Th
Hamblin Bay Fault
Tmv
55
Qal
Thrc
828T
BM/B 1618

SE ROA 43058

Spring 17 – Cottonwood Spring

Topographic base: 7.5' Callville Bay Quadrangle
Geology references: Anderson (1973), Campagna (1990) unpublished mapping

Cottonwood Spring is located approximately 2.5 km north of Hamblin Mountain and 1.5 km southeast of North Shore Road. in a wash channel that is tributary to Callville Wash. It appears that spring discharge has in the past occurred from alluvial sediments in the northwest-trending wash channel just downstream of a 3-m high dry waterfall. There are two cottonwood trees located here and evidence of several holes dug by bighorn sheep, burros, or horses in search of water. However, surface discharge was not evident at this location during either of our visits (10-3-95 and 2-6-96). The only discharge evident from the area was from a steel pipe into a metal tank about 40 m southwest of the cottonwood trees. On 10-3-95, the tank was only partially full. indicating some leakage through the sides and insufficient spring discharge to keep it completely full. On 2-6-96, the tank was completely full and overflowing, suggesting that discharge was somewhat greater than observed during the 10-3-95 visit. The tank is useful to wildlife, as we observed several desert bighorn sheep during the 10-3-95 visit. Samples were collected from the pipe as it discharged into the tank.

The orifice is located at a north-south-trending fault contact of the Tertiary Rainbow Gardens basal conglomerate (on the east) with the Triassic upper red unit of the Moenkopi Formation (on the west). The basal conglomerate is approximately 10 to 20 m thick in the area of the spring. The alluvium filling the wash is probably less than 10 m thick.

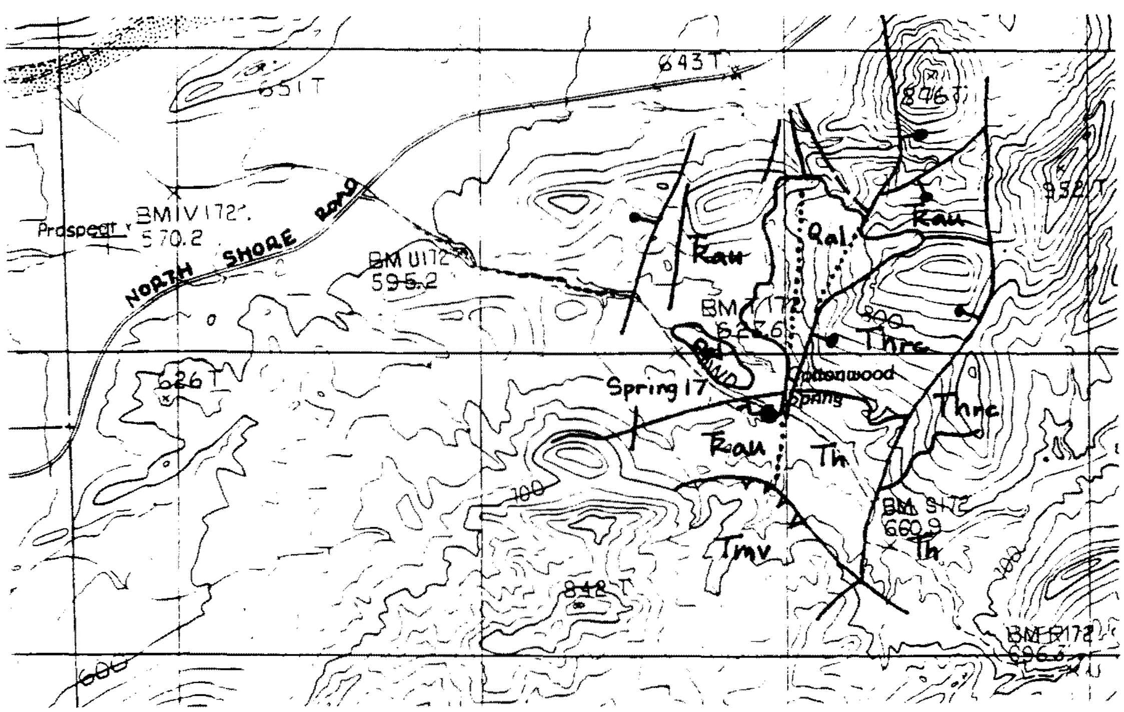

Spring 18 – Gypsum Spring

Topographic base: 7.5' Frenchman Mtn. Quadrangle
Geology references: Bohannon (1978), Longwell *et al.* (1965)

The spring is located approximately 6 km east southeast of Sunrise Mountain and about 1.5 km southwest of Gypsum Cave. The surface discharge is characterized by several seeps and pools in a 3-m-deep, north-south-trending wash channel. The pools were less than 1 m in diameter at both visits (10-2-95 and 2-6-96) and surface flow was present for less than 15 m downstream of the highest orifice. Very dense stands of tamarisk and reeds surround the orifice and line the banks of the wash channel. Samples were collected from surface flow as it emerges from dense vegetation near the orifice.

Gypsum Spring issues from gypsum beds of the Thumb Member about 0.5 km south of a ridge composed of Triassic and older rocks. The spring discharge appears to be controlled by the intersection of the water-bearing unit with land surface: no structural control is evident. Although the elevation of the spring is lower than water levels in the carbonate aquifer to the north in Dry Lake Valley, stable isotopic data indicate that the carbonates are not the source for discharge at Gypsum Spring. Rather, this spring plots in the region of low-elevation precipitation which indicates that its flow was recharged locally. As with other locally-derived springs, the absence of detectable atmospheric tritium in the spring water indicates that despite the local origin, travel times are long and the discharge does not simply represent discharge of groundwater recharged during recent precipitation events.

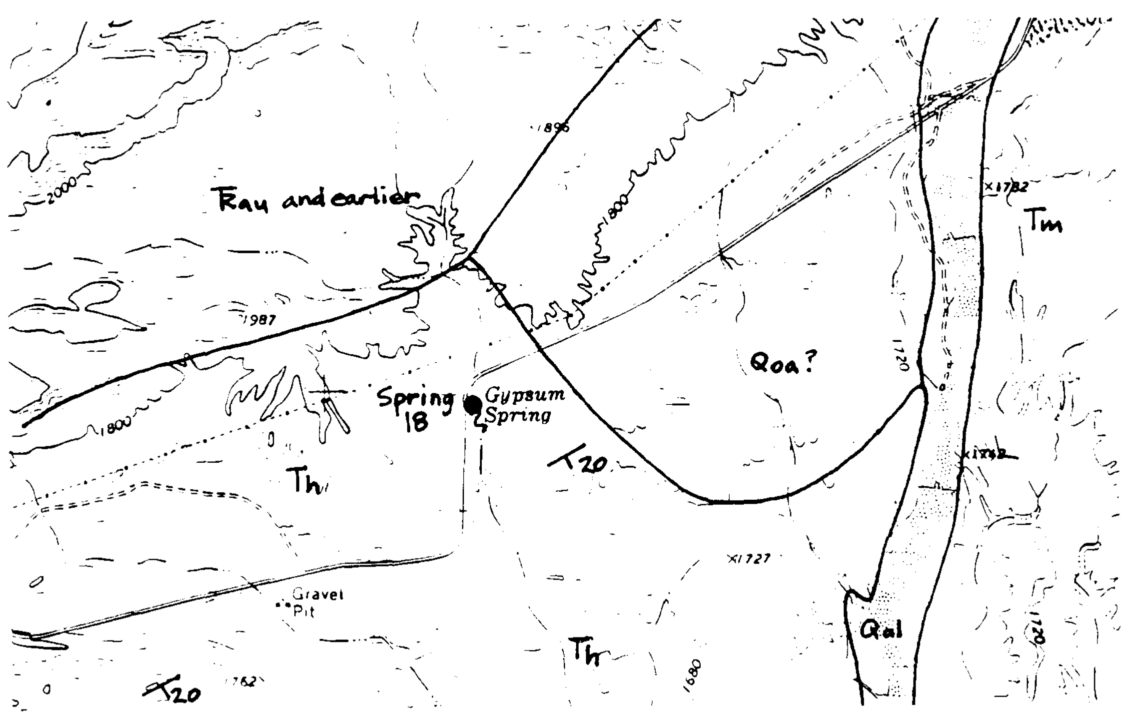

SE ROA 43060

Spring 19 – Unnamed spring south of Rainbow Gardens

Topographic base: 7.5' Henderson Quadrangle
Geology references: Bell and Smith (1980)

The spring is located at the southern end of Rainbow Gardens and about 1.75 km north of Las Vegas Wash. The spring issues from Quaternary alluvial fan deposits in the bottom of a 5-m-deep wash channel incised in the fan surface. The surface flow originates from a single orifice but the area around the spring supports thick tamarisk, mesquite, and grasses; presumably related to shallow groundwater throughout the area. Flow is at the surface for approximately 10 m before it infiltrates into the alluvial deposits. A pipe and circular concrete tank suggest that the spring has been utilized as a water supply in the past, but both are presently filled with sediment.

The spring is near a step-over in a major northwest-trending strike-slip fault (Bell and Smith, 1980). The fault forms a boundary between the Tertiary Horse Spring Formation to the northeast and Quaternary alluvial fan deposits and Tertiary Muddy Creek Formation to the southwest.

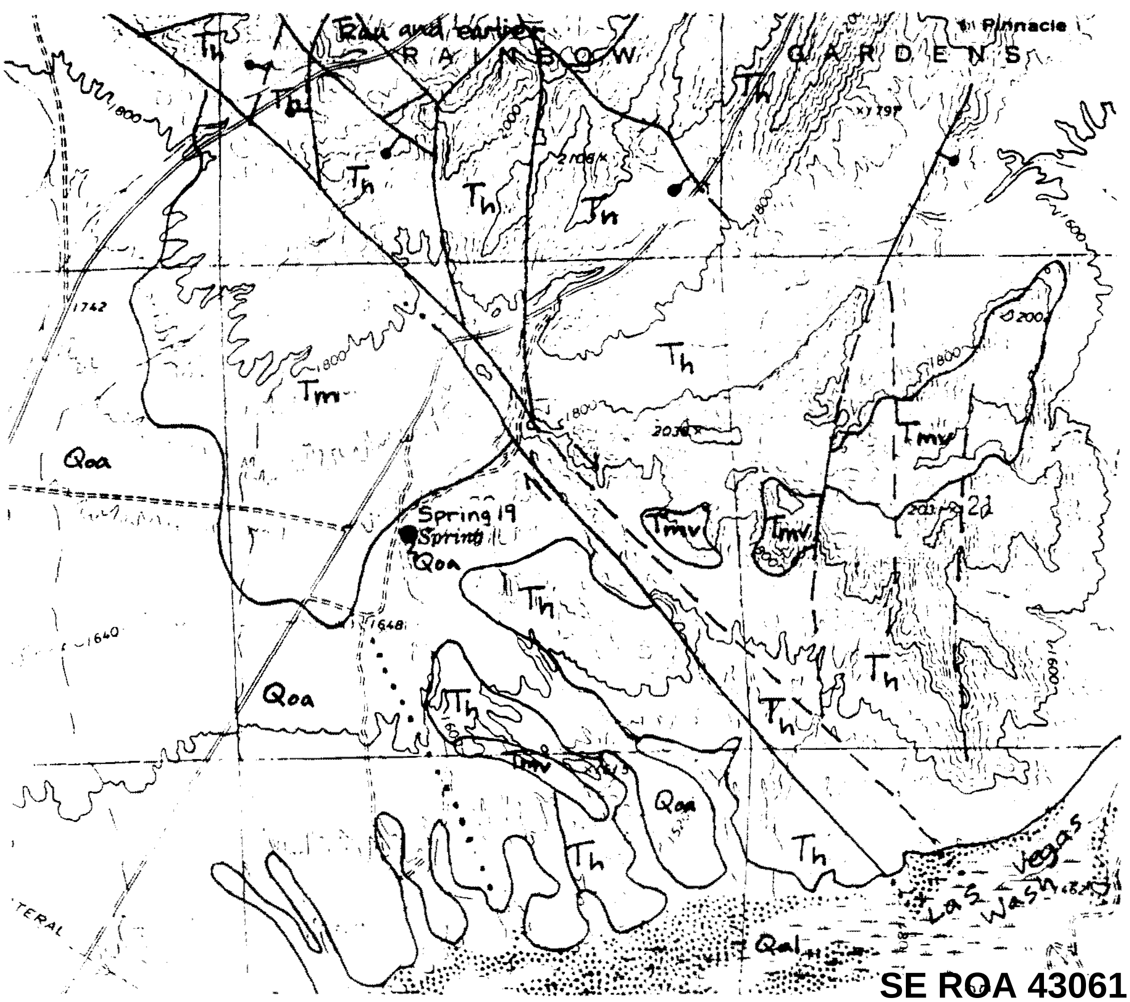

Spring 20 – Pupfish Spring

Topographic base: 7.5' Hoover Dam Quadrangle
Geology references: Mills (1994)

The main spring is 30 m upslope of a concrete tank, which is located on the west side of the Lower Portal Road, just above the tunnel to the base of Hoover Dam. The pool issues as a 6-m-high waterfall into a 4-m-diameter pool. The top of the waterfall was inaccessible, so samples were collected from the pool. Dense vegetation surrounds the pool and the channel that leads to the river. Measurements of flow rate were made just above where the channel enters the river. In addition to the main spring, there are numerous seeps along the cliff face between the spring and the river.

Spring 21 – Arizona Hot Spot

Topographic base: 7.5' Hoover Dam Quadrangle
Geology references: Mills (1994)

Several seeps and springs issue from the Arizona side of the river, about 1.6 km downstream of Hoover Dam. The largest of these is the furthest downstream and is located almost directly across the river from the mouth of Goldstrike Canyon. Samples were collected from an orifice at the margin of a talus slope, about 10 m above the river.

The springs issue from Miocene Patsy Mine volcanics (undifferentiated).

Spring 22 – Sauna Cave

Topographic base: 7.5' Hoover Dam Quadrangle
Geology references: Mills (1994)

Sauna Cave is a shaft mined into the wall of Black Canyon on the Nevada side of the river, and is located 1.4 km below the dam. Groundwater discharges at the back end of the shaft and flows out of the mouth. Samples were collected at the point of discharge at the back end of the shaft. Flow measurements were made at the mouth.

The shaft is mined into the Boulder City Pluton and intersects a north-south-trending fault.

Spring 23 – Nevada Hot Spring

Topographic base: 7.5' Hoover Dam Quadrangle
Geology references: Mills (1994)

Several springs issue from the floor and walls of Goldstrike Canyon about 600 m upstream from the river. Although most of the discharge into the channel is relatively diffuse, we sampled from a point orifice at the base of the north wall, about 100 to 150 m below the highest point of discharge. Discharge measurements were conducted about 75 m upstream from the concrete dam at the riverbank.

The spring issues from a north-south-trending high angle fault in the Miocene Boulder City Pluton.

Spring 24 – Nevada Hot Spot

Topographic base: 7.5' Hoover Dam Quadrangle
Geology references: Mills (1994)

The spring issues into a small cove on the Nevada side of the river, about 1.6 km below Hoover Dam. There are two main orifices above the river, but many seeps and drips, and possible subsurface discharge to the river. Large ferns overhang the river.

The spring issues from a north-south-trending high angle fault in the Miocene Boulder City Pluton.

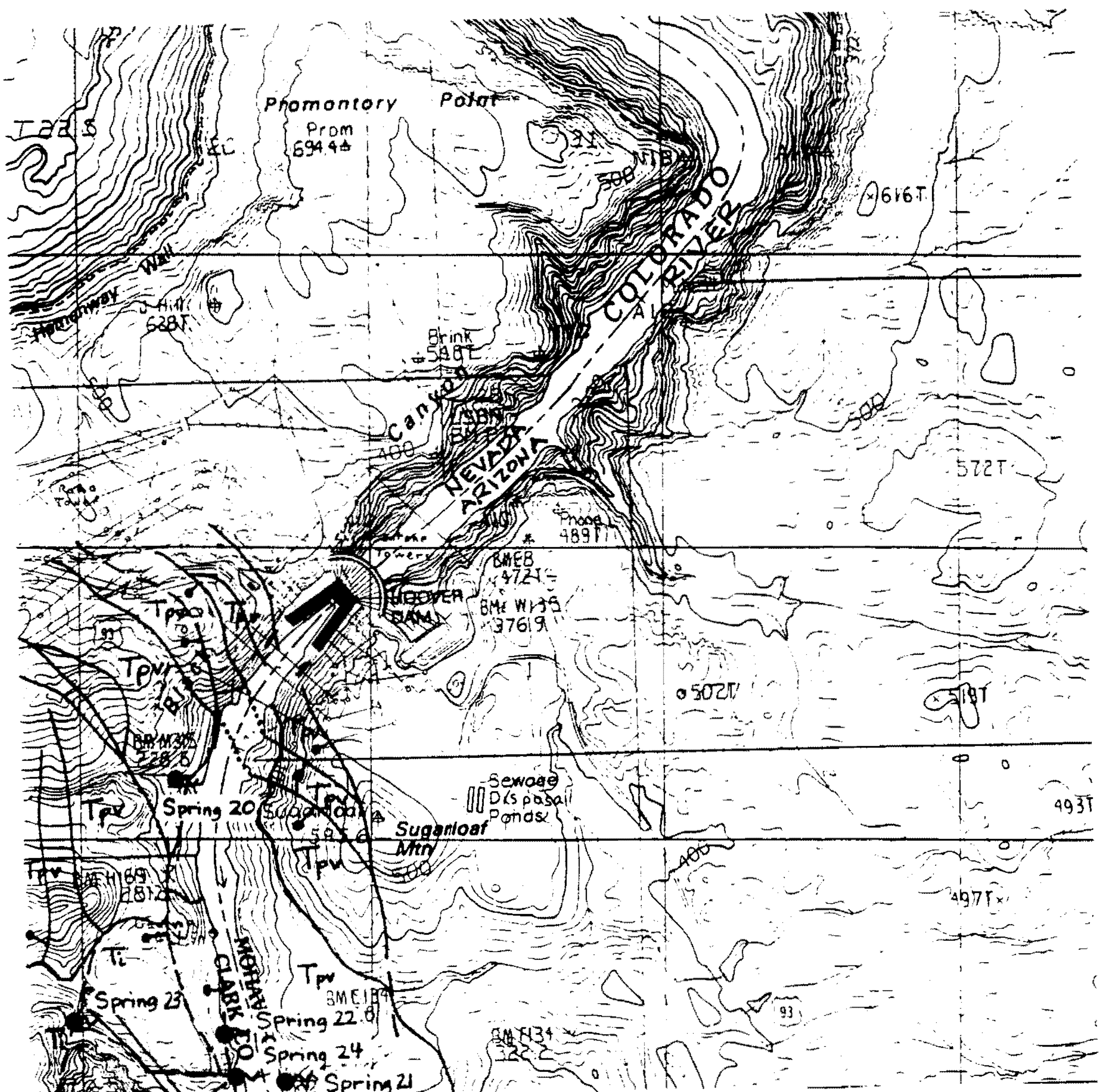

Spring 25 – Palm Tree, Hot

Topographic base: 7.5' Ringbolt Rapids Quadrangle
Geology references: Anderson (1978)

This spring is located about 100 m from the river in a ravine that meets the river about 2.25 km below the dam. The spring issues as diffuse flow from the banks of the ravine. A cold spring (Palm Tree Cold) issues about 100 m upstream of the hot spring. The floor of the ravine is covered by very dense tamarisk. The combined surface flow of the warm and cold springs extends down the ravine to the river.

The spring issues from Miocene Patsy Mine volcanics (undifferentiated) near a northwest trending right lateral strike-slip fault.

Spring 26 – Palm Tree, Cold

Topographic base: 7.5' Ringbolt Rapids Quadrangle
Geology references: Anderson (1978)

This spring is located about 200 m from the river in a ravine that meets the river about 2.25 km below the dam. A warm spring (Palm Tree Hot) issues about 100 m below the cold spring. The floor of the ravine is covered by very dense tamarisk, making access to the cold spring very difficult. An area of reeds grows just above the highest orifice of the cold spring, where the ravine widens and the floor flattens. Surface flow extends down the ravine to the warm spring, and the combined flow extends to the river.

The spring issues from Miocene Patsy Mine volcanics (undifferentiated) near a northwest trending right lateral strike-slip fault.

Springs 28 and 29 – Boy Scout Canyon

Topographic base: 7.5' Ringbolt Rapids Quadrangle
Geology references: Anderson (1978)

There are a number of springs and seeps in Boy Scout Canyon, and a wide variety of temperatures. Boy Scout Canyon is on the Nevada side and meets the river about 3.5 km below the dam. The lowest point of discharge is about 400 m up the canyon from the river. At this location, cold water discharge forms a waterfall about 12 m high and warm water discharge issues from seeps just above the floor of the canyon. The highest area of warm discharge occurs as seepage from an overhanging wall about 50 m upstream from the springs just described. The surface flow above this point is cold and passes over several waterfalls. Samples were collected of both the warm and cold discharge. Note that despite their difference in temperature, these springs have very similar geochemical and isotopic composition.

Although the discharge rate from this spring is relatively high, only a small fraction of the surface flow reached the river on our visit of 2-2-97. Several reaches of the channel carried no surface flow. The discharge measurement was made at the farthest downstream location of channel flow over a bedrock bench.

The springs issue from the Miocene Boulder City pluton at points where near vertical, north-south-trending faults intersect from below an unconformable barrier. This unconformity appears to act as a "ceiling", preventing further flow within the plutonic rocks.

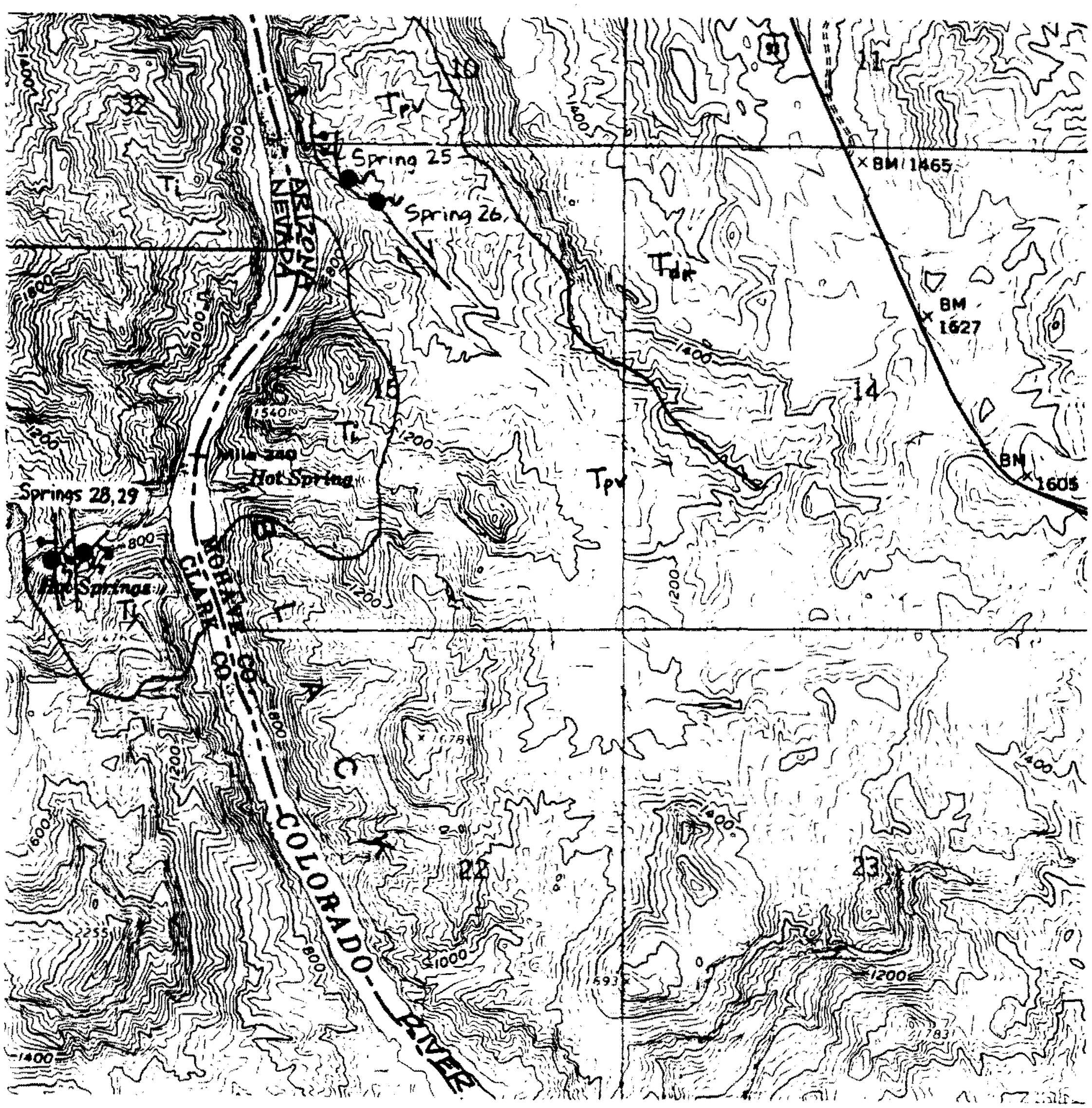

SE ROA 43065

Spring 27 – Unnamed Spring in Horsethief Canyon

Topographic base: 7.5' Ringbolt Rapids Quadrangle
Geology references: Anderson (1978)

Horsethief Canyon extends into the west side of Mount Wilson of the Black Mountains in Arizona. Several springs and seeps occur in the canyon above a dry waterfall, supporting a wide variety of vegetation. At the time of our visit (2-3-97), the highest flow rate occurred about 1 km upstream from the waterfall, and supported a stand of cottonwood trees, reeds, and other vegetation. Surface flow was discontinuous over a total length of several hundred meters. Flow was on the surface in reaches where bedrock benches formed the base of the canyon, or where the alluvial deposits were thin. In other reaches, flow presumably occurs within the alluvial deposits.

The spring issues from Tertiary intrusive granite of the Wilson Ridge pluton (described by Anderson *et al.*, 1972).

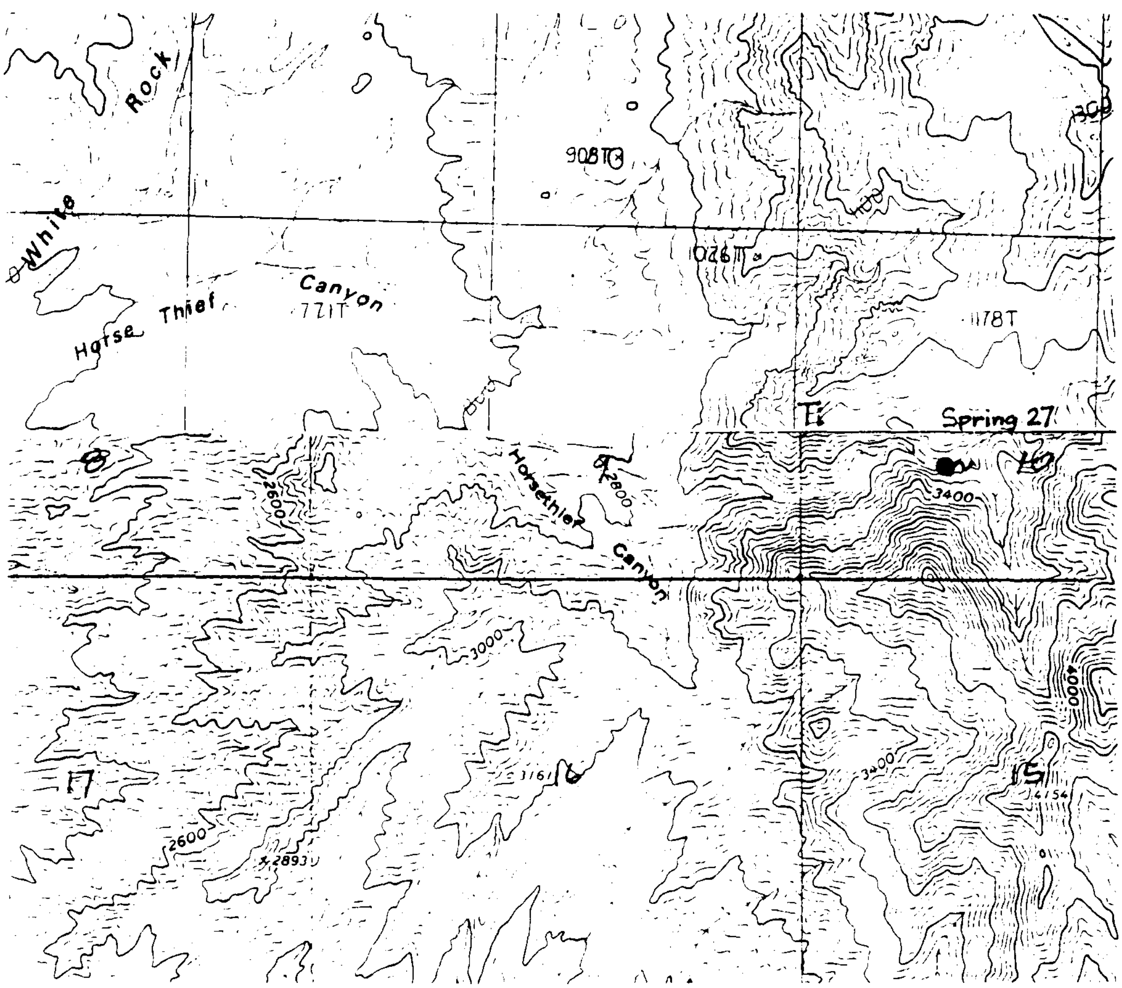

Spring 30 – Arizona Hot Spring

Topographic base: 7.5' Ringbolt Rapids Quadrangle
Geology references: Anderson (1978)

Arizona Hot Spring is located in a dramatic slot canyon that meets the river just downstream of Ringbolt Rapids, and about 6.6 km downstream of the dam. The spring issues into several manmade pools that are located about 300 m up the canyon from the river. The canyon walls near the pools are nearly vertical and 2 to 3 m apart at the base. Above the pools, the canyon opens up and the walls slope gently away from the alluvium-filled channel. Surface flow extends about 150 m down the canyon from the pools, much of it in a bedrock channel, but infiltrates when the channel passes over alluvial gravels.

The spring issues from Miocene Patsy Mine volcanics (undifferentiated) near a northwest trending right lateral strike-slip fault. This fault is offset by a north-south-trending normal fault and the spring issues from near the intersection of the two faults.

Spring 31 – Unnamed cold spring near Arizona Hot Spring

Topographic base: 7.5' Ringbolt Rapids Quadrangle
Geology references: Anderson (1978)

The spring is located about 20 m up the canyon from the highest (man-made) pool of Arizona Hot Spring. Above this spring, the canyon is wide, the walls slope gently, and the floor is covered by alluvium. Below the spring, the canyon narrows dramatically (forming a "slot canyon"), the walls are nearly vertical, and the floor is scoured bedrock. The flow issues from alluvium in the base of the canyon, just above the point where the channel enters the slot canyon.

Spring 32 – Nevada Falls

Topographic base: 7.5' Ringbolt Rapids Quadrangle
Geology references: Anderson (1978)

Nevada Falls spring is located in a small cove on the Nevada side, approximately 8.2 km below the dam. Surface flow originates about 11 m above the gravel bank of the river, and drops to the river in a series of waterfalls. Only the highest pool contains vegetation. Samples were collected from the second pool up from the riverbank, which is about 3 m above the bank.

The flow issues from a north-south trending fault in the Miocene Patsy Mine volcanics (undifferentiated), about 100 m east of a contact with Tertiary Mount Davis lavas.

Spring 33 – Bighorn Sheep Spring

Topographic base: 7.5' Ringbolt Rapids Quadrangle
Geology references: Anderson (1978)

Bighorn Sheep spring is located in a steep-sided canyon that meets the river 8.4 km below the dam. The main orifice forms a 5-m-high waterfall on the north side of the canyon, about 600 m up the canyon form the river. Because the orifice was inaccessible, the samples were collected near the base of this waterfall. Additional discharge occurs at several small seeps located upstream of the main orifice, all discharging from the north wall of the canyon. Surface flow is present in the channel to within 100 m of the river, but did not reach the river on our 2-2-97 visit. Dense stands of tamarisk extend from the orifice all the way to the river.

The spring issues from a northeast-trending fault in the Tertiary lavas (Mount Davis Volcanics).

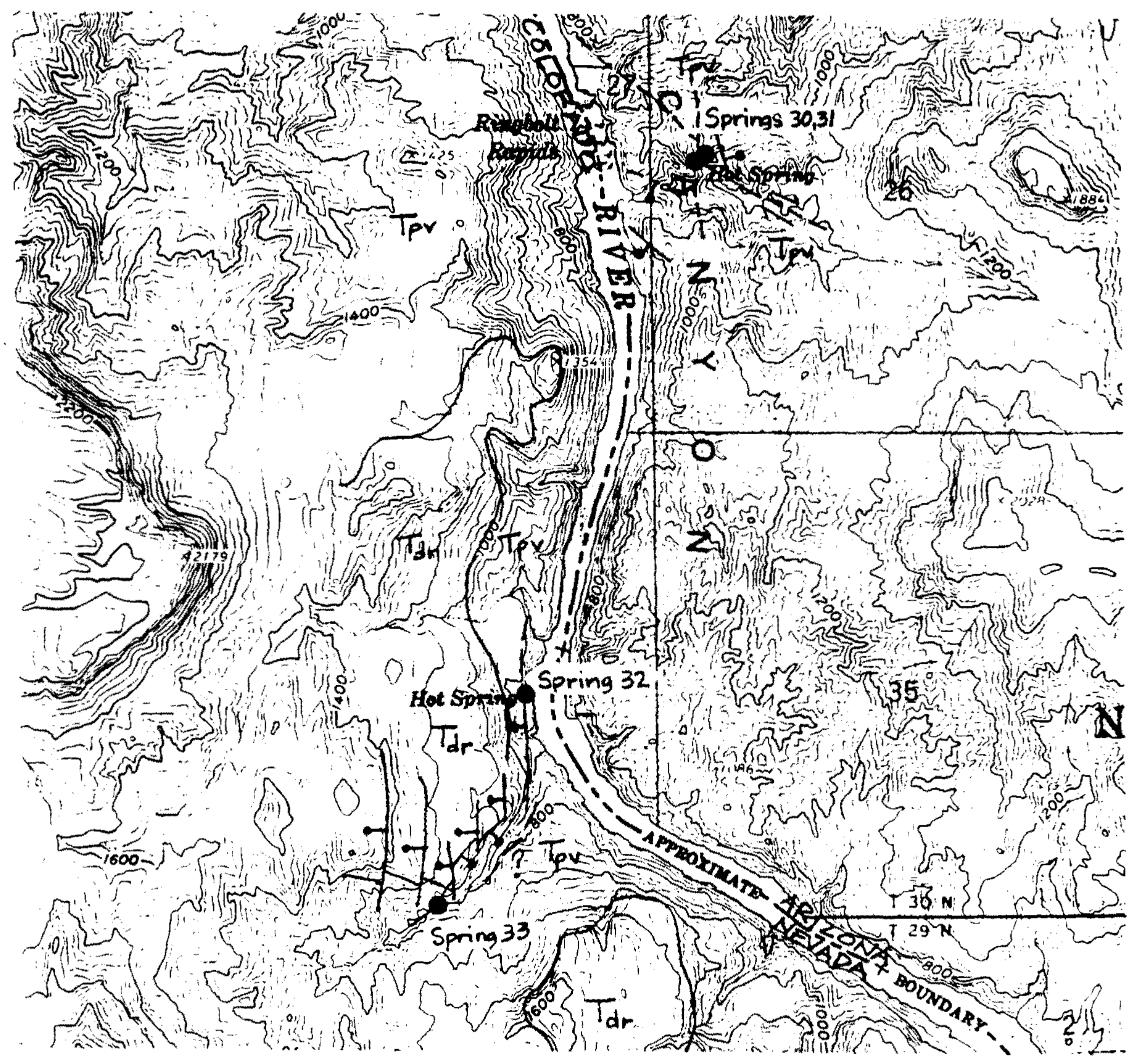

SE ROA 43068

Spring 34 – Arizona Seep

Topographic base: 7.5' Ringbolt Rapids Quadrangle
Geology references: Anderson (1978)

Arizona seep is 11.3 km below Hoover Dam, on the Arizona side of the river. The spring issues as drips and seeps from a rock overhang ("rain cave"), about 20 m above the river. There is no main orifice. The moist soil resulting from the spring discharge supports thick vegetation that extends down to the river. Samples were collected from the seeps with the highest discharge rate.

The spring issues from Miocene Patsy Mine volcanics (undifferentiated) near several northwest trending right lateral strike-slip faults. These faults offset low-angle faults, which produce the spring flow. A north-south trending high angle fault is located 0.5 km to the east of the spring.

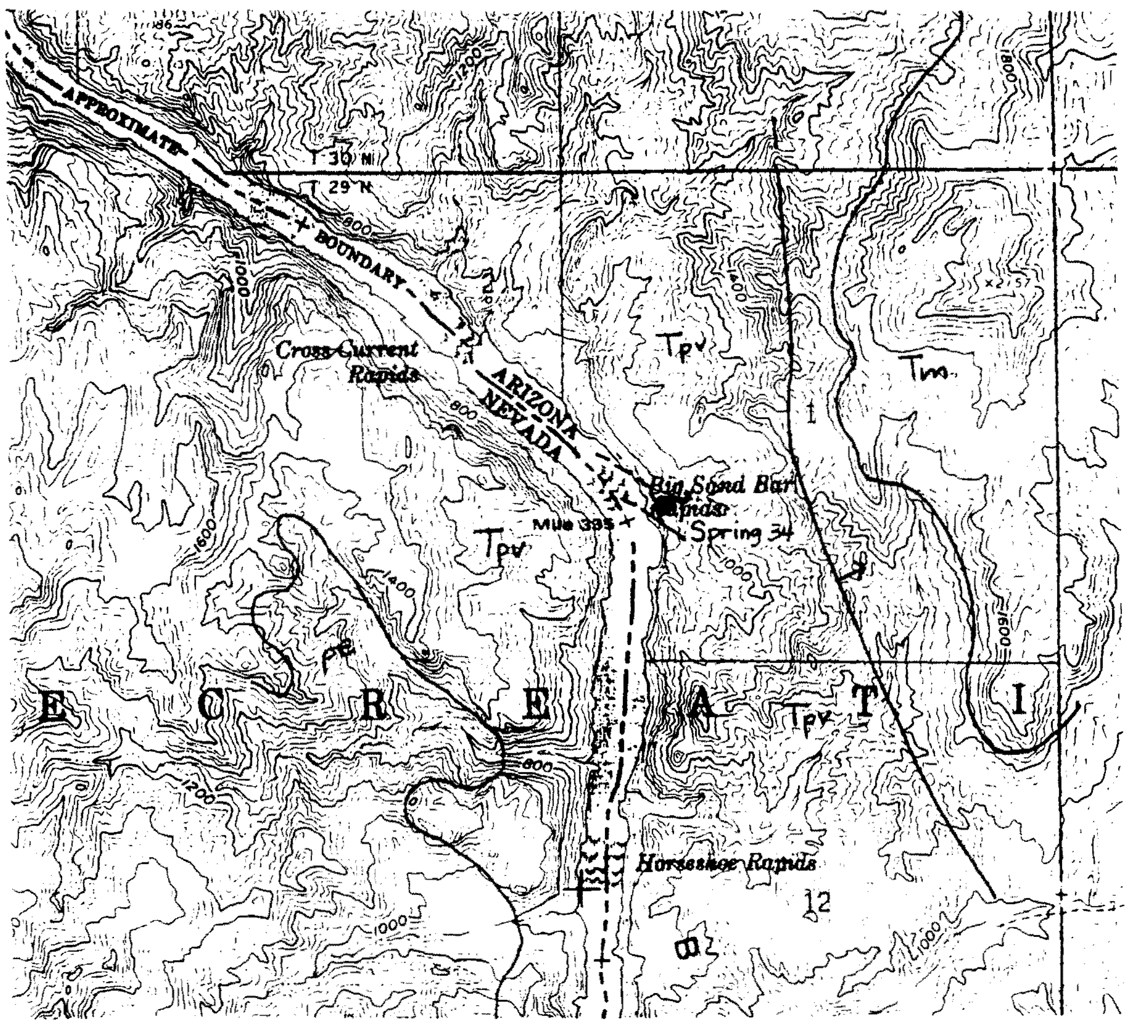

Spring 35 – Latos Pool

Topographic base: 7.5' Willow Beach Quadrangle
Geology references: Anderson (1978)

Latos Pool is located in Burro Wash on the eastern slope of the Eldorado Mountains, and about 1.6 km west of the Colorado River. Three pools fill a narrow portion of the wash, where the channel cuts through consolidated conglomerate. The two lower pools are connected and are both about 4 m long, 2 m wide, and over 1.5 m deep. The lowest pool is almost completely filled with reeds. The upper pool is smaller and is located about 15 m upstream. Another seepage area is located about 200 m upstream in a drainage extending from the southwest. This seep supports a thick stand of mesquite and grass. A third seepage area is located on a bench above the wash channel and about 100 m south of the pools. This seep also supports a thick stand of mesquite and grasses. Samples were collected from surface flow in the channel, below a seep area in the ravine walls and about 50 m below the pools. At the time of our visit (5-6-97), surface flow was discontinuous for about 100 m below the pools. However, evidence of recent surface flow (dried algae and salt deposits) extended from where the power line road crosses Burro Wash all the way upstream past the three pools.

Latos Pool is located on a fault trending N 15° W within a consolidated conglomerate of the Tertiary Muddy Creek Formation.

SE ROA 43070

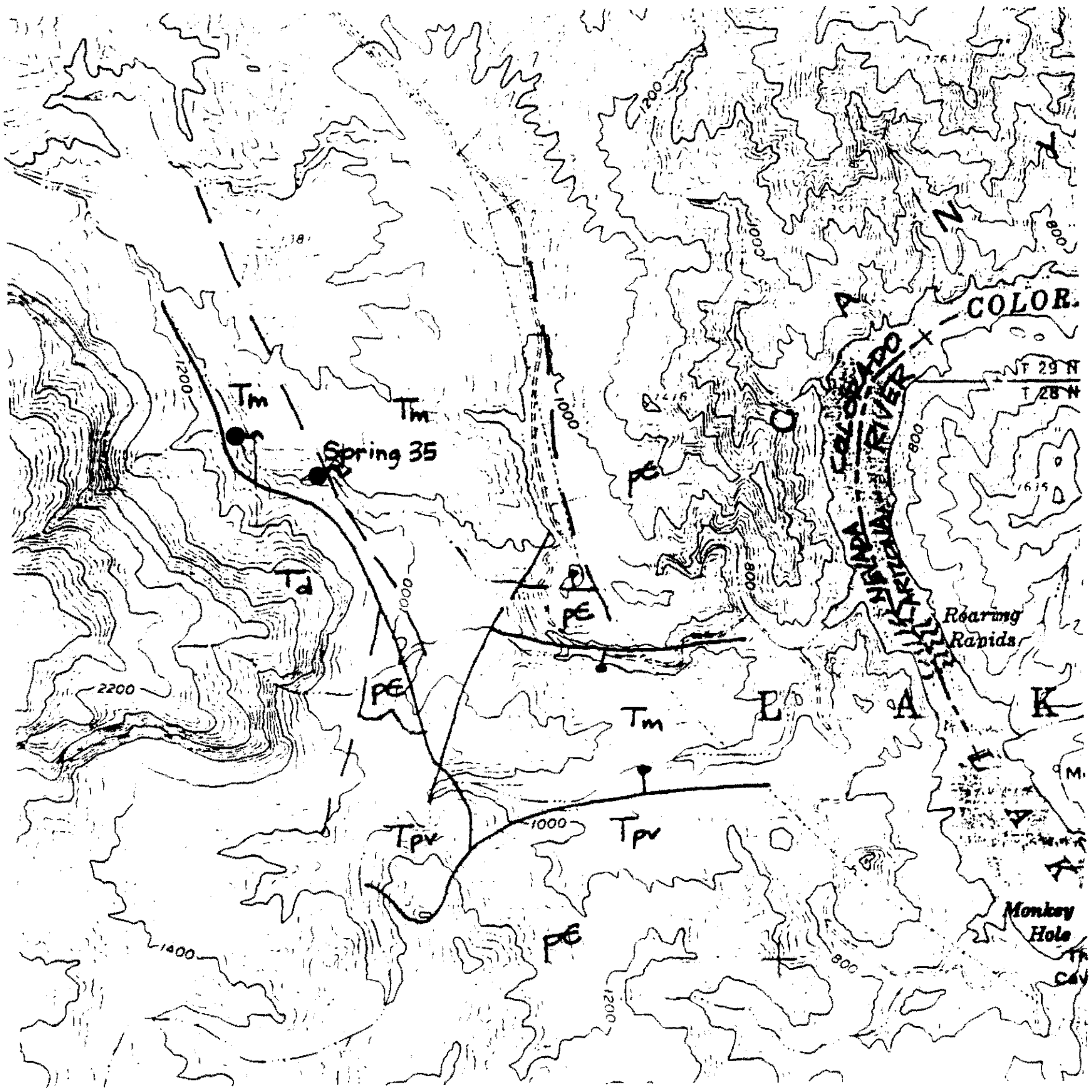

Tm
Tm
Spring 35
Td
pЄ
pЄ
pЄ
pЄ
Tm
Tpv
Tpv
COLOR.
COLORADO
RIVER
NEVADA
ARIZONA
T 29 N
T 28 N
Roaring
Rapids
L
A
K
Monkey
Hole
2200
1400
1200
1000
800

SE ROA 43071

Spring 36 – Unnamed Spring in Aztec Wash

Topographic base: 7.5' Nelson Quadrangle
Geology references: Longwell (1963)

Aztec Wash extends out of the Eldorado Mountains toward Lake Mohave, south of Nelson, Nevada. The spring issues as seeps from alluvial deposits and directly from fractures in the granite walls of the channel, and flows discontinuously at the surface for about 150 m. The highest point of discharge was about 100 m upstream from a small concrete dam in the wash channel at our visit of 2-5-96. A pipe extends from the dam about 2 km down Aztec wash, although its poor condition prevents it from conveying any water. In addition, the channel behind the dam is filled with alluvial deposits. At the time of our second visit (2-11-97) the highest point of discharge was downstream about 20 m, and the discharge rate was lower. Grass and reeds line the banks of the ravine where a soil layer has developed; other areas consist of exposed granite with no soil or vegetation. Vegetation is sparse above the spring, suggesting that groundwater is deeper below ground surface.

The spring issues from steeply-dipping fractures in the Precambrian Rapakivi granite.

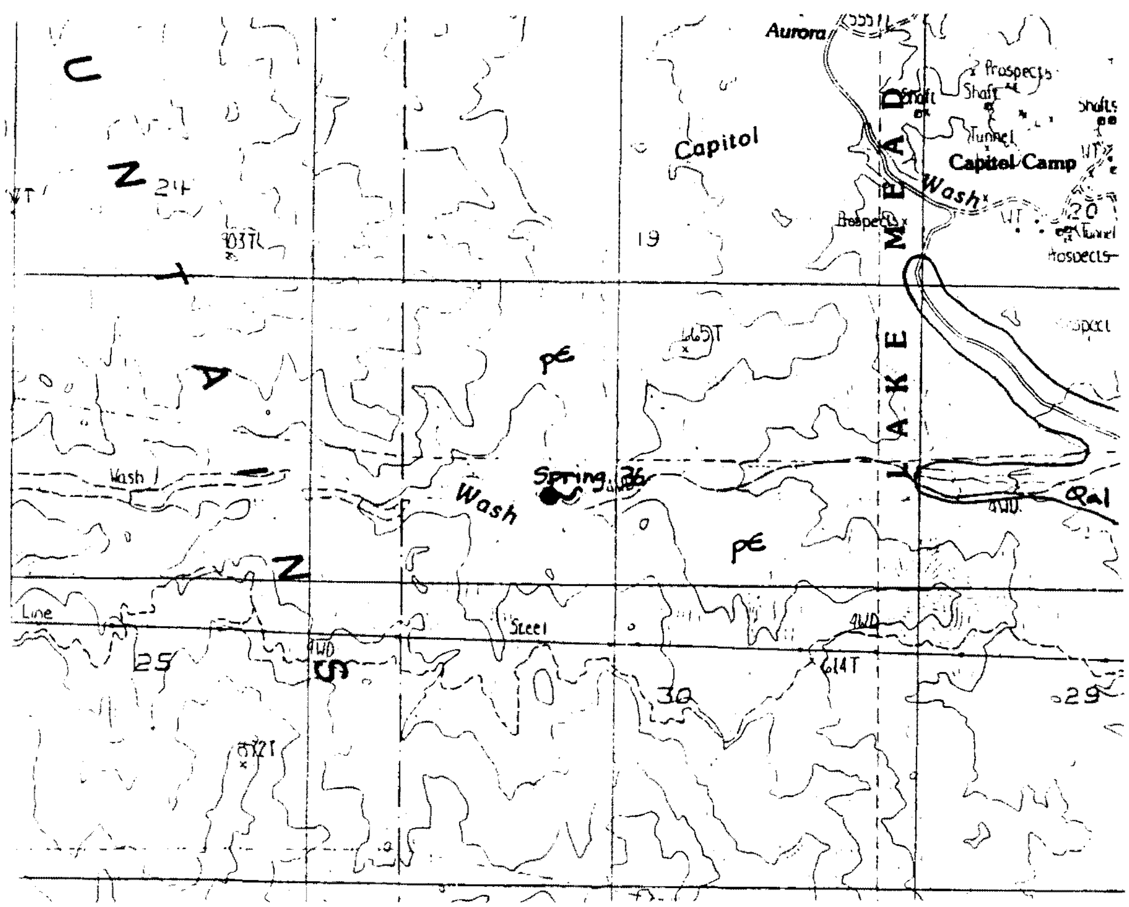

SE ROA 43072

JA_12952

APPENDIX C

ISOTOPIC DATA FOR SELECTED SOUTHERN NEVADA GROUNDWATERS

Table C-1. Isotope Composition of Selected Southern Nevada Groundwaters. Values shown are averages if multiple samples are available. Number in parentheses is number of samples, if greater than one.

Site Name	Latitude (d m s)	Longitude (d m s)	Altitude of Land Surface (m AMSL)	δD (SMOW, ‰)	$\delta^{18}O$ (SMOW, ‰)	$\delta^{13}C$ (PDB, ‰)	PMC (uncor-rected)	^{3}H (pCi/L)	Source[1]
McCullough Range, Eldorado Mountains, Highland Range, New York Mountains									
Crescent Spring	35 28 43	115 10 47	1292	-73.0	-9.4	—	—	—	c
Ora Hana Spring	35 37 25	115 04 07	1170	-72.0	-8.4	—	—	—	c
McClanahan Spring	35 41 42	115 11 05	902	-67.0	-7.2	-7.0	68.1	—	c
Rand Spring	35 42 03	114 51 20	1140	-78.0	-9.5	—	—	24.0	b
Bridge Spring	35 43 36	114 49 06	1032	-77.0	-9.2	—	—	19.0	b
Mormon Mountains									
Huckberry Spring	36 55 04	114 26 16	1580	-87	-12.3	—	—	—	c
Horse Spring	36 56 29	114 26 47	1750	-89	-12.7	—	—	—	c
Davies Spring	36 57 56	114 30 07	1825	-89	-12.5	—	—	—	c
East Mormon Mountains									
Peach Spring	36 57 16	114 17 23	950	-76.5	-10.4	—	—	—	c
Gourd Spring	36 57 31	114 17 30	950	-76.5	-10.6	—	—	—	c
Central Spring Mountains									
Trout Spring	36 13 22	115 40 59	2360	-97.7(19)	-13.6(22)	-8.1(5)	90.8(1)	257(3)	c
Cold Creek Spring	36 24 05	115 44 20	1930	-100.1(16)	-13.8(18)	-9.6(5)	76.0(4)	92(4)	c
Southern Spring Mountains									
Bird Spring	35 53 20	115 22 12	1326	-88.0	-11.7	-7.8	67.5	—	c
Sandstone Spring #1	36 03 47	115 28 09	1207	-89.0	-12.2	-10.6(2)	49.8(2)	<15(1)	c
BLM Visitors Center Well	36 07 44	115 26 03	1152	-89.0	-12.25	-9.3	46.0	9.0	c
Red Spring	36 08 40	115 25 10	1116	-89.0	-12.25	-10.5(2)	62.4(2)	3.0	c
Willow Spring	36 09 41	115 29 51	1402	-90.5	-12.3	—	—	—	c
White Rock Spring	36 10 27	115 28 43	1469	-91.0	-12.5	-12.0	—	<2.0	c
Castillo Well	35 50 02	115 26 09	1140	-94.0	-12.5	-9.3	39.4	—	c
Sheep Range									
Wiregrass Spring	36 38 00	115 12 29	—	-94.3(9)	-12.8(9)	-10.2	96.8	89.6	c
Moorman Well Spring	36 38 38	115 05 52	1963	-91.8	-12.7	-9.9	—	—	c
Cow Camp Spring	36 35 01	115 18 26	—	-92.0	-12.6	—	—	—	c
Lamb Spring	36 56 42	115 06 21	1700	-92.5	-13.15	—	—	—	c
Sawmill Spring	36 40 50	115 10 34	—	-92.0	-12.85	—	—	—	c
Sheep Spring	36 53 42	115 06 53	—	-96.0	-13.35	—	—	—	c
Meadow Valley Wash Flow System									
Wells and Springs	—	—	—	-87.3(14)	-11.8(13)	—	—	—	c
Lower White River Flow System									
Hiko Spring	37 35 54	115 12 49	—	-109.0	-13.8	-5.4	—	<10	e
Crystal Spring	37 31 58	115 13 50	—	-108(d)	-14.3(d)	-5.3	6.2	<10	e
Ash Spring	37 27 49	115 11 34	1102	-108.0	-14.1	-6.7	6.3	0.0	c
Big Muddy Spring	36 43 20	114 42 48	542	-97.8(3)	-12.9(3)	-6.0	6.7	<1.0	c
M–8 Spring	36 43 15	114 43 39	—	-99.0	-12.75	—	—	—	c
M–9 Spring	36 43 33	114 43 38	—	-96.5	-12.45	—	—	—	c

SE ROA 43074

Table C-1. Isotope Composition of Selected Southern Nevada Groundwaters. Values shown are averages if multiple samples are available. Number in parentheses is number of samples, if greater than one (Continued).

Site Name	Latitude (d m s)	Longitude (d m s)	Altitude of Land Surface (m AMSL)	δD (SMOW, ‰)	$\delta^{18}O$ (SMOW, ‰)	$\delta^{13}C$ (PDB, ‰)	PMC (uncor-rected)	^3H (pCi/L)	Source[1]
Lower White River Flow System Continued									
Pederson's Warm Spring	36 42 36	114 42 54	555	-97.0	-12.75	—	—	—	c
Iverson's Spring	36 42 37	114 42 43	—	-97.0	—	—	—	—	c
CE–VF–2 Well	36 52 30	114 56 44	752	-101.0(2)	-13.0(2)	-6.1	7.0	<1.0	c
CE–DT–6 Well	36 46 04	114 47 13	693	-97.0	-12.95	-8.0	8.4	1.8	c
CSV–2 Well	36 46 50	114 43 20	666	-98.0	-12.85	-5.5	8.4	4.0	c
Dry Lake Valley Well	36 27 18	114 50 38	638	-97.5	-13.3	-4.2	3.0	7.0	c
GP Apex Well	36 20 28	114 55 36	753	-98.0	-13.45	-5.5	2.7	<.3	c
CE–DT–4 Well	36 47 44	114 53 32	662	-101.0	-13.0	—	7.6	<2.0(1)	c
CE–DT–5 Well	36 47 44	114 53 32	661	-101.0	-13.0	—	7.6	<2.0(1)	c
Genstar Well	36 23 29	114 54 14	661	-97.0	-13.05	-4.9	1.5	<1.0	c
South Hidden Valley Well	36 33 08	114 55 30	807	-90.5	-11.2	—	—	—	c
CSV–3 Well	36 41 27	114 55 30	736	-75.0	-10.3	—	—	—	c
Weiser Wash Flow System									
EH–3 Well (Tmc)	36 41 32	114 31 32	530	-90.7(3)	-11.9(3)	—	—	—	d
EH–7 Well (Tmc)	36 40 14	114 31 53	512	-91.0	-12.3	—	—	—	d
EH–3 Well (below Tmc)	36 41 32	114 31 32	530	-92.0	-12.9	—	—	—	d
EH–7 Well (below Tmc)	36 40 14	114 31 53	512	-93.0	-12.8	—	—	—	d
Eldorado Valley									
Eldorado Substation Well	35 48 13	115 00 14	550	-96.0	-12.0	-7.8	7.75	<10	b
Colorado River									
Below Hoover Dam	36 00 35	114 44 40	200	-102.0	-12.7	-5.7	—	51.0	f
Valley of Fire									
Valley of Fire Well	36 25 21	114 32 52	683	-82.0	-10.6	-8.5	18.7	—	c
Northeast Las Vegas Valley									
Nellis AFB Well #13	36 12 44	115 03 00	552	-98.0	-13.8	-8.0	—	—	c
Lake Mead Base Well #3	36 14 21	115 00 16	568	-101.5	-13.8	-5.3	5.6	<.3	c
Nellis AFB #4	36 14 56	115 00 15	585	-95.0	-13.2	-6.3	21.0	—	c
Southwest Las Vegas Valley									
Sky Harbor Airport	35 58 16	115 08 50	—	-95.0	-13.1	-6.8	—	—	c
Showboat Country Club #2	36 02 51	115 04 48	—	-97.0	-13.3	—	—	—	c
Jean Prison Well	35 47 18	115 20 43	—	-95.0	-12.1	-7.6	2.4	—	c
Sunset Park Well	36 03 49	115 05 51	—	-94.0	-12.7	-6.7	4.0	—	c

[1] Sources of data:
a Thomas *et al.*, 1991
b SNWA, unpublished data
c Thomas, *et al.*, 1997
d DRI, unpublished data
e Hershey and Mizell, 1995
f This study

SE ROA 43075

desert research institute

University and Community College System of Nevada

Water Resources Center

Investigation of the Origin of Springs in the Lake Mead National Recreation Area

Karl F. Pohlmann
David J. Campagna
Jenny B. Chapman
Sam Earman

March 1998

Publication No. 41161

prepared by
Water Resources Center
Desert Research Institute
University and Community College System of Nevada

prepared for
National Park Service, Water Resources Division

Figure 2 Cross Section of the Littlefield Limestone across the river from Littlefield

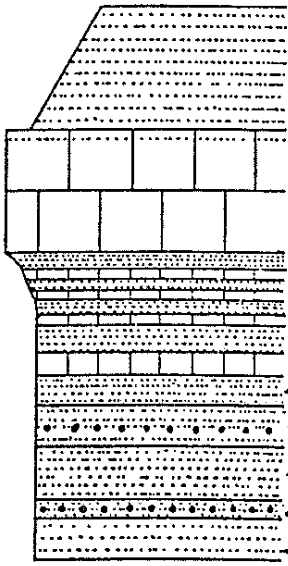

Red Brown Sandstone

White Limestone, massive micrite with some inclusions of sand.

Interbedded silty Sands and Limestone

Gray to White siltstone, poorly cemented.

Brown Sandstone, medium to pebble grained.

Interbedded Brown Siltstone, Sandstone, and Silty Sandstone.

Conglomeratic Sandstone

Brown Sandstone, fine grained.

Figure 3 Cross Section of the Littlefield Limestone Downstream of "Reber" Spring

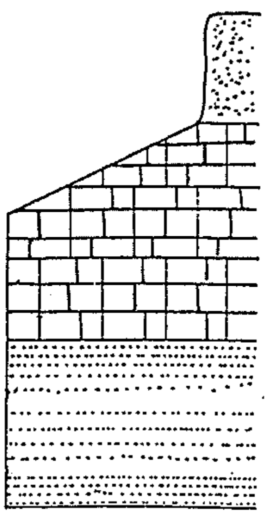

Tan Sandstone, fine to coarse grained, well cemented ($CaCO_3$).

White Limestone, thin bedded, sparudite, porous.

White to Yellow Brown siltstone

Vertical Scale 0 5 10 feet

Figure 4 Cross Section of the Littlefield Limestone Upstream of Leavitt Ranch Spring

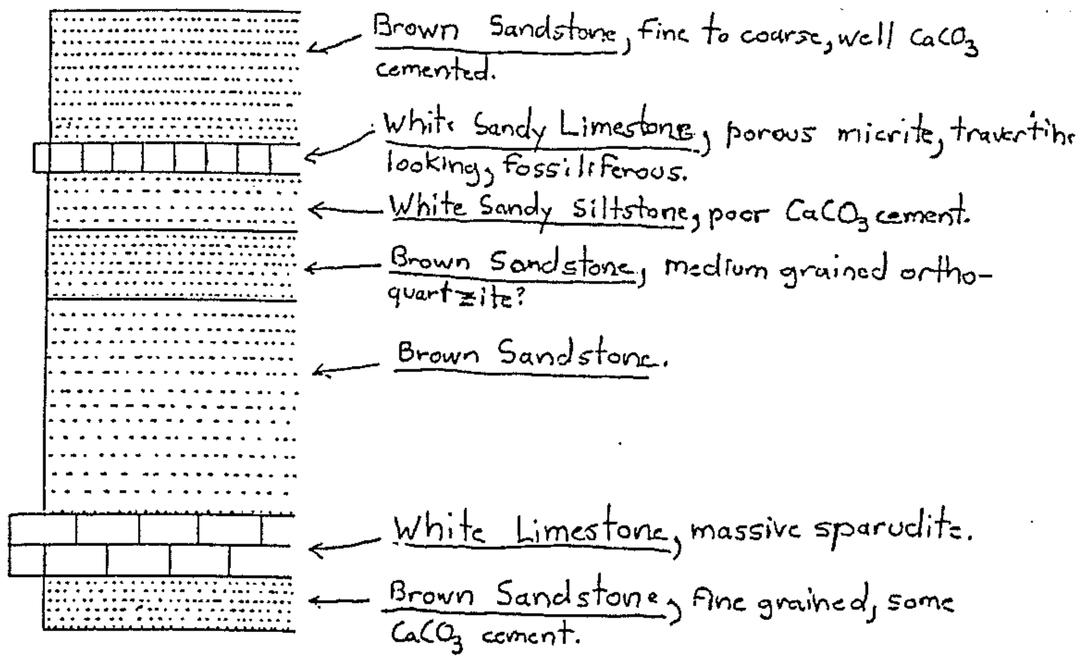

Figure 5 Cross Section of the Littlefield Limestone Downstream of mouth of the Gorge.

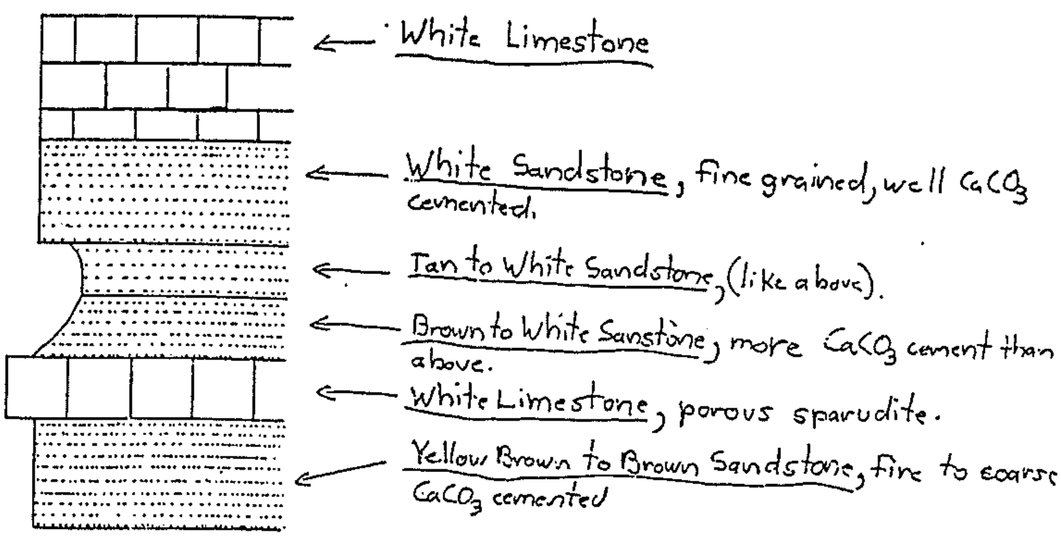

Above X-sections are located on Plate 2. Sections underlain Littlefield Conglomerate. Vertical Scale 0 5 10 feet

APPENDIX B

HYDROLOGY DATA

TABLE 1

DISCHARGE MEASUREMENTS ALONG THE VIRGIN RIVER AND ITS TRIBUTARIES
(in cfs)

Gaging Location		1/17 1975		1/18 1975	8/5 1975		3/27 1976		6/17 1976	6/18 1976	6/24 1976	7/7 1976	7/20 1976	7/27 1976	7/28 1976	7/30 1976
Virgin River at Washington-St.George canal crossing									955 12					84	50	71
Virgin River at I-15 bridge near Bloomington,Utah									1200 14		650 11 4200	1016 10 4300		1520 34 2500	813 50	1700 71
Virgin River at gage at First Narrows.						1130 15 2750	1200 21 2750	1300 20 2750	1400 0		1150 0			1060 66 66 2800 (0.5)	1125 52 52 (0.4)	1015 41 41 (.53)
Virgin River at junction with Black Rock Gulch						1513 0 2550	1545 10 2550									
Black Rock Gulch														745 5 1900	700 .4 .4	
Virgin River opposite the Cedar Pocket Rest Area						1710 2 2700	1730 2 2700									
Virgin River above first springflow	1304 82	1555 83	2200 73	325 63	1400 0	1800 0				630 0	630 0	700 0	1400 0	1500 0	1200 0	
Virgin River at gage below first springflow										630 .3				1730 <1	1310 .7	720 64
Virgin River at the Mouth of the Gorge	1310 102	1655 118	2235 100	400 80						800 20	915 22 3400	1320 21				
Virgin River near Leavitt Ranch Spring(#70)					1400 42					930 40	1125 45	1600 48 3450	1630 46			
Beaver Dam Wash at Gage					1500 .6					1415 1.3	1355 .9	1700 1.1 480	1340 .8 450		1600 .6	
Virgin River at Littlefield	1400 141	1600 149	2200 149	400 134	1600 52					1525 65	1530 57	1900 60	1445 59		1700 56	1610 98
Petrified Springs Weir(#89)											1700 2					

Upper number is time,middle number is flow in cfs, lower number is specific conductance(SC) in micromhos at 25 degrees C, number in parentisis is river stage in feet.

TABLE 2

BEAVER DAM WASH STAGE/DISCHARGE DURING SUMMER 1976

	June		July		August		September	
	Stage ft.	Discharge cfs	Stage ft.	Discharge cfs	Stage ft.	Discharge cfs	Stage ft.	Discharge cfs
Date								
1	.06	.85	.05	.75	.12	1.50	.05	.75
2	.06	.85	.05	.75	.12	1.50	.05	.75
3	.06	.85	.09	1.20	.12	1.50	.05	.75
4	.05	.75	.10	1.30	.12	1.50	.07	1.00
5	.05	.75	.10	1.30	.12	1.50	.10	1.30
6	.06	.85	.11	1.40	.12	1.50	.09	1.20
7	.06	.85	.15	1.80	.07	1.00	.07	1.00
8	.06	.85	.10	1.30	.06	.85	.06	.85
9	.06	.85	.05	.75	.06	.85	.05	.75
10	.07	1.00	.05	.75	.05	.75	.10	1.30
11	.07	1.00	.05	.75	.05	.75		
12	.08	1.10	.05	.75	.05	.75		
13	.08	1.10	.05	.75	.05	.75		
14	.08	1.10	.05	.75	.05	.75		
15	.08	1.10	.05	.75	.05	.75		
16	.09	1.20	.05	.75	.06	.85		
17	.09	1.20	.05	.75	.06	.85		
18	.09	1.20	.05	.75	.07	1.00		
19	.09	1.20	.06	.85	.07	1.00		
20	.09	1.20	.06	.85	.07	1.00		
21	.08	1.10	.07	1.00	.07	1.00		
22	.05	.75	.07	1.00	.07	1.00		
23	.05	.75	.07	1.00	.07	1.00		
24	.05	.75	.07	1.00	.08	1.10		
25	.05	.75	.07	1.00	.08	1.10		
26	.05	.75	.07	1.00	.08	1.10		
27	.05	.75	.07	1.00	.09	1.20		
28	.05	.75	.08	1.10	.09	1.20		
29	.05	.75	.12	1.50	.08	1.10		
30	.05	.75	.21	?	.06	.85		
31	.05	.75	.42	?	.06	.85		
Sum =		27.70		27.10		23.20		8.35
Mean =		.92		.97		.97		.93

SE ROA 43081

APPENDIX C

HYDROCHEMICAL DATA

TABLE 1 WATER QUALITY ANALYSIS OF THE LITTLEFIELD SPRINGS

ANALYSIS IN EPM (SIO2 IN PPM)

SPRING NO.	DATE SAMPLED	SAMPLED BY	TEMP C	PH	EC	CA2+	MG2+	NA+	K+	CL-	(SO4)=	(HCO3)=	SIO2
76	[illegible]-25-76	DRI/WRC	25.	7.68	[illegible]	20.96	10.44	12.61	.86	12.01	27.73	7.30	
[illegible]	3-17-76	DRI/WRC	22.	7.46	[illegible]	20.24	10.26	12.28	.81	11.84	27.36	7.30	
37	3-17-75	DRI/WRC	24.	6.19	[illegible]	20.66	16.12	12.96	.81	11.64	28.90	5.10	19.90
76	3-17-75	DRI/WRC	22.	7.59	3850.	20.96	16.12	13.01	.79	11.65	27.11	7.34	19.60
75	[illegible]	USGS	24.	[illegible]	[illegible]	17.37	10.51	12.63		12.13	26.65	2.03	
77	2-[illegible]	USGS	24.	7.72	[illegible]	26.31	10.12	12.23		11.99	26.03	5.21	
7[illegible]	[illegible]	USGS	24.	3.56	[illegible]	19.66	13.94	14.92		12.24	27.07	5.36	
	11-16-[illegible]	USGS	25.	[illegible]	[illegible]	22.65	10.12	13.49		12.01	26.65	7.60	
	[illegible]-75	DRI/WRC	29.	7.6[illegible]	[illegible]	14.97	8.55	15.57	.55	9.67	19.13	6.02	21.30
76	[illegible]-75	DRI/WRC	24.	7.40	[illegible]	19.24	16.12	12.79	.91	11.73	27.09	6.60	20.10
43	[illegible]-17-75	DRI/WRC	27.	6.78	[illegible]	19.8[illegible]	9.75	17.79	.80	11.70	26.52	5.62	19.10
7[illegible]	[illegible]	DRI/WRC	26.	7.24	3590.	21.81	19.23	12.44	.64	11.67	26.34	7.29	17.70
76	[illegible]-75	DRI/WRC	26.	7.49	3721.	20.50	10.20	12.66	.65	11.87	26.48	7.49	17.70
59	9-23-76	DRI/WRC	27.	7.60	[illegible]	21.51	10.44	12.09	.83	12.01	24.88	7.49	
65	[illegible]-25-75	DRI/WRC	24.	7.[illegible]	3360.	19.71	10.44	12.09	.82	11.82	26.32	5.39	
?	[illegible]-12-[illegible]	EPA	25.	7.79	3790.	22.21	10.36	12.14	.59	11.93	27.48	7.16	
?	2-07-[illegible]	EPA	25.	7.44	3710.	20.76	16.53	12.63	.62	11.49	26.66	5.95	
?	[illegible]	EPA	25.	7.46	3760.	20.81	10.63	12.27	.64	11.67	25.66	6.36	
?	[illegible]-31-[illegible]	EPA	25.	7.60	3476.	21.96	10.44	12.27	.47	11.95	24.65	6.49	
?	[illegible]-19-[illegible]	UNR AG STA	24.	7.70		22.01	10.53	13.79		11.31	26.71	8.34	16.00
?	5-19-[illegible]	UNR AG STA	24.	7.70		21.26	10.20	14.56		11.73	26.77	8.00	26.00
?	5-1[illegible]	UNR AG STA	24.	7.75		21.56	10.28	14.56		11.93	26.15	8.47	22.00
?	[illegible]	NEVADA STA	24.	7.70		21.21	11.08	13.44		12.18	26.44	7.60	15.00
?	[illegible]-23-[illegible]	USBR	24.	7.50	3730.	23.10	10.30	12.60		11.90	27.00	7.28	
?	[illegible]-23-[illegible]	USBR	24.	7.70	3730.	22.90	10.60	13.00		12.00	27.10	7.24	

101

SE ROA 43083

TABLE I CONT.

SPRING NO.	DATE SAMPLED	SAMPLED BY	TEMP C	PH	EC	CA2+	MG2+	NA+	K+	CL-	(SO4)-	(HCO3)-	SIO2
[illegible]	[illegible]-23-40	USBR	24.	7.50	3730.	21.00	10.40	11.90		11.10	25.60	7.20	
[illegible]	[illegible]-23-46	USBR	24.	7.50	3720.	24.70	10.50	12.50		11.76	26.60	7.19	
?	2-2[illegible]-69	USBR	[illegible]	7.50	[illegible]	13.70	6.47	8.17		7.66	16.70	3.91	
75	7-30-75	USBR	26.	6.90	3693.	21.75	8.20	12.92	[illegible]	11.76	23.17	7.34	17.00
[illegible]	9-10-74	USBR	26.	6.90	[illegible]	21.56	9.38	12.92	.85	11.65	24.28	7.34	17.00
41	6-30-75	USBR	26.	6.65	3704.	21.65	8.01	13.05	.91	12.24	22.32	8.11	17.00
2	6-25-75	USBR	24.	6.70	3705.	23.35	7.36	12.40	.81	10.90	23.26	7.97	16.00
2	9-0[illegible]-74	USBR	26.	7.70	3690.	24.45	9.29	13.62	.89	12.01	27.54	7.51	17.00
79	9-09-74	USBR	26.	7.5[illegible]	36[illegible]0.	19.61	9.42	13.57	.94	12.10	26.63	5.51	18.00
85	9-09-74	USBR	26.	7.24	3690.	20.96	8.80	13.57	.93	11.90	24.68	6.42	16.00
76	7-30-75	USBR	23.	7.30	3590.	26.21	9.13	13.22	.89	11.90	24.44	5.79	17.50
79	7-30-75	USBR	26.	6.96	3520.	21.36	9.21	13.22	.85	11.70	24.80	7.28	17.00
76	8-27-75	USBR	23.	6.80	3706.	21.56	8.20	13.65	.90	11.93	24.19	7.47	17.00
75	8-27-75	USBR	2[illegible].	7.50	3601.	23.76	8.72	12.92	.95	11.65	24.86	5.96	17.00
75	8-27-75	USBR	23.	6.76	3605.	21.91	8.47	13.04	.94	11.76	24.44	7.10	17.00
64	8-27-75	USBR	24.	7.60	3625.	20.65	7.76	13.79	.91	11.70	24.11	5.36	16.00
?	8-27-75	USBR	26.	6.60	3600.	23.35	7.50	12.79	.91	11.70	23.94	8.10	16.00
65	8-29-75	USBR	26.	6.70	3714.	22.21	7.90	12.53	.88	11.59	23.61	7.92	17.00
65	8-29-75	USBR	26.	6.66	3716.	21.56	8.96	12.53	.89	11.84	23.11	7.80	17.00
79	8-28-75	USBR	26.	6.60	3730.	22.21	8.47	12.65	.89	11.76	24.28	7.88	17.00
79	8-28-75	USBR	24.	7.50	3645.	19.71	8.88	12.42	.89	11.70	24.11	5.33	17.00
69	8-26-75	USBR	24.	7.40	3663.	20.56	8.60	12.44	.90	11.59	23.51	7.01	17.00
78	7-24-73	USBR	24.	7.20		21.77	9.23	13.50	.91	11.72	26.00	7.45	
78	7-31-73	USBR	24.	7.20	3720.	22.79	8.13	13.60	.91	12.07	25.70	7.43	
78	8-21-73	USBR	24.	7.50	3740.	23.09	8.50	13.27	.84	11.75	25.99	7.33	

SE ROA 43084

TABLE 1 CONT

STATION NO	DATE SAMPLED	SAMPLED BY	TEMP C	PH	EC	CA++	MG++	NA+	K+	CL-	(SO4)-	(HCO3)- SIO2
72	3-23-74	USBR	24.	7.30	3750.	24.49	6.94	12.16	.96	11.01	25.66	7.36
75	9-09-74	USBR	24.	7.50	3640.	19.45	5.64	13.32	.55	12.11	25.09	5.68
75	7-24-73	USBR	25.	7.70	3780.	22.19	9.19	13.03	.91	11.82	26.25	7.55
75	7-31-73	USBR	24.	7.54	3720.	22.99	7.93	13.50	.91	12.07	25.85	7.45
77	8-21-73	USBR	25.	7.30	3740.	23.15	[illegible]	13.27	.85	11.84	26.18	7.23
79	3-29-74	USBR	24.	7.90	3750.	[illegible]	[illegible]	13.15	.96	11.91	24.93	7.34
75	9-09-74	USBR	26.	7.50	3630.	19.70	4.32	12.65	.94	11.91	24.89	5.55
79	8-23-73	USBR	24.	7.60	3610.	24.63	3.45	13.17	.65	11.94	25.43	4.60
7	8-27-73	USBR	24.	7.50	3610.	22.44	7.24	13.19	.69	11.64	26.65	5.02
79	[illegible]-20-73	USBR	24.	7.40	3510.	25.73	4.07	13.54	.87	12.34	25.99	6.75
79	[illegible]-14-73	USBR	24.	7.70	3760.	21.90	7.8[illegible]	14.2[illegible]	.93	12.49	26.14	3.35
65	5-14-73	USBR	25.	7.10	3740.	27.49	4.63	[illegible]	.91	11.82	25.66	7.33
65	6-14-73	USBR	25.	7.10	3740.	24.63	7.05	13.14	.91	12.42	25.40	7.23
85	5-23-73	USBR	24.	7.59	3670.	24.85	3.49	13.17	.84	12.84	26.43	5.85
85	6-28-73	USBR	24.	7.50	3630.	21.69	6.63	13.30	.88	11.70	26.27	4.75
89	6-21-73	USBR	24.	7.70	3700.	25.24	5.96	14.03	.83	11.65	25.43	7.25
85	6-21-73	USBR	24.	7.50	3740.	23.75	[illegible]	13.97	.65	11.84	26.18	7.26
74	5-26-73	USBR	24.	7.50	3630.	21.44	7.62	13.39	.69	11.64	26.46	4.70
2	6-20-73	USBR	24.	7.60	3530.	23.75	4.56	12.69	.76	11.10	24.40	6.45
3	5-23-73	USBR	24.	7.56	3680.	22.54	7.63	13.11	.81	11.45	25.25	6.95
13	5-21-73	USBR	24.	7.30	3600.	23.53	7.71	13.02	.79	11.15	25.66	7.70
33	5-21-73	USBR	24.	7.50	3600.	24.36	7.60	13.87	.87	11.75	26.77	7.60
33	5-21-73	USBR	24.	7.46	3630.	24.63	7.54	13.47	.67	11.64	26.74	7.60
1	4-10-74	USBR	26.	7.50	2980.	15.84	7.37	10.74	.66	9.63	19.18	5.55
2	5-28-73	USBR	24.	7.70	3290.	18.62	6.54	12.32	.77	10.66	23.47	3.95

103

TABLE 1 (CONT)

SAMPLE NO.	DATE	SAMPLED BY	[illegible]	[illegible]	[illegible]	[illegible]	[illegible]	[illegible]	[illegible]	CL-	[illegible]	(HCO3)-	SIO2
[illegible]	[illegible]-73	USB	24.	7.70	2[illegible]	[illegible].25	[illegible]	[illegible].25	.53	7.56	15.94	5.2[illegible]	
[illegible]	[illegible]-75	USBR	24.	7.86	370[illegible]	24.54	[illegible]	13.33	.9[illegible]	11.86	26.10	[illegible].53	
[illegible]	[illegible]-74	USBR	[illegible]	[illegible]	3790.	22.[illegible]	[illegible]	[illegible]	.96	11.81	[illegible]	5.29	
[illegible]	[illegible]-76	USBR	[illegible]	7.5[illegible]	37[illegible]	21.[illegible]	3.57	12.7[illegible]	.96	11.[illegible]	[illegible]	6.83	
SUM			[illegible]	593.27	[illegible]	[illegible]	691.	[illegible]021.	[illegible]	[illegible]	[illegible]	[illegible]	[illegible]
MEAN			24.	[illegible]	[illegible]	[illegible]	[illegible]	[illegible]	[illegible]	11.66	25.31	6.62	17.96
[illegible]			[illegible]	[illegible]	74	[illegible]	[illegible]	[illegible]	[illegible]	[illegible]	79	79	[illegible]
STD DEV.N			1.	[illegible]	2.[illegible]	2.5[illegible]	1.71	.97	[illegible]	.79	2.16	1.25	2.14

FOR DESCRIPTION OF SAMPLE LOCATION SEE APPENDIX D

104

SE ROA 43086

JA_12966

LOG OF TEMPERATURE AND SPECIFIC CONDUCTANCE

The following includes temperature and specific conductance measurements on the Littlefield Springs, Virgin River, and tributaries that this author collected. The numbers shown correspond to numbers used in the spring location log. Temperature was measured to within ±.5° C with a pocket thermometer, or within ±1° F with the Beckman portable conductivity meter. All values were converted to centrigrade. The meter was also used to measure the conductivity to within ±50 micromhos for the periods up to August 19 after which the meter was reading low by about 300 micromhos. Readings have been adjusted appropriately. The readings are good within ±100 micromhos. The following two tables are for the 1976 field season.

TABLE 2

SPRING TEMPERATURE AND SPECIFIC CONDUCTANCE LOG

Spring Location No.	Time/Date	Temperature Degrees C	Specific Conductance Micromhos at 25 C
1	7/07/76	23	2850
(Riprap)	7/12/76	22	2900
	1200 7/20/76	22	2850
	1310 7/28/76	22	2750
	1030 8/03/76	22	2700
	1430 8/10/76	21.9	2780
	1200 8/17/76	22	2700
	1620 9/06/76	21.9	2900
	1320 9/23/76	22.5	2850
1	7/07/76	23	2850
(Spring from	7/12/76	23.3	2900
Bed)	1200 7/20/76	24	2875
	1310 7/28/76	23.3	2800
	1430 8/10/76	22.5	2800
	1200 8/17/76	22.5	2750
	1630 9/06/76		2800
2	910 9/20/76	24.5	3100
	same	24.5	3300
3	9/20/76	24	3100
5	2/14/76	23	
	9/20/76		3200
6	2/14/76	23.5	
	9/20/76	23.5	3300
7	1318 2/14/76	21.5	
	9/20/76	24.5	3300
8	1333 2/14/76	23.5	
	same	24.0	
	9/20/76	23.5	3200
9	1015 9/20/76	23.5	3250
10	9/20/76	24.0	3300
12	9/20/76	24.0	3300

TABLE 2 CON'T

Spring Location No.	Time/Date		Temperature Degree C	Specific Conductance Micromhos at 25 C
13	1045	9/20/76	24.5	3300
14	800	7/07/76	24.4	3375
		7/29/76	24.5	3100
	1315	8/17/76	24.7	3150
		9/20/76	24.5	3350
16	1140	9/20/76	25.0	3300
17		9/20/76	25.0	3300
22	1215	9/20/76	25.2	3300
24		9/20/76	26.5	3350
25	1230	9/20/76	25.0	3100
27	1240	9/20/76	24.5	3300
28	1352	2/14/76	24.0	
	1245	9/20/76	24.9	3350
29	1412	2/14/76	24.0	
	1300	9/20/76	24.9	3310
31		9/20/76	25.2	3350
32	1415	2/14/76	24.5	
33	1320	9/20/76	26.8	3400
35	1433	2/14/76	25	
		2/14/76	25	
	1723	2/14/76	25	
	805	2/15/76	25	
	1403	2/15/76	25	
	815	7/07/76	25.8	3425
	1430	7/29/76	25.5	3200
	1100	8/03/76	26.5	3300
	1520	8/10/76	25.8	3600
	1330	8/17/76	26.1	3225
		9/20/76	26.0	3400
37		9/20/76	24.5	3300

TABLE 2 CON'T

Spring Location No.	Time/Date		Temperature Degree C	Specific Conductance Micromhos at 25 C
38	1145	3/28/76	25.5	
(Bedrock)	1340	9/20/76	26.9	3400
41	1510	2/14/76	25.5	
	820	2/15/76	25.5	
		6/24/76	26.5	3400
	1400	9/20/76	26	3400
43	1315	3/28/76	25.5	3500
(Spring at Mouth)		7/29/76	26.5	3300
	1115	8/03/76	27.0	3400
	1545	8/10/76	26.7	3430
	1410	8/17/76	26.5	3250
		9/20/76	26.9	3375
	1430	9/23/76	26.5	3350
	915	9/25/76	27.0	3400
45		6/24/76	25.5	3350
		7/07/76	26.7	3450
		7/29/76	26.5	3350
	1430	9/20/76	26.5	3400
48		9/20/76	27	
49		9/20/76	27.5	
51		2/14/76	25.5	
	1530	9/20/76	27.2	
	1000	9/25/76	27.2	3450
53		9/25/76	27.0	3450
55	1630	9/20/76	27.2	
56		9/20/76	27.5	
58		9/20/76	27.5	
59		9/20/76	27.5	
60		9/20/76	27.2	
61		9/20/76	27.2	

TABLE 2 CON'T

Sample Location No.	Time/Date	Temperature Degree C	Specific Conductance Micromhos at 25 C
62	9/20/76	27.2	
65	9/25/76	23.0	3400
68	9/23/76	23.5	3300
69	9/23/76	24.5	3300
70	1245 7/20/76	25.6	3350
		25.6	3400
	7/29/76	25	3300
		25.6	3200
	1330 8/10/76	24.5	3410
	1443 8/17/76	24.5	3050
	1545 9/06/76	24.5	3300
	1640 9/13/76	24.5	3100
	1625 9/23/76	23.5	3100
73	1255 2/15/76	24.5	
	1345 3/28/76	24.5	3500
	1310 9/25/76	25.5	3250
74	1320 9/25/76	23.5	3450
78	1640 2/14/76	25.0	
	715 2/15/76	25.0	
	820 7/08/76	26.1	3400
	7/29/76	26.5	3300
	8/03/76	27.0	3300
79	1640 2/14/76	25.0	
	715 2/15/76	25.0	
	3/28/76	24.0	3500
	7/12/76	27.0	3400
	1600 7/20/76	27.0	3275
	1200 8/10/76	26.5	3390
84	1500 9/25/76	26.1	3250
85	1714 6/24/76	25.5	
	8/19/76	23.9	
83	1745 8/12/76	24.0	3300

TABLE 2 CON'T

Sample Location No.	Time/Date		Temperature Degree C	Specific Conductance Micromhos at 25 C
90	1745	8/12/76	24.0	3300
		8/20/76	25.0	3300
	1207	9/25/76	24.5	3300

TABLE 3

VIRGIN RIVER AND TRIBUTARY TEMPERATURE
AND SPECIFIC CONDUCTANCE LOG

Sample Location	Time of Sample	Sample Temperature °C	Specific Conductance mmhos at 25°C
Virgin River near Washington Fields	4/02/76	16.0	2700
Virgin River near Bloomington at I-15 Bridge	4/02/76	18.5	3300
	6/ /76	31.1	4700
	0650 6/24/76	14.5	4200
	1015 7/07/76	31.1	4500
	1520 7/27/76	33.3	2900
Virgin River at Gage at First Narrows	1200 3/27/76	20.0	2750
	4/02/76	24.0	3200
	1310 7/27/76	33.3	2900
Virgin River at Cedar Pocket Rest Area	1710 3/27/76	13.1	2700
Virgin River at Confluence with Black Rock Gulch	1515 3/27/76	13.5	2550
Black Rock Gulch	0745 7/27/76	24.4	1900
Virgin River at Gage below First Spring Flow	7/12/76	32.2	3000
	7/20/76	35.6	2875
	1730 7/27/76	12.2	2800
	1310 7/28/76	32.2	2800
	1400 8/ /76		3700
	1035 8/03/76	23.5	3200
Virgin River at the Mouth of the Gorge	1315 3/28/76	25.6	3400
	4/02/76	25.5	3500
	0915 6/24/76	23.2	3400
	7/07/76	29.4	3475
	1115 8/03/76		3600
	1430 8/10/76		3000
Virgin River above Leavitt Ranch Spring	1125 6/24/76	27.2	3450
	1600 7/07/76	31.1	3450

TABLE 3 CON'T

Sample Location	Time of Sample		Sample Temperature °C	Specific Conductance mmhos at 25°C
Beaver Dam Wash	1355	6/24/76	25.0	700
	1700	7/07/76	25.6	480
	1340	7/20/76	26.7	450
	1600	7/28/76	25.6	475
	1110	8/10/76	26.7	460
	1448	9/06/76	25.0	450

APPENDIX D

SPRING LOCATION LOG

SPRING LOCATION LOG

The reader is referred to the map of spring location which shows the location numbers which correspond to the numbers in the log below. In general, this represents the majority of the visible springflow that this author could delineate during the field seasons during the summer of 1975 and the summer of 1976. This author has mapped springflow and not the abundant seeps which occur throughout the map area unless that seep had some importance. Specific conductances and temperature were gathered from 1975 to the summer of 1976 with the Beckman electrical conductivity meter and with a pocket mercury thermometer. Accuracy of measurements are within ±50 micromhos on the conductivity meter and within $\pm .5^{o}$ C on the thermometer. In some cases the temperature of the water was measured with the Beckman meter, in which case the accuracy is within $\pm 2^{o}$ F.

1. First occurence of spring flow. Water is visible upstream of here, but this represents the first visible springflow. At least 8 springs are visible with the maximum flow being from Riprap spring which is greater than 2 gallons per minute (gpm). Springs occur at, below, and above river low stage from the north bank. The maximum height of discharge of water above the river low stage is 1 foot. Springs are occurring from cemented highway riprap and alluvium. There is a fault crossing the river here and the springs are probably fault related. This site of springs is called Riprap spring and Spring from Bed. As stated, Riprap spring is the largest discharging spring which occurs from the riprap, while just upstream of it is the spring from the river bed that always has a substantial pool developed, which is called the Spring from the Bed. There is one other substantial spring from the bed just upstream. This site corresponds to the USBR site 25 and 26.

2. Springs underneath and near the second highway bridge from the mountains' front. At least 8 springs are estimated to flow greater than 5 gpm. Springs occur at, below, and above the river low stage. Springs occur from beneath the bridge pilings, from the highway riprap, and alluvium along the north bank. The springs are possibly fracture related or highway construction related. Springs are within 2 feet of river low stage. This includes USBR sites 22 and 23. The river is flowing about 1-2 cfs at this location.

3. Springs about 1 gpm occurs from south bank near alluvium bedrock contact. Spring is related to fracture/fault that passes here (USBR site 24).

4. Springs, two flowing at about one gpm. Springs occurring from Limestone along a fracture above the river low stage from north bank.

5. Springs at least 4 from 1-5 gpm and seeps above river level in Quaternary alluvium from south bank. One spring observed from beneath south bridge pilings. This is USBR site 21.

6. Springs in alluvium at least five at about one gpm. Springs occur up to five feet above river low stage. Springs occur near limestone outcrop which is in fracture zone. Springs probably fracture related.

7. Springs at least three at one gpm occur at river low stage from south bank in highway riprap.

8. Springs at least 10 flowing greater than 2 gpm. Springs occur at, below, and above river low stage along south bank from highway riprap. Note many of these springs are under pressure and spurt out into the air. Presence of numerous solution cavities in outcrops in this area.

9. Springs at least two at one gpm occur where interbedded shale and limestone plunges beneath river flood plain along the north bank. Springs stratigraphically controlled and occur from carbonate along bedding plain. Flow in the river estimated to be around three cfs.

10. Springs, 2 large springs one .25 cfs, the other .18 cfs occur from alluvium about 1 foot above river low stage from south bank. Modified parshall flume (3 inch) readings .28 and .31 feet. Probably fault related (see geologic map).

11. Springs at least three about one gpm occurring from south bank in alluvium near river low stage.

12. Large spring, .36 cfs from carbonate rock from north bank about 2 feet above river low stage. Spring appears to be fault/fracture related (see geologic map). Flume measurement .48 feet.

13. Spring from south bank from alluvium flowing at .29 cfs. Flume reading .42 feet. Probably related to fault which crosses the area near here.

14. Springs at least three, less than one gpm occurring near river low stage from alluvium along south bank. Series of seeps along north bank.

15. Trough spring, actually series of springs collected into a channel. Flow is about 1-1.5 cfs and occurs from alluvium up to 8-10 feet above the river low stage from south bank. Springs originate near undivided carbonate section outcrop and probably related to a fault which crosses area. Flow from springs exceeded capacity of the flume. This is USBR site 27.

16. Springs, at least 10 around 1 gpm. Springs occur from riprap at, above, and below river low stage from highway riprap along south bank. Springs probably related to fault outcropping on other side of river.

17. Springs at least five, one gpm occurring from highway riprap along south bank. Springs occur up to two feet above river low stage.

18. Springs at least three, one gpm occurring from highway riprap along the south bank. Springs occur up to two feet above river low stage; springs under some pressure and shoot up into air.

19. Spring greater than one gpm occurs from fault/fracture in undivided carbonate section along north bank of river above river low stage.

20. Seeps along bedding plane from thinly bedded limestone in undivided section from north bank. Seeps above river low stage up to five feet and are stratigraphically controlled.

21. Springs at least three, one gpm occurring from bedrock from north bank near river low stage.

22. Springs at least 3, 2 collect into channel and the flow is .31 cfs. Springs occur from south bank from highway riprap about 2 feet above river low stage. Springs are believed to be related to fracture which passes between the highway and the river. Flume measurement .44 feet.

23. Springs at least three, one gpm occur from north bank in alluvium above river low stage.

24. Spring flowing at .23 cfs occurring from the Thunder Springs member of the Redwall Limestone. Spring occurs at 2 to 3 feet above river low

stage from north bank. Springs related to fractures occurring here. Note large cave, probably fracture solution cavity related. Flume measurement .36 feet.

25. Springs at least three, one gpm occurring from Thunder Springs member of the Redwall Limestone and from alluvium up to three feet above river low stage from north bank. These springs occur along fractures.

26. Dripping seeps occurring from the Thunder Springs member of the Redwall Limestone up to five feet above the river low stage from north bank.

27. Springs at least five, greater than one gpm occurring from the south bank alluvium near river low stage.

28. Spring .5-.75 cfs occurs from alluvium from south bank just downstream of major fault. Spring is probably fault related. Spring occurs within 2 feet of river low stage. Flume reading .8 feet.

29. Springs at least 5, greater than 2 gpm from alluvium along south bank. Springs occur up to 3 feet above river low stage and occur just downstream of a major fault.

30. Seeps from the Thunder Springs member of the Redwall Limestone and from the undivided section of carbonate rocks from the north bank. Many of the seeps are fracture related and occur up to 10 feet above river low stage.

31. Springs collecting in channel and flowing at .38 cfs. Springs occur in alluvium from south bank up to 5 feet above river low stage. Springs probably fault fracture related. Flume reading .5 feet.

32. Springs at least 5, greater than 2 gpm and 1 at .33 cfs. Springs occur from south bank between the first and second set of bridge pillars as one goes downstream. Springs occur from bank material (alluvium/construction) up to 5 feet above river low stage. Large spring occurs near Thunder Springs outcrop. Springs probably related to faulting in the area. Flume reading .46 feet.

33. Springs at least 10, 1 gpm occurring from fractured Thunder Springs member of the Redwall Limestone from the north bank. Springs probably related to fault that crosses the river just upstream of here. This is USBR site 28.

34. Springs issuing from beneath river low stage and from alluvium from north bank. Two springs issuing from where major fault crosses the river, both around one gpm.

35. Springs at least 10 of which 3 are .25 cfs or larger, the rest are greater than 2 gpm. Springs occur from alluvium and riprap up to 3 feet above the river low stage from the south bank beneath the west end of the bridge. One of the springs here was a January 1976 temperature station. Springs are probably fault/construction related.

36. Springs at least three, one gpm from alluvium from south bank near river low stage.

37. Two springs one gpm and some seeps occur above river low stage from south bank in alluvium.

38. Bedrock spring and 2 other springs. Bedrock spring flow is greater than 5 gpm and occurs along a fracture about 5-8 feet above river low

stage while the 2 other springs are about 1 gpm and occur at the undivided carbonate section contact with the stream alluvium along a fracture. This is USBR site 29.

39. Seeps from the undivided section and the Redwall Limestone along fractures from the north bank of the river up to five feet above the river low stage. One spring one gpm stratigraphically controlled by the Thunder Springs member dipping beneath the river.

40. Occasional seep in the undivided section along fractures from the north bank.

41. Springs at least 10, several discharge greater than 10 gpm, the rest greater than 2 gpm from riprap, and alluvium along the south bank. Springs discharge at, below, and up to 2 feet above river low stage. Note a January 1976 temperature gaging station was located in this stretch, however, it no longer exits. Fracturing evident here. This is USBR site 19 and 20.

42. Seeps along fractures in the Redwall Formation along the north side of the river.

43. Spring at Mouth of Gorge. Spring .28 cfs from alluvium 2-3 feet above the river low stage from the south bank. Spring is just upstream of January 1975 gaging station. Flume measurement .42 feet at 14:10 on August 17, 1975, .41 feet at 18:35 on August 17, 1976.

44. Springs at least three, one gpm from south bank in alluvium up to three feet above river low stage.

45. Spring near January 1975 gaging station. Spring is first major spring downstream of gage flowing at .4-.47 cfs. Spring is from south bank from alluvium 3 feet above river low stage. Flume reading .57 feet at 18:35 on August 17, 1976, and .52 feet at 9:30 on August 18,1976 with much leakage.

46. Springs at least three, greater than two gpm occurring from alluvium from south bank three feet above river low stage.

47. Springs two, one gpm and seeps occurring from north bank from alluvium at two feet above river low stage.

48. Springs, two greater than two gpm beneath second culvert from last outcrop of rock between highway and river. Springs from beneath river low stage.

NOTE: Have just passed out of the mouth of the gorge and am now in the Virgin River Valley and the Transition Zone hydrogeologic province.

49. Seeps and 3 small springs 1 gpm occur from sandstone within the Littlefield Conglomerate. Conglomerate appears to have much sand beds in it. Springs occur along bedding plane in sandstone up to 15-20 feet above river low stage from the north bank. Note near the change in slope at the flood plain there is dense growth and a pond of water. This is below the Littlefield Limestone.

50. Spring from beneath river low stage along south bank.

NOTE: What follows is a series of eight large springs called the Rattlesnake Springs. These springs are closely spaced along the river, occur from the alluvium no more than two feet above the river low stage from the south bank. There are numerous smaller springs in this area but they are not mentioned because of insignificance compared to the springs mentioned. The springs are listed in order of occurence. Each spring is marked on the map.

51. Flow estimated to be between one and two cfs; flow exceeds capacity of flume.

52. Flow estimated to be between 1-1.5 cfs; flow exceeds capacity of flume, but not as much as 51. Note there are springs occurring beneath bed of river here.

53. Flow estimated to be 1.5-3 cfs, spring greatly exceeds the flume capacity. This spring is the spring that has been sampled and called Rattlesnake Spring.

54. Large spring with 2 tributaries, 1 tributary gaged at flume capacity .92 feet, the tributary gaged at .66 feet with much leakage total flow estimated to be 1-1.5 cfs.

55. Flow gaged at .6-.7 cfs, flume reading .5 feet.

56. Flow gaged at .5-.6 cfs, flume measured .58 feet with leakage.

57. Flow gaged .2-.3 cfs, flume measured .33 feet with leakage.

58. Flow measured .6-.9 cfs, flume measured .7 feet with leakage.

59. Spring one gpm and seep from Littlefield Conclomerate along north bank of river.

60. Springs 2, 1 at .8-1.0 cfs, the other .4-.6 cfs occurring from alluvium along south bank. Springs are near the river low stage. The flume measurements are .92 feet with leakage and .54-.7 feet respectively.

61. Spring one to two cfs occurring from south bank in stream alluvium. The spring exceeded the capacity of the flume.

62. Springs 3, 5 gpm, .48 cfs, and .6-.7 cfs occurring from river alluvium along south bank. The 2 springs were flumed at .58 feet with no leakage and .66 feet with leakage.

63. Spring around two gpm from alluvium in south bank approximately two feet above river low stage.

64. Spring around two gpm same as above.

65. Cold Spring, this spring is the collection of at least 2 springs occurring from south bank in alluvium 6 to 8 feet above river low stage. Spring estimated at .5 cfs, and discharges into river via a waterfall. Spring originates halfway between river and conglomerate cliff.

66. Springs, two less than one gpm and seepage from sandstone in the Littlefield Conglomerate about five feet above river low stage from the south bank.

67. Spring about one gpm about two feet above the floor of a wash in the Littlefield Conglomerate. No visible discharge to river.

68. Springs, at least two, one gpm occur from the Littlefield Conglomerate. The springs due discharge to the Virgin River. The springs occur about four feet above river low stage.

NOTE: This marks the end of the Transition Zone in the Virgin River Valley. The Virgin River Valley hydrogeologic province begins past this last spring.

69. Spring less than 1 gpm occurs about 2 feet below the contact of the sandstone in the Littlefield Limestone and the Littlefield Conglomerate. Travertine deposits here. Spring picks up flow downstream in this wash. It collects into trough and has flow of .22 cfs with flume measurement of .35 feet. No visible discharge to the river.

70. Leavitt Ranch Spring. Spring occurs about 4 feet below the contact between the sandstone of the Littlefield Limestone and the Littlefield Conglomerate. Note gage was installed 30 feet downstream of where springflow first occurs.

Time		Head	Discharge
14:10	1/17/1975	.155 feet	27 gpm
15:55		.16	28
21:35		.15	26
00:55	1/18/1975	.16	28
03:20		.16	28
08:30	8/05/1975	.145	24
14:15		.145	24

Discharge measurements made by WRC/DRI. No visible discharge to the river.

71. Springs at least 2 each greater than 1 gpm originating in travertine mound about 15-20 feet below top of rim near contact of Littlefield Limestone with Littlefield Conglomerate. Springs start 1 gpm and gain flow as it goes downhill. There is no visible discharge to the river.

72. Springs at least 3, at 5 gpm occurring from talus material around 15-20 feet from top of rim near Littlefield Limestone and Littlefield conglomerate contact. No visible discharge to the river.

73. Reber Spring also known as Camp Wash Spring. Spring has been developed by Burdett Reber by blasting trenches (2) perpendicular to the river within a limestone bed in the Littlefield Limestone. The channels have since been covered up. Water was occurring from fracture within the Littlefield Limestone. The system was developed because Mr. Reber was unable to pump sufficient quantities of water from 2 adjacent wells. Following flow is collection of 2 ditches:

Time		Head	Discharge
13:40	1/17/1975	.58 feet	390 gpm
16:00		.56	368
21:25		.56	368
00:40	1/18/1975	.56	368
03:30		.56	368
08:45	8/05/1975	.66-.71	430-450

Flow measurements by WRC/DRI made with 6 inch Parshall Flume. In 1975 spring was developed and then covered.

74. Stalagtite spring. Spring a collection of at least 3 springs occurring from unconsolidated material covering the Littlefield Limestone. Total flow estimated to be around .25 cfs. Stalagtites are formed where this spring cascades off cliff and discharges into pond at base of cliff formed by Reber and this spring's discharge. There is discharge to river.

75. Seep occurs from Littlefield Conglomerate about three feet above river low stage.

76. Petrified #1 and another spring. The other spring has about 1 gpm discharge. These springs occur in wash, collect together and gain in flow as one approaches the river. Springs are occurring in unconsolidated material stratigraphically at the Littlefield Limestone level. There is travertine in this wash and along seeping wall which has abundant growth

where the springs cascade to a ponded area in the river flood plain. The USBR has sampled the discharge to the river from the ponded area which is also fed by Petrified #2 springs and others. This is site #16.

Time		Head	Discharge
11:35	1/17/1975	.22 feet	47 gpm
15:35		.215	45
17:45		.22	47
21:10		.22	47
24:00		.22	47
04:00	1/18/1975	.22	47
08:15	8/05/1975	.22	47
10:00		.195	37
14:30		.195	37

Flow measurements by WRC/DRI, made with 3 inch modified Parshall Flume. There is discharge to the river.

77. Spring about one gpm occurs from unconsolidated material in wash. Spring is stratigraphically occurring from Littlefield Limestone, but does not discharge to the river.

78. Petrified Spring #2. Actually the collection of flow from several springs. The USGS has sampled here. The spring occurs from unconsolidated material along ditch along the north side of the interstate highway. Spring occurs stratigraphically from the Littlefield Limestone. This spring has been sampled by the USGS and it is Bureau site 1. The following flow is the collection of the majority of the flow. There may be some gain downstream.

Time		Head	Discharge
13:00	11/17/1975	.57 feet	381 gpm
15:45		.575	386
18:00		.57	381
21:20		.57	381
00:25	11/18/1975	.57	381
04:10		.57	381

The following measurements made by the WRC/DRI with a 6 inch modified Parshall Flume. There is discharge to the river.

79. Petrified #3. Spring occurring from unconsolidated material from the south side of the interstate highway in a ditch. The spring is stratigraphically in the Littlefield Limestone formation and like the spring across the highway is actually a collection of springs. This spring receives flow from the other side of the highway via a culvert. The spring is estimated to be about 1 cfs of flow similar to that across the highway. The USGS has sampled here and so has the USBR. This is USBR site 2, 3, 5, and 6. There is discharge to the river.

80. Springs 2, 1 at less than 1 gpm and the other at greater than 1 gpm. The springs occur from unconsolidated material and travertine about 15-20 feet below the top of the rim here. Stratigraphically occurring near the Littlefield Limestone/Conglomerate contact. These springs have been sampled by the USBR. No visible discharge to the river.

81. Spring greater than 1 gpm occurs from unconsolidated material 10-15 feet above rim. Stratigraphically occurs at the base of the Littlefield Limestone. There is no visible discharge to the river.

82. Springs, 2, 2 gpm and less than 1 gpm occurring from unconsolidated material, 10-15 feet below rim stratigraphically from the Littlefield Limestone. No visible discharge to the river

83. Spring, one gpm occurring in small cave in travertine. Spring occurs above large travertine mound mapped in the area. Stratigraphically occur from the Littlefield Conglomerate. There is no visible discharge to the river.

84. Springs collect in a channel and flow at .31 cfs. Springs are occurring at contact of travertine mound with cliff face. Springs stratigraphically occur from the Littlefield Conglomerate. Flume measured .44 feet at 18:00 on August 21, 1976, and .44 feet at 20:00 on August 21, 1976. There is discharge to the river.

85. Farm Springs (or the Petrified Springs of the USGS) 2 large springs of flow 2 cfs gaged on June 24, 1976. The USGS has flow measurements on these springs and the channel into which it flows. Springs occur at base of cliff at river flood plain contact. Springs occur from unconsolidated material and from travertine. Springs occur stratigraphically from the Littlefield Conglomerate. This is USBR site 8, 9, 10, and 12.

86. Springs, two, one gpm and less than one gpm occur above the base of the cliff and river flood plain contact. Springs occur in calcium carbonate cemented sandstone material which is probably spring formed. Stratigraphically the spring is occurring from the Littlefield Conglomerate. No visible discharge to the river or the Petrified Springs Canal.

87. Spring, less than 10 gpm occurring near base of cliff and flood plain contact from unconsolidated material. Stratigraphically the spring is occurring from the Littlefield Conglomerate. No visible discharge to the river or the Petrified Springs Canal.

88. Series of springs and seeps occurring along this wash. Largest flow of total collected flow of springs appears to be around 10 gpm. Springs' flow begins near contact between Littlefield Limestone and Conglomerate and picks up as it flows downstream. Springs occur throughout this wash area are usually small, 1 gpm. No visible discharge

to the river or the Petrified Springs Canal. Note find very damp soil 6 inches beneath surface in Littlefield Conglomerate stratigraphic zone. This is USBR site 11.

89. Springs three, five gpm near base of cliff at the flood plain. The springs feed the Petrified Springs irrigation ditch. Springs stratigraphically occur from the Littlefield Conglomerate although they occur from the unconsolidated material.

90. Last occurrence of Spring Flow, springs three, one gpm and seeps from unconsolidated material. Springs stratigraphically occur from the Littlefield Limestone. Note this is also the last occurence of the Littlefield Formation on this side of the river. No visible discharge to the river or to the Petrified Springs Canal.

APPENDIX E

PULSE TRAIN RESULTS

Figure 1

Stage vs. Time Virgin River at the First Narrows

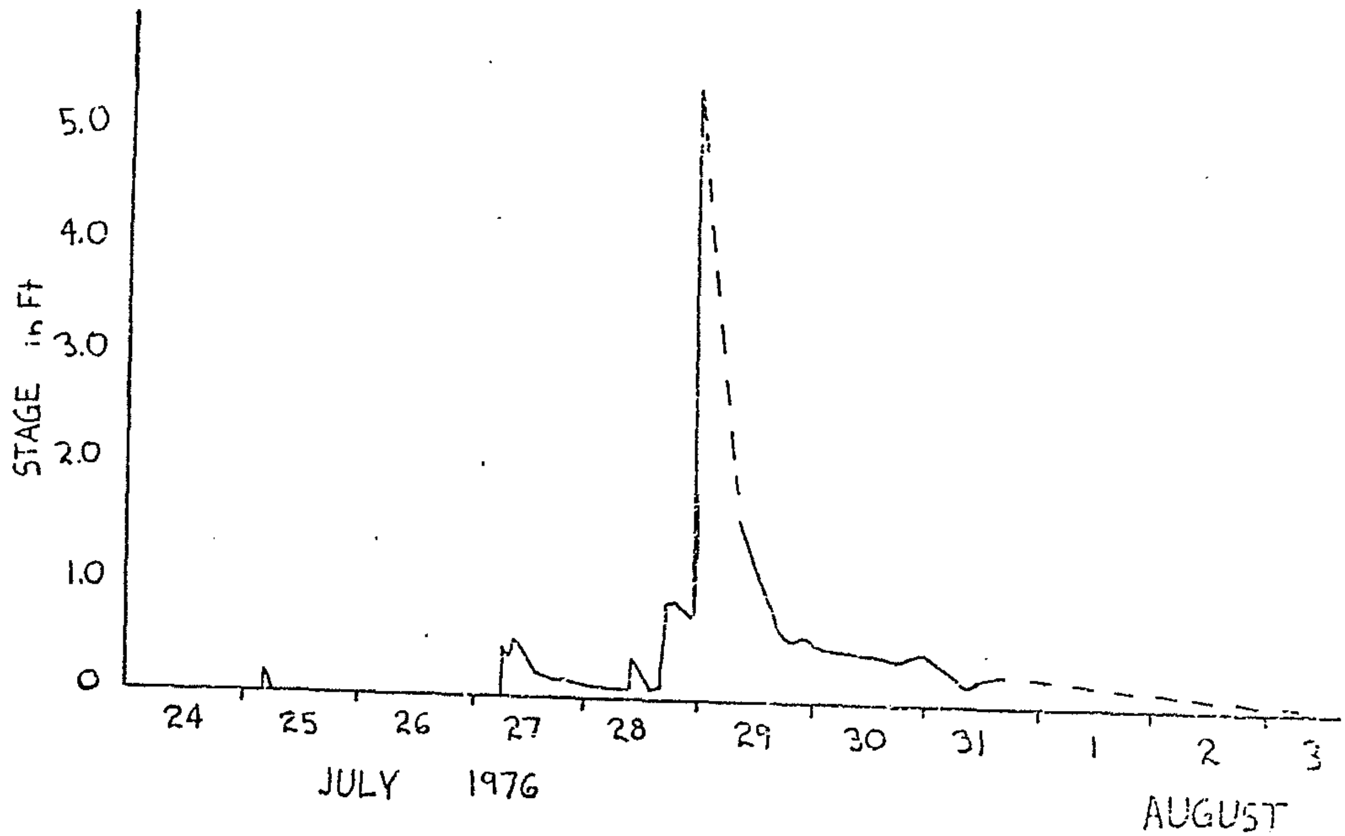

Figure 2

Stage vs. Time Virgin River at the First Narrows

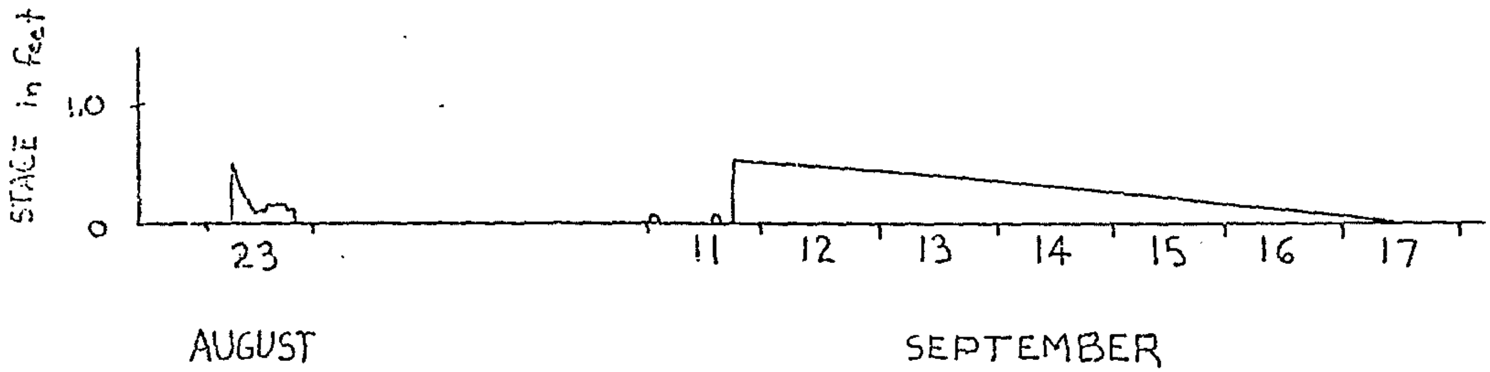

132

Figure 3

EC vs. Time Leavitt Ranch Spring (#70)

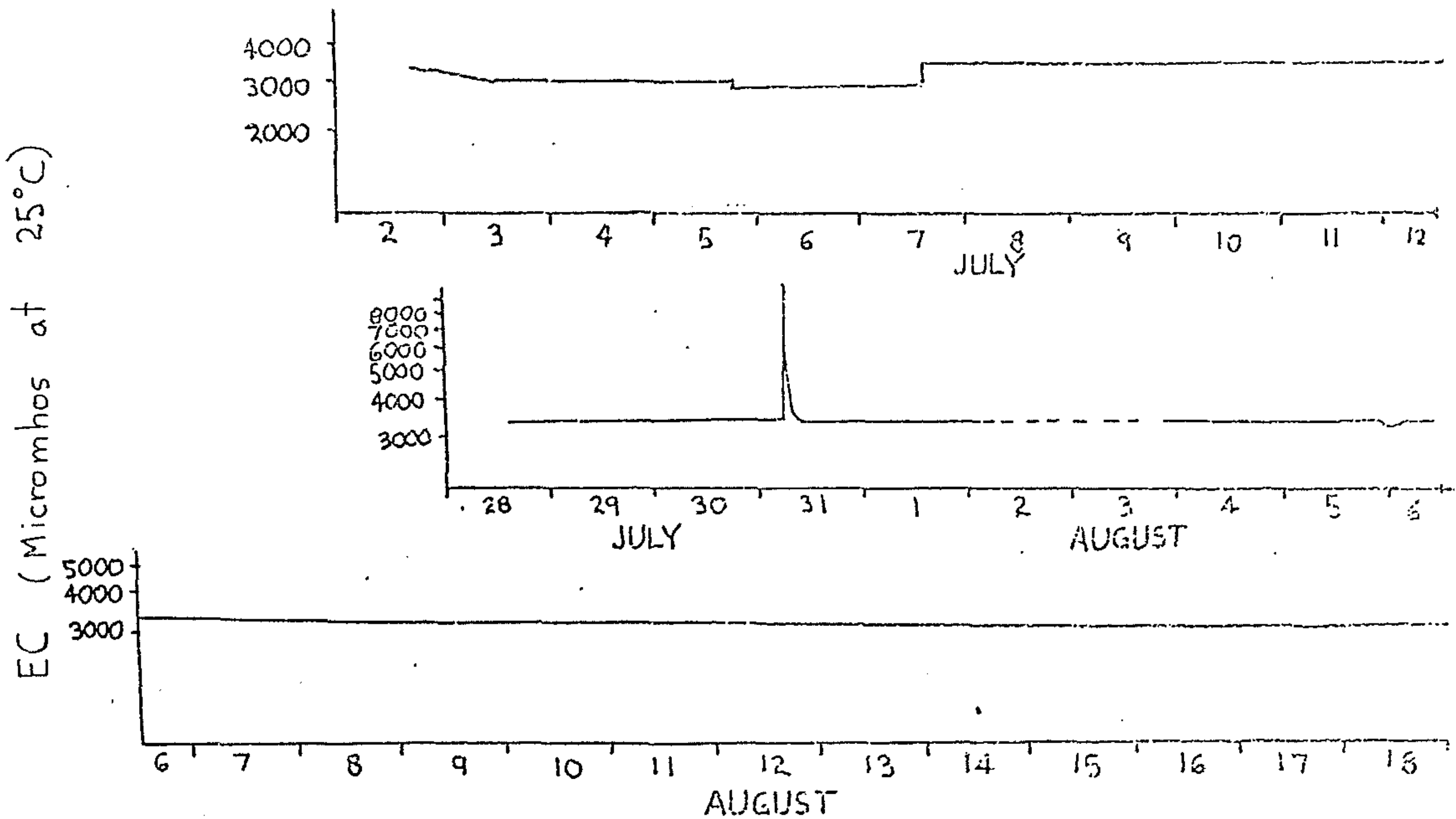

Figure 4

EC vs. Time Leavitt Ranch Spring (#70)

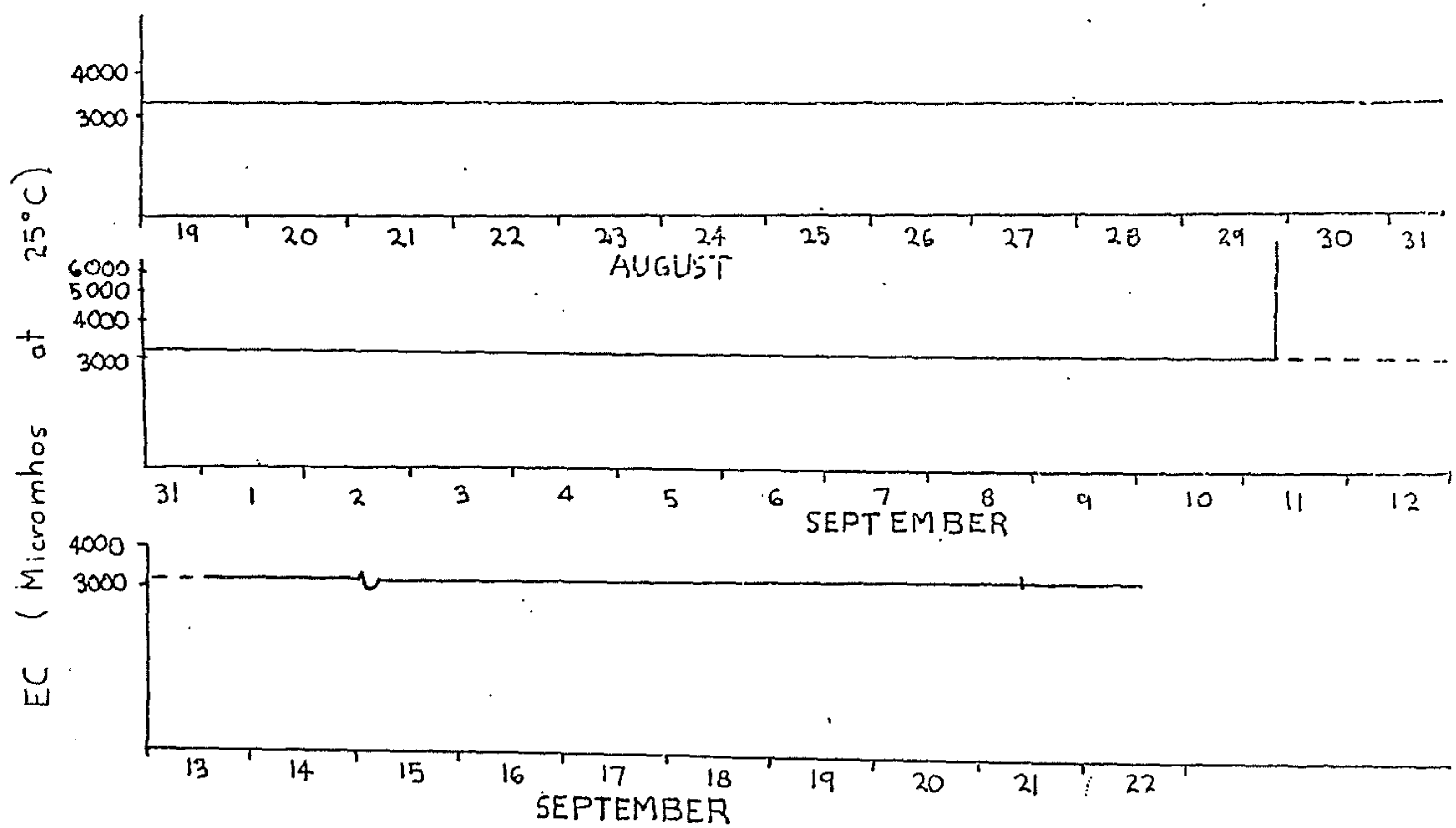

134

TABLE 1

STAGE LEAVITT RANCH IN FEET

Day	June	July	August	September
1		.36	.36	.24
2		.36	.36	.24
3		.36*	.36*	.24
4		.36*	.36*	.24
5		.36*	.33*1	.24
6	.36	.36*	.31	.24
7	.36*	.36*	.29	.24
8	.36*	.36*	.28	.24
9	.36*	.36*	.27	.24
10	.36*	.36*	.27	.24
11	.36	.36*	.27	.35*3
12	.36	.36*	.26	
13	.36	.36	.26	
14	.36	.36	.26	
15	.36	.36	.26	
16	.36	.36	.26	
17	.36	.36	.25	
18	.36	.36	.25	
19	.36	.36	.24*2	
20	.36	.36	.24	
21	.36	.36	.24	
22	.36	.36	.24	
23	.36	.36	.24	
24	.36	.36	.24	
25	.36	.36	.24	
26	.36	.36	.24	
27	.36	.36	.24	
28	.36	.36	.24	
29	.36	.36	.24	
30	.36	.36	.24	
31		.36	.24	

* Poor record due to leakage or silting, record corrected
*1 Leakage around flume begins
*2 Leakage stabalized, but continues
*3 Peak of .8++

Note: Stage is distance in feet above inlet to stilling well.

Note: To obtain flow H = stage - .07 feet = feet
Then use formula for 90° V-notch Weir
$Q(ft^3/sec) = (2.5H)^{5/2}$ for period from August 5-19 correct stage to .36 feet. For period August 19-September 10 use stage .36 feet.

TABLE 2

STAGE VIRGIN RIVER BELOW FIRST SPRINGFLOW

Day	June	July	August	September
1		.08*	1.00	.06
2		.08*	.68	.06
3		.08*	.35	.06
4		.08*	.15	.06
5		.08*	.07	.06
6		.08*	.07	.07
7		.08*	.07	.07
8		.08*	.07	.07
9		.08*	.07	.07
10		.08*	.07	.08
11		.08*	.06	.25
12	.09	.08*	.06	
13	.09	.08*	.06	
14	.09	.08*	.06	
15	.09	.08*	.06	
16	.09	.08	.06	
17	.08*	.08	.06	
18	.08*	.08	.06	
19	.08*	.08	.06	
20	.08*	.08	.06	
21	.08*	.08	.05	
22	.08*	.08	.05	
23	.08*	.08	.07	
24	.08*	.08	.07	
25	.08*	.08	.07	
26	.08*	.08	.07	
27	.07	.15	.07	
28	.08	.45	.06	
29	.08	1.70	.06	
30	.08	.95	.06	
31		.60	.07	

* Poor record due to unstabilized stilling well. Stage estimated.

Note: All of record poor

Geology and Geophysics of Spring, Cave, Dry Lake, and Delamar Valleys, White Pine and Lincoln Counties and Adjacent Areas, Nevada and Utah: The Geologic Framework of Regional Groundwater Flow Systems

PRESENTATION TO THE OFFICE OF THE NEVADA STATE ENGINEER

Prepared by

SOUTHERN NEVADA WATER AUTHORITY

June 2011

Suggested citation:
Rowley, P.D., Dixon, G.L., Burns, A.G., Pari, K.T., Watrus, J.M., and Ekren, E.B., 2011, Geology and geophysics of Spring, Cave, Dry Lake, and Delamar valleys, White Pine and Lincoln Counties and adjacent areas, Nevada and Utah: The geologic framework of regional groundwater flow systems: Presentation to the Office of the Nevada State Engineer: Southern Nevada Water Authority, Las Vegas, Nevada.

Geology and Geophysics of Spring, Cave, Dry Lake, and Delamar Valleys, White Pine and Lincoln Counties and Adjacent Areas, Nevada and Utah: The Geologic Framework of Regional Groundwater Flow Systems

Submitted to:
Jason King, P.E., State Engineer
State of Nevada
Department of Conservation & Natural Resources
Division of Water Resources
901 S. Stewart Street, Suite 2002
Carson City, Nevada 89701

Pertaining to:
Groundwater Applications 54003 through 54021 in
Spring Valley
and
Groundwater Applications 53987 through 53992 in
Cave, Dry Lake, and Delamar Valleys

June 2011

Prepared by:
Southern Nevada Water Authority
Water Resources Division
P.O. Box 99956
Las Vegas, Nevada 89193-9956

Peter D. Rowley, Geologist — Date: June 4, 2011

Gary L. Dixon, Principal Geologist — Date: June 2, 2011

CONTENTS

CONTENTS (CONTINUED)

CONTENTS (CONTINUED)

SE ROA 43124

JA_13004

CONTENTS (CONTINUED)

FIGURES

FIGURES (CONTINUED)

FIGURES (CONTINUED)

SE ROA 43128

JA_13008

FIGURES (CONTINUED)

PLATES

NUMBER **TITLE**

SE ROA 43130

JA_13010

This Page Left Intentionally Blank

TABLES

NUMBER **TITLE** **PAGE**

This Page Left Intentionally Blank

ACRONYMS

2D	two-dimensional
AMT	audiomagnetotelluric
BARCASS	Basin and Range Carbonate Aquifer System Study
EIS	environmental impact statement
GBNP	Great Basin National Park
HGU	hydrogeologic unit
I-15	Interstate Highway 15
LVVSZ	Las Vegas Valley Shear Zone
MT	magnetotelluric
NPS	National Park Service
NTS	Nevada Test Site
NSE	Nevada State Engineer
POD	point of diversion
PSZ	Pahranagat Shear Zone
SNWA	Southern Nevada Water Authority
SR	State Route
US 50	U.S. Highway 50
US 6	U.S. Highway 6
US 93	U.S. Highway 93
USGS	U.S. Geological Survey
WCWCD	Washington County Water Conservancy District

ABBREVIATIONS

afy	acre-feet per year
ft	foot
Ga	billion years
gpm	gallons per minute
km	kilometer
m	meter
Ma	million years
mg	milligram
mi	mile
mi^2	square mile
ohm-m	ohm-meter [unit of electrical resistivity]

This Page Left Intentionally Blank

1.0 INTRODUCTION

This report describes the geologic framework of an area of east-central and southeastern Nevada and adjacent western Utah. Included are geologic, hydrogeologic, and geophysical data collected throughout the study area, and updated geologic and hydrogeologic maps and cross sections based on the same presented in Dixon et al. (2007a). These updates were prompted by the analyses of new data collected within the study area since 2007, and the evaluation of more recent published and unpublished literature that, in some instances, required updating interpretations of selected features of the geologic framework. The new data were compiled from new geophysical studies employed and analyzed to better understand the structural framework of the area, and from borehole data from the Southern Nevada Water Authority (SNWA) exploratory drilling and hydraulic-testing program. The study area and Project Basins (Spring, Cave, Dry Lake, and Delamar valleys) are presented in Figure 1-1. Details regarding the Project background and the administrative history regarding the SNWA applications are presented in the Conceptual Plan of Development (SNWA, 2011) and Holmes et al. (2011), respectively.

1.1 Purpose and Scope of Geologic Investigation

The purposes of this report, as with the report by Dixon et al. (2007a), are to (1) provide an overview of the geology for an area encompassing the Project Basins, including a description of how that geology relates to the hydrogeology of the area; (2) present the geologic and hydrogeologic framework of the Project Basins and surrounding area; and (3) evaluate the framework to assess the potential for groundwater flow at selected boundaries.

The scope of this geologic investigation and that which led to the report by Dixon et al. (2007a) included significant data compilation and acquisition, and development of geologic and hydrogeologic surface maps and cross sections. This investigation also included gravity surveys of the Project Basins conducted by the U.S. Geological Survey (USGS) through joint funding agreements with SNWA. Significant fieldwork was done by the authors to improve the geologic understanding of selected areas. The scope of work was defined, in part, to differentiate between aquifers and confining zones, that is, hydrogeologic units (HGUs) with high and low hydraulic conductivity, respectively. The geologic investigation also focused on identifying areas where confining zones of sufficient thickness are present and inhibit groundwater flow.

1.2 Document Organization

This document consists of the following eight sections and Appendix A, which presents photos of the study area and selected points of interest.

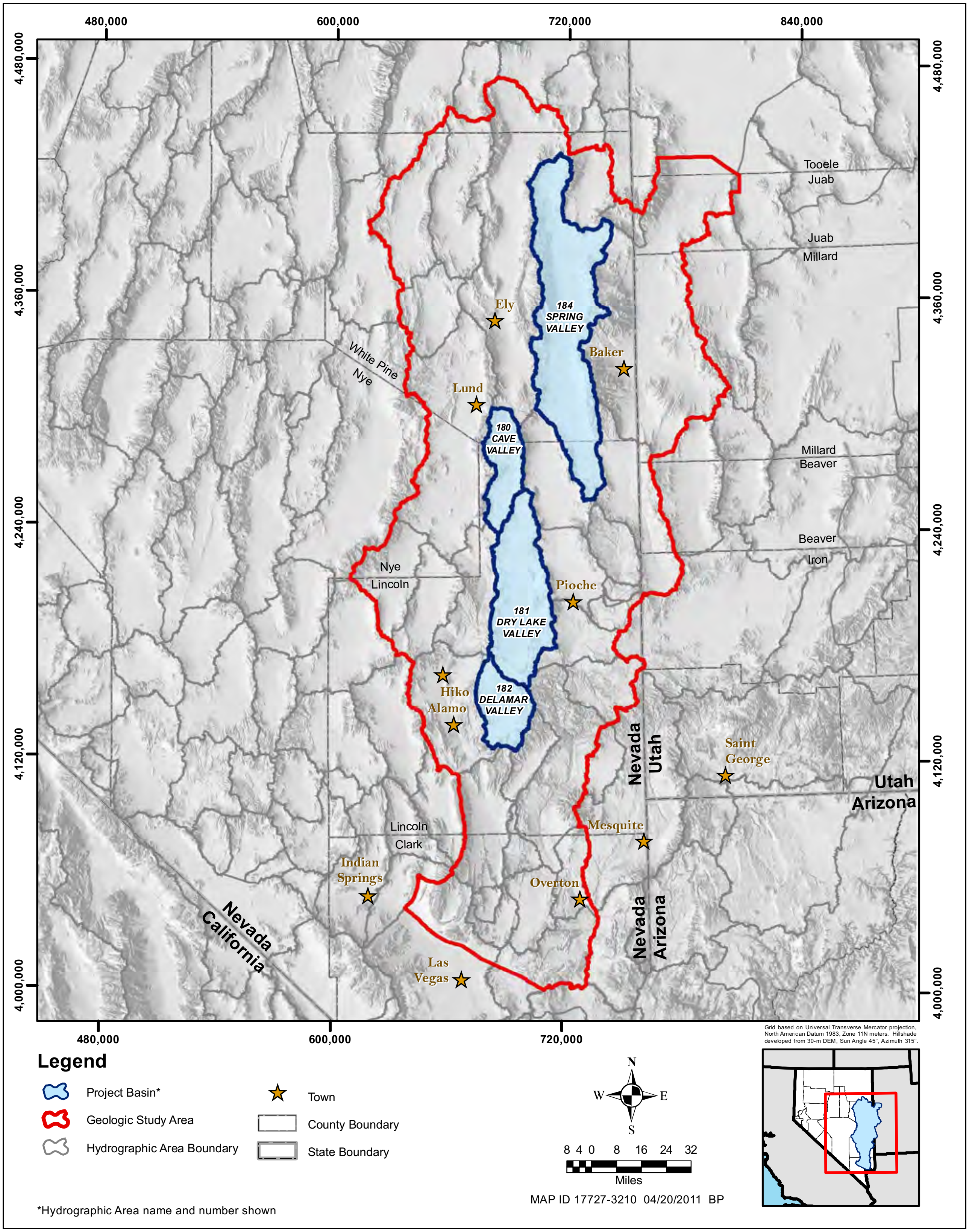

Figure 1-1
Location of Project Basins and Other Hydrographic Areas

- Section 1.0 provides a description of the Project background, the purpose and scope of the geologic investigation, and an overview of the contents of this report.

- Section 2.0 summarizes hydrogeologic concepts used and the geologic setting of the area, including the regional geologic features and drainage (Section 2.1). Section 2.2 discusses features of the geologic framework that affect the movement of groundwater.

- Section 3.0 describes the methodology applied in the geologic analysis, including a description of the objectives of the analysis and technical approach.

- Section 4.0 discusses the geology and hydrogeology of the geologic study area and some of the surrounding basins and ranges that could be in hydrogeologic connection with the basins of the geologic study area (Figure 1-1). Section 4.0 is divided into subsections describing the various aspects of the geology and hydrogeology, as follows:

  - Section 4.1 discusses the general geology and detailed stratigraphy of the geologic study area of this report, notably the geologic units in the study area.

  - Section 4.2 discusses the HGUs of the geologic study area and how they relate to the geologic units.

  - Section 4.3 discusses the evolution of the geologic structure in the geologic study area and how that structure impacts the hydrogeology.

  - Section 4.4 describes the geology in terms of the mountain ranges and adjacent basins within the geologic study area and how the specific geology in these areas affects the hydrogeology.

- Section 5.0 discusses the geophysics of the geologic study area.

- Section 6.0 discusses professional opinions on previous studies in the project area.

- Section 7.0 is a summary of the general geology and general hydrogeology of the geologic study area.

- Section 8.0 provides a list of references cited in the document as well as a list of references used in making the geologic maps and cross sections.

This Page Left Intentionally Blank

2.0 GEOLOGIC PRINCIPLES IN THE STUDY AREA

The study area for the geologic investigation encompasses the Project Basins and adjacent basins that may or may not be hydraulically connected to the Project Basins due to the nature of the geologic framework at their boundaries. The principles governing the development of the geologic framework model are discussed in this section, including descriptions of how the geologic framework can affect groundwater flow.

The area covered by this geologic investigation is hereafter referred to as the geologic study area, as delineated by a thick red line on Figure 2-1. The geologic study area is irregular in shape because it is made up of many hydrographic areas, which are individual valleys or basins identified and defined by surface-water drainages. Hydrographic areas are the boundaries named, numbered, and described by Federal, State, and local agencies and used in the administration of their responsibilities. Most hydrographic areas consist of a single topographic basin surrounded by ranges. The four Project Basins are the hydrographic areas that are the main focus of our attention.

2.1 Geologic Setting and Background

The geologic study area (Figure 2-1) is within the Great Basin subprovince of the Basin and Range physiographic province, characterized by north-trending basins and ranges that are formed by generally north-striking basin-range normal faults. The area has been subjected to several periods of deformation since Precambrian time. The most recent episode of deformation, which produced the present topography, is the basin-range episode of normal faulting. Most springs in the area are controlled by basin-range faults (Volume 3 of SNWA, 2008). The present topography consists of a number of closed basins and partially closed basins, typical of the Great Basin region where surface-water flow is restricted to that region. Exceptions occur only along the southeastern Great Basin boundary, where a few basins have surface water exiting to the Colorado River. These exceptions include the Virgin River, Muddy River, Las Vegas Wash, and the associated basins in which these streams occur.

During wetter periods of Pleistocene time, the latest of which was about 10,000 to 15,000 years before present, ancestral streams connected some closed basins, commonly through a series of ancestral lakes. For instance, the White River and its tributaries flowed southward through much of the western portion of the map area and integrated many of these basins, apparently by overflowing closed basins one by one (Figure 2-2) (Tschanz and Pampeyan, 1970). During this time, the White River joined other perennial streams that flowed southward to join the Colorado River at the vicinity of present-day Lake Mead, at the southern edge of the area. At the present time, over most of its course and as far south as Moapa, Nevada, the White River is intermittent.

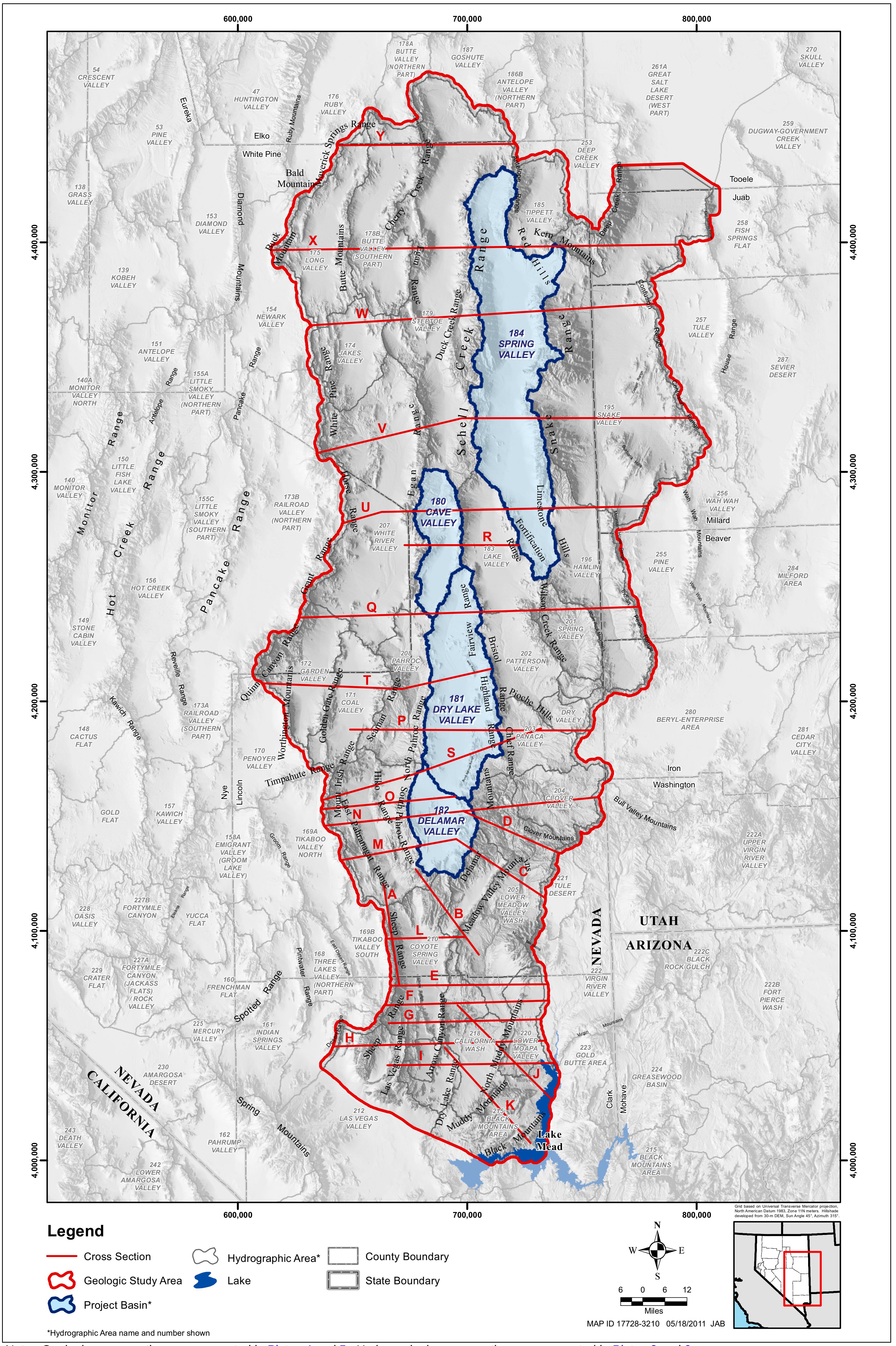

Note: Geologic cross sections are presented in Plates 4 and 5. Hydrogeologic cross sections are presented in Plates 8 and 9.

Figure 2-1
Hydrographic Basins, Ranges, and Locations of Cross Sections

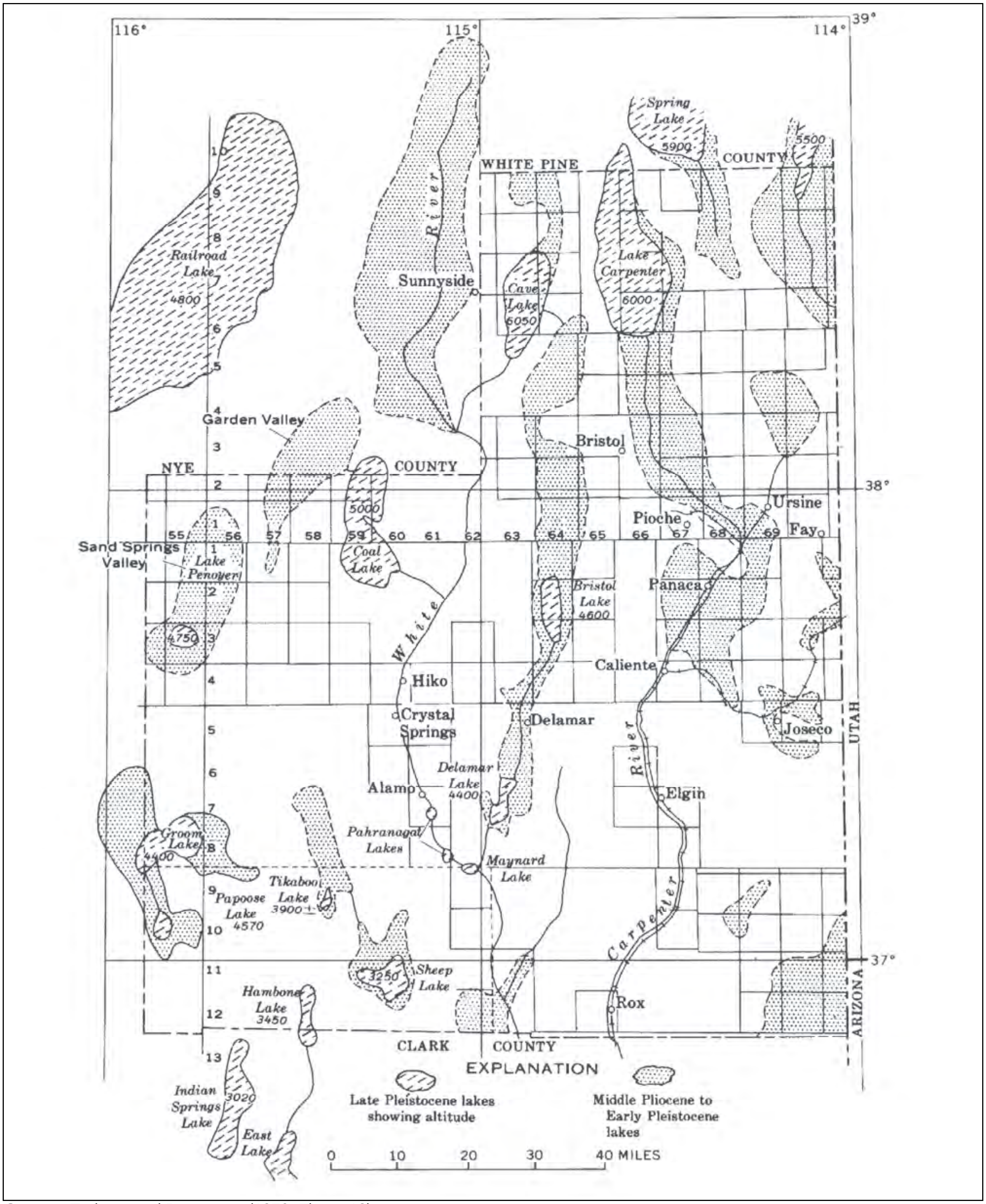

Source: Tschanz and Pampeyan (1970, Figure 18)

Figure 2-2
Map of Pliocene and Pleistocene Lakes and Streams in Lincoln County and Adjacent Areas, Nevada

Despite the intermittent nature of surface water, groundwater occurs at different depths beneath most of the map area. The groundwater exists in aquifers within and between a number of groundwater basins, and it flows through these aquifers and ultimately to areas of groundwater discharge. Together, these aquifers make up the groundwater basin of the hydrographic area. When one hydrographic area is hydraulically connected to that of an adjacent area, and the groundwater in both flows toward a common low discharge area, a groundwater flow system is defined. Some groundwater flow systems consist of many hydrographic areas, and these are called regional groundwater flow systems. Adjacent to these regional groundwater flow systems may be other hydrographic areas that are parts of separate groundwater flow systems. The geologic study area lies within the Carbonate-Rock Province of eastern Nevada and Western Utah as described by Plume and Carlton (1988), and is underlain by an interconnected regional carbonate-rock aquifer. The geologic study area was selected of sufficiently large size so as to allow the investigation of the geologic framework to assess the potential hydraulic continuity or discontinuity between the Project Basins and adjacent areas.

Groundwater flow directions and magnitudes are controlled, in large part, by the geologic framework. The primary regional aquifers in the flow systems consist of Paleozoic carbonate rocks, volcanic rocks (generally Tertiary ash-flow tuffs), and Miocene to Holocene basin-fill sediments. The primary regional confining zones within the flow systems are Precambrian to Cambrian schist, quartzite, slate, and shale, Mississippian shale, Mesozoic clastic sedimentary rocks, and Jurassic to Tertiary plutonic rocks. Attributes of the geologic framework that influence groundwater flow are described in the following section.

2.2 Geologic Controls Affecting the Movement of Groundwater

Several factors affect the movement of groundwater in the study area (Figure 2-3). Of these, porosity, permeability, and fractures/joints dominate and determine the rate and amount of flow in the principal aquifers. In basin filled-aquifers, overburden pressures have an undetermined affect on movement of groundwater through the saturated sediments, although permeability is presumed to decrease with depth due to the overburdened pressure.

Groundwater moves by two mechanisms, porous-media flow and fracture flow. Porous-media flow is often considered the primary mechanism of groundwater flow, and the most commonly applied analytical models to quantify the amounts and rates of flow are based on porous-media flow. While it is a significant, if not dominant, component of groundwater movement in many areas, fault-related fracture flow is of greater significance in the Basin and Range.

Fracture flow (also called fracture-dominated flow), in which groundwater moves along open fractures (secondary porosity/permeability) in rocks and sediments, predominates in the geologic study area because all rock units and sediments in the area are heavily faulted. The process of faulting creates not only faults of all sizes but also joints, which are fractures along which there has been no relative movement along the joint surface except for its opening perpendicular to the surface. Most groundwater movement may actually be along fault-caused joints. Joints that are formed by faults are generally oriented parallel to the fault that caused them. Most faults are basin-range, high-angle normal faults, which trend north or within 30 degrees of north and have an average dip at about 60 degrees. The location of faults is found by geologic mapping. Because faults are uneven in

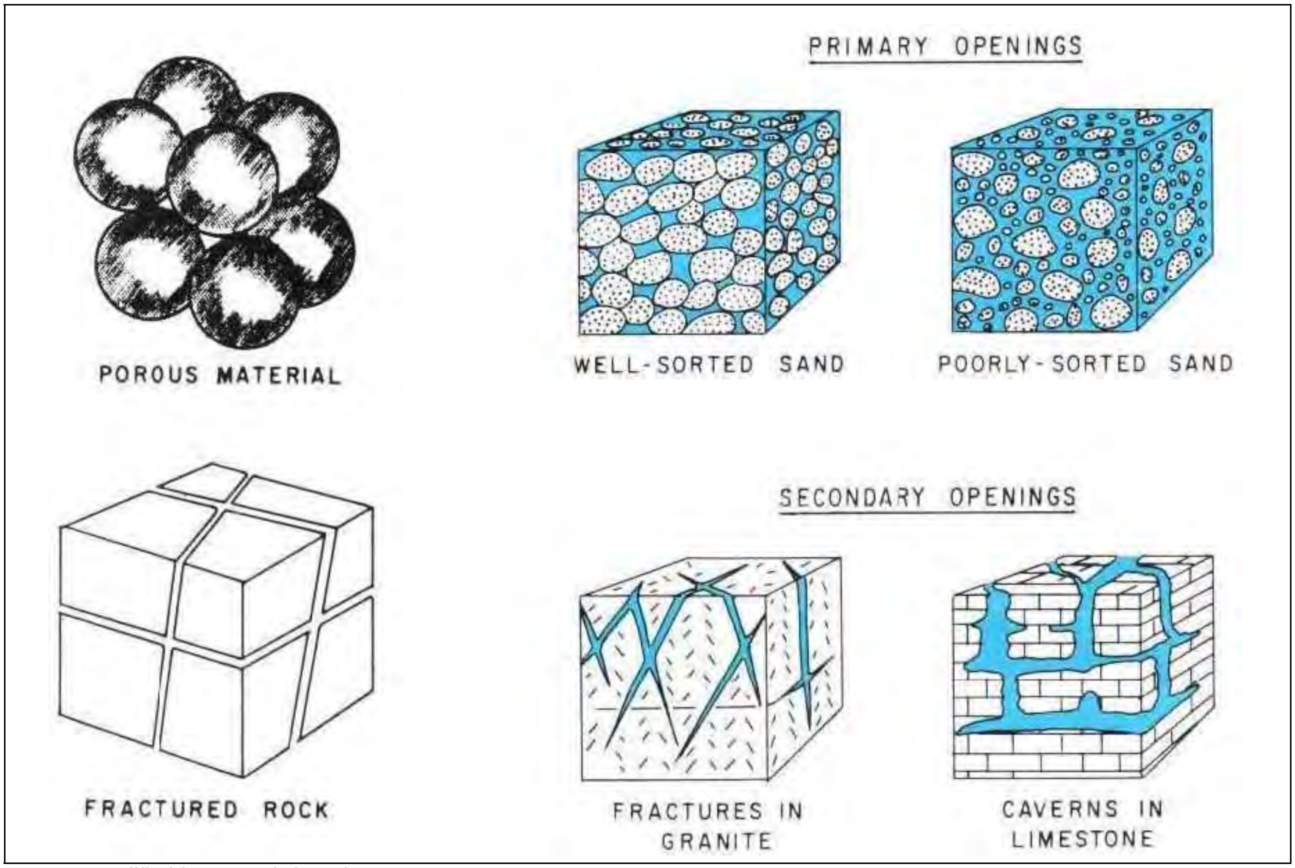

Source: Modified from Heath (1983)

Figure 2-3
Schematic of Primary and Secondary Porosities/Permeabilities of Rock Matrices

their size and distribution across an area, groundwater movement along them is not uniform and therefore cannot be approximated by a formula. Therefore, predictions of flow volumes and rates from fracture flow correspondingly are more approximated than those from porous-media flow. Nonetheless, volumes and rates from fracture flow are considered to be significantly greater than those by porous-media flow. Most regional flow is by fracture flow. In the Basin and Range, fracture flow is especially important within brittle rock types, especially carbonates and ash-flow tuffs, although groundwater movement even in unconsolidated sediments appears to be enhanced and presumably increases in importance as sediments become progressively more consolidated (older). Movement of groundwater is enhanced by fracture flow even in confining zones.

2.2.1 Geologic Controls Affecting Primary and Secondary Porosities

2.2.1.1 Rock Lithology

Rock type partly determines whether groundwater flow will be along primary or secondary porosity. Rock type in turn depends upon the depositional environment, age, and degree of consolidation and brittleness of rock units.

Unconsolidated rocks, which are made up primarily of young (Quaternary) sediments of many depositional environments and exposed at and just beneath the surface, contain fewer fractures by virtue of not being through as many earthquakes (faulting events) as older rocks and not being able to fracture like consolidated rocks. When these unconsolidated deposits are made up of clastic material (that is, particles such as sand or gravel) from a depositional environment such as stream alluvium or multiple sand dunes, they form an aquifer through which fluids are more likely to move by porous-media flow. The younger, near-surface part of the basin-fill sediments in the geologic study area is in this category. Below one or two hundred feet, however, lower (older) basin-fill deposits are progressively more consolidated and therefore progressively more fractured. Yet in the Basin and Range, even young unconsolidated sediments have locally been extensively faulted, and enhanced flow by fractures results. If the unconsolidated deposits are fine-grained sediments such as silt or clay, from a depositional environment such as a flood plain, playa lake, or deep marine basin, they will form a confining unit that, lacking fractures, will not allow movement of measurable groundwater through it.

Consolidated rocks in the Basin and Range, including older parts of the basin fill, will fracture no matter their depositional environment. Consolidated clastic rocks deposited in many ancient depositional environments, as with unconsolidated rocks, are likely to form aquifers whereby some groundwater moves by porous-media flow but most moves by fracture flow. Some consolidated rocks are particularly brittle and therefore will fracture readily. These include carbonate rocks from both marine and lake environments. Marine carbonates, unlike lake carbonates, are thousands of feet thick and widespread in the Basin and Range province, resulting in the great Paleozoic carbonate aquifer in and beyond the geologic study area. Both ash-flow tuffs and basalt lava flows deposited on the surface in volcanic environments are similarly brittle and generally widespread in the Basin and Range province, but in the geologic study area tuffs are rarely more than 1,000 ft thick and basalt flows are either thin or absent.

Many consolidated rocks have had their pores closed by heat and pressure (metamorphic and intrusive rocks) or by cementation of material in their pores (quartzite, which was formerly sandstone but now contains few remaining pore spaces). Other consolidated rocks, such as ancient marine shales, consist of clay minerals that are too fine-grained to allow groundwater through them. These consolidated rocks in the geologic study area are fractured but where thick, as with the Precambrian basement rocks and Neoproterozoic to Early Cambrian quartzites that underlie the entire area and the Mississippian Chainman Shale, are in most places confining units whether fractured or not. In some places, however, these rock types are cut by major fault zones that allow groundwater to move through them. Quartzite commonly is brittle and, where thin and sandwiched between aquifer rocks, may shatter like a plate of glass during basin-range faulting, resulting in a fracture-flow aquifer in its own right. The Eureka Quartzite of Ordovician age, which ranges between 600 and 800 ft thick through the geologic study area, is such a unit. Details of rock types and ages of rock units versus their properties as aquifers or confining units in the geologic study area are discussed in Sections 4.1 and 4.2.

2.2.1.2 Structural Controls

The main concept in understanding the movement of groundwater in the geologic study area is that groundwater flows through rock fractures with high-angle faults, in other words, fracture flow. With few exceptions, these faults are the basin-range normal faults associated with basin-range extension of the past 20 million years and that created the present topography of the Great Basin, as discussed in greater detail in Sections 4.1.5.2 and 4.3.2.4. Recognition, understanding, and documentation of this concept have increased for decades, motivated by fracture flow's important role in such topics as isolation of radioactive waste in underground repositories, groundwater transport of radionuclides, cleanup of toxic waste, exploitation of petroleum and geothermal reservoirs, and, of course, movement of groundwater (Haneberg et al., 1999; Faybishenko et al., 2005a and b). Unfortunately, many details in the physics and mathematics of fracture flow are unknown; therefore, only limited success has occurred in constructing mathematical models of fracture flow (Faybishenko et al., 2005b). One of the biggest problems has been that "numerical predictions often do not match field observation results" (Faybishenko et al., 2005a, p. vii). To resolve these issues, field and theoretical case studies have increased in number, especially in the last decade. These studies have been undertaken more commonly for fluid flow in jointed rocks (Faybishenko et al., 2005a) than in the more complicated case of in faulted rocks (e.g., Haneberg et al., 1999). To date, however, models based on the study of fracture flow have been conceptual, theoretical, and engineering-based.

Most of what we know about fracture flow began with U.S. Department of Energy-funded studies, primarily by the USGS, on the Nevada Test Site (NTS) so as to trace movement of contaminated groundwater resulting from hundreds of above- and below-ground nuclear tests (Winograd and Thordarson, 1968, 1975; Laczniak et al., 1996; Leahy and Lyttle, 1998; Rowley and Dixon, 2004). These studies began in the 1950s and resulted in publications on the geology, detailed geologic mapping of the entire NTS, and conclusions from well tests and other hydrologic data. The studies resulted in the discovery of the huge Death Valley regional groundwater flow system (Harrill et al., 1988; Laczniak et al., 1996; Harrill and Prudic, 1998; D'Agnese et al., 2002; Workman et al., 2002a and b; Belcher, 2004). In this flow system, recharge originated in the broad, high mountains of central Nevada, and flow terminated as spring discharge in Ash Meadows, Oasis Valley, and Death Valley. Among the scores of reports that resulted, the words structural "barriers" and "conduits" were introduced (Winograd and Thordarson, 1968, p. 35) to describe faults and other fractures that respectively create dams to flow across them and exhibit high transmissibilities along them.

The most useful studies specific to the conceptualization of the role of faults on flow were those of Caine et al. (1996) and Sibson (1996, 2000) because they dealt with the geology of fracture flow. These studies were done independently of each other. Sibson (1996, 2000) discussed shear mechanisms and large-volume movement of hydrothermal fluids along high-angle faults that result in hydrothermal ore deposits, whereas Caine et al. (1996) applied the work to groundwater flow. Caine et al. (1996) broke high-angle faults into (1) a central core zone (p. A-5 of Appendix A), which is generally of low permeability across it because of gouge and foliation in clay minerals formed along the axis of fault deformation, and (2) outer damage zones on each side of the core, which is likely to be of high permeability across and along them because they consist largely of joints and small faults that are generally parallel to the core zone (Figure 2-4). They pointed out that central core zones are in many places cut by synchronous or later faults and joints, so local flow is hardly unusual across them. Nonetheless, they found that faults generally tend to retard flow across (perpendicular to) them and provide conduits to flow laterally along (parallel to) them. Caine and Forster (1999) and Caine et al. (2010) expanded on these conclusions by adding more field examples and constructing computer models of faults and simulations of fluid flow in these models.

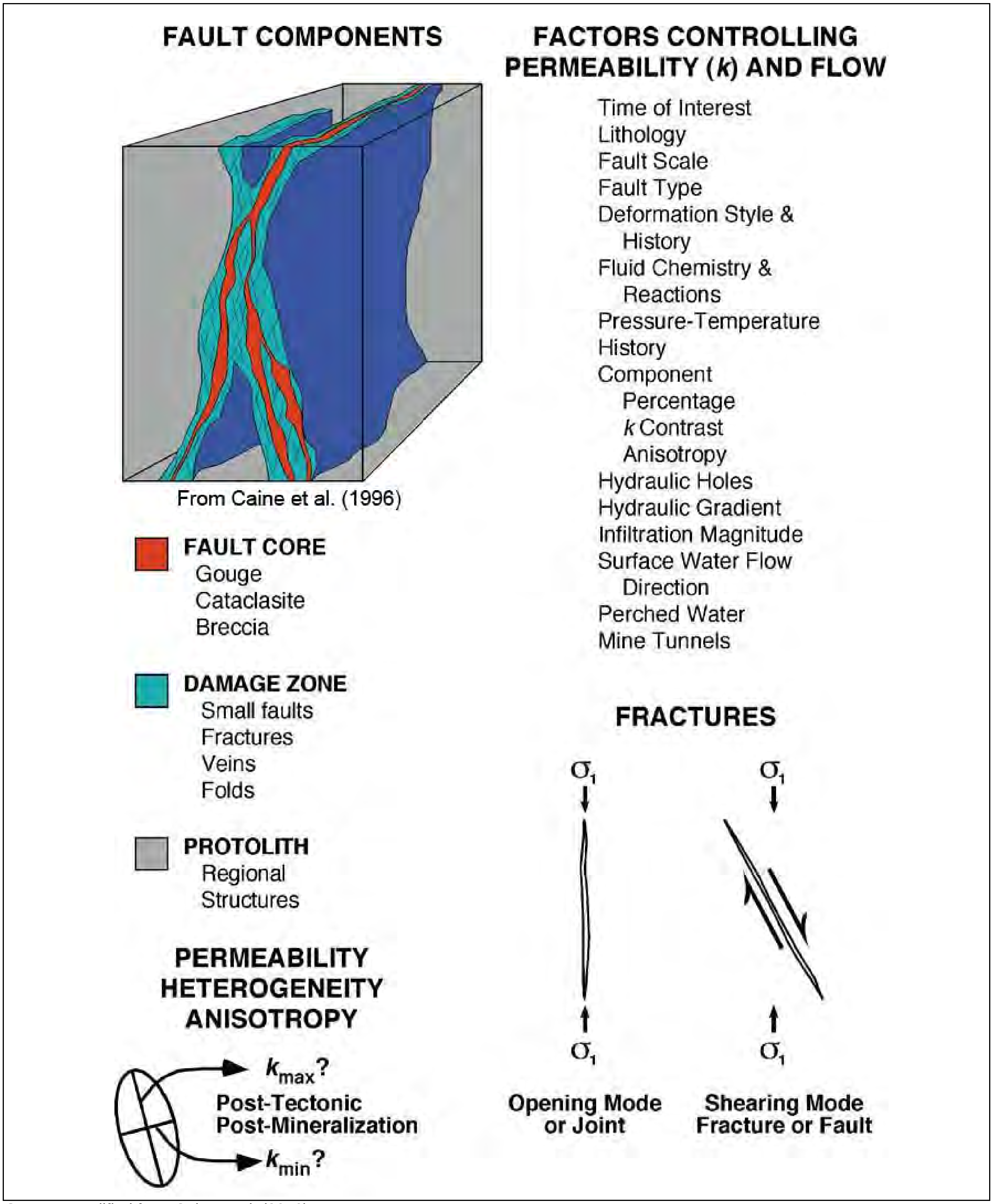

Source: Modified from Caine et al. (2010)

Figure 2-4
Conceptualization of Fault Components and Factors Controlling Permeability and Groundwater Flow

In the last decade, the literature on fracture flow and the role of faults as barriers and/or conduits has become voluminous, but it is beyond the scope of this report to summarize these conclusions. Brief summaries of some of this literature, however, are provided by Rowley and Dixon (2004) and Rowley et al. (2009). Perhaps more important, the authors have published several practical studies for water districts in or adjacent to the geologic study area that have used the concept of faults as barriers and conduits to site production water wells and well fields by drilling faults. For example, parts of the Mesquite basin were geologically mapped at 1:24,000 scale (Williams, 1996, 1997) for the Virgin Valley Water District, and all of the basin was mapped at 1:100,000 scale (Dixon and Katzer, 2002). The purpose of this mapping was to describe the geometry of basin-range faults that provide conduits for southward groundwater flow from the primary recharge area in the broad Clover Mountains north of the basin (Plates 1 and 2). Then Dixon and Katzer (2002) sited production water wells on faults in poorly consolidated basin-fill deposits (Muddy Creek Formation). Well yields of as much as 1,700 gpm and averaging 1,500 gpm were documented by Johnson et al. (2002). Later, a 1:250,000-scale geologic map of this and adjacent areas was prepared by Page et al. (2005a) to portray and discuss fracture-flow concepts of a large area that later became the southeastern parts of Plates 1 and 2.

Additional practical documentation of faults as conduits resulted in additional successful projects east of Mesquite, in Utah. Here, the groundwater resources of the Gunlock well field northwest of St. George were re-evaluated in terms of southward conduit flow along the north-trending Gunlock fault zone (Rowley, 2002; Rowley and Dixon, 2004). The study concluded that wells progressively closer to the Gunlock fault were progressively better producers (as much as 1,400 gpm) and that the well field had sufficient water for increased pumping by the city. High yields in several other well fields in the St. George area can be explained by basin-range faults that pass beneath the well fields, carrying groundwater from high-altitude recharge areas to the north (Biek et al., 2007). The Sand Hollow well field east of St. George, which was designed and constructed, and is managed, by Washington County Water Conservancy District (WCWCD), is artificially recharged by Sand Hollow Reservoir, which lies entirely on the aquifer, the Jurassic Navajo Sandstone. To site additional wells in the field, geologic mapping was done at 1:12,000 scale to find fault conduits in the area, then wells were proposed for WCWCD to drill (Rowley et al., 2004). The first of these drilled was tested at 2,500 gpm (Cram, pers. comm., 2006). The same concept of mapping and siting wells was done for the proposed WCWCD Anderson Junction Reservoir that will artificially recharge the Anderson Junction well field, along Interstate Highway I-15 (I-15) halfway between Cedar City and St. George (Rowley and Dixon, 2010).

For purposes of this report, Figure 2-5 provides a synopsis of whether flow of groundwater is enhanced or impeded by certain types of structures in the geologic study area. Classic basin-range normal faults, which trend mostly north and form during extension (pulling apart) in an east-west direction, provide conduits (enhanced flow) to groundwater flow north or south, assuming that the hydraulic gradient is in these directions, as is the case in virtually the entire geologic study area. Yet these same faults provide barriers (impeded flow) to groundwater flow to the east or west (see Section 4.3.2.4). Innumerable examples of likely conduits created by basin-range normal faults are mapped in the geologic study area (Plate 1), including the major bounding faults on the eastern and western sides of the four project basins. These same faults form likely full or partial barriers to flow east or west through the north-trending ranges and hills on either side of the basins that are defined by the faults.

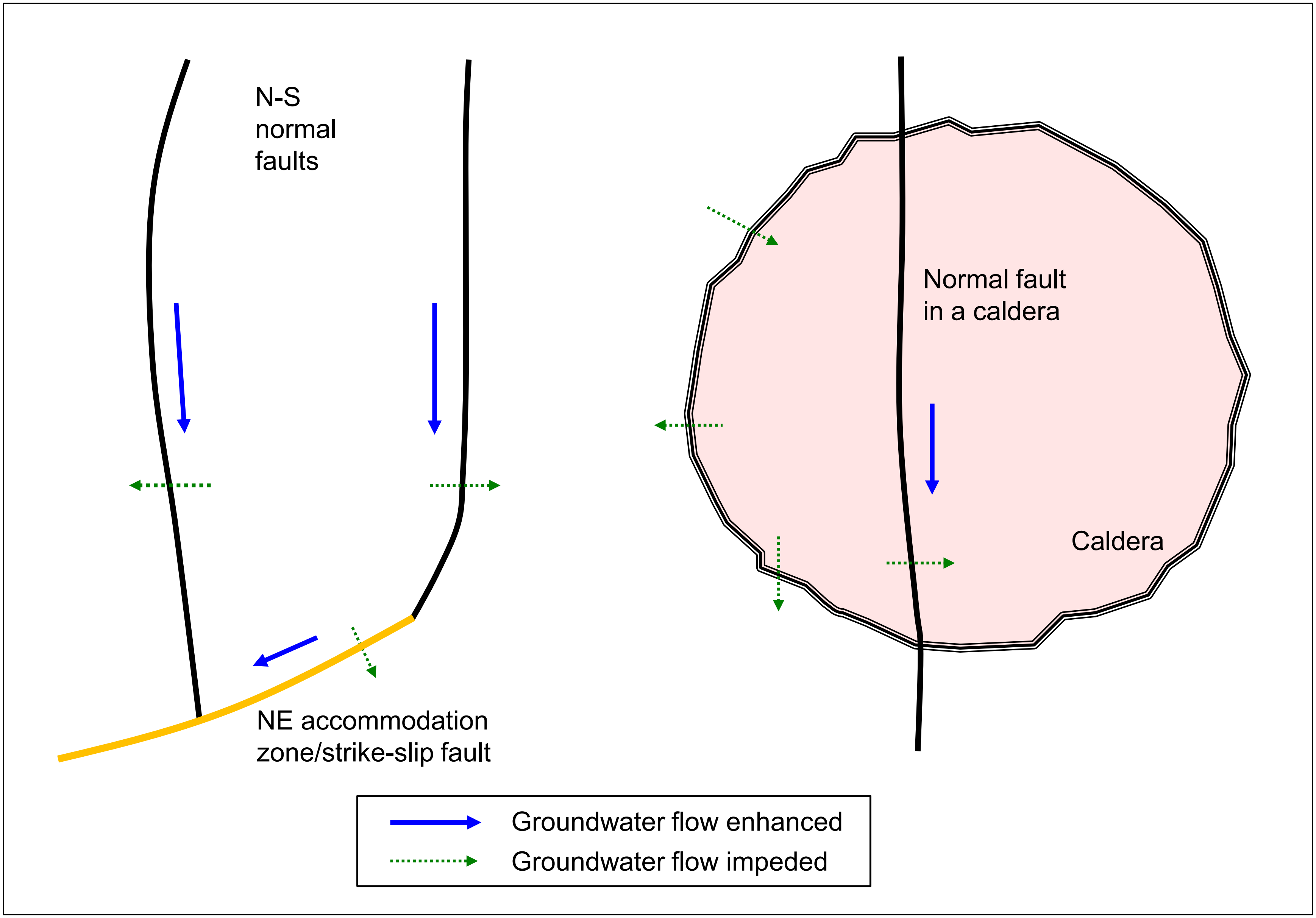

Figure 2-5
Map Showing Enhancement/Impedance of Groundwater Flow along or across Faults and Calderas

In some parts of the geologic study area, such as the Pahranagat Shear Zone (PSZ) at the southern end of Delamar and Pahranagat valleys (Sections 4.4.16 and 4.4.12; Figure 4-12), northeast- or north west-trending faults accommodate the east-west basin-range extension by strike-slip movement (see Section 4.3.2.4). For these accommodation zones, conduits are oriented northeast or northwest and barriers are oriented perpendicular to conduits (Figure 2-5).

Calderas are huge semi-circular collapsed areas above vents for ash-flow tuffs, which are the most voluminous Tertiary volcanic rock type in the Great Basin (see Sections 4.1.5.2 and 4.3.2.3). The semi-circular caldera margin and an aquitard of intrusions that underlies the caldera provide barriers to groundwater flow, except where the caldera is cut by normal faults (Figure 2-5). The caldera margins of the Indian Peak and Caliente caldera complexes are examples that are expected to provide barriers to flow through them, although the Indian Peak caldera complex is in turn truncated by large younger basin-range normal faults that allow northerly flow through its margin (Plate 1).

2.2.1.3 Width of Faults and its Relevance to Groundwater Flow

Faults of small displacement, width, and length can form significant lateral flow conduits along the hydraulic gradient, whether in consolidated or unconsolidated deposits. Faults of large displacement, width, and length can form still larger conduits, especially on the downthrown side, known as a hanging wall (Shipton and Cowie, 2001; Minor and Hudson, 2006). For these reasons, Plates 1 and 2 show regional (major) and subsidiary (smaller) faults, distinguished by geologic mapping based on their amount of offset and their fault length and width.

With respect to the influence of large faults on groundwater flow, what do we know about the width of faults in and near the geologic study area? The literature on the width of large faults in the Great Basin is limited because fault zones consist of broken, sheared, and altered rock that commonly can be disaggregated by one’s hands, so the rocks in these fault zones are easily removed by erosion from view in the field. Nonetheless, several examples known to the authors can be given where exposures are especially good. West of the geologic study area, Dixon et al. (1972) mapped north-northeast-striking oblique-slip fault zones, each made up of a series of individually mapped, parallel faults of the same displacement, on either side of the Park Range, west of Little Smoky Valley, Nye County, Nevada; each zone was locally more than half a mile wide and more than 12 mi long. Not far away, along the west side of Hot Creek Valley, Nye County, Ekren et al. (1973) mapped a zone of range-front faults and parallel Quaternary faults of the same normal displacement just east of the range front that is as much as 2.5 mi wide and more than 10 mi long. The major north-northeast-trending oblique-slip Kane Springs Wash fault zone in Kane Springs Valley (Plates 1 and 2, east of the Delamar Range) is about 1.25 mi wide and many miles long (Swadley et al., 1994). The Grand Wash fault zone, a normal fault separating the Colorado Plateau from the Great Basin along the eastern side of Lake Mead, is shown by parallel north-trending bedrock and Quaternary faults at least 1 mi wide (Billingsley and Workman, 2000). Detailed, high-quality geophysics, including seismic and audiomagnetotellurics (AMT) profiles and also gravity and aeromagnetic anomalies, provides even better estimates of fault widths (see Section 5.0). These large faults are almost always shown as zones of disrupted beds and blocks, commonly several miles wide. Hundreds of examples could be cited.

Based on the authors' experience, the influence of faults on groundwater flow is proportional to the width of fault zones, and in turn the width of fault zones is proportional to the magnitude of displacement of fault zones. However, this generalization applies only to high-angle faults, and their influence on groundwater partly depends upon the type and age of the high-angle fault. High-angle normal faults, for example, form in an extensional stress regime (pulling apart, in an east-west direction for basin-range faults), so fractures tend to be more open. Strike-slip faults form during lateral shear so fractures may be tighter. Oblique-slip faults would have properties intermediate between normal and strike-slip faults. Transverse faults (Section 4.3.1) probably are akin to strike-slip faults so can be expected to be relatively tight to groundwater flow. In addition to these qualifiers to the general rules, the age of a fault influences how open its fractures are. An active (seismic) fault, such as many of the range-front faults in the geologic study area, breaks rocks—especially brittle rocks—with each fault movement, whereas an inactive fault, especially one that is pre-Miocene in age, may have been sealed or partly sealed by precipitation of minerals carried by groundwater. In other words, a Holocene fault can be expected to be especially transmissive to groundwater flow.

3.0 METHODOLOGY

The objectives of the geologic analysis and the methods applied in developing the products accompanying this report are described in the following sections. Work products developed as part of this analysis include 1:250,000-scale digital geologic maps (Plates 1 and 2), an explanation of map units (Plate 3), and cross sections (Plates 4 and 5). HGUs were derived by combining geologic stratigraphic units based on their hydraulic properties and spatial distribution as described in Volume 1 of SNWA (2008, Section 4.2, Table 4-1 p. 4-20). The digital geologic maps were then simplified accordingly to construct hydrogeologic maps (Plates 6 and 7) and cross sections (Plates 8 and 9). The geologic map area (red line, Figure 2-1) covers most of White Pine County and Lincoln County, Nevada, as well as large parts of adjacent counties in Nevada and Utah.

3.1 Objectives

The primary objective of this geological analysis was to develop a digital geologic and hydrogeologic framework to further our understanding of the hydrogeology of the study area and to serve as the foundation for developing conceptual and numerical models groundwater flow models of the Project Basins and adjacent areas. The geologic information provided data on the locations of potential boundary flow, extents of HGUs, basin geometries, and important geologic features comprising the framework that may affect local and/or regional groundwater flow. Some of these data were used to describe the geologic setting of selected regional springs, the descriptions of which are presented in Volume 3 of SNWA (2008). The geologic framework model also provides aquifer and aquitard thicknesses for the geologic study area. Geologic evaluations outside of the Project Basins (Figure 2-1) provided a basis for interpretations of groundwater interactions across the basin boundaries. This geologic analysis was manifested through the creation of geologic and hydrogeologic maps and cross sections of the study area.

The data compilation included the distribution, geometry, thickness, composition, and physical properties of geologic units used to define HGUs and potential aquifers and confining zones. Such information was considered in ascertaining the rock units that are most likely to provide pathways for groundwater flow and which rock units are most likely to retard or divert flow.

An important aspect of the geologic maps is the portrayal of the distribution and attitude of faults, especially those formed during the youngest (basin-range) episode of deformation. Faults may serve as barriers and/or conduits to groundwater flow as described in Section 2.0 and presented in Figures 2-4 and 2-5. In the geologic study area, most faults trend northerly, parallel to the ranges. Thus, basin-range faults may serve as significant conduits to groundwater flow in the north-south direction. In other parts of the geologic study area, basin-range faults may either direct groundwater flow through a system of barriers and conduits, and/or impede groundwater flow, toward otherwise down-gradient groundwater basins. Part of the objective of this report was to evaluate the potential

SE ROA 43152

JA_13032

for these faults to influence groundwater flow, especially how they might act as either barriers or conduits to groundwater flow.

3.2 Technical Approach

The approach used in this investigation was to combine published and unpublished geologic information from dozens of references collected, compiled, and reviewed by the authors. In addition, an evaluation was conducted of borehole information from oil and gas test wells, monitor wells, such as those drilled during the U.S. Air Force's MX missile-siting program of the early 1980s, and borehole information from exploratory test wells and monitor wells constructed by SNWA in support of the Project. Other sources of information included geophysical studies of the region published by USGS and other entities, particularly data from gravity surveys performed by the USGS. These latter studies have given insight as to the framework geometry and thickness of basin fill and depth to underlying rocks within several basins in Lincoln and White Pine counties, Nevada. A final source of evidence is geologic field work performed by the authors of this report.

Based on the evaluation of the compiled data and the expertise of the authors involved in this investigation, geologic maps were constructed for the area (Plates 1 and 2). Geologic cross sections were constructed (Plates 4 and 5) from the geologic maps. Because of the complexity of the geology of eastern Nevada, these maps and cross sections represent a work in progress, inasmuch as new data on crosscutting faults, attitude of bedding surfaces, intrusions, volcanic sequences, and other geologic units and geologic relationships must be continuously evaluated as new information becomes available.

The geologic units were combined into HGUs of similar hydraulic properties and spatial extent. These broad units make up the aquifers, confining zones, and units of intermediate permeability of the area described by this report. These HGUs are displayed in Plates 6 and 7. Cross sections of these units were compiled using the geologic cross sections of Plates 4 and 5 as a basis; these hydrogeologic cross sections are displayed in Plates 8 and 9. Based on the hydrogeologic maps and cross sections, the extents of aquifers, confining zones, and intermediate-permeability rocks could be evaluated, along with potential fault barriers and fault conduits to groundwater flow. The hydrogeologic maps, cross sections, and hydrogeologic interpretations were used to compile the geologic framework model. The hydrogeologic maps and cross sections were also interpreted to evaluate probable groundwater flow paths and flow barriers.

3.3 Geologic Data Compilation

Geologic data were derived from a number of sources, including literature review, review of Nevada and Utah State Engineers' records, and well databases. Well data were obtained from well logs, databases associated with oil and gas test wells drilled within the geologic study area, and from records of exploratory test and monitor wells drilled by SNWA in upper Moapa, Coyote Spring, Delamar, Dry Lake, Cave, and Spring valleys. Not every well had geologic information, but most of them did have useful information to assist in compiling the geologic and hydrogeologic cross sections. As part of the data compilation, geologic experts who have worked within the study area were consulted and studies completed by the USGS were evaluated. This information was reviewed and compared with all other sources of geologic information prior to incorporation into the geologic maps and cross sections.

3.4 Preparation of Geologic Maps and Sections

The geology of the southern part of the study area (Figure 3-1) has been discussed by Page et al. (2005a). In this report the geology for this area was digitally mapped at 1:250,000 scale (Plate 2). To the west of this area, digital geologic and tectonic maps were also published at a 1:250,000 scale (Workman et al., 2002a and b), and include some of the southwestern portions of Plates 1 and 2. These geologic maps included significant new and unpublished geologic mapping.

For the maps (Plates 1 and 2), much of the Nevada surface geology was compiled from county 1:250,000-scale geologic maps and the Nevada 1:500,000-scale state geologic map (Stewart and Carlson, 1978). From west to east and north to south, the Nevada counties covered by these maps are southern Elko County (Roberts et al., 1967), eastern Nye County (Cornwall, 1972; Kleinhampl and Ziony, 1985), White Pine County (Hose and Blake, 1976), Lincoln County (Tschanz and Pampeyan, 1970), and Clark County (Longwell et al., 1965). Most of the Utah surface geology was compiled from four 1:100,000-scale maps (Hintze and Davis, 2002a and b; Rowley et al., 2006 and 2008; Biek et al., 2007), two 1:250,000-scale maps (Morris, 1987; Steven et al., 1990), and the Utah 1:500,000-scale state geologic map (Hintze, 1980a). Summary reports on the geology of Millard County (Hintze and Davis, 2003) and the geology of Utah (Hintze, 2005; Hintze and Kowallis, 2009) were also valuable. Both the Nevada and Utah state geologic maps were digitized and re-released as digital files, but not updated with respect to maps and reports published since 1978 and 1980, respectively, by Hess and Johnson (1997), Raines et al. (2003), and Crafford (2007) for Nevada and as Hintze et al. (2000) for Utah.

Nearly all of the regional geologic maps (Figure 3-1) were published decades ago. A significant part of the entire map area was compiled by Terrascan Group, Inc. (Howard, 1978), but it compiled the same county maps without updating them. As part of the USGS Basin and Range carbonate-rock aquifer system study (BARCASS), Sweetkind et al. (2007a) compiled a 1:500,000-scale, digital geologic map of a large area that includes all but the eastern edge of the area of Plate 1. However, their map was compiled from Stewart and Carlson (1978), Hintze (1980a), Hintze et al. (2000), and Raines et al. (2003), from which all faults were removed. To that file, Sweetkind et al. (2007a) added some gravity interpretations, some dotted “geophysically determined faults,” and some sketched faults. Two diagrammatic cross sections accompanied this map, but neither matched the topography, geology, or geophysics of their map.

The plates and text of this report incorporate all known revisions and reinterpretations of previously published reports and geologic maps that were deemed necessary. Small-scale geologic maps used in the creation of Plates 1 and 2 are indexed in Figure 3-1. Commonly, new maps and reports were more detailed (published at larger scale). Not all of these maps and reports are cited in the text because of their large number, although all of them are listed in Section 8.0. In addition, Plates 1 and 2 include some new, unpublished field observations and geologic mapping.

The geologic and hydrogeologic maps and sections and the explanation of geologic units of this study area (Plates 1 through 9) cover an area of about 25,000 mi^2. The compilation of the geologic maps of

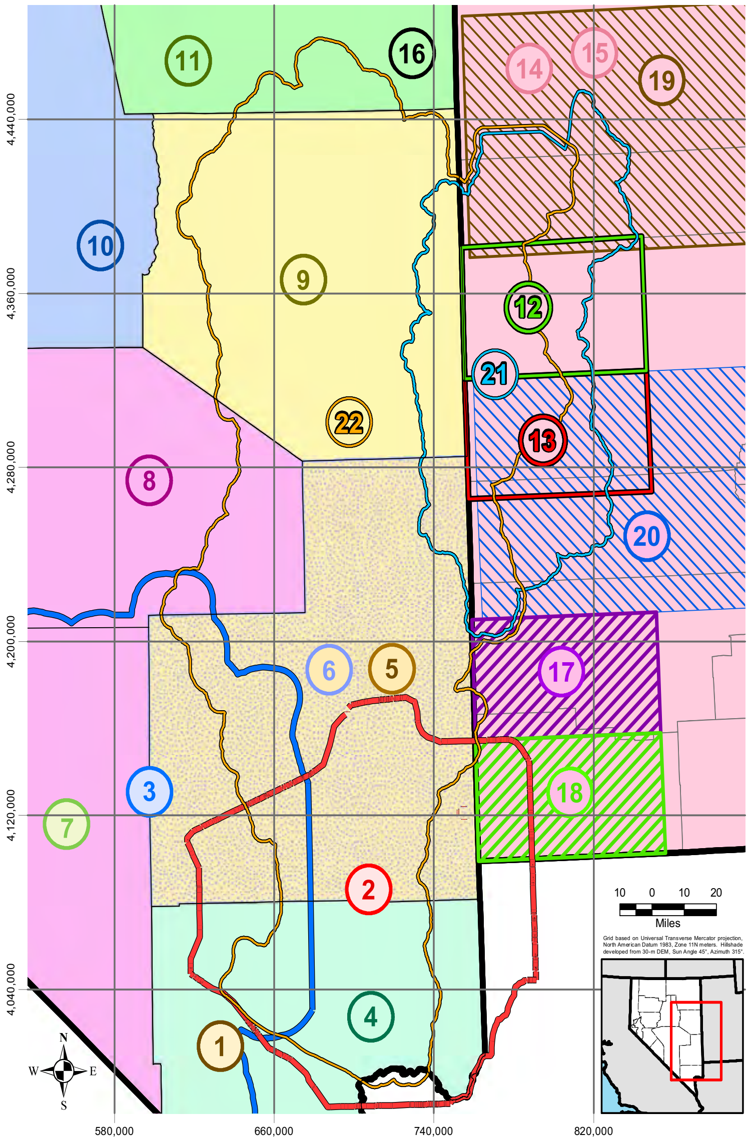

Source Maps:

1. Page, W.R., Lundstrom, S.C., Harris, A.G., Langenheim, V.E., Workman, J.B., Mahan, S.A., Paces, J.B., Dixon, G.L., Rowley, P.D., Burchfiel, B.C., Bell, J.W., and Smith, E.I., 2005, Geologic and Geophysical maps of the Las Vegas 30' × 60' quadrangle, Clark and Nye Counties, Nevada, and Inyo County, California: U.S. Geological Survey Scientific Investigations Map 2814, 55 p., scale 1:100,000.
2. Page, W.R., Dixon, G.L., Rowley, P.D., and Brickey, D.W., 2005, Geologic map of parts of the Colorado, White River, and Death Valley ground-water flow systems: Nevada Bureau of Mines & Geology Map 150, scale 1:250,000. Digital GIS data provided.
3. Workman, J.B., Menges, C.M., Page, W.R., Taylor, E.M., Ekren, E.B., Rowley, P.D., Dixon, G.L., Thompson, R.A., and Wright, L.A., 2002, Geologic map of the Death Valley ground water model area, Nevada and California: U.S. Geological Survey Miscellaneous Field Studies MF-2381-A, scale 1:250,000. Digital GIS data provided.
4. Longwell, C.R., Pampeyan, E.H., Bowyer, B., and Roberts, R.J., 1965, Geology and mineral deposits of Clark County, Nevada: Nevada Bureau of Mines and Geology Bulletin 62, 218 p., scale 1:250,000.
5. Tschanz, C.M., and Pampeyan, E.H., 1970, Geology and Mineral deposits of Lincoln County, Nevada: Nevada Bureau of Mines and Geology Bulletin 73, 187 p., scale 1:250,000.
6. Ekren, E.B., Orkild, P.P., Sargent, K.A., and Dixon, G.L., 1977, Geologic map of Tertiary rocks, Lincoln County, Nevada: U.S. Geological Survey Miscellaneous Investigations Series Map I-1041, scale 1:250,000.
7. Cornwall, H.R., 1972, Geology and mineral deposits of southern Nye County, Nevada: Nevada Bureau of Mines and Geology Bulletin 77, 49 p., scale 1:250,000.
8. Kleinhampl, F.J., and Ziony, J.I., 1985, Geology of northern Nye County, Nevada: Nevada Bureau of Mines and Geology Bulletin 99A, 172 p., scale 1:250,000.
9. Hose, R.K., and Blake, Jr., M.C., 1976, Geology and mineral resources of White Pine County, Nevada, Part 1, Geology: Nevada Bureau of Mines and Geology Bulletin 85, p. 1-35., scale 1:250,000.
10. Roberts, R.J., Montgomery, K.M., and Lehner, R.E., 1967, Geology and mineral resources of Eureka County, Nevada: Nevada Bureau of Mines and Geology Bulletin 64, 152 p., scale 1:250,000.
11. Coats, R.R., 1987, Geology of Elko County, Nevada: Nevada Bureau of Mines and Geology Bulletin 101, 112 p., scale 1:250,000.
12. Hintze, L.F., and Davis, F.D., 2002, Geologic map of the Tule Valley 30' × 60' quadrangle and parts of the Ely, Fish Springs, and Kern Mountains 30' × 60' quadrangles, northwest Millard County, Utah: Utah Geological Survey Map 186, scale 1:100,000.
13. Hintze, L.F., and Davis, F.D., 2002, Geologic map of the Wah Wah Mountains North 30' × 60' quadrangle and part of the Garrison 30' × 60' quadrangle, southwest Millard County and part of Beaver County, Utah: Utah Geological Survey Map 182, scale 1:100,000.
14. Hintze, L.F., Willis, G.C., Laes, D.Y.M., Sprinkel, D.A., and Brown, K.D., 2000, Digital Geologic Map of Utah, Utah Geological Survey Map 179DM, scale 1:500,000.
15. Hintze, L.F., 1980, Geologic map of Utah: Utah Geological and Mineralogical Survey, scale 1:500,000.
16. Hess, R.H., and Johnson, G.L., 1997, Nevada Bureau of Mines and Geology County Digital Mapping Project, Open File report 97-1, Nevada Bureau of Mines and Geology, scale 1:250,000. These data were digitized from the county Geology and Mineral Resource Bulletins published by the NBMG. Digital products cover Clark, Lincoln, White Pine, Southern Nye, Northern Nye, Elko and Eureka counties.
17. Rowley, P.D., Williams, V.S., Vice, G.S., Maxwell, D.J., Hacker, D.B., Snee, L.E., and Mackin, J.H., 2006, Interim geologic map of the Cedar City 30' × 60' quadrangle, Iron and Washington Counties, Utah: Utah Geological Survey Open-File Report 476DM, scale 1:100,000. Rowley, P.D., Hacker, D.B., Maxwell, D.J., Maxwell, J.D, and Boswell, J.T., 2008, Interim geologic map of the Utah part of the Deer Lodge Canyon, Prohibition Flat, Uvada, and Pine Park quadrangles (east part of the Caliente 30' × 60' quadrangle), Iron and Washington Counties, Utah: Utah Geological Survey Open-File Report 530, scale 1:24,000.
18. Biek, R.F., Rowley, P.D., Hacker, D.B., Hayden, J.M., Willis, G.C., Hintze, L.F., Anderson, R.E., and Brown, K.D., 2007, Geologic map of the St. George and east part of the Clover Mountains 30' × 60' quadrangles, Washington and Iron Counties, Utah: Utah Geological Survey Map 242, scale 1:100,000.
19. Morris, H.T., 1987, Preliminary geologic map of the Delta 2° quadrangle, Tooele, Juab, Millard, and Utah Counties, Utah: U.S. Geological Survey Open-File Report 87-185, scale 1:250,000.
20. Steven, T.A., Morris, H.T., and Rowley, P.D., 1990, Geologic map of the Richfield 1° × 2° quadrangle, west-central Utah: U.S. Geological Survey Miscellaneous Investigations Series Map I-1901, scale 1:250,000.
21. Rowley, P.D., Dixon, G.L., Burns, A.G., and Collins, C.A., 2009, Geology and hydrogeology of the Snake Valley area, western Utah and eastern Nevada, *in* Tripp, B.T., Krahulec, Ken, and Jordan, J.L., eds., Geology and geologic resources and issues of western Utah: Utah Geological Association Publication 38, CD, p. 251-269 + Plate 1 (scale 1;250,000).
22. This study and Dixon, G.L, Rowley, P.D., Burns, A.G., Watrus, J.M., and Donovan, D.J., Ekren, E.B., 2007, Geology of White Pine and Lincoln Counties and adjacent areas, Nevada and Utah—The geologic framework of regional groundwater flow systems: Southern Nevada Water Authority, Las Vegas, Nevada, Doc. No. HAM-ED-0001, variously paginated, scale 1:250,000.

Figure 3-1
Previous Large-Scale Mapping Used to Evaluate Geology and to Create the Geologic and Hydrogeologic Maps of Plates 1 and 2

Plates 1 and 2 required many name changes to specific geologic units throughout this large geologic study area. Map scale required some lumping of units with others. New names or new correlations required other changes. In many places, facies changes resulted in major changes in the lithology of a specific unit, and in other places, different formation names were used essentially for the same unit. In some instances, a specific unit thinned in certain areas and was included as a member of another unit or as an inconsequential bed within another unit. An example is the Mississippian Chainman Shale, which is a major shale confining unit in the north, as in White Pine County (Hose and Blake, 1976), but a generally inconsequential shale horizon included within other units in the southern map area, as in Clark County (Longwell et al., 1965). During compilation of the geologic map, separate stratigraphic columns were used for different counties, along with a stratigraphic column for units in western Utah. Correlations between specific geologic units are commonly given in the literature and these correlations were generally used to associate units of the same or similar age in different parts of the map area. An example is the correlation between the Devonian Guilmette Formation and the Devils Gate Limestones (Hose and Blake, 1976).

During map compilation, a hard copy of the available digital file—generally the county map—was modified by hand, then digitized. Before this compilation, all available new geologic data about the area were accumulated, assimilated, and evaluated. The new data included reports, different concepts, detailed or regional maps, geophysics, and well logs. Some new interpretations conflicted with old interpretations, necessarily resulting in different placement of contacts and faults. Decisions on the eventual linework were based on what appeared to be scientifically the most reasonable alternative and depended primarily on the judgement and experience of the authors.

The maps (Plates 1 and 2) include 25 new geologic cross sections (Plates 4 and 5), most of which generally trend east-west. In addition, geologic cross sections were drawn through many springs in the geologic study area (Volume 3 of SNWA, 2008). The cross sections on Plates 4 and 5 are roughly evenly spaced across the map area at the same scale as the map and at locations chosen to best show specific geologic and structural relationships important to the interpretation of the hydrogeology. In addition, hydrogeologic maps (Plates 6 and 7) and hydrogeologic cross sections (Plates 8 and 9) were constructed, where geologic units with similar hydrologic properties such as porosity and permeability were combined into HGUs, distinct from the geologic units that comprise them. Few of the reports and maps used to compile the geologic maps had associated geologic cross sections, so the cross sections for this report are based on interpretations of the county geologic maps along with all other available maps and reports of the map areas. A geologic map by Terrascan Group, Inc. (Howard, 1978) presented associated cross sections that were used to help interpret some of the cross sections in this report. In addition, the geologic map of Elko County (Coats, 1987) was used to help interpret Cross Section Y—Y' (Plate 4), along the northern edge of the map area. The cross sections of Page et al. (2006) aided in constructing the cross sections in the southern part of the geologic study area. The cross section of Smith et al. (1991) was useful in constructing Cross Section X—X' (Plate 4) near the northern margin of the geologic study area.

Unlike compilation of the geologic map, most cross sections are newly authored for this report. The first step in the construction of cross sections is to satisfy the three-dimensional geometry of the rocks at depth based on the types, attitudes, and thicknesses of rocks and structures on the surface. The most difficult part of making cross sections is dealing with the near absence of subsurface information. Therefore, geophysics and well logs near the line of section are valuable. Fortunately, aeromagnetic and gravity geophysical data were available for much of the area. Unfortunately, well logs, AMT profiles, and seismic profiles are rare. Where local information on the third dimension is not available, analogies are made with areas in other parts of the Great Basin where seismic and drill-log data provide ideas about how the rocks and structures look at depth. And here, as in compilation of geologic maps, the judgment and experience of the authors are of paramount importance.

All cross sections incorporated lithologic information from available oil- and water-well logs. Oil-well logs in Nevada are available online from the Nevada Bureau of Mines and Geology or through their publications. Garside et al. (1988) compiled geologic data from oil and gas wells drilled in Nevada from 1907 through 1988. This compilation was supplemented by Hess (2001). This information was supplemented again in 2004 (Hess, 2004). Oil-well logs in Utah were obtained from the Utah Division of Oil, Gas, and Mining website (UDOGM, 2006). Water-well logs in Utah were obtained from the Utah Division of Water Rights website (UDWR, 2006).

Geophysical studies, notably gravity maps (Saltus, 1988a and b; Cook et al., 1989; Ponce, 1992; Saltus and Jachens, 1995; Ponce et al., 1996), aeromagnetic maps (Hildenbrand and Kucks, 1988a and b), and seismic sections (Allmendinger et al., 1983; Hauser et al., 1987; Alam, 1990; Alam and Pilger, 1991), were used to aid in the interpretation of geologic cross sections and structure sections. Gravity maps and AMT profiles were completed by USGS as part of USGS/SNWA joint funding agreements (Mankinen et al., 2006, 2007, and 2008; McPhee et al., 2005, 2006a and b, 2007, 2008, and 2009; Mankinen and McKee, 2009 and 2011; Scheirer, 2005; Scheirer et al., 2006). The gravity data were converted to depth-to-basement data and were used to aid in constructing the cross sections.

A technical review of the entire text and plates was done by M.A. Kuntz, Emeritus Geologist of the USGS, Denver, Colorado. At least 90 percent of his suggestions were accepted by the authors. This resulted in many improvements to the text and plates.

4.0 GEOLOGY AND HYDROGEOLOGY

4.1 Geology and Stratigraphy

4.1.1 Overview

The geology of the geologic study area (Figure 2-1, Plates 1 and 2) is characterized by a thick stratigraphic sequence of rocks from Proterozoic to Holocene age that has been structurally deformed during several tectonic episodes. The thick sequence includes three major assemblages that are important aquifers:

- Carbonate aquifer of Paleozoic age
- Volcanic rocks of Tertiary age
- Basin-fill sediments of Tertiary to Quaternary age.

Along with the aquifers are moderate to thick confining units or low-permeability units, including:

- Early to Late-Proterozoic metamorphic and igneous rocks
- Late Proterozoic to Lower Cambrian quartzite and shale
- Shale, sandstone, and conglomerate of Mississippian age
- Triassic to Cretaceous shale, siltstone, and sandstone
- Mesozoic and Cenozoic plutons.

Three tectonic episodes, plus an intervening episode of extensive volcanism, have affected the hydrogeology of the region. The oldest tectonic episode is the Antler deformation (Late Devonian to Late Mississippian). This episode included east-verging thrust sheets. The second tectonic episode was the Sevier deformation (Jurassic through early Cenozoic) that resulted in east-verging thrust sheets in which Paleozoic carbonate rocks were placed over each other and over younger rocks.

In Eocene to middle Miocene time, volcanism resulted in the development of thick blankets of ash-flow tuff and related lava flows, including many scattered calderas that were the sources of the tuffs. The caldera margins formed new groundwater flow paths and barriers.

The third tectonic episode is the middle Miocene to Holocene basin-range deformation that shaped the current topography of the Great Basin, including most of Nevada and parts of western Utah and southeastern California. Basin-range faulting produced graben and horst topography, resulting in deep basins and relatively high mountain ranges, generally oriented north-south. The mountain ranges provided areas of groundwater recharge, and accumulations of alluvial fill within the basins provided areas of aquifer storage and avenues of groundwater flow. Basin-range faults may provide hydrogeologic barriers to groundwater flow. But more commonly, basin-range faults provide conduits to groundwater flow, especially from north to south. These north-south conduits may also double as barriers to east or west flow.

The age of the rocks in the geologic study area is summarized in a Geologic Time Scale chart (Figure 4-1). The oldest rocks are Early Proterozoic (Paleoproterozoic) and Late Proterozoic (Neoproterozoic) metamorphic and igneous units. These rocks are overlain by thick sequences of quartzite and subordinate shale, which are locally metamorphosed to slate and schist, of Neoproterozoic age. The Proterozoic rocks pass conformably upward into rocks of similar type and thickness, though less metamorphosed, that are Neoproterozoic to Early Cambrian in age. During Middle Cambrian time, carbonate deposition was initiated, and thick sequences of marine limestone and dolomite were deposited from the Middle Cambrian through the Permian Periods. These rocks make up the carbonate aquifer of Nevada and adjacent parts of Utah and range in thickness between 5,000 and 30,000 ft throughout this area (Harrill and Prudic, 1998).

Locally, marine sandstone and shale are intertongued with the carbonates. These units generally do not form significant impediments to regional groundwater flow, with the exception of the Chainman Shale and related shale and sandstone of Late Mississippian age. This unit locally exceeds 2,000 ft in thickness, and in all but the southern part of the geologic study area, this unit divides the carbonate aquifer into two distinct aquifers, the lower and upper carbonate aquifers. The Chainman Shale and related clastic units were derived from erosion of a structural highland, the Antler Highland, in and northwest of the geologic study area. The highland, made up in large part of the Roberts Mountain allochthon, was produced by the Antler compressive deformational event.

Mesozoic rocks in the geologic study area are largely nonmarine clastic rocks, thin where deposited and in most places they have been removed by erosion. Mesozoic and older rocks were deformed during the Sevier deformational event. At this time, the geologic study area was a highland, also known as a hinterland, and an episode of erosion of the area removed most Mesozoic rocks.

Plutons of Late Jurassic to Paleocene age were intruded during Sevier deformation. These plutons probably had associated extrusive volcanic units, but all of these units have been removed by erosion. Mesozoic plutons commonly led to significant mineralization in the geologic study area.

Middle Tertiary (Eocene to middle Miocene) time marked the continuation of calc-alkaline intrusion and resulting volcanism, the terminal product of relatively rapid subduction beneath western North America that began in the Triassic Period (Atwater, 1970; Lipman et al., 1972; Hamilton, 1995; Schellart et al., 2010). Above individual source plutons, vent deposits included andesitic and dacitic lava flows and volcanic mudflow breccia that locally exceeded several thousand feet of thickness. Caldera deposits consist of dacitic to rhyolitic ash-flow tuffs, which are at least several thousand feet thick within individual calderas. Farther outward from the vents above the plutons, lava flows are sparse because they do not flow more than a few miles from their vents; outflow ash-flow tuffs, on the other hand, traveled as far as 100 mi from their source caldera, so accumulated to aggregate thicknesses exceeding 1,000 ft in most of the geologic study area.

Starting at about 20 Ma ago (middle Miocene), subduction ceased or slowed and extensional deformation increased in the Great Basin (Christiansen and Lipman, 1972; Christiansen and Yeats, 1992; Rowley and Dixon, 2001; Schellart et al., 2010). Basin-range deformation, characterized by

ERA	PERIOD	EPOCH	TIME	PROCESSES AND ROCK TYPES
Cenozoic	Quaternary	Holocene Pleistocene	Present 2.6 Ma	Valley-Fill Alluvium
	Tertiary	Pliocene Miocene Oligocene Eocene Paleocene	5.3 *Ma* 23 *Ma* 33.9 *Ma* 55.8 *Ma* 65.5 Ma	Start Basin-Range Faulting (20 Ma) Volcanics and Older Sediments Emplacement of Calderas
Mesozoic	Cretaceous Jurassic Triassic		251 Ma	Sevier Orogeny, Intrusions Continental Sediments
Paleozoic	Permian Pennsylvanian Mississippian Devonian Silurian Ordovician Cambrian		542 Ma	Antler Orogeny, Intrusions Chainman Shale, Carbonates
Precambrian			~4.5 Ga	Quartzite and Shale

Source: Adapted from GSA (1999)

Figure 4-1
Geologic Time Scale, Including Rock Type and Tectonic Events

vertical (normal) faulting, began to form alternating mountain ranges and valley basins. The main pulse of this basin-range faulting began about 10 Ma ago, during which time the present topography formed. As valleys formed, they were filled by debris eroded from the adjacent mountain ranges, creating basin-fill deposits.

Individual rock units, structures, basins, and ranges are described in the following sections. Thicknesses of most units are from the county reports of the area where the unit is exposed. The relationships between geologic units in the different areas of the map can be determined from Figures 4-2 to 4-5. These figures illustrate geologic columns for Lincoln (Figure 4-2), White Pine (Figure 4-3), and Clark counties (Figure 4-5), Nevada, and western Utah (Figure 4-4). The Utah area consists of western Iron, Beaver, and Millard counties and the southwestern corner of Juab County.

4.1.2 Proterozoic Rocks

The oldest rocks are in and adjacent to the southern part of the geologic study area in the Beaver Dam Mountains, Mormon Mountains, Virgin Mountains, northeastern Spring Mountains, and the Desert Range (Plate 2) (Tschanz and Pampeyan, 1970; Longwell et al., 1965). These rocks are crystalline metamorphic rocks of Paleoproterozoic age (Page et al., 2005a) that have been mapped in this report as Precambrian rocks (p€). Over most of the geologic study area, however, the oldest rocks are Neoproterozoic to Lower Cambrian quartzite. These Neoproterozoic to Cambrian units appear to be the initial deposits of the Cordilleran miogeocline, a western belt of offshore carbonate-shelf and intertidal deposits (Page et al., 2005a). These units were deposited in shallow marine waters along a passive continental margin of what is now western North America (Stewart and Poole, 1974; Stewart, 1976).

In White Pine County and adjacent Utah, the principal Neoproterozoic unit is the McCoy Creek Group. The assemblage consists of well-bedded, resistant feldspathic quartzite and subordinate slate and argillite more than 9,000 ft thick in the Schell Creek Range (Plate 1) and about 7,600 ft thick in the Deep Creek Range, Utah. The metamorphic grade of these units is low to moderate, locally producing schist. The unit is mapped in the Deep Creek Range with the underlying Trout Creek Group, also of Neoproterozoic age and similar in appearance. The Trout Creek Group is estimated at 11,600 ft thick (Hintze and Kowallis, 2009) and of higher metamorphic grade. Link et al. (1993) concluded that both of these sequences range in age from 780 to 560 Ma and that the upper part of the McCoy Creek Group may be correlative with the Johnnie Formation of southern Nevada, which is as much as 4,000 ft thick. In Lincoln County and at least in parts of White Pine County, the basal units of the overlying Prospect Mountain Quartzite are considered to be partly Neoproterozoic. The McCoy Creek and Trout Creek units are mapped in the geologic study area as Precambrian rocks (p€).

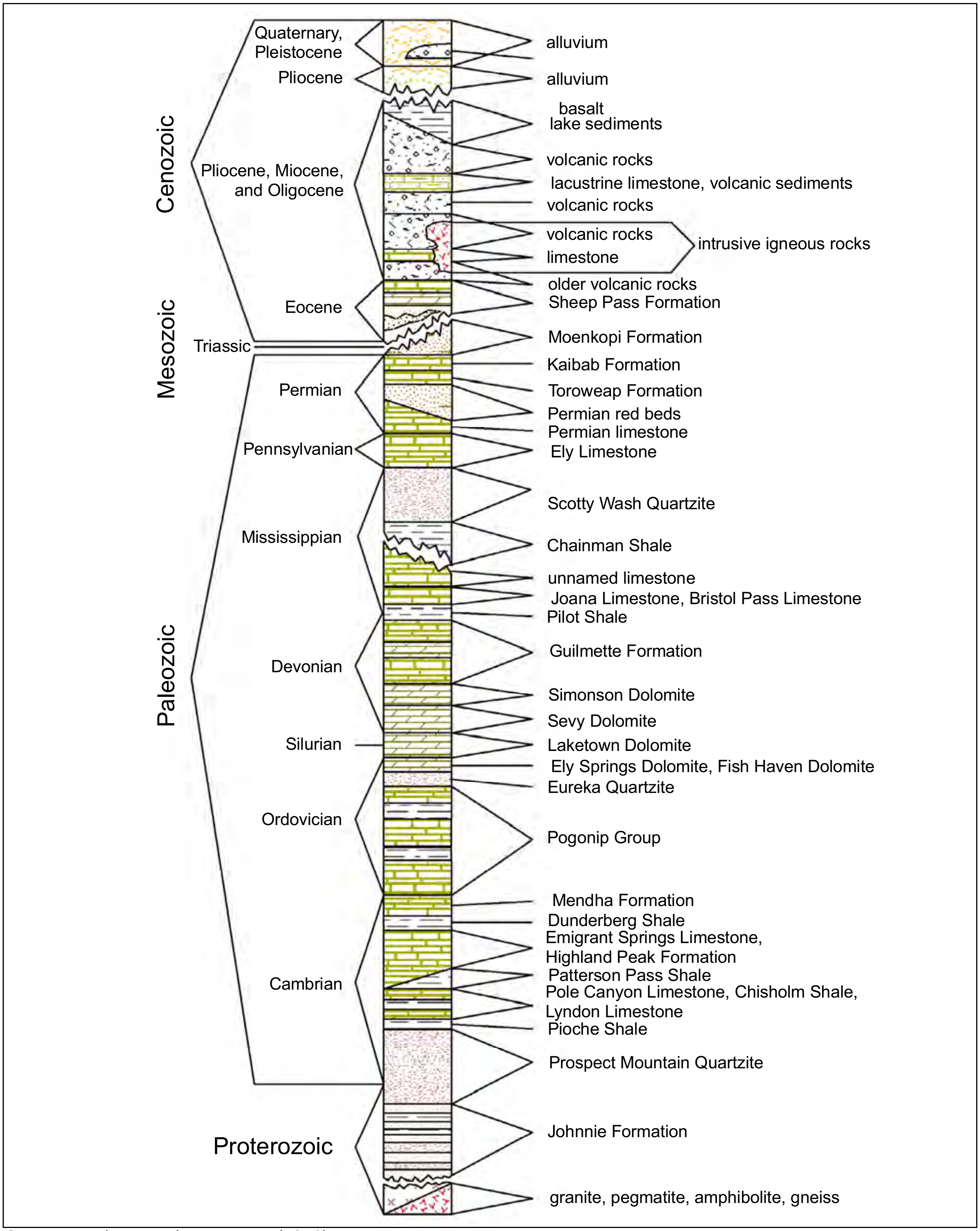

Source: Tschanz and Pampeyan (1970)

Figure 4-2
Geologic Units of Lincoln County, Nevada

SE ROA 43162

JA_13042

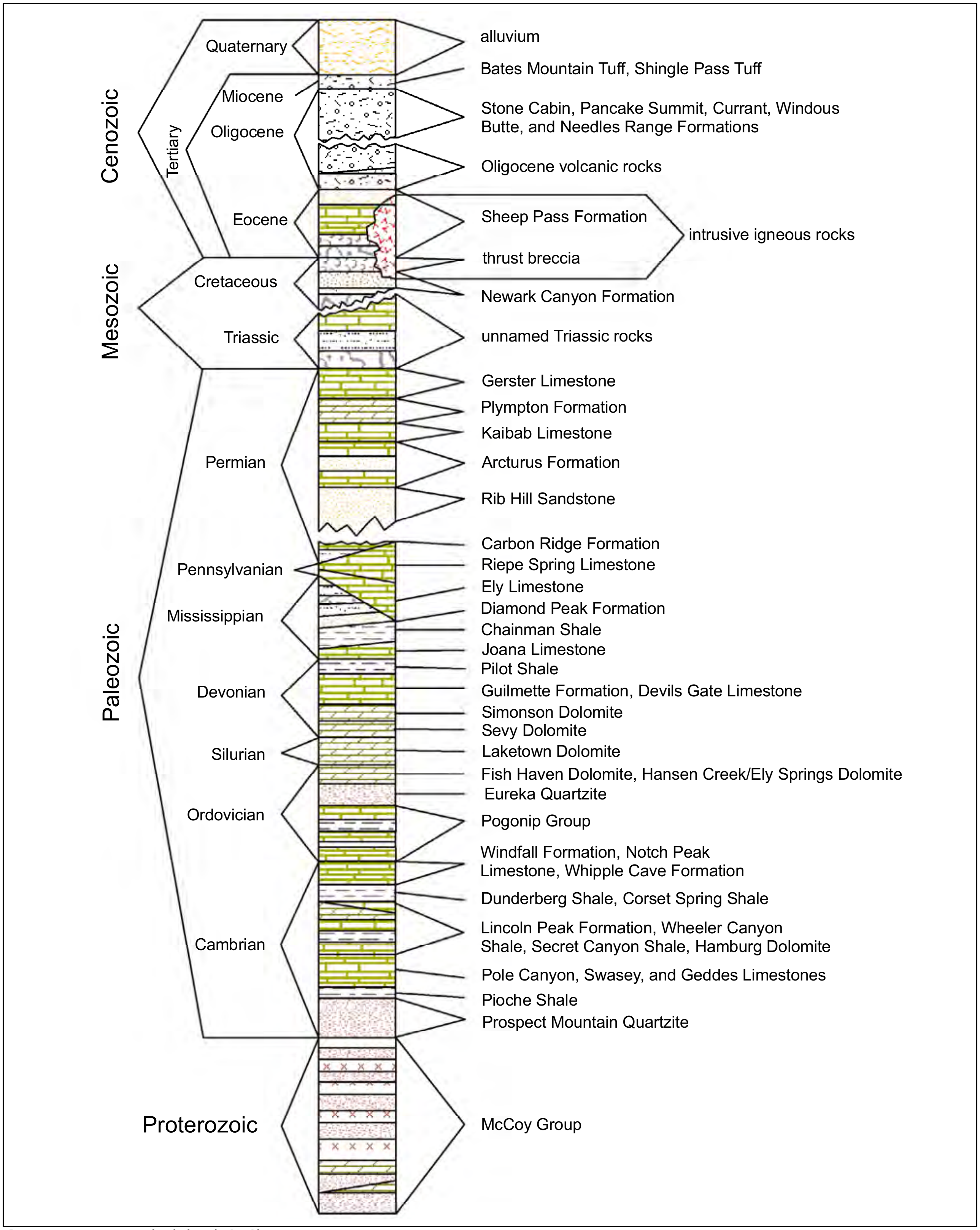

Source: Hose and Blake (1976)

Figure 4-3
Geologic Units of White Pine County, Nevada

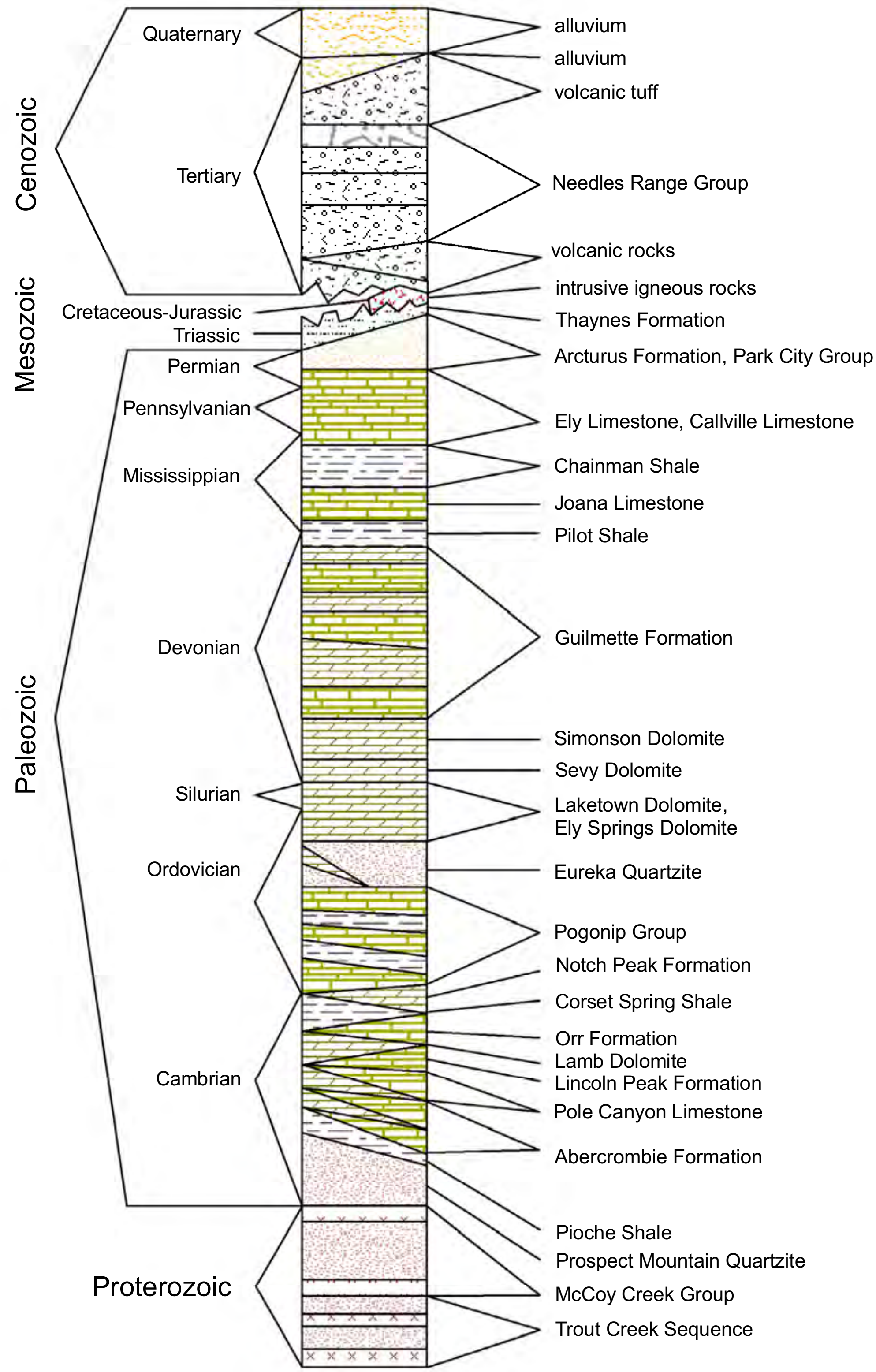

Source: after Hintze and Kowallis (2009, Charts 45 and 46)

Figure 4-4
Geologic Units of Western Utah

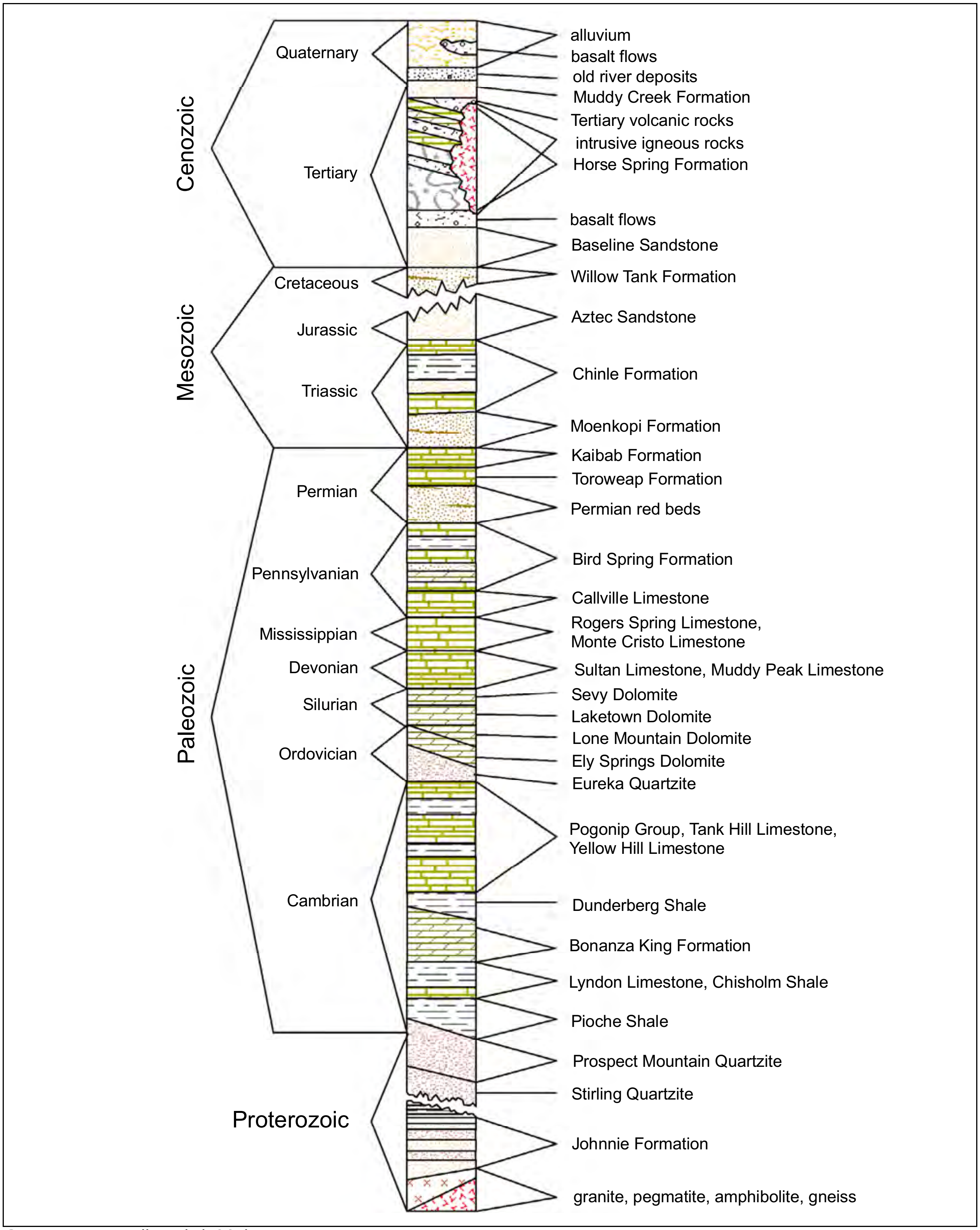

Source: Longwell et al. (1965)

Figure 4-5
Geologic Units of Clark County, Nevada

4.1.3 Paleozoic Rocks

4.1.3.1 Cambrian Rocks

The Prospect Mountain Quartzite (Cambrian to Precambrian sedimentary rocks, Єp€s) overlies the McCoy Creek Group in White Pine County. The Prospect Mountain consists of well-bedded, resistant quartzite and subordinate shale, commonly weakly metamorphosed. It has been generally considered to be Early Cambrian, although it is not well characterized by age or correlation from place to place, and at least in the southern part of the geologic study area is partly Neoproterozoic. In the study area, complete sections are uncommon, but the unit ranges from 3,000 to nearly 8,000 ft thick (Tschanz and Pampeyan, 1970). Thickness decreases southward to just a few hundred feet in the Mormon Mountains. The Prospect Mountain Quartzite in the southern half of the geologic study area is correlated with three units mapped in and west of the southern part of the geologic study area: the Stirling Quartzite (Neoproterozoic and Early Cambrian), the Wood Canyon Formation (Early Cambrian), and the Zabriskie Quartzite (Early Cambrian) (Stewart, 1970, 1974, and 1984; Rowley et al., 1994).

In the southern part of the geologic study area, the Stirling Quartzite is at least 2,000 ft thick and the base is not exposed. Link et al. (1993) considered the Stirling Quartzite to postdate the Neoproterozoic McCoy Creek Group. In the Desert Range and above the Gass Peak thrust in the Las Vegas Range, the Wood Canyon Formation, a quartzite, is 1,000 to 3,000 ft thick.

Above the Prospect Mountain Quartzite are, from base to top, the Pioche Shale (Lower and Middle Cambrian, 200 to 1,000 ft thick), Lyndon Limestone (Middle Cambrian, 150 to 400 ft thick), and Chisholm Shale (Middle Cambrian, 100 to 300 ft thick). These three units are combined in many places with the Prospect Mountain Quartzite, as Єp€s in White Pine County. These rocks are partly correlative with the Carrara Formation at the NTS and in portions of Clark County.

Cambrian carbonate rocks range in thickness from almost 5,000 ft over most of the geologic study area to about 7,500 ft just southwest of the study area. The map unit is mostly middle Cambrian labeled Єm. In the southern half of the geologic study area, the most widespread and best studied of the Cambrian carbonate rocks is the Highland Peak Formation, consisting of Middle and Late Cambrian, well-bedded limestone and dolomite about 4,500 ft thick (Tschanz and Pampeyan, 1970). To the west, in the Groom mining district, it is 5,400 ft thick.

In the northern part of the geologic study area, the Cambrian carbonate rocks consist of many named units of generally similar lithology, total thickness, and age (Hose and Blake, 1976). Just to the northwest, in the Eureka area, these were originally named, from base to top, the Eldorado Dolomite, the Geddes Limestone, the Secret Canyon Shale, and the Hamburg Dolomite (Roberts et al., 1967). In the Snake Range, these are, from base to top, the Pole Canyon Limestone, the Lincoln Peak Formation, and the Johns Wash Limestone. These latter names are now preferred in the northwestern part of the geologic study area and areas to the west. In the Cherry Creek Mountains and extending into western Utah, the units making up the entire sequence of Middle Cambrian carbonate rocks are, from base to top, the Dome Formation, Swasey Limestone, Wheeler Shale, Marjum Limestone, Weeks Limestone, Trippe Limestone, Wah Wah Summit Formation, Orr Formation, and others (Hose and Blake, 1976; Hintze and Davis, 2003). The overall Middle Cambrian carbonate sequence is roughly equivalent to the Bonanza King Formation to the south (Longwell et al., 1965). See Figures 4-2 to 4-5 for geologic sections in different areas of the map.

Above the Middle Cambrian carbonate section in Nevada is an Upper Cambrian to Lower Ordovician(?) sequence that includes a lower unit, the Dunderberg Shale, and an unnamed upper unit of limestone and dolomite (Tschanz and Pampeyan, 1970). The rocks are mapped as an upper part of the Cambrian section (Ꞓu); in some cross sections, the map unit is combined with Ꞓm as Cambrian carbonate rocks, undivided (Ꞓc). In White Pine County and in Utah, the Ꞓu limestone unit has been variously referred to as the Windfall Formation, Orr Formation, Notch Peak Limestone, and Whipple Cave Formation. In the southern part of the geologic study area, the Ꞓu limestone unit is the Nopah Limestone. See Figures 4-2 to 4-5 for geologic sections. The Dunderberg Shale generally is about 300 ft thick over most of the geologic study area, but it is as much as 1,400 ft thick in the southern Ruby Mountains (Hose and Blake, 1976). The overlying limestone ranges in thickness from 400 to 4,000 ft, generally being thickest on the western side of the geologic study area (Tschanz and Pampeyan, 1970).

4.1.3.2 Ordovician to Devonian Rocks

The Ordovician to Silurian parts of the rock column in the geologic study area are shown as a lower unit (Middle and Lower Ordovician, symbol Ol) and an upper unit (Silurian and Upper Ordovician, symbol SOu). The lower unit in the area consists in ascending order of the Pogonip Group and the Eureka Quartzite. The Pogonip Group consists of interbedded thick-bedded limestone, sandy to silty limestone, conglomerate, and shale, generally about 2,000 to 3,500 ft thick in the geologic study area. The Eureka Quartzite is a distinctive white, resistant, brittle, vitreous, fine- to medium-grained quartzite that thins southward from 600 to 800 ft thick in the Confusion Range to 200 ft in southern Lincoln County (Hose and Blake, 1976; Tschanz and Pampeyan, 1970). The Eureka Quartzite is a major marker bed throughout most of the geologic study area (Plates 1 and 2). Just northwest of the geologic study area, the lower unit includes the Vinini and Valmy formations.

The upper unit (SOu) generally consists in ascending order of the Hansen Creek Formation, Ely Springs Dolomite, Fish Haven Dolomite, and Laketown Dolomite. The Ely Springs Dolomite is mostly a poorly resistant, gray to dark-gray carbonate unit that occurs over most of the area of Plate 1 in Lincoln County (Tschanz and Pampeyan, 1970). The Ely Springs Dolomite in Lincoln County overlaps into northern Nye and Eureka counties, where it is locally called the Hansen Creek Formation, a dark dolomite and/or limestone unit that thins southward from 500 to 100 ft (Tschanz and Pampeyan, 1970; Kleinhampl and Ziony, 1985). In White Pine County, the Ely Springs Dolomite is called the Fish Haven Dolomite and ranges between 200 and 850 ft thick. The Silurian Laketown Dolomite is lithologically similar to the Ely Springs Dolomite and Fish Haven Dolomite and ranges between 600 and 1,850 ft thick.

In Eureka and Nye counties, the Laketown Dolomite is underlain by, and partly equivalent in age to, the Lone Mountain Formation, a unit with reef limestone and dolomite that is not present farther east in Lincoln and White Pine counties (Kleinhampl and Ziony, 1985). In Nye County, these units, particularly the Lone Mountain Formation, overlie and interfinger with the Roberts Mountain Formation. The Roberts Mountain Formation is a western facies of deep-water sediments and is comprised of shaly limestone, dolomite, and shale with a thickness of 500 to 1,900 ft (Kleinhampl and Ziony, 1985). See Figures 4-2 to 4-5 for geologic sections in different areas of the map.

Devonian carbonate rocks over most of the geologic study area have been mapped as, in ascending order, the Sevy Dolomite, Simonson Dolomite, and Guilmette Formation, all of which formed on a shallow-water marine carbonate platform. Where combined, they are mapped as Devonian rocks, undivided (Du) or, when local Silurian rocks are included, as Devonian and Silurian sedimentary rocks, undivided (DS). In the southern part of the geologic study area, this map unit includes the Muddy Peak Limestone (Upper and Middle[?] Devonian). In most places, however, the three formations are mapped as the Sevy and Simonson Dolomites (Ds) and Guilmette Formation (Dg). Sandberg et al. (1997) redefined the upper part of the Simonson Dolomite in Nevada, or the lower part of the Guilmette Formation in Utah (Hintze and Kowallis, 2009), as the Fox Mountain Formation. The Sevy Dolomite is a resistant, gray dolomite, commonly argillaceous and with a sandstone unit near the top. This dolomite increases in thickness southward across the geologic study area from about 450 ft in the Snake Range to 1,300 ft in the Limestone Hills and southward (Tschanz and Pampeyan, 1970). This thickness decreases south of the Pahranagat Range, and the unit disappears south of the Delamar Mountains. The Simonson Dolomite is resistant, dark- and light-gray dolomite about 900 to 1,200 ft thick over most of the geologic study area, but it thins to less than 700 ft in the southeastern part of the map area, continuing to decrease in thickness farther south. The Simonson Dolomite is about 500 ft thick in the Snake Range (Tschanz and Pampeyan, 1970), although both the Simonson and Sevy dolomites were locally reduced in thickness by faulting. The Fox Mountain Formation consists of thin (generally 100 to 150 ft), gray limestone except for dolomite in its upper part.

The Guilmette Formation (Dg) is a mostly resistant, fossiliferous limestone and dolomite, with biostromes and bioherms, and commonly sandy with minor sandstone layers. The unit ranges in thickness from about 1,050 to 3,500 ft and appears to decrease in thickness in all directions from its thickest occurrences in north-central Lincoln County (Tschanz and Pampeyan, 1970; Hose and Blake, 1976). The middle part of the Guilmette Formation consists of the Alamo Breccia Member, which is as thick as 300 ft northwest of Alamo, Nevada. It was formed by the cataclysmic Alamo bolide impact event (Warme et al., 2008). In Clark County, the Guilmette map unit includes the Sultan Limestone, which is made up of a lower dolomite unit and an upper limestone unit with a thickness of 1,800 ft (Longwell et al., 1965). The Sultan Limestone is equivalent to the Muddy Peak Limestone in the Muddy Mountains.

In Eureka County and northern Nye County, the rocks of the Sevy, Simonson, and lower Guilmette units are called the Nevada Formation (Dn), which is about 2,500 ft thick. This map unit locally includes the Cockalorum Wash Formation. In Eureka and northern Nye counties, the upper Guilmette Formation is called the Devils Gate Limestone (Dd), which is about 2,000 ft thick (Roberts et al., 1967; Hose and Blake, 1976; Kleinhampl and Ziony, 1985).

4.1.3.3 Mississippian to Lower Permian Rocks

In White Pine County, a distinctive sequence of clastic rocks consists, in ascending order, of the Pilot Shale, Joana Limestone, Chainman Shale (Mc), and Diamond Peak Formation (Md). In Lincoln County, only the Pilot Shale is recognized (Tschanz and Pampeyan, 1970). These map units represent products of the Antler deformation, which took place in Late Devonian to Late Mississippian time and resulted in the Antler Highland located along the western side and northwest of the geologic study area. The basin of deposition of these units was to the east of the highland (Poole and Sandberg, 1977 and 1991; Larson and Langenheim, 1979, Figures 7 and 8). Where these four units are thin, they are categorized on the map as Mississippian to Devonian rocks (MDd). But in most places, Chainman Shale and Diamond Peak Formation are mapped separately and Pilot Shale and Joana Limestone are combined as unit MD. The Pilot Shale, Late Devonian to Early Mississippian, is mostly a poorly resistant, gray, thin-bedded dolomitic siltstone and limestone containing little shale. This unit is generally from 100 to 400 ft thick, but locally, in northern White Pine County and western Utah, it is 500 to 900 ft thick (Hose and Blake, 1976; Tschanz and Pampeyan, 1970; Hintze and Davis, 2002a and b). The Joana Limestone (Lower Mississippian) is a mostly resistant, bluish-gray limestone about 100 to 1,000 ft thick.

The Monte Cristo Group of southern Nevada, which is Upper and Lower Mississippian, is considered equivalent to the Joana Limestone. The Monte Cristo Group overlies the Sultan Limestone. The Monte Cristo is a dark-gray to light-gray limestone containing abundant chert and is about 750 ft thick. In the Muddy Mountains, the Mississippian Rogers Spring Limestone has a similar lithology and is considered to be equivalent in age to the Monte Cristo (Longwell et al., 1965). The general equivalent of the Chainman Shale southwest of the geologic study area is the Eleana Formation (Mississippian and Upper Devonian), which is several thousand feet thick (Workman et al., 2002a). The Monte Cristo, Rogers Spring, and Eleana are included with the MD map unit. The map unit also includes local units Mercury Limestone and Bristol Pass Limestone (both mostly in White Pine County), Webb Formation (Elko County), Ochre Mountain Limestone (Utah), and West Range Limestone (Upper Devonian) in northern Lincoln County, Nevada.

The Upper Mississippian Chainman Shale is a soft, black, impermeable shale that is between 200 and 2,000 ft thick. This unit is mapped as unit Mc over the northern part of the geologic study area, but the Chainman is thin in the southern part of the geologic study area and here is included within a sequence of more permeable carbonate rocks. It is a regional confining unit (called the "upper aquitard") separating the lower carbonate aquifer from the upper carbonate aquifer over all except the southern part of the geologic study area. Paleotopography during deposition and post-depositional erosion resulted in substantial variations in Chainman thickness. The unit was mapped (Hintze and Davis, 2002a) in the Confusion Range as having thicknesses greater than 2,000 ft. A similar thickness is reported from an oil-well log in Lake Valley (Hess, 2004). Although these two locations are distal from the source area, they represent localized depositional basins.

In the northwestern part of the geologic study area, the Upper Mississippian Diamond Peak Formation is mapped as unit Md above the Chainman Shale. The Diamond Peak Formation is a poorly resistant, gray siltstone, claystone, sandstone, and conglomerate that ranges in thickness from 600 to 2,500 ft (Hose and Blake, 1976; Kleinhampl and Ziony, 1985). The unit thins and pinches out eastward in north-central White Pine County. The Diamond Peak Formation is derived from erosion of the Antler Highland and generally included in the upper aquitard with Chainman. The Diamond Peak is generally equivalent to the Scotty Wash Quartzite in the southern part of the geologic study area. The Scotty Wash Quartzite is made up of interbedded sandstone, shale, and local limestone of limited extent. The Scotty Wash is included with the Md map unit.

Much of the geologic study area is underlain by the Ely Limestone, which is mostly Pennsylvanian but includes Mississippian rocks at its base and Permian rocks at its top. The Ely Limestone is mapped as Pennsylvanian rocks (ℙ). In the Utah part of the geologic study area, the Ely Limestone is 1,850 to 2,000 ft thick (Hintze and Davis, 2002a and b). The map unit is called the Wildcat Peak Formation in the northwestern part of the geologic study area and the Callville Limestone in the southern and eastern part of the geologic study area. The Ely Limestone is overlain by a Lower Permian limestone of similar lithology in northern White Pine County (Hose and Blake, 1976). All units are resistant, gray limestone sequences that collectively range in thickness from 1,900 to 3,000 ft thick. The overlying Lower Permian limestone is called the Riepe Spring Limestone. Where both Ely and Riepe Spring are mapped together in the northern part of the geologic study area, they are shown as Permian and Pennsylvanian rocks, undivided (Pℙ). The rocks in the Pℙ unit are unnamed in Lincoln County and range from 3,500 to more than 5,000 ft thick (Tschanz and Pampeyan, 1970). The Ely and Riepe Spring Limestones are overlain by, and partly equivalent to, the Carbon Ridge Formation, a Lower Permian, nonresistant, thin-bedded limestone and shale that is 1,400 to 2,300 ft thick. The Carbon Ridge is locally mapped separately in the northwestern part of the geologic study area as Pc, or where thinner is included within the Pℙ map unit.

The Bird Spring Formation is an Upper Mississippian to Lower Permian limestone in the southern part of the geologic study area that is roughly equivalent in age to the combined Ely Limestone, Riepe Spring Limestone, and Carbon Ridge Formation of White Pine County (Longwell et al., 1965; Tschanz and Pampeyan, 1970). The Bird Spring is a sequence of limestone beds with sandstone and dolomitic limestone layers. The formation is as much as 8,000 ft thick in the Spring Mountains and Las Vegas Range (Page et al., 2005b) and at least 5,400 ft thick in the Meadow Valley Mountains (Pampeyan, 1993). The Bird Spring is included in the Pℙ map unit, as is the Brock Canyon Formation in the northwestern part of the geologic study area and the Oquirrh Group (Lower Permian and Pennsylvanian) in the northeastern part of the geologic study area.

The Lower Permian Rib Hill Sandstone (Pr) overlies the Carbon Ridge Formation in the northwestern part of the geologic study area (Hose and Blake, 1976). The Rib Hill is a nonresistant sandstone and dolomite 500 to 1,400 ft thick. In northern White Pine County and adjacent parts of Utah, the Lower Permian Arcturus Formation (Pa) is the name for a sequence of poorly resistant, gray limestone, sandstone, and siltstone that is 2,700 to 3,400 ft thick (Hose and Blake, 1976). In the northwestern part of the geologic study area, the Arcturus Formation overlies the Rib Hill Sandstone. Where the two are combined in the mapping, they are shown as unit Par. In Elko County, this map unit includes the Pequop Formation. In the southern part of the geologic study area, the Par map unit includes a redbed sequence, and in the southeastern part of the map, the map unit includes the Queantoweap Sandstone.

4.1.3.4 Park City Group

The Park City Group (Pp) is a distinctive, resistant, light-gray Lower Permian limestone and dolomite sequence that is exposed only locally. The scattered nature of the outcrops suggests that the unit was originally fairly extensive in the geologic study area but has been partly removed by erosion over most of its original extent. In White Pine County and adjacent western Utah, the group is made up, from base to top, of the Kaibab Limestone, Plympton Formation, and Gerster Limestone. The Kaibab

Limestone is 50 to 600 ft thick, the Plympton is 700 to 900 ft thick, and the Gerster is as thick as 1,100 ft (Hose and Blake, 1976). These rocks are not found in Eureka or Nye counties.

In Lincoln County and east of the geologic study area in Utah, the east platform part of the sequence consists of the Toroweap Formation, the Kaibab Limestone, and locally the Plympton Formation (Tschanz and Pampeyan, 1970). In Lincoln County, these units have a combined thickness of between 250 and 450 ft. The Toroweap is a cherty, thin-bedded, shaly limestone, and the Kaibab limestone is a cherty, sandy, light-gray limestone. The Kaibab Limestone and Toroweap Formation in Clark County have a maximum combined thickness of 1,300 ft in the Muddy Mountains (Bohannon, 1983). In Clark County, their lithology is dominated by cherty limestone, sandstone, and red shale, with local gypsum beds (Bohannon, 1983; Page et al., 2005b).

4.1.4 Mesozoic Rocks

Mesozoic rocks were deposited locally or have been largely removed by erosion in the geologic study area. However, they are exposed in some ranges and are widespread east and south of the map area. Most of these rocks are continental clastic rocks deposited in fluvial, lacustrine, eolian, and marginal marine environments. The Thaynes Formation (Lower Triassic) is a soft, gray, thin-bedded claystone and limestone that is locally about 1,900 ft thick in western Utah in the northeastern part of the geologic study area (Hintze and Davis, 2002a). The overlying Moenkopi Formation (Lower Triassic) is a mostly soft, red and gray, thin-bedded siltstone, limestone, sandstone, and shale, commonly gypsiferous, and locally about 2,000 ft thick in western Utah. The Thaynes and Moenkopi Formations are thin in the Nevada portion of Plate 1 and are not separated on this map. In Clark County, however, the Moenkopi Formation is about 2,000 ft thick and of similar lithology, with gypsum beds in the upper part of the formation (Page et al., 2005b).

The Upper Triassic Chinle Formation includes a basal unit, the Shinarump Conglomerate Member, which is a resistant gray sandstone and conglomerate that ranges from 10 to 250 ft thick. The balance of the formation is of soft, variegated mudstone and siltstone that is widely exposed above the Moenkopi in the southern part of the geologic study area (Bohannon, 1983; Page et al., 2005b). This mudstone and siltstone have been measured to be about 1,000 to 3,300 ft thick within the geologic study area. The Luning Formation (Upper Triassic) is locally exposed northwest of the area. All Triassic rocks in the geologic study area have been combined as Triassic sedimentary rocks (Ꞧs).

Jurassic sedimentary rocks (Js) are exposed in the southern part of the geologic study area. These rocks are dominated by the Lower Jurassic Aztec Sandstone, a brick-red, buff, and light-gray, fine- to medium-grained eolian sandstone containing large-scale cross beds. The Aztec is 600 to 3,600 ft thick. The equivalent Navajo Sandstone is about 2,000 ft thick in the southeastern part of the geologic study area. It is here underlain by the Moenave (lower) and Kayenta (upper) Formations, both of Early Jurassic age and mostly made up of fine-grained sandstone and siltstone of eolian and fluvial origin, with a combined thickness of 500 to 3,000 ft. The Navajo is here overlain by the Temple Cap (lower) and Carmel (upper) Formations, both of Middle Jurassic age and made up of sandstone, limestone, siltstone, and shale of mostly marginal marine origin and with a combined thickness of about 900 ft. The map unit also includes the Dunlap Formation (Lower Jurassic) in the northwestern part of the geologic study area.

Cretaceous synorogenic sedimentary rocks (Ks) are present but uncommon in the geologic study area. Most of this area was a highland undergoing erosion at that time. The Lower Cretaceous Newark Canyon Formation is exposed in the northwestern part of the geologic study area as a poorly exposed, reddish-brown to gray, fresh-water limestone, siltstone, conglomerate, and sandstone from 1,400 to 1,800 ft thick (Hose and Blake, 1976). Upper Cretaceous sedimentary rocks, shed east from erosion of Sevier highlands in and north of the geologic study area, are thin and patchy in the map area but extensive and thick east and south of the area. Upper Cretaceous through Paleocene fault breccias, primarily from thrust faults related to Sevier deformation, are locally exposed in the geologic study area.

In Clark County, Cretaceous sedimentary units include from older to younger the Willow Tank Formation (Lower Cretaceous) and the Baseline Sandstone. The Willow Tank Formation is 300 to 450 ft thick and consists of a basal conglomerate and overlying fine-grained sediments, including bentonitic clay, and is primarily restricted to the Muddy Mountains. The Baseline Sandstone consists of about 3,000 to 5,000 ft of gray and red, well-bedded sandstone and conglomerate. In the southeastern (Utah) part of the geologic study area, the Upper Cretaceous Cedar Mountain Formation and overlying Iron Springs Formation consist of mudstone, shale, sandstone, and conglomerate about 3,000 ft thick.

Plutonic rocks related to the Middle Jurassic through Paleocene Sevier deformational event are exposed locally throughout the geologic study area (Maldonado et al., 1988). Of these, much of the southern Snake Range is intruded by a Middle and Upper Jurassic batholith (Miller et al., 1999) and Jurassic quartz monzonite and diabase that have been identified in the House Range and in the Burbank Hills, respectively, both in Utah near the eastern edge of the geologic study area (Hintze and Davis, 2002a and b, and 2003). Other plutons of quartz monzonite to granodiorite, mostly of Middle Jurassic age, form a north-trending belt along the eastern edge of White Pine County, Nevada, extending from the southern Snake Range to the Clifton Hills of western Utah. A north-trending plutonic belt of Cretaceous age is exposed in eastern White Pine County, Nevada, extending into the Deep Creek Range of western Utah and including the main mass of the large Kern Mountains granite batholith of apparent Cretaceous and Eocene age (Best et al., 1974; Miller et al., 1999). On the geologic maps, these plutonic rocks are shown as Jurassic (Ji), Cretaceous (Ki), Tertiary to Cretaceous (TKi), or Tertiary (Ti) intrusive rocks. Geophysics shows that the batholith extends eastward, downthrown beneath Snake Valley and buried by basin-fill sediments (Mankinen and McKee, 2009). An east-trending string of small Lower Cretaceous plutons extends from Eureka through Ely, Nevada.

4.1.5 Cenozoic Rocks

Cenozoic rocks in the geologic study area belong to three main sequences: (1) locally exposed, mostly thin, older continental sedimentary rocks; (2) generally voluminous, calc-alkaline volcanic rocks and their source plutons; and (3) rocks that formed during regional basin-range extension, namely thin bimodal-composition (basalt and high-silica rhyolite) lava flows and locally thick basin-fill sediments. On the geologic maps, most of these rocks are separated into several rock types based on age, following the mapping strategy of Ekren et al. (1977). The basalts and basin-fill sedimentary rocks, including surficial sediments, of the youngest of the three main sequences, however, are mapped respectively as Quaternary to late Tertiary basaltic rocks (QTb) and Quaternary to late Tertiary alluvium (QTa).

4.1.5.1 Latest Cretaceous to Miocene Sedimentary Rocks

The oldest Cenozoic sedimentary rocks (Ts1) are thin and poorly exposed in the geologic study area but are more common in eastern Clark County and southwestern Utah. These units were deposited with, or unconformably deposited on, rocks deposited and deformed during the Sevier orogeny. In eastern Nevada, the principal Ts1 unit is the Sheep Pass Formation of Eocene to Oligocene age (Hose and Blake, 1976; Druschke et al., 2009). The Sheep Pass Formation occupies a basin about 15,000 mi^2 in size over an area extending south from Ely and Eureka, Nevada, to Penoyer and northern Pahranagat valleys (Fouch et al., 1991; Druschke et al., 2009). The unit is mostly nonresistant, gray conglomerate, sandstone, mudstone, and limestone, with a thickness of 600 to 3,000 ft in the geologic study area.

In the southeastern part of the geologic study area, the mostly resistant Grapevine Wash Formation and overlying Claron Formation are included within the Ts1 map unit. The Grapevine Wash Formation, poorly constrained in age as Late Cretaceous to early Tertiary but considered by Hintze et al. (1994) to postdate Sevier deformation, consists of as much as 2,000 ft of gray, tan, and red conglomerate and sandstone. The Claron Formation, also poorly constrained in age but likely of a restricted age ranging between Paleocene and Oligocene, is sandstone, limestone, and conglomerate as much as 2,000 ft thick.

Similar sedimentary rocks (Ts2, Ts3, and Ts4) of various names and ages, from Oligocene to Miocene, are exposed in the geologic study area. These include the Gilmore Gulch Formation of about 30 Ma (Ts2), exposed in the northwestern part of the area. The Horse Spring Formation, about 12 to 20 Ma, and the red sandstone unit, 11 to 12 Ma, that overlies it are mapped as Ts4 in the southern part of the geologic study area (Bohannon, 1983 and 1984). The Horse Spring Formation consists of conglomerate, sandstone, siltstone, claystone, limestone, dolomite, tuff, and gypsum as much as 10,000 ft thick.

4.1.5.2 Tertiary Volcanic Rocks

Volcanic rocks make up the primary Cenozoic rock type in the geologic study area. The older (Eocene to middle Miocene) sequence of calc-alkaline rocks consists of andesite to low-silica rhyolite that are mapped as different units separated by rock type and age. Tertiary plutonic rocks, which are the sources for the volcanic rocks, are mapped as unit Ti whether of calc-alkaline or bimodal origin.

The calc-alkaline sequence is made up largely of regional ash-flow tuff sheets derived from widely scattered calderas. The oldest tuffs are mapped as Tt1 (Eocene and Oligocene) that predate the Needles Range Group (about 32 Ma). The next younger group of tuffs, consisting mostly of the Needles Range Group, is mapped as Tt2 (Oligocene), from about 32 Ma to 27 Ma, the latter the age of the Isom Formation. The next younger tuffs are mapped as Tt3 (Oligocene and Miocene), ranging in age from that of the Shingle Pass Tuff (about 27 Ma) to the youngest calc-alkaline tuffs (about 18 Ma). Individual calderas are filled with thick intracaldera ash-flow tuffs that are at least several thousand feet thick. Their outflow sheets are typically thin, generally less than 1,000 ft, but the aggregate thickness of all of these tuffs is several thousand feet in many places. Isopach (thickness) maps of most tuffs in the study area were given by Sweetkind and duBray (2008).

The outflow tuffs are interspersed with locally distributed but thick central stratovolcano deposits made up of lava flows and volcanic mudflow breccia generally deposited above their source plutons. Where these calc-alkaline flows and breccia are largely andesite, they are mapped as Ta1, Ta2, Ta3, and Ta4 based on ages that correspond to those of the related ash-flow tuffs. Unit Ta4 is made up of andesitic (calc-alkaline) flows of post-18 Ma that are exposed in the southern part of the geologic study area. Where calc-alkaline flows and breccia are largely low-silica rhyolite, they are mapped as Tr1, Tr2, and Tr3 based on ages that correspond to those of the tuffs.

The tectonic environment during calc-alkaline magmatism was generally one of east-west extension in the Great Basin. The direction of principal maximum compressive stress was generally north-south, creating an environment of strike-slip and oblique-slip faults. The orientation and size of mountains during this time are poorly known, but the outpouring of large volumes of volcanic ash-flow tuff probably resulted in a subdued landscape with topographic variations caused by the uneven distribution of these units.

In the Great Basin, vents—notably calderas—for Tertiary calc-alkaline volcanic rocks occur in generally east-west igneous belts that become younger from north to south (Ekren et al., 1976 and 1977; Stewart and Carlson, 1976; Stewart et al., 1977; Rowley, 1998; Rowley and Dixon, 2001). These igneous belts are partly controlled by transverse zones and underlain by batholiths whose cupolas provide the vents for the volcanic rocks. The oldest volcanic rocks in the map area belong to the Ely-Tintic igneous belt (belt names from Rowley [1998]) in the northern part of the geologic study area. The ages of vents in this belt are about 38 Ma and locally older (Eocene) along the northern margin of the area, and 36 Ma farther south (Rowley, 1998). An east-trending gap in vent areas, about 30 to 60 mi wide north-south, occurs south of Ely and Preston, Nevada, and a volcanic plain of thin outflow tuffs underlies the gap. The axis of the next igneous belt to the south, the Pioche-Marysvale igneous belt, is south of Pioche, Nevada. The volcanic centers here are about 32 to 31 Ma on the northern side of the belt and about 28 to 27 Ma along the southern part. About 12 mi south of the Pioche-Marysvale belt is the Delamar-Iron Springs igneous belt, of about 24 Ma along its northern side and 16 Ma along its southern side. Its southern edge is just south of the latitude of Pahranagat Valley, Nevada.

In the Ely-Tintic igneous belt, the most voluminous volcanic unit is the Kalamazoo Tuff (35 Ma), an ash-flow tuff sequence deposited over an east-west elongated area 90-mi-long and 25 mi wide. Its caldera source has not been found but Gans et al. (1989) suggested that it may be buried beneath northern Spring Valley, which is near the center of the area of deposition of the Kalamazoo Tuff. Gravity data (Section 5.1.1) gave no support for this hypothesis but hint that it is more plausible that the caldera is buried beneath southern Tippett Valley. Other ash-flow tuffs and lava flows underlie and overlie the Kalamazoo Tuff, and the overall thickness of the volcanic rocks in the igneous belt is about 500 to 1,500 ft. Plutons of a 45 to 30 Ma age range are scattered throughout the belt; most of these represent source areas of volcanic rocks that have since been removed by erosion. One of these plutons (Best et al., 1974) is at the eastern end of the composite-age Kern Mountains pluton. This and other Eocene to Oligocene plutons and batholiths in the northern Snake Range, Kern Mountains, and

Deep Creek Range represent initial calc-alkaline magmatism beneath these ranges (Miller et al., 1999) that later were uplifted during basin-range extension.

In the Pioche-Marysvale belt, volcanic rocks are thicker and more widespread than in the Ely-Tintic belt because calderas are more abundant and larger and the volcanic rocks are somewhat younger and thus less eroded. Most volcanic rocks are regional ash-flow tuffs from calderas, but lava flows and mudflow breccia erupted from volcanoes in and along the margins of calderas or from isolated volcanoes such as the Seaman Range volcanic center. The largest vent area in the belt is the Indian Peak caldera complex (Best et al., 1989a) in the southeastern part of the geologic study area. It erupted ash-flow tuffs and related rocks of the Needles Range Group (Oligocene, about 32 to 28 Ma) and the Isom Formation (27 to 26 Ma). This may be the largest caldera complex in the world; ash-flow tuffs from this complex are spread over an area of about 200 mi east-west by 150 mi north-south.

Intracaldera megbreccia deposits result from landsliding of the outside wall of a caldera margin into a caldera following rapid eruption of huge ash-flow tuff sheets and the collapse of the caldera floor to fill the erupted parts of the underlying magma chamber. These megabreccia deposits (Tmb) are mapped only in the Indian Peak caldera complex on the geologic map (Plate 1) and cross section Q—Q' (Plate 4), but on the hydrogeologic map (Plate 6) and cross sections (Plate 8) these rocks are included within the Tertiary volcanic rocks (Tv). Megabreccia deposits (Tmb) are also mapped in and west of the southern Sheep Range on the geologic map (Plate 2) and cross section H—H' (Plate 5), and these deposits do not include significant volcanic rocks, but instead result from large gravity slides off the Sheep Range. On the hydrogeologic map (Plate 7) they are mapped with Tertiary older sediments (Tos), but on hydrogeologic cross section H—H' (Plate 9) they are too thin to be shown so are included in surficial deposits (QTs).

A cluster of smaller calderas west of the Indian Peak caldera complex also belongs to the Pioche-Marysvale igneous belt. These calderas produced, from oldest to youngest and generally from north to south, regional ash-flow tuffs known as the Stone Cabin Formation (35.3 Ma), Pancake Summit Tuff (34.8 Ma), Windous Butte Formation (31.3 Ma), tuff of Hot Creek Canyon (29.7 Ma), Monotony Tuff (27.3 Ma), tuff of Orange Lichen Creek (26.8 Ma), Shingle Pass Tuff (26.7 to 26 Ma), tuff of Lunar Cuesta (25.4 Ma), tuff of Goblin Knobs (25.4 Ma), tuff of Big Ten Peak (25 Ma), Pahranagat Tuff (22.6 Ma), and Fraction Tuff (18.3 Ma) (Best et al., 1989b and 1993). Most of this cluster of calderas was referred to as the “central Nevada caldera complex” (Best et al., 1993; Scott et al., 1995). However, the feature is not a classic caldera complex because all of it has not subsided following tuff eruptions but, instead, individual calderas (subsided areas) are locally separated by pre-caldera Phanerozoic sedimentary rocks that are currently exposed outside the margins of individual calderas. Within calderas in the geologic study area, intracaldera ash-flow tuffs and subordinate lava flows and mudflow breccia are several thousand feet thick and are underlain by intracaldera source plutons. Outside the calderas, the thickness of volcanic rocks in the belt in the area is about 1,500 to 3,000 ft, but locally more. A few plutons of the same age range, likely representing sources for volcanic rocks that have been removed by erosion, occur in the Grant Range and many other parts of the geologic study area.

In the Delamar-Iron Springs igneous belt, at the southern edge of the geologic study area, the largest igneous centers are the Caliente and Kane Springs Wash caldera complexes. The Caliente caldera

SE ROA 43175

JA_13055

complex erupted ash-flow tuffs that spread over an area about 150 mi east-west by 100 mi north-south. It had an unusually long history of activity, at least 10 Ma. The regional ash-flow tuffs derived from it include the Swett (23.7 Ma) and Bauers (22.8 Ma) Tuff Members of the Condor Canyon Formation, Racer Canyon Tuff (18.7 Ma), Hiko Tuff (18.3 Ma), tuff of Tepee Rocks (17.8 Ma), tuff of Dow Mountain (17.4 Ma), tuff of Acklin Canyon (17.1 Ma), tuff of Rainbow Canyon (15.6 Ma), Ox Valley Tuff (13.5 Ma), and probably the Leach Canyon Formation (23.8 Ma) (Rowley et al., 1995; Scott and Swadley, 1995; Snee and Rowley, 2000). The Kane Springs Wash caldera complex, just to the south, erupted the tuff of Narrow Canyon (15.8 Ma), tuff of Boulder Canyon (15.1 Ma), and Kane Wash Tuff (14.7 to 14.4 Ma) (Scott et al., 1995 and 1996; Scott and Swadley, 1995). The total thickness of volcanic rocks in the igneous belt generally does not exceed 1,000 ft outside the caldera complexes.

The younger (middle Miocene to Quaternary) bimodal sequence, which postdates the calc-alkaline sequence, is made up of small basalt lava flows and cinder cones as well as small high-silica rhyolite volcanic domes, lava flows, ash-flow tuffs, and airfall tuffs. The basalts are categorized on the geologic map as unit QTb, rhyolite domes and flows as Tr4, and tuffs as Tt4. All the volcanic rocks derived from the Kane Springs Wash caldera complex, and those that postdate the tuff of Tepee Rocks from the Caliente caldera complex, are included within the bimodal assemblage. The tectonic environment during bimodal magmatism was east-west extension, with the direction of principal maximum compressive stress generally oriented vertically, creating an environment of north-south normal faults. Bimodal magmatism coincided with basin-range deformation, in which the present topography was created and previous tectonic features and topography were deformed and obscured.

4.1.5.3 Miocene to Holocene Sediments

With the start of basin-range deformation at about 20 Ma, north-striking normal faults created the present ranges and basins. Erosion of the ranges, as they were faulted up, resulted in basin-fill sediments that accumulated to thicknesses of locally more than 10,000 ft in down-faulted basins. In most places, the basin-fill sediments are unnamed. These units are referred to as middle Miocene alluvium Holocene (QTa) and are considered to be aquifers, especially where fractured by faulting.

The bimodal volcanic rocks that were deposited at the same time were either high-silica rhyolite lava flows and tuffs or basalt lava flows and tuffs. Their distribution in the geologic study area is spotty and their thickness is rarely more than several hundred feet, except for their source volcanic domes or cinder cones. Where thin, they may be combined in the cross sections with the older, much thicker calc-alkaline volcanic rocks or with thick interbedded basin-fill sediments.

The basin-fill sediments (QTa) were largely deposited by streams in closed basins. In general, coarse-grained materials accumulated around the edges of the mountain fronts, whereas finer materials accumulated toward the center of the basins. In some basin interiors, fine-grained sediments accumulated in ephemeral playa lakes. The largest lakes were pluvial lakes of Pleistocene age, including the latest Pleistocene Bonneville and Lahontan lakes that had water depths of as much as 1,000 ft, resulting in deposition of clay and saline sediments in many basins (Mifflin and Wheat, 1979; Currey, 1982; Currey et al., 1984). These lakes, however, were short lived and produced fine-grained materials that rarely exceeded a few tens of feet in thickness. Quaternary basin-fill deposits are mostly thin (several hundred feet) and overlie Pliocene and upper Miocene basin-fill sediments that may be thousands of feet thick, depending on the throw of the basin-range faults that produced the basins. Data from boreholes in Snake Valley indicate several hundred feet of Tertiary evaporites within the deepest part of the basin.

The concept that extensional basins contain coarse-grained sediments on their margins and fine-grained sediments in their interiors may be valid for periods of time that are geologically short (thousands of years) but is invalid for larger periods (tens of thousands of years) because of the vagaries of the sizes of storms that deposit sediments, of climate changes, of integration of some basins, and of timing of the deformation of basin-bounding versus within-basin faults. In other words, basin margins may become basin centers and vice versa, over 10 Ma. Therefore, in practice, the stratigraphy of basin-fill sediments is characterized by a complex intertonguing of beds of all lithologies. Within-basin faults commonly produced horsts (hills) of soft basin-fill sediments that were then eroded away by streams and redeposited as younger basin-fill sediments. Sweetkind et al. (2007b), in a short chapter on the hydrogeologic setting of the BARCASS area, endorsed the conceptual model of coarse- versus fine-grained deposits depending on distance from basin margins. They proposed two hydrogeologic units for extensional basins: coarse-grained basin-fill deposits (their hydrogeologic unit CYSU) from the margins of closed basins and fine-grained basin-fill deposits (unit FYSU) from the interiors, with the former an aquifer and the latter a confining unit. Mapping experience in the Great Basin, especially revealing where deposits in closed basins have been eroded following drainage integration by a through-flowing stream so that underlying deposits are now visible, shows that no vertical plug of fine-grained sediments is in the interiors of basins as envisioned by Sweetkind et al. (2007b). Plate 1 includes thin surficial deposits in and on the flanks of the ranges, such as stream deposits, landslides, and spring deposits, that are not individually separated in this report or on the maps because of their limited extent.

In some places the basin-fill sediments have local names that were categorized as QTa on the geologic map. One such local unit is the Muddy Creek Formation (Bohannon, 1984) of 5 to 11 Ma in southern Lincoln and Clark counties. The Muddy Creek consists of locally gypsiferous shale, siltstone, and fine-grained sandstone. Another named unit is the Panaca Formation, consisting of about 2- to 10-Ma sandstone, siltstone, shale, and conglomerate, and located in the central part of the geologic study area (Rowley and Shroba, 1991). Other units of similar lithology to the Panaca Formation are the Horse Camp Formation in the northwestern part of the area (Brown and Schmitt, 1991) and the Salt Lake Formation northeast of the area. All these units are generally more than 1,000 ft thick and locally as much as 10,000 ft thick.

4.2 Hydrogeologic Units

HGUs are rock units grouped so that they are more useful for hydrogeologic studies. As given on Plates 6 and 7 and listed in Table 4-1, HGUs are a set of geologic formations that are grouped into aquifers or confining units based on their physical properties. By defining HGUs, the evaluation of groundwater occurrence and movement is facilitated as is the development of conceptual and numerical models of groundwater flow. The geologic units (Plate 3) that make up each HGU are listed below under the discussion of HGUs. This grouping reflects lithologic properties rather than more traditional geologic groups, which are based on genetic sequences.

Table 4-1
Brief Summary of Hydrogeologic Units

QTs	Quaternary and Tertiary sediments - Includes sediments younger than the volcanic section but may include older sediments where volcanic rocks are minor or nonexistent. Also includes playa deposits. Generally moderate permeability but may be high where fractured.
QTb	Quaternary and Tertiary basalt - Quaternary and late Tertiary mafic volcanic rocks. Generally permeable but not hydrologically significant regionally because mostly thin.
Tv	Tertiary volcanic rocks - Miocene to Eocene volcanic rocks. Good to moderate permeability, commonly a significant aquifer.
Tos	Older Tertiary sediments - Primarily created for the cross sections; includes the older Tertiary alluvial and lacustrine section below the volcanic section and megabreccia deposits west of the Sheep Range. Of moderate permeability where fractured.
TJi	Tertiary to Jurassic intrusive rocks - Includes all plutons. Generally impermeable except where fractured.
KŦs	Cretaceous to Triassic siliciclastic rocks - Thicker where near the Colorado Plateau and generally of low permeability. More abundant in the southern part of the geologic study area. A confining unit of limited extent.
Pℙc	Permian and Pennsylvanian carbonate rocks - Includes Ely Limestone, Bird Spring Formation, Park City Group, and other units. May include thin Triassic carbonate rocks in the Butte Mountains. Also includes Permian red beds, undifferentiated. A highly permeable aquifer.
Ms	Mississippian siliciclastic rocks - Includes Chainman Shale, Scotty Wash Quartzite, Diamond Peak Formation, and Eleana Formation. The Chainman Shale and Scotty Wash Quartzite are not differentiated in Lincoln County, except in the Egan and Schell Creek Ranges. Where mapped, is a confining unit of low permeability, but where thin were combined with adjacent aquifer units.
MOc	Mississippian to Ordovician carbonate rocks - Joana Limestone (Monte Cristo Formation) to Pogonip Group, also includes thin Chainman Shale in most of Lincoln and Clark counties. The Pilot Shale, Eureka Quartzite, Guilmette Formation, Simonson Dolomite, Sevy Dolomite, and Laketown Dolomite are also included. A highly permeable aquifer.
Ꞓc	Cambrian carbonate rocks - Includes the Bonanza King, Highland Peak, Lincoln Peak, and Pole Canyon formations. A highly permeable aquifer.
ꞒpꞒs	Cambrian and Precambrian siliciclastic rocks - Includes the Wood Canyon Formation, Prospect Mountain and Stirling quartzites, Chisholm Shale, Lyndon Limestone, and Pioche Shale. Generally impermeable except where fractured.
pꞒm	Precambrian metamorphic rocks - Precambrian X, Y, and Z high-grade metamorphic rocks, generally Paleoproterozoic. It also includes the Johnnie Formation in the south and the McCoy Creek and Trout Creek groups in the Schell Creek, Deep Creek, and Snake ranges. Impermeable except where fractured.

HGUs must be distinguished from hydrostratigraphic units (Maxey, 1964; Seaber, 1992; Donovan, 1996), which are based on the material properties of porosity and permeability. Hydrostratigraphic units are independent of age, formation boundaries, and saturation.

HGUs, as opposed to hydrostratigraphic units, reflect geologic history, conform to informal and formal formation boundaries, and define many of the large-scale differences and spatial distributions of porosity and permeability. HGUs largely define units that could be called regional aquifers and confining zones and would be of Group or Supergroup rank in formal stratigraphic terminology because they are made up of units of formation rank. These formal distinctions are not critical in the context of this report because the units are informal and conform to geologic unit boundaries, but this discussion should give the reader a sense of the purpose, scale, and general approach used to develop the units and the challenges in developing traditional geologic correlations. The geologic and hydrogeologic maps and cross sections were developed concurrently in preparation of this report.

4.2.1 Precambrian Metamorphic Rocks

Precambrian rock units (p€m) consist primarily of moderately to intensely metamorphosed Precambrian "basement" rocks, forming the most significant aquitard in the geologic study area because it underlies the entire geologic study area (Page et al., 2005a; Hintze and Kowallis, 2009). The largest exposure in the area of Plate 6 is on the eastern side of the Schell Creek Range, north of U.S. Highway 50 (US 50) and on the western side of the Snake Range, north and south of US 50. This unit includes the Proterozoic rock units up through the McCoy Group. The permeability of the unit is low, except in areas where fractured or weathered. Additional Precambrian basement rocks are on Plate 7 in the southern part of the geologic study area in the Mormon Mountains, the Desert Range, and the Black Mountains at Lake Mead. These rocks include Precambrian metamorphic and crystalline rocks, the McCoy Creek Group, Trout Creek Group, and the Johnnie Formation. On the geologic maps and cross sections (Plates 1 and 2), this map unit has the symbol p€.

4.2.2 Cambrian to Precambrian Siliciclastic Rocks

The Cambrian to Precambrian clastic rock unit (€p€s) is non-metamorphosed to moderately metamorphosed siliciclastic rock deposited in the Neoproterozoic and Early Cambrian. The unit is quartzite with a substantial thickness of shale also present, thus a major aquitard. The unit is thickest in the southwest where it is estimated to exceed 10,000 ft, and it is thinnest in the north and southeast where it is estimated to be about 5,000 ft thick or locally less. The thickness of the unit is approximate because the base is rarely exposed, but the estimate is consistent with the amount of section that is exposed. In most places, the youngest formation within this unit is the Pioche Shale, and the bulk of the unit is mapped as the Prospect Mountain Quartzite. The permeability of the unit is low except in areas where fractured or weathered. The difference in permeability between p€m and €p€s in exposed sections is considered minor, although the €p€s unit is expected to be slightly more permeable than the older p€m (Belcher et al., 2001). On the geologic maps and cross sections, this unit consists of the symbol €p€s.

4.2.3 Cambrian Carbonate Rocks

The Cambrian carbonate unit (€c) consists of Middle and Upper Cambrian carbonate rocks, notably the Bonanza King, Highland Peak, and Pole Canyon formations. The units are interpreted to be thicker in the south (~8,000 ft) and thinner (~5,000 ft) in the north. This unit is mostly carbonate with a limited thickness of clastic sections. It has high permeability, especially where faulted, and therefore is a major aquifer. In the southern part of the geologic study area, the unit constitutes about half the thickness of the Paleozoic section. The Cambrian carbonate aquifer includes a thin, spatially limited confining unit, the Dunderberg Shale. This unit is of limited extent and is too thin to be considered capable of limiting flow on a regional basis. On the geologic maps and sections, this unit consists of the rocks with the symbols of both €m and €u and, on the cross sections, also the rocks with the symbol €c.

4.2.4 Mississippian to Ordovician Carbonate Rocks

The Mississippian to Ordovician carbonate rock unit (MOc) consists of the middle part of the Paleozoic carbonate section. The unit can exceed 12,000 ft as on Plate 8, Cross Section P—P' but has a wide variation in thickness as on Plate 8, Cross Section N—N' due to paleotopographic influences during deposition and post-depositional erosion. The unit includes the section from the Mississippian Joana or Monte Cristo Limestone to the Ordovician Pogonip Group or Antelope Valley Formation and therefore includes the Pilot Shale and Eureka Quartzite. This unit is characterized as carbonate with limited clastic rocks. It is generally very permeable, especially where faulted.

The Mississippian to Ordovician carbonate aquifer includes the Ordovician Eureka Quartzite and Pilot Shale, which are confining zones. Neither of these formations is considered a significant aquitard at the scale of Plates 6 to 9, and the brittle Eureka Quartzite, where fractured, can be an aquifer nearly as permeable as the carbonates. This section of rocks also includes the Guilmette, Sultan, Sevy, and Simonson formations of Devonian Age and the Lone Mountain Dolomite of Silurian age. These rocks are predominately dolomite. From oldest to youngest, the symbols for the rocks on the geologic maps and sections that are combined in this HGU are the following: Ol, SOu, SO, Ds, Dg, Dn, Dd, Du, DO, DS, MD, and MDd.

4.2.5 Mississippian Siliciclastic Rocks

The Mississippian clastic rock unit (Ms) includes the Diamond Peak Formation, Chainman Shale, Scotty Wash Quartzite, and equivalent siliciclastic rock units. The first two formations listed are not differentiated in this report in Lincoln County, except in the Egan and Schell Creek ranges, and are not differentiated in Clark County because they are thin. The clastic rock unit is derived from erosion of highlands in north-central Nevada associated with the Antler upland. It is thickest (about 3,500 ft) on the western side of Plate 8, Cross Section Y—Y'. The permeability of the unit is low, and the unit is an important confining layer in the Paleozoic section north of the North Pahroc Range (about 38 degrees north latitude). In the Snake Range, the rock unit is too thin to comprise a confining unit. On the geologic maps and sections, the unit consists of the rocks with the symbols Mc and Md.

4.2.6 Permian and Pennsylvanian Carbonate Rocks

The Permian and Pennsylvanian carbonate unit (PIPc) includes the Ely Limestone and Bird Spring Formation. It is nominally equivalent to the upper carbonate aquifer of Winograd and Thordarson (1975) at the NTS. In the northern part of the geologic study area, these rocks are continuous with the Arcturus and Park City groups, which are predominantly carbonate rocks. In the Butte Mountains in the northwestern part of the area, a small section of Triassic rocks is included in this unit. The unit is thickest near Robinson Summit in the Egan Range, with a thickness of ~10,000 ft at Plate 8, Cross Section W—W'. This unit is mostly carbonate, with a minimal thickness of clastic rocks. It is generally very permeable on a regional scale, especially where faulted. It is hydrologically similar to the lower carbonate section but separated from it by the Mississippian confining unit, unit Ms. The unit includes Permian carbonate and red beds in the southern part of the geologic study area. From oldest to youngest, the symbols for the rocks on the geologic maps and sections that are combined in this HGU are the following: IP, PIP, Pr, Pa, Par, and Pp.

4.2.7 Cretaceous to Triassic Siliciclastic Rocks

The Cretaceous to Triassic clastic unit (KŦRs) consists of Mesozoic rocks in eastern Lincoln and Clark counties. The unit includes the Triassic Moenkopi and Chinle formations and the Jurassic Aztec and Navajo sandstones. These units are locally beneath thrust faults that carry overlying older Paleozoic carbonates thrust from the west during Sevier deformation, and this unit may be 10,000 ft thick or more. The rocks of this unit are generally much less permeable than the carbonate aquifers. The symbols for the rocks on the geologic maps and sections that are combined in this HGU are ŦRs, Js, and Ks.

4.2.8 Tertiary to Jurassic Intrusive Rocks

The Tertiary to Jurassic intrusive unit (TJi) includes all plutons in the geologic study area. Mesozoic plutons form either a significant part of, or the bulk of, several large ranges in the northeastern part of the area, including the Snake, Schell Creek, Egan, and Kern ranges. In addition, extensive Tertiary plutons exist beneath all calderas. The permeability of the unit is low except in areas where fractured or weathered. The symbols for the rocks on the geologic maps and sections that are combined in this HGU are Ji, Ki, TKi, and Ti.

4.2.9 Older Tertiary Sediments

The older Tertiary sedimentary unit (Tos) consists mostly of older Tertiary clastic sediments (Eocene to Oligocene age) below the volcanic section. The unit reaches a maximum thickness of 4,000 ft in Railroad Valley, west of the geologic study area, and a similar thickness in the southern part of the area. The permeability is moderate, especially where well fractured. On the geologic map and cross sections, the unit consists of the rocks with the symbol Ts1 where they underlie the Tertiary volcanic rocks HGU, and includes megabreccia with the symbol Tmb on the geologic map on and west of the southern Sheep Range.

4.2.10 Tertiary Volcanic Rocks

The Tertiary volcanic unit (Tv) includes large volumes of middle Tertiary (Eocene to middle Miocene), mostly intermediate to felsic volcanic rocks. It also includes thin sedimentary rocks and local tuffaceous sediments that are interbedded with the volcanic units. Most of the exposed bedrock in Delamar, Dry Lake, Patterson, Little Spring, Rose, Eagle, Kane Spring, and Clover valleys are of volcanic rock. Outflow rocks are generally less than 3,000 ft thick, but intracaldera rocks may locally be more than 10,000 ft thick.

The Tertiary volcanic unit consists of a number of units of variable permeabilities: ash-flow tuffs are brittle and generally permeable, whereas lava flows are less permeable. In general, the permeability is considered good to moderate, but where faulted, the unit is more permeable and in some places, it may be an important aquifer. From oldest to youngest, the symbols for the rocks on the geologic maps that are combined in this HGU are the following: Tmb in the Indian Peak caldera complex but not west of the southern Sheep Range, Ta1, Ta2, Ta3, Ta4, Tr1, Tr2, Tr3, Tr4, Tt1, Tt2, Tt3, and Tt4. The symbol for the rocks on the geologic sections is Tv.

SE ROA 43181

JA_13061

4.2.11 Quaternary and Tertiary Basalt

The Quaternary and Tertiary basalt unit (QTb) resulted from Quaternary and late Tertiary mafic volcanism. The deposits are thin but locally cover significant areas. The unit is of possible hydrologic significance as a separate unit only where divided from the older volcanic rocks by alluvium. It is separated from the alluvium largely because it is a distinct rock type. The largest outcrops are located in north-central Nye County (Plate 1), and there are also extensive outcrops of this unit in southern Lincoln and northern Clark counties (Plate 2). Basalt is brittle and has high permeability, but because of the limited thickness and distribution, it does not have regional significance as a HGU. On the geologic maps and cross sections, the unit consists of the rocks with the same symbol (QTb).

4.2.12 Quaternary and Tertiary Sediments

The Quaternary and Tertiary sedimentary sequence (QTs) consists mostly of basin-fill sediments younger than the volcanic section. This unit may include older Tertiary sediments where the volcanic rocks are thin or nonexistent and these older units are too thin or too localized to separate out. In some places, these older units consist of sands and gravels that are difficult to distinguish from the younger alluvial sediments, and these units are, therefore, lumped together.

The QTs unit is interpreted to be thicker than 10,000 ft in some down-faulted grabens (valleys), such as Dry Lake and Panaca valleys on Plate 8, Cross Section P—P'. The unit is composed of conglomerate, fresh-water limestone, sand, silt, gravel, and clay, and therefore it has a large range of permeability. Also included in this unit are playa deposits that are too thin to show on cross sections but are an obvious surface feature throughout the Great Basin. Overall, the map unit has moderate permeability but may be high where fractured. The symbols for the rocks on the geologic maps that are combined in this HGU are Ts2, Ts3, Ts4, and QTa. On the cross sections, the symbol for the rocks in this HGU is QTs.

4.3 Structural Geology

This section discusses the structural framework of the geologic study area. This presentation is followed by an analysis of the effect of specific structures on the hydrogeology of the region. This analysis covers structures as both groundwater flow conduits and flow barriers as conceptualized in Section 2.0.

4.3.1 Evolution of the Regional Structure

Three main structural events affected the geologic study area: (1) Late Devonian to Late Mississippian Antler compressive deformation, (2) Late Jurassic to early Tertiary Sevier compressive deformation, and (3) late Cenozoic basin-range extensional deformation. In addition to these structural events, middle Cenozoic time was characterized by mild extension (Rowley, 1998; Miller et al., 1999; Rowley and Dixon, 2001) and voluminous calc-alkaline volcanism that profoundly affected the topography and hydrology of the geologic study area.

The Late Devonian to Late Mississippian Antler compressive deformation affected the northwestern part of the geologic study area, creating a north-trending highland (Larson and Langenheim, 1979; Carpenter et al., 1994; Poole and Sandberg, 1977 and 1991). This event formed folds and thrusts of the Roberts Mountain allochthon, which was at least 8,000 ft thick and passed through Eureka, Nevada (Carpenter et al., 1994; Saucier, 1997). The thrusts transported deeper-water sedimentary rocks eastward as much as 100 mi. Coarse synorogenic siliceous clastic detritus was shed from the highland into the foreland basin to the east, transitioning to shale farther east. The main synorogenic rock units that resulted were the Chainman Shale and Diamond Peak Formation, and farther south the Scotty Wash Quartzite.

The second structural event, the Middle Jurassic to early Tertiary Sevier compressive deformation, resulted in generally north- to north-northeast-striking, east-verging folds and thrust faults. Scattered Middle Jurassic to lower Tertiary plutons were emplaced in many mountain ranges of the geologic study area. Eastward-directed overthrusts emplaced Neoproterozoic to middle Paleozoic rocks over Neoproterozoic to Mesozoic rocks (Armstrong, 1968). At least a half dozen large thrusts are well exposed in the Las Vegas area, each with displacements ranging from several to 20 mi (Page et al., 2005b). Tectonic shortening caused by thrusting in southern Nevada is at least 22 to 45 mi (Stewart, 1980; Burchfiel et al., 1974). Except for the southern part of the geologic study area, most of the area has been considered to be the western hinterland of the deformation. In other words, Sevier deformation created Late Cretaceous to early Tertiary highlands (hinterlands) that in turn shed most major thrusts and clastic debris primarily to the east (Vandervoort and Schmitt, 1990; Druschke et al., 2009). Some of the thrusts, including the Gass Peak, however, have been projected northward into the hinterland in the central and northern part of the geologic study area, including the Timpahute Range, Worthington Mountains, Golden Gate Range, Grant Range, Pancake Range, and Newark Valley (Vandervoort and Schmitt, 1990; Dobbs et al., 1994; Taylor et al., 2000). Most of the thrusts in the Confusion Range appear to represent minor movement along bedding planes in weak beds during tight folding of Sevier age. Anderson (1983), however, interpreted the faults to have formed by gravity sliding into the axis of a synclinorium. Sevier-type deformation is shown schematically on Figure 4-6, and the Sevier-age Glendale/Muddy Mountains thrust in the Muddy Mountains is shown on Figure 4-7.

East-striking faults and folds, alignments of plutons and volcanic vents, alignments of geophysical anomalies, local alignments of basins and ranges, hot springs, hydrothermally altered rocks, and mineral deposits have been noted in the Great Basin for years, primarily by geologists of the mining industry. Ekren et al. (1976 and 1977), Rowley et al. (1978), and Stewart et al. (1977) called these alignments “lineaments” with an origin similar to transform faults in the ocean basins. Ekren et al. (1976) also suggested that the lineaments began to form in the Cretaceous, if not earlier, and continued to be active throughout both Tertiary calc-alkaline magmatism and basin-range deformation. Like transform faults, these lineaments seem to represent boundaries between areas to the north and south that had different amounts, rates, and types of structural deformation. Rowley (1998) and Rowley and Dixon (2001) referred to them as transverse zones, and we follow their terminology here. They are poorly known and have been mapped in detail only locally, so they are projected with limited evidence between the areas where they are known. Therefore, transverse zones are delineated as speculative zones of potential disruption on Plates 1 and 2.

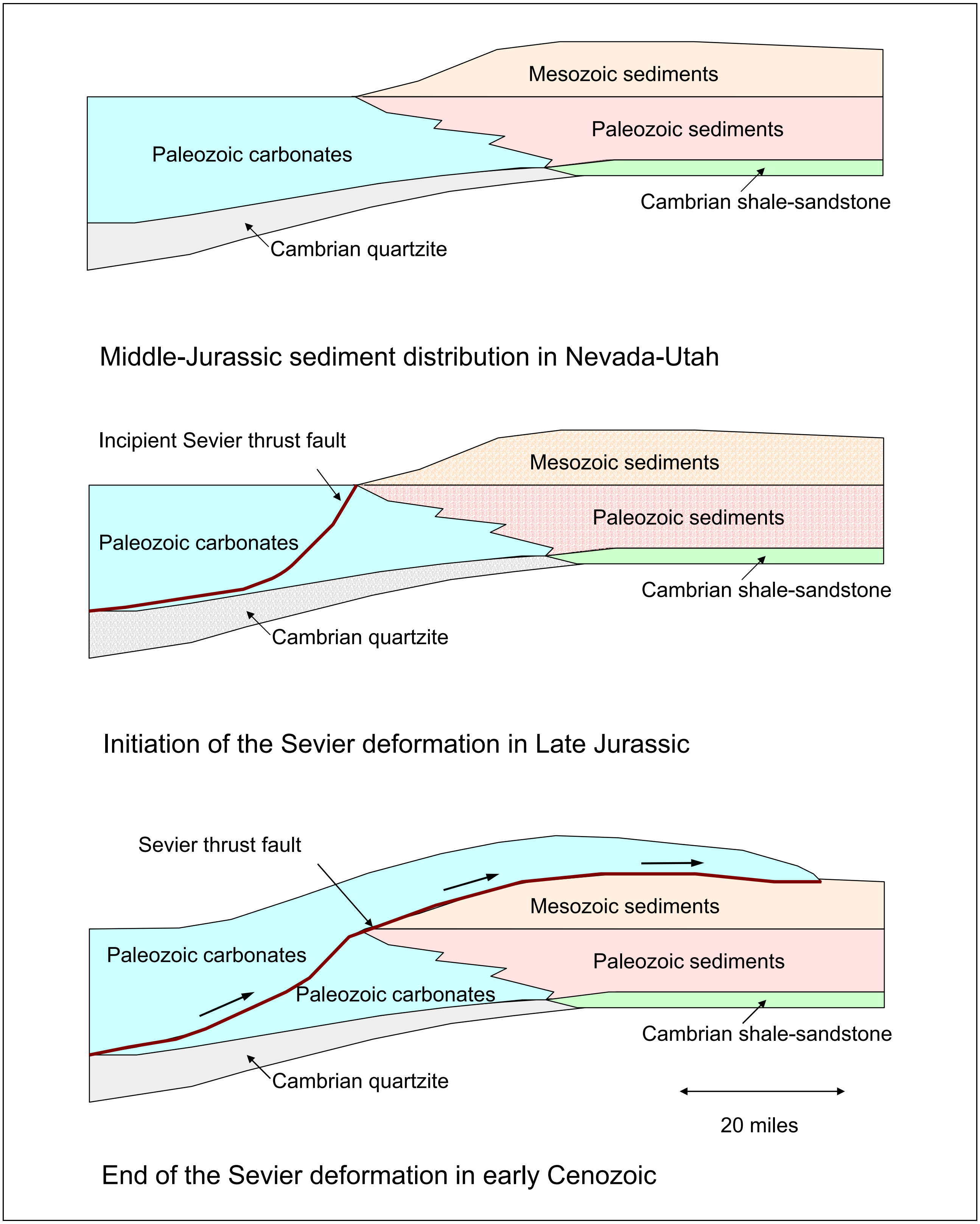

Figure 4-6
Schematic Diagram of Sevier Thrust Sheets, Illustrating the Movement of Paleozoic Carbonates over Cratonic Sediments

SE ROA 43184

JA_13064

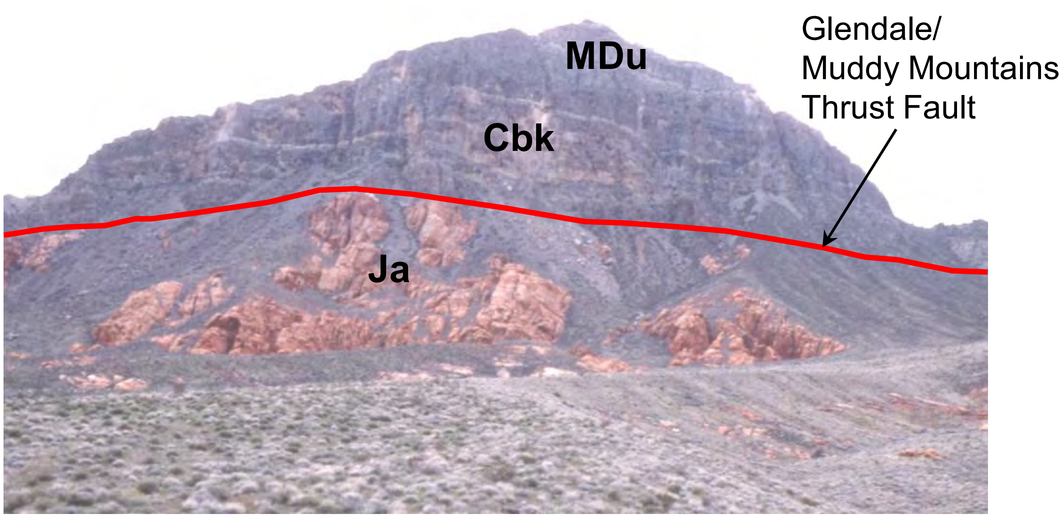

Ja – Jurassic Aztec Sandstone
MDu – Mississippian-Devonian carbonates, undifferentiated
Cbk – Cambrian Bonanza King Formation

Figure 4-7
Paleozoic Carbonates Thrust over Jurassic Aztec Sandstone in the Muddy Mountains near Muddy Peak

Transverse zones bound parts of most igneous belts in the Great Basin. They also define the northern and southern sides of the Caliente caldera complex, representing structures by which this caldera spread east and west to a degree much more profound than most other caldera complexes in the Great Basin. Transverse zones are poorly known and have been mapped in detail only locally, so they are projected with limited evidence between areas where they are known. Some transverse zones seem to be discontinuous along strike (along their east-west trend), so they may be present for several miles or tens of miles, then be absent or buried for miles, then be present again. Such is the case with the Sand Pass transverse zone (Rowley, 1998; Rowley and Dixon, 2001), which bounds the northern and southern side of the Kern Mountains but progressively to the east is buried beneath the surficial sediments of Snake Valley, absent through the carbonate bedrock of the northern Confusion Range and western Middle Range (Plates 1 and 6), and present in the carbonate bedrock and basin-fill sediments of the central and eastern Middle Range and of Sand Pass (Rowley et al., 2009, Plate 1). Farther east, east-trending features are absent in the Drum Mountains and Thomas Range (Rowley et al., 2009, Plate 1), but they are prominent east of the Thomas Range most of the way to and east of the Wasatch front in central Utah (Stoeser, 1993; Rowley, 1998; Rowley and Dixon, 2001).

The third structural event, the basin-range episode of extensional deformation, began at about 20 Ma and continues today. It is characterized by east-west extension and resulted primarily in north-striking normal faults. Over some parts of the Great Basin, early phases of this deformation produced north-striking basins and ranges due partly to gentle folding. Sediments were deposited in basins formed by these early faults and broad warps, but these basins were not necessarily in the same locations as they are today. The present topography was produced later, during the main pulse of basin-range deformation that began after 10 Ma for most parts of the Great Basin. The orientation of axes of basins and ranges since 10 Ma were commonly different from those created during the early phase of deformation. Some parts of the older basins were uplifted as part of the new ranges and some parts of the older ranges were downthrown as part of the new basins. An example is the presence of Miocene lacustrine limestones and associated clastics in the North Pahroc and Pahranagat ranges (Tschanz and Pampeyan, 1970) that were originally deposited in one or more basins.

The dominant fault type since major deformation began (about 10 Ma) continued to be north-striking normal faults, but locally strike-slip and oblique-slip faults accommodated the east-west extension. Examples of such accommodation zones are the east-northeast, left-lateral PSZ at the southern end of Pahranagat Valley and the northeast-trending, left-lateral Kane Spring fault zone west of the Meadow Valley Mountains (Ekren et al., 1977). Vertical displacement on some normal faults in the study area far exceeded 10,000 ft. In and near the study area, the dominant topography is alternating complex horsts and grabens (Mankinen and McKee, 2009; McPhee et al., 2009). An alternative view of basin-range structure, in which the abundance of and amount of displacement on normal faults and their effect on groundwater flow is much less than presented here, is given by Sweetkind et al. (2007b, Figure 9), who envisioned a topography of tilt blocks faulted on only one side. East-striking transverse faults continued to be active at the same time, segmenting the Great Basin into broad east-trending corridors of different types and amounts of east-west pulling apart.

In some parts of the map area, low-angle faults were previously mapped as thrust faults (e.g., Hazzard and Turner, 1957; Misch, 1960; Nelson, 1966), yet these geologists correctly recognized that the faults partly followed weak beds in the Pioche Shale. The rocks above these faults, however, were not thickened and compressed as above thrust faults but instead were stretched and attenuated, and younger rocks were emplaced on older rocks (Hose and Blake, 1976). The first workers to recognize the significance of the faults were Moores et al. (1968) and Armstrong (1972), from work west of the study area. These workers concluded that most of these low-angle faults are Tertiary expressions of structural extension. The faults formed after rapid uplift of the ranges, in which the tops of the uplifted blocks were structurally stripped (or attenuated or denuded) by low-angle faults that verged into the adjacent low areas, much like large gravity slides. They called them attenuation or denudation faults. Most formed during the basin-range episode of deformation.

In and west of the study area, the major low-angle fault, called the Snake Range decollement, emplaced Middle Cambrian carbonates and some younger rocks over Middle Cambrian carbonates and Lower Cambrian to Neoproterozoic quartzite. Whitebread (1969) mapped this feature over a large part of the southern Snake Range that includes Great Basin National Park (GBNP). Coney (1974) mapped small-scale structures in the fault plane in the Snake Range and found that upper-plate rocks on the east side of the range traveled eastward, and those on the west side of the range traveled westward. Hose and Blake (1976) showed the decollement as it was then known. Following a comprehensive study, Miller et al. (1983) and Gans et al. (1985, 1989) reinterpreted the fault as an Eocene to Miocene low-angle fault caused by stretching and thinning during uplift as a metamorphic core complex. They suggested that the decollement may represent the ductile-brittle transition zone uplifted by the core complex (see Figure 4-8) (Miller et al., 1983; Gans et al., 1985, Gans, 2000b). Rocks have been thinned by the elimination of strata due to the faulting.

Later work indicated that, whereas the decollement had an older (late Eocene and early Oligocene) history, most displacement on it was middle Miocene and later, coinciding with basin-range

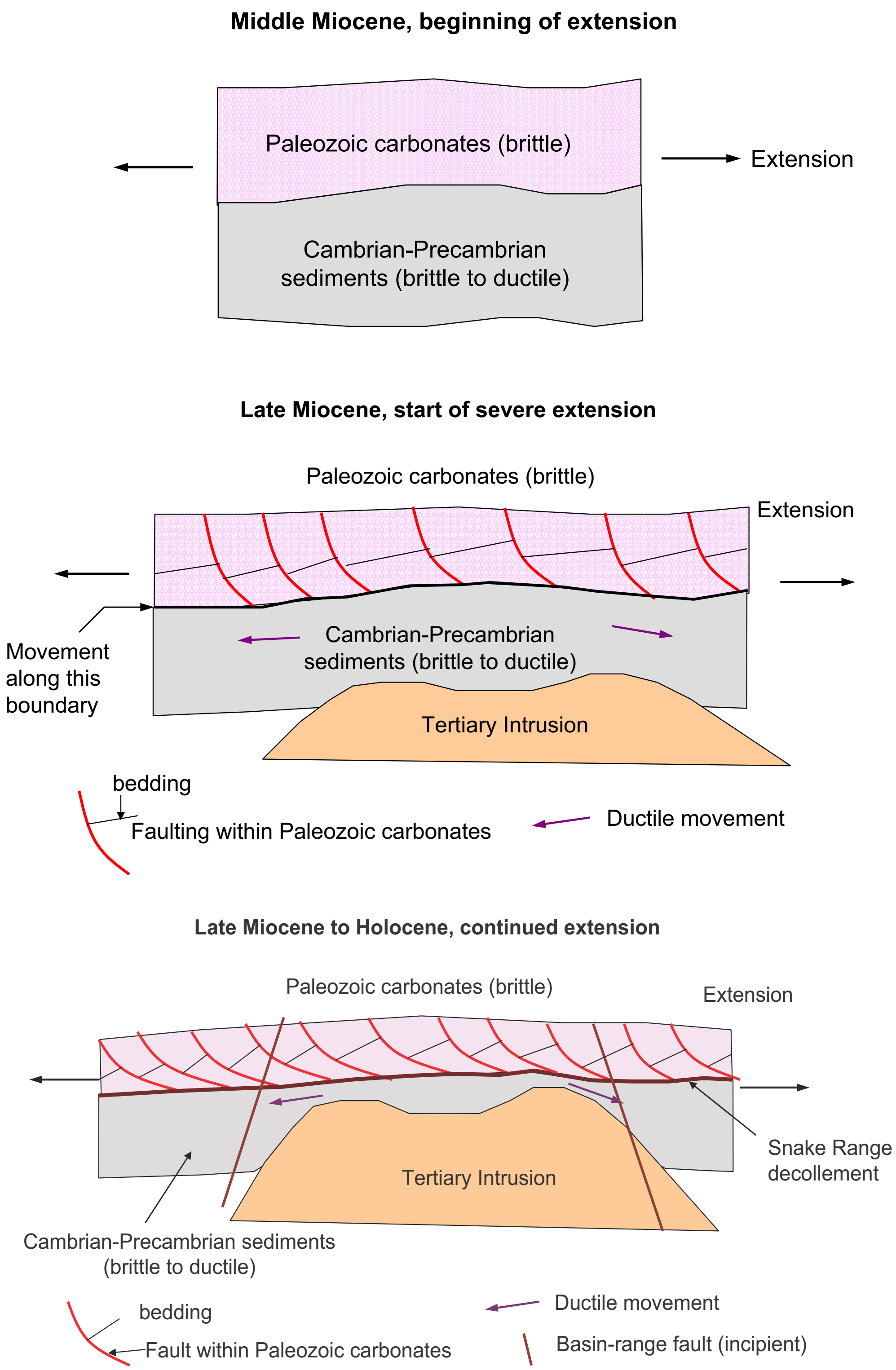

Source: Gans et al. (1985)

Figure 4-8
One Scenario for Development of the Snake Range Decollement during Late Cenozoic Extension

deformation (Miller et al., 1999). Some geologists (Allmendinger et al., 1983; Bartley and Wernicke, 1984; Kirby and Hurlow, 2005; Sweetkind, 2007a) interpreted the decollement to be a major detachment fault in the Great Basin and to have many miles (37 mi according to Bartley and Wernicke, 1984, p. 652) of eastward displacement of the upper plate relative to its underlying footwall. However, Gans and Miller (1985, p. 411) pointed out that the fault plane occupies the same stratigraphic position (top of the Pioche Shale) and does not "cut downsection to the east," so they therefore concluded that it could not have "a large amount of translation" and more likely represents "decoupling along the stratigraphic horizon in the Pioche Shale." Miller et al. (1999) later reinterpreted the amount of eastward translation on the decollement on the crest and eastern side of the Snake Range to about 7 to 9 mi, although they acknowledged that movement on the decollement on the western side of the range was westward, as first recognized by Coney (1974).

Probably the decollement represents movement along a weak stratigraphic horizon on the steep upper flanks of rapidly rising ranges (Figure 4-8). Finally, in their most recent conclusions about the structure, Miller et al. (1999, p. 902) suggested that the Snake Range decollement may not be a normal fault at all but instead a "highly complex structural boundary developed above a rising and extending mass of hot crystalline rocks."

4.3.2 Effect of Structures on Groundwater Flow

This section evaluates the effect of the three episodes of structural deformation and one episode of volcanism on the groundwater flow in the geologic study area. This analysis covers structures as both groundwater flow conduits and flow barriers, in other words how they guide flow along and across a general flow path.

4.3.2.1 The Antler Deformation

The Antler episode of compressive deformation probably had the least direct effect on groundwater flow of any structural event. Most of the thrust faults associated with this tectonic event are west and northwest of the geologic study area. Instead, the deformational event had more of an effect on the types of sediment deposited than on any structural controls on groundwater flow. The deformation created a highland west of the map region, and sandstone and shale, including the Chainman Shale, were deposited mostly within the northern half of the geologic study area, forming a lithologic aquitard. Most of the tectonic features developed during this event were themselves deformed and changed in subsequent tectonic episodes.

4.3.2.2 The Sevier Deformation

The Sevier episode of compressive deformation had a stronger effect on groundwater flow in the region than the Antler event. The Sevier event resulted in major thrust faults, especially in the southern part of the geologic study area but locally in the central and northern part of the area. Gouge and mylonitic zones along these thrusts have created barriers to groundwater flow, particularly in the Sheep Range, the Pahranagat Range, the Delamar Mountains, and in several other ranges in the southern part of the area. Furthermore, these thrust faults brought western assemblage carbonates over eastern assemblage cratonic clastic sedimentary rocks of Triassic through Cretaceous age. These cratonic confining units generally also are flow barriers. Some of these geologic barriers to flow are several thousand feet thick, as in the Muddy, Meadow Valley, and Clover mountains. In other places, thrust faults brought Precambrian and Cambrian siliciclastic rocks over the carbonate units, as in the Sheep and Las Vegas ranges along the Gass Peak thrust and in the Delamar Mountains along the Delamar thrust. In contrast to barriers to flow caused by the Sevier deformation, northerly conduits may have resulted from a concentration of fractures developed along the axes of open shallow anticlines, most of which trend north.

4.3.2.3 The Eocene-Miocene Episode of Calc-Alkaline Volcanism

The third episode of landscape change was during the Eocene, Oligocene, and Miocene epochs, when the area was drastically affected by voluminous calc-alkaline volcanism, mild extension, and high-angle strike-slip faults and high- to low-angle normal faults. The topography became dominated by calderas, which capped mountainous areas formed by uplift and inflation of the crust due to the rise of underlying source batholiths and stocks. Ash-flow tuffs that erupted from the calderas blanketed and subdued the topography. Stratovolcanoes and other volcano edifices fed lava flows and mudflows. The geometry, extent, strike, size, and type of fault structures that formed during this time are poorly known but likely included strike-slip and normal faults, including detachment faults. The region appears to have been characterized by mild east-west extension and strike-slip faults of northeast and northwest strikes. The caldera complexes and their associated ring faults and other margin structures were mostly barriers to groundwater flow. Perhaps more important than the caldera margins themselves are the intracaldera intrusions that underlie the calderas, which caused hydrothermal clay to form by heating and convective overturn of ancient groundwater and contact metamorphism of intracaldera ash-flow tuff. Faults and associated joints that postdate and cut the calderas locally provide conduits for groundwater flow through the calderas.

4.3.2.4 The Miocene-Quaternary Basin-Range Episode of Extension

The basin-range episode of extensional faulting began in the middle Miocene and is continuing today. The faults that formed during this episode are generally moderate to steeply dipping normal faults that are generally north trending. They formed most of the topography we see today. High-angle oblique-slip and local strike-slip faults that had trends at high angles to the extension direction formed as accommodation zones during the same east-west extension. The north-striking high-angle faults and resultant fractures generally provide conduits to groundwater flow north or south along the hydraulic gradient, rather than flow barriers (e.g., Rowley and Dixon, 2004). In areas where groundwater flow is directly across these fault zones, such as between Spring and Hamlin valleys, groundwater flow may be limited by gouge in the core zones of the faults but not prevented by these structures (Figures 2-4 and 2-5). The hydrologic effect produced by faults largely results from joints that the faults cause, with larger-displacement faults resulting in more joints and thus greater fracture flow. However, for brittle rocks such as carbonates, welded ash-flow tuff, and basalt flows, even small faults—which are many times more abundant in the Great Basin than the large faults we have mapped—create rock fractures, acting like a hammer on a plate of glass. These brittle rocks in the Great Basin cannot help but be significantly fractured throughout, commonly creating important aquifers (Winograd and Thordarson, 1975; Dettinger, 1992; Dettinger et al., 1995; Burbey, 1997; Rowley and Dixon, 2004).

Some normal faults are low-angle—that is, denudation, detachment, or attenuation faults. Their effect on groundwater flow is much less important than that from high-angle faults. These low-angle fault zones may result either from brittle or plastic deformation, resulting respectively in gouge or mylonitic zones along the faults. Gouge and mylonite may provide barriers to groundwater flow. An example is the Snake Range decollement that formed as the Snake and Schell Creek ranges were uplifted and intruded. The low-angle faults of the Snake Range decollement may locally prevent rainfall from infiltrating the range. But a more profound effect on infiltration is caused by the underlying Proterozoic and Cambrian metamorphic rocks and quartzite, which also provide barriers to east or west flow through the ranges.

4.4 Descriptions of Basins and Ranges and Potential for Interbasin Groundwater Flow

This study concentrated on specific basins or hydrographic areas within or adjacent to the geologic study area. The basins and ranges, their structure and geometry, and the potential for interbasin groundwater flow between them are described in this section. Mountain ranges adjacent to the basins are described in more detail than the valleys themselves due to their greater exposures of pre-Quaternary geologic units. Because of this, the discussion below is organized by ranges, and the adjacent basins are discussed within these sections going from north to south and west to east, starting in the northwestern part of the map

The potential for interbasin groundwater flow is discussed within the text and is illustrated by Figure 4-9. The figure shows the likelihood of groundwater flow across boundaries between hydrographic areas based primarily on lithology and structure. Smaller boxes on the figure show areas where more detailed maps and cross sections are provided. On Figure 4-9, the potential for interbasin groundwater flow is geologically classified as likely, permissible, or unlikely. The hydrographic area boundaries identified as likely or permissible zones for groundwater flow are approximate locations and are not meant to represent the exact location of interbasin groundwater flow. More specific flow routes and their estimated volumes of groundwater are provided in the accompanying hydrologic report (Burns and Drici, 2011). A similar investigation of flow routes and volumes, but with different interpretations, was given in the results of the BARCASS (Knochenmus et al., 2007; Welch et al., 2007); their interpretations will be discussed in Section 6.0.

Specific flow pathways are controlled by topographic and geologic features, whose accurate, detailed geologic mapping and understanding are critical to interpreting flow routes between basins. Where the potential for such interbasin flow is classified as likely, the basin boundary is generally topographically low, the bedrock at and beneath the surface of the boundary is an aquifer or otherwise permeable due to fracturing, and the orientation of structures (mostly faults but also the dip of beds) is favorable (parallel to the trend of faults and beds) instead of unfavorable (perpendicular to the faults and beds) with respect to the boundary orientation, allowing groundwater to pass through the boundary. However, locally, water-level or hydraulic-gradient data at such a boundary may indicate groundwater flow away in both directions from the boundary, one type of groundwater divide. Where the potential for interbasin flow is classified as unlikely, the basin boundary is generally topographically high, the bedrock making up the subsurface of the boundary is commonly, although not necessarily, a confining unit, and the orientation of structures at the boundary is unfavorable with respect to the orientation of the boundary. Where the potential for interbasin flow is classified as

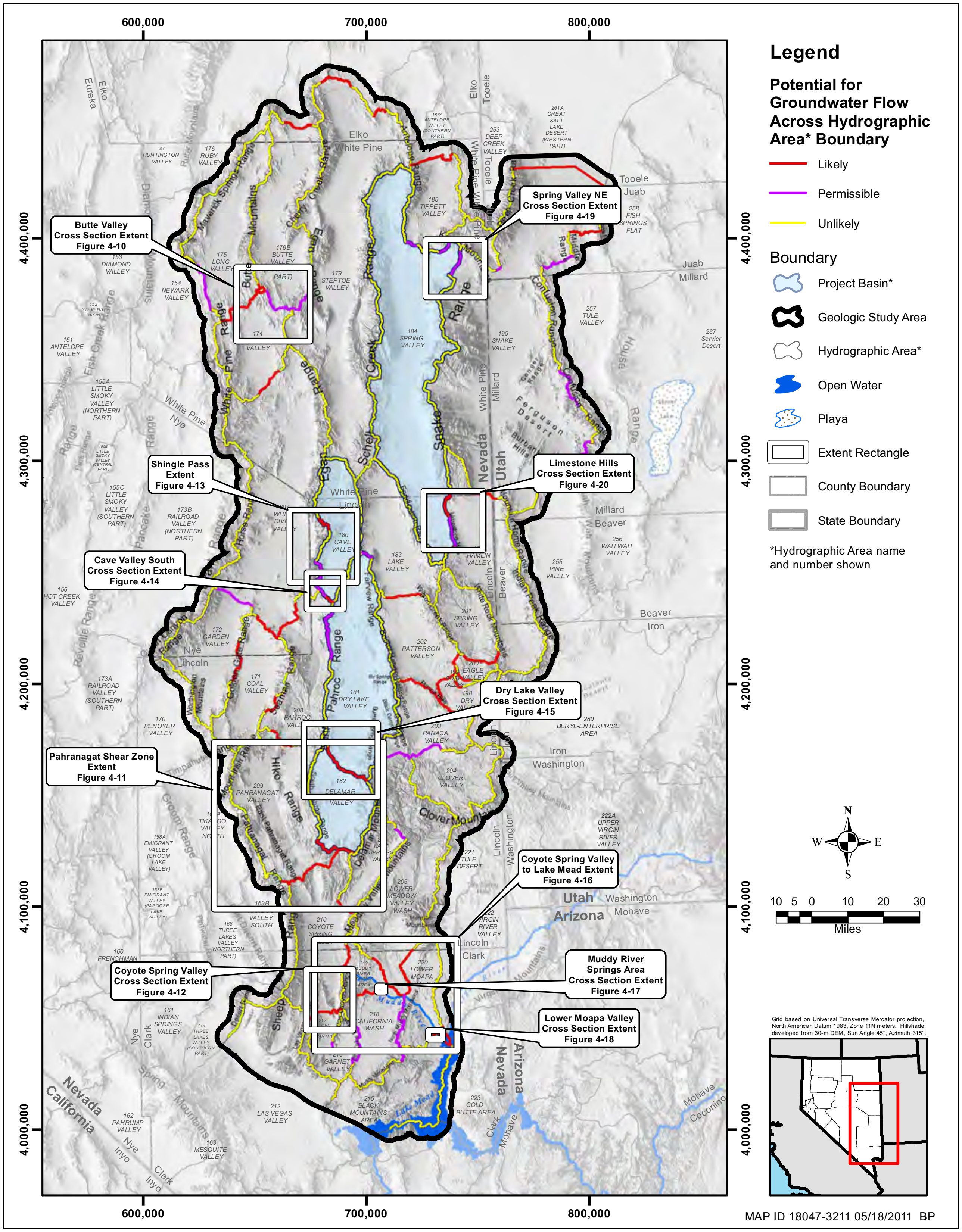

Figure 4-9
Potential for Interbasin Groundwater Flow within the Geologic Study Area

SE ROA 43191
JA_13071

permissible, the basin boundary has been evaluated with respect to topographic and geologic data and determined to have a significant likelihood for flow through it.

4.4.1 Ruby Mountains, Bald Mountain, and Buck Mountain

The Ruby Mountains, just west of the geologic study area, is a horst in which large amounts of vertical uplift resulted in detachment (attenuation) faults along the margins. In other words, the range is a metamorphic core complex formed during major uplift (Howard et al., 1979; Wright and Snoke, 1993). Most rocks in the range dip east and are early Paleozoic in age. The Ruby Mountains is cored by a Jurassic to Miocene batholith and Precambrian to Lower Cambrian rocks, which constitute confining zones.

Bald Mountain consists of east-dipping lower Paleozoic rocks cored by Jurassic intrusions that formed major deposits of gold, silver, and other metals (Hitchborn et al., 1996). Bald Mountain joins Buck Mountain, a horst of subhorizontal middle Paleozoic rocks. A low, south-trending narrow arm of Buck Mountain joins the White Pine Range to the south, and flow is permissible from Long Valley into Newark Valley through Beck Pass in the arm (Figure 4-9; Section 4.4.2). The intrusions provide a barrier to flow across Bald Mountain.

Ruby Valley is a deep graben bounded by the Ruby Mountains to the west, the Maverick Springs Range (Section 4.4.2) to the east, and Bald Mountain to the south. Probably this graben is locally about 5,000 ft deep. On the western side of the Ruby Mountains and Bald Mountain is Huntington Valley, a graben that is several thousand feet deep. This valley is bounded on the west by the Diamond Mountains. A groundwater divide is present between Huntington Valley and Newark Valley (Harrill et al., 1988). Newark Valley is bounded by the Diamond Mountains to the west and by Bald and Buck mountains to the east. This valley is another graben with locally more than 5,000 ft of valley fill (Plates 4 and 8, Cross Section X—X'); it is further described in Section 4.4.3. Seismic profiles disclose Sevier thrusts beneath the basin-fill deposits (Dobbs et al., 1994).

4.4.2 Maverick Springs Range

The Maverick Springs Range of northern White Pine County, Nevada, is a low, northeast-trending range of mostly east-dipping upper Paleozoic rocks uplifted along a normal fault on the western side. The range bounds the southeastern edge of Ruby Valley. The eastern side of the Maverick Springs Range is bounded by a normal fault, down to the east, that separates it from Long Valley to the east. The northern end of the Maverick Springs Range is cored by a Tertiary pluton (Plates 4 and 8, Cross Section Y—Y') that continues north into Elko County, Nevada, as a broad series of hills, floored by cupolas of a Tertiary stock or batholith. The southern half of the Maverick Springs Range joins Buck Mountain to the south, separated by a down-to-the-west normal fault in the Alligator Ridge area, site of a major gold deposit (Nutt, 2000). The pluton in the Maverick Springs Range is a barrier to groundwater flow east or west across the northern part of the range, and flow is theoretically possible but considered unlikely through carbonate rocks above and around the pluton. The east dip of the beds would preferentially cause mountain recharge to flow eastward.

Long Valley, at the northwestern part of the study area, is narrow and shallow at its northern end but it widens and deepens to at least 3,000 ft to the south. The fault zone that bounds the western side of the Maverick Springs Range in Ruby Valley passes south through Mooney Basin (between the southern Maverick Springs Range and the Bald Mountain-Buck Mountain ridge) and is potentially a conduit for groundwater flow between southern Ruby Valley and western Long Valley. Most groundwater in Long Valley flows southward along north-trending faults and fractures in the valley, then into Jakes Valley to the southeast (Figure 4-9) (Harrill et al., 1988). One potential exception to all flow passing from southern Long Valley to Jakes Valley is a flow path from southwestern Long Valley through Beck Pass (north of the White Pine Range) into Newark Valley to the west. Such a path was suggested by Harrill et al. (1988), although they did not assign a volume to that flow. This route is classified as permissible because Beck Pass is low with respect to the two valleys and is underlain by surficial sediments of unknown although probably small thickness. Furthermore, most rocks at and beneath the pass are aquifers consisting of upper Paleozoic carbonates and lower Tertiary ash-flow tuff. Although no west-trending structure has been mapped at or near the pass, the rocks are potentially fractured due to north-trending range-front faults on either side of the pass. Such range-front faults, as well as the north-striking beds, are likely to be barriers to significant flow across the basin boundary.

4.4.3 Butte Mountains and White Pine Range

The Butte Mountains is located east of Long Valley; the range is west of central and southern Butte Valley. The Butte Mountains is a 40-mi-long, north-trending horst of east-dipping to anticlinally folded, upper Paleozoic sedimentary rocks (Hose and Blake, 1976; Otto, 2008). Southward, the Butte Mountains joins the eastern side of the north-trending, 50-mi-long White Pine Range across a low range of hills of upper Paleozoic carbonate rocks and Tertiary volcanic rocks. The southern end of the Butte Mountains also joins with several repeated fault ridges of the Egan Range (Section 4.4.9) to the east across a similarly low range of volcanic hills that forms the southern end of Butte Valley.

The northern White Pine Range is a generally low, broad series of horsts and grabens (Gans, 2000a). One of the grabens becomes Long Valley to the north, and the eastern horst becomes the Butte Mountains to the north. The northern White Pine Range is underlain largely by upper Paleozoic rocks, but middle Paleozoic rocks underlie some of the horsts (Lumsden et al., 2002) and Tertiary volcanic rocks underlie some of the grabens (Plates 4 and 8, Cross Section W—W'). The middle Paleozoic rocks included repeated fault blocks containing the Chainman Shale. The Chainman shale and faults of the horsts and grabens form a groundwater barrier between Jakes Valley and Railroad Valley to the west. The southern end of the White Pine Range has considerable elevation (as much as 11,500 ft) and is made up mostly of east-dipping, lower to middle Paleozoic rocks. The range here has a large eastward bulge, the White River caldera, which includes an underlying resurgent dome that undoubtedly is responsible for the high relief of the range (Plates 4 and 8, Cross Section V—V'). West of the caldera, the rocks include Cambrian to Precambrian siliciclastic rocks intruded by a Tertiary pluton. The north-trending axis of the caldera contains a narrow, north-striking graben; it is likely that the graben transmits groundwater flow between Jakes Valley and the White River Valley (Figure 4-9), respectively north and south of the caldera. The siliciclastic and intrusive rocks of the southern White Pine Range form a groundwater barrier between White River Valley and Railroad Valley. East-dipping sedimentary rocks in the range allow recharge to flow preferentially eastward from the range into the White River Valley.

Butte Valley, east of the Butte Mountains, is a graben similar to Long Valley. Butte Valley contains upper Paleozoic rocks at a shallow depth, with overlying Tertiary volcanic rocks in the southern part of the valley. The valley fill is a maximum of about 4,000 ft thick, in turn overlying less than 1,000 ft of Tertiary volcanic rocks. A narrow horst is within the northern end of Butte Valley (Plates 4 and 8, Cross section Y—Y').

Based on the geologic framework, a flow path at the northern boundary of Jakes Valley is likely, with permissible boundaries extending south and east from there (Figure 4-9). This area is shown on a detailed geologic map of the volcanic hills that extend from the southern Butte Mountains across several western ridges of the Egan Range to define the southern end of Butte Valley (Figure 4-10). The flow path is along faults and fractures, from the southwestern part of Butte Valley into Jakes Valley. The geologic cross section (boundary flow profile) across the western part of the volcanic hills (Figure 4-10) is drawn perpendicular to this flow path.

In places, the volcanic rocks south of Butte Valley have been eroded off, exposing underlying Triassic and upper Paleozoic carbonate rocks. The profile is drawn generally parallel to the basin boundary and perpendicular to the permissible flow path. A detailed analysis of gravity anomalies was performed by Mankinen and McKee (2011) of the USGS to further understand possible flow paths (Section 5.1.2 and Figure 5-8). The analysis suggests that the primary structure is the large fault at the left (northwest) end of the cross section. This fault shows up as a prominent structure identified by maxspots on the isostatic residual gravity map (Figure 5-8). Summit Spring, along the fault near the basin boundary, suggests the presence of water in the fault zone. Another major fault, shown at the southeastern end of the profile, may also provide a conduit for groundwater to Jakes Valley.

A second permissible flow path, from southeastern Butte Valley southeastward to Steptoe Valley along the range-front fault on the western side of the Egan Range (eastern edge of Figure 4-10), would be in part within fractured volcanic rocks on the western downthrown side of this fault zone. If so, flow would pass beneath a low, unnamed pass between the headwaters of north-flowing Combs Creek and those of south-flowing Smith Valley.

Jakes Valley, south of the Butte Mountains, may be as deep as 6,500 ft (Plates 4 and 8, Cross Section W—W'), with Tertiary volcanic rocks and upper Paleozoic carbonate rocks beneath about 5,000 ft of basin-fill sediments. Most of interbasin flow to Jakes Valley is thought to come from Long Valley (Harrill et al., 1988), with some smaller amount likely from Butte Valley as previously described. However, as part of BARCASS, Knochenmus et al. (2007) and Welch et al. (2007) suggested an additional but significant volume passes from Steptoe Valley northwest beneath the northern business district of Ely, Nevada, then through the northern Egan Range to Jakes Valley; this hypothesis is discussed in Section 6.0. However, this boundary is interpreted here as a boundary of unlikely flow. Groundwater out of southern Jakes Valley is likely to travel to the southeast beneath the ephemeral surface-water outlets (Jakes Wash area) from Jakes Valley to White River Valley, as well as southward along parts of the graben in the White River caldera.

West of the White Pine Range, Newark Valley is a shallow graben, narrowing and becoming shallower to the south, as described in Section 4.4.1. West of the southern end of the White Pine Range, Newark Valley opens out southward into Railroad Valley, a broad deep graben. East of the axis of the White River caldera, the White Pine Range is dropped down by many down-to-the-east

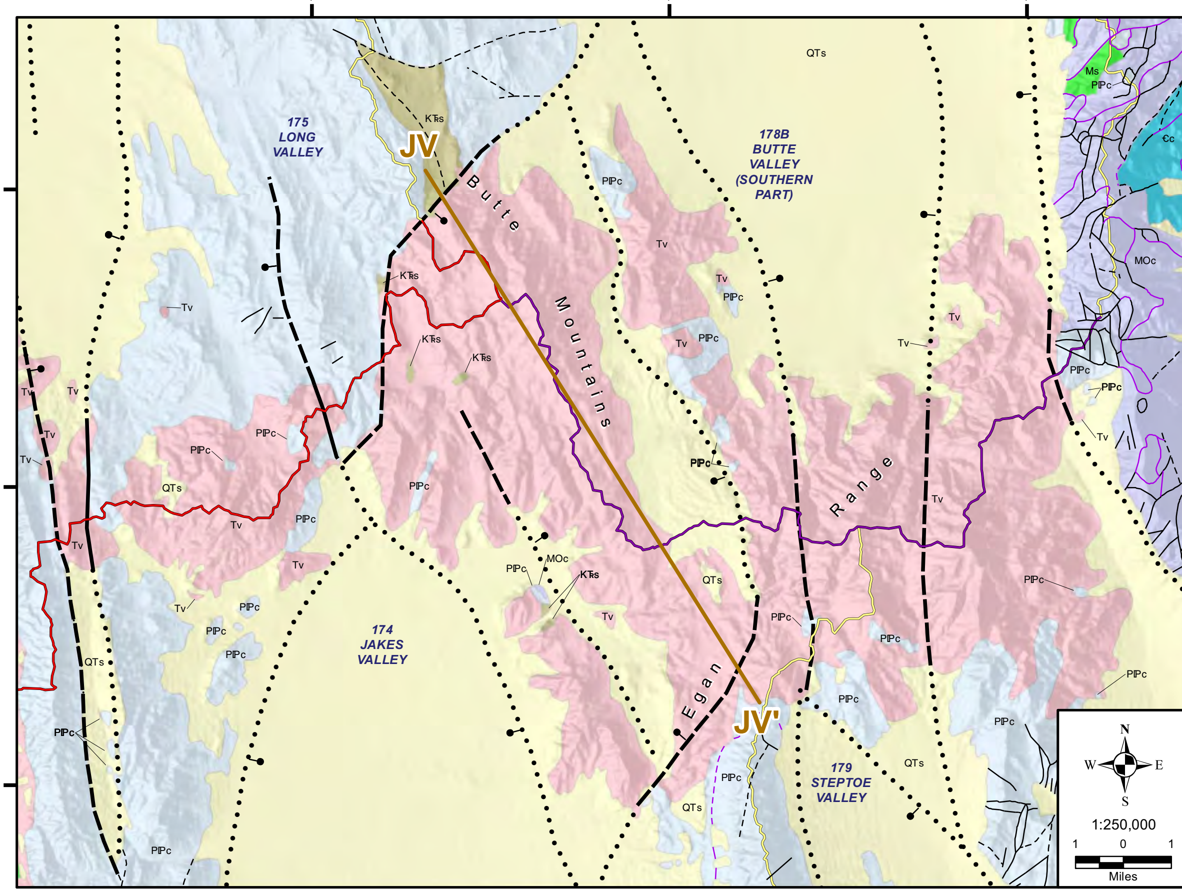

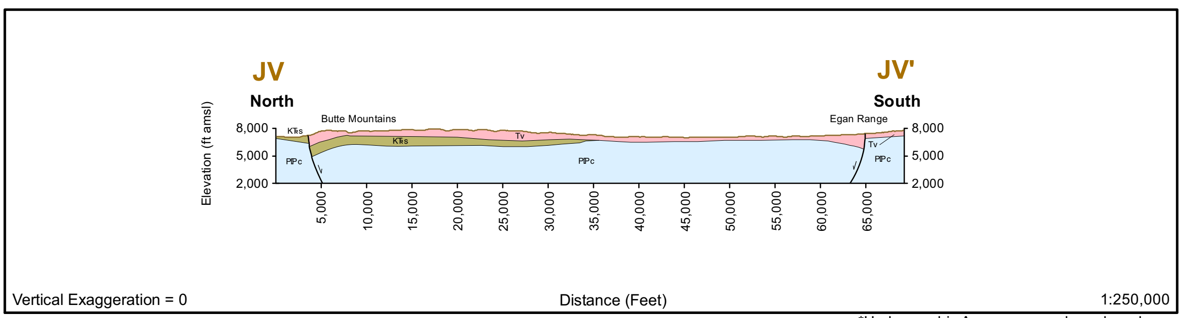

*Hydrographic Area name and number shown

Legend

Hydrogeology

Map Unit - Description

QTs	Quaternary-Tertiary sediments
Tv	Tertiary volcanic rocks
KTRs	Cretaceous-Triassic clastic rocks
PIPc	Permian-Pennsylvanian carbonate rocks
Ms	Mississippian clastic rocks
MOc	Mississippian-Ordovician carbonate rocks

Regional Faults

Normal fault

Solid where known; dashed where inferred; dotted where concealed. Bar and ball on downthrown side of fault.

Subsidiary Faults

Normal fault

Detachment fault

Solid where known; dashed where inferred; dotted where concealed; dotted and queried where uncertain. Bar and ball on downthrown side of fault.

Cross Section profile

Potential for Groundwater Flow Across Hydrographic Area* Boundary

Permissible

Likely

Unlikely

Grid based on Universal Transverse Mercator projection, North American Datum 1983, Zone 11N meters. Hillshade developed from 30-m DEM, Sun Angle 45°, Azimuth 315°.

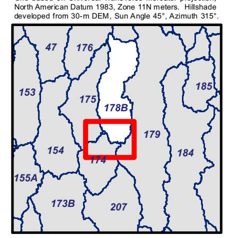

MAP ID 18073-3210 05/25/2011 BP

Figure 4-10
Hydrogeologic Map and Cross Section of Area between Butte Valley and Jakes Valley

normal faults that also create White River Valley to the east. Although relatively shallow at this latitude, near Preston and Lund, Nevada, White River Valley widens and becomes a deep, broad graben to the south, with a depth of more than 5,000 ft (see Section 4.4.4).

4.4.4 Horse, Grant, and Quinn Canyon Ranges

At the southern side of the White River caldera in northern Nye County, Nevada, the east-striking, oblique-slip Currant Summit fault zone (Moores et al., 1968; Williams and Taylor, 2002), part of the Prichards Station transverse zone, structurally separates the White Pine Range to the north from the small, 20-mi-long, north-trending Horse Range to the south. The Horse Range consists of east-dipping, lower to middle Paleozoic sedimentary rocks (Plates 4 and 8, Cross Section U—U'). The Horse Range is uplifted on its western side against thick, east-dipping volcanic rocks and basin-fill sediments to the west. The basin-fill sediments fill Horse Camp Basin (Moores et al., 1968; Brown and Schmitt, 1991), and the volcanic rocks form the eastern flank of the northern Grant Range and underlie the basin.

The Grant Range is 40 mi long, increasing in width southward. It, in turn, passes into the high, broad Quinn Canyon Range to the south, which is 15 mi north-south by 20 mi east-west. These ranges are bounded on the west by the deep graben of Railroad Valley, whereas the Horse and Grant ranges are bounded on the east by the large, deep graben of White River Valley. The Grant Range is underlain mostly by east-dipping Cambrian through Permian carbonate rocks (Lumsden et al., 2002) cut by several east-verging Sevier thrust faults (Taylor et al., 2000) and, in turn, intruded by a large Tertiary pluton in the central and southern parts of the range (Plates 4 and 8, Cross Section Q—Q'). Low-angle Tertiary detachment faults dip into Railroad Valley from both sides, especially the Grant Range on the east. Many subsurface detachments were detected during widespread exploration for oil in Railroad Valley (Lund et al., 1991; Schalla and Johnson, 1994; French and Schalla, 1998; Ehni and Faulds, 2002). The carbonate rocks plunge generally northward in the range, so Cambrian and Precambrian siliciclastic rocks and the Tertiary intrusive rocks form the core of the southern Grant Range and likely act as a barrier to groundwater flow between Railroad and White River valleys.

The Quinn Canyon Range, south of the Grant Range, is bordered by Garden Valley to the east, the southern end of Railroad Valley to the north and northwest, and Penoyer Valley (Sand Spring Valley) to the south. Garden Valley is a narrow graben several thousand feet deep, between the Quinn Canyon and Golden Gate Ranges (Plates 4 and 8, Cross Sections T—T' and Q—Q'). The Quinn Canyon Range is underlain by all or parts of several calderas (Ekren et al., in press), making up the southeastern part of what is referred to on Plate 1 as the central Nevada caldera complex. This feature, called a caldera complex by Best et al. (1993) and Scott et al. (1995), is not, however, a true caldera complex because not all of it has subsided as a caldera; instead, individual calderas are separated by pre-caldera rocks, so it might better be considered a cluster of adjacent calderas. The southwestern end of the Quinn Canyon Range, including the southern edge of the "caldera complex," passes into Lincoln County, where it is a narrow prong of outflow volcanic rocks. East of this prong and south of the main massive part of the range underlain by the caldera is Penoyer Valley (Sand Spring Valley), which is the single-basin Penoyer Valley Flow System (Harrill et al., 1988).

The calderas of the main mass of the Quinn Canyon Range are underlain by intracaldera (resurgent) plutons (see Plates 4 and 8, Cross Section T—T') that likely limit east-west groundwater flow between Railroad Valley and White River/Garden valleys. Fault conduits between Railroad Valley and Penoyer Valley are likely limited due to the presence of a buried caldera margin and perhaps the strong range-front fault along the western side of the Quinn Canyon Range.

Gravity surveys on the eastern side of White River Valley (Scheirer, 2005) suggest that the valley is underlain by many thousands of feet of basin-fill sediments and volcanic and carbonate rocks. We interpret that the White River Valley contains at least as much as 5,000 ft of valley fill (Dixon et al., 2007a and c) (Plates 4 and 8, Cross Sections Q—Q' and U—U'). The valley narrows southward east of the Seaman Range (here called Pahroc Valley) as the ephemeral White River was incised into Pleistocene basin-fill sediments during canyon cutting following drainage integration with the Colorado River (Dixon, 2007) (Plates 4 and 8, Cross Section T—T'). White River Valley receives its primary interbasin flow from Jakes Valley (Harrill et al., 1988). However, Welch et al. (2007) suggested an additional but significant contribution from Steptoe Valley that passes southwest through the southern part of Ely, then through the northern Egan Range (see, however, Section 6.0). In the southwest part of White River Valley, the geology is such that groundwater flow is permissible from southwestern White River Valley to Garden Valley. Also, it is likely for groundwater to flow from southwestern White River Valley into Coal Valley, and beneath the intermittent White River east of the Seaman Range into Pahroc Valley.

Springs are abundant in White River Valley, especially in the center of the valley and near Nevada Highway 318, which is west of the eastern side of the valley. Those in the center of the valley are warm and hot springs, some of which supply lakes that together were grouped and set aside as the Wayne Kirch Wildlife Management Area, managed by the Nevada Department of Wildlife. As far as we can tell, virtually all springs in White River Valley come up along north-trending basin-range faults, many of them with Quaternary displacement. Hydrologic data and geologic cross sections of most springs in White River Valley are discussed in Volume 3 of SNWA (2008), including Hot Creek Spring in the Kirch Wildlife Management Area (see also Section 6.2.2.1).

4.4.5 Worthington Mountains and Timpahute Range

The northern end of the narrow, 15-mi-long, north-trending Worthington Mountains is just southeast of the Quinn Canyon Range. The Worthington Mountains define the northeastern side of Penoyer Valley and the western side of southern Garden Valley. The Worthington Mountains consists mostly of west-dipping Ordovician through Mississippian rocks that are uplifted along a north-striking fault on the eastern side of the range. The range contains the east-verging Freiburg thrust, which placed Ordovician rocks on Ordovician and Devonian rocks during Sevier deformation (Taylor et al., 2000).

The Worthington Mountains extend southward into the Timpahute Range, an east-trending block of heavily faulted mountains. The Timpahute Range separates the southeastern side of Penoyer Valley from northern Tikaboo Valley. The Timpahute Range is underlain by Upper Cambrian through Permian sedimentary rocks, unconformably overlain by Tertiary volcanic rocks. The Paleozoic rocks are cut by several Sevier thrusts, the lowest of which places Devonian rocks over Devonian through Permian rocks. The uppermost thrust places Cambrian through Ordovician rocks above younger rocks (Taylor et al., 1994). The western end of the range includes the Tempiute mining district of tungsten and silver, associated with two Tertiary granite stocks. The range is heavily broken by north-south basin-range faults and synchronous east-west faults. The east-west faults, which define the southern margin of the range, are part of the Timpahute transverse zone, which also controls the northern side of the Caliente caldera complex.

Garden Valley, east of the Worthington Mountains, terminates southward against the eastern Timpahute Range. Garden Valley is a graben containing about 3,000 ft of basin-fill sediment (Plates 4 and 8, Cross Section T—T'). Penoyer Valley is bounded on the east by a range-front fault and on the south by the east-west Timpahute transverse zone. Penoyer Valley probably contains several thousand feet of basin-fill sediments.

Groundwater flow to the west of the southern Worthington Mountains is theoretically possible through the fractured Paleozoic carbonate and Tertiary volcanic rocks because of the north-northeast-striking faults connecting Garden Valley with Penoyer Valley at the northern end of the Worthington Mountains. This flow, however, has been considered minor by Belcher (2004) and for the purposes of this study is deemed unlikely (Figure 4-9). The eastern Timpahute Range is underlain by a granitic pluton and, therefore, groundwater flow between Garden Valley and the eastern arm of northern Tikaboo Valley is unlikely.

4.4.6 Golden Gate Range, Mount Irish, Pahranagat Range, and Northern Sheep Range

The Golden Gate Range is a 40-mi-long, string of low north-trending faulted hills that passes southward into Mount Irish, a 10-mi by 10-mi range bounded by east-striking faults. Mount Irish is the northernmost part of the larger, 35-mi-long Pahranagat Range, which continues southward to the 50-mi-long Sheep Range. The northern end of the Golden Gate Range, located in Nye County, Nevada, forms the western side of White River Valley and the eastern side of Garden Valley. The main part of this range forms the boundary between Garden and Coal valleys in Nye and Lincoln counties. In Nye County, the Golden Gate Range consists of Devonian through Pennsylvanian rocks overlain by Tertiary volcanic rocks. Here and farther south, the range is a west-tilted horst; the main controlling normal fault is on the eastern side. In Lincoln County, the rocks of the Golden Gate Range are Devonian to Pennsylvanian sedimentary deposits, of which Ordovician through Devonian rocks are thrust over Devonian to Mississippian rocks (Plates 4 and 8, Cross Section T—T'). In the central Golden Gate Range, the range is cross cut by two faults along related gaps that would allow groundwater to flow in a west to east direction into Coal Valley (Figure 4-9).

The Mount Irish Range is a stubby, east-trending block that is the eastern continuation of the Timpahute Range and is controlled by east-striking faults of the Timpahute transverse zone. Mount Irish is made up of Ordovician through Mississippian rocks containing the same thrusts including the Gass Peak thrust that occur in the Timpahute Range (Plates 4 and 8, Cross Sections O—O' and S—S') (Taylor et al., 1994 and 2000). The Mount Irish block closes the southern end of Coal Valley and it is unlikely that north-striking faults through the block allow groundwater flow at this location.

The Pahranagat Range, including a separate parallel structural block along the eastern side that is called the East Pahranagat Range, is bounded by Tikaboo Valley on the west and shallow Pahranagat Valley (Tingley et al., 2010) on the east. The Pahranagat Range (Page et al., 2005a; Jayko, 1990 and 2007) is a horst bounded on both sides by major normal faults (Plates 4 and 8, Cross Sections M—M' and N—N'). In the north, the range dips gently west but in the south it is a syncline. The east-verging

Gass Peak thrust of Sevier age runs the length of the range, placing Middle Cambrian to Devonian rocks on Devonian to Mississippian rocks. The East Pahranagat Range locally consists of an overturned fold of Devonian to Pennsylvanian rocks. Tertiary volcanic rocks unconformably overlie the folded and thrust-faulted Paleozoic rocks and are thickest where downfaulted into a graben between the Pahranagat Range and East Pahranagat Range. At their southern ends, the Pahranagat and East Pahranagat Ranges are separated from the northern Sheep Range by a series of east-northeast-striking splays of the predominantly left-lateral PSZ (Ekren et al., 1977; Johnson, M. 2007a). Figure 4-11 shows the PSZ with respect to basin boundaries and topographic features. The southern splay of the PSZ is the Maynard Lake fault zone (Plates 5 and 9, Cross Section A—A') (Tschanz and Pampeyan, 1970; Jayko, 1990 and 2007). The western part of this fault is interpreted to join the main north-south normal fault that defines the western side of the Sheep Range, and the eastern part of the fault is interpreted to join the main north-south normal fault that defines the western side of the Delamar Mountains (Figure 4-11). In this interpretation, the Maynard Lake zone—like the others of the PSZ—is an accommodation or transfer fault that transfers east-west extension (pulling apart) into left-lateral shear. In this scenario, in those places where faults strike north, all east-west extension is taken up by normal movement down the dip of the fault plane, and where faults strike northeast, east-west pulling apart is taken up by mostly left-lateral movement.

The northern Sheep Range is a narrow, abrupt mountain mass of Cambrian and Ordovician sedimentary rocks that make up the leading edge of the Gass Peak thrust fault of Sevier age (Plates 5 and 9, Cross Section L—L'; Page et al., 2005a). It is geologically likely that the subparallel faults of the PSZ provide conduits from southern Pahranagat Valley through the Pahranagat Range to Tikaboo Valley South. The most likely of these fault conduits is through the unnamed low pass between the Pahranagat Range and the Sheep Range, where the largest left-lateral fault zone, the Maynard Lake fault zone, cuts through brittle Tertiary ash-flow tuffs and Devonian dolomite at the pass (Figure 4-11).

Pahranagat Valley (see also Section 4.4.12), between the East Pahranagat Range on the west and the Hiko Range on the east, is a remarkably well-watered valley containing the agricultural communities of Hiko and Alamo, Nevada, and two large lakes that are the home of the Pahranagat National Wildlife Refuge (U.S. Fish and Wildlife Service). Structurally the valley is a shallow graben (Plates 4 and 8, Cross Sections S—S', O—O', N—N', and M—M'). Several large regional springs, including Hiko and Crystal springs and Ash Spring (Section 6.2.3.3), are controlled by basin-range faults (Dixon and Van Liew, 2007; Volume 3 of SNWA, 2008).

4.4.7 Southern Sheep Range, Las Vegas Range, and Elbow Range

The southern Sheep Range is underlain by mostly Cambrian and Ordovician carbonate rocks that dip eastward (Plates 5 and 9, Cross Sections E—E', F—F', G—G', and H—H') (Guth, 1980). The range is a large tilt block uplifted along major north-striking, basin-range normal faults on its western side. The range is on the upthrown western side of the low-angle, west-dipping Gass Peak thrust. The thrust transported Neoproterozoic to Cambrian quartzite and Cambrian to Devonian carbonate rocks eastward over Cambrian to Mississippian rocks. Within the Sheep Range, north-striking basin-range faults are abundant, but some cross-faults that strike east to east-northeast also have been mapped. Quaternary basin-range faults define much of the eastern side of the range (Dohrenwend et al., 1996).

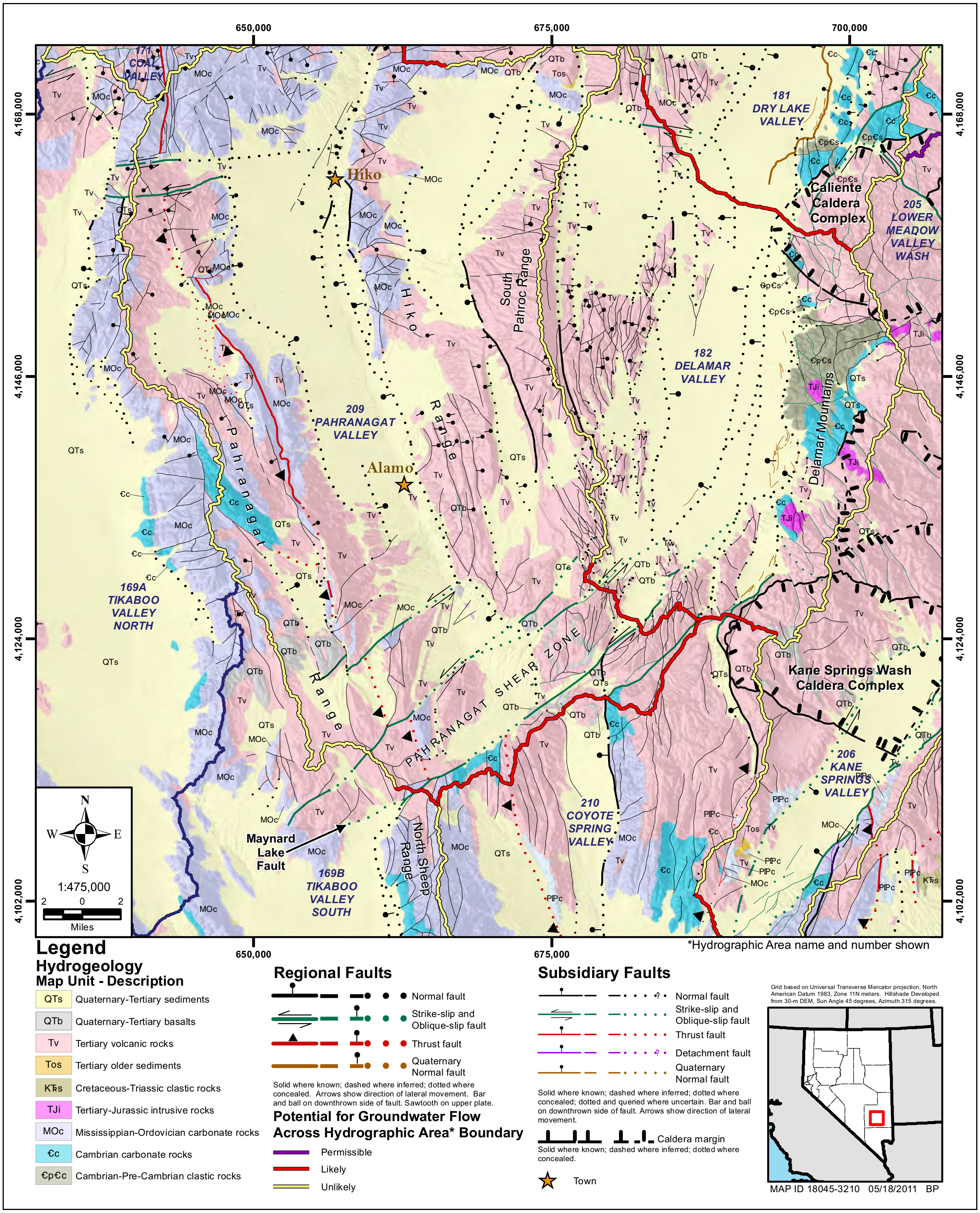

Figure 4-11
Hydrogeologic Map and Basin Boundaries of Pahranagat and Delamar Valleys and Vicinity

SE ROA 43200

JA_13080

A small, north-trending range (Figure 4-11) lies east of the northwestern arm of Coyote Spring Valley and west of Pahranagat Wash, U.S. Highway 93 (US 93), and the northeastern arm of Coyote Spring Valley. The small range is considered part of the northern Sheep Range but is separated from the high Sheep Range to the west by the northwestern arm of Coyote Spring Valley. The northern end of this small range terminates against the Maynard Lake fault zone of the PSZ. This small basin-range tilt block consists largely of east-dipping volcanic rocks (Jayko, 1990 and 2007) that rest unconformably on Pennsylvanian and Permian carbonate rocks. North-striking normal faults within, west, and east of the small range pass into the Maynard Lake fault zone and transfer their normal slip to oblique slip. The buried north-striking trace of the Gass Peak thrust fault passes beneath the normal faults near the western side of the small range.

The Las Vegas Range northwest of Apex is defined by the Gass Peak thrust, which transported rocks as old as the Cambrian Wood Canyon Formation eastward over Mississippian, Pennsylvanian, and Permian carbonate rocks of the Bird Spring Formation (Plates 5 and 9, Cross Sections F—F', G—G' H—H', and I—I') (Maldonado and Schmidt, 1991). Most of the range is made up of folded Bird Spring limestone, with the Gass Peak thrust exposed along its western side (Maldonado and Schmidt, 1991; Page, 1998). The small Elbow Range, which bounds the Las Vegas Range on the northeast, is made up of thrusted and folded Bird Spring Formation (Page and Pampeyan, 1996) that has been uplifted as a horst (Plates 5 and 9, Cross Sections E—E' and F—F'). The southern ends of the Sheep Range and Las Vegas Range, and continuing east, of the Arrow Canyon Range (Section 4.4.17), Dry Lake Range (Section 4.4.21), and Muddy Mountains (Section 4.4.21) terminate against the west-northwest-striking, oblique-slip (right-lateral and normal) Las Vegas Valley Shear Zone (LVVSZ), which defines the northern side of the Las Vegas basin (Workman et al., 2002a and b; Page et al., 2005a and b; Beard et al., 2007).

Faults of the PSZ, notably the Maynard Lake fault zone, provide likely flow paths from southern Delamar Valley (Section 4.4.12) to the southern boundary of Pahranagat Valley. The Maynard Lake fault zone provides a partial barrier to southward flow from southern Pahranagat and Delamar valleys, effectively damming the groundwater at this location (Rowley and Dixon, 2001; Rowley et al., 2001; Dixon et al., 2007a; Johnson, M. 2007b). Significant groundwater, however, works its way south through the barrier into Coyote Spring Valley (Harrill et al., 1988), largely along the north-trending normal faults and fractures bounding the small north-trending range west of US 93 and along the large north-trending normal fault east of US 93 that defines the eastern side of the northeastern arm of Coyote Spring Valley (Figure 4-12). All these north-trending faults join the Maynard Lake fault zone. In addition, some groundwater from Delamar Valley may follow the conduit into Coyote Spring Valley created by the unnamed fault of the PSZ south of the Maynard Lake fault.

The many basin-range faults that underlie and define the sides of Coyote Spring Valley provide the pathways for southward groundwater flow (Harrill et al., 1988; Schmidt and Dixon, 1995). About 15 mi south of the northern end of Coyote Spring Valley, faults on the western side of the Elbow Range and eastern side of the Sheep Range (Figure 4-12) provide pathways for groundwater flow to the south and Hidden Valley. Gravity data in Coyote Spring Valley (Phelps et al., 2000) indicate that much of Coyote Spring Valley is relatively shallow except for deeper internal grabens downthrown along faults just west of the Meadow Valley Mountains and west of the northern Arrow Canyon Range (see Section 5.2). The deeper graben just west of the Meadow Valley Mountains is oriented

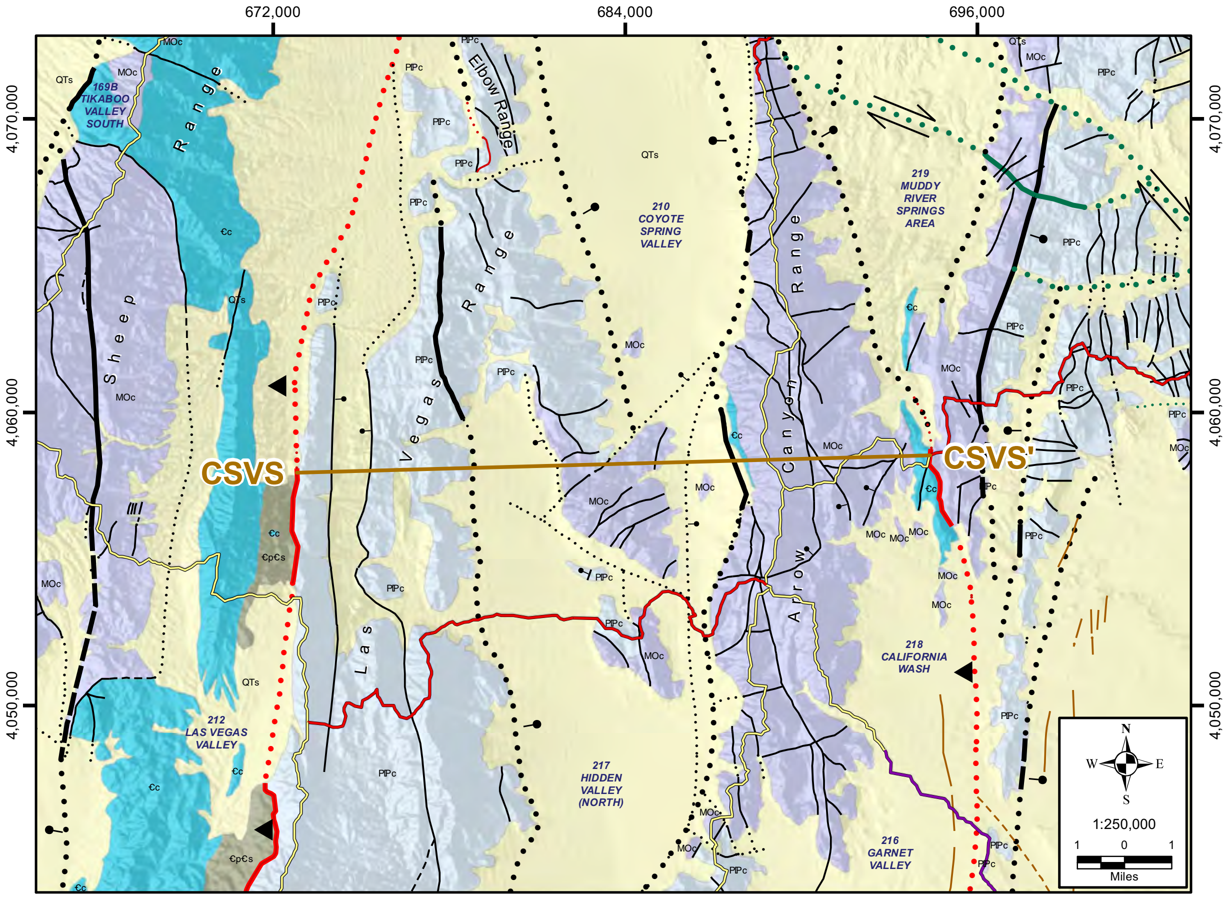

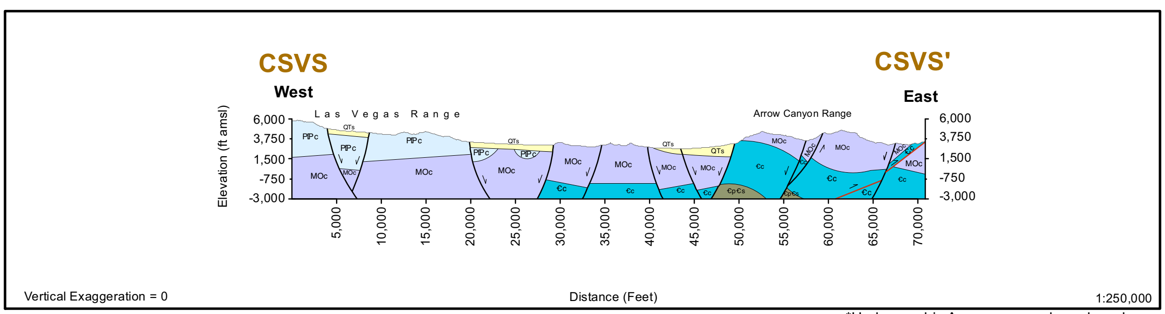

*Hydrographic Area name and number shown

Legend

Hydrogeology

Map Unit - Description

- QTs — Quaternary-Tertiary sediments
- PIPc — Permian-Pennsylvanian carbonate rocks
- MOc — Mississippian-Ordovician carbonate rocks
- Єc — Cambrian carbonate rocks
- ЄpЄs — Cambrian-Pre-Cambrian clastic rocks

Regional Faults

- Normal fault
- Strike-slip and Oblique-slip fault
- Thrust fault

Solid where known; dashed where inferred; dotted where concealed. Sawtooth on upper plate. Arrows show direction of lateral movement. Bar and ball on downthrown side of fault.

Potential for Groundwater Flow Across Hydrographic Area* Boundary

- Permissible
- Likely
- Unlikely

Subsidiary Faults

- Normal fault
- Strike-slip and Oblique-slip fault
- Thrust fault
- Quaternary Normal fault

Solid where known; dashed where inferred; dotted where concealed and queried where uncertain. Bar and ball on downthrown side of fault.

- Cross Section profile

MAP ID 18165-3211 05/18/2011 BP

Grid based on Universal Transverse Mercator projection, North American Datum 1983, Zone 11N meters. Hillshade developed from 30-m DEM, Sun Angle 45°, Azimuth 315°.

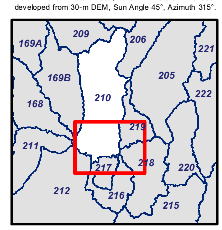

Figure 4-12
Hydrogeologic Map and Cross Section of Southern Coyote Spring Valley and Hidden Valley

SE ROA 43202

JA_13082

north-northwest, indicating that the controlling buried faults have the same trend. These faults serve to carry most groundwater beneath Pahranagat Wash and the eastern part of Coyote Spring Valley along a path that generally follows the Wash east, past the northern end of the Arrow Canyon Range and into small Table Mountain basin (Harrill et al., 1988). From there, most of this groundwater continues southeast and east-southeast, partly beneath and partly parallel to, but south of, Nevada Highway 168 along structurally-controlled flow paths to Muddy River Springs, then along structurally-controlled flow paths as underflow beneath the Muddy River to the Overton Arm of Lake Mead. This flow path is described in Sections 4.4.17 and 4.4.21.

It is likely that some of the groundwater beneath Coyote Spring Valley continues southward, parallel to US 93, along faults west of the western side of the Arrow Canyon Range and both east and west of the Elbow Range. A geologic map and cross section (Figure 4-12) shows many north-trending basin-range faults west of the Arrow Canyon Range that may carry groundwater. Groundwater in the vicinity of the cross section is known to be deep (700 to 800 ft), but it would be moving in Cambrian to Permian carbonate rocks that are locally heavily fractured along the faults, creating many likely flow paths. Perhaps the most important of these conduits shown on the cross section is the large western frontal fault of the Arrow Canyon Range, which would allow access of groundwater from southern Coyote Spring Valley into Hidden Valley.

4.4.8 Cherry Creek Range

The high Cherry Creek Range is in northern White Pine and southern Elko Counties. The range is a large horst of gently west-dipping Precambrian through Permian sedimentary rocks. Basin-range faults separate it from Butte Valley on the west and from Steptoe Valley on the east; the bigger fault is on the east.

A thin sliver of bedrock cored by a Tertiary intrusion connects the Cherry Creek Range with the northern Egan Range. A northeast-striking oblique-slip fault, left-lateral and down-to-the-west, cuts through the southern end of this sliver. Despite the suggestion of Harrill et al. (1988), it is unlikely that this fault provides an avenue for minor groundwater to flow from Butte Valley South to Steptoe Valley (Figure 4-9). This pluton, along with Precambrian and Cambrian quartzite into which it was intruded, form a likely barrier to groundwater flow north of the fault. The west dip of the rocks in the Cherry Creek Range would facilitate flow of recharge westward toward Butte Valley.

4.4.9 Northern Egan Range

Like the Cherry Creek Range to the north, the Egan Range is a high, north-trending horst of Precambrian through Permian rocks, unconformably overlain by Tertiary volcanic rocks. The major basin-range fault zone that uplifted the Egan Range is along the eastern side. The vertical displacement along this fault is as much as 20,000 ft. The range continues southward for 70 mi in White Pine County, then another 40 mi in Lincoln County. In the northern end of the range, the rocks dip westward and are intruded by Tertiary stocks. The Snake Range decollement is present here as a thin skin of Paleozoic rocks at the crest of the range and along its western slope (Plates 4 and 8, Cross Section X—X'). The decollement is a Tertiary denudation/attenuation fault that transported rocks as

SE ROA 43203

JA_13083

old as Middle Cambrian eastward and placed them on top of older rocks. Butte Valley is to the west and Steptoe Valley is to the east of the northern Egan Range.

About 20 mi south of the northern end of the Egan Range, the range becomes considerably wider and lower as the Butte Mountains join it from the west and Butte Valley closes. Here the range is broken into a series of horsts and grabens (Plates 4 and 8, Cross Section W—W'). The downthrown areas on the western side of the Egan Range are underlain by Tertiary volcanic rocks that form low ridges and hills that connect with the southeastern Butte Mountains. The towns of Ely and Ruth, Nevada, occur in this broad, low, heavily faulted part of the Egan Range, in areas called Copper Flat and Smith Valley. A major mining district, the Robinson district, was developed on a series of east-trending ore deposits of copper, molybdenum, lead, zinc, silver, and gold associated with a middle Cretaceous pluton. Barren Eocene rhyolite plutons and volcanic rocks also are present in the area and extend to Ely on the eastern side of the Egan Range adjacent to Steptoe Valley (Brokaw and Shawe, 1965; Brokaw and Heidrick, 1966; Brokaw and Barosh, 1968; Brokaw, 1967, Brokaw et al., 1973; Jones, 1996; Gans et al., 2001; Tingley et al., 2010). Southwest of the mining district, a series of low hills extends southwest to the White River caldera of the White Pine Range. These hills provide the southeastern margin of Jakes Valley and the north-northwestern margin of White River Valley (Figure 2-1).

South of the Robinson mining district, the Egan Range continues southward for almost 30 mi to the latitude of Lund as a single, high horst of east-dipping Cambrian through Permian rocks that together are more than 30,000 ft thick (Plates 4 and 8, Cross Section V—V') (Kellogg, 1963 and 1964; Taylor et al., 1991). Patches of volcanic rocks overlie the Paleozoic rocks on the eastern edge of the range. Several small plutons also are exposed. Major faults of the horst separate the Egan Range from the White River Valley to the west and southern Steptoe Valley to the east. Steptoe Valley is a deep graben containing as much as 8,000 ft of basin-fill sediments. Thus, it is one of the deepest grabens in the central Great Basin.

4.4.10 Southern Egan Range

At the latitude of Lund, Nevada, a narrow ridge of Cambrian to Permian rocks extends southeastward from the main part of the Egan Range to the Schell Creek Range to the east. This ridge, at Bullwhack Summit, forms the southern end of Steptoe Valley and the northern end of Cave Valley. The Egan and Schell Creek Ranges continue southward, with Cave Valley between them. Along the western side of Cave Valley (Plates 4 and 8, Cross Section U—U'), the Egan Range is a complexly faulted horst of east-dipping Cambrian to Permian rocks, overlain by Tertiary volcanic rocks. White River Valley is west of the Egan Range. Halfway southward down Cave Valley, at a latitude about 20 mi south of Lund, a northeast-striking oblique-slip fault passes through the Egan Range at Shingle Pass (Plates 4 and 8, Cross Section R—R') to join the western range-front fault of the Egan Range. Farther south, the Egan Range remains an east-tilted horst of Cambrian through Tertiary rocks, then bends southeast to join the southern end of the Schell Creek Range. Here Cave Valley terminates where the Egan and Schell Creek ranges join each other in a complex of north-northeast- and north-northwest-striking normal and oblique-slip faults. Farther south, the combined Egan and Schell Creek ranges become a low, narrow, north-northwest-striking horst of faulted Paleozoic sedimentary rocks and Tertiary volcanic rocks (Plates 4 and 8, Cross Section Q—Q') that topographically continues southward to the northern end of the North Pahroc Range.

Cave Valley consists of two distinct but connected portions, separated by the oblique-slip fault at Shingle Pass. One of these portions, northern Cave Valley, is a narrow graben containing mostly east-dipping Cambrian rocks at shallow depth overlain by relatively thin volcanic rocks and in turn basin-fill sediments (Plates 4 and 8, Cross Section U—U'). Gravity data (Scheirer, 2005) and oil test well logs (Hess, 2004) indicate that the base of the combined basin-fill sediments and volcanic rocks is about 3,000 ft below the valley floor of northern Cave Valley.

The fault at Shingle Pass likely provides a conduit for groundwater flow from northern Cave Valley into White River Valley (Figure 4-9). Shingle Pass is formed by the intersection of several major faults, but primarily it is defined by a northeast-striking, oblique-slip (left lateral and normal) fault zone (Figure 4-13). At the western end of Shingle Pass, this fault zone cuts through upper Paleozoic limestone on its northern side and lower Paleozoic limestone on its southern side. These rocks are brittle so the faults could be conduits to southwestward flow.

Southern Cave Valley is in Lincoln County and south of where the valley narrows to about 2 mi wide. The narrowing is due to a northeast-trending tilt block bounded on the northwest by the fault at Shingle Pass and striking northeast across most of Cave Valley. The block is buried but continues in the subsurface to the northeast to the large north-trending range-front fault zone that uplifts the Schell Creek Range (Plates 4 and 8, Cross Section R—R'). To the southwest, the tilt block swings into the main north-trending part of the Egan Range, which continues to the south. The tilt block consists of southeast-dipping Cambrian through Mississippian rocks that includes the Mississippian Chainman Shale, which is buried along the southeastern edge of the block. These relationships are supported by oil-test-well drilling, gravity surveys, seismic surveys and AMT profiles (Hess, 2004; McPhee et al., 2005, 2006a and b; Mankinen et al., 2006; Scheirer, 2005). Details are provided in Sections 5.1.4, 5.2.3, and 5.3. Despite the narrowing of the valley, a groundwater connection between northern and southern Cave Valley is considered certain because of flow along the north-striking, western range-front fault of the Schell Creek Range. Southern Cave Valley generally contains less than 3,000 ft of basin-fill sediments and volcanic rocks. In a narrow, central, north-trending axial part of the valley, however, these Cenozoic rocks are 6,000 ft or more thick. McPhee et al. (2005 and 2007) provided information on faults on the eastern side of the basin based on AMT profiles.

At the southern end of Cave Valley, a series of north-northwest-trending right-lateral oblique-slip faults and north-northeast-trending, left-lateral oblique-slip faults forms the boundary between southern Cave Valley, northern Pahroc Valley, and northern Dry Lake Valley. These faults provide likely and permissible groundwater pathways out of southern Cave Valley (Figure 4-9) into northern Pahroc Valley, and then potentially into northern Dry Lake Valley. A geologic map and cross section (Figure 4-14), oriented parallel to the basin boundary and perpendicular to flow, show several faults that may be conduits to southward flow through the Cave Valley boundary. The range-front, oblique-slip fault (left-lateral and normal) zone at the eastern end of the cross section juxtaposes Devonian dolomite against intrusive rocks. These rocks are brittle; they fracture easily and may form a significant fault conduit. The two faults farther west in the cross section cut through upper Paleozoic limestone, largely overlain by a relatively thin veneer of Tertiary ash-flow tuffs; such rocks also are brittle and would form permissible fault conduits.

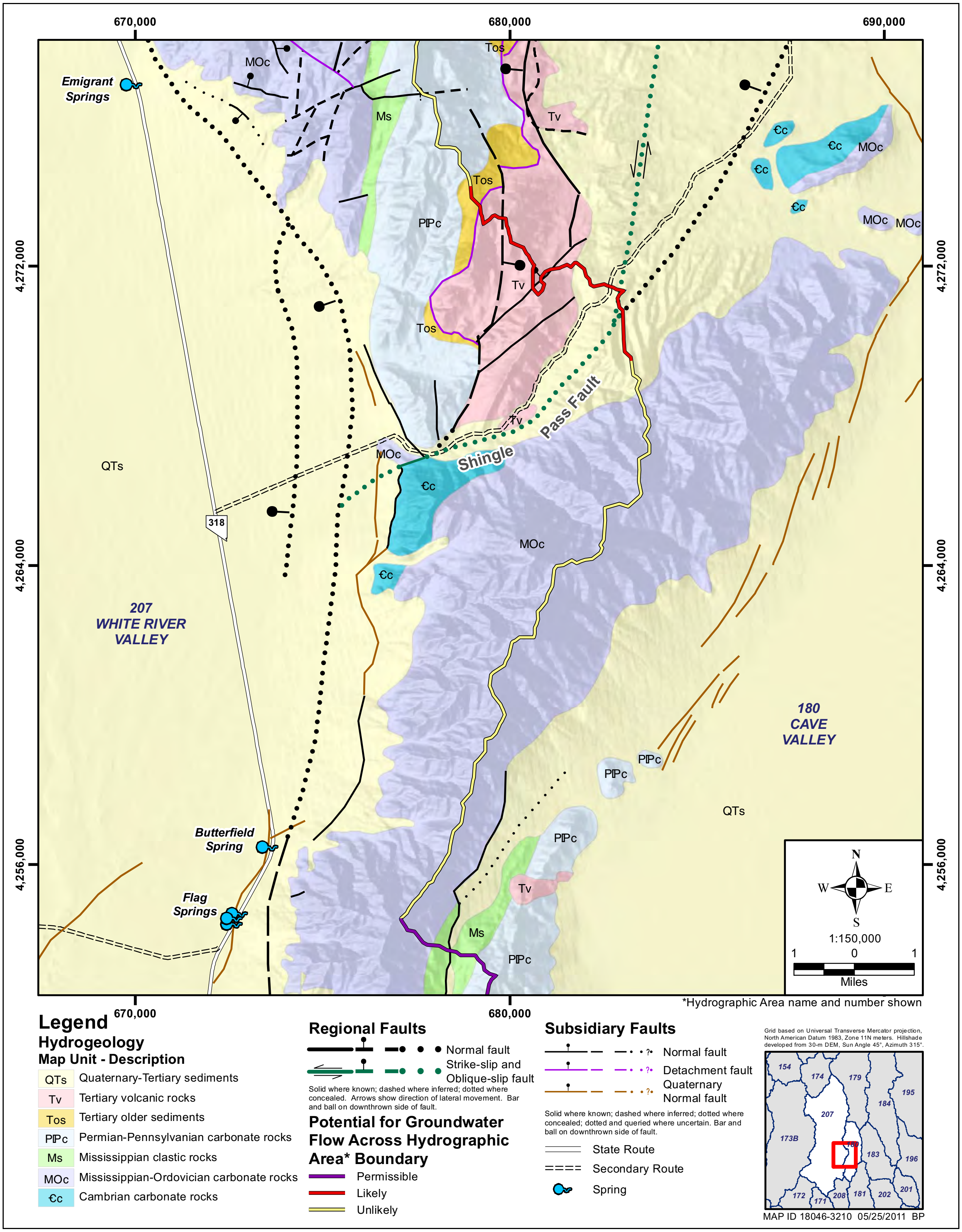

Figure 4-13
Hydrogeologic Map and Basin Boundaries of Shingle Pass Area

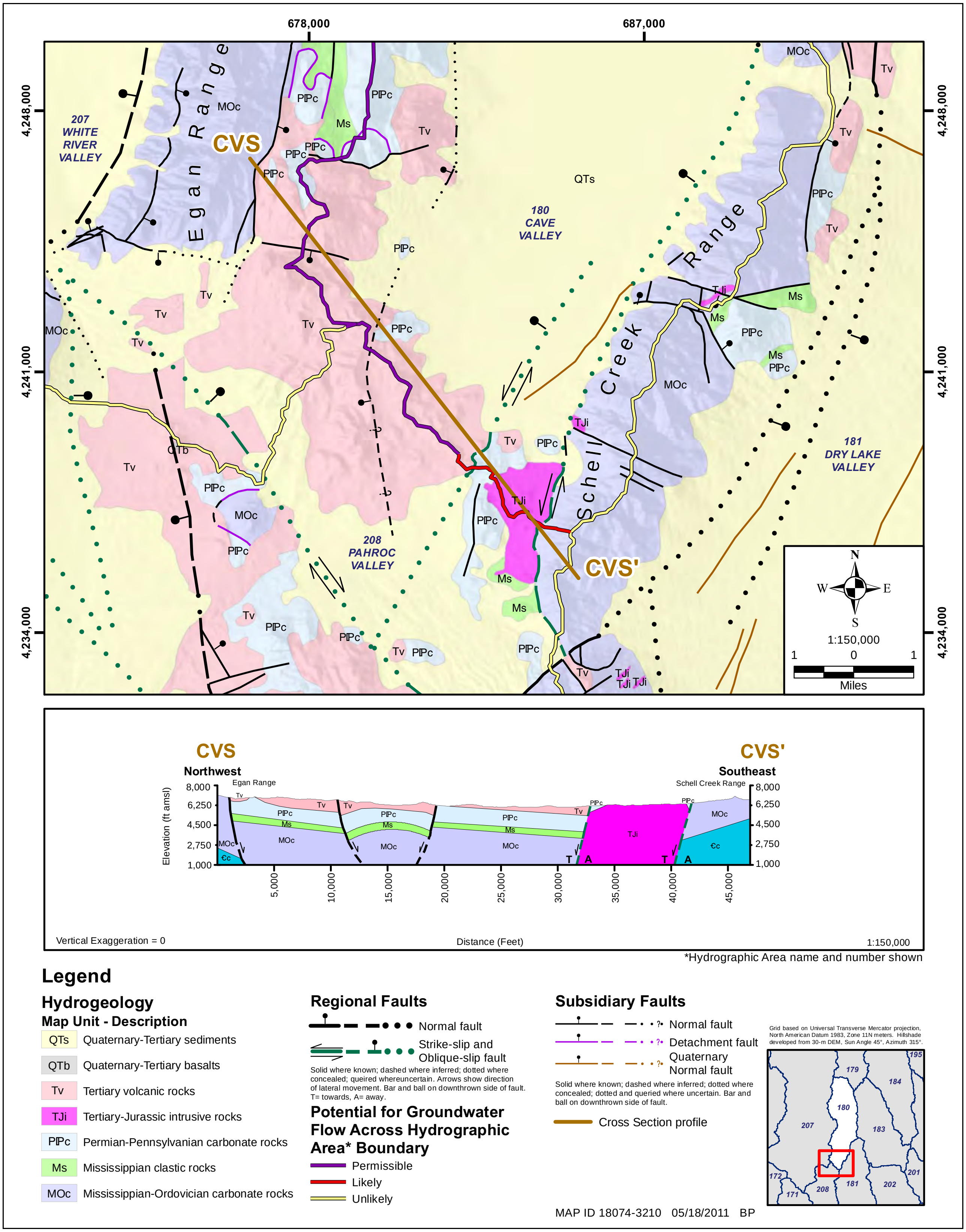

Figure 4-14
Hydrogeologic Map and Cross Section of Southern Cave Valley and Vicinity

SE ROA 43207
JA_13087

4.4.11 Seaman Range

The 35-mi-long, heavily-faulted Seaman Range, located in Nye and Lincoln counties, is a horst that trends north and northwest and joins the Golden Gate Range at the northern end of both ranges (Section 4.4.6). Coal Valley, between the two ranges, is a graben containing several thousand feet of basin-fill sediments (Plates 4 and 8, Cross Section T—T'). The valley is bounded on the south by the Timpahute Range. At its northern end, the Seaman Range is low and bounds the southern end of the White River Valley. In Nye County, the Seaman Range is made up of Devonian to Pennsylvanian sedimentary rocks, overlain unconformably by Tertiary volcanic rocks (duBray and Hurtubise, 1994). In Lincoln County, the Seaman Range is made up of gently west-dipping Ordovician to Pennsylvanian rocks that are unconformably overlain by Tertiary volcanic rocks. The Tertiary volcanic rocks include the dacitic to rhyolitic Seaman volcanic center of flows, subordinate tuffs, and a central plug (duBray and Hurtubise, 1994). It is likely that northwest-trending faults along Seaman Wash (southern end of the range) form conduits for movement of groundwater between Coal Valley and Pahroc Valley (Figure 4-9).

4.4.12 North Pahroc, South Pahroc, and Hiko Ranges

The North Pahroc Range extends south for 40 mi from the junction with the southern Egan and Schell Creek ranges. It is separated from the smaller South Pahroc Range by east-trending belt of faulted rocks of low relief formed by the east-striking Timpahute transverse zone. This zone of faulted rocks is also the boundary between Dry Lake Valley to the north and Delamar Valley to the south. The Seaman (Section 4.4.11) and the North Pahroc are separated by Pahroc Valley but the ranges join together at their southern ends; the Hiko Range continues south of this intersection. The Hiko Range is a small range parallel to and west of the South Pahroc Range and east of northern Pahranagat Valley. The South Pahroc Range is south of the North Pahroc Range and forms the western boundary of Delamar Valley. The South Pahroc Range connects with the Hiko Range at their southern ends to form the eastern boundary of southern Pahranagat Valley. The ephemeral channel of the White River is present along the western side of the North Pahroc Range. The channel is deeply incised through Tertiary volcanic rocks at White River Narrows, then enters the Pahranagat Valley north of the town of Hiko, where the ephemeral channel is called Pahranagat Wash. Pahranagat Valley (Section 4.4.6) is a graben west of the Hiko Range that contains volcanic and Paleozoic bedrock at shallow depth (Plates 4 and 8, Cross Sections S—S', O—O', and N—N').

The North Pahroc, South Pahroc, and Hiko ranges are complex horsts. The North Pahroc Range consists of upper Paleozoic rocks overlain by Tertiary volcanic rocks. These rocks dip west off major faults along the eastern side of the range. The South Pahroc Range is a series of west-tilted blocks of volcanic rocks; the main faults are on the eastern side of the range. The Hiko Range consists of Devonian rocks and overlying volcanic rocks that dip east off the normal fault that separates the range from the floor of Pahranagat Valley. The South Pahroc and Pahranagat ranges terminate to the south against the east-northeast-trending PSZ, which also terminates Pahranagat and Delamar valleys.

Dry Lake Valley is a deep graben (Plates 4 and 8, Cross Sections T—T', P—P', and S—S') east of the southern Schell Creek Range and North Pahroc Range that contains, in most places, 3,000 to 5,000 ft of basin-fill sediments (Mankinen et al., 2006; Dixon and Rowley, 2007d) but locally along the axis of the graben as much as 10,000 ft of sediments and underlying downfaulted volcanic and carbonate rocks (Scheirer, 2005). Delamar Valley, just south of Dry Lake Valley, is a southward-deepening graben with a general maximum thickness of more than 3,000 ft of basin-fill sediments east of the South Pahroc Range (Mankinen et al., 2006; Dixon and Rowley, 2007d) but locally as much as 5,000 ft of sediments and underlying downfaulted volcanic and carbonate rocks (Scheirer, 2005). AMT profiles that show some details of the faults in Dry Lake and Delamar valleys are given in Sections 5.2.4 and 5.2.5, respectively.

Groundwater flow is southward in Dry Lake and Delamar valleys (Harrill et al., 1988; Brothers et al., 1996; Dixon and Rowley, 2007d). The basin boundary between Dry Lake Valley and Delamar Valley is so low as to be imperceptible to a person standing on the ground. Here US 93 runs east-west along the boundary, traversing what appears to be a continuous north-trending valley. Bedrock made up of east-striking fault blocks of Tertiary ash-flow tuffs and lava flows are exposed along the basin boundary both west (Scott and Swadley, 1992; Scott et al., 1995) and east (Swadley and Rowley, 1994) of the valley, and regional tectonic studies (Rowley, 1998; Rowley and Dixon, 2001) indicate that the buried Timpahute transverse zone passes beneath the valley beneath US 93 and is exposed to the east and west of the valley. The depth-to-basement map (Figure 5-13) shows that the thickness of basin-fill sediments and volcanic rocks along the basin boundary is from 2,500 to 6,500 ft thick. This thickness at the basin boundary, as well as continuation through the basin boundary between Dry Lake Valley and Delamar Valley of north-trending basin-range that bound the ranges on either side of the combined valleys, indicate that any basin boundary is indeed superficial and that most groundwater continues on its southerly route across the boundary into Delamar Valley.

To shed more light on the likely path between Dry Lake Valley and Delamar Valley, a boundary-flow profile (geologic cross section), oriented crudely parallel to the basin boundary and perpendicular to the likely flow paths, is given in Figure 4-15. The geologic map and profile show range-front faults on either side of the combined valley and other major faults internal to the valley, all of which are likely conduits for groundwater flow from north to south.

The southern end of Delamar Valley is structurally complicated. It is defined by the northeast-trending PSZ (Ekren et al., 1977; Scott et al., 1995), which has at least 5 parallel, left-lateral faults, spread across a width of about 10 mi. Three of these faults enter southern Delamar Valley, where they pass into north-trending normal faults (Figure 4-11). In addition, other north-trending normal faults, some feeding into faults of the shear zone, define the east and west sides of Delamar Valley; some continue southward into Coyote Spring Valley. Harrill et al. (1988) expressed the complex nature of the faults when he showed three southward flow paths out of southern Delamar Valley. Two of the fault zones of the PSZ that enter southern Delamar Valley are the Delamar Lake fault to the north and the Maynard Lake fault to the south. The Maynard Lake fault continues southwestward to define the southern end of Pahranagat Valley and the Pahranagat Range and the northern end of the Sheep Range, then the fault enters Tikaboo Valley. AMT profiles made across both faults in southern Delamar Valley show (Section 5.2.5, Figures 5-27 and 5-28, respectively) that both are large subvertical faults that exhibit high conductivity. Flow along both faults is geologically classified as likely. Of these flow paths, the most significant is along or north of the larger fault, the Maynard Lake fault. Near Maynard Lake, some of the fractures in the fault zone served as vents for late Cenozoic basalt lava flows, so in addition to its central gouge zone, the fault is likely a barrier in most places to flow to the south. Thus the fault creates a natural dam that impounds southern Pahranagat Lake, in the southern end of Pahranagat Valley. In addition, the fault barrier allows some

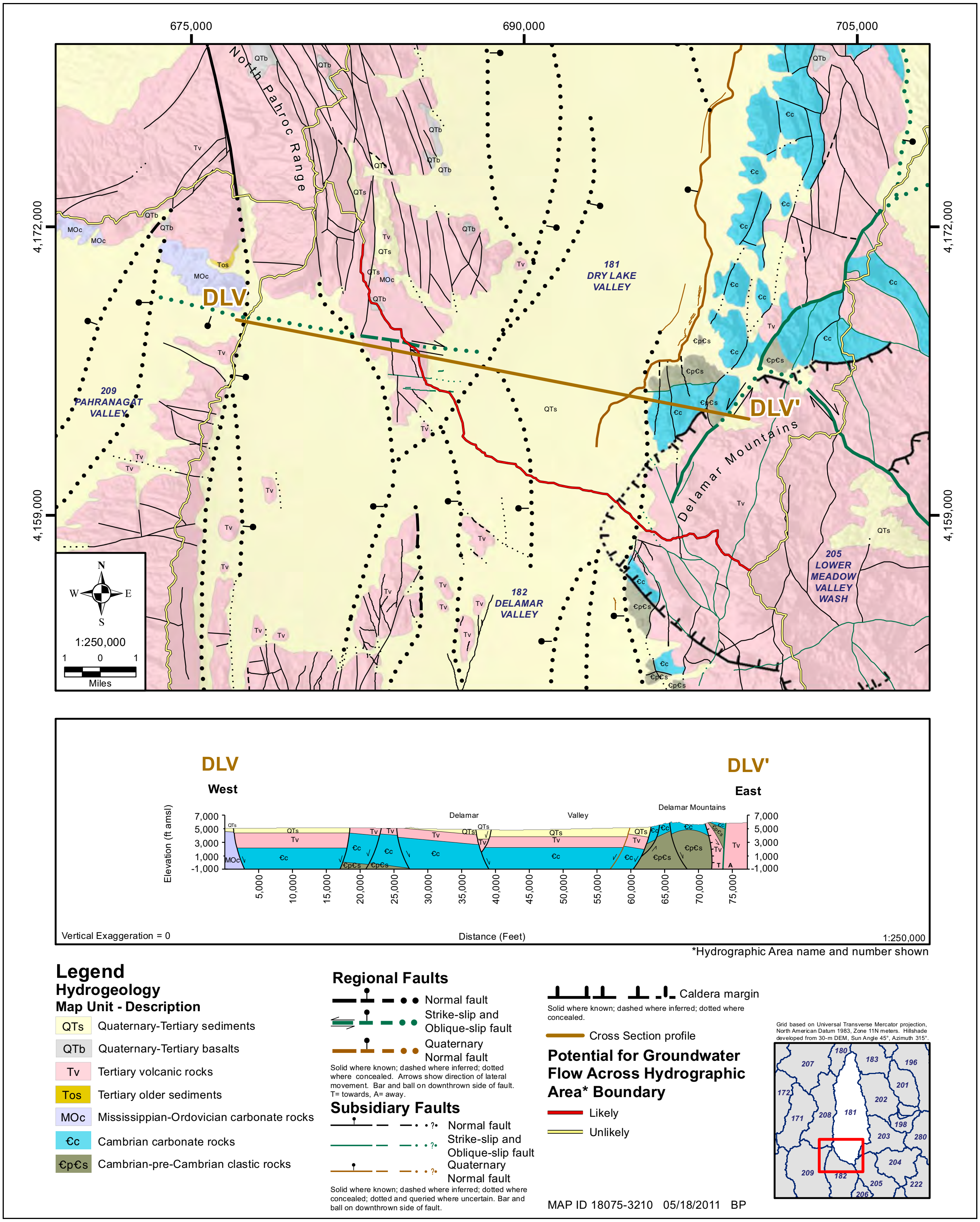

Figure 4-15
Hydrogeologic Map and Cross Section of Southern Dry Lake Valley and Northern Delamar Valley

SE ROA 43210

JA_13090

groundwater to pass along its northwest side into Tikaboo Valley (Section 4.4.6). Nonetheless, significant groundwater from Delamar and Pahranagat valleys passes southward through the Maynard Lake fault and along other left-lateral or normal faults into Coyote Spring Valley, although the exact multiple paths have yet to be determined (Rowley and Dixon, 2001, 2004; Johnson, M. 2007a).

4.4.13 Schell Creek Range

The northern end of the Schell Creek Range is just south of the northern border of White Pine County. The range continues south for 120 mi, mostly as a high, narrow, north-striking horst. Steptoe and Cave valleys are on the west, and Spring Valley, northern Lake Valley, and northern Dry Lake Valley (Muleshoe Valley) are on the east. The northern part of the Schell Creek Range is made up of a west-dipping sequence of Precambrian through Permian rocks (Lumsden et al., 2002), with overlying Tertiary volcanic rocks along the faulted western flank of the range (Plates 4 and 8, Cross Section X—X'). Small Tertiary intrusions are exposed locally along the range. The main bounding basin-range fault is on the eastern side of the range. The Snake Range decollement is locally exposed at the crest of the Schell Creek Range. This denudation/attenuation fault transported Middle Cambrian and younger rocks westward and eastward over Lower Cambrian and older rocks (Figure 4-8). About 10 mi northeast of Ely, two north-northeast-striking faults form a graben, Duck Creek Valley, in the range (Plates 4 and 8, Cross Section W—W'). The southern half of the Schell Creek Range along Cave Valley contains a narrow, heavily faulted sequence of Precambrian through Tertiary rocks that dips east. Here the dominant fault is on the western flank of the range. West of the Geyser Ranch (Johnson, M. 2007b) (Plates 4 and 8, Cross Section U—U') the rocks are mostly Neoproterozoic and Cambrian quartzite (Van Loenen, 1987), but farther south the rocks are dropped down along an east-trending fault at Patterson Pass and are mostly of middle to upper Paleozoic and Tertiary age (Plates 4 and 8, Cross Section R—R'). Where the Schell Creek Range joins the Egan Range, a Tertiary pluton has mineralized adjacent carbonate rocks at the Silver King Mine (Plates 4 and 8, Cross Section Q—Q').

Spring Valley is a broad, deep graben. On the southwestern side of Spring Valley, a thin ridge of gently northeast-dipping Pennsylvanian and Permian carbonate rocks extends southeast from the central Schell Creek Range to the Fortification Range; here the low pass traversed by US 93 is called Lake Valley Summit. Spring Valley continues southeast on the eastern side of the Fortification Range. South of the thin carbonate ridge is Lake Valley (Johnson, M. 2007a), between the Schell Creek Range and the Fortification Range. Lake Valley contains at least 2,000 ft of basin-fill sediments throughout its 60-mi length but locally the sediments may be much thicker (Plates 4 and 8, Cross Sections U—U', R—R', and Q—Q') (Scheirer, 2005). At the thin bedrock ridge between the Fortification Range and the Schell Creek Range, the combination of carbonate rocks here and a north-south fault cutting through would seem to create the potential for significant groundwater flow between southern Spring and northern Lake valleys, but the Chainman Shale, at shallow depth beneath the thin ridge, probably creates a barrier to flow, and we consider flow through the ridge unlikely. Water levels, in fact, suggest that the ridge is a groundwater divide (Burns and Drici, 2011). In contrast, Knochenmus et al. (2007) considered flow to be possible through it. The Schell Creek Range forms the northwestern boundary of Lake Valley for about 20 mi southward until it bends south-southwest to join the Egan Range.

Because much of the Schell Creek Range is covered by Precambrian to Cambrian quartzite, the range forms a barrier to flow between much of Steptoe Valley and Spring Valley. Knochenmus et al. (2007) and Welch et al. (2007), however, proposed two flow routes east through the Schell Creek Range from southern Steptoe Valley (see Section 6.0). Gravity data analyzed in Section 5.1.3 provide no support for these hypotheses.

On the eastern side of northern Cave Valley, the Schell Creek Range is cored by Precambrian to Cambrian quartzite, creating a likely barrier to flow between northern Cave Valley and Lake Valley (Figure 4-9). Farther south, at Patterson Pass, the quartzite sequence is down-faulted and carbonate and volcanic rocks and cross faults are present, but it is unlikely that groundwater flows between southern Cave Valley and Lake and northern Dry Lake valleys. Range-front faults on both sides of the southern Schell Creek Range further inhibit this flow.

Northern Dry Lake Valley, also known as Muleshoe Valley, lies east of the southern Schell Creek Range. This valley contains at least several thousand feet of basin-fill sediments (Plates 4 and 8, Cross Section Q—Q'), and gravity surveys (Scheirer, 2005) indicate that about 3,000 to more than 6,000 ft of basin-fill sediments plus underlying downfaulted volcanic rocks underlie most of the valley. A seismic profile across the valley is discussed in Section 5.3. It is permissible that some groundwater flows southward from Lake Valley through fault conduits at Muleshoe Pass, between the Schell Creek Range and the northern Fairview Range (Figure 4-9). Fault conduits provide pathways for groundwater flow from northern Dry Lake Valley to the south and into Delamar Valley.

4.4.14 Fairview, Bristol, West, Ely Springs, Highland, Black Canyon, Burnt Spring, and Chief Ranges, and Pioche Hills

From north to south, the Fairview, Bristol, Highland, and Chief Ranges are a 60-mi-long group of north-trending, heavily faulted ranges of mostly east-dipping rocks. These in-line horsts and tilt blocks lie west of Lake and Panaca (Meadow) valleys. From north to south, the West, Ely Springs, Black Canyon, and Burnt Spring ranges are small horsts along the western side of the Bristol, Highland, and Chief ranges. Northern Dry Lake (Muleshoe) Valley is west of the Fairview Range, and the rest of Dry Lake Valley is west of the West, Ely Springs, Black Canyon, and Burnt Spring ranges. The Pioche Hills, which extends southeast from the eastern side of the southern Bristol Range, separates Lake Valley on the north from Panaca (Meadow) Valley on the south. All the ranges are uplifted by normal and oblique-slip (left-lateral and right-lateral, normal) faults.

The Fairview Range touches the Schell Creek Range across Muleshoe Pass, through which runs the range-front faults for both the Schell Creek and Fairview Ranges. The Fairview Range is a horst made up of Devonian to Pennsylvanian rocks at both the northern and southern ends of the range. The central part of the range consists of the western lobe of the Indian Peak caldera complex. The low pass between the Fairview Range and the Bristol Range is cut by numerous east-striking faults of the Blue Ribbon transverse zone, which crosses the entire Great Basin at about this latitude (Rowley, 1998; Rowley and Dixon, 2001).

The Bristol Range is a horst that consists mostly of an east-dipping sequence of Cambrian carbonate rocks. The range is cored by a Tertiary pluton on the northern end that is associated with silver deposits of the Jackrabbit and Bristol districts. A low angle, west-dipping denudation or gravity-slide

SE ROA 43212

JA_13092

fault that placed Devonian rocks on Cambrian rocks is exposed in the northwestern part of the range (Page and Ekren, 1995). The Highland Range, the southward continuation of the Bristol Range, consists of east-dipping Cambrian carbonate rocks, underlain by Precambrian and Cambrian quartzite. A moderately west-dipping, down-to-the-west fault on the western side of the range, the breakaway part of the Highland detachment fault, placed the younger carbonate rocks on the older quartzite. The Chief Range, south of the Highland Range, is made up of east-dipping Precambrian and Cambrian quartzite that is unconformably overlain by Tertiary volcanic rocks and cut by a Tertiary pluton that controls the small Chief gold district (Rowley et al., 1994). The faults that lift the range on the western side consist of an oblique-slip fault (right lateral and normal) and the west-dipping Highland detachment fault.

The small West Range, to the west of the northern Bristol Range, consists of Devonian sedimentary rocks and Tertiary volcanic rocks on which Devonian rocks are emplaced by a low-angle fault that can be interpreted as either a denudation fault or a gravity-slide plane (Plates 4 and 8, Cross Section T—T') (Page and Ekren, 1995). The Ely Springs Range, south of the West Range and northwest of the Highland Range, consists of Cambrian through Silurian rocks, overlain by Tertiary volcanic rocks. The Black Canyon Range, south of the Ely Springs Range and southwest of the Highland Range, consists of Cambrian sedimentary rocks and Tertiary volcanic rocks (Plates 4 and 8, Cross Section P—P'). The Burnt Springs Range, southwest of the Black Canyon Range, is made up of Cambrian sedimentary rocks unconformably overlain by Tertiary volcanic rocks (Plates 4 and 8, Cross Section S—S').

The Pioche Hills consists of Cambrian sedimentary rocks unconformably overlain to the northeast by Tertiary volcanic rocks (Dixon and Rowley, 2007b). The hills contain the major Pioche lead-zinc-silver mining district, which is controlled by its proximity to the margin of the Indian Peak caldera complex. The margin includes caldera-collapse megabreccia and caldera ring dikes. Panaca (Meadow) Valley, south of the Pioche Hills, is probably at least 5,000 ft deep (Plates 4 and 8, Cross Section P—P') and is filled with Pliocene to upper Miocene basin-fill sediments of the Panaca Formation (Rowley and Shroba, 1991).

The presence in the Bristol, Highland, and Chief ranges of near-surface Neoproterozoic to Cambrian quartzite results in a barrier to groundwater flow between Lake, Patterson (southern Lake) and Panaca (Meadow) valleys to the east and Dry Lake Valley to the west (Figure 4-9). Across the Fairview Range, a barrier to flow results from the Indian Peak caldera complex due to probable subsurface intracaldera intrusions and their contact metamorphic and hydrothermal products. A permissible fault conduit from Lake to Dry Lake valleys exists for flow through Muleshoe Pass at the northern end of the Fairview Range (Figure 4-9).

4.4.15 Delamar Mountains

The Delamar Mountains extends southward for 40 mi from the Burnt Springs Range, forming the western side of Delamar Valley and continuing to Coyote Spring Valley. The boundary between the Delamar and Burnt Spring ranges is the northern caldera wall of the Caliente caldera complex, here controlled by the east-trending Timpahute transverse zone (Ekren et al., 1976; Swadley and Rowley, 1994; Rowley, 1998). The eastern side of the northern Delamar Mountains is bounded by the perennial, south-flowing Meadow Valley Wash, which drains Panaca (Meadow) Valley, passes south through Caliente, Nevada, and then creates beautiful Rainbow Canyon that separates the Delamar Mountains from the Clover Mountains to the east (Dixon and Rowley, 2007c; Tingley et al., 2010). The stream becomes ephemeral at the southern end of Rainbow Canyon, but in the Pleistocene it was part of through-flowing drainage that joined the Muddy River at Glendale, Nevada, and from there to the Colorado River. The eastern side of the southern Delamar Mountains is Kane Springs Valley, to the east of which is the Meadow Valley Mountains.

The Delamar Mountains consists of east-dipping Neoproterozoic to Cambrian rocks and Tertiary volcanic rocks. The range, however, is dominated by Tertiary caldera complexes. The western end of the Caliente caldera complex is in the northern part of the range, and the Kane Springs Wash caldera complex is in the central part of the range (Plates 4 and 8, Cross Sections N—N', D—D', and C—C') (Rowley et al., 1995; Scott et al., 1995 and 1996; Dixon et al., 2007b). The main bounding fault of the Delamar Mountains is the down-to-the-west normal fault on the western side, and this is joined from the southwest by several splays of the left-lateral and normal PSZ (Ekren et al., 1977). In Kane Springs Valley, the bounding fault is the oblique (left-lateral and normal down-to-the-west) Kane Springs Wash fault zone (Swadley et al., 1994). Flow from southern Delamar Valley is likely through the PSZ and north-striking normal faults into Pahranagat and Coyote Springs valleys (see Figure 4-9 and Figure 4-12).

Neoproterozoic to Cambrian quartzite and shale and Tertiary caldera complexes form an effective barrier to groundwater flow between Delamar Valley and valleys to the east (Figure 4-9). The calderas are barriers primarily because of their underlying intracaldera intrusions and both hydrothermal clays and contact-metamorphic rocks formed by emplacement of the intrusions into intracaldera tuffs. North- and northeast-striking basin-range faults just west of the calderas provide geologically likely conduits for groundwater to southern Pahranagat and northern Coyote Springs valleys.

4.4.16 Meadow Valley Mountains

The Meadow Valley Mountains constitutes a narrow, generally low, north-northeast-trending range about 40-mi-long. The northern 30 mi of the range consists mostly of outflow ash-flow tuffs and part of the Kane Springs Wash caldera complex (Plates 4 and 8, Cross Section C—C'). The southern end of the Meadow Valley Mountains, just east of Coyote Spring Valley, is made up of mostly thrust-faulted and normally faulted Paleozoic rocks (Plates 4 and 8, Cross Sections C—C', Plates 5 and 9, Cross Sections B—B', E—E', and F—F') (Pampeyan, 1993; LVVWD, 2001). The Meadow Valley Mountains is separated from the Delamar Mountains on the west by Kane Springs Valley, a shallow valley underlain along the eastern side by the oblique-slip (normal, left-lateral) Kane Springs Wash fault zone (Swadley et al., 1994; Harding et al., 1995; Scott et al., 1996). The broad, deep valley of Meadow Valley Wash lies east of the Meadow Valley Mountains and west of the Mormon Mountains (Schmidt, 1994).

The Kane Springs caldera, north-northeast-striking oblique faults, and thrusts likely prevent groundwater flow between Kane Springs Valley and the valley of Meadow Valley Wash.

4.4.17 Arrow Canyon Range

The Arrow Canyon Range is a sharp, narrow, north-trending range consisting of a syncline of Cambrian to Mississippian carbonate rocks. It is uplifted along its western side by normal faults of the Arrow Canyon Range fault zone (Plates 5 and 9, Cross Section I—I') (Schmidt and Dixon, 1995; Page and Pampeyan, 1996; Page, 1998). The trace of the north-striking Dry Lake thrust, which carries Cambrian rocks over Silurian through Permian carbonate rocks, is exposed and projected north just east of the range (Page and Dixon, 1992; Schmidt and Dixon, 1995; LVVWD, 2001). East of the Dry Lake thrust, the Silurian through Permian rocks form a series of low, unnamed, north-trending hills. These hills are controlled by north-striking normal faults, along some of which are Pleistocene carbonate spring-mound deposits that indicate that the faults formerly carried significant groundwater (Schmidt and Dixon, 1995).

Coyote Spring Valley, on the western side of the range, is underlain by thin basin-fill sediments, generally less than 1,000 ft thick (Plates 5 and 9, Cross Sections L—L', E—E', F—F', and G—G'; Section 5.2). Groundwater moves south beneath Coyote Spring Valley (Section 4.4.7). A major part of that groundwater flows southeast, between the northern end of the Arrow Canyon Range and the southwestern end of the Meadow Valley Mountains (Figure 4-16; Harrill et al., 1988). Here it flows past the MX-4 and high-yield (3,400 gpm) MX-5 wells, drilled in the 1980s by the military adjacent to Pahranagat Wash during the MX Missile Program (Buqo, 2007). Pahranagat Wash is currently an intermittent stream but was perennial after White River Valley was integrated with the Colorado River, at least ten thousand years ago. Some groundwater also may flow through the Arrow Canyon Range in its carbonate rocks. It is well known that the southeast-flowing groundwater is the principal source of many large springs in the Muddy River Springs area, which currently create the surface flow in the perennial part of the Muddy River below the springs (Schmidt and Dixon, 1995; Donovan et al., 2004; Buqo, 2007; Donovan, 2007; Johnson, J. 2007).

The details of the groundwater flow to Muddy River Springs were determined in part from the geologic mapping by Page and Pampeyan (1996), Schmidt et al. (1996), and Donovan et al. (2004), and the geophysics of Scheirer et al. (2006). The mapping recognized that, following stream integration during the late Pleistocene, ancestral Pahranagat Wash flowed southeast—as it does now—through a small basin (Table Mountain basin) just east of the northern Arrow Canyon Range that is underlain by the Muddy Creek Formation and younger Holocene to late Miocene surficial and basin-fill sediments. Many of the younger sediments were deposited from spring discharge. From that basin, the ancestral river continued southeast, parallel to and south of Nevada Highway 168, through an unnamed ridge of north-trending, east-dipping, upper Paleozoic carbonates. The ridge is the southward continuation of the southeastern prong of the Meadow Valley Mountains. Here the ancestral stream cuts spectacular Arrow Canyon, which is currently dry; at Muddy River Springs, dry Pahranagat Wash becomes the Muddy River.

Additional geologic mapping by SNWA showed that the bedrock ridge continues, although locally buried, for 20 mi south of Arrow Canyon to become the Dry Lake Range (Plates 2 and 5, Cross Sections F—F', G—G', H—H', and I—I'). The bedrock ridge is uplifted on both sides by north-trending basin-range faults, the largest being on the western side. These faults, plus others that parallel them on the east, served as groundwater conduits that carried groundwater southward, forming several upper Pleistocene spring mounds north of I-15 and west of the railway stop of Ute.

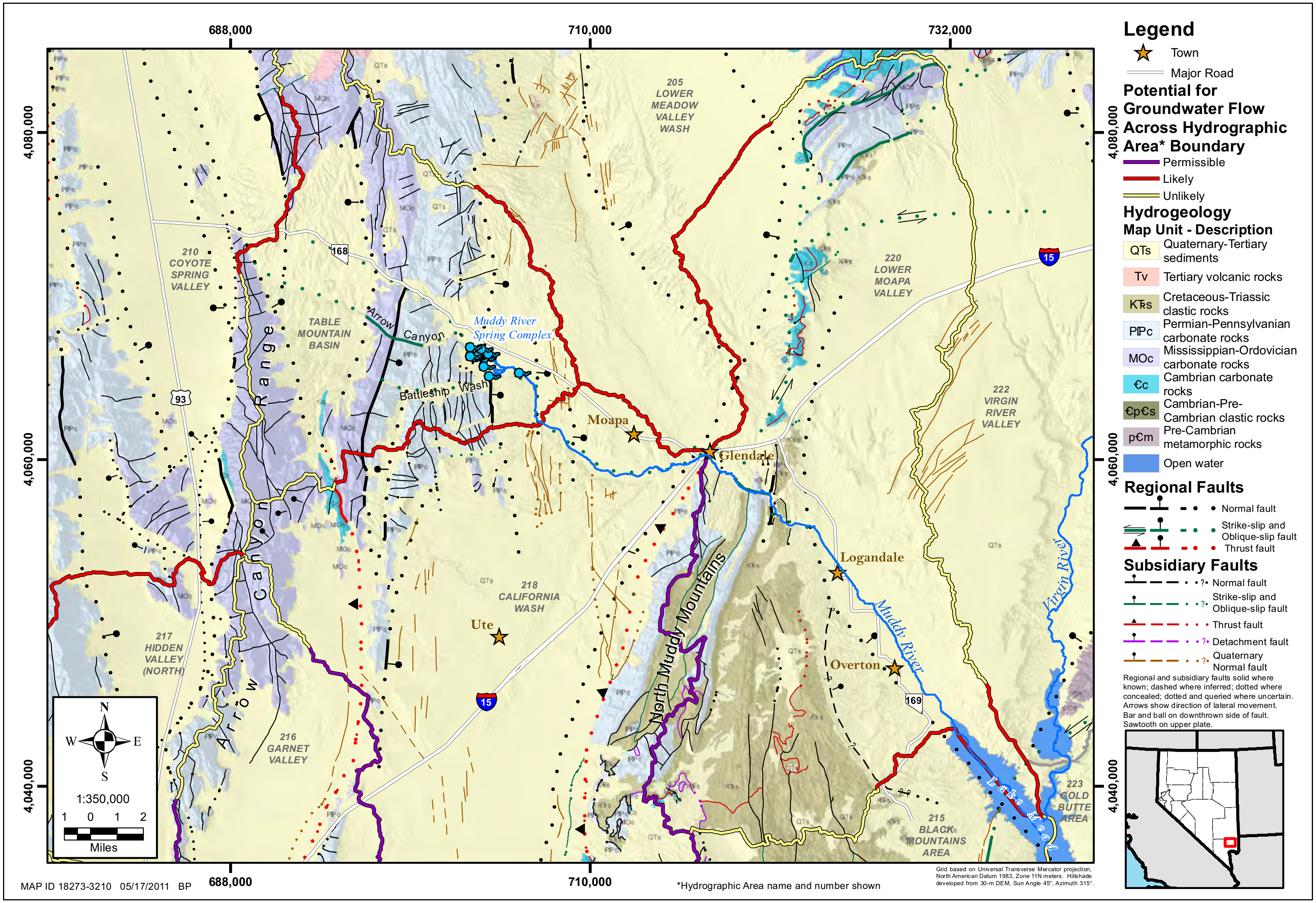

Figure 4-16
Hydrogeologic Map of Coyote Spring Valley to Lake Mead

SE ROA 43216

JA_13096

Within the bedrock ridge, east-trending faults are abundant, including some that control Arrow Canyon and Battleship Wash just to the south. These faults act as conduits that allow groundwater to pass eastward through the ridge to Muddy River Springs. In addition, mapping suggests that a west-northwest-trending fault zone, probably with right-lateral motion, formed a broad canyon now followed by Highway 168 that was probably another large ancestral stream that carried surface water, with groundwater beneath it. The geologic map presented on Figure 4-17 shows these details. The large, north-trending, down-to-the-east, normal fault at the western end of the cross section is the main control on Muddy River Springs. Virtually all springs in the Muddy River Springs complex are at fault intersections of east-, north-, and northwest-trending faults. Locally the faults created abrupt Pleistocene scarps, some of which failed as landslides (Donovan et al., 2004). White, post-Muddy Creek Formation (Pliocene) sediments were deposited by spring discharge east-southeast of Muddy River Springs, in upper Moapa Valley. Current groundwater flow continues southeast of Muddy River Springs as underflow beneath the Muddy River. The new mapping indicated that west- to northwest-trending faults appear to control nearly the entire course of the Muddy River between Muddy River Springs and Logandale (Figure 4-16), including the course of the river through the North Muddy Mountains (at Jackman Narrows). At Glendale, groundwater beneath Meadow Valley Wash combines with that beneath the Muddy River, then continues through The Narrows to Logandale, and from there to Overton and Lake Mead (Harrill et al., 1988). The passage through the North Muddy Mountains to Logandale is interpreted to be as surface flow and underflow in fractures beneath the fault-controlled passageway at and east of The Narrows. As described in Section 4.4.21, north-northwest-trending faults probably controlled the course of the Muddy River from Logandale to Overton, as well as the Overton Arm of Lake Mead (Figures 4-16 and 4-18).

Some of the faults suggested by new mapping between Table Mountain basin and Lake Mead are buried by surficial sediments. To test the likelihood of faults in these areas, Scheirer and Andreasen (2008) interpreted gravity data that they collected along traverses oriented perpendicular to buried parts of some of the possible faults. The gravity data supported faults beneath Pahranagat Wash in Table Mountain basin (gravity line 2 of Scheirer and Andreasen, 2008), along Nevada 168 in Table Mountain basin (gravity lines 1 and 2) and perhaps north of Muddy River Springs (gravity line 3), perhaps at Muddy River Springs (gravity line 3), beneath the Muddy River south of Moapa (gravity line 4se), and perhaps in three places near Overton (gravity line 12).

4.4.18 Fortification Range, Wilson Creek Range, and White Rock Mountains

The Fortification Range is a narrow, locally high, north-northwest-trending range about 20-mi-long. The range is a horst bounded on both sides by normal faults. Northern Lake Valley is on the west, and the southern end of Spring Valley is on the east. The northern half of the Fortification Range is a series of faulted, upper Paleozoic carbonate rocks including, at the northern end, a narrow, low, north-northwest-trending, northeast-dipping cuesta that joins the eastern side of the Schell Creek Range. This low ridge, which separates Spring Valley on the northeast from Lake Valley on the southwest, is a groundwater divide, as noted in Section 4.4.13. Geological reasons for the ridge being a groundwater divide are that the ridge is bounded on the northeastern side by a northwest-striking fault and the ridge is underlain by the Chainman Shale, which is probably more than 1,000 ft thick (Plates 4 and 8, Cross Sections U—U'). The northern Fortification Range is complexly faulted and contains repeated sections of the Chainman Shale beneath the surface. The presence of the Chainman in the fault blocks likely prevents groundwater flow through the northern half of the range.

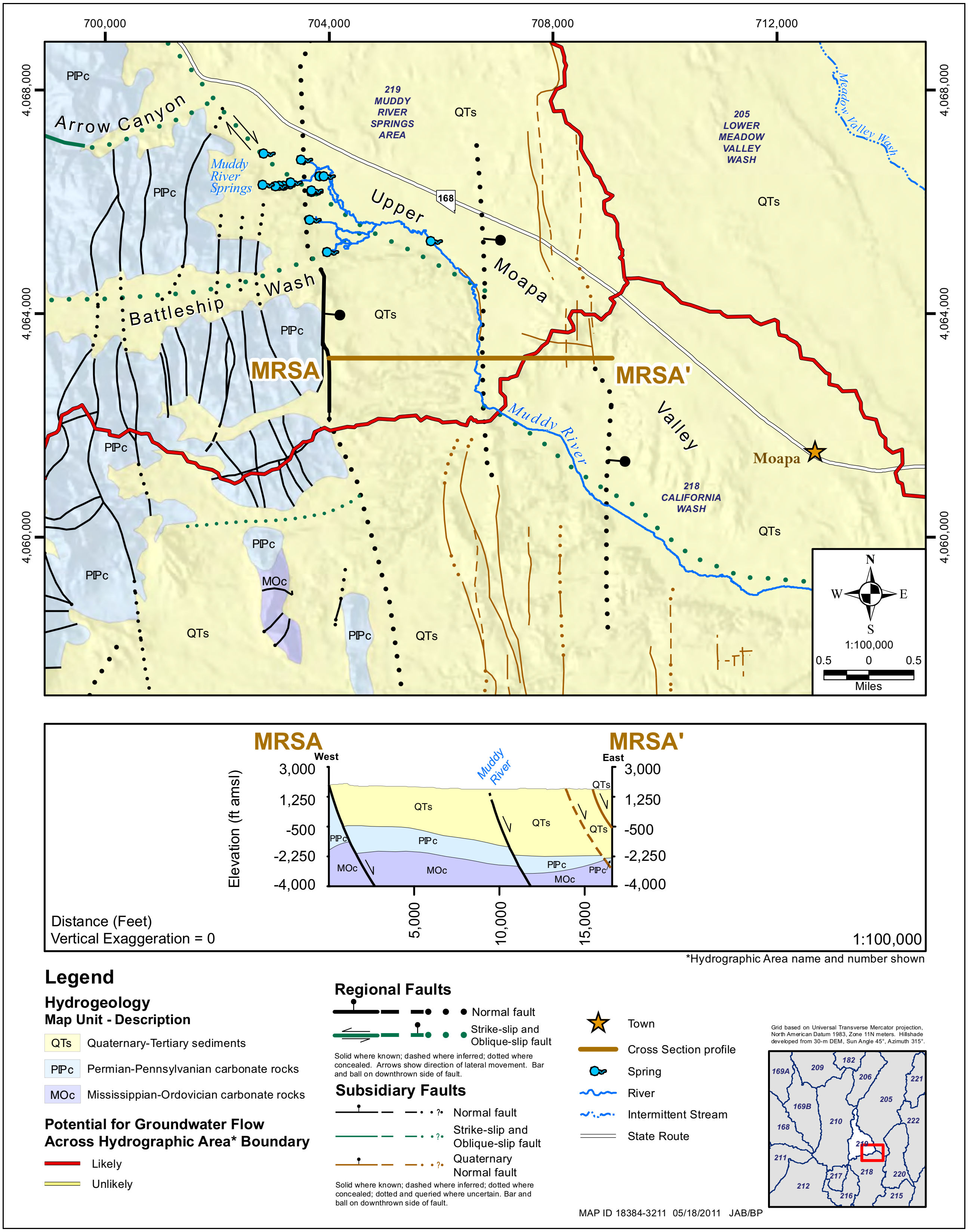

Figure 4-17
Hydrogeologic Map and Cross Section of the Muddy River Springs Area

SE ROA 43218

JA_13098

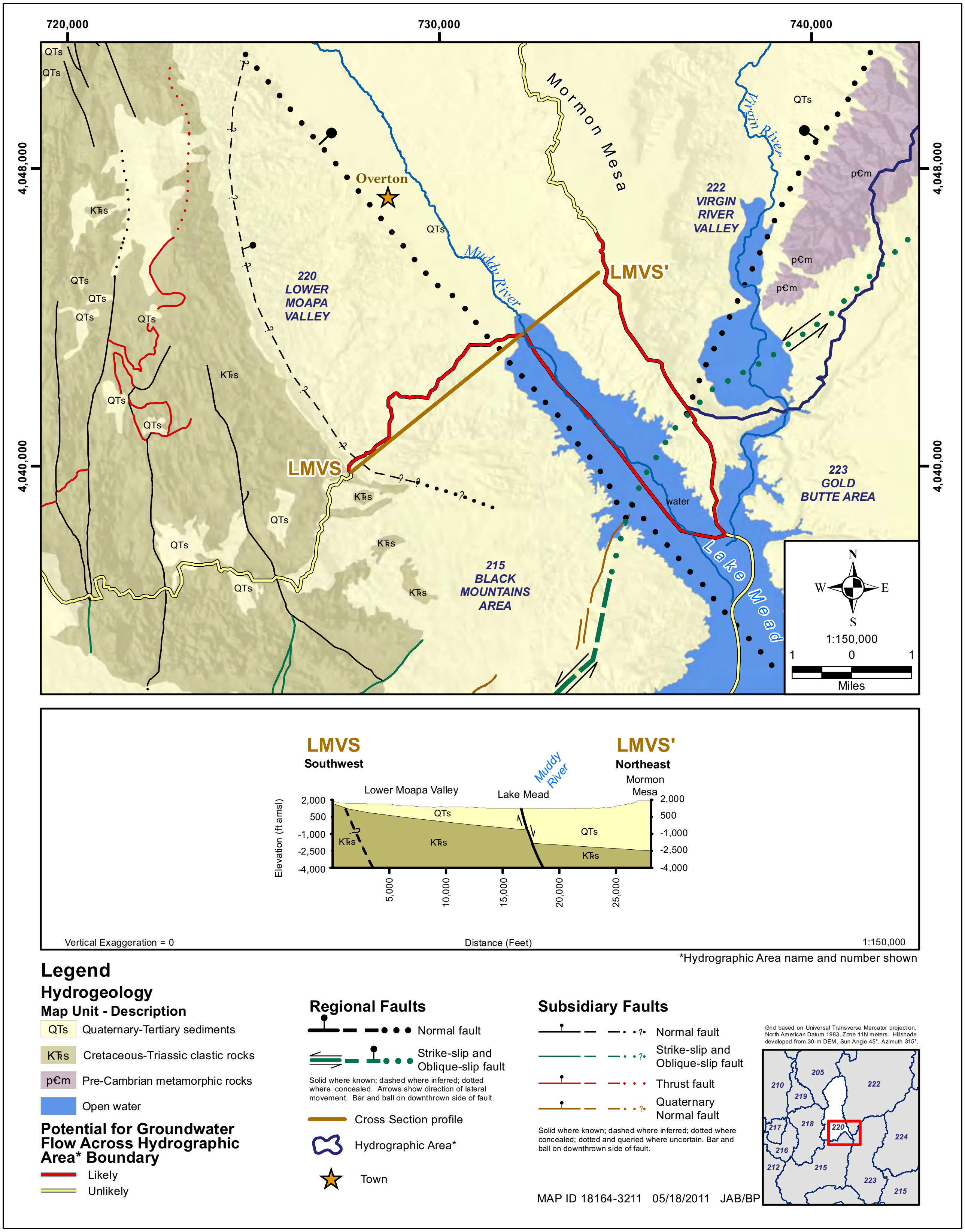

Figure 4-18
Hydrogeologic Map and Cross Section of the Lower Moapa Valley

The southern half of the Fortification Range consists of east-dipping volcanic rocks (Loucks et al., 1989), part of which are interpreted to be intracaldera rocks of the Indian Peak caldera complex. Due to the Chainman Shale in the northern part of the range and the caldera in the southern part, the entire range likely is a barrier to groundwater flow. The Fortification Range connects at its southern end with the broad Wilson Creek Range beyond a low pass. This pass, at the mining town of Atlanta, Nevada, is partly underlain by an east-striking fault, which may permit groundwater flow.

The Wilson Creek Range is a complexly faulted, north-northwest-trending range that forks southward, with the continuation of the Wilson Creek Range on the west and with the White Rock Mountains on the east. A small central valley (graben), named Spring Valley, separates the two ranges. This valley is called “little” Spring Valley in this report to distinguish it from the much larger Spring Valley to the north. The Wilson Creek Range and White Rock Mountains are each about 35-mi-long and consist entirely of intracaldera volcanic rocks, probably floored by an unexposed intracaldera (resurgent) intrusion of the Indian Peak caldera complex (Willis et al., 1987; Best et al., 1989c). The western side of the Wilson Creek Range is bounded by its main normal fault. The valleys to the west of the range are northern Lake and Patterson (southern Lake) valleys; the southern half of northern Lake Valley and all of Patterson Valley are within the Indian Peak caldera. The White Rock Mountains is a horst, with its main fault on the eastern side. The southern ends of the Wilson Creek Range and White Rock Mountains pass into a series of mostly unnamed, generally low fault blocks of intracaldera volcanic rocks (Best and Williams, 1997; Williams et al., 1997). These fault blocks continue southward for 10 mi to the southern wall of the Indian Peak caldera. The fault blocks of the southern end of the White Rock Mountains extend eastward to join the southern Needle Range (Indian Peak Range), thereby closing off Hamlin Valley east of the White Rock Mountains. More fault blocks extend southward another 15 mi as outflow volcanic rocks to the Clover Mountains, which is underlain by the Caliente caldera complex. Panaca Summit, traversed by Nevada State Route (SR) 319 and 10 mi east of Panaca, is a pass through these hills of outflow volcanic rocks.

Because of its assumed underlying intracaldera intrusions, the Indian Peak caldera complex probably is a low-permeability unit with limited groundwater flow through it. However, north-south faults, particularly the range-front faults along Lake, Patterson, and Hamlin valleys, likely provide conduits for southward (Lake and Patterson valleys) and northward (Hamlin Valley) groundwater flow (Figure 4-9).

4.4.19 Clover Mountains and Bull Valley Mountains

The Clover Mountains, Bull Valley Mountains, and northern Delamar Mountains represent a poorly defined, broad, east-trending, 60-mi-long series of low mountains made up of heavily faulted volcanic rocks. North-south Rainbow Canyon is a narrow erosional cut made by Meadow Valley Wash near the western part of the mountains. The Clover Mountains extends from Rainbow Canyon on the west for about 30 mi to the Utah/Nevada border on the east and from the Panaca (Meadow) Valley on the north to about 25 mi to the Tule Desert on the south. The Bull Valley Mountains extends eastward about 20 mi from the Utah/Nevada border and is about 20 mi north to south. The entire east-trending mountain mass passes into north-trending ranges on all sides. This massif gets its unusual easterly trend because it is cored by the 50-mi by 20-mi Caliente caldera complex (Ekren et al., 1977; Rowley et al., 1995), one of the largest calderas in the United States.

The east-elongated Caliente caldera complex is bounded on the north and south by east-trending transverse zones, the Timpahute on the north and the Helene on the south. Locally, the transverse zones are caldera margins. These transverse zones facilitated differential east-west growth (spreading) of the caldera, driven by east-west extension and caldera eruptions. Rowley and Anderson (1996) referred to the complex as a syntectonic caldera. The caldera complex is floored by an intracaldera intrusion of batholithic dimensions, but it is exposed in few places (Plates 4 and 8, Cross Sections N—N' and D—D'). South of the caldera complex, the Clover Mountains is underlain by Paleozoic carbonate rocks cut by a Sevier thrust fault and many high-angle normal faults, but these rocks are blanketed by a thick cover of outflow ash-flow tuff, and they are remote and poorly studied and mapped.

The batholith and the east-trending faults present a likely barrier to southward groundwater flow, but the entire mountain mass is heavily cut by north- and northwest-trending faults, so it is geologically permissible that these provide conduits to some flow. Rainbow Canyon allows surface water to move southward via Meadow Valley Wash.

4.4.20 Mormon Mountains

The Mormon Mountains is a nearly circular range, about 18 mi across, east of lower Meadow Valley Wash. The Mormon Mountains represents a dome of mostly Cambrian to Permian rocks, underlain by Paleoproterozoic crystalline metamorphic rocks. East-verging Sevier thrust faults placed Cambrian rocks above Cambrian to Mississippian rocks. The range subsequently underwent major uplift, and it now is underlain by prominent positive aeromagnetic and gravity anomalies. Wernicke et al. (1985) interpreted the range to contain west-verging detachment faults that resulted from late Tertiary extension above a metamorphic core complex. Wernicke et al. (1985) suggested that these detachment faults followed thrust faults within the mountains. Anderson and Barnhard (1993) disputed the detachment hypothesis, and they instead emphasized footwall deformation along normal and oblique-slip, generally high-angle faults that flatten upward and formed during the major domal uplift. Carpenter and Carpenter (1994a) also disputed the detachment hypothesis, partly on seismic data unavailable to Wernicke and colleagues. Carpenter and Carpenter (1994a and b) argued for Tertiary extension along high-angle normal faults and explained Wernicke's low-angle structures as representing gravity slides. Walker et al. (2007) discussed data that supported the gravity-slide concept. These interpretations based on the findings since 1985 have been largely adopted by Page et al. (2005a), Scheirer et al. (2006), Anderson et al. (2010), and by this report.

The broad valley of Meadow Valley Wash, to the west and northwest of the Mormon Mountains, is underlain by three geophysical sub-basins, the northern two of which contain basin-fill sediments and underlying volcanic rocks as thick as 6,000 ft, whereas the southern geophysical basin contains basin-fill and volcanic rocks as thick as 9,000 ft (Scheirer et al., 2006). Well logs suggest that the component of basin-fill sediments in these sub-basins is as much as 3,000 ft (Plates 5 and 9, Cross Section E—E'). Northwest of the Mormon Mountains, two buried thrust faults have been hypothesized (Plates 4 and 8, Cross Section C—C'). Southwest of the Mormon Mountains, buried Paleozoic carbonate rocks may be present beneath Meadow Valley Wash (Plates 5 and 9, Cross Section B—B'). A band of hills continuing southward from the Mormon Mountains is underlain by Paleozoic sedimentary rocks that are cut by Sevier thrust faults, including the Glendale/Muddy Mountains thrust (Plates 5 and 9, Cross Sections E—E' and F—F').

The Mormon Mountains represents a barrier to groundwater flow between the eastern side of Meadow Valley Wash and the Tule Desert to the east. However, a low divide north of the Mormon Mountains might allow minor volumes of such eastern flow. Southwest of the Mormon Mountains, flow is likely from lower Meadow Valley Wash to California Wash at Glendale, Nevada (Section 4.4.21).

4.4.21 North Muddy Mountains, Muddy Mountains, and Dry Lake Range

The southeastern corner of the geologic study area contains the North Muddy Mountains and, to the south, the Muddy Mountains (Plates 5 and 9, Cross Sections H—H', I—I', and K—K') (Bohannon, 1983). The North Muddy Mountains separates the California Wash area on the west from the Mesquite basin (Virgin River Valley) on the east. The Muddy Mountains occupies the northern side of Lake Mead. West of the Muddy Mountains, the map area includes the small Dry Lake Range east of Apex. This range is made up mostly of Bird Spring carbonate rocks. A narrow arm of bedrock extending west from Apex connects with the southern Arrow Canyon Range/Las Vegas Range. A thin finger of Quaternary sediments at Apex, just west of the Dry Lake Range, most probably was a pathway for Tertiary and Quaternary basin-fill sediments entering the Las Vegas Valley in the southwestern corner of the map area. The finger also is along the trace of the north-northeast- striking Dry Lake thrust (Page and Dixon, 1992). Basin-fill sediments to the northeast along the I-15 corridor (California Wash area) belong to an east-tilted half graben that reaches depths of 9,000 to 12,000 ft (Langenheim et al., 2001, 2010; Scheirer et al., 2006). The California Wash area does not appear to have been connected with the Las Vegas basin because, based on limited mapping in the area, the basin sediments are not correlated with those in the Las Vegas Valley.

In the Muddy Mountains and North Muddy Mountains, high-angle faults strike north-northeast (Bohannon, 1983; Beard et al., 2007), and the east-west gap between the two ranges, now occupied by Tertiary and Quaternary basin-fill sediments, is also likely underlain by fractures of the same strike. The northern Muddy Mountains and North Muddy Mountains contain significant Jurassic sedimentary rocks (Bohannon, 1983; Beard et al., 2007), including the Aztec Formation. The Aztec Formation and other Jurassic sandstone units have low permeability and thus form a confining zone. The northwestern side of the North Muddy Mountains is made up of upper Paleozoic carbonate rocks, which suggests that it is geologically permissible that they allow southward and southeastward groundwater flow (Figure 4-9) (Eichhubl et al., 2004). Mesozoic sedimentary rocks in the eastern North Muddy Mountains and the Muddy Mountains may also allow southward flow to Lake Mead. A possible flow barrier is provided by east-striking faults of the northern Muddy Mountains. These faults include the northeast-verging Glendale/Muddy Mountains thrust (Figures 4-6 and 4-7) (Bohannon, 1983; Carpenter and Carpenter, 1994b; Beard et al., 2007). Bohannon interpreted this structure as the northern continuation of the Keystone thrust zone, which has been displaced approximately 40 mi right laterally by the LVVSZ (see Section 4.4.7). As with the Keystone/ Glendale/Muddy Mountains thrust zone, the Dry Lake thrust just west of the Keystone/ Glendale/Muddy Mountains thrust has been displaced 40 mi by the same shear zone; its southern equivalent is the Deer Creek thrust in the Spring Mountains. Farther east in the North Muddy Mountains, the Summit/Willow Tank thrust is exposed (Plates 5 and 9, Cross Section J—J') (Bohannon, 1983, 1984, and 1992; Carpenter and Carpenter, 1994b; Beard et al., 2007). At the southeastern end of the Muddy Mountains and northern side of Lake Mead, the LVVSZ passes eastward into the northeast-striking, oblique-slip (left-lateral and normal) Lake Mead fault zone, both part of Quaternary and late Tertiary east-west extension in the area (Anderson and Barnhard, 1993; Workman et al., 2002a and b; Page et al., 2005a and b; Beard et al., 2007, 2010; Langenheim et al., 2010).

Lower Moapa Valley, in the southeastern edge of the geologic study area and northwest of where the Muddy and Virgin rivers enter the Overton Arm of Lake Mead, is clearly an area of groundwater discharge (Harrill et al., 1988). Surficial sediments, dominated by Quaternary and Pliocene river deposits of the ancestral and present Virgin and Muddy rivers and resistant calcretes, respectively, underlie the valley and Mormon Mesa. The surficial deposits are underlain by Pliocene and upper Miocene basin-fill deposits making up the southwestern end of Mesquite basin. Surficial and basin-fill sediments are lumped as the QTa and QTs units in Plates 2 and 7, respectively, but in this area most basin-fill sediments are represented by the Horse Springs and Muddy Creek formations, which are exposed as low hills west of the river lowlands at Longandale and Overton. The Black Mountains and Gold Butte areas, respectively southwest and east of Lake Mead, contain Proterozoic metamorphic rocks that extend northeastward to the southwestern Virgin Mountains. Numerous fault zones have been mapped here and in the north Muddy Mountains. These faults include northeast-striking faults of the Lake Mead fault zone that are discharge points for Rogers and Blue Point springs in the Lake Mead National Recreation Area.

Figure 4-18 shows a geologic map and cross section in the southern part of lower Moapa Valley. Although not distinguished on the map from Tertiary basin-fill deposits, deposits of the ancestral and present-day Virgin and Muddy rivers are likely to be hundreds of feet thick, inasmuch as both rivers have been carrying and depositing sediments since at least the Pliocene. Permeability in the deposits is probably considerably greater than the underlying finer-grained Muddy Creek Formation but probably not the Horse Springs Formation. A large northwest-trending, down-to-the-northeast, normal fault is interpreted to partly control the axis of the basin and the linear nature of Overton arm of Lake Mead. Gravity line 12 (Scheirer and Andreasen, 2008) imaged three density contrasts that might represent splays of the fault, even though density contrasts would be expected to be small between different beds in the underlying basin sediments. This fault downthrows river deposits on the northeast against Muddy Creek Formation on the southwest. Such a fault would provide significant conduits for groundwater flow. Southwest of that fault, the poorly exposed Muddy Creek Formation may be dropped down against the Horse Spring Formation by a queried normal fault. These rock units, as well as underlying Mesozoic rocks west of them, dip northeast into the basin.

4.4.22 Antelope Range, White Pine County

The Antelope Range, in northeastern White Pine County, Nevada, is a relatively small, low range of faulted, Tertiary volcanic rocks that unconformably overlie west-dipping Silurian to Permian sedimentary rocks, dominantly carbonate rocks. It is a horst between the narrow, northern part of Spring Valley on the west, and Tippett Valley (Antelope Valley) on the east. At its northern end, Spring Valley contains about 2,000 ft of basin-fill sediments. Tippett Valley contains at least 1,000 ft of basin-fill sediments, with thick volcanic rocks beneath these sediments; geophysical data indicate that the depth to the pre-volcanic rocks locally is as much as 18,000 ft (5.5 km).

The Antelope Range likely is a barrier to groundwater flow through it (Figure 4-9), for flow in northern Spring Valley appears to head south, whereas flow in Tippett Valley appears to head north

(Harrill et al., 1988). Low passes separate Tippett Valley from northeastern Spring Valley. Some flow is permissible between Spring Valley and Tippett Valley, given the presence of north-trending faults that may be conduits to flow in the low passes, the direction of flow is equivocal. Harrill et al. (1988) suggested minor flow southward, but Knochenmus et al. (2007) suggested minor flow northward. Gans et al. (1989) and Sweetkind et al. (2007a) speculatively showed the caldera source of the largest ash-flow tuff in the area, the 35-Ma Kalamazoo Tuff, to be buried beneath northern Spring Valley just south of the Antelope Range and southwest of the Red Hills. If present here, this feature might retard groundwater flow to or from Tippett Valley. To address groundwater flow in and south of Tippett Valley, detailed gravity data were collected and analyzed by Mankinen and McKee (2011) of the USGS, through a cooperative agreement with SNWA (Section 5.1.1). The gravity anomalies (Figures 5-4 and 5-6) and depth-to-basement data (Figure 5-5) do not corroborate a caldera there, but suggest alternative caldera sites within Tippett Valley (see also Sections 4.4.23 and 5.1.1).

4.4.23 Kern Mountains and Adjacent Small Ranges

The Kern Mountains is a 17-mi-long, east-trending range that was structurally controlled by the Sand Pass transverse zone; east-striking faults occur on both the northern and southern sides of the range (Rowley, 1998; Rowley and Dixon, 2001). The granite core of the Kern Mountains is made up of three separate plutons. These plutons are all biotite-bearing; the largest pluton also contains primary muscovite. The plutons range in age from 75 to 35 Ma (Best et al., 1974; Ahlborn, 1977; Miller et al., 1999). A separate, shallow Tertiary pluton erupted lava flows on the southeastern side of the range (Gans et al., 1989). The batholith that underlies the Kern Mountains is considered by Miller et al. (1999) to represent part of an underlying core complex that formed the Snake and Deep Creek ranges and their attenuation/denudation faults. The Red Hills, a small north-trending range south of the western end of the Kern Mountains, consists mostly of complexly faulted and mineralized Paleozoic rocks. A narrow east-draining valley, Pleasant Valley, separates the Kern Mountains and the Deep Creek Range to the north. This valley may have as much as 3,000 ft of valley fill (Plates 4 and 8, Cross Section X—X'). A broad unnamed valley between the Kern Mountains and the Snake Range contains white, coarse-grained, basin-fill sediments at its eastern end but these rocks appear to be relatively thin.

Because of its core of plutonic rocks, the Kern Mountains forms a likely barrier to groundwater flow through it. However, it is geologically permissible that limited eastward flow takes place along east-striking fault conduits, carbonate rocks, and basin-fill sediments south of the mountain block (Nichols, 2000, Plate 4; Katzer and Donovan, 2003). This flow would have to cross many buried north-south faults across its path, so the path would have to be circuitous. Nichols (2000) noted that water-level data in northern Spring Valley are ambiguous in evaluating the volume he proposed. Gillespie (2008) concluded that water geochemistry and isotopes provide no support for any interbasin flow. Welch et al. (2007), in contrast, suggested a steep eastward gradient and a large flow in carbonate rocks beneath the basin fill (see Section 6.0). In an attempt to shed light on this possible flow path, Mankinen and McKee (2011) of the USGS prepared a detailed isostatic residual gravity map and maxspots of the area (Figure 5-6), as interpreted in Section 5.1.1. This analysis suggests that the Red Hills presents a barrier to interbasin flow from Spring Valley and from Tippett Valley. A boundary-flow profile (geologic cross section) oriented perpendicular to the possible flow path and parallel to the permissible basin boundary is given as Figure 4-19. The thin clastic sediments of the late Cenozoic basin fill (QTs) and the west-northwest fault may allow groundwater to move eastward,

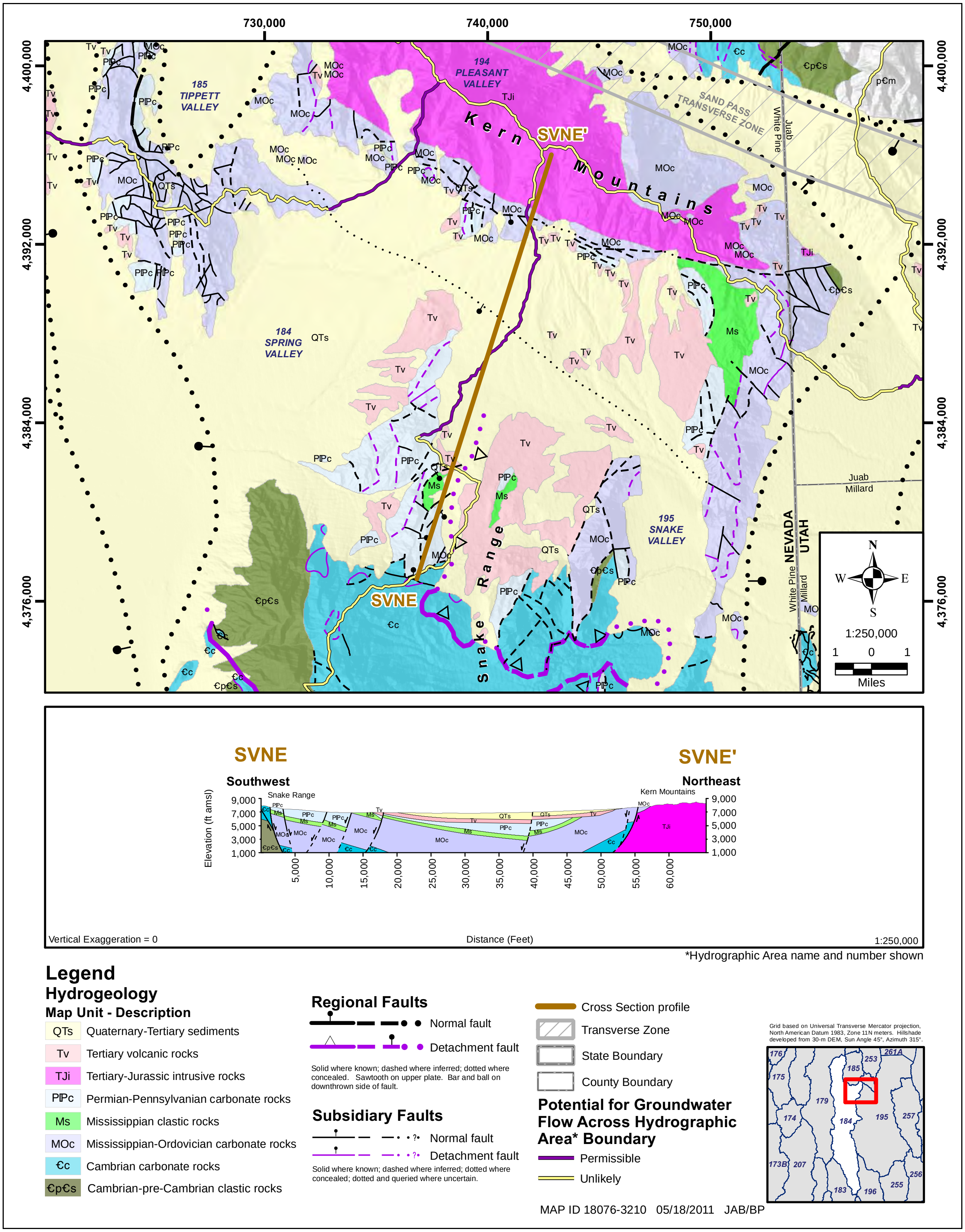

Figure 4-19
Hydrogeologic Map and Cross Section of Northeastern Spring Valley

but possible north-trending fault barriers, which likely are more significant than indicated on the map because they are buried, would present impediments to this flow. It is more likely that any interbasin contribution from Spring or Tippett valleys is small. Probably most groundwater in the shallow basin(s) between the Kern Mountains and the Snake Range (Figure 5-6) is from local recharge, in other words, from precipitation on the Kern Mountains and northern end of the Snake Range. This local recharge would be the source of tritium (modern water) that is found at Gandy Warm Springs in Snake Valley (Acheampong et al., 2009; Kistinger et al., 2009; Section 4.4.25).

4.4.24 Deep Creek Range, Utah

The Deep Creek Range is a high (as much as 12,000 ft altitude), north-trending range about 40-mi-long just east of the Nevada-Utah border and northeast of the Kern Mountains. The Deep Creek Range is a horst bounded by north-striking normal faults on either side that separate it from Deep Creek Valley to the west and northern Snake Valley and the Great Salt Lake Desert to the east. The fault on the eastern side of the Deep Creek Range appears to be the main basin-range fault controlling the range, and has vertical displacement of at least 10,000 ft, based on the height of the range and the Precambrian and plutonic rocks on its crest. The basin-range fault on the western side is also significant, for it drops Deep Creek Valley, which contains as much as 5,000 ft of basin-fill sediments.

Geologic mapping of the Deep Creek Range began with Nolan's (1935) classic report on the Gold Hill mining district at the northern end of the range. Here, Jurassic, Eocene, and Miocene plutons formed gold, tungsten, arsenic, silver, lead, copper, and zinc deposits in limestone of mostly Pennsylvanian and Mississippian age (Nolan, 1935; Robinson, 1993). Nolan mapped many east-striking faults that he called "transverse faults" and recognized that they cut the range in many places. Rocks in the northern part of the mountains dip east and range from Proterozoic to Cambrian quartzite on the east to Devonian dolomite on the west. In the central part of the range, another Tertiary pluton, the Ibapah granite of 39 Ma (Miller et al., 1999) spans the width of the range. The southern part of the range consists of highly deformed Neoproterozoic quartzite and schist of the McCoy Creek and Trout Creek groups. These Precambrian units have a combined thickness estimated at 19,000 ft (Nutt et al., 1990; Hintze and Kowallis, 2009). West of the southern part of the range, Paleozoic sedimentary rocks dip westward. These rocks range from Neoproterozoic and Cambrian quartzite through Cambrian and Devonian carbonate rocks and Mississippian Chainman Shale. They are cut by many low- to high-angle faults subparallel to the north-northeast-striking beds. The faults include detachments that may represent attenuation deroofing of the Deep Creek Range during its uplift (Miller et al., 1999).

The quartzite and plutons that make up the core of the Deep Creek Range form a likely barrier to groundwater flow between Snake and Deep Creek valleys (Figure 4-9). Groundwater flows north in these valleys. In fact, Snake Valley passes northward into the Great Salt Lake Desert at the latitude of the central Deep Creek Range. The Great Salt Lake Desert is the ultimate sink for groundwater in this area (Harrill et al., 1988).

4.4.25 Snake Range and Limestone Hills

The Snake Range is a broad, high, north-trending range. It contains Wheeler Peak, more than 13,000 ft high and within GBNP. The range is about 65-mi-long, nearly all of it in White Pine County, but with the low southern end in Lincoln County. The range is a complexly faulted horst, bounded on both sides by major high-angle normal fault zones. South of the Snake Range, the Limestone Hills is a narrow, low, heavily-faulted cuesta of mostly Devonian carbonate rocks about 20 mi long.

Spring Valley, west of the Snake Range, is a 100-mi-long, broad, deep graben containing about 6,000 ft of basin-fill sediments and defined by basin-range faults of at least 10,000 ft of vertical displacement (McPhee et al., 2005, 2006a and b; Mankinen et al., 2006; Dixon and Rowley, 2007a; Mankinen, 2007; McPhee, 2007) (Plates 4 and 8, Cross Sections X—X', W—W', V—V', and U—U'). Details on the faults bounding and within the valley are given by isostatic residual gravity and maxspots (Figure 5-4) and depth to pre-Cenozoic basement (Figure 5-5), as discussed in Section 5.1.1. About 25 AMT profiles, many of them discussed in Section 5.2.1, locate range-front and subsidiary faults and depth to bedrock (Pari and Baird, 2011).

Snake Valley, east of the Snake Range, is a 95-mi-long, broad, deep graben that passes southward into Hamlin Valley. Basin-fill sediments are locally more than 5,000 ft thick beneath Snake Valley but local holes in the basin contain thicker (10,000 ft) basin-fill and volcanic rocks (Plates 4 and 8, Cross Sections X—X', W—W', and V—V') (Allmendinger et al., 1983; Saltus and Jachens, 1995; Davis, 2005; Kirby and Hurlow, 2005). Seismic sections (Alam, 1990; Alam and Pilger, 1991) and logs of five deep oil wells in Snake Valley support these thicknesses (Herring, 1998a and b; Herring et al., 1998; Schalla, 1998; Hintze and Davis, 2002a; Hess, 2004; UDOGM, 2008). Additional information on faults is given from gravity data (Section 5.1.1) and AMT profiles (Section 5.2.2). Surficial sediments of Spring Valley and northern Snake Valley are dominated by deposits of late Pleistocene lakes (Currey, 1982).

Hamlin Valley, southeast of the Snake Range and south of, and tributary to, Snake Valley, is about 55 mi long. Gravity data indicate that the maximum thickness of basin-fill deposits and underlying volcanic rocks beneath Hamlin Valley is about 10,000 ft (Mankinen and McKee, 2009), with the basin-fill deposits being at least 4,000 ft thick. Seismic profiles and oil-test boreholes provide details to these interpretations (Alam, 1990; Alam and Pilger, 1991; Hess, 2004).

Except for the southern end, the Snake Range is cored by Neoproterozoic to Cambrian quartzite that is intruded by a massive composite batholith formed apparently by multiple episodes of intrusion in Middle and Late Jurassic and Tertiary time (Whitebread, 1969; Miller et al., 1994, 1995 and 1999; Gans et al., 1999a and b; Lee et al., 1999a, b, and c; Miller and Gans, 1999; Gans, 2000b). The range was uplifted along its high-angle faults and the roof stretched apart so that its rocks failed along bedding planes in the Pioche Shale and moved down the flanks of the range as the Snake Range decollement (Section 4-8). The decollement places complexly faulted Middle Cambrian carbonate and younger rocks over a lower plate of Middle Cambrian carbonate rocks, Lower Cambrian clastic rocks, and older rocks. Most development of the decollement was synchronous with basin-range extension (Miller et al., 1999; Gans, 2000a). The decollement is exposed on the top and eastern side of the northern half of the range (Tingley et al., 2010) (Plates 4 and 8, Cross Section W—W'). East of the range, the decollement has been imaged by seismic profiles (Allmendinger et al., 1983; Miller et al., 1999) as it passes eastward beneath the surface of Snake Valley. Allmendinger et al. (1983) and Kirby and Hurlow (2005) suggested that the eastern frontal fault of the Snake Range, separating the range from Snake Valley, is the low-angle Snake Range decollement. Geophysics (Mankinen and McKee, 2009; McPhee et al., 2009) and the straight range front argue instead for our interpretation of a high-angle normal fault that bounds the eastern side of the range (Plates 1 and 6). Rodgers (1987), Alam (1990), Smith et al. (1991), Alam and Pilger (1991), McGrew (1993), and Miller et al. (1999, Figure 10) also showed such a high-angle basin-range fault that is younger than, and thus cuts, the decollement (Plates 4 and 8, Cross Section W—W').

The central part of the Snake Range is narrower and becomes progressively lower southward, and detachment faults are not exposed. Where U.S. Highway 6 (US 6)/US 50 crosses over Sacramento Pass, north-striking, east-dipping listric normal faults drop down to the east Miocene basin-fill sediments that are about 6,500 ft thick (Gans et al., 1989; Miller et al., 1994, 1995, and 1999). The area south of Sacramento Pass includes GBNP (Sweetkind, 2007b), the centerpiece of which is Wheeler Peak, the second highest mountain in Nevada. The northern part of the Park was geologically mapped by Whitebread (1969) at 1:48,000 scale. In his mapping, he recognized the Snake Range decollement, which he left unnamed but referred to it not as a thrust but as a low-angle fault that placed younger rocks on older rocks. He considered all faults in the area to be of low angle and of the same structural event, although it is not clear whether he considered it of Sevier or Tertiary age. This mapping was compiled at 1:250,000 scale by Hose and Blake (1976). Following comprehensive detailed mapping in mostly the northern Snake Range (Miller et al., 1994 and 1995; Gans et al., 1999a and b; Lee et al., 1999a, b, and c; Miller and Gans, 1999), Miller et al. (1999) summarized the geology of the Snake Range decollement. Miller and her colleagues continued their mapping southward to include the entire Park, resulting in an unpublished, unauthored, and unreviewed draft digital 1:24,000-scale geologic map of the park, on file in 2008 with the National Park Service (NPS). It compiled, with some modifications, and expanded the mapping of Whitebread. Because the emphasis of their project was the Snake Range decollement, their mapping—as with Whitebread (1969)—of surficial (Quaternary) and basin-fill (Quaternary to Miocene) deposits was superficial, and high-angle basin-range normal faults that define and uplift the range and also are abundant within the range were not recognized. Updating the geology of the Snake Range on Plates 1 and 6 required examination of 1:40,000-scale aerial photos and Google Earth images as well as limited field work and a review of more recent publications, including those on young and active high-angle faults in the area (Black et al., 2003). Many previously unrecognized high-angle, generally north-trending, basin-range faults, some cutting Quaternary and Pliocene surficial and basin-fill deposits, were added to the map.

The southern end of the Snake Range is a low series of tilt-block cuestas of Devonian and Mississippian sedimentary rocks faulted against Tertiary volcanic rocks (Plates 4 and 8, Cross Section U—U'). These tilt blocks become progressively lower in elevation to the south, and the eastern tilt blocks plunge beneath the valley fill. The western tilt blocks continue southward to become the Limestone Hills, which consists mostly of east-dipping Devonian carbonate rocks bounded by normal faults on the western and eastern sides. The Limestone Hills continues southward into the Wilson Creek Range (Section 4.4.18). The southern end of the Limestone Hills forms part of the northern wall of the Indian Peak caldera complex. Here the Atlanta silver-gold mining district is in Silurian to Ordovician carbonate rocks along the east-striking caldera margin.

Because of its core of plutons and quartzite, the Snake Range is a groundwater barrier to east or west flow for nearly its entire length. In the Sacramento Pass area in the center of the range, however, it is geologically conceivable that minor groundwater might flow eastward through the range along an east-striking fault and adjacent carbonate and volcanic rocks. But we consider such flow unlikely because any flow would have to be at least 1,500 ft below the surface to surmount the pass.

Spring Valley is made up of at least two geophysical sub-basins (Figure 5-5), as indicated by gravity data discussed in Section 5.1.1. The northern of these is about 90 mi long. It is structurally deepest at its northern end, west of the Antelope Range, where it is also a separate small basin. Harrill et al. (1988) suggested that water from this part passes southward. The southern end of the northern geophysical sub-basin is near the northeastern end of the Fortification Range, where depth-to-basement data (Figure 5-5) shows a shallow buried east-west bedrock ridge connecting the northern Fortification Range with the southern Snake Range. Near the central part of this northern geophysical sub-basin, just south of where US 6/50 crosses Spring Valley, Rattlesnake Knoll protrudes above the valley. This Knoll, investigated by Mankinen et al. (2006), may be the surface expression of another, but narrower (Figure 5-5), buried east-west ridge whose hydrologic significance is unknown.

Groundwater seems to pool in the northern geophysical sub-basin (Harrill et al., 1988). Some flow, however, is permissible to or from Tippett Valley (Section 4.4.22) or to Snake Valley between the southern Kern Mountains and northern Snake Range, although the Red Hills would seem to block flow out of Spring Valley (Section 4.4.23).

The southern geophysical sub-basin is about 20 mi long, between the Fortification Range and the Limestone Hills (Section 5.1.1). It is part of the same surface-drainage basin as the northern geophysical sub-basin, with surface flow northward into the low part of the northern sub-basin.

It has long been suggested that the faulted carbonate rocks that form the low Limestone Hills and its adjacent passes provide the only significant likely pathway for groundwater flow from Spring Valley; this flow goes eastward to northern Hamlin Valley (Harrill et al., 1988) (Figure 4-9). Yet, north-south faults bound the Limestone Hills on its east and west sides, so these present partial barriers to eastward flow. Therefore, flow along this route was estimated to be only 4,000 afy by Hood and Rush (1965), Rush and Kazmi (1965), Harrill et al. (1988), Brothers et al. (1994), and Katzer and Donovan (2003). Nichols (2000) suggested a flow of between 8,000 and 12,000 afy if one uses a greater hydraulic conductivity value for carbonate rocks in the area. Gillespie (2008) found that any interbasin flow “cannot be confirmed or rejected based on the current data and modeling constraints.” Welch et al. (2007), however, suggested a volume of 33,000 afy (see Section 6.2.1.4).

To test the hypothesis that groundwater moves from Spring Valley to Hamlin Valley via the Limestone Hills, Figure 4-20 gives a boundary-flow profile (cross section) drawn parallel to the basin boundary and perpendicular to the possible flow direction. The cross section suggests that flow is likely at both the northern and southern ends of the Limestone Hills, with permissible flow in between. The geologic map shows that the Limestone Hills is a horst, defined on either side by two north-trending basin-range, range-front faults that lifted the horst up with respect to the basins on either side. Both faults probably are partial barriers to easterly flow through them. At the northern likely flow route, two regional faults are shown cutting through the lowest pass along the basin

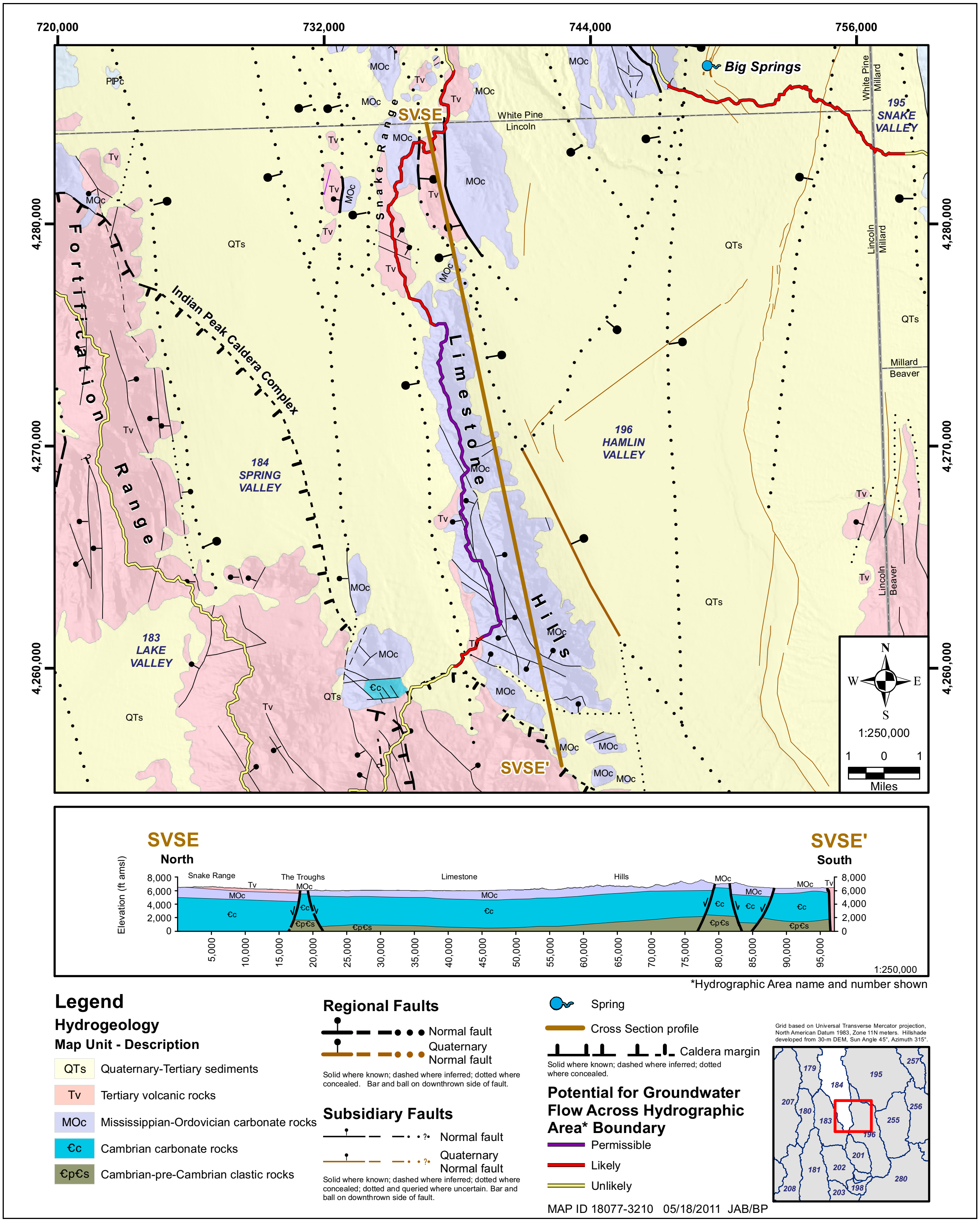

Figure 4-20
Hydrogeologic Map and Cross Section of the Southern Snake Range and Limestone Hills and Vicinity

boundary, known as The Troughs (see also Figures 5-7 and 5-20). Both are splays of the eastern range-front fault of the Limestone Hills and are possible conduits in one of two areas considered likely for groundwater to move through the Limestone Hills. Two subsidiary, west-northwesterly-trending faults are shown on the map just west of The Troughs. East-trending faults, too small to be mapped at this scale, may cut entirely through the narrow horst of the Limestone Hills at various places, including the area of The Troughs.

The southern likely flow path through the Limestone Hills would be at the southern part of the Hills. Here two west-northwest-trending faults cut through lower Paleozoic carbonate rocks just north of where the parallel-trending margin of the Indian Peak caldera complex separates the Limestone Hills to the north from the White Rock Mountains to the south. The southern of the two faults underlies a low pass at that locality, so it may be a small conduit for flow. All rocks shown in the cross section, except those at great depth, are aquifers, amenable to flow through them. Therefore interbasin flow is considered likely or permissible, although no evidence yet supports a flow that is large. Whatever the flow is, the southern geophysical sub-basin of Spring Valley, west of the Limestone Hills, would seem to be the only source for the groundwater.

From northern Hamlin Valley, groundwater passing through the Limestone Hills combines with north-flowing groundwater from southern Hamlin Valley, then flows northward into Snake Valley (Davis, 2005) then farther northward to the Great Salt Lake Desert (Harrill et al., 1988; Knochenmus, 2007). Groundwater in Snake Valley flows northward along mostly high-angle, north-striking normal faults in both the basin-fill and carbonate-rock aquifers. Not only is the valley bounded on both sides by range-front faults, forming a graben, but the interior part of the valley itself and its basin-fill sediments are cut by innumerable faults (Mankinen and McKee, 2009; McPhee et al., 2009; Rowley et al., 2009), few of which have been shown in previous mapping and only some of which can be shown on Plates 1 and 4 because of scale.

Several springs in Hamlin and Snake valleys owe their presence to faults. Big Springs occurs on the southeastern flank of the Snake Range at the edge of northwestern Hamlin Valley (Figures 4-20 and 5-7). Like most other springs in the Great Basin, it is controlled by north-trending basin-range faults (Sections 5.1.1 and 5.2.2), which allow groundwater to move to the surface from the underlying water table.

4.4.26 Confusion Range, Conger Range, Burbank Hills, and Tunnel Spring Mountains

The Confusion Range and small ranges of similar rocks form the entire eastern (Utah) side of Snake Valley. The area includes hills (Middle Range) connected to and east of the northern end of the Confusion Range. The Confusion Range proper is 60-mi-long, with a general northerly trend. Tule Valley is east of the Confusion Range. The Conger Range is a 15-mi-long, southwest-diverging fork in the southern Confusion Range, located northeast of the small communities of Baker, Nevada, and Garrison, Utah. The Burbank Hills is a 15-mi-long range south of the Conger Range and southeast of Baker and Garrison. The Burbank Hills is separated from the Conger Range by a northwest- trending valley known as the Ferguson Desert; the Desert may contain several thousand feet of basin-fill deposits (Plates 1 and 6, Plates 4 and 8, Cross Section V—V'). The Tunnel Spring Mountains is a narrow, 20-mi-long range southeast of the Burbank Hills and east of northern Pine Valley. Northern Pine Valley connects with the southeastern end of the Ferguson Desert.

All of these ranges consist almost entirely of north-striking, folded, thrusted, and attenuated, middle to upper Paleozoic rocks and Triassic rocks that together form a synclinorium, in other words a combination of synclines and anticlines that overall appear as a broad syncline (Plates 1 and 6, Plates 4 and 8, Cross Sections W—W' and V—V') (Hose, 1977; Hintze and Davis, 2002a and b, and 2003). The Mississippian Chainman Shale, 1,000 to 2,000 ft thick in the area, is repeated and thus exposed on both sides of and beneath all these ranges because it is deformed into north-striking folds (Hintze and Davis, 2002a and b, and 2003). Tertiary regional ash-flow tuffs formerly covered most of the area to a thickness of as much as 500 ft, but erosion has left only patches of these tuffs, notably the Oligocene Needles Range Group, derived from the Indian Peak caldera complex (Best et al., 1989a and b). Basin-range faults cut all these ranges, but most are of small displacement so individual stratigraphic units are remarkably coherent and continuous over this large area. The most significant basin-range fault is the northerly-trending fault zone that defines the eastern side of Snake Valley. Basin-range faults that separate the Confusion Range from Tule Valley have moderate vertical offset.

The Chainman Shale underlies, at shallow depth, all of these areas except the southern Confusion Range. The entire area is underlain at shallow depth by north-striking thrust faults. The folded Chainman, and perhaps the thrusts, probably are significant barriers to groundwater flow to the east or west. Other barriers to east or west flow are the north-striking basin-range faults. The only flow from west to east that is permissible is in the southern Confusion Range, where lower Paleozoic carbonate rocks are exposed and the range is low (Harrill et al., 1988). East-trending transverse faults of the Sand Pass transverse zone were mapped in the central and eastern Middle Range and through Sand Pass, but none extended westward to Snake Valley. The available water- level data suggest that most groundwater flow in Snake Valley and Tule Valley, and perhaps in the Confusion and related ranges, is northward, most likely along the north-striking faults and north-striking beds.

4.4.27 Needle Range and Wah Wah Mountains

The Needle Range, just east of the Nevada-Utah state line, is about 50-mi-long and consists of two subranges, the Mountain Home Range to the north and the Indian Peak Range to the south. The Mountain Home Range merges with the Burbank Hills to the north. Hamlin Valley, to the west, separates the Needle Range from the southern Snake Range, Limestone Hills, and White Rock Mountains to the west. To the east of the Needle Range is Pine Valley and to the south is the Escalante Desert. The Wah Wah Mountains is a parallel tilt block of similar length to, and located east of, the Needle Range, east of the geologic study area. The Wah Wah Mountains is the southward continuation of the Confusion Range. Wah Wah Valley is east of the Wah Wah Mountains and west of the San Francisco Mountains.

The northern part of the Needle Range consists of folded, middle to upper Paleozoic rocks (Hintze and Davis, 2002b). Locally, lower Paleozoic carbonate rocks are thrust over upper Paleozoic carbonate rocks (Best et al., 1987a and b). Most of the Needle Range, however, consists of east-dipping outflow ash-flow tuffs derived primarily from the Indian Peak caldera complex. The southeastern caldera margin passes through much of the southern part of the range (Williams et al., 1997). The Needle Range is a faulted horst, with the main basin-range fault separating Hamlin Valley from the Needle Range (Plates 1 and 6, Cross Sections U—U' and Q—Q'). Hamlin Valley contains at least 4,000 ft of basin-fill sediments (Plates 4 and 8, Cross Sections U—U' and Q—Q'). The basin-fill sediments in the southern half of Hamlin Valley are underlain by the Indian Peak caldera complex (Plates 4 and 8, Cross Section Q—Q'). A significant basin-range fault separates the eastern side of the Needle Range from Pine Valley.

The northern Wah Wah Mountains, like the southern Confusion Range just to the north, consist of gently folded and locally thrusted, lower to middle Paleozoic carbonate rocks. Farther south, east-dipping Neoproterozoic to Cambrian quartzite and overlying Cambrian carbonate rocks form most of the range (Hintze and Davis, 2002b; Rowley et al., 2009, Plate 1). An oil well drilled by Hunt Oil Company in the southern Wah Wah Mountains was spudded in the Prospect Mountain Quartzite and penetrated 12,500 ft of rocks, including several thrust zones (Erskine, 2001). Other thrust faults that place lower Paleozoic rocks over middle and upper Paleozoic rocks are well exposed and unconformably overlain by east-dipping, Tertiary ash-flow tuffs (Abbott et al., 1983). Near the southern end of the range, other Sevier thrusts place Cambrian rocks above the Jurassic Navajo Sandstone (Best et al., 1987c). The southeastern part of the Indian Peak caldera complex cuts the southwestern end of the Wah Wah Mountains (Williams et al., 1997). As with the Needle Range, the dominant structure controlling the range is a basin-range fault zone on the western margin, beneath Pine Valley. Pine Valley is a graben underlain by basin-fill sediments perhaps as much as several thousand feet thick but generally less (Davis, 2005). The southern ends of both the Needle Range and Wah Wah Mountains merge with each other (Best et al., 1987c) and, still farther southwest, these merge with the White Rock Mountains. These southern range margins form the northern margin of Escalante Desert and the southern margin of the Indian Peak caldera complex (Best, 1987).

4.4.28 Fish Springs and House Ranges

The 20-mi-long Fish Springs Range, near the northeastern edge of the geologic study area, extends south from the Great Salt Lake Desert. The southward continuation of the Fish Springs Range is the 60-mi-long House Range. The two ranges form the eastern boundary of Tule Valley, which is just east of the study area and contains basin-fill sediments that in most places are 1,000 to 2,000 ft thick but have been estimated to be locally more than 6,000 ft thick (Davis, 2005). The surficial deposits in Tule Valley consist largely of lacustrine deposits of Lake Bonneville and of alluvial fans (Sack, 1990).

The Fish Springs Range is a highly faulted but generally gently west-dipping horst consisting of Middle Cambrian to Middle Devonian carbonate rocks that rest on Lower Cambrian siliciclastic rocks (Plates 4 and 8, Cross Section X—X') (Kepper, 1960; Hintze, 1980a and b; Morris, 1987; Hintze et al., 2000; Hintze and Kowallis, 2009). The range is bounded by large basin-range faults on its western and eastern sides, with the main fault being the one on the eastern side. This fault is still active and has components of Holocene and Pleistocene movement (Oviatt, 1991; Black et al., 2003). East-striking, oblique-slip faults have been mapped throughout the range (Hintze, 1980a and b). Some of them partly control the Fish Springs zinc-lead-silver-tungsten mining district on the northwestern side of the range (Oliveira, 1975; Christiansen, 1977); a newly discovered, buried Eocene quartz monzonite pluton also controls this district (Puchlik, 2009). A concentrated series of east-striking faults occurs at Sand Pass, which separates the southern end of the Fish Springs Range from the northern end of the House Range. This east-trending fault zone is part of the Sand Pass transverse zone, which extends intermittently as far to the east as the Wasatch front and as far to the west as the Kern Mountains (Stoeser, 1993; Rowley, 1998; Rowley and Dixon, 2001). At Sand Pass, the transverse zone contains small intrusions (Chidsey, 1978) and causes profound structural differences (the rocks have opposite dips and the main fault is on opposite sides) between the two ranges, as in some other transverse zones (Faulds and Varga, 1998).

The high House Range is a tilt block, bounded on the western side by a major basin-range fault beneath eastern Tule Valley and on the eastern side by a fault of lesser displacement. The faults uplift the range and tilt it several degrees east (Hintze and Davis, 2002a; Rowley et al., 2009, Plate 1). Like the main bounding fault zone of the Fish Springs Range, the main fault zone of the House Range is an active fault zone of large displacement that includes Holocene and Pleistocene movement (Sack, 1990; Black et al., 2003), but this fault zone is on the western side of the House Range. The range, famous among paleontologists for its trilobites, consists mostly of Cambrian strata, which include clastic sedimentary rocks at the western base of the range and carbonate rocks above. The central part of the range is intruded by the Notch Peak quartz monzonite pluton of Jurassic age.

Neoproterozoic to Cambrian quartzite along the western side of the Fish Springs and House ranges forms a likely eastward groundwater barrier between Tule Valley and the valleys to the east, including the Sevier Desert. Northward flow, of course, likely dominates in this entire area in conduits provided by basin-range faults, including the fault zone along the western sides of the Fish Springs and House ranges (Stephens, 1977).

This Page Left Intentionally Blank

5.0 GEOPHYSICS

In an effort to provide additional data to interpret the subsurface of the geologic framework, SNWA contracted with the USGS Geophysical Unit at Menlo Park, California to collect and analyze geophysical data in the geologic study area. The analysis of geophysical measurements throughout the project area defines the overall shape and thickness of basins, identifies buried faults that may be either barriers or conduits to groundwater flow, provides estimates of the depth to pre-Cenozoic basement rocks, helps characterize interbasin flow as to likely, unlikely, or permissible interbasin flow, and assists in describing aquifers.

5.1 Gravity Surveys

For hydrogeology, the most critical type of geophysical information is data on the gravity of rocks measured at the surface. Within the geologic study area, more than 5,000 gravity measurements (Snyder et al., 1981 and 1984; Bol et al., 1983; Ponce, 1992 and 1997) had previously been made, but more detail was needed in many areas. In 2000, the USGS collected 224 gravity stations along 5 profiles in Coyote Spring Valley (Phelps et al., 2000). Between 2003 and 2007, the USGS collected another 1,632 gravity stations and issued analysis reports (Scheirer, 2005; Mankinen, 2007; Mankinen et al., 2006, 2007, 2008). In 2002, with funding from the Virgin Valley Water District, NPS, and the USGS, the USGS collected 344 gravity stations in Meadow Valley Wash basin and California Wash basin and, just east of the map area, in the Tule Desert (Scheirer et al., 2006). In 2008, Mankinen and McKee (2009) collected 206 gravity stations, primarily in Snake Valley and, just east of the geologic study area, in Tule Valley and Fish Springs Flat, and interpreted the anomalies. In the fall of 2010, additional gravity data (99 new gravity stations) were measured in several key areas in and adjacent to Spring Valley by Mankinen and McKee (2011) and their analysis is included here. The sections below summarize the geophysical results for each basin, discussed from north to south. A brief analysis of gravity data from California Wash Basin and lower Meadow Valley Wash, which have less significance for the four Project Basins, are discussed in Sections 4.4.20 and 4.4.21. At gravity stations on bedrock, samples were collected for density and magnetic-susceptibility properties. In this section, we use metric measurements because they were used in the USGS studies.

New gravity stations were collected within coverage gaps of the prior data, especially within and adjacent to the Project Basins. Values of observed gravity at the new stations were calculated by accounting for fluctuations related to tidal accelerations and for instrument drift constrained at the beginning and end of each day. Gravity observations were processed to account for the predictable effects of latitude, elevation, and terrain variations. Because available gravity data for the study area were made by many different observers at different times, the data set was examined to remove duplicate entries. Major station elevations were compared with elevations interpolated from 10- and 30-m digital elevation models. Large elevation differences indicate possible errors in station location or elevation, and each station so identified was examined individually to confirm the discrepancy

SE ROA 43236

JA_13116

before omitting it from the data set. The revised data set, including all new gravity observations, was gridded at a spacing of 0.5 km using a minimum curvature algorithm (Webring, 1985). Gravity data were reduced using standard gravity corrections (Blakely, 1995) to produce the complete Bouguer gravity anomaly. A regional isostatic field was subtracted from the Bouguer anomaly, thus removing long-wavelength variations in the gravity field that are inversely related to topography. The resulting isostatic gravity field is a reflection of local density distributions in the middle and upper crust. Gravity lows (cool colors) generally indicate low-density sedimentary basin-fill deposits and volcanic rocks in the basins; gravity highs (warm colors) generally reflect pre-Cenozoic basement rocks in the basins.

Gridded isostatic gravity anomaly data were used to guide the gravity analysis in two modes: (1) to detect significant lateral density interfaces in the subsurface using a maximum horizontal gradient technique (Blakely and Simpson, 1986) and (2) to create models of the depth to pre-Cenozoic basement using the anomaly separation technique of Jachens and Moring (1990). The magnitude of the gradient is a function of the depth to the density boundary and the size of the density contrast.

The depth-to-basement technique, in turn, involves two steps: (a) to separate contributions to the isostatic gravity anomaly that arise from Cenozoic sedimentary and volcanic deposits and those from pre-Cenozoic rocks and (b) to convert the contributions from the lower density deposits into a model of basin depth (Jachens and Moring, 1990). In other words, the isostatic residual gravity field reflects a pronounced contrast between dense pre-Cenozoic rocks and significantly less dense overlying strata. Because of this relationship, the gravity inversion method (Jachens and Moring, 1990) can be used to separate the isostatic residual anomaly into pre-Cenozoic "basement" and younger "basin" fields, thus allowing an estimate of thickness of Cenozoic basin fill. Because upper Cenozoic sedimentary alluvial fill and underlying Tertiary volcanic rocks have similar densities, they cannot be geophysically discriminated from each other, so geophysically (in this section only) they are lumped together as "basin fill" within an area. The accuracy of thickness estimates derived by the gravity inversion technique is dependent on (1) the assumed density-depth relation of the Cenozoic basin fill and (2) the initial density assigned to the basement rocks. Density of basement rocks is generally assumed to be 2.67 mg/m^3, and this value is considered appropriate in this area, where major exposures consist of Neoprecambrian through upper Paleozoic marine carbonate and siliciclastic sedimentary rocks. Subvolcanic Cenozoic intrusions are included here as part of the basement because their physical properties are similar to most of the older rocks, and they differ strongly from those of the eruptive and basin-fill sequences. The density-depth function used here is the same as used in an earlier basin-depth analysis of the Basin and Range province (Saltus and Jachens, 1995). The gravity inversion method also allows the input of basement depths determined from deep drill-holes and seismic data.

Gravity data can be enhanced in a number of ways (e.g., Blakely, 1995) to better characterize causative sources of their anomalies. Gravity anomalies can be analytically upward-continued by 1 to 3 km (Hildenbrand, 1983) to de-emphasize surface and near-surface features and enhance the contribution from deeper sources. Horizontal gradients can then be calculated for the long-wavelength gravity anomalies identified by the upward-continued data (e.g., Cordell, 1979; Blakely, 1995). When calculated for two-dimensional (2D) data grids, horizontal gradients will place narrow ridges, called "maxspots," over significant changes in gravity. The method of Blakely and Simpson (1986) was used to calculate maximum values of these gravity and magnetization gradients, the locations of which tend to overlie the edges of causative bodies with abrupt, near-vertical contacts. For non-vertical contacts between geologic units of contrasting properties, maximum values of the horizontal gradients will be displaced down-dip and away from the edges of the body. These maxima, along with the gradient "ridges" containing them, identify density contrasts that can help delineate deep-seated crustal structures, primarily faults, separating major tectonic domains. Zones between these domains can potentially locate Cenozoic tectonic features and, indeed, many examples can be seen where the maxspots closely track faults that have been mapped at the surface. Where lines of maxspots from deeper levels are displaced from each other toward the basin, a basin-dipping fault is suggested (Figure 5-1). In other words, when progressively deeper maxspots are projected vertically (that is, upward continued) to the surface, onto the map of the isostatic residual gravity field, they are progressively farther on the downdip side of a fault than the actual surface trace of the fault (see Figure 5-5 and others). The less a fault dips, the farther apart are the maxspots from the various depths, as opposed to a vertical fault, where the maxspots that are upward continued from different depths are on top of each other.

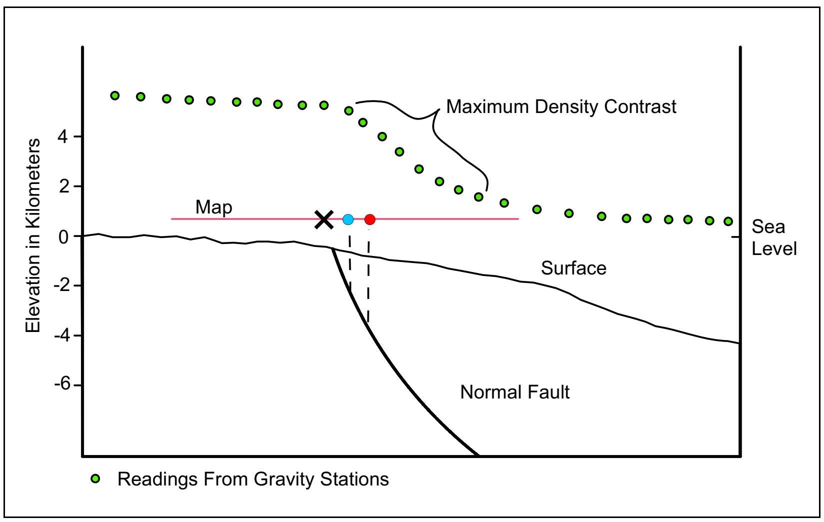

Note: X at surface, blue dot from 2 km depth, red dot from 3 km depth.

Figure 5-1
Geologic Cross Section of a Normal Fault Interpreted from a Gravity Profile across It (Black Dots), Showing Upward-Continued Maxspots Projected onto a Map

5.1.1 Gravity Data for Spring and Snake Valleys

Mankinen et al. (2006) interpreted the gravity data in Spring and Snake valleys (Figure 5-2), including 545 new gravity stations (Figure 5-3) collected primarily in Spring Valley, the northern Limestone Hills, northern Hamlin Valley, and southern Tippett (Antelope) Valley. The isostatic gravity field for Spring and Snake valleys is shown on Figure 5-4. The depth to basement, calibrated by 11 oil and gas wells, is shown on Figure 5-5. The topographic contour interval in these figures is 400 m. Later, Mankinen et al. (2007) collected additional data in Tippett Valley and Spring Valley as well as areas to the south; and Mankinen and McKee (2009) reinterpreted the gravity data in Snake Valley, Hamlin Valley, and areas farther east of the geologic study area based on 206 new gravity stations in these regions. In the fall of 2010, additional gravity data were collected by Mankinen and McKee (2011) in northern Spring Valley, Tippett Valley, and the unnamed valley between the Kern

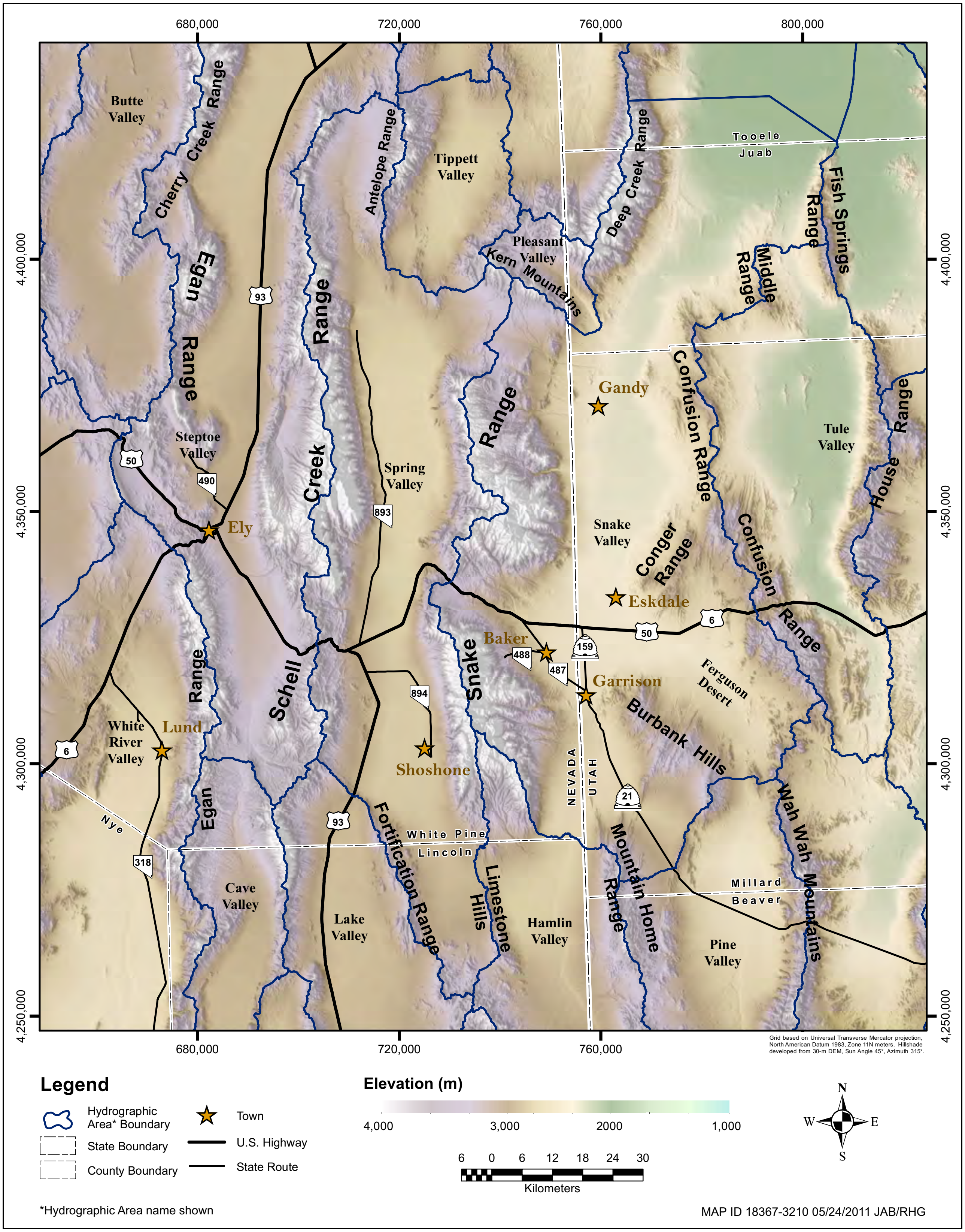

Figure 5-2
Shaded Relief Map of Spring and Snake Valleys and Vicinity, Nevada and Utah

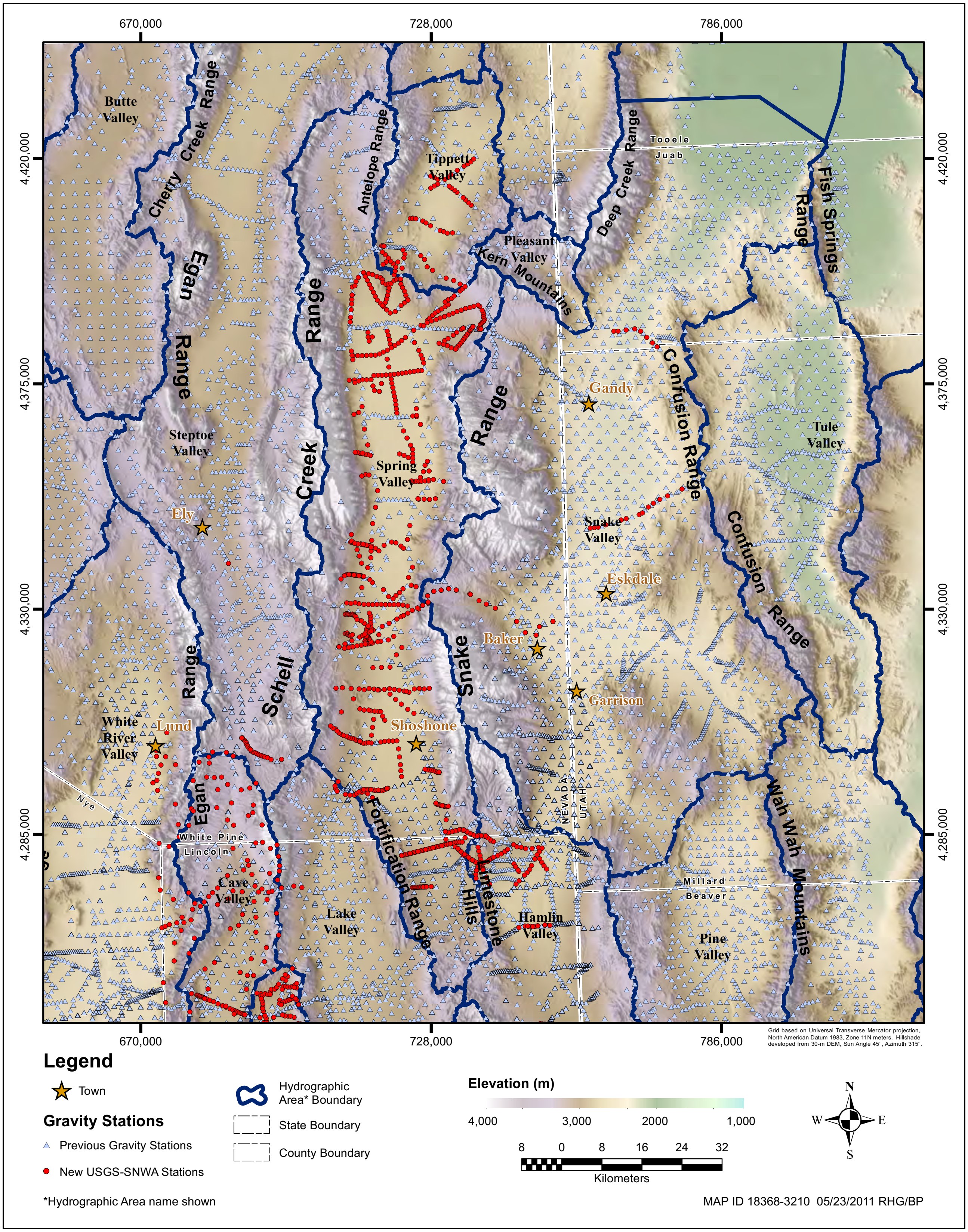

Figure 5-3
Gravity Stations in Spring and Snake Valleys and Vicinity, Nevada and Utah

SE ROA 43240

JA_13120

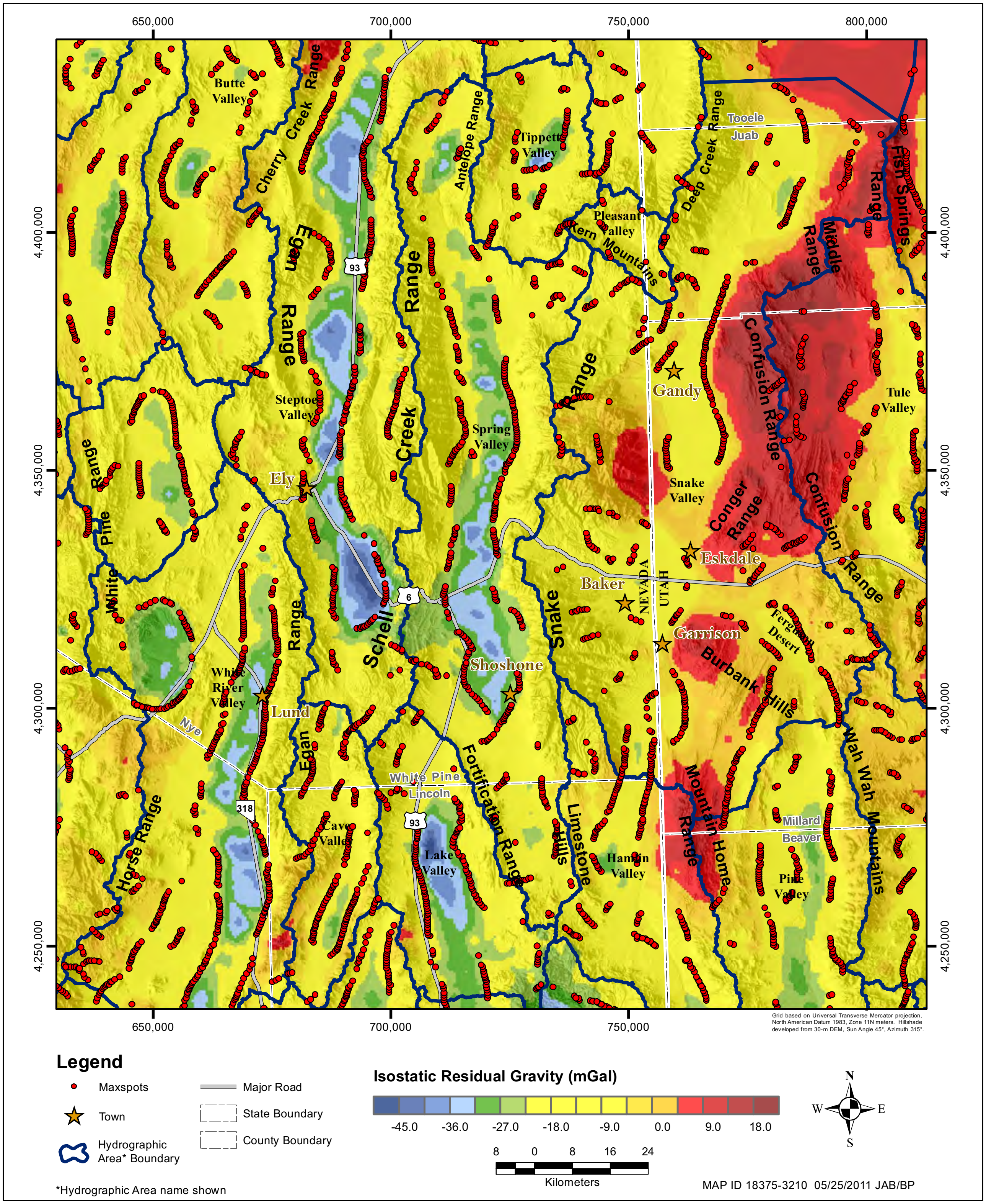

Note: Maxspots calculated from the 3-km upward-continued gravity grid.

Figure 5-4
Isostatic Residual Gravity Field and Maxspots in Spring and Snake Valleys and Vicinity, Nevada and Utah

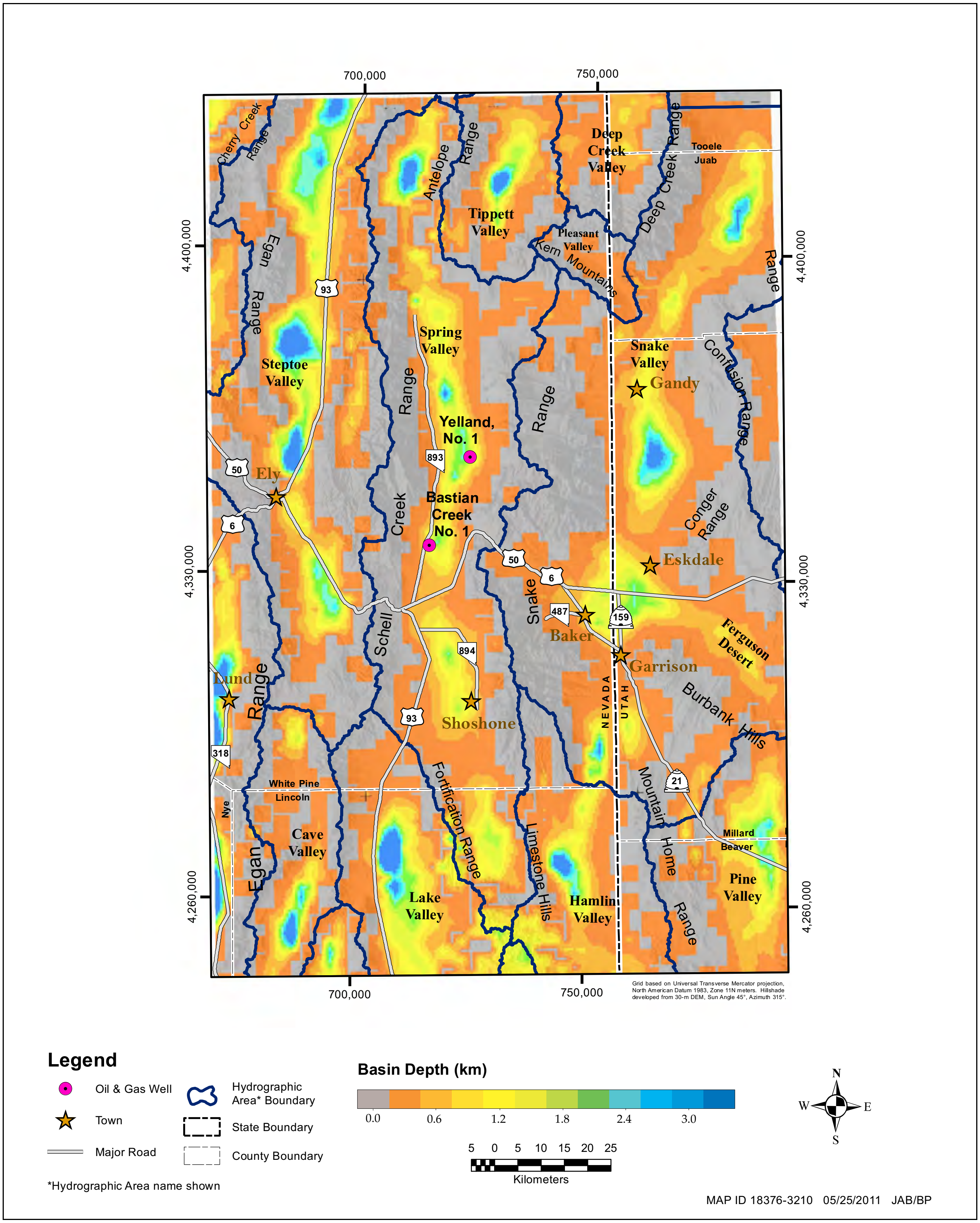

Figure 5-5
Depth to Pre-Cenozoic Basement in Spring and Snake Valleys and Vicinity, Nevada and Utah

Mountains and Snake Range. Our discussion below and all figures include these new data, although the final USGS reports giving them will soon be released.

The gravity inversion method indicates that the maximum thickness of basin fill (alluvium and volcanic rocks) in the principal valleys of interest is generally 2 km or more (Figure 5-5). Note, however, that the deepest areas of Spring and Hamlin valley are much narrower than the deepest areas in both Steptoe and Snake valleys. Absolute values of basin depths are estimated using a density-depth profile calibrated by deep oil and gas wells, some of which penetrated pre-Cenozoic basement. Maximum depths to pre-Cenozoic basement in Spring, Steptoe, and Hamlin valleys are interpreted to be between 3 and 3.5 km, except for the northernmost parts of Steptoe and Spring valleys (39°45′ N to 40°N), which appear to have maximum depths near 4 km. The approximately 4 km of fill in these areas are comparable to the deepest parts of Snake Valley. Maximum depths in Duck Creek Valley northeast of McGill range from approximately 1.5 to 2.0 km. There appears to be a particularly deep basin beneath Tippett Valley (Antelope Valley), where depths appear to be generally greater than 3 km, and in some areas these depths max extend to between 5 and 5.5 km.

Depth-to-basement data (Figure 5-5) indicate that Spring Valley has a maximum depth (basin-fill sediments plus volcanic rocks) of almost 4 km west of the Antelope Range, but elsewhere is generally 1.5 to 2 km deep, and locally 3 km (Mankinen et al., 2006). Two oil test wells (Yelland No. 1 and Bastian Creek No. 1) in northern Spring Valley give depths to basement of 1.5 and 1.2 km, respectively (Hess, 2004). Figure 5-5 also suggests two geophysical sub-basins to Spring Valley. The northern geophysical sub-basin extends from west of the Antelope Range southward to just northeast of the Fortification Range. In its northern part, just south of the Antelope Range, Gans et al. (1989) and Sweetkind et al. (2007a) suggested that the caldera source of the Kalamazoo Tuff was buried beneath the valley here. However, the relatively high gravity at this location would tend to argue against this hypothesis inasmuch as most calderas are marked by substantial gravity lows. In the central part of the northern geophysical sub-basin, where the valley is crossed by US 6/US 50, a small hill (Rattlesnake Butte) made up of bedded volcanic breccia protrudes from near the middle of the valley and is the site of a former fluorspar mine. Mankinen et al. (2006) collected gravity, ground magnetic, and paleomagnetic data here that suggests a narrow and subtle, buried east-west bedrock ridge that connects with the Snake Range to the east (Figure 5-5).

The southern geophysical sub-basin of Spring Valley is south of an inter-valley bedrock ridge that is entirely buried by basin-fill alluvium. This interpreted ridge has no bedrock at the surface but has an obvious expression in the gravity data as a broad ridge at less than 0.4 km depth (Figure 5-5) that appears to extend entirely across Spring Valley between the northern Fortification Range and the southwestern Snake Range. The southern sub-basin located west of the Limestone Hills, has a maximum depth of about 1.6 km.

During data collection, special attention was paid to several boundaries to Spring Valley where groundwater-flow volumes or directions were poorly known or in debate. These included (1) Tippett Valley, (2) the area between Tippett Valley and Spring Valley, (3) the area between the Kern Mountains and the Snake Range, and (4) the area of and north of the Limestone Hills. For area #1, #2, and #3, Figure 5-6 shows the isostatic gravity, including maxspots, from Mankinen and McKee (2011). Two deep lows in Tippett Valley are shown here, both marked by curved structures on their southern sides that clearly define the lows. The curved lines in either area could be faults

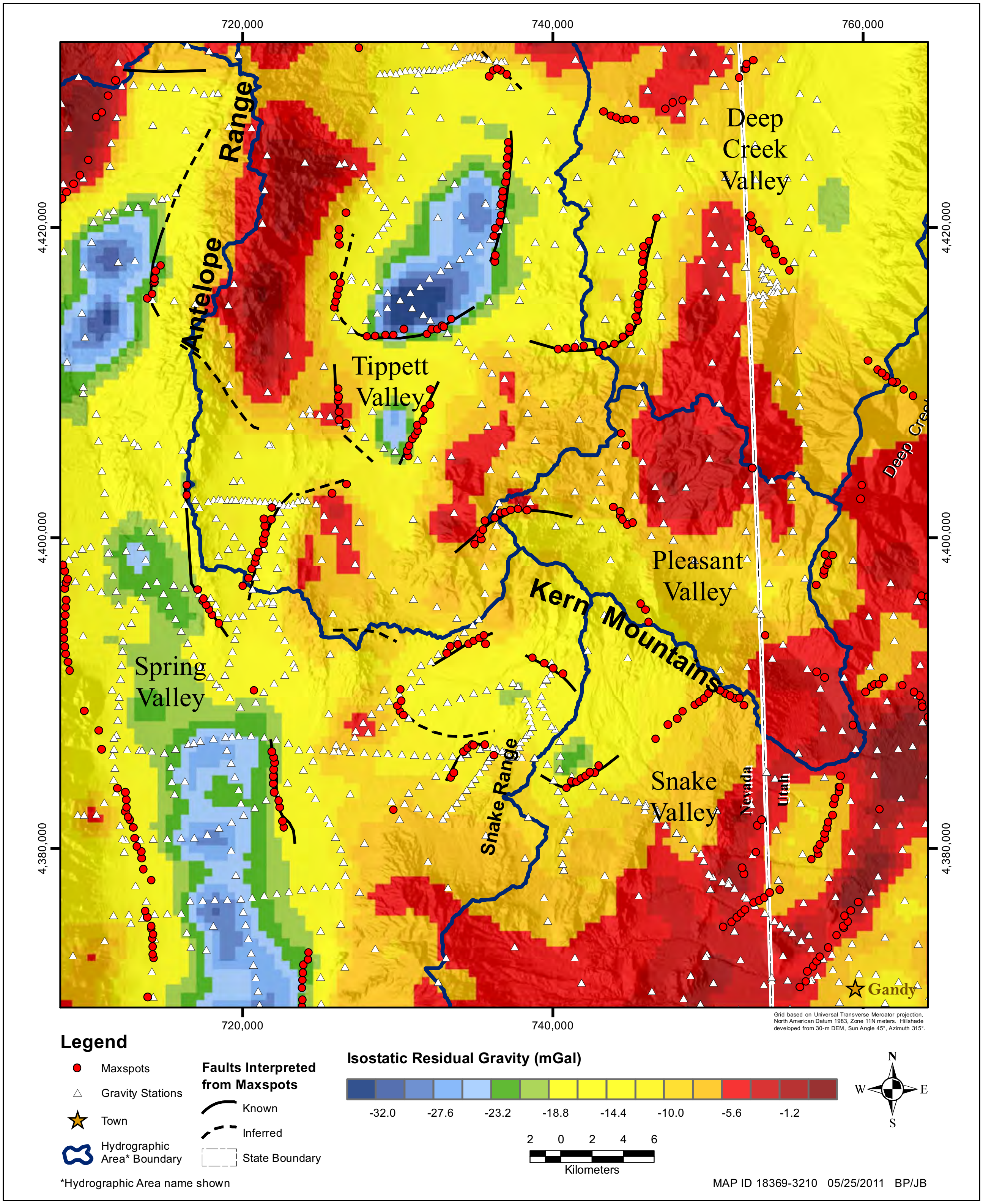

Note: Red maxspots are upward-continued from 3 km depth. Black lines are faults interpreted from maxspots.

Figure 5-6
Isostatic Residual Gravity Field and Maxspots in Tippett Valley, Western Kern Mountains, and Vicinity, Nevada

downthrown into the center of the basin or the boundaries of the caldera that erupted the Kalamazoo Tuff. Maxspots on these curved lines and on the north-trending structure on the northeastern side of the larger, northern low clearly define structures that dip into the basins; the one on the northeastern side of the northern low is a major down-to-the-west basin-range fault. In the western part of the map area, gravity data define two segments of the main, north-trending, mostly west-dipping, graben-bounding fault on the eastern side of Spring Valley and another north-to-northeast-trending range-front fault that bounds the western side of the central to northern Antelope Range; the three faults probably connect with each other.

Farther south, the east-central part of the map area (Figure 5-6) shows the western end of the Kern Mountains, including an east-trending fault defined by gravity data on the northern side. South of the Kern Mountains, the western part of the basins between the Kern Mountains and Snake Range (southeastern part of the map area) was downthrown along faults that have east-northeast and west-northwest components but result in one or two east-west basins. The low range southwest of the Kern Mountains is the Red Hills, whose western and eastern sides are defined by north-trending basin-range faults. Isostatic gravity data show that these north-trending faults not only define the Red Hills but appear to continue as buried faults that define shallow bedrock both north and south of the range. It might be argued that groundwater could move eastward from Spring Valley south of the Red Hills, but the isostatic gravity data suggest that buried pre-Tertiary rocks underlie the area south of the Red Hills and likely constitute a barrier for such a flow path. In conjunction with the depth-to-basement map (Figure 5-5), it seems more reasonable that any interbasin contribution of groundwater to the basin(s) between the Kern Mountains and Snake Range would be small or nil.

Figure 5-7 shows the isostatic gravity map and maxspots for area #4, from Mankinen and McKee (2011). The map shows the northern Limestone Hills and southern Snake Range, and the low pass between them that is south of the center of the map (contour interval is 400 m). The high-gravity areas (red) are underlain by exposed Devonian carbonate rocks, whereas the basins of Spring Valley on the west and northern Hamlin Valley on the east (yellow to blue) are underlain by upper Cenozoic alluvium and basin-fill deposits and in turn by volcanic rocks (compare with the geologic map, Plates 1 and 6). The two main north-trending, range-front, basin-range faults are shown by gravity data on either side of the Snake Range and Limestone Hills. The ranges are intensely internally broken, especially by north-trending faults, as indicated by Plates 1 and 6, but few of these faults are discriminated by gravity. One that is discriminated separates the large eastern high from the large central to southern high to the west, with a small graben of alluvial-fan and underlying volcanic rocks between the two highs of carbonates; this fault clearly continues south and probably joins the main eastern range-front fault. At the low pass (i.e., The Troughs) between the southern Snake Range and the Limestone Hills, the large central gravity high (red) has a northwest-trending embayment on its eastern side. This embayment probably marks an east-trending or northwest-trending fault that displaces the gravity high. This structure may provide a pathway for groundwater to flow from Spring Valley to northern Hamlin Valley. In the northeastern part of the map area, Big Springs is a large local spring controlled by a north-trending Quaternary fault subsidiary to the main range-front fault due west.

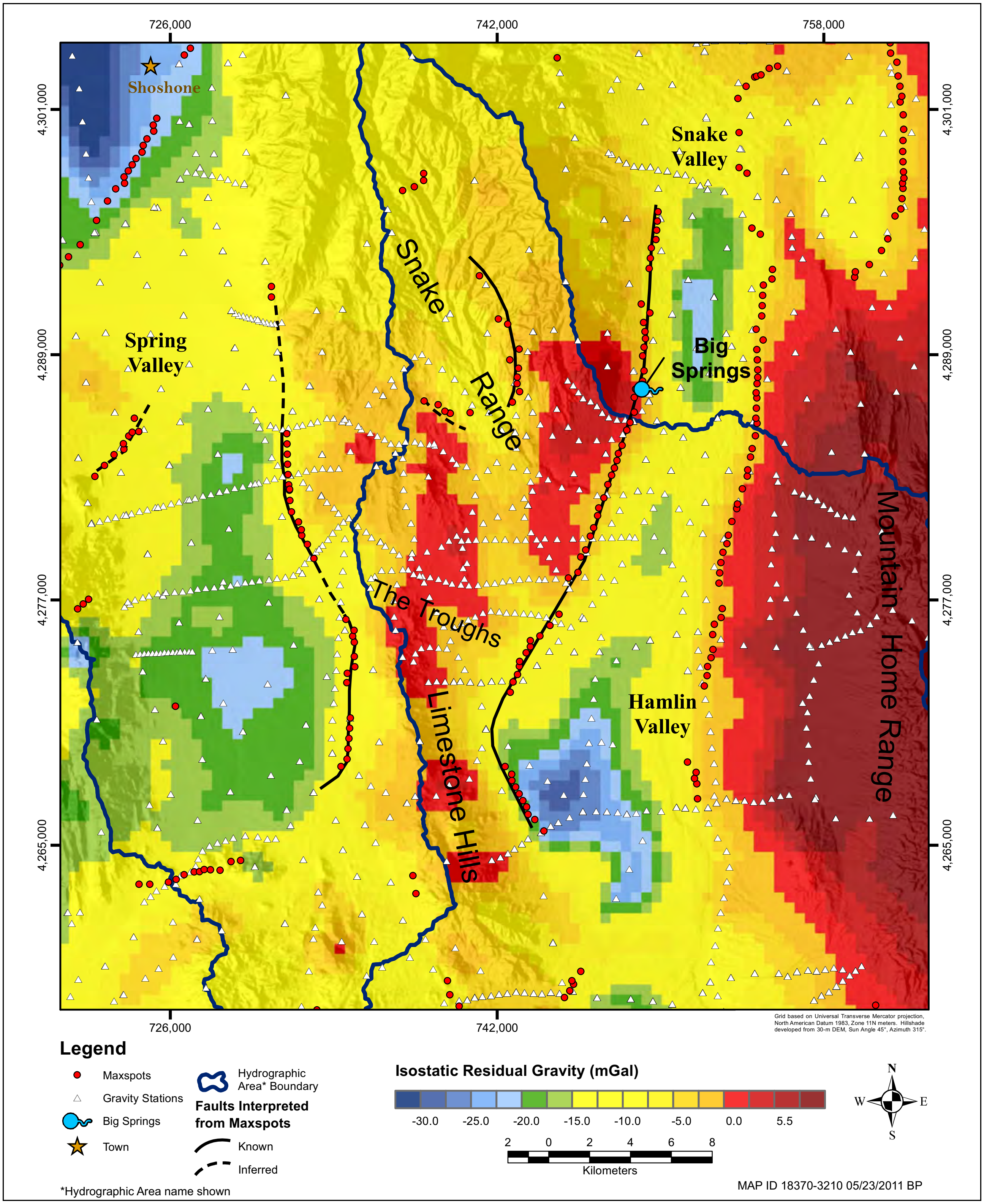

Note: Red maxspots are upward-continued from 3 km depth. Black lines are faults interpreted from maxspots.

Figure 5-7
Isostatic Residual Gravity Field and Maxspots in the Southern Snake Range and Northern Limestone Hills, Nevada

5.1.2 Gravity Data for Butte Valley and Jakes Valley

In order to help better understand the boundary conditions between south Butte and Jakes valleys, we analyzed the isostatic gravity in these two valleys and the low hills between them (Figure 5-8). Butte Valley consists of three deep gravity low areas (blue), or geophysical sub-basins, two that trend northeast and are joined in the northeastern part of the figure, and the other a deep low 20 km to the south, just south of the southwestern-extending end of the Cherry Creek Range, and also trending largely northeast. The two northern geophysical sub-basins are defined on both sides by major, northeast-striking normal basin-range faults, and the northwestern side of the southern sub-basin is similarly defined by a major northeast-striking normal fault. These faults are interpreted from maxspots. Gravity data show that the fault controlling the southern geophysical sub-basin, located between the sub-basin and the Cherry Creek Range, continues southwestward beneath southern Butte Valley. Clearly the bedrock in the southwestern end of the Cherry Creek Range also continues as a buried ridge beneath Butte Valley, and connects with the southeastern Butte Mountains on the western side of the valley.

The northeast-striking basin-bounding fault that defines the southern geophysical sub-basin (Figure 5-8) is dashed to the southwest along the southeastern edge of the Butte Mountains and low hills of volcanic rocks just to the southeast of the Butte Mountains. The fault is dashed because the change in gravity across it is considerable but the data (gravity stations) are not closely spaced here to constrain the gradient, which therefore is not as obvious or as significant as the gradient farther northeast where it bounds the sub-basin. The dashed part of the geophysically-determined fault is also shown by a mapped fault on the geologic map (Figure 4-10). A gravel road between Butte and Jakes Valley (its eastern part follows Thirtymile Wash) parallels the fault, with Summit Spring along the road controlled by the fault near the low pass between the Butte Mountains and the hills to the southeast.

5.1.3 Gravity Data for the Southern End of Steptoe Valley

In an attempt to look for possible outlets for groundwater flow from southernmost Steptoe Valley, Mankinen and McKee (2011) compiled detailed gravity data for the area consisting of southern Steptoe Valley, southwestern Spring Valley, northern Cave Valley, and northern Lake Valley. Figure 5-9 illustrates the isostatic gravity anomalies for this area. Southernmost Steptoe Valley, shown as green in the northwestern corner of the map, appears to be relatively shallow. In fact, in the middle of Steptoe Valley about 5 km north of the map area, oil test well Titan Federal No. 1 penetrated basin-fill sediments and volcanic rocks to a depth of 940 m (Hess, 2004). Southwestern Spring Valley in the northeastern part of the map and northern Lake Valley in the southeastern part of the map are significantly deeper, as indicated by blue. Only a small sub-basin of Cave Valley, at and south of the low pass, called Bullwhack Summit, which separates Steptoe Valley from Cave Valley, appears to contain significant basin-fill sedimentary rocks or volcanic rocks, whereas basin-fill and volcanic rocks are thin in more southern parts of Cave Valley on the map (see also Figure 5-5). Maxspots in Figure 5-9 show that this northern sub-basin to Cave Valley is defined on its southern side by a northeast-trending, northwest-dipping normal fault. This fault continues northeast and it and its northeast continuation (green northwest of it, and yellow southeast of it) may partly uplift the Schell Creek Range. To the east, other north- to northeast-trending normal faults that dip east to southeast mark another prominent fault zone that defines the eastern side of the Schell Creek Range.

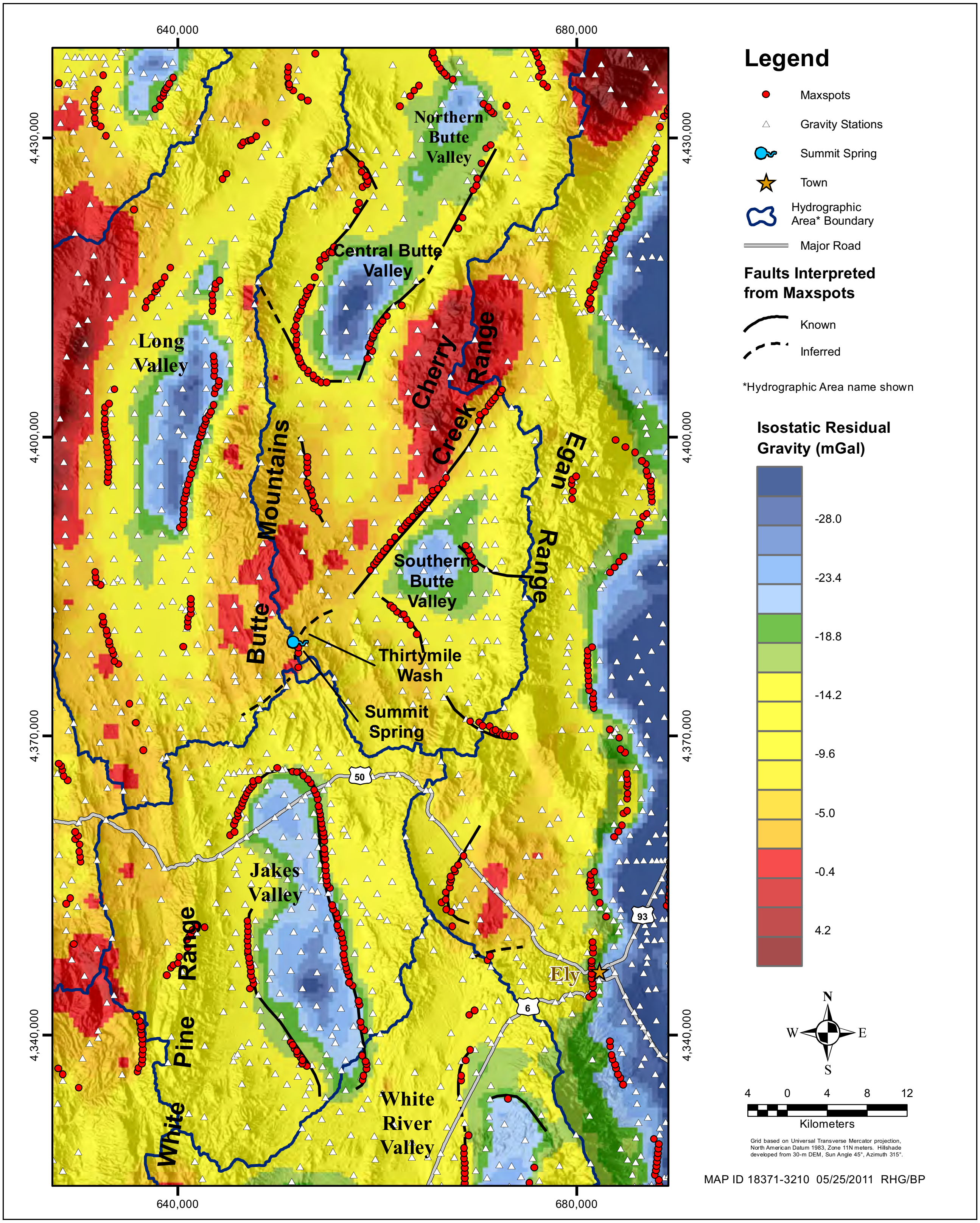

Note: Red maxspots are upward-continued from 3 km depth. Black lines are faults interpreted from maxspots.

Figure 5-8
Isostatic Residual Gravity Field in Butte and Jakes Valleys and Vicinity, Nevada

SE ROA 43248

JA_13128

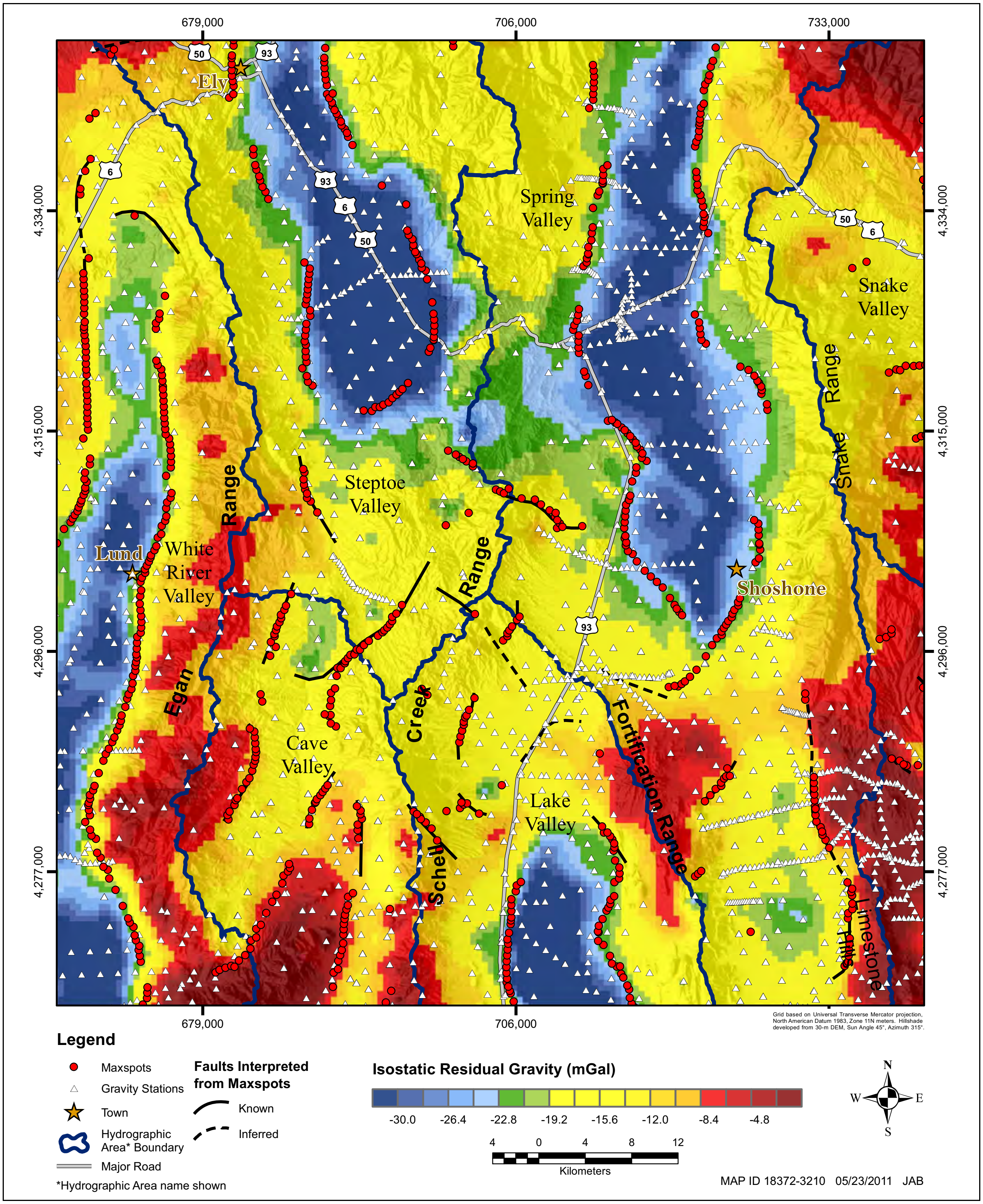

Note: Red maxspots are upward-continued from 3 km depth. Black lines are faults interpreted from maxspots.

Figure 5-9
Isostatic Residual Gravity Field and Maxspots in Southern Steptoe Valley and Vicinity, Nevada

SE ROA 43249
JA_13129

The main mass of the range, between these faults marking its east and west sides, are made up of relatively high-gravity rocks (yellows, with some reds) that correlate on the geologic map (Plate 1) with heavily faulted Paleozoic carbonates and the Chainman Shale.

5.1.4 Gravity Data for Cave, Dry Lake, and Delamar Valleys

In 2003 and 2004, with support from SNWA, Scheirer (2005) collected 468 new gravity stations in Cave, Dry Lake, and Delamar valleys to supplement about 3,500 stations in the area that had been previously collected (Snyder et al., 1981 and 1984; Bol et al., 1983; Ponce, 1992 and 1997). Scheirer's study was updated in 2006 with the collection of 434 additional stations in Spring and northern Dry Lake valleys (Mankinen et al., 2007). In 2007, another 185 gravity stations in central to southern Dry Lake and Delamar valleys (Mankinen et al., 2008) were obtained.

The figures and some of the interpretations of the gravity anomalies in the three valleys follow that of Mankinen et al. (2008). Figures 5-10 and 5-11 (Figures 1and 3, respectively, of Mankinen et al., 2008) provide, respectively, the shaded relief index map and the isostatic gravity field. Figure 5-12 (Figure 4 of Mankinen et al., 2008) shows maxspots on the isostatic gravity field. The calculated maximum values of the horizontal gradients are given as small crosses, whereas colored dots are maximum values of the horizontal gradients after analytically upward-continuing the observed anomalies to 2 km.

Figure 5-13 (Figure 7 of Mankinen et al., 2008), the depth to pre-Cenozoic basement, shows that all basins are asymmetrical in cross section and in their placement beneath the valley, reflecting basin-range extension that is rarely symmetrical in time and space. Dry Lake Valley is characterized by a slot-like graben in its center, whereas the deep portions of Cave and Delamar valleys are more bowl-shaped. The figure shows that southern Cave Valley (south of the Shingle Pass fault) is significantly deeper than Cave Valley north of the Shingle Pass fault and that the deepest parts of Dry Lake and Delamar valleys are in their southern parts. Northern Dry Lake Valley (Muleshoe Valley) is relatively shallow compared to the rest of Dry Lake Valley, and the buried bedrock ridge separating them, along the east-trending Blue Ribbon transverse zone, is apparent in the depth-to-basement data (Figure 5-13). Using the depth-to-basement algorithm, the general depth of the basin beneath southern Cave Valley extends down to 3 to 5 km, that beneath northern Dry Lake (Muleshoe) Valley to 2 km, that beneath southern Dry Lake Valley to 3 to 5 km and perhaps locally to 6.5 km, and that beneath southern Delamar Valley to 2 to 3 km (Scheirer, 2005; Mankinen et al., 2008). The ranges surrounding Dry Lake and Delamar valleys are dominated by volcanic rocks that may produce lower-density basin infill, which, in turn, would make the maximum depth estimates somewhat less. Significant parts of the basins are shallow (less than 1 km deep).

The east-trending Timpahute transverse zone shows up well in gravity data (Figure 5-12) across Dry Lake Valley and east and west of it, but a possible bedrock ridge that might separate southern Dry Lake Valley from northern Delamar Valley is indeed subtle, in the depth-to-basement data (Figure 5-13). In contrast, a buried north-trending bedrock ridge between the North Pahroc and South Pahroc ranges is obvious (Figure 5-13).

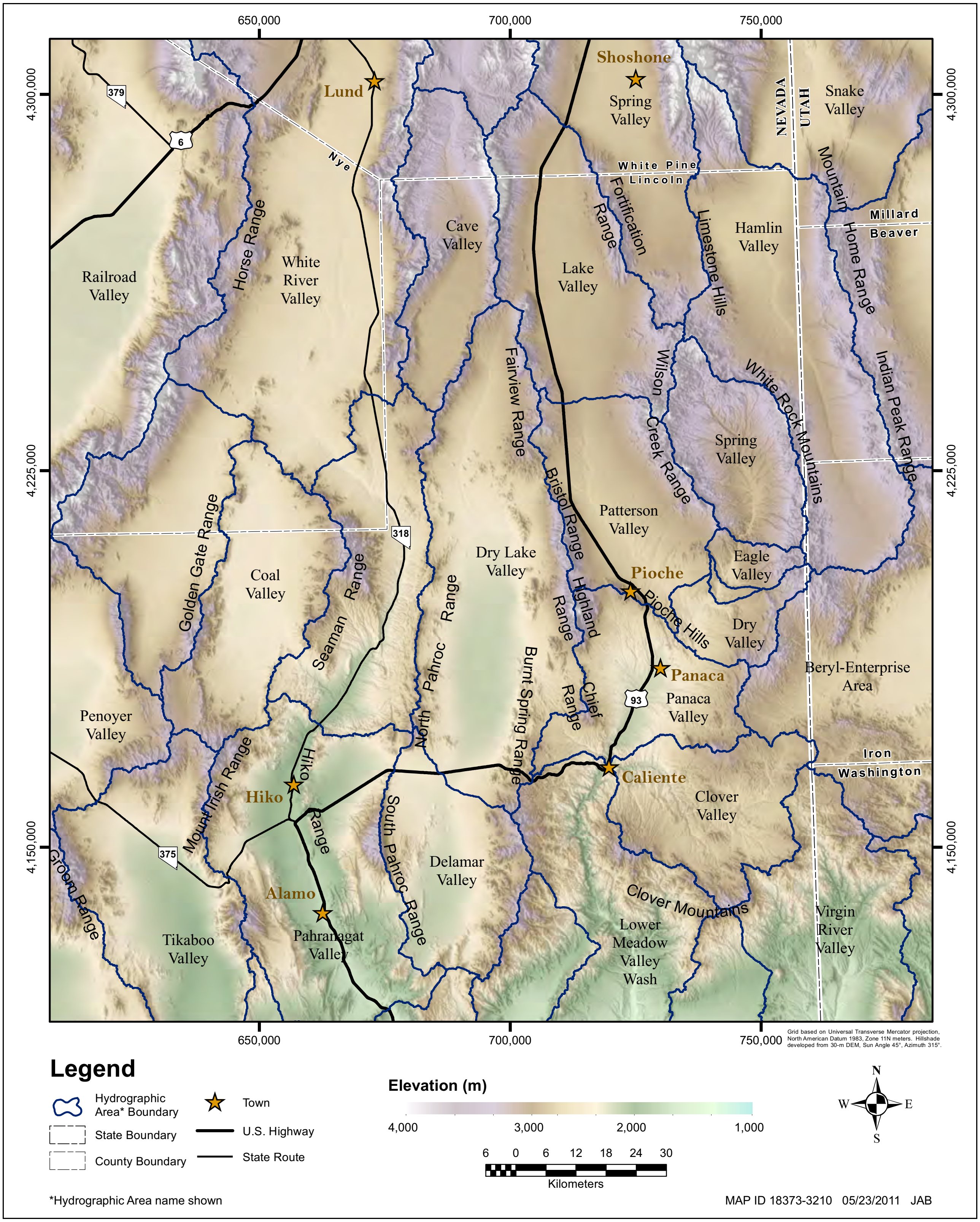

Source: Mankinen et al. (2008)

Figure 5-10
Shaded Relief Map of Cave, Dry Lake, and Delamar Valleys and Vicinity, Nevada

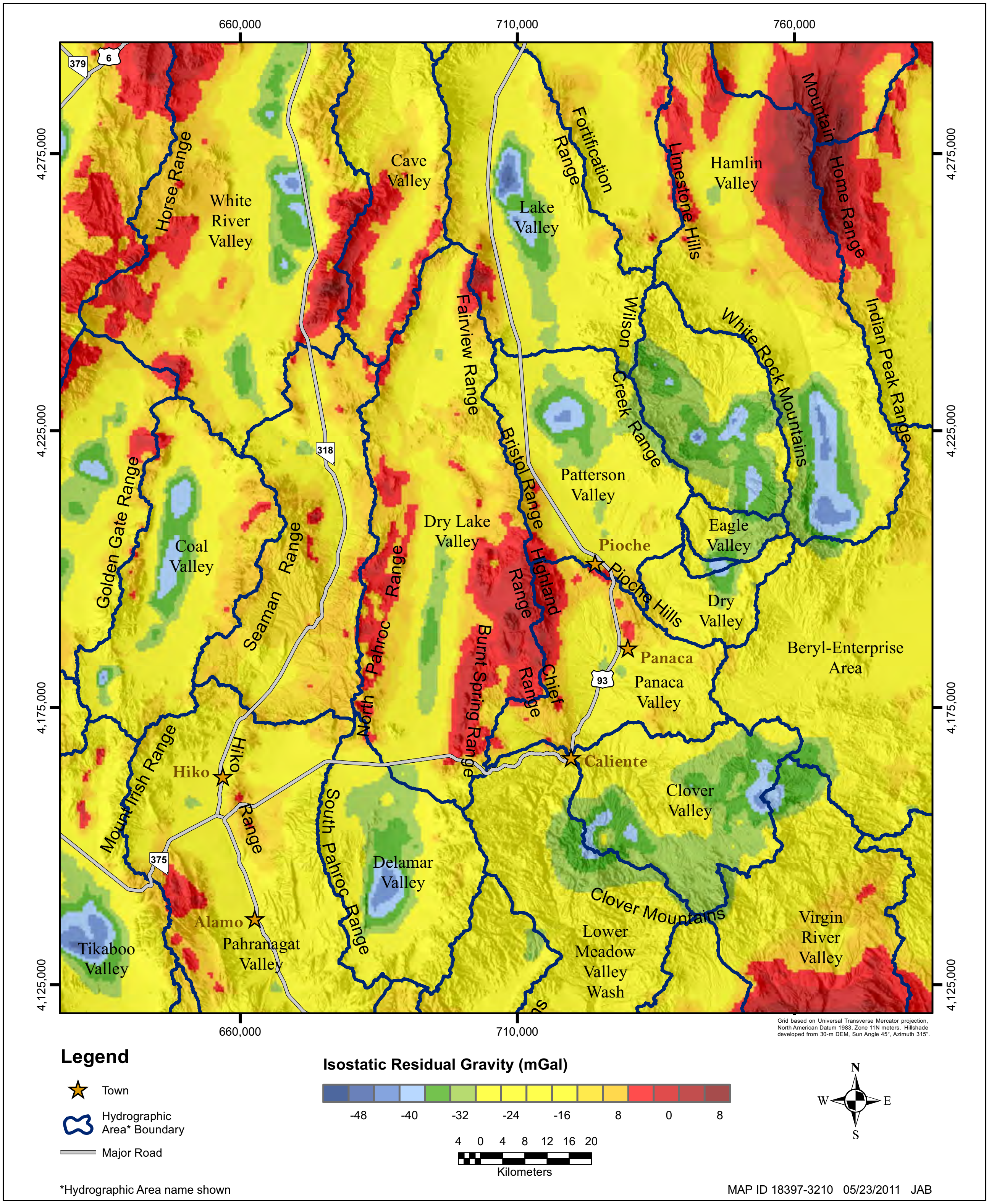

Source: Mankinen et al. (2008)

Figure 5-11
Isostatic Residual Gravity Field of Cave, Dry Lake, and Delamar Valleys and Vicinity, Nevada

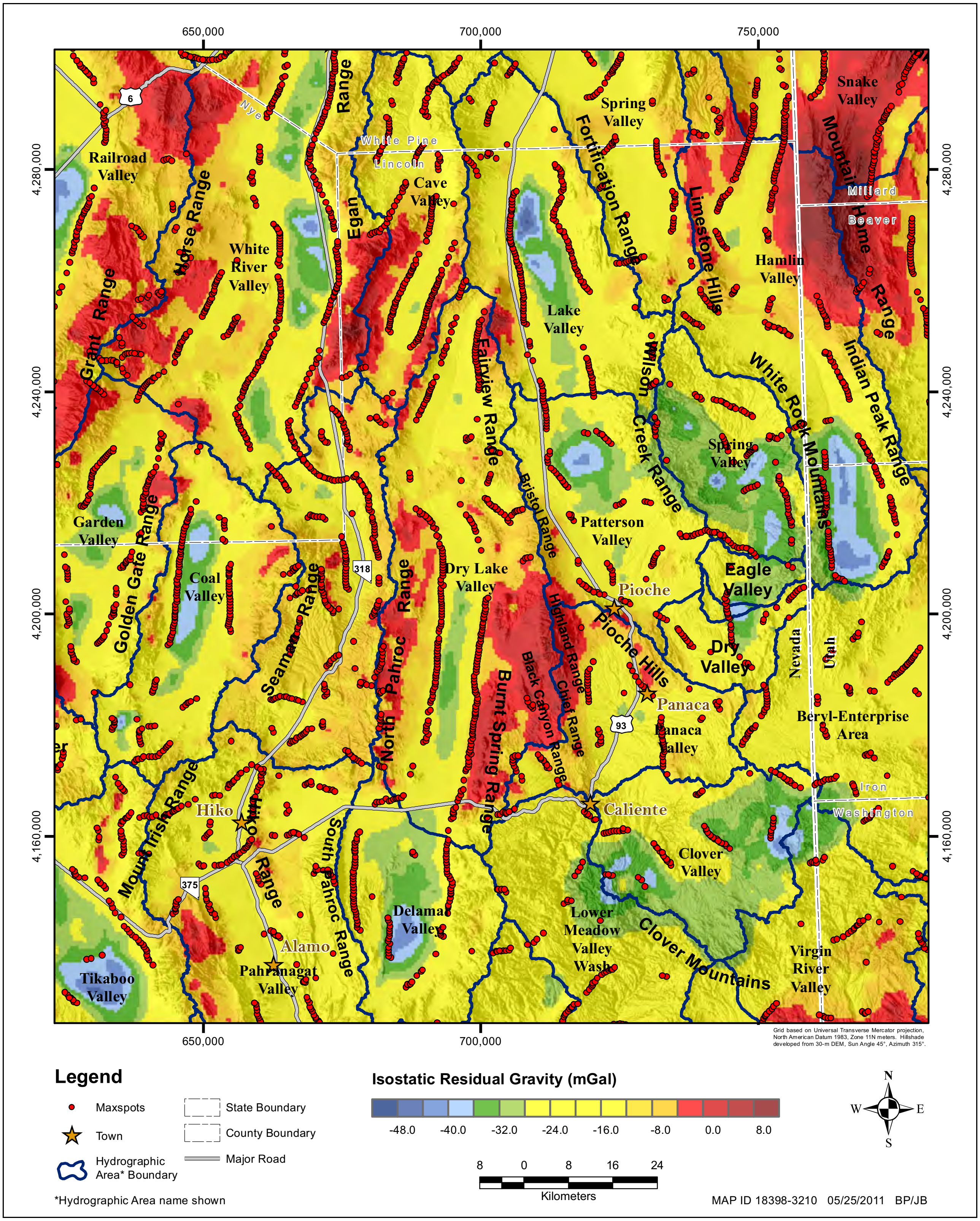

Source: Mankinen et al. (2008)

Figure 5-12
Isostatic Residual Gravity Field Showing Maxspots

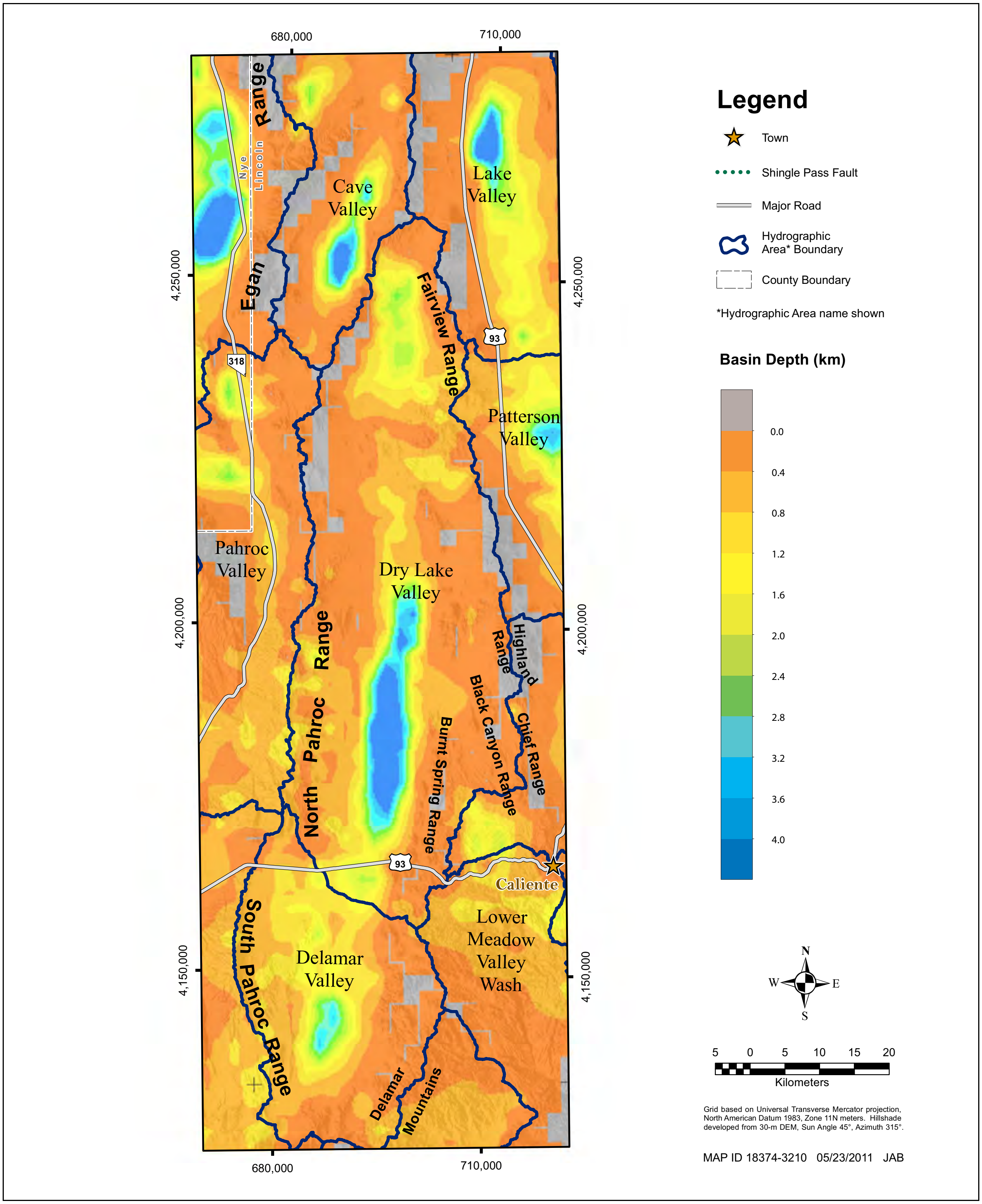

Source: Mankinen et al. (2008)

Figure 5-13
Depth of pre-Cenozoic Basement of Cave, Dry Lake, and Delamar Valleys and Vicinity, Nevada

5.2 Audiomagnetotelluric Studies

In conjunction with the gravity studies, AMT surveys were performed targeting faults and stratigraphy within the valleys, as well as estimates of depth to pre-Cenozoic basement. AMT technology detects variations in shallow, subsurface electrical resistivity, which is largely dependent on the fluid content, porosity, density, fractures, and conductive mineral content of the subsurface geology. The results are presented as a cross section along a linear profile, providing information on the third dimension in the geologic framework.

Under funding from SNWA, the USGS (McPhee, 2007; McPhee et al., 2005, 2006a and b) concluded that the technology serves as a valuable tool for mapping subsurface faults and lithology at shallow depths in basins (above about 300 m). In addition, when compared to the basement-surface estimates derived from the inversion of gravity data (Section 5.1), AMT technology proves successful in estimating the depth to bedrock. That the AMT data are consistent with the gravity data enhances confidence in both depth estimates. Dixon et al. (2007a) reproduced and interpreted three of the profiles of McPhee and her colleagues. The results of some of these later studies were published by McPhee et al. (2007, 2008, 2009), whereas other profiles have been and are being prepared by SNWA, which also interpreted the profiles (Pari and Baird, 2011).

AMT uses the magnetotelluric (MT) method, a geophysical technique that applies the earth's natural electromagnetic fields as an energy source to investigate the electrical resistivity structure of the subsurface (Telford et al., 1990; Vozoff, 1991). Within the earth's upper crust, the resistivity of geologic units is largely dependent upon their fluid content, porosity, density, degree of fracturing, temperature, and conductive mineral content (Keller, 1987). Saline fluids within pore spaces and fracture openings can reduce bulk resistivity by several orders of magnitude relative to dry rock. Resistivity can also be lowered by the presence of conductive clay minerals, graphite, and metallic sulfide mineral deposits. Tables of electrical resistivity for a variety of rocks, minerals, and geological environments may be found in Keller (1987) and Palacky (1987). For example, marine shale, mudstone, Pleistocene lake beds, and clay-rich alluvium are normally conductive, having values of a few to tens of ohm-m (ohm-meters). Fault zones can appear as low-resistivity (i.e., high-conductivity) units of less than 100 ohm-m when they are composed of rocks fractured enough to host fluids and clay alteration minerals (Eberhart-Phillips et al., 1995). Carbonate and clastic rocks are moderately to highly resistive, having values of hundreds to thousands of ohm-m depending on their fluid content, porosity, fractures, and impurities. Unaltered, metamorphic, nongraphitic rocks are moderately to highly resistive. Unaltered, unfractured igneous rocks normally are resistive and have values greater than 500 ohm-m or greater.

Using the same principles as the MT method, the AMT method estimates the electrical resistivity of the earth over depth ranges of a few meters to about one kilometer, depending upon site conditions, using a high-frequency range (Zonge and Hughes, 1991), whereas MT typically uses a lower frequency range. In areas where the resistivity distribution does not change rapidly from station to station, resistivity soundings provide a reasonable estimate of the resistivity layering beneath the site.

AMT data were collected using a Geometrics Stratagem EH4 system, which applies both natural- and controlled-source electromagnetic signals to obtain a continuous electrical sounding of the earth beneath the measurement site (Geometrics, 2007; McPhee et al., 2006a and b). Profiles were from

0.7 to 12.7 km long, with station spacing between 100 and 400 m. They are discussed below in basins generally from north to south, then west to east. The first AMT studies in the project area were done by McPhee et al. (2005, 2006a and b) along two profiles in southern Spring Valley, both of which (Profiles A and B) are reproduced below.

5.2.1 AMT Data for Spring Valley

A total of twenty-five, generally east-trending, AMT profiles (2D inversion models) were completed in Spring Valley to define faults, interpret the stratigraphy, and aid in siting drill hole locations. The work was done by the USGS, SNWA, and Layne GeoSciences. All profiles are discussed by Pari and Baird (2011). Only some of the profiles, however, are displayed here; the locations of these are shown on Figures 5-14.

About 8 km north of US 6/US 50 and just east of SR 893, the AMT data for Profile POD 54011 (abbreviated as POD 54011) were collected by Layne Geosciences (2009) along a line 1.6 km long in order to determine the geologic framework at SNWA point of diversion (POD) well application 54011. The geophysical data were reprocessed and interpreted by Pari and Baird (2011). Figures 5-15 presents the geologic map and interpreted profile. The profile reveals two buried interbasin basin-range normal faults, which are east of the main range-front fault west of SR 893. The two faults in the profile displace basin-fill sediments down to the east between stations S2 and S3 and near station S7. The highly conductive nature of the sediments suggests that they are lake sediments.

Profile 10 consists of two profiles about 10 km south of US 6/US 50 and separated by the main north-south highway here, US 93. Profile 10 West (SVN10West) is 3.2 km long, passing along the northern side of several large hills of carbonate rocks (the high resistivity material in the profile) dropped down along multiple large, north-trending, down-to-the-east normal faults that define the east side of the Schell Creek Range. The profile was collected by Layne Geosciences (2009) and reprocessed and interpreted by Pari and Baird (2011). The geologic map and interpreted profile (Figure 5-16) shows a complicated series of normal faults.

AMT data in Profile B (SVNB) were collected on a line about 3 km east of where US 93 crosses a low pass (Lake Valley Summit) that separates Spring Valley from Lake Valley to the south. The data in Profile B (SVNB) were published by McPhee et al. (2006a) and interpreted by McPhee et al. (2005) and SNWA, as shown in Figure 5-17. The low, northwest-trending ridge (in the southwest part of the map) is made up of Permian rocks and Pennsylvanian Ely Limestone that strike northwest and dip northeast; the ridge connects the southern Schell Creek Range with the northern Fortification Range. SNWA test well 184W103, just north of the western end of the line, was drilled to a depth of 310 m in the Ely Limestone. The AMT profile, about 2.3 km long, images a prominent west-northwest-trending, range-front fault that defines the low ridge and is the southeastward continuation of the fault zone that defines the eastern side of the Schell Creek Range.

Profile A (SVNA) is 12.7 km long, spanning southern Spring Valley between the eastern edge of the Fortification Range and the western edge of the Limestone Hills (McPhee et al., 2005, 2006a and b). The 2D inversion model and its geologic interpretation are shown in Figure 5-18. Two SNWA monitoring wells are shown on the geologic map; the western one is projected to the profile. SNWA

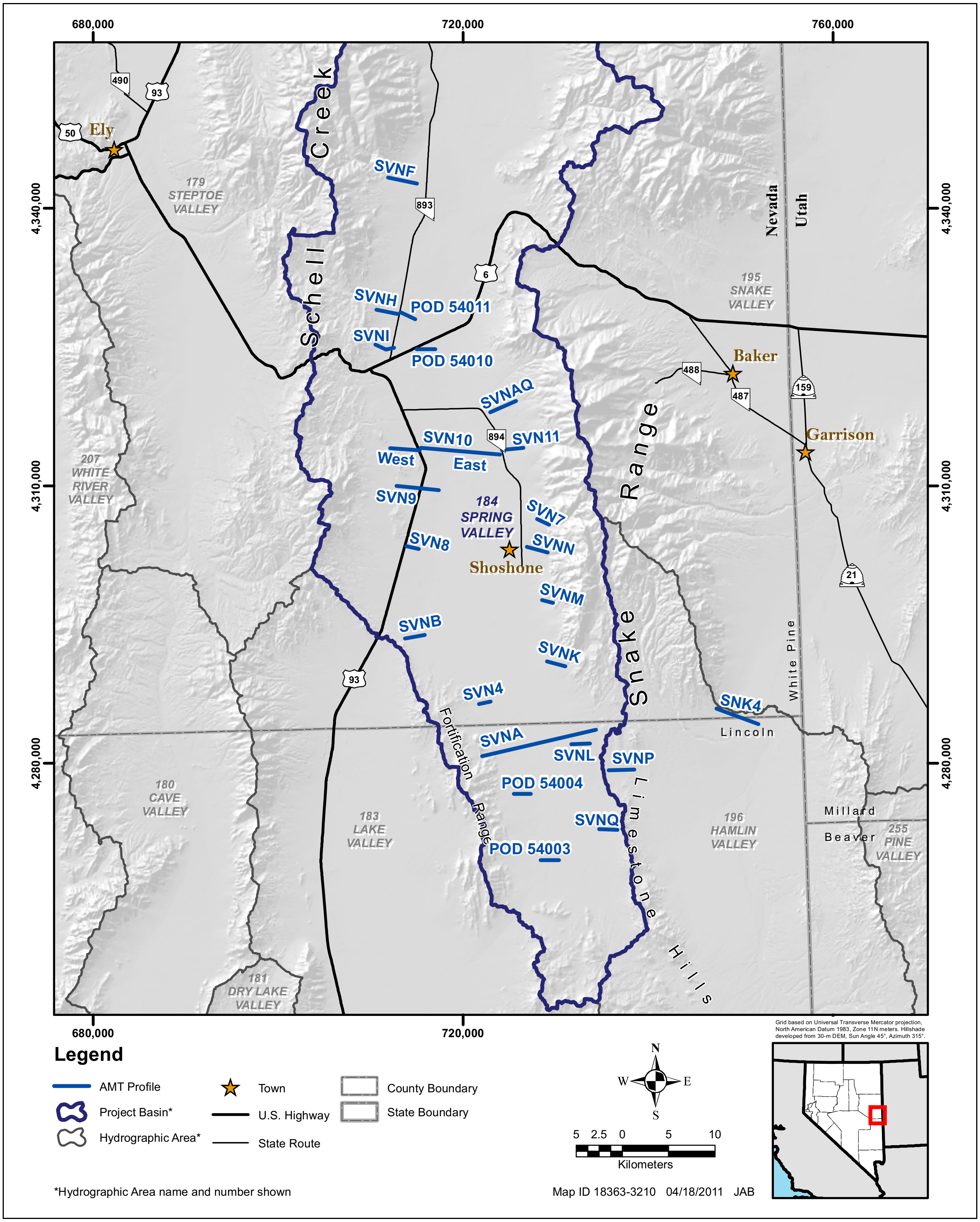

Figure 5-14
Map of Spring Valley and Vicinity, Nevada Showing Locations of AMT Profiles

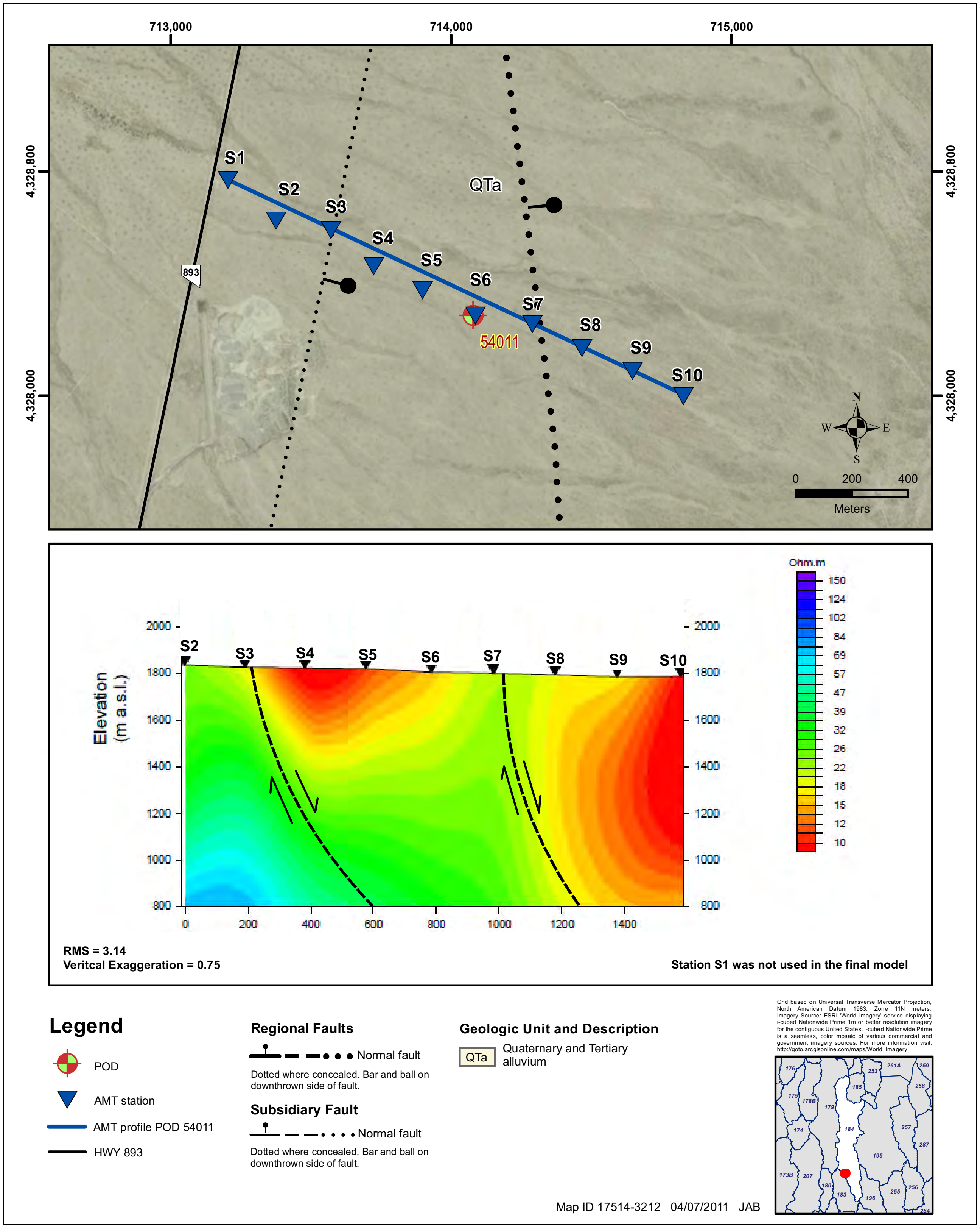

Source: Pari and Baird (2011)

Figure 5-15
Map and 2D Model of Area of POD 54011

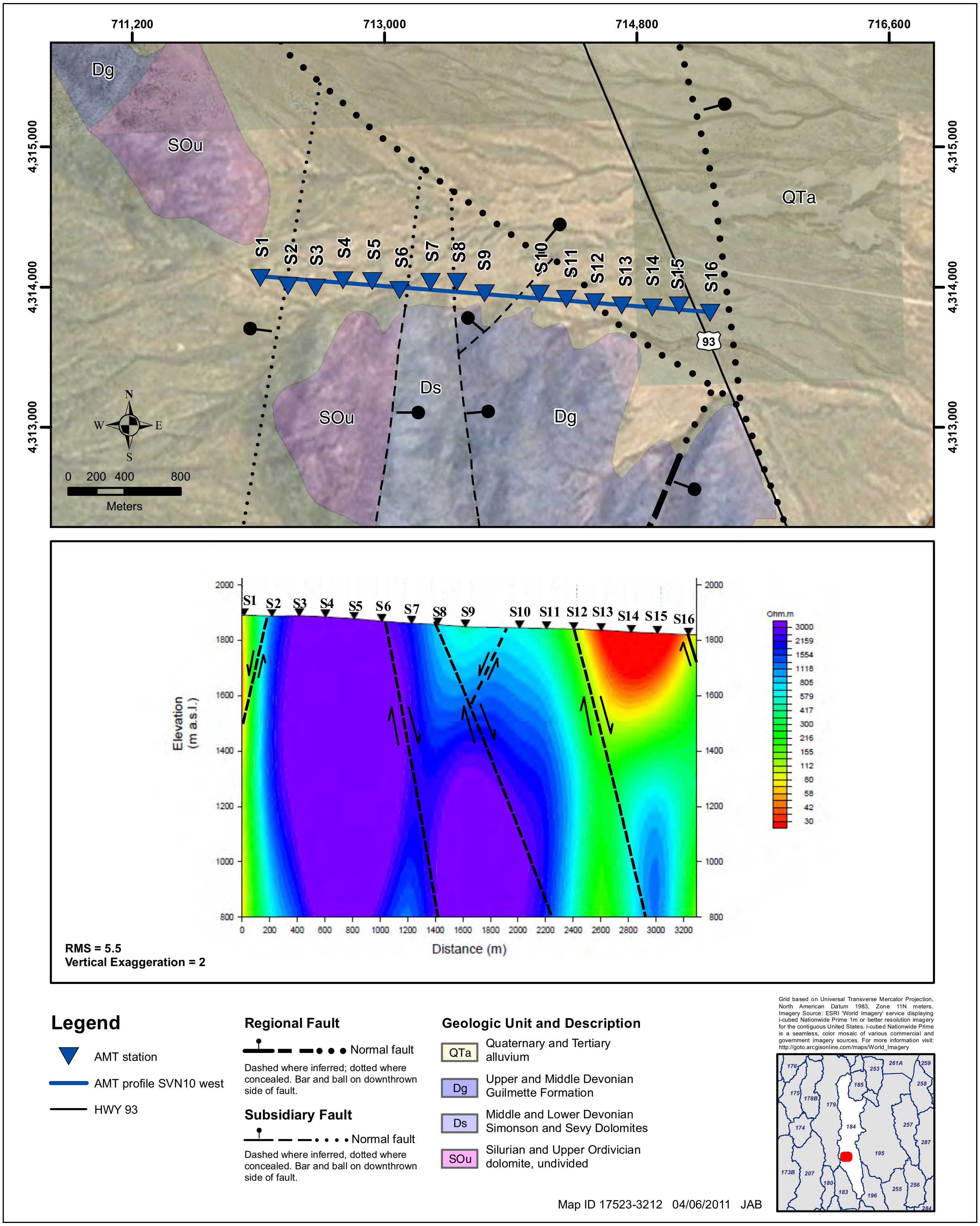

Source: Pari and Baird (2011)

Figure 5-16
Map and 2D Model of SVN10 West

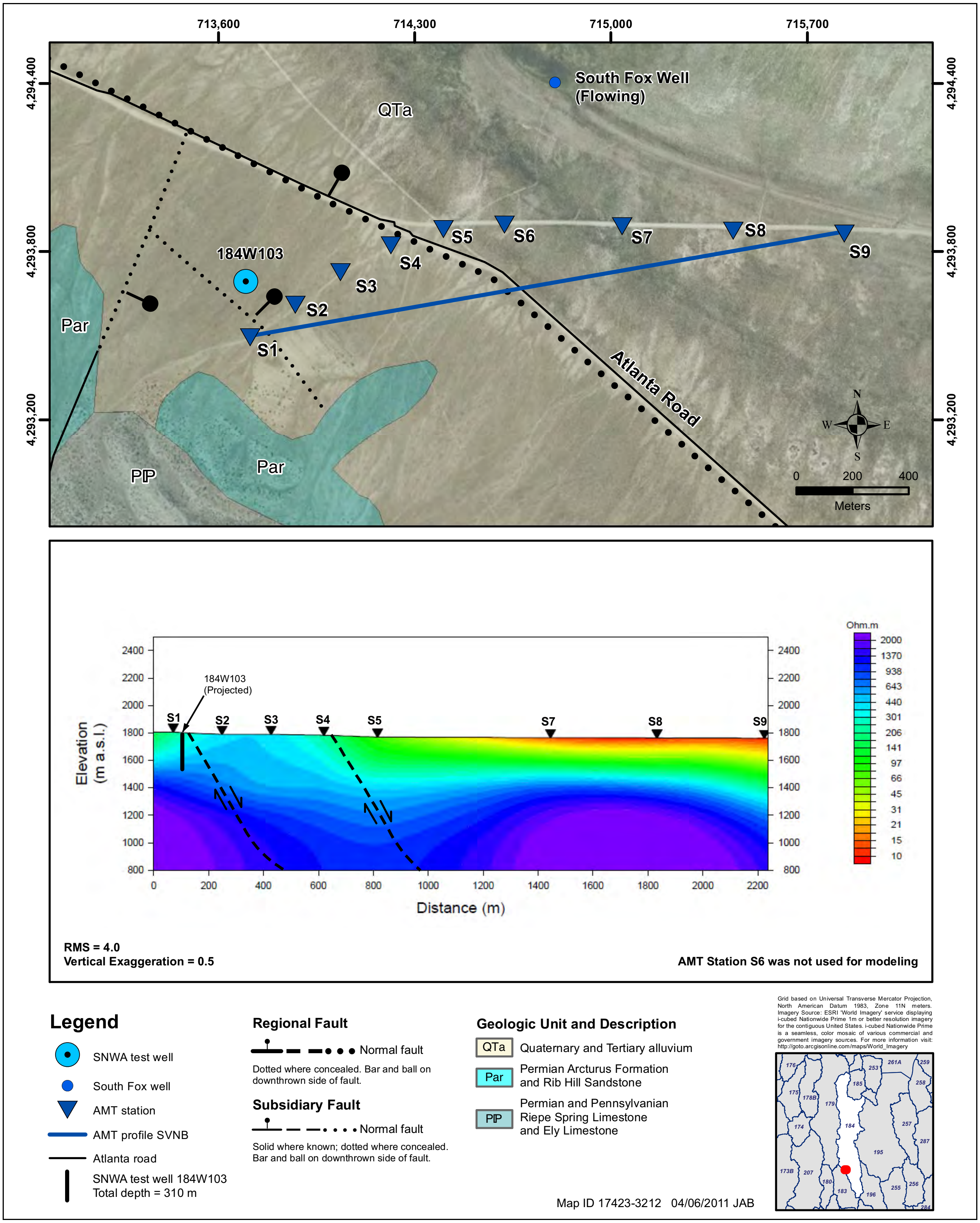

Source: Pari and Baird (2011)

Figure 5-17
Map and 2D Model of SVNB

SE ROA 43260

JA_13140

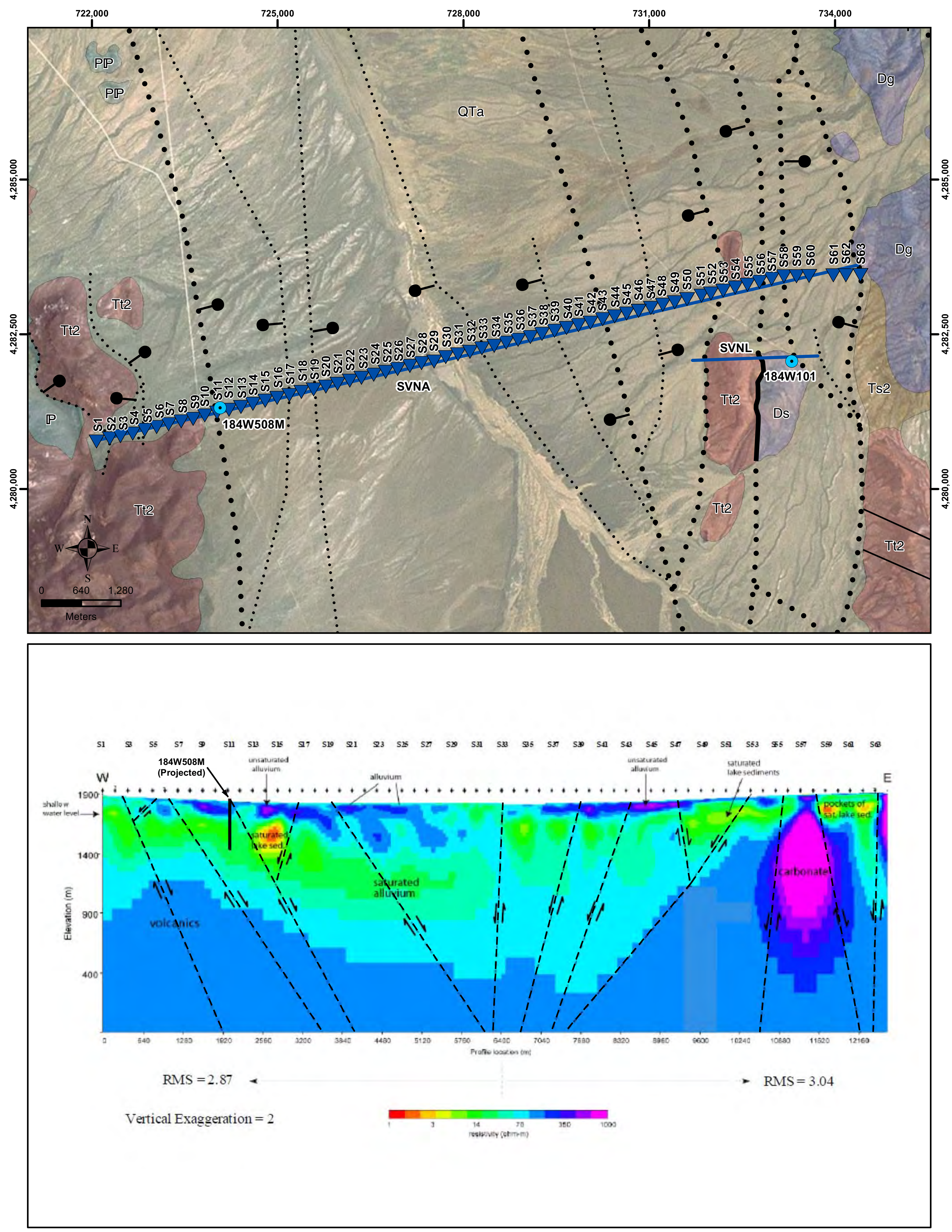

Legend

- AMT station
- AMT profile SVNA
- SNWA well
- SNWA monitor well 184W508M

Regional Fault

Normal fault

Solid where known; dotted where concealed. Bar and ball on downthrown side of fault.

Subsidiary Fault

Normal fault

Solid where known; dotted where concealed. Bar and ball on downthrown side of fault.

Geologic Unit and Description

- QTa — Quaternary and Tertiary alluvium
- Ts2 — Tertiary, mostly tuffaceous sandstone and bedded airfall tuff
- Tt2 — Tertiary, poorly-densly welded ash-flow tuff and interbedded airfall tuff
- IP — Pennsylvanian Ely Limestone
- PIP — Permian and Pennsylvanian Riepe Spring Limestone and Ely Limestone
- Dg — Upper and Middle Devonian Guilmette Formation
- Ds — Middle and Lower Devonian Simonson and Sevy Dolomites

Grid based on Universal Transverse Mercator Projection, North American Datum 1983, Zone 11N meters. Imagery Source: ESRI 'World Imagery' service displaying i-cubed Nationwide Prime 1m or better resolution imagery for the contiguous United States. i-cubed Nationwide Prime is a seamless, color mosaic of various commercial and government imagery sources. For more information visit: http://goto.arcgisonline.com/maps/World_Imagery

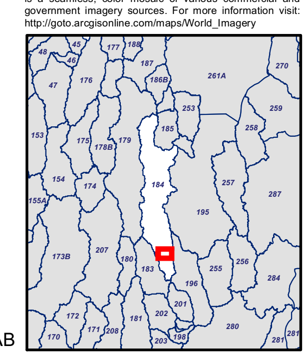

Map ID 17526-3212 04/06/2011 JAB

Source: Pari and Baird (2011)

Figure 5-18
Map and 2D Model of SVNA

Well 184W508M is near AMT station S11 near the western end of the profile and SNWA Well 184W101 is south of station S56 near the eastern end of the profile. The western well was drilled to a depth of 360 m, encountering non-welded and moderately welded ash-flow tuffs throughout. The eastern well was drilled to a depth of 538 m, encountering carbonate rocks. The profile shows 10 interpreted faults as black lines. A clear transition between unsaturated (200 to 500 ohm-m) alluvium above and saturated alluvium/volcanic rocks (20 to 50 ohm-m) below is present at roughly 100 m depth in many parts of Profile A. Highly resistive (greater than 1,000 ohm-m) carbonate rocks are clearly defined at the eastern end of Profile A under the Limestone Hills, and the locations and dips of several range-front and interbasin faults that lack surface expression can be interpreted throughout the upper 1-km portion of the section image. The interpreted surface between the alluvium/basin-fill sediments and underlying volcanic rocks is shown on the cross section.

About 1 km south of the eastern end of Profile A (SVNA), AMT data were collected along Profile L (SVNL; see Figure 5-19) by McPhee et al. (2007), but the data were not interpreted. The profile, which is 2.0 km long, was compiled to add detail to fault interpretations in Profile A (SNVA), to test electrical responses in volcanic versus carbonate rocks, and to interpret the data in SNWA test well 184W101, west of the Limestone Hills. The geologic map and profile, interpreted by Pari and Baird (2011) are shown in Figure 5-19. The profile images four basin-range faults. Test Well 184W101, near station S9, had a total depth of 536 m, wholly in carbonate rocks.

About 4 km south of Profile A (SVNA), AMT data were measured by McPhee et al. (2008) for Profile Q (SVNQ) through a pass between the southern Snake Range and the northern Limestone Hills. This pass, at The Troughs, is one of the two most likely routes for any groundwater moving from Spring Valley to Hamlin Valley to the east. Profile P (SVNP) was published by McPhee et al. (2008), who did not interpret the geology. The geologic map and the profile, interpreted by Pari and Baird (2011), are shown on Figure 5-20. At its eastern edge, the profile images a prominent buried, down-to-the-west and west-dipping normal fault that forms the eastern side of an axial graben of Tertiary volcanic rocks. Farther west, between stations S10 and S11, a prominent east-dipping and down-to-the-east normal fault forms the western side of the graben. This fault continues north and south of the map area; south of the map area, this fault is the eastern range-front fault of the Limestone Hills. Farther west along the profile, between stations S9 and S10, a west-dipping and down-to-the-west normal fault is imaged. AMT data for two other profiles were collected in the area of The Troughs, one of which was attempted to look for east-trending faults in the pass, but the results were not conclusive (McPhee et al., 2007, 2008). Gravity data, discussed in Section 5.1.1, were more diagnostic in an attempt to image east-trending structures near The Troughs. A less detailed geologic map and cross section is provided as Figure 4-20 and discussed in Figure 4.4.25.

5.2.2 AMT Data for Snake Valley

Under contract from SNWA, the USGS completed four generally east-trending AMT profiles in Snake Valley. SNWA has collected AMT data for additional profiles that are being processed and interpreted. Of the four USGS profiles, preliminary profiles of three of them, whose imaged geology was not interpreted, were published by McPhee et al. (2007). Later, AMT data for the fourth profile (Figure 5-21) were collected, then all four profiles were interpreted and published by McPhee et al. (2009). The southern of these, Profile 4 (SNK4) in the Big Springs area along the southeastern flank of the Snake Range (Figure 5-14) is reproduced here as Figure 5-21. It was done to identify

SE ROA 43262

JA_13142

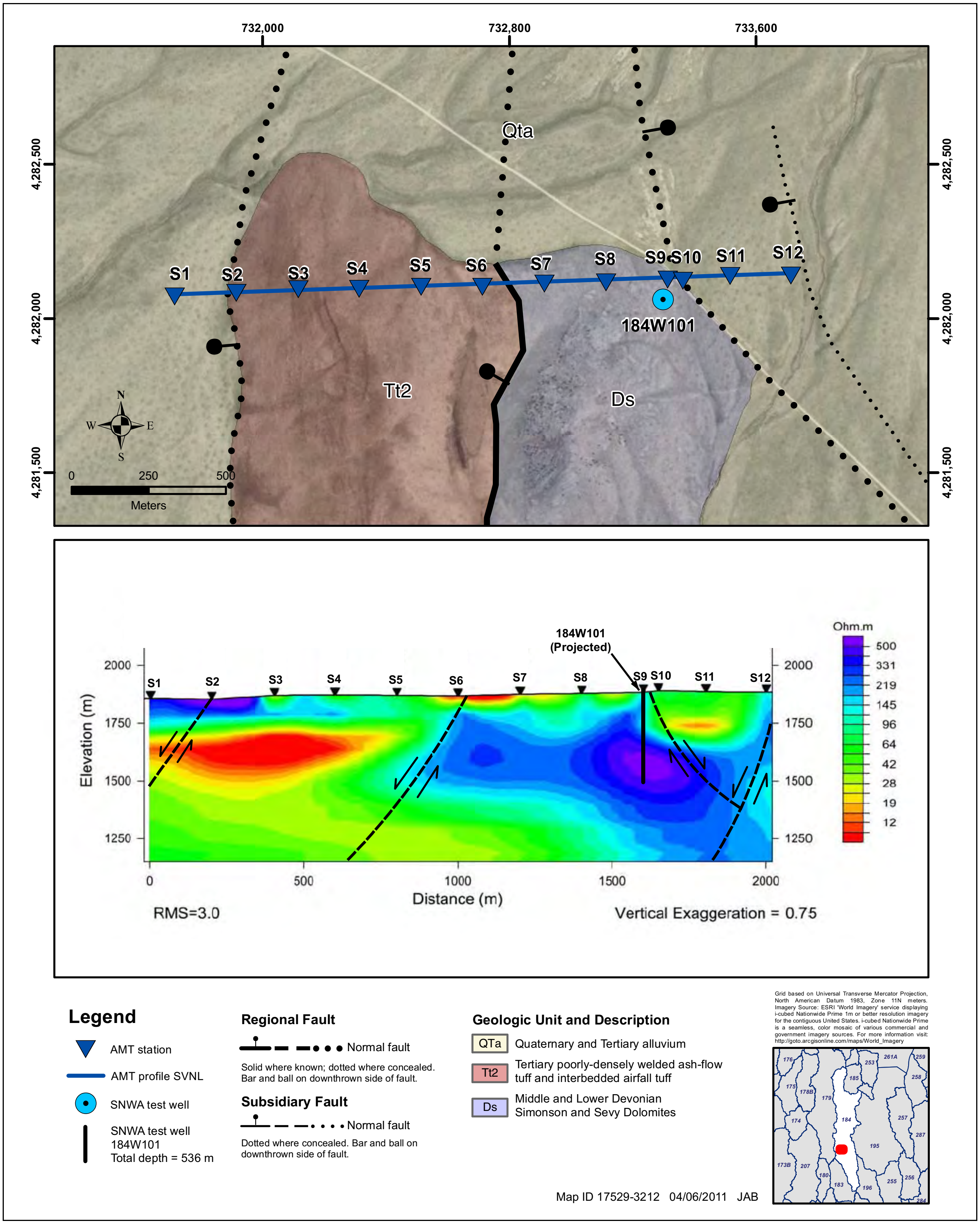

Source: Pari and Baird (2011)

Figure 5-19
Map and 2D Model of SVNL

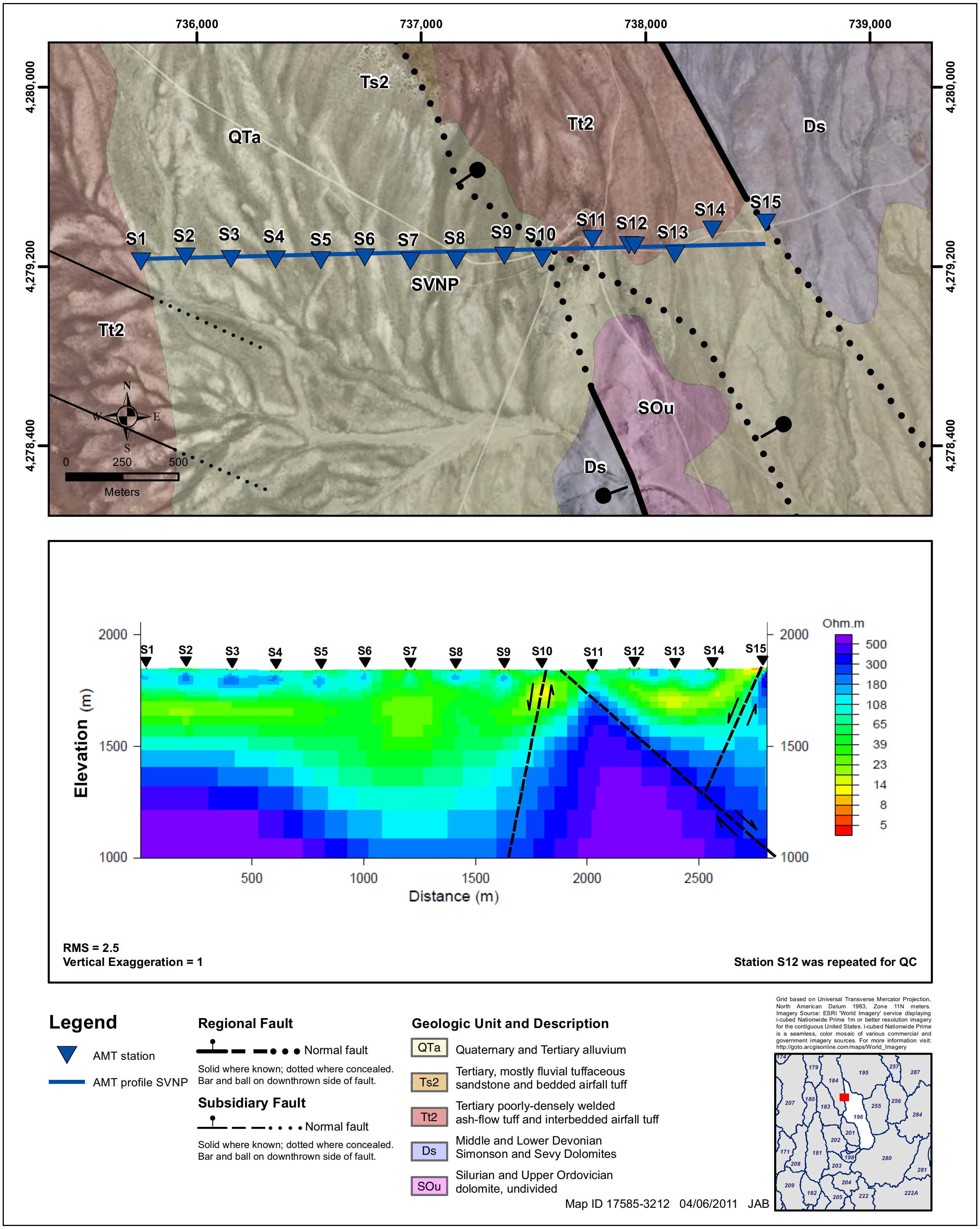

Source: Pari and Baird (2011)

Figure 5-20
Map and 2D Model of SVNP

SE ROA 43264

JA_13144

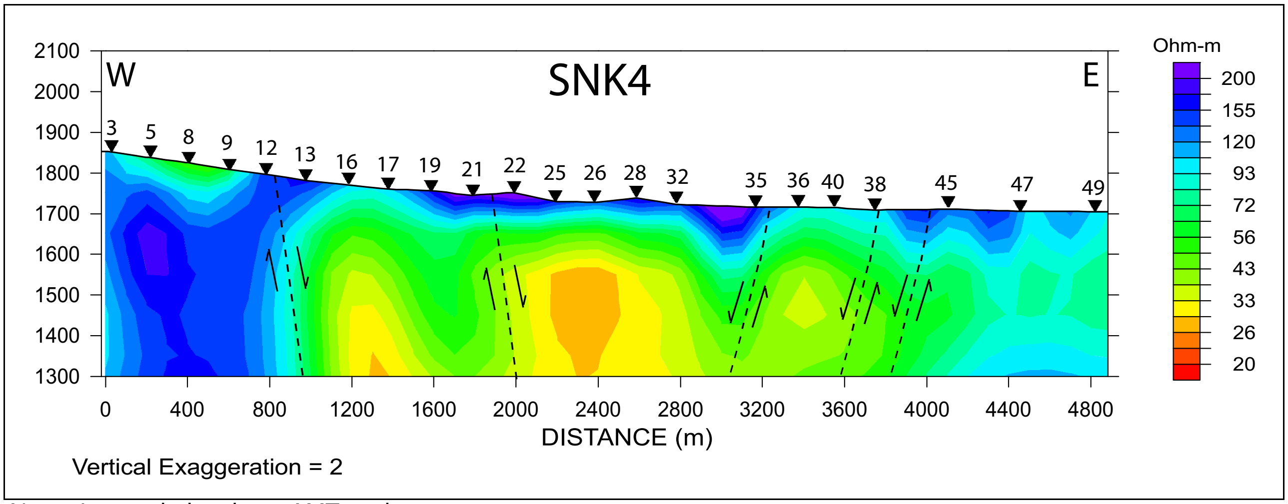

Note: Inverted triangles = AMT stations.

Figure 5-21
2D Inverse Model Computed from the Transverse-Magnetic-Mode Data along Profile SNK4 in Western Snake Valley, Nevada (RMS = 3.0)

structures that control the springs. Most of these structures are Quaternary faults that were mapped cutting alluvial-fan deposits. The line, which extends for 5.0 km, is about 4 km south of the Big Springs complex and 1 to 3 km south of South and North Little Spring, respectively. The interpreted profile McPhee et al. (2009) provides a spectacular example of the usefulness of AMT geophysics, with at least 5 basin-range faults imaged. The main down-to-the-east, range-front fault zone is the western one in the profile, near station 12. The other faults, farther east, suggest why springs are abundant in the area.

5.2.3 AMT Data for Cave Valley

AMT data were collected along a single east-trending line, Profile E (CVE) against the eastern side of southern Cave Valley and west of Sidehill Pass. The location is shown on Figure 5-22. Profile E (CVE), collected and interpreted by McPhee et al. (2005, 2006a and b), has a length of 3.4 km. The geologic map and profile (Pari and Baird, 2011) are shown on Figure 5-23. Profile E clearly images the western range-front basin-range fault of the Schell Creek Range. Other buried interbasin faults, including one between stations S2 and S3, are less clear but probable.

Profile E (CVE) compares favorably with existing drill holes and with the adjacent industry seismic profile (Scheirer, 2005) discussed in Section 5.3. Existing SNWA well 180W504M, drilled south of the line of Profile E (CVE) and east of the main range-front fault, penetrated basin-fill sediments to a depth of 150 m, then passed into carbonate rocks to a total depth of 272 m. Sidehill Pass Federal No. 18-13 (see also Section 5.3), drilled north of the line of Profile E (just north of the map in Figure 5-23) and west of the main range-front fault, penetrated about 1,550 m of basin-fill sediments before passing into the Mississippian Joana Limestone, which continued to a total depth of about 2,000 m (Hess, 2004).

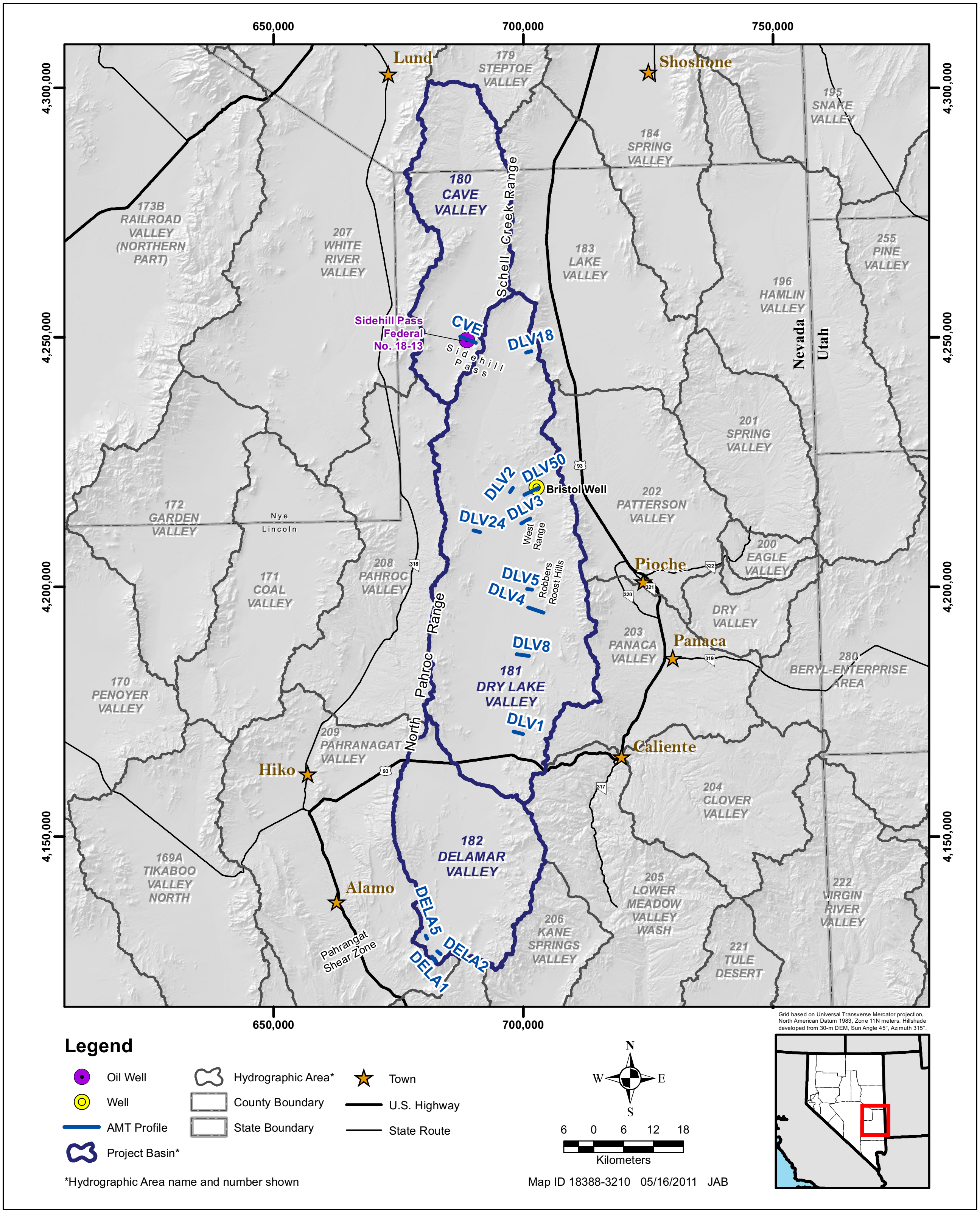

Figure 5-22
Map of Cave, Dry Lake, and Delamar Valleys, Nevada and Utah, Showing Location of AMT Profiles

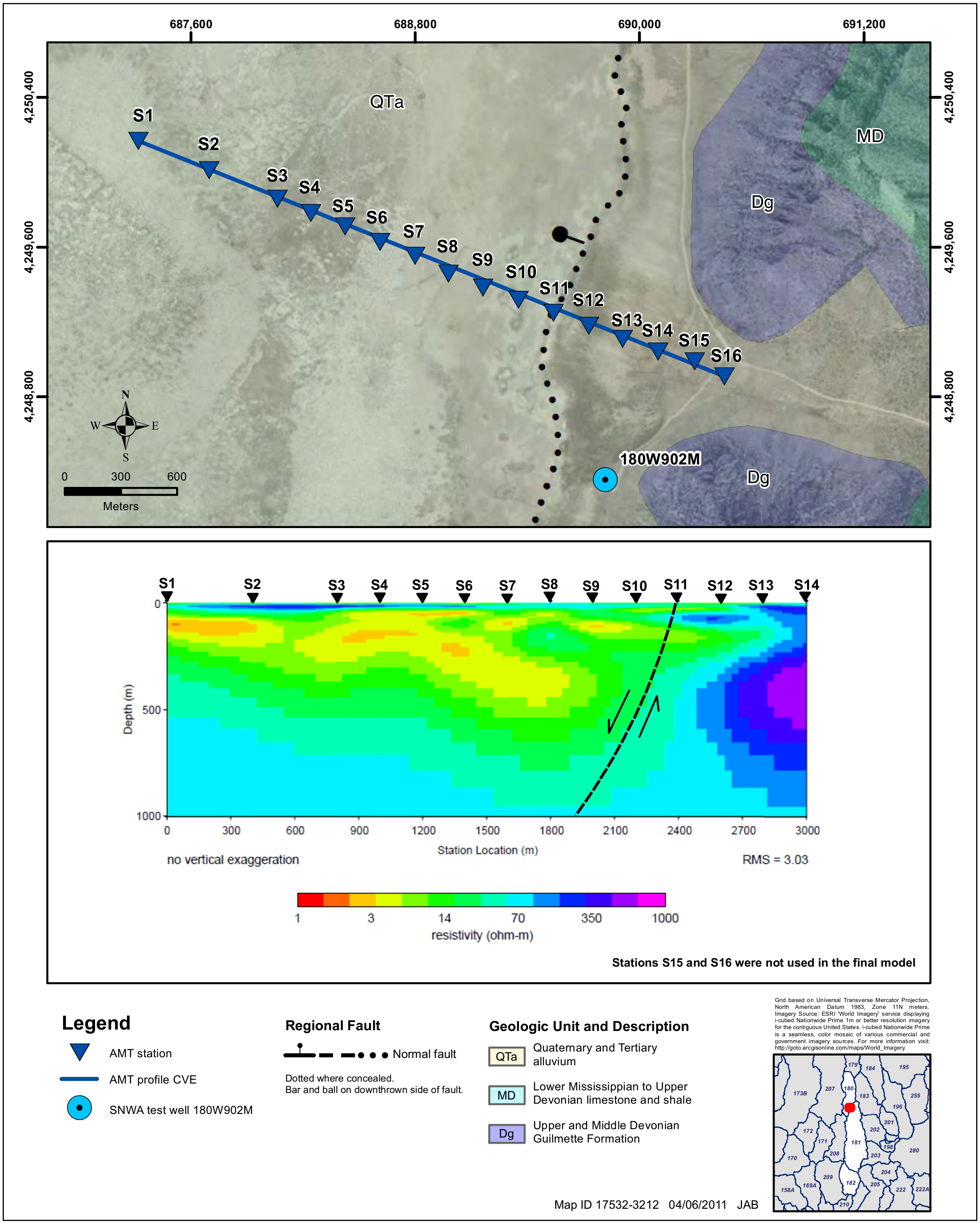

Source: Pari and Baird (2011)

Figure 5-23
Map and 2D Model of CVE

SE ROA 43267

JA_13147

5.2.4 AMT Data for Dry Lake Valley

A total of nine, generally east-trending, AMT profiles were completed in Dry Lake Valley, seven by the USGS (McPhee et al., 2008) and two by SNWA. All profiles were interpreted and discussed by Pari and Baird (2011). Only some of the profiles, however, are discussed here; the locations of these are shown on Figure 5-22.

Just east of Dry Lake Valley, AMT data were collected by SNWA in a structurally complex area west of Bristol Wells and just east of the West Range to test the AMT technique where Tertiary ash-flow tuffs are faulted against Devonian and Ordovician carbonate rocks. The data in Profile 50 (DLV50), which has a length of 3.2 km, shows that the technique clearly displayed large buried structures whether they cut volcanic or carbonate rocks. However, stations S1 through S3 were omitted from the profile due to poor data quality. The profile was interpreted by Pari and Baird (2011), as shown in Figure 5-24. Both the western end of the profile (station S4) and the eastern part (between stations S13 and S14) of the profile show mapped buried right-lateral faults. In between these two faults, the profile clearly shows a still larger buried right-lateral fault between stations S7 and S8, characterized by its vertical nature. Although not mapped because of the scale (1:250,000) of the geologic map (Plate 1), this strike-slip fault was mapped at a scale of 1:24,000 by Page and Ekren (1995). It is clearly a major structure that contains highly conductive hydrothermal clay, fault gouge, and groundwater.

Farther south, AMT data were collected along a single line on the western side of Dry Lake Valley, at the northern end of the North Pahroc Range. The data in Profile 24 (DLV24), which has a length of 1.4 km, were collected, but not interpreted geologically, by McPhee et al. (2008). The geologic map and interpreted profile, by Pari and Baird (2011), are shown in Figure 5-25. Three faults are imaged by Profile 24 (DLV24), one a mapped but buried right-lateral fault between stations S1 and S2, and two buried normal faults that define a graben between stations S4 and S8.

About 32 km to the south, on the western side of the Robber Roost Hills, AMT data were obtained from a line 2.5 km long, but not geologically interpreted, by McPhee et al. (2008). The geologic map and Profile 8 (DLV8) were interpreted by Pari and Baird (2011), as shown in Figure 5-26. Two major splays of the range-front fault zone on the eastern side of Dry Lake Valley were imaged, a major fault that includes Quaternary displacement near station S5, and a buried major splay farther east, at station S11. Two smaller faults were identified to the west. The fault that includes Quaternary movement is clearly a major fault, for it contains highly conductive material, probably hydrothermal clay and fault gouge, and it probably contains significant groundwater. About 10 km north of the profile, historic open fissures formed by movement along the Quaternary fault were mapped by Swadley (1995).

5.2.5 AMT Data for Delamar Valley

Three AMT profiles (Pari and Baird, 2011) were performed in the southwestern Delamar Valley to image northeast-trending, left-lateral strike-slip faults of the PSZ (Ekren et al., 1977; Scott et al., 1993), which mostly displaces Tertiary ash-flow tuffs. Two of the profiles, whose locations are shown on Figure 5-22, are given here. The faults of the PSZ pass into north-trending basin-range normal faults at both ends so the faults of the PSZ can be looked upon as accommodation zones during east-west basin-range extension. In other words, their slip where they trend northeast is

SE ROA 43268

JA_13148

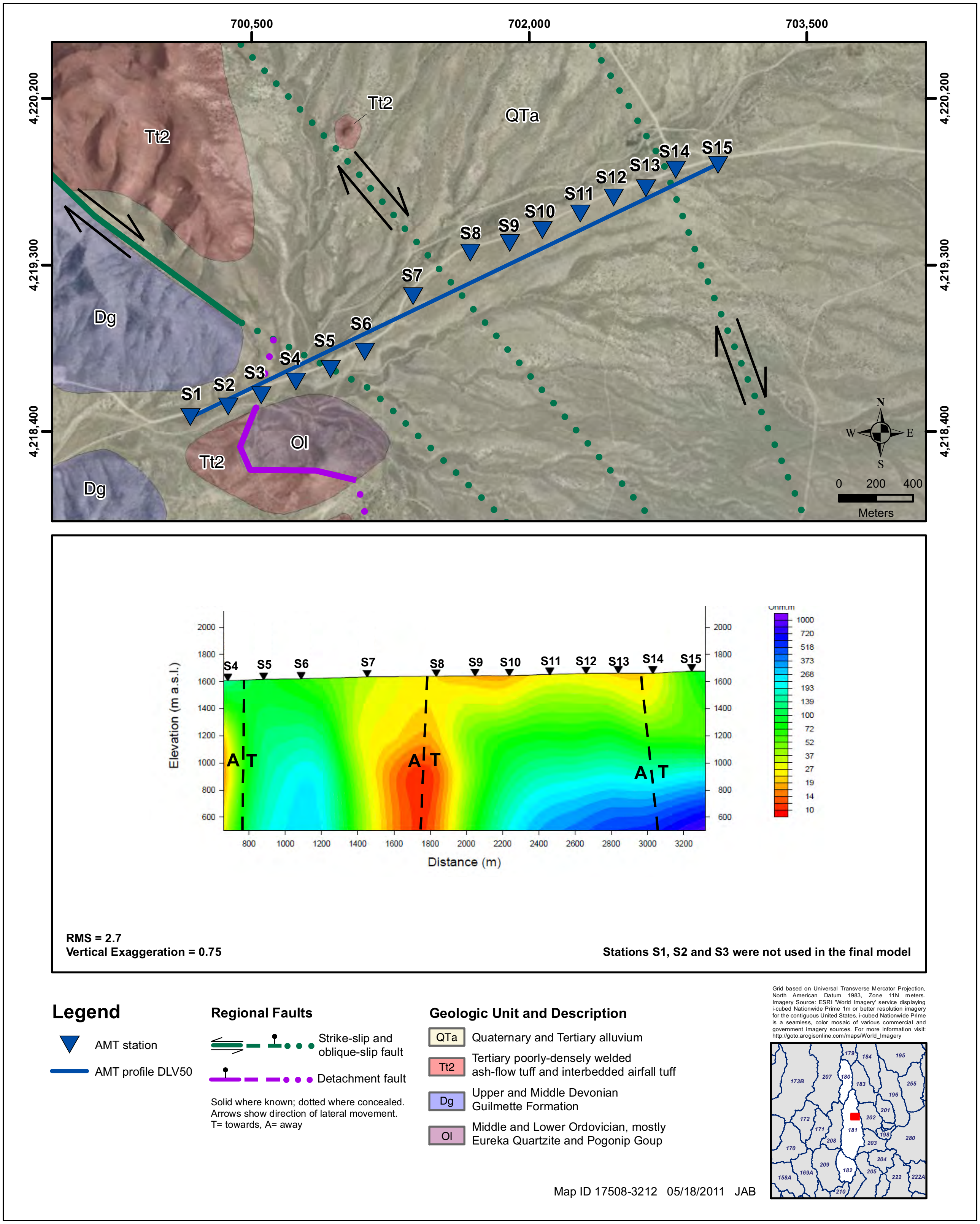

Source: Pari and Baird (2011)

Figure 5-24
Map and 2D Model of DLV50

SE ROA 43269

JA_13149

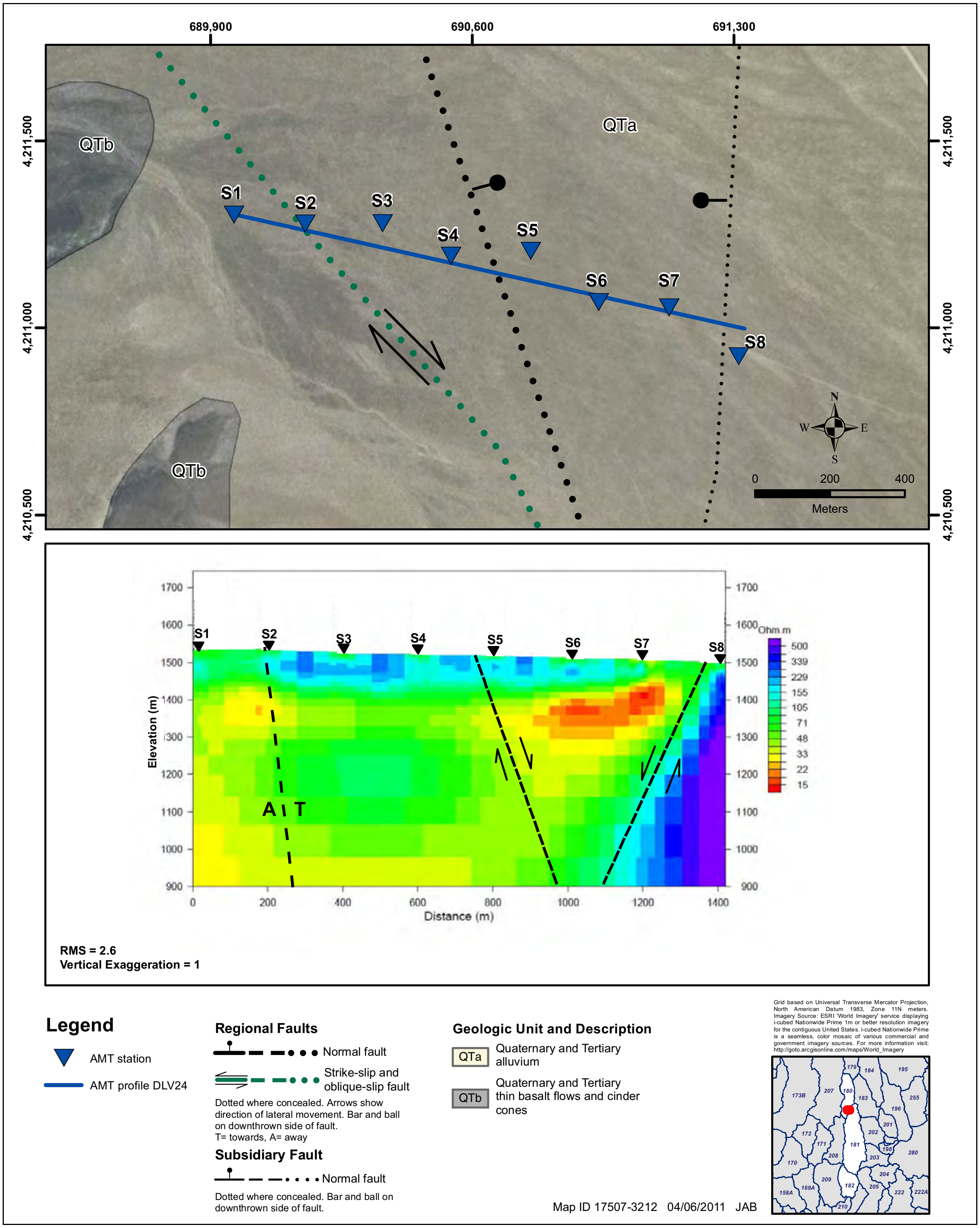

Source: Pari and Baird (2011)

Figure 5-25
Map and 2D Model of DLV24

SE ROA 43270

JA_13150

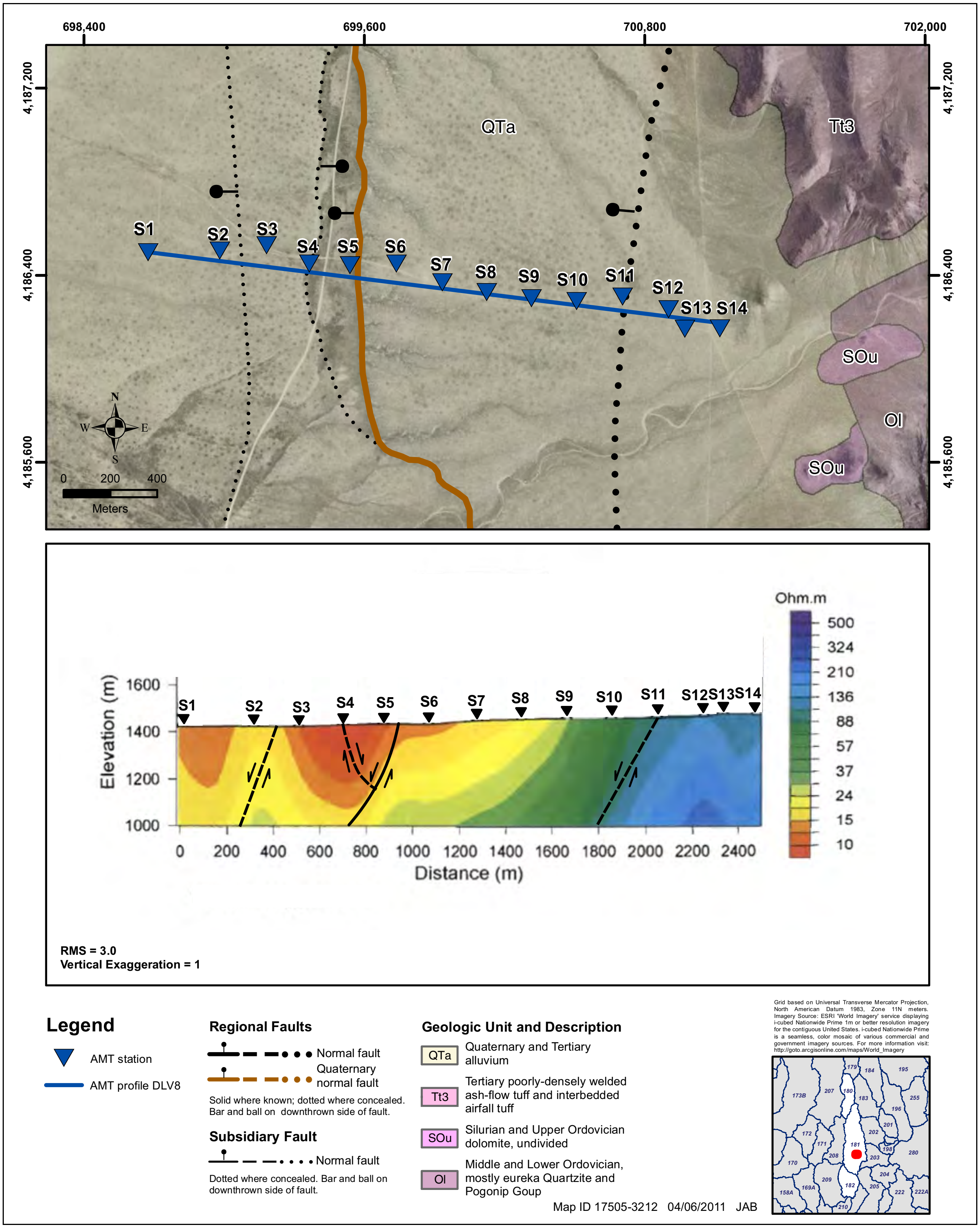

Source: Pari and Baird (2011)

Figure 5-26
Map and 2D Model of DLV8

largely strike slip and where they trend north their displacement is largely dip slip. The dip of purely strike-slip faults is generally vertical, whereas the dip of normal faults is on average 60 degrees.

The northern of the three profiles, Profile 5 (DELA5) from south of Delamar Lake, crossed the buried projection of the Delamar Lake fault of the PSZ and has a length of 0.7 km, oriented perpendicular to the fault. The AMT data were compiled by McPhee et al. (2008) but the profile was not geologically interpreted. The geologic map and profile were interpreted by Pari and Baird (2011), as shown in Figure 5-27. The profile images a wide, steeply southeast-dipping fault zone between stations S3 and S4. The fault zone is marked by conductive material, probably representing hydrothermal clay, fault gouge, and groundwater in the fault zone.

About 5 km south of Profile 5, AMT data were measured by McPhee et al. (2008) along a line 1.2 km long, across the Maynard Lake fault, which is the main fault of the PSZ. The data in this profile, known as Profile 1 (DELA1), were not geologically interpreted by McPhee and her colleagues but were interpreted by Pari and Baird (2011). Figure 5-28 reproduces the geologic map and profile. Profile 1 (DELA1) images a broad subvertical strike-slip fault beneath stations S5 and S6. The lesser conductivity in the central core of the fault may be due to fault gouge (see Section 2.2.1.2).

5.3 Seismic Studies

An additional view into the subsurface structure of southern Cave Valley and northern Dry Lake (Muleshoe) Valley is provided by a portion of the industry-shot ECN-01 seismic reflection line (Scheirer, 2005) (Figure 5-29). The seismic line crosses near the maximum depth position of Cave Valley. The seismic reflection image illustrates the asymmetric character of Cave Valley, with a steeper eastern side where the range-front fault of the Schell Creek Range lies and a less-steep western floor leading up to the dip-slope of the Egan Range. Strong reflectors mark the base of Cave Valley, and a discordant and more horizontal packet of reflectors characterizes much of the deeper valley fill. Weaker subhorizontal reflectors are present in the upper valley fill. The reflectors in the shallow portions of Muleshoe Valley are weak or absent, but in its deeper section they exhibit characteristics similar to those of the Cave Valley reflectors.

These seismic data are displayed in travel time, so a quantitative appraisal of seismic depths to basement is not possible. Nevertheless, the basin structure inferred from gravity analysis (Figure 5-29) shares a number of similarities with the seismic image: Cave Valley is asymmetric and reminiscent of a half-graben (Scheirer, 2005). The overall shapes of Cave versus Muleshoe, in deeper portions, appear similar in the seismic and gravity models. Location and depth of American Petroleum Institute (API) well 27-017-05221 are superimposed schematically on Figure 5-29 to illustrate its general agreement with the gravity depth-to-basement estimate and to show its position with respect to the seismic structures.

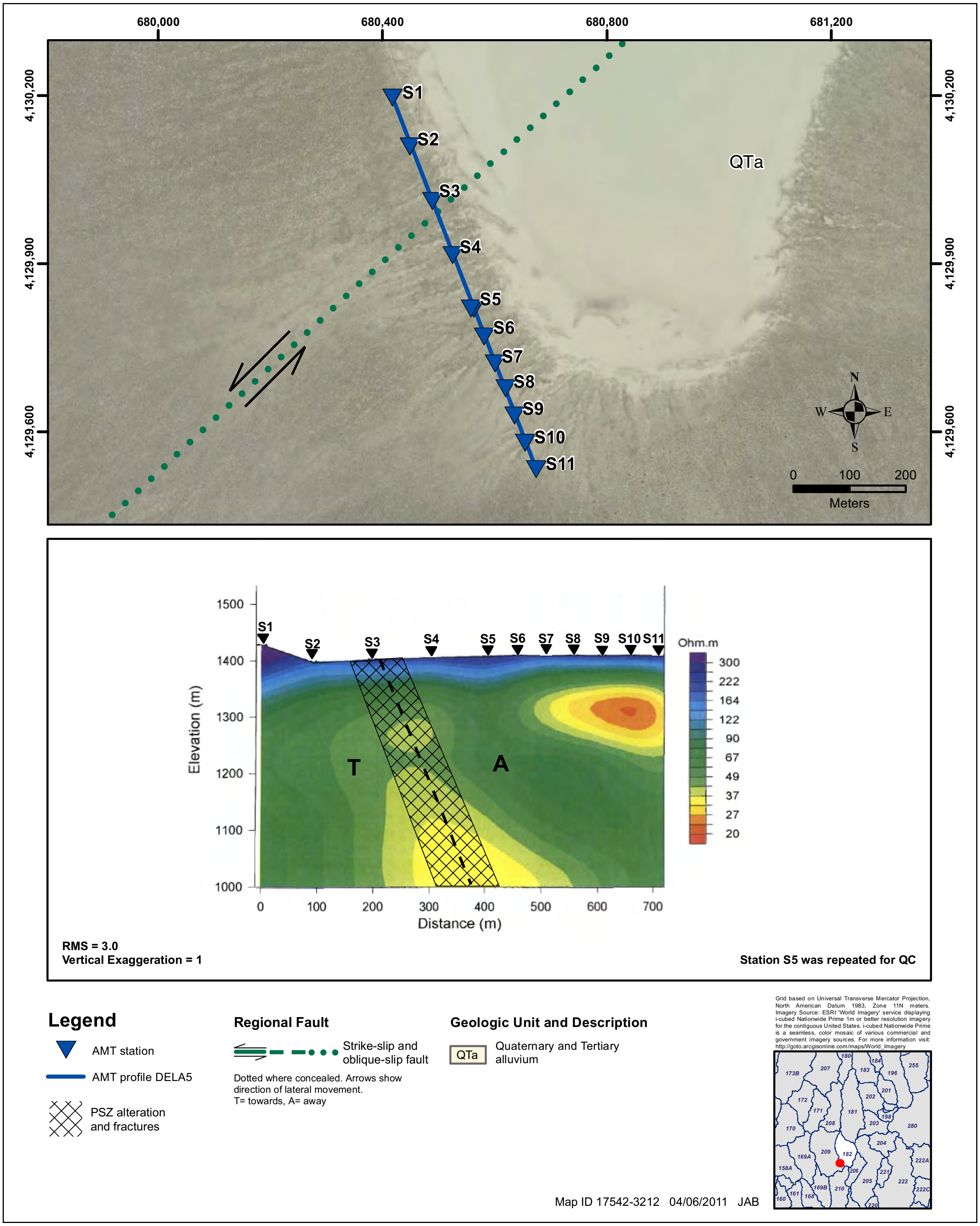

Source: Pari and Baird (2011)

Figure 5-27
Map and 2D Model of DELA5

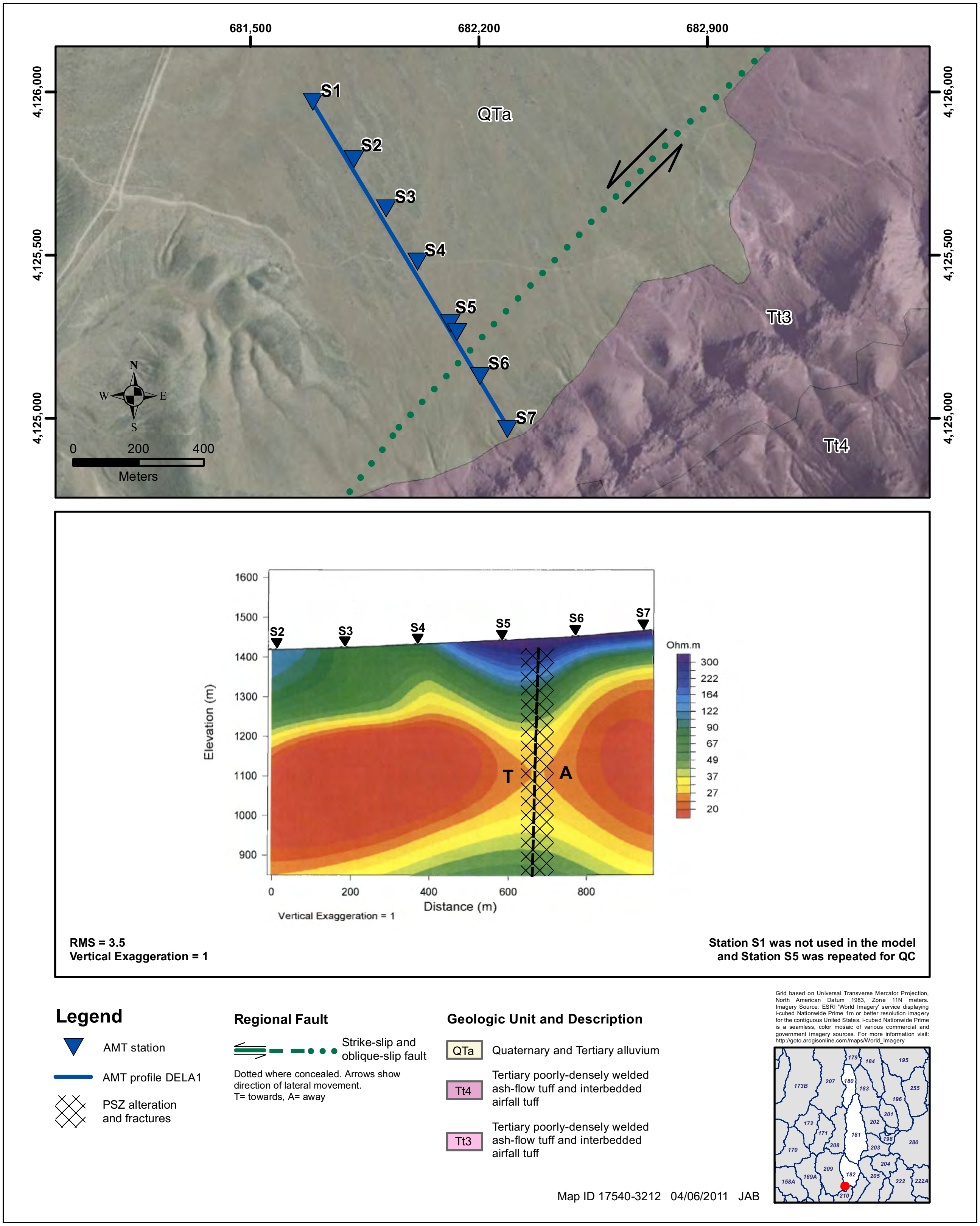

Source: Pari and Baird (2011)

Figure 5-28
Map and 2D Model of DELA1

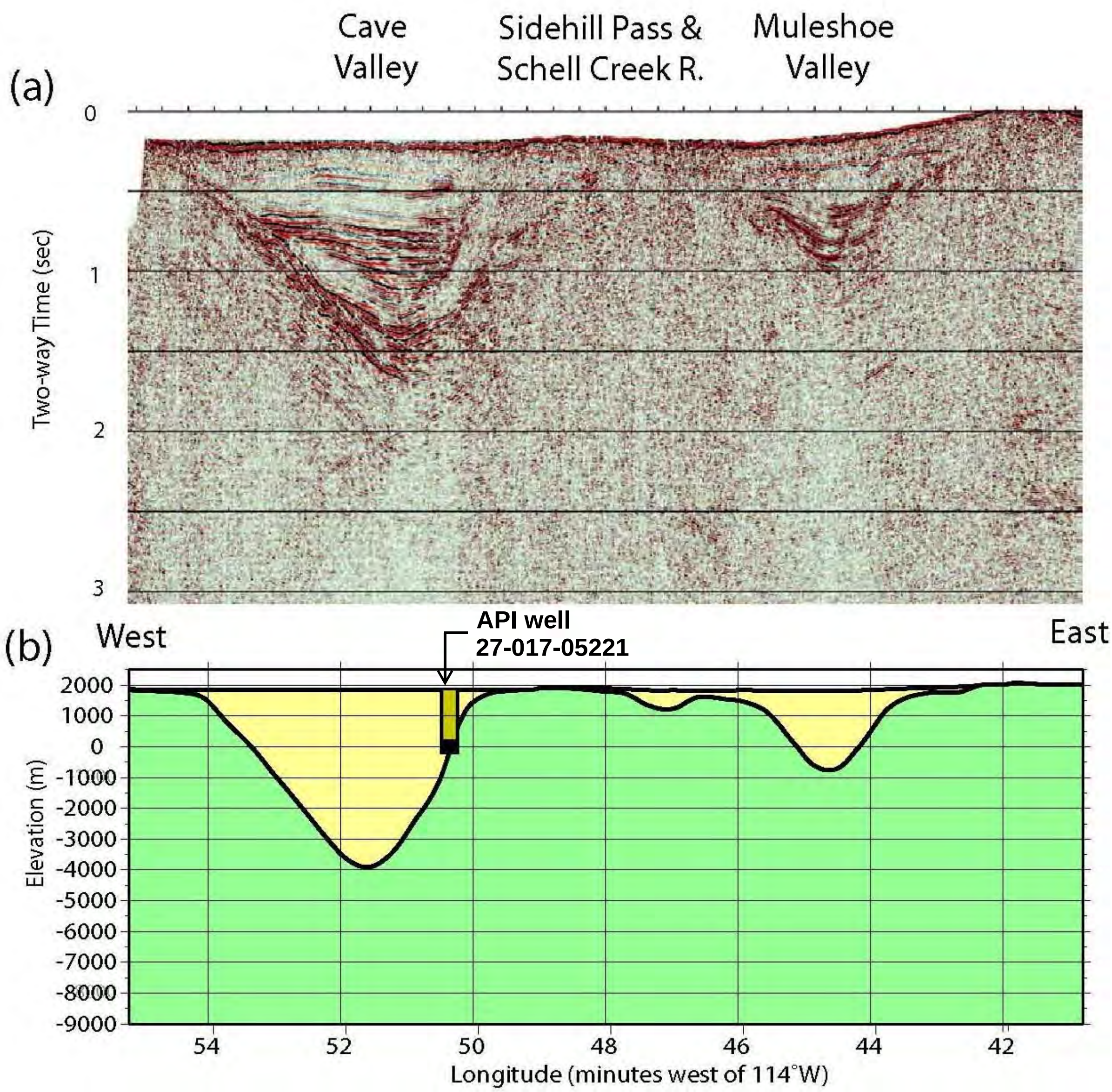

(a) Cross section of southern Cave and northern Muleshoe valleys ECN-01 seismic reflection section displayed in time. (b) Results of gravity depth-to-basement inversion with low-density basin fill in yellow. API well 27-017-05221 is displayed on the section, and its alluvial interval is shown in dark yellow. Vertical exaggeration = 1.5.

Source: after Scheirer (2005)

Figure 5-29
(a) ECN-01 Seismic Reflection Section Displayed in Time
(b) Results of Gravity Depth-to-Basement

6.0 PROFESSIONAL OPINIONS ON PREVIOUS STUDIES IN THE PROJECT AREA

Several previous studies on the hydrogeology in the project area have resulted in conclusions that, in part, differ from those of this SNWA report. In addition, some testimony, cross-examinations, and arguments by protesting parties during past hearings have questioned conclusions made in hydrogeological reports or testimony by SNWA. We anticipate that protestants in the upcoming proceedings by the Nevada State Engineer (NSE) will raise a number of these same issues relating to the geology of Spring, Delamar, Dry Lake, and Cave valleys. Therefore this section identifies several of those issues and discusses whether the anticipated positions of protestants, based upon previous studies, are supported by the geology of the region. First we summarize the pertinent, previously published and unpublished reports on studies containing positions we disagree with. Then we cover the issues raised by these studies or previous testimony, basin by basin, from north to south and west to east, starting with the project basins of Spring, Delamar, Dry Lake, and Cave valleys.

6.1 Previous Studies

6.1.1 The BARCASS Report

In 2004, the U.S. Congress funded the BARCASS to investigate the hydrogeology, recharge and discharge, groundwater flow, geochemistry of the aquifer system, and groundwater budgets for White Pine County, Nevada, and adjacent areas in Nevada and Utah. The work was done by the USGS, with minor collaboration from the Desert Research Institute and the Utah Department of Natural Resources. A main report (Welch et al., 2007) and six accompanying reports resulted. Some subsections and maps in the main report were separately authored. The most important hydrogeologically of these were the 1:500,000-scale geologic map (Sweetkind et al., 2007a), hydrogeologic conclusions (Sweetkind et al., 2007b), and classification of basin boundaries into three categories of likely flow, possible flow (comparable to our use of permissible flow in Figure 4-9), and no flow likely (Knochenmus et al., 2007).

Welch et al. (2007) proposed interbasin groundwater flow routes and volumes as part of the BARCASS effort to balance basin water budgets. As a result, recharge and evapotranspiration estimates drive the BARCASS interbasin-flow estimates regardless of the geology of the hydrographic-area boundaries. Other SNWA reports will discuss the accuracy of the BARCASS water budget based on its recharge and evapotranspiration estimates.

In their classification of flow boundaries, Knochenmus et al. (2007) relied heavily on their geologic map (Sweetkind et al., 2007a) but its compilation at that large a scale required simplistic portrayal of the geology that removed almost all faults and some confining units. A major confining unit in the map area, the Chainman Shale (their "upper siliciclastic rock unit"), has a maximum thickness of about 2,000 ft, so that when dipping steeply or dissected by faults, it cannot be shown at their map scale, leading them to erroneous conclusions about flow paths. Furthermore, the geology that Sweetkind et al. (2007a) compiled was obsolete, for it came from State geologic maps (Stewart and Carlson, 1978; Hintze, 1980a). Even though more up-to-date geologic maps had long been published, virtually none of these post-1980 references (for example, those in our map bibliography of Section 8.0) were used or cited. In addition, the report of Dixon et al., 2007a had been released and was available to BARCASS authors, but it also was ignored. The Sweetkind map contains two cross sections taken from the literature but neither matches the map. Therefore reliance on the Sweetkind map, coupled with the use of water budgets rather than measured data, led Knochenmus et al. (2007) and Welch et al. (2007) to erroneous conclusions about the likelihood, as well as specific paths and volumes, of interbasin flow. In addition, Welch et al. (2007, p. 37-38) assumed that the carbonate aquifer is in most places hydraulically connected within ranges and beneath basins because the geologic map of Sweetkind et al. (2007a) showed only a few faults. In fact, geologic evidence shows that most ranges are hydraulically separated from adjacent basins by high-angle faults of thousands of feet of dip-slip and strike-slip displacement, and basins and ranges are internally broken by faults of large and small magnitude that not only may create barriers in their own right but juxtapose aquifers against confining units. In other words, most basins, ranges, and even small pieces of both may be compartmentalized with respect to their neighbors in terms of groundwater flow. With respect to the project basins that the BARCASS addressed, their hydrogeologic map, hydrogeology conclusions, and flow routes across basin boundaries are largely in error.

6.1.2 Reports by Elliott and Other USGS Authors

In 2006, Elliott et al. published the results of a USGS study of the surface-water resources of GBNP, under contract from the NPS. The study covered two years (October 2002 to October 2004) of stream-flow measurements, short as surface-water studies go. The release of the report took place four months before the start of hearings on Spring Valley for the NSE in September 2006, and most conclusions addressed groundwater issues rather than surface-water issues. Specifically, the report suggested repeatedly that any SNWA pumping in the basin-fill aquifer or underlying carbonate aquifer of Spring or Snake valleys “might” dry up perennial streams in the Park. In fact, the report contained few data that addressed groundwater, such as water levels, drill data, pump tests, groundwater flow volumes or directions or groundwater chemistry or isotopes. Hypothetical statements such as “might” are generally used when an author has little or no supporting evidence, inasmuch as a conclusion that anything “might” happen is a conclusion without any meaning and fails to add to existing knowledge.

Elliott et al. (2006) based their conclusions, in part, on obsolete geologic mapping that did not recognize high-angle basin-range faults in Spring Valley, the Snake Range, and Snake Valley. Therefore their groundwater speculations that SNWA pumping “might” affect GBNP streams were erroneous. A view of a basin without faults is simplistic, leading to a model in which the sedimentary basin fill in Spring and Snake Valleys is generally isotropic and homogeneous, therefore porous-media flow concepts only apply. A later report by Prudic (2006) defended the conclusions of Elliott et al. (2006), continued the use of the hypothetical “might” with respect to the effects on GBNP streams from SNWA pumping, and suggested “evidence” that consisted of analogies with supposedly close surface water/groundwater interactions in areas outside Nevada. The simplistic and obsolete USGS geologic framework of Elliott et al. (2006) was maintained by the 2007 USGS BARCASS study (Section 6.1.1).

In a grant proposal to NPS for additional study of GBNP, the USGS (2008) claimed that the Elliott report had "identified" that some of the streams and springs in GBNP were "susceptible to ground-water withdrawals" by anticipated SNWA groundwater pumping. The objectives of the 2008 USGS proposal included attempts to (1) find evidence for the conclusions already made by Elliott et al (2006) that SNWA pumping would lead to depletion of GBNP streams, and (2) improve the geologic framework. Funding was approved by the NPS. Some USGS studies have been completed, and others are continuing. To address objective (1), USGS studies included additional work on the hydrology and alluvial thicknesses of GBNP streams. Two masters students, Jackson (2010) and Dotson (2010), whose studies built upon previous students in GBNP (Acheampong, 1992; Glonek, 2001), were supported by the USGS. Jackson (2010) and Dotson (2010) found that loss rates along several GBNP perennial streams at issue were low because the stream gravels were sealed by calcium carbonate, and therefore that there was no connection between GBNP streams and the groundwater beneath Snake Valley. A study of springs was made by Prudic (2007) and Prudic and Glancy (2009), but no connection was found between these springs and Snake Valley groundwater. Allander and Berger (2010) used seismic refraction methods to determine alluvial thicknesses along three profiles adjacent to Baker Creek but found that the creek is disconnected from the groundwater.

For objective (2), Asch and Sweetkind (2010 and 2011) collected AMT data along two profiles along Lehman Creek and south of Kious Spring, in Snake Valley southeast of the GBNP headquarters west of Baker. In their literature review, they noted that earlier reports (dePolo, 2008; dePolo et al., 2009) had discovered Quaternary faults in this area. The two profiles identified one of these, a mostly buried high-angle Quaternary fault that they had not previously recognized or factored into their groundwater interpretations. They interpreted the fault to be of minor displacement and too young to have much of a bearing on the uplift and development of the Snake Range. This fault zone, however, had been previously identified and mapped (Dixon et al., 2007a, Plate 1; Rowley et al., 2009, Plate 1). Its location was constrained by gravity data (Mankinen et al., 2006; Mankinen and McKee, 2009) and previous AMT profiles (McPhee et al., 2009). It was interpreted (Dixon et al., 2007a; Mankinen and McKee, 2009; McPhee et al., 2009, Figure 1; Rowley et al., 2009) to be the main eastern range-front basin-range fault of the Snake Range. Asch and Sweetkind (2010 and 2011) neither acknowledged or cited these previous reports. Nonetheless, their improved understanding of the geologic framework makes it unlikely that they will argue for any drawdown of GBNP streams by SNWA pumping because high-angle faults tend to compartmentalize basins into separate hydraulically-connected parts. Whether for object (1) or (2), the introductions of nearly all these USGS reports continued to state that SNWA pumping "might" dewater GBNP streams, but the conclusions of all reports admitted that they found no evidence of this effect. Even Prudic (2006, p. 3) admitted that "most of the Park's surface-water resources likely would not be affected by pumping because of either low-permeability rocks or because groundwater is sufficiently deep as to not be directly in contact with the streambeds."

6.1.3 Myers' Unpublished Reports

Dr. Tom Myers, Hydrologic Consultant from Reno, Nevada, wrote a number of reports as a consultant for protestants in the Hearings of the NSE. There are four hearings reports, two (Myers, 2006a and b) for the Spring Valley hearings and two (Myers, 2007b and c) for the Delamar Valley/Dry Lake Valley/Cave Valley hearings. In addition, Myers (2007a) wrote a review of SNWA reports for the Bureau of Land Management Environmental Impact Statement (EIS) Project. Two of the hearings reports (Myers, 2006a, 2007b) developed conceptual groundwater-flow models. Speaking only to the hydrogeology in the five reports, we are of the opinion that the hydrogeology is simplistic and that Myers largely ignored geology input for his own reports and misunderstood the geology that SNWA submitted. In addition, the geologic map that Myers cited is obsolete, taken from the 1:500,000-scale State geologic map (Stewart and Carlson, 1978). In Myers (2006a), all faults from Stewart and Carlson (1978) were removed, the units generalized, and the resulting map shown at page-size 1:1,000,000 scale, thus largely illegible and unintelligible. In Myers (2007b), three page-size figures of the three valleys were reproduced at nearly 1:1,000,000 scale. Only about a single page of text in both reports (Myers, 2006a and 2007b) covered topographic setting and hydrogeology, and most citations to the geology are from several hydrologic publications that contain minimal coverage of geology. His apparent lack of understanding of the importance of the geologic framework of the subject basins led Myers to erroneous conclusions regarding routing and amounts of interbasin flow and potential effects of pumping.

In his rebuttal report for SNWA's positions on Spring Valley, Myers (2006b) had no criticisms of SNWA's concepts on geology or interbasin flow. But Myers (2007c) rebuttal for the hearings on Dry Lake, Delamar, and Cave valleys disputed SNWA's positions on interbasin flow between (1) northern and southern Cave Valley, (2) southern Cave to Pahroc valleys, (3) Delamar to Coyote Spring valleys, (4) Delamar to Pahranagat valleys, and (5) Coyote Spring Valley to Lake Mead. Myers' rebuttal contains no supporting evidence. His arguments stem largely from his misunderstanding of fracture flow and the geology of basin boundaries. They will be discussed in the sections below, except for #5, which is discussed in Sections 4.4.17 and 4.4.21.

The review of SNWA's EIS documents by Myers (2007a) dealt only in part with geology, and his only substantive comments disputed the concept of fracture flow, which he referred to as an "opinion." Myers (2007c, p. 14) disputed the fundamental principle of fracture flow that faults can be both conduits and barriers in his particularly revealing comment that "SNWA cannot have it [barrier and conduit flow] both ways." Section 2.2 of this report stated the scientific principals of fracture flow to show that this theory is generally accepted by geologists and hydrogeologists and is not the mere opinion of the authors.

6.2 Issues in Basins within the Project Area

6.2.1 Issues in Spring Valley

6.2.1.1 Flow to or from Tippett Valley

Knochenmus et al. (2007) showed the entire Antelope Range as well as the basin boundary between Tippett and Spring valleys as a boundary of likely flow, and Welch et al. (2007, Figure 41) showed northeastward flow of 2,000 afy from Spring Valley to Tippett Valley.

Geologic evidence (Plates 1 and 6, Section 4.4.22) shows that the high Antelope Range is a complexly faulted horst of Paleozoic rocks, including the Chainman Shale confining unit, and of Tertiary volcanic rocks. The range is bounded on both sides by large range-front faults. These faults and most faults internal to the range are oriented northerly, therefore tend to create barriers to flow east to west. The southern end of Tippett Valley is bounded by the complexly faulted Red Hills (Plates 4 and 8, Cross Section X—X'), of similar rocks and structures to the Antelope Range. Most groundwater is in the low main aquifer, that of the basin-fill sediments of Spring and Tippett valleys. Gravity data (Section 5.1.1) show thick basin fill and clear buried faults oriented mostly perpendicular to possible flow in passes between Tippett and Spring valleys.

Our opinion is that interbasin flow is confined to a narrow path between two passes at the southern end of Tippett Valley, on either side of the Red Hills. Considering the lack of water-level data, flow direction is inconclusive and the boundary may just be a groundwater divide.

6.2.1.2 Flow to Snake Valley between the Kern Mountains and Snake Range

Knochenmus et al. (2007) showed a steep eastward gradient in carbonate rocks across the northern Spring Valley basin boundary, then beneath the shallow basin fill in basin(s) between the southern Kern Mountains and northern Snake Range, to Snake Valley. Yet they gave no data points and stated that the flow route is only "possible". Welch et al. (2007, Figure 41) showed a flow of 16,000 afy along this path.

Gravity data (Section 5.1.1) indicate that barriers to flow are presented by prominent faults and buried bedrock ridges north and south of the Red Hills. In addition, the barriers caused by the Red Hills (Plates 4 and 8, Cross Section X—X') make it more likely that no groundwater passes eastward from northern Spring Valley. Furthermore, geologic and geophysical evidence (Sections 4.4.25 and 5.1.1) suggests that Spring Valley consists of geophysical sub-basins that are separated by buried bedrock ridges that may restrict flow from one sub-basin to another. The best explanation is that the water in the basin(s) between the Kern Mountains and Snake Range more likely is from local recharge from the high Kern Mountains and the high northern end of the Snake Range rather than from basins to the west.

Our opinion is that Welch et al. (2007) are premature in their suggestion for a large volume of flow shown in Figure 41. Some flow is permissible from northeastern Spring or Tippett valleys to the basin(s) between the Kern Mountains and the Snake Range, but such flow would hardly be in the volumes suggested by Welch et al. (2007).

6.2.1.3 Flow from Steptoe Valley to Southern Spring Valley

Welch et al. (2007) proposed four flow routes from Steptoe Valley, two to the east and two to the west, through the high ranges that bound the basin on either side.

All previous workers (e.g., Harrill et al., 1988) have considered all groundwater flow within Steptoe Valley to be northward. The two paths to the east, from the southern end of the valley through the Schell Creek Range, are discussed north to south in this and the next (6.2.1.4) sections.

Both paths to the east proposed by Welch et al. (2007) are through parts of the range where Knochenmus et al. (2007) considered flow to be possible. The northern of these, calculated to have flow of 4,000 afy along a path to southern Spring Valley, is about 10 mi south of Connors Summit, the pass where US 6/US 50 crosses the Schell Creek Range.

The geologic map (Plates 1 and 6) shows that the Schell Creek Range at the suggested northern path is high (at least 1,600 ft of relief between any possible passes and Steptoe Valley) and broad (more than 10 mi). The range here is bounded on both sides by large range-front faults oriented perpendicular to the flow suggested by Welch et al. (2007) and internally complexly deformed by faults that contain fault blocks and slivers of Chainman Shale, a major confining unit (Plates 4 and 8, Cross Section V—V'; Section 4.4.13). Gravity data show the Schell Creek Range to be massive and of relatively high density, with no breaks or faults that might be interpreted to be flow paths (Section 5.1.3). The geologic map of Sweetkind et al. (2007a), however, showed only lower and upper Paleozoic carbonate rocks, with no Chainman Shale or range-front or internal faults, because their map scale did not allow these complexities to be given. The result is that their map gives the false impression that there are no barriers to groundwater flow.

In our opinion, groundwater flow through the entire Schell Creek Range is unlikely. There is no geological or gravity-data support for any groundwater flow along the northern of the two paths from southern Steptoe Valley to southern Spring Valley.

6.2.1.4 Flow from Steptoe Valley to Lake, Spring, and Hamlin Valleys

The southern of the two paths (see Section 6.2.1.3 for the northern one) proposed by Welch et al. (2007) for flow to the east from southern Steptoe Valley is 16 mi south of Connors Summit. Here the volume of flow was proposed to be 20,000 afy (Welch et al., 2007, Figure 41) to northern Lake Valley.

The geologic map (Plates 1 and 6) shows that the Schell Creek Range is made up of lower Paleozoic carbonate rocks that have been complexly faulted, with few faults oriented parallel to the BARCASS flow path that could act as conduits. No passes through the range here are lower than 7,900 ft elevation, a relief of more than 300 ft from Steptoe Valley. It is unreasonable to expect groundwater to pass beneath broad, high ranges such as the Schell Creek Range, in part, because the lithostatic pressure from the weight of rocks above any flow path hydraulically connected to groundwater in adjacent basins would tend to close prospective flow paths. The geologic map of Sweetkind et al. (2007a) shows only carbonates, with no faults, because their map scale did not allow such details to be given. Gravity data (Section 5.1.3) show a relatively high-gravity, homogeneously dense range with no discernible density breaks or faults that may be interpreted to be flow paths.

It is our opinion not only that the flow path proposed by Welch et al. (2007) does not exist, nor is there any groundwater flow anywhere out of southern Steptoe Valley.

As a consequence of their flow path containing 20,000 afy from Steptoe Valley to Lake Valley, Welch et al. (2007) proposed another flow path, from Lake Valley through the central Fortification Range—at the county line between White Pine and Lincoln Counties—to southern Spring Valley. They considered this flow to be 29,000 afy. Knochenmus et al. (2007) classified flow anywhere across the Fortification Range to be possible, even south of the county line.

SE ROA 43281

JA_13161

The geologic map (Plates 1 and 6) shows the basin boundary of the central Fortification Range to be high and abrupt, and at the flow path (Plates 4 and 8, Cross Section U—U') suggested by Welch et al. (2007) to consist of mostly upper Paleozoic carbonates but with Chainman Shale likely at shallow depth and below the water table in repeated fault blocks (Section 4.4.18). Several miles south of the county line, the range is underlain by a caldera of the Indian Peak caldera complex (Plates 4 and 8, Cross Section Q—Q' and R—R'). The range is bounded on both sides by range-front faults and is cut internally by additional north-trending faults. Sweetkind et al. (2007a), in contrast to our more detailed geologic map, showed only upper Paleozoic carbonates cut by a single fault on the western side.

In our opinion, the flow path proposed by Welch et al. (2007) through the Fortification Range does not exist. There is no evidence for any flow through the high Fortification Range, which we classify as unlikely with respect to flow through it. The existence of the Chainman Shale and the Indian Peak caldera complex underlying the range creates impermeable barriers that would prevent the passage of any groundwater along that path.

The next downgradient flow path that Welch et al. (2007) hypothesized is a path from southern Spring Valley eastward through the basin boundary of the Limestone Hills and into Hamlin Valley. They considered this path to support 33,000 afy of groundwater.

The geologic map (Plates 1 and 6; Figure 4-20) shows that the rocks in the Limestone Hills consist of lower Paleozoic limestone and Tertiary ash-flow tuffs bounded on both sides by north-trending, range-front normal faults and internally broken by small faults of the same trend (Plates 4 and 8, Cross Section U—U'; Section 4.4.25). Gravity and AMT studies (Sections 5.1.1 and 5.2.1) supports these structural interpretations. Sweetkind et al. (2007a), however, showed the rocks to consist of lower Paleozoic carbonates bounded on the west side by a single fault, as befits the lack of detail that his map scale allows.

It is our opinion that flow through the Limestone Hills is permissible and, locally at lower passes in the north and south, likely. However, the volume (33,000 afy) proposed by Welch et al. (2007) is unreasonably high. The geologic framework can support some flow through cross faults in carbonate rocks, but the north-trending faults that define the range present partial barriers. Furthermore, the groundwater from Spring Valley is from only the southern geophysical sub-basin (see discussions in Sections 4.4.25 and 5.1.1). As noted in the previous paragraphs, we find no support for any contribution to this geophysical sub-basin from Lake Valley.

6.2.2 Issues in Cave Valley

6.2.2.1 Shingle Pass Fault

Knochenmus et al. (2007) showed the entire southern Egan Range as a hydrographic boundary for possible flow through it and Welch et al. (2007, Figure 41) ascribed a volume of 9,000 afy passing westward along a flow path 6 mi north of Shingle Pass through the Egan Range. Myers (2007c, p. 11) however, suggested that all groundwater in northern Cave Valley is blocked from passing southward into southern Cave Valley by the footwall block (southern side) of the Shingle Pass fault because the *fault block contains Chainman Shale and extends northeastward across Cave Valley. Therefore Myers (2007b, p. 3) reasoned that all groundwater in northern Cave Valley passes through Shingle Pass, where it supplies Moon River and Hot Creek springs in the middle of White River Valley. He concluded that any SNWA pumping in Cave Valley will decrease discharge in these springs.*

Geologic evidence (Plates 1 and 6, Plates 4 and 8, Cross Section R—R'; Section 4.4.10) indicates that the Egan Range north of Shingle Pass consists of nearly the entire stratigraphic succession in this part of Nevada, including the Chainman Shale and other confining units, all dipping eastward. As a result, we show the entire southern Egan Range as an unlikely flow boundary (Figure 4-9), except for a permissible path at Shingle Pass.

Groundwater in Cave Valley flows from north to south. The Shingle Pass fault is a large, northeast-trending, oblique-slip (left-lateral and normal) accommodation fault that breaks the Egan Range at Shingle Pass, then continues northward as the eastern, down-to-the-east, primarily normal, range-front fault of the Egan Range. We interpret that a second large fault, but a down-to-the-west normal fault, continues northeast from Shingle Pass, crossing northern Cave Valley and joining the western down-to-the-west, range-front normal fault of the Schell Creek Range. The second fault serves to separate the northern Cave Valley sub-basin from the southern Cave Valley sub-basin because the footwall (southern) side of the fault reaches almost entirely across Cave Valley. The Shingle Pass fault provides a permissible outlet for some groundwater to pass from northern Cave Valley southwestward into White River Valley. But all the groundwater in northern Cave Valley will not pass through Shingle Pass (with an elevation of somewhat less than 7,000 ft) because an easier and lower-elevation conduit exists in the large north-trending, range-front fault (Plates 4 and 8, Cross Section R—R') that bounds the base of the entire western side of the Schell Creek Range at an elevation of less than 6,500 ft elevation (Section 4.4.10 and Figure 4-12). This large range-front fault, clearly imaged multiple times by geophysics (Sections 5.1.4, 5.2.3, and 5.3), downthrows the footwall block of the second fault. This fault effectively removes the footwall block of the second fault from blocking southward groundwater flow because the north-trending fault along the western Schell Creek Range creates a broad avenue of north-trending fractures, between the downthrown hanging wall and the Schell Creek range front.

Moon River and Hot Creek springs are hot regional springs in the middle of White River Valley controlled by north-trending faults that get their groundwater from more northern parts of the valley (Burns and Drici, 2011; Thomas and Mihevc, 2011). In a comprehensive summary of springs throughout and near the geologic study area, Volume 3 of SNWA (2008) summarized the hydrology, geology, geologic cross sections, and results of monitoring many springs in White River Valley, including Hot Creek Spring. Moon River Spring, which is 2.6 mi southwest of Hot Creek Spring, is probably controlled by the same down-to-the-west, basin-range fault that controls Hot Creek Spring. There is no geologic evidence that these springs get any water from Cave Valley.

It is our opinion that Knochenmus et al. (2007) are incorrect in showing the entire southern Egan Range as a boundary that allows possible flow. It is also our opinion that Welch et al. (2007, Figure 41) was not correct in ascribing a volume of 9,000 afy passing westward through the Egan Range along a flow path 6 mi north of Shingle Pass. Furthermore, it is our opinion that Myers (2007c) erred in suggesting that all groundwater from northern Cave Valley is blocked from passing into southern Cave Valley by the footwall block of the second fault. Finally, Myers (2007b) was incorrect in suggesting that all groundwater in northern Cave Valley passes through Shingle Pass. He also is wrong in suggesting that any groundwater from Cave Valley will supply Moon River and Hot Creek springs. While the Shingle Pass fault may allow minor amounts of groundwater to flow to White River Valley (Section 4.4.10; Figure 4-13), there is no evidence that supports a large flow. It is our opinion that the western range-front fault of the Schell Creek Range provides the primary conduit for groundwater flow in Cave Valley.

6.2.2.2 Flow through Southern Cave Valley

Myers (2007c, p. 11) maintained not only that no groundwater flowed from northern to southern Cave Valley (Section 6.2.2.1) but that, because recharge to southern Cave Valley is small, little groundwater would go south from southern Cave Valley. Myers stated that most of that flow would end up in Pahranagat Valley.

In our opinion and consistent with our conclusions in Section 6.2.2.1, most groundwater in northern Cave Valley finds its way to southern Cave Valley along the western range-front fault of the Schell Creek Range. From there, groundwater passes southward through several north-trending normal- and oblique-slip faults, and fractured carbonate and volcanic rocks along and between the faults, from southern Cave Valley, then into Pahroc Valley to the west and Dry Lake Valley to the east (see Section 4.4.10; Plates 4 and 8, Cross Section Q—Q'; Figure 4-13).

6.2.3 Issues in Dry Lake and Delamar Valleys

6.2.3.1 The Timpahute Transverse Zone

Some protestants have questioned the possible hydrologic effect of the east-trending Timpahute transverse zone, which crosses the project area (Plates 1 and 6), including the low, virtually imperceptible divide between Dry Lake Valley and Delamar Valley, where the zone is roughly coaxial with US 93.

Transverse zones are defined and described in Section 4.3.1, and several of them are mapped on Plates 1 and 6, including the Timpahute transverse zone. Transverse zones are poorly known and controversial. Because they separate areas north and south of them that have undergone different amounts, rates, and types of east-west basin-range extension, much like east-striking transform faults in the ocean basins, they are discontinuous along strike. Perhaps this is because they are not always expressed as faults and, because they are primarily boundaries, they may be expressed as discrete narrow east-west zones in some places, jump north or south in other places, and be miles wide in still other places. Furthermore, transverse zones are in general deep-seated structures, so in many places they are not likely to be expressed as obvious features at the surface.

Detailed geologic mapping (Section 4.4.12) and gravity surveys (Section 5.1.4) have identified parts of the east-trending Timpahute transverse zone in the bedrock on both (western and eastern) sides of the valley where Dry Lake Valley passes into Delamar Valley. East-trending faults may be traced to the west as far west as Pahroc Summit Pass, between the North and South Pahroc ranges where US 93 crosses into Sixmile Flat and north of which a SNWA monitoring well was sited. The Timpahute transverse zone, however, has not been identified in the Sixmile Flat area (Plates 4 and 8, Cross Section S—S'). Furthermore, water levels at the monitoring well along the transverse zone do not indicate any flow west across Pahroc Summit Pass. More importantly, chemistry and isotopes for water from wells in Delamar and Dry Lake valleys are different from those for groundwater in Pahranagat Valley (Burns and Drici, 2011). Perhaps most telling is the cross section (basin-boundary profile) and geologic map of Plates 1 and 6 and Figure 4-15, which show a series of large, north-trending normal faults that define the range fronts on either sides of Dry Lake and Delamar valleys and bifurcate the valley itself. These faults, oriented parallel to the potentiometric gradient, are conduits to southward groundwater flow and barriers to westward flow.

In our opinion, no groundwater passes along the Timpahute transverse zone into Pahranagat Valley.

6.2.3.2 Flow from Delamar Valley to Pahranagat Valley

Myers (2007b, p. 1) hypothesized that "the entire amount [of discharge from Dry Lake and Delamar valleys] discharges as interbasin flow to Pahranagat Valley." He furthermore seemed to suggest flow paths at various places through the basin boundary, in addition to the Pahranagat shear zone (Myers, 2007b, p. 1-2, 44; Myers, 2007c, p. 13-15).

Although the South Pahroc and Hiko ranges, which separate Delamar Valley from Pahranagat Valley, are relatively low and largely made up of volcanic and underlying carbonate rocks, these two north-trending ranges are defined by innumerable north-trending basin-range faults that would present barriers to flow across them (Plates 1 and 6; Plates 4 and 8 Cross Sections M—M', N—N', and O—O',). Flow would more likely continue south in conduits provided by north-trending faults within and on either side of Delamar Valley rather than swing west into Pahranagat Valley. In Pahranagat Valley north of Alamo, Nevada, Crystal Springs (Dixon and Van Liew, 2007), Hiko Springs, and Ash Springs are regional springs (Section 4.4.6, Volume 3 of SNWA, 2008) controlled by north-trending basin-range faults (Plates 4 and 8 Cross Sections O—O'). Chemistry and isotopes from water at these and other springs in Pahranagat Valley north of Alamo are consistent with a source from White River Valley but are different from water in Dry Lake and Delamar valleys (Thomas et al., 2001; Burns and Drici, 2011; Thomas and Mihevc, 2011). Although the PSZ clearly brings some groundwater (see section below) from southern Delamar Valley to southern Pahranagat Valley, the hydraulic gradient in Pahranagat Valley is southward and the PSZ enters only southern Pahranagat Valley south of Alamo (Figure 4-11), from where this groundwater continues to flow southward into Coyote Spring Valley.

It is our opinion that Myers (2007b) is wrong in stating that the entire amount of discharge from Dry Lake and Delamar valleys discharges as interbasin flow to northern and central Pahranagat Valley. Our opinion is based on the presence of barriers created by many north-trending basin-range faults, between Delamar and Pahranagat valleys, the isotopic evidence, and the entry of the PSZ into only southern Pahranagat Valley. The only possible flow path from Delamar Valley to Pahranagat Valley is that described in Section 6.2.3.3, below.

6.2.3.3 Flow along the Pahranagat Shear Zone

Myers (2007c, p. 13) claimed that SNWA's proposed route for groundwater flow from southern Delamar Valley southwestward to Coyote Spring valleys "does not make sense." Although he seemed to accept flow along the PSZ to southern Pahranagat Valley, he questioned how flow could cross the shear zone and continue southward into Coyote Spring Valley (Myers, 2007c, p. 13-15). He gave no evidence that groundwater from southern Pahranagat moves northward against the hydraulic gradient to supply more northern parts of Pahranagat Valley. Nor did he offer alternatives as to where the groundwater in Coyote Spring Valley comes from.

We discussed the geologic evidence for groundwater movement from southern Delamar Valley to southern Pahranagat and northern Coyote Spring valleys in Section 4.4.6. The area is underlain mostly by brittle volcanic rocks at the surface and continuing below the water table, and these rocks are fractured not only by the northeast-striking left-lateral faults of the PSZ (Plates 5 and 9, Cross Sections B—B') but by north-striking normal faults that feed into the shear zone both north and south of it. All these faults are connected because the PSZ is an accommodation fault zone that developed during basin-range extension so it is connected with, and formed during, the same deformational episode as basin-range faults (Sections 4.3.1 and 4.4.6). As an accommodation zone, the northeast-trending faults of the PSZ connect with north-trending normal faults on both sides, so groundwater moves through the whole system.

It is our opinion that the PSZ provides a likely flow path that would allow groundwater to travel from southern Delamar Valley to southern Pahranagat Valley. Presently available scientific information is not available to pinpoint the exact routes for water from Delamar and southern Pahranagat valleys to northern Coyote Spring Valley, but there are doubtless many paths.

6.2.4 Issues in Steptoe Valley

6.2.4.1 Flow from Steptoe Valley to Jakes Valley

Of the four groundwater flow paths proposed by Welch et al. (2007, Figure 41) west and east (see Sections 6.2.1.3 and 6.2.1.4) out of southern Steptoe Valley, two were considered to pass westward through high parts of the Egan Range west of Ely, Nevada. The Egan Range at both these flow paths was judged by Knochenmus (2007) to be a hydrographic boundary of likely flow. Presumably this conclusion was guided by the compilation of Sweetkind et al. (2007a) that showed nearly all rocks in the range here to be upper Paleozoic carbonates, with no faults shown bounding or within the range. The northern of these two paths is the subject of this section; the southern path is described in Section 6.2.4.2. The northern path was shown in Figure 41 to cross the western of three prongs of the range about 10 mi northwest of Ely, allowing 14,000 afy of groundwater into Jakes Valley. Apparently the proposed path from Steptoe Valley follows or is north of US 50, which goes through the main business district of Ely, then northwest across a pass into Copper Flat before bearing west across the western prong of the Egan Range.

It is our opinion that the Egan Range beneath both westward flow paths is a boundary of unlikely flow. Regarding the northern of these two proposed paths, geologic evidence shows that the prong of the Egan Range is an overturned strike ridge of upper Paleozoic carbonate rocks, with 500 to 1,500 ft of relief, that is bounded on both sides by range-front normal faults oriented perpendicular to the BARCASS-hypothesized flow path (Plates 1 and 6; Section 4.4.3). These faults would likely block any westerly groundwater flow. Southeastern Copper Flat and the pass to Ely, along the possible flow path, are underlain by the northern part of the huge, active Ruth copper mining district, an area of complex geology where confining zones of many types can be found. The district includes Cretaceous and Tertiary plutons that probably pass into batholiths at depth, as well as faulted pieces of the Chainman Shale that act as barriers to flow. Metamorphosed rocks and hydrothermally altered rocks formed by the plutons are dense and rich in clay minerals, resulting in additional confining units. It is our opinion that no westward flow paths exist in the Ruth copper mining district area.

6.2.4.2 Flow from Steptoe Valley to White River Valley

Welch et al. (2007, Figure 41) proposed another west-flowing path for groundwater from Steptoe Valley to the White River Valley, located 11 mi south of the one described in Section 6.2.4.1. The path is similarly depicted through a part of the Egan Range considered by Knochenmus et al. (2007) to be a basin boundary where flow is likely through it. The path that Welch et al. (2007) showed follows US 6 through the southern part of Ely, Nevada, then southwest to cross the range at Murry Summit, 700 ft above Ely. Welch et al. (2007) suggested that 8,000 afy moves by this path into White River Valley.

Geologic evidence shows that the flow path proposed by BARCASS goes through mostly west-dipping upper Paleozoic carbonates underlain on their eastern side by buried Chainman Shale (Plates 1 and 6; Section 4.4.4). But the flow path passes along the southern part of the Ruth mining district, likely underlain by buried plutons and metamorphosed and mineralized rocks, all of which are likely confining zones. The range here is bounded on both sides by large range-front faults oriented perpendicular to the supposed flow path, and these faults would act as barriers to any westward groundwater flow. In addition, the range is internally broken by many small- to moderate-displacement faults also oriented mostly perpendicular to flow.

It is our opinion that no flow path exists from Steptoe Valley to the White River Valley through this part of the Egan Range.

6.2.5 Issues in Snake Valley

6.2.5.1 Impact of Pumping in Great Basin National Park

Elliott et al. (2006) and subsequent USGS workers in GBNP hypothesized that SNWA pumping in Spring or Snake valleys “might” lead to a drawdown of surface water in GBNP.

Except for some lower Paleozoic carbonates in fault blocks, most rocks that underlie GBNP are Cambrian and Precambrian confining units (Plates 1 and 6; Plates 4 and 8, Cross Sections V—V'; Section 4.4.25). The carbonates themselves are hydraulically compartmentalized by being displaced against the more abundant confining units by low-angle normal faults recognized by the USGS hydrologists and by more common high-angle normal faults mapped on Plates 1 and 6.

Pumping by SNWA in Spring or Snake valleys would be from groundwater in basin-fill sedimentary rocks. This groundwater is not physically hydraulically connected to the surface water in GBNP, (Kistinger et al., 2009, p. 311) except perhaps rarely where streams debouch from bedrock canyons into Spring and Snake valleys. In fact, in most places where perennial streams derived from the Park drain into the valleys, the water table in the basin fill is well below the surface water. The streams in these locations here become losing streams and soon lose their flow into the basin-fill deposits by natural processes instead of by pumping. In the rare short reaches where the water table is at the level of stream flow, stream gravels have been cemented by calcium carbonate, effectively sealing them and preventing any surface water/groundwater connection (Dotson, 2010; Jackson, 2010).

Basing conclusions on previous, mostly obsolete geologic maps, the USGS (Elliott et al., 2006) did not recognize that the Snake Range is a basin-range horst uplifted along huge, high-angle range-front normal faults on the eastern and western sides of the range. Nor did they study the surficial and basin-fill deposits in Snake and Spring valleys, so they did not notice abundant young (Pleistocene to Holocene) faults that cut the deposits. Therefore, the USGS geologic framework in which groundwater moves was incomplete and largely incorrect. Asch and Sweetkind (2010 and 2011), however, used AMT geophysics to find one large buried fault cutting basin-fill deposits, the same one previously recognized and mapped by Dixon et al. (2007a, Plate 1), McPhee et al. (2009, Figure 1), and Rowley et al. (2009, Plate 1). These studies were not cited by Asch and Sweetkind. This fault, however, is just one of hundreds of large- to medium-displacement, high-angle normal faults that cut the basin fill east and west of GBNP and contributed to the uplift of the Snake Range (Dixon et al., 2007a; Mankinen and McKee, 2009; McPhee et al., 2009; Rowley et al., 2009; Sections 5.1.1 and 5.2.2; Plates 4 and 8, Cross Section V—V'). Therefore, even if the basin-fill deposits had shallow water tables and GBNP streams were hydraulically connected to the groundwater, the many faults have compartmentalized the basin fill, so that any groundwater pumping would have many barriers to any hydraulically connected streams.

In our opinion, the hypothesis by Elliott et al. (2006) and subsequent USGS workers that pumping by SNWA anywhere in Spring or Snake valleys would affect surface water flows in GBNP perennial streams is wrong.

This Page Left Intentionally Blank

7.0 SUMMARY

7.1 Summary of Approach

In developing the geologic framework that is described in this report, we compiled and interpreted significant amounts of data while building the geologic and hydrogeologic maps and cross sections presented here. This has allowed us to produce a digital hydrogeological framework that has provided the foundation for developing conceptual and numerical models of groundwater flow of portions of the area covered by this geologic analysis.

We developed the 1:250,000-scale digital geologic maps (Plates 1 and 2) using data that included the distribution, geometry, thickness, composition, and physical properties of geologic units used to define aquifers, HGUs, and potential confining units. When combined with the geographic breadth of our map coverage, the 1:250,000 scale provides a more detailed and comprehensive picture of the region's geology than any other map in existence. As noted in this report, many earlier maps produced by others use a 1:500,000 scale or larger (e.g., Sweetkind et al., 2007a, which the USGS used in support of its BARCASS study), but such a scale does not typically capture many of the geologic features identified here. Of course, a 1:250,000 scale may not capture all details in geologic features that affect groundwater flow either, but this report incorporates all available map scales of even greater scale in our mapping and analysis, as well as focusing new field observations on all problem areas we can identify.

We evaluated the maps presented here in conjunction with information provided by geologic data, gravity surveys, AMT investigations, and other sources to identify likely pathways for groundwater flow. More specifically, we identified faults that might serve as conduits or barriers (or both) to groundwater flow, and we evaluated the potential for specific faults to serve as conduits or barriers. The region's predominantly north-south faults are excellent conduits to groundwater flow in those directions, but those same faults typically act as barriers to east-west flow. An understanding of faults is critical to evaluating whether groundwater could possibly flow from one basin to another, and also in determining where groundwater might be located within certain basins.

7.2 Summary of Opinions on Key Issues

As described in more detail in Section 6.0, we have evaluated the likelihood of a number of possible flow paths identified by others in previous reports. For each suggested flow path across boundaries of hydrographic areas, we have reviewed our geologic framework, maps, cross sections, and data to determine whether groundwater flow would be likely, permissible, or unlikely along the path, and whether any possible flows would be volumetrically limited by the geology of the area. In the case of nearly every flow path suggested in the other reports described (e.g., BARCASS and Myer's multiple reports), we found that the geologic framework of the area supports either no possible groundwater flow or flow in amounts far less than the amounts suggested by others.

7.2.1 Spring Valley

In Spring Valley, we found that flow between Tippett Valley and Spring Valley is permissible but far from likely and, if it exists at all, is confined to a small permissible southward flow path on the northeast side of the Red Hills.

We also found that some flow is possible from northeastern Spring Valley or Tippett Valley to the basin(s) between the Kern Mountains and the Snake Range, but that such flow would be far less than the 16,000 afy suggested by Welch et al. (2007) (Section 6.2.1.2). The geology of the area, which includes prominent faults and buried bedrock ridges north and south of the Red Hills, makes it more likely that no groundwater moves eastward from northern Spring Valley.

We also found no geologic support for the proposition that groundwater flows from Steptoe Valley to Spring Valley through the Schell Creek Range, as that high range is generally bounded by various confining zones, including large north-south range-front faults that are perpendicular to the suggested flow path (Sections 6.2.1.3 and 6.2.1.4). Similarly, we see no geologic evidence that would support the existence of a flow path from Steptoe Valley to Lake Valley, then Spring Valley, as the suggested flow path in those areas crosses at right angles to many large- to medium-displacement faults and strike ridges of the impermeable Chainman Shale and a caldera of the Indian Peak caldera complex (Section 6.2.1.4).

Some flow is permissible and even likely from Spring Valley to Hamlin Valley through the Limestone Hills, but the volume of 33,000 afy proposed by Welch et al. (2007) is unreasonable and is unsupported by the geology of the area. We believe that the existence of faults in the Limestone Hills are at least partial barriers to flow, and the source of groundwater may be relatively small (the southern geophysical sub-basin of Spring Valley), and therefore that the estimate of others that for flow through this path is more reasonable (Rush and Kazmi, 1965; Nichols, 2000; Burns and Drici, 2011) (Section 6.2.1.4).

7.2.2 Cave Valley

We found that although Shingle Pass may allow minor amounts of groundwater to pass to the White River Valley, no evidence has demonstrated such flow (Section 6.2.2.1). Additionally, we found that a large, north-trending, range-front fault on the eastern side of Cave Valley along the Schell Creek Range acts as a significant southward conduit of groundwater from northern to southern Cave Valley (Section 6.2.2.2). That fault likely serves as the primary conduit of water in Cave Valley, despite the existence of Chainman Shale in the hanging wall (west) of the fault that extends across most of Cave Valley. That hanging-wall block does not impede the primary conduit (i.e., the north-south fault) that likely transports most groundwater southward.

7.2.3 Dry Lake and Delamar Valleys

We found that the geologic framework does not support significant groundwater flow from Dry Lake and Delamar valleys into northern and central Pahranagat Valley (Section 6.2.3.1). North-trending faults in the area of the Timpahute transverse zone appear to be conduits to southward groundwater flow and barriers to westward flow. It is far more likely, based on the geologic framework, that the majority of groundwater in Pahranagat Valley comes from basins to the north and west (i.e., Garden, Coal, and Pahroc valleys).

We also found that the only likely flow path from Delamar Valley to Pahranagat Valley is through the PSZ to southern Pahranagat Valley south of Alamo (Section 6.2.3.2). Furthermore, the clear southward hydraulic gradient in Pahranagat Valley argues that any groundwater entering southern Pahranagat Valley along the PSZ must go southward and westward from southern Pahranagat Valley.

7.2.4 Steptoe Valley

We found that the geology does not support a flow path from Steptoe Valley to Jakes Valley, as range-front faults on both sides of the Egan Range, in concert with smaller faults within the range and many confining units in and adjacent to the Ruth mining district, act as barriers to possible flow (Section 6.2.4.1). Furthermore, we found that no flow path exists from Steptoe Valley to White River Valley for the same reasons (Section 6.2.4.2).

7.2.5 Snake Valley and Great Basin National Park

The hypothetical suggestion by Elliott et al. (2006) and subsequent USGS reports that SNWA pumping in Spring or Snake valleys “might” lead to decreased surface water flows in GBNP is not supported by the geologic framework of the region (Section 6.2.5.1). The groundwater of those valleys is not geologically or hydraulically connected in any significant way to the streams in GBNP, particularly as hundreds of large- to medium-displacement, high-angle normal faults provide barriers between valley groundwater and GBNP streams. Elliott et al. and subsequent USGS investigators have failed to consider their hypothetical statements through the lens of a complete and accurate geologic framework.

7.3 Conclusions

The geologic framework developed through the data interpretation and map construction described in this report is the most accurate, comprehensive, and up-to-date representation yet done of the Project Basins and surrounding area. No other reports or studies have addressed the region in this comprehensive manner or identified the region’s geologic features with the same level of detail as in this report. We believe that our approach provides ample support for our evaluation of possible flow paths discussed above, groundwater occurrence and movement, and the development of conceptual and numerical models of groundwater flow.

This Page Left Intentionally Blank

8.0 REFERENCES

The following geologic maps and reports are cited in the text of the report. This list is followed by a map bibliography consisting of the geologic maps and reports used to construct the plates, whether these references were cited in the text or not.

Abbott, J.T., Best, M.G., and Morris, H.T., 1983, Geologic map of the Pine Grove-Blawn Mountain area, Beaver County, Utah: U.S. Geological Survey Miscellaneous Investigations Series Map I-1479, scale 1:24,000.

Acheampong, S.Y., 1992, Isotope hydrology of Lehman and Baker Creeks Drainages, Great Basin National Park, Nevada [M.S. thesis]: University of Nevada, Las Vegas, 105 p.

Acheampong, S.Y., Farnham, I.M., and Watrus, J.M., 2009, Geochemical characterization of ground water and surface water of Snake Valley and the surrounding areas in Utah, *in* Tripp, B.T., Krahulec, K., and Jordan, J.L., eds., Geology and geologic resources and issues of western Utah: Utah Geological Association Publication 38, p. 325-344.

Ahlborn, R.C., 1977, Mesozoic-Cenozoic structural development of the Kern Mountains, eastern Nevada-western Utah [M.S. thesis]: Brigham Young University Geology Studies, Vol. 24, Pt. 2, p. 117–131.

Alam, A.H.M.S, 1990, Crustal extension in the southern Snake Range and vicinity, Nevada-Utah: An integrated geological and geophysical study [Ph.D. dissertation]: Louisiana State University, 126 p.

Alam, A.H.M.S., and Pilger, Jr., R.H., 1991, An integrated geologic and geophysical study of the structure and stratigraphy of the Cenozoic extensional Hamlin Valley, Nevada-Utah, *in* Raines, G.L., Lisle, R.E., Schafer, R.W., and Wilkinson, W.H., eds., Geology and ore deposits of the Great Basin: Geological Society of Nevada, Symposium Proceedings, April 1–5, 1990, Vol. 1, p. 93–100.

Allander, K.K., and Berger, D.L., 2009, Seismic velocities and thicknesses of alluvial deposits along Baker Creek in the Great Basin National Park, east-central Nevada: U.S. Geological Survey Open-File Report 2009-1174, 14 p.

Allmendinger, R.W., Sharp, J.W., Von Tish, D., Serpa, L., Brown, L., Kaufman, S., Oliver, J., and Smith, R.B., 1983, Cenozoic and Mesozoic structure of the eastern Basin and Range province, Utah, from COCORP seismic-reflection data: Geology, Vol. 11, No. 9, p. 532–536.

SE ROA 43294

JA_13174

Anderson, R.E., 1983, Cenozoic structural history of selected areas in the eastern Great Basin, Nevada-Utah: U.S. Geological Survey Open-File Report 83-504, 47 p.

Anderson, R.E., and Barnhard, T.P., 1993, Heterogeneous neogene strain and its bearing on horizontal extension and horizontal and vertical contraction at the margin of the extensional orogen, Mormon Mountains area, Nevada and Utah: U.S. Geological Survey Bulletin 2011, 43 p.

Anderson, R.E., Felger, T.J., Diehl, S.F., Page, W.R., and Workman, J.B., 2010, Integration of tectonic, sedimentary, and geohydrologic processes leading to a small-scale extension model for the Mormon Mountains area north of Lake Mead, Lincoln County, Nevada, *in* Umhoefer, P.J., Beard, L.S., and Lamb, M.A., eds., Miocene tectonics of the Lake Mead region, central Basin and Range: Geological Society of America Special Paper 463, p. 395–426.

Armstrong, R.L., 1968, Sevier orogenic belt in Nevada and Utah: Geological Society of America Bulletin, Vol. 79, No. 4, p. 429–458.

Armstrong, R.L., 1972, Low-angle (denudation) faults, hinterland of the Sevier orogenic belt, eastern Nevada and western Utah: Geological Society of America Bulletin, Vol. 83, No. 6, p. 1729–1754.

Asch, T.H., and Sweetkind, D.S., 2010, Geophysical characterization of range-front faults, Snake Valley, Nevada: U.S. Geological Survey Open-File Report 2010-1016, 226 p.

Asch, T.H., and Sweetkind, D.S., 2011, Audiomagnetotelluric characterization of range-front faults, Snake Range, Nevada: Geophysics, Vol. 76, p. B1-B7.

Atwater, T., 1970, Implications of plate tectonics for the Cenozoic tectonic evolution of western North America: Geological Society of America Bulletin, Vol. 81, p. 3513–3536.

Bartley, J.M., and Wernicke, B.P., 1984, The Snake Range decollement interpreted as a major extensional shear zone: Tectonics, Vol. 3, No. 6, p. 647–657.

Beard, L.S., Anderson, R.E., Block, D.L., Bohannon, R.G., Brady, R.J., Castor, S.B., Duebendorfer, E.M., Faulds, J.E., Felger, T.J., Howard, K.A., Kuntz, M.A., and Williams, V.S., 2007, Preliminary geologic map of the Lake Mead 30′ × 60′ quadrangle, Clark County, Nevada, and Mohave County, Arizona: U.S. Geological Survey Open-File-Report 2007-1010, 109 p., 3 plates, scale 1:100,000. [http://pubs.usgs.gov/of/2007/1010/].

Beard, L.S., Campagna, D.J., and Anderson, R.E., 2010, Geometry and kinematics of the eastern Lake Mead fault system in the Virgin Mountains, Nevada and Arizona, *in* Umhoefer, P.J., Beard, L.S., and Lamb, M.A., eds., Miocene tectonics of the Lake Mead region, central Basin and Range: Geological Society of America Special Paper 463, p. 243–274.

Belcher, W.R., ed., 2004, Death Valley regional ground-water flow system, Nevada and California—Hydrogeologic framework and transient ground-water flow model: U.S. Geological Survey Scientific Investigations Report 2004–5205, 408 p.

Belcher, W.R., Elliott, P.E., and Geldon, A.L., 2001, Hydraulic-property estimates for use with a transient ground-water flow model of the Death Valley Regional Ground-Water Flow System, Nevada and California: U.S. Geological Survey Water-Resources Investigations Report 01-4210, (revised August 1, 2002), 28 p.

Best, M.G., 1987, Geologic map and sections of the area between Hamlin Valley and Escalante Desert, Iron County, Utah: U.S. Geological Survey Miscellaneous Investigations Series Map I-1774, scale 1:50,000.

Best, M.G., and Williams, V.S., 1997, Geologic map of the Rose Valley quadrangle, Lincoln County, Nevada: U.S. Geological Survey Geologic Quadrangle Map GQ-1765, scale 1:24,000.

Best, M.G., Armstrong, R.L., Graustein, W.C., Embree, G.F., and Ahlborn, R.C., 1974, Mica granites of the Kern Mountains pluton, eastern White Pine County, Nevada: Remobilized basement of the Cordilleran miogeosyncline?: Geological Society of America Bulletin, Vol. 85, p. 1277–1286.

Best, M.G., Christiansen, E.H., and Blank, Jr., R.H., 1989a, Oligocene caldera complex and calc-alkaline tuffs and lavas of the Indian Peak volcanic field, Nevada and Utah: Geological Society of America Bulletin, Vol. 101, p. 1076–1090.

Best, M.G., Christiansen, E.H., Deino, A.L., Grommé, C.S., McKee, E.H., and Noble, D.C., 1989b, Eocene through Miocene volcanism in the Great Basin of the western United States *in* Chapin, C.E., and Zidek, J., eds., Field excursions to volcanic terranes in the western United States, Volume II: Cascades and Intermountain West: New Mexico Bureau of Mines and Mineral Resources Memoir 47, p. 91–133.

Best, M.G., Grant, S.K., Hintze, L.F., Cleary, J.G., Hutsinpiller, A., and Saunders, D.M., 1987a, Geologic map of the Indian Peak (southern Needle Range), Beaver and Iron Counties, Utah: U. S. Geological Survey Miscellaneous Investigations Series Map I-1795, scale 1:50,000.

Best, M.G., Hintze, L.F., and Holmes, R.D., 1987b, Geologic map of the southern Mountain Home and northern Indian Peak Ranges (central Needle Range), Beaver County, Utah: U.S. Geological Survey Miscellaneous Investigations Series Map I-1796, scale 1:50,000.

Best, M.G., Morris, H.T., Kopf, R.W., and Keith, J.D., 1987c, Geologic map of the southern Pine Valley area, Beaver and Iron Counties, Utah: U.S. Geological Survey Miscellaneous Investigations Series Map I-1794, scale 1:50,000.

Best, M.G., Scott, R.B., Rowley, P.D., Swadley, W.C., Anderson, R.E., Grommé, C.S., Harding, A.E., Deino, A.L., Christiansen, E.H., Tingey, D.G., and Sullivan, K.R., 1993, Oligocene-Miocene caldera complexes, ash-flow sheets, and tectonism in the central and southeastern Great Basin, *in* Lahren, M.M., Texler, Jr., J.H., and Spinosa, C., eds., Crustal evolution of the Great Basin and Sierra Nevada—Field trip guidebook: Geological Society of America, Cordilleran and Rocky Mountain sections meeting, p. 285–311.

Best, M.G., Toth, M.I., Kowallis, J.B., Willis, J.B., and Best, V.C., 1989c, Geologic map of the northern White Rock Mountains-Hamlin Valley area, Beaver County, Utah, and Lincoln County, Nevada: U.S. Geological Survey Miscellaneous Investigations Series Map I-1881, scale 1:50,000.

Biek, R.F., Rowley, P.D., Hacker, D.B., Hayden, J.M., Willis, G.C., Hintze, L.F., Anderson, R.E., and Brown, K.D., 2007, Interim geologic map of the St. George 30' × 60' quadrangle and east part of the Clover Mountains 30' × 60' quadrangle, Washington and Iron Counties, Utah: Utah Geological Survey Open-File Report 478, scale 1:100,000, 2 sheets.

Billingsley, G.H., and Workman, J.B., 2000, Geologic map of the Littlefield 30' × 60' quadrangle, Mohave County, northwestern Arizona: U.S. Geological Survey Geologic Investigations Series Map I-2628, scale 1:100,000.

Black, B.D., Hecker, S., Hylland, M.D., Christenson, G.L., and McDonald, G.N., 2003, Quaternary fault and fold database and map of Utah: Utah Geological Survey Map 193DM, scale 1:500,000. (CD-ROM).

Blakely, R.J., 1995, Potential theory in gravity and magnetic applications. New York, Cambridge University Press.

Blakely, R.J., and Simpson, R.W., 1986, Approximating edges of source bodies from magnetic or gravity anomalies: Geophysics, Vol. 51, No. 7, p. 1494–1498.

Bohannon, R.G., 1983, Geologic map, tectonic map and structure sections of the Muddy and Northern Black Mountains, Clark County, Nevada: U.S. Geological Survey Miscellaneous Investigations Series Map I-1406, scale 1:62,500.

Bohannon, R.G., 1984, Nonmarine sedimentary rocks of Tertiary age in the Lake Mead region, southeastern Nevada and northwestern Arizona: U.S. Geological Survey Professional Paper 1259, 72 p.

Bohannon, R.G., 1992, Geologic map of the Weiser Ridge quadrangle, Clark County, Nevada: U.S. Geological Survey Geologic Quadrangle Map GQ-1714, scale 1:24,000.

Bol, A.J., Snyder, D.B., Healey, D.L, and Saltus, R.W., 1983, Principal facts, accuracies, sources, and base station descriptions for 3672 gravity stations in the Lund and Tonopah 1° × 2° quadrangle, Nevada: U.S. Department of Commerce, National Technical Information Service, PB83-202-671, 86 p.

Brokaw, A.L., 1967, Geologic map and sections of the Ely quadrangle, White Pine County, Nevada: U.S. Geological Survey Geologic Quadrangle Map GQ-697, scale 1:24,000.

Brokaw, A.L., and Barosh, P.J., 1968, Geologic map and sections of the Riepetown quadrangle, White Pine County, Nevada: U.S. Geological Survey Geologic Quadrangle Map GQ-758, scale 1:24,000.

Brokaw, A.L., and Heidrick, T., 1966, Geologic map and sections of the Giroux Wash quadrangle, White Pine County, Nevada: U.S. Geological Survey Geologic Quadrangle Map GQ-476, scale 1:24,000.

Brokaw, A.L., and Shawe, D.R., 1965, Geologic map and sections of the Ely 3 SW quadrangle, White Pine County, Nevada: U.S. Geological Survey Miscellaneous Geological Investigations Map I-449, scale 1:24,000.

Brokaw, A.L., Bauer, H.L., and Breitrick, R.A., 1973, Geologic map of the Ruth quadrangle, White Pine County, Nevada: U.S. Geological Survey Geologic Quadrangle Map GQ-1085, scale 1:24,000.

Brothers, K., Bernholtz, A.J., Buqo, T.S., and Tracy, J.V., 1994, Hydrology and steady state ground-water model of Spring Valley, Lincoln and White Pine counties, Nevada: Las Vegas Valley Water District, Las Vegas, Nevada, Cooperative Water Project Report No. 13, 69 p.

Brothers, K., Katzer, T., and Johnson, M., 1996, Hydrology and steady state ground-water model of Dry Lake and Delamar valleys, Lincoln County, Nevada: Las Vegas Valley Water District, Las Vegas, Nevada, Cooperative Water Project Report No. 16, 48 p.

Brown, C.L., and Schmitt, J.G., 1991, Horse Camp Formation: Record of Miocene-Pliocene extensional basin development, northern Grant Range, Nevada, *in* Flanigan, Donna M.H., Mike Hansen and T. Edward Flanigan, (eds.), Geology of White River Valley, the Grant Range, Eastern Railroad Valley and Western Egan Range, Nevada: 1991 Fieldtrip Guidebook, Nevada Petroleum Society Inc., Reno, p. 7–13.

Buqo, T., 2007, Carbonate development in the Muddy Springs area, *in* Coache, R., ed., Regional tour of the carbonate system guidebook: Nevada Water Resources Association, Clark County, Nevada, June 18-20, 2007, p. 5–6.

Burbey, T.J., 1997, Hydrogeology and potential for ground-water development, carbonate-rock aquifers, southern Nevada and southeastern California: U.S. Geological Survey Water-Resources Investigations 95–4168, 65 p.

Burchfiel, B.C., Fleck, R.J., Secor, D.T., Vincelette, R.R., and Davis, G.A., 1974, Geology of the Spring Mountains, Nevada: Geological Society of America Bulletin, Vol. 85, No. 7, p. 1013–1022.

Burns, A.G., and Drici, W., 2011, Hydrology and water resources of Spring, Cave, Dry Lake, and Delamar valleys, Nevada and vicinity: Presentation to the Office of the Nevada State Engineer: Southern Nevada Water Authority, Las Vegas, Nevada.

Caine, J.S., Evans, J.P., and Forster, C.B., 1996, Fault zone architecture and permeability structure: Geology, Vol. 24, No. 11, p. 1025–1028.

Caine, J.S., and Forster, C.B., 1999, Fault zone architecture and fluid flow: Insights from field data and numerical modeling, *in* Haneberg, W.C., Mozley, P.S., Moore, J.C., and Goodwin, L.B., eds., Faults and subsurface fluid flow in the shallow crust: American Geophysical Union Geophysical Monograph 113, p. 101–127.

Caine, J.S., Manning, A.H., Berger, B.R., Kremer, Y., Guzman, M.A., Eberl, D.D., and Schuller, K., 2010, Characterization of geologic structures and host rock properties relevant to the hydrogeology of the Standard Mine in Elk Basin, Gunnison County, Colorado: U.S. Geological Survey Open-File Report 2010–1008, 56 p.

Carpenter, J.A., and Carpenter, D.G., 1994a, Analysis of Basin-Range and Fold-Thrust Structure, and Reinterpretation of the Mormon Peak Detachment and Similar Features as Gravity Slide Systems: Southern Nevada, Southwest Utah, and Northwest Arizona, *in* Dobbs, S.W., and W.J. Taylor, eds., Structural and Stratigraphic Investigations and Petroleum Potential of Nevada, with Special Emphasis South of the Railroad Valley Producing Trend: Nevada Petroleum Society Conference Volume II, p. 15–52.

Carpenter, J.A., and Carpenter, D.G., 1994b, Fold-Thrust Structure, Synorogenic Rocks, and Structural Analysis of the North Muddy and Muddy Mountains, Clark County Nevada, *in* Dobbs, S.W., and W.J. Taylor, eds., Structural and Stratigraphic Investigations and Petroleum Potential of Nevada, with Special Emphasis South of the Railroad Valley Producing Trend: Nevada Petroleum Society Conference Volume II, p. 65–94.

Carpenter, J.A., Carpenter, D.G., and Dobbs, S.W., 1994, Antler Orogeny: Paleostructural Analysis and Constraints on Plate Tectonic Models with a Global Analogue in Southeast Asia, *in* Dobbs, S.W., and W.J. Taylor, eds., Structural and Stratigraphic Investigations and Petroleum Potential of Nevada, with Special Emphasis South of the Railroad Valley Producing Trend: Nevada Petroleum Society Conference Volume II, p. 187–240.

Chidsey, Jr., T.C., 1978, Intrusions, alteration, and economic implications in the northern House Range, Utah: Brigham Young University Geology Studies, Vol. 25, Pt. 3, p. 47–65.

Christiansen, W.J., 1977, Geology of the Fish Springs mining district, Juab County, Utah [M.S. thesis]: Salt Lake City, University of Utah, 66 p.

Christiansen, R.L., and Lipman, P.W., 1972, Cenozoic volcanism and plate-tectonic evolution of the western United States: II. Late Cenozoic: Royal Society of London Philosophical Transactions A, Vol. 271, No. 1213, p. 249–284.

Christiansen, R.L., and Yeats, R.S., 1992, Post-Laramide geology of the U.S. Cordilleran region, *in* Burchfiel, B.C., Lipman, P.W., and Zoback, M.L., eds., The Cordilleran Orogen: Conterminous U.S.: Boulder, Colorado, Geological Society of America, The Geology of North America, V. G-3, p. 261–406.

Coats, R.R., 1987, Geology of Elko County, Nevada: Nevada Bureau of Mines and Geology Bulletin 101, 112 p.

Coney, P.J., 1974, Structural analysis of the Snake Range décollement, east-central Nevada: Geological Society of America Bulletin, Vol. 85, No. 6, p. 973–978.

Cook, K.L., Bankey, V., Mabey, D.R., and DePangher, M., 1989, Complete Bouguer gravity anomaly map of Utah: Utah Geological and Mineral Survey Map 122, scale 1:500,000.

Cordell, L., 1979, Gravimetric expression of graben faulting in Santa Fe Country and the Española Basin New Mexico, *in* Ingersoll, R.V., ed., Guidebook of Santa Fe Country, 30th Field Conference: New Mexico Geological Society, October 4–6, 1979, p. 59–64.

Cornwall, H.R., 1972, Geology and mineral deposits of southern Nye County, Nevada: Nevada Bureau of Mines and Geology Bulletin 77, 49 p.

Crafford, A.E.J., 2007, Geologic Map of Nevada: U.S. Geological Survey Data Series 249, 1 CD-ROM, 46 p., 1 plate.

Cram, C., 2006, Personal communication to P. Rowley (consultant to Southern Nevada Water Authority) regarding yields of new wells at Sand Hollow State Park, Utah, Washington County: Water Conservancy District, St. George, Utah.

Currey, D.R., 1982, Lake Bonneville: Selected features of relevance to neotectonic analysis: U.S. Geological Survey Open-File Report 82-1070, 30 p.

Currey, D.R., Atwood, G., and Mabey, D.R., 1984, Major levels of Great Salt Lake and Lake Bonneville: Utah Geological Survey Map 73, scale 1:750,000.

D'Agnese, F.A., O'Brien, G.M., Faunt, C.C., Belcher, W.R., and San Juan, C., 2002, A three-dimensional numerical model of predevelopment conditions in the Death Valley regional ground-water flow system, Nevada and California: U.S. Geological Survey Water-Resources Investigations Report 02–4102, 114 p.

Davis, F.D., 2005, Water resources of Millard County, Utah: Utah Geological Survey Open-File Report 447, 27 p.

dePolo, C.M., 2008, Quaternary faults in Nevada: Nevada Bureau of Mines and Geology Map 167, scale 1:1,000,000.

dePolo, C.M., Johnson, G.L., Price, J.G., and Mauldin, J.M., 2009, Quaternary faults in Nevada—Online interactive map: Nevada Bureau of Mines and Geology Open-File Report 09-9, scale 1:1,000,000.

Dettinger, M.D., 1992, Geohydrology of areas being considered for exploratory drilling and development of the carbonate-rock aquifers in southern Nevada—preliminary assessment: U.S. Geological Survey Water-Resources Investigations Report 90–4077, 35 p.

Dettinger, M.D., Harrill, J.R., Schmidt, D.L., and Hess, J.W., 1995, Distribution of carbonate-rock aquifers and the potential for their development, southern Nevada and adjacent parts of California, Arizona, and Utah: U.S. Geological Survey Water-Resources Investigations Report 91–4146, 100 p.

Dixon, G.L., 2007, Geology of White River Narrows and Pahroc Valley, *in* Coache, R., ed., Regional tour of the carbonate system guidebook: Nevada Water Resources Association, Clark County, Nevada, June 18-20, 2007, p. 17–18.

Dixon, G.L., and Katzer, T., 2002, Geology and hydrology of the lower Virgin River Valley in Nevada, Arizona, and Utah: Virgin Valley Water District, Mesquite, Nevada, Report VVWD-01, 126 p.

Dixon, G.L., and Rowley, P.D., 2007a, Hydrogeology of Caliente and lower Meadow Valley Wash, *in* Coache, R., ed., Regional tour of the carbonate system guidebook: Nevada Water Resources Association, Clark County, Nevada, June 18-20, 2007, p. 65–66.

Dixon, G.L., and Rowley, P.D., 2007b, Hydrogeology of Dry Lake and Delamar valleys, *in* Coache, R., ed., Regional tour of the carbonate system guidebook: Nevada Water Resources Association, Clark County, Nevada, June 18-20, 2007, p. 69–70.

Dixon, G.L., and Rowley, P.D., 2007c, Hydrogeology of Pioche, Panaca and Caliente areas, *in* Coache, R., ed., Regional tour of the carbonate system guidebook: Nevada Water Resources Association, Clark County, Nevada, June 18-20, 2007, p. 63–64.

Dixon, G.L., and Rowley, P.D., 2007d, Hydrogeology of Spring Valley, *in* Coache, R., ed., Regional tour of the carbonate system guidebook: Nevada Water Resources Association, Clark County, Nevada, June 18-20, 2007, p. 35–36.

Dixon, G.L., Donovan, D.J., and Rowley, P.D., 2007b, Geology of Oak Springs Summit, *in* Coache, R., ed., Regional tour of the carbonate system guidebook: Nevada Water Resources Association, Clark County, Nevada, June 18-20, 2007, p. 71–72.

Dixon, G.L., Donovan, D.J., and Rowley, P.D., 2007c, Hydrogeology of White River Valley, *in* Coache, R., ed., Regional tour of the carbonate system guidebook: Nevada Water Resources Association, Clark County, Nevada, June 18-20, 2007, p. 21–22.

Dixon, G.L., Hedlund, D.C., and Ekren, E.B., 1972, Geologic map of the Pritchards Station quadrangle, Nye County, Nevada: U.S. Geological Survey Miscellaneous Geologic Investigations Map I-728, scale 1:48,000.

Dixon, G.L., Rowley, P.D., Burns, A.G., Watrus, J.M., Donovan, D.J., and Ekren, E.B., 2007a, Geology of White Pine and Lincoln counties and adjacent areas, Nevada and Utah: The geologic framework of regional groundwater flow systems: Southern Nevada Water Authority, Las Vegas, Nevada, Doc. No. HAM-ED-0001, 157 p.

Dixon, G.L., and Van Liew, B., 2007, Hydrogeology of Crystal Springs, *in* Coache, R., ed., Regional tour of the carbonate system guidebook: Nevada Water Resources Association Clark County, Nevada, June 18–20, 2007, p. 13–14.

Dobbs, S.W., Garbee, Jr., J.J., Stuart, C.K., and Nelson, S.L., 1994, Intergrated [sic] Geological and Geophysical Interpretation in the Newark Valley Area, Eureka Fold-and-Thrust Belt, East-Central Nevada, *in* Dobbs, S.W., and W.J. Taylor, eds., Structural and Stratigraphic Investigations and Petroleum Potential of Nevada, with Special Emphasis South of the Railroad Valley Producing Trend: Nevada Petroleum Society Conference Volume II, p. 241–253.

Dohrenwend, J.C., Schell, B.A., Menges, C.M., Moring, B.C., and McKittrick, M.A., 1996, Reconnaissance photogeologic map of young (Quaternary and late Tertiary) faults in Nevada, *in* Singer, D.A., ed., An analysis of Nevada's metal-bearing mineral resources: Nevada Bureau of Mines and Geology Open-File Report 96–2, p. 9-1–9-12.

Donovan, D.J., 1996, Hydrostratigraphy and allostratigraphy of the Cenozoic alluvium in the northwestern part of Las Vegas Valley, Clark County, Nevada [M.S. thesis]: University of Nevada, Las Vegas, 199 p.

Donovan, D.J., 2007, Geology of Muddy River Springs, *in* Coache, R., ed., Regional tour of the carbonate system guidebook: Nevada Water Resources Association, Clark County, Nevada, June 18-20, 2007, p. 1–2.

Donovan, D.J., Dixon, G.L., and Rowley, P.D., 2004, Detailed geologic mapping in the Muddy Springs area, Clark County, Nevada [abs.]: Nevada Water Resources Association Annual Conference, Mesquite, Nevada, February 24–26, 2004, p. 23.

Dotson, K.E., 2010, Geochemical analysis of calcium carbonate cementation and its role in reducing loss rates along Snake Creek, southern Snake Valley, White Pine County, Nevada [M.S. thesis]: University of Nevada, Reno, 72 p.

Druschke, P., Hanson, A.D., Wells, M.L., Rasbury, T., Stockli, D.F., and Gehrels, G., 2009, Synconvergent surface-breaking normal faults of Late Cretaceous age within the Sevier hinterland, east-central Nevada: Geology, Vol. 37, No. 5, p. 447–450.

duBray, E.A., and Hurtubise, D.O., 1994, Geologic map of the Seaman Range, Lincoln and Nye counties, Nevada: U.S. Geological Survey Miscellaneous Investigations Series Map I-2282, scale 1:50,000.

Eberhart-Phillips, D., Stanley, W.D., Rodriguez, B.D., and Lutter, W.J., 1995, Surface seismic and electrical methods to detect fluids related to faulting: Journal of Geophysical Research, Vol. 100, No. B7, p. 12919–12936.

Ehni, W., and Faulds, J., eds., 2002, Detachment and attenuation in eastern Nevada and its application to petroleum exploration: Nevada Petroleum Society 2002 Field Trip Guidebook, 163 p.

Eichhubl, P., Taylor, W.L., Pollard, D.D., and Aydin, A., 2004, Paleo-fluid flow and deformation in the Aztec Sandstone at the Valley of Fire, Nevada—Evidence for the coupling of hydrogeologic, diagenetic, and tectonic processes: Geological Society of America Bulletin, Vol. 116, p. 1120–1136.

Ekren, E.B., Bucknam, R.C., Carr, W.J., Dixon, G.L., and Quinlivan, W.D., 1976, East-trending structural lineaments in central Nevada: U.S. Geological Survey Professional Paper 986, 16 p.

Ekren, E.B., Hinrichs, E.N., Quinlivan, W.D., and Hoover, D.L., 1973, Geologic map of the Moores Station quadrangle, Nye County, Nevada: U.S. Geological Survey Miscellaneous Geologic Investigations Map I-756, scale 1:48,000.

Ekren, E.B., Orkild, P.P., Sargent, K.A., and Dixon, G.L., 1977, Geologic map of Tertiary rocks, Lincoln County, Nevada: U.S. Geological Survey Miscellaneous Investigations Series Map I-1041, scale 1:250,000.

Ekren, E.B., Rowley, P.D., Dixon, G.L., Page, W.R., and Brandt, J.M., in press, Geology of the Quinn Canyon Range and vicinity, Nye and Lincoln Counties, Nevada: Southern Nevada Water Authority, Las Vegas, Nevada.

Elliott, P.E., Beck, D.A., and Prudic, D.E., 2006, Characterization of surface-water resources in the Great Basin National Park area and their susceptibility to ground-water withdrawals in adjacent valleys, White Pine County, Nevada: U.S. Geological Survey Scientific Investigations Report 2006-5099, 156 p. Available at URL:http://pubs.water.usgs.gov/sir2006-5099.

Erskine, M.C., 2001, Structural overlap of passive continental margin stratigraphic packages onto the Colorado Plateau cratonic package in southwestern Utah, *in* Erskine, M.C., Faulds, J.E., Bartley, J.M., and Rowley, P.D., eds., The geologic transition, High Plateaus to Great Basin—A symposium and field guide: The Mackin Volume: Utah Geological Association Publication 30, and American Association of Petroleum Geologists Publication GB78, September 20–22, 2001, p. 365–377.

Faulds, J.E., and Varga, R.J., 1998, The role of accommodation zones and transfer zones in the regional segmentation of extended terranes, *in* Faulds, J.E., and Stewart, J.H., eds., Accommodation zones and transfer zones: The regional segmentation of the Basin and Range province: Geological Society of America Special Paper 323, p. 1–45.

Faybishenko, B., Witherspoon, P.A., and Gale, J., eds, 2005a, Dynamics of fluids and transport in fractured rock: American Geophysical Union Geophysical Monograph 162, 207 p.

Faybishenko, B., Witherspoon, P.A., Bodvarsson, G.S., and Gale, J. eds., 2005b, Emerging issues in fractured-rock flow and transport investigations: Introduction and overview, *in* Faybishenko, B., Witherspoon, P.A., and Gale, J., eds., Dynamics of fluids and transport in fractured rock: American Geophysical Union Geophysical Monograph 162, p. 1–11.

Fouch, T.D., Lund, K., Schmitt, J.G., Good, S.C., and Hanley, J.H., 1991, Late Cretaceous(?) and Paleogene sedimentary rocks and extensional(?) basins in the region of the Egan and Grant ranges, and White River and Railroad valleys, Nevada: Their relation to Sevier and Laramide contractional basins in the southern Rocky Mountains and Colorado Plateau, *in* Flanigan, Donna M.H., Mike Hansen and T. Edward Flanigan, eds., Geology of White River Valley, the Grant Range, Eastern Railroad Valley and Western Egan Range, Nevada: 1991 Fieldtrip Guidebook, Nevada Petroleum Society Inc., p. 15–28.

French, Don E., and Schalla, Robert A., (eds.), 1998, Hydrocarbon habitat and special geologic problems of the Great Basin: 1998 Field Trip Guidebook, Nevada Petroleum Society, 109 p.

Gans, P.B., 2000a, The northern White Pine Range, *in* Gans, P.B., and Seedorff, E., eds., Geology and ore deposits 2000: The Great Basin and beyond: Geological Society of Nevada, Symposium Proceedings, May 15–18, 2000, p. 83–95.

Gans, P.B., 2000b, The Snake Range metamorphic core complex—Geologic overview of the northern Snake Range, *in* Gans, P.B., and Seedorff, E., eds., Geology and ore deposits 2000: The Great Basin and beyond: Geological Society of Nevada, Symposium Proceedings, May 15–18, 2000, p. 99–117.

Gans, P.B., and Miller, E.L., 1985, Comment on "The Snake Range decollement interpreted as a major extensional shear zone" by John M. Bartley and Brian P. Wernicke: Tectonics, Vol. 4, No. 4, p. 411-415.

Gans, P.B., Mahood, G.A., and Schermer, E., 1989, Synextensional magmatism in the Basin and Range province: A case study from the eastern Great Basin: Geological Society of America Special Paper, Vol. 233, 53 p.

Gans, P.B., Miller, E.L., Huggins, C.C., and Lee, J., 1999b, Geologic map of the Little Horse Canyon quadrangle, Nevada and Utah: Nevada Bureau of Mines and Geology Field Studies Map 20, scale 1:24,000.

Gans, P.B., Miller, E.L., and Lee, J., 1999a, Geologic map of the Spring Mountain quadrangle, Nevada and Utah: Nevada Bureau of Mines and Geology Field Studies Map 18, scale 1:24,000.

Gans, P.B., Miller, E.L., McCarthy, J., and Ouldcott, M.L., 1985, Tertiary extensional faulting and evolving ductile-brittle transition zones in the northern Snake Range and vicinity: New insights from seismic data: Geology, Vol. 13, p. 189–193.

Gans, P.B., Seedorff, E., Fahey, P.L., Hasler, R.W., Maher, D.J., Jeanne, R.A., and Shaver, S.A., 2001, Rapid Eocene extension in the Robinson district, White Pine County, Nevada: Constraints from 40Ar/39Ar dating: Geology, Vol. 29, No. 6, p. 475–478.

Garside, L.J., Hess, R.H., Fleming, K.L, and Weimer, B.S., 1988, Oil and gas developments in Nevada: Nevada Bureau of Mines and Geology Bulletin 104, 136 p.

Geological Society of America, 1999, 1999 Geologic Time Scale [Internet], [accessed December 9, 2010], available from http://www.geosociety.org/science/timescale/timescl-1999.pdf.

Geometrics, 2007, Operation manual for Stratagem systems running IMAGEM Version 2.19 [Internet], [accessed December 7, 2010], available from ftp://geom.geometrics.com/pub/GeoElectric/Manuals/EH4_manual_F.pdf.

Gillespie, J.M., 2008, A conceptual model of groundwater flow in Spring Valley, NV, and Snake Valley, NV-UT [M.S. thesis]: Brigham Young University, Provo, Utah, 80 p.

Glonek, L.A., 2001, Estimating effective discharge at Lehman Creek, Great Basin National Park, Nevada [M.S. thesis]: University of Nevada, Las Vegas, 223 p.

GSA, see Geological Society of America.

Guth, P.L., 1980, Geology of the Sheep Range, Clark County, Nevada [Ph.D. dissertation]: Massachusetts Institute of Technology, Cambridge, Massachusetts, 189 p.

Hamilton, W.B., 1995, Subduction systems and magmatism, *in* Smellie, J.L., (ed.), Volcanism Associated with Extension at Consuming Plate Margins: Geological Society Special Publication No. 81, p. 3–28.

Haneberg, W.C., Mozley, P.S., Moore, J.C., and Goodwin, L.B., eds., 1999, Faults and subsurface fluid flow in the shallow crust: American Geophysical Union Geophysical Monograph 113, 222 p.

Harding, A.E., Scott, R.B., Mehnert, H.H., and Snee, L.W., 1995, Evidence of the Kane Springs Wash caldera in the Meadow Valley Mountains, southeastern Nevada, *in* Scott, R.B., and Swadley, W.C., eds., Geologic studies in the Basin and Range–Colorado Plateau transition in southeastern Nevada, southwestern Utah, and northwestern Arizona, 1992: U.S. Geological Survey Bulletin 2056, p. 135–180.

Harrill, J.R., Gates, J.S., and Thomas, J.M., 1988, Major ground-water flow systems in the Great Basin region of Nevada, Utah, and adjacent states: U.S. Geological Survey Hydrologic Investigations Atlas HA-694-C, scale 1:1,000,000, 2 sheets.

Harrill, J.R., and Prudic, D.E., 1998, Aquifer systems in the Great Basin region of Nevada, Utah, and adjacent states—summary report: U.S. Geological Survey Professional Paper 1409-A, 66 p.

Hauser, E., Potter, C., Hauge, T., Burgess, S., Burtch, S., Mutschler, J., Allmendinger, R., Brown, L., Kaufman, S., and Oliver, J., 1987, Crustal structure of eastern Nevada from COCORP deep seismic reflection data: Geological Society of America Bulletin, Vol. 99, p. 833–844.

Hazzard, J.C., and Turner, E.F., 1957, Decollement-type overthrusting in south-central Idaho, northwestern Utah, and northeastern Nevada [abs.]: Geological Society of America Bulletin, Vol. 68, No. 12, p. 1829.

Heath, Ralph C., 1983, Basic ground-water hydrology: U.S. Geological Survey Water-Supply Paper 2220, 86 p.

Herring, D.M., 1998a, Drilling results for the Balcron Oil #12-36 Cobra State dry hole, Millard County, Utah, *in* French, Don E., and Schalla, Robert A., (eds.), Hydrocarbon habitat and special geologic problems of the Great Basin: 1998 Field Trip Guidebook, Nevada Petroleum Society, p. 88–89.

Herring, D.M., 1998b, Drilling results of the EREC #31-22 Mamba Federal dry hole, Millard County, Utah, *in* French, Don E., and Schalla, Robert A., (eds.), Hydrocarbon habitat and special geologic problems of the Great Basin: 1998 Field Trip Guidebook, Nevada Petroleum Society, p. 85–86.

Herring, D.M., Greene, D.C., French, D.E., Schalla, R.A., and Taylor, W.J., 1998, 1998 Nevada Petroleum Society Field Trip—Day 3: Ely to Snake Valley, *in* French, Don E., and Schalla, Robert A., (eds.), Hydrocarbon habitat and special geologic problems of the Great Basin: 1998 Field Trip Guidebook, Nevada Petroleum Society, p. 81–101.

Hess, R., 2001, Nevada oil and gas well map: Nevada Bureau of Mines and Geology Open-File Report 2001–07.

Hess, R., 2004, Nevada oil and gas well database (NVOILWEL): Nevada Bureau of Mines and Geology Open-File Report 04–01, 240 p.

Hess, R.H., and Johnson, G.L., 1997, Nevada Bureau of Mines and Geology county digital mapping project: Nevada Bureau of Mines and Geology Open-File Report 97–1, scale 1:250,000.

Hildenbrand, T.G., 1983, FFTFIL: A filtering program based on two-dimensional Fourier analysis of geophysical data: U.S. Geological Survey Open-File Report 83–237, 60 p.

Hildenbrand, T.G., and Kucks, R.P., 1988a, Filtered magnetic anomaly maps of Nevada: Nevada Bureau of Mines and Geology Map 93B, scale 1:000,000, 5 sheets.

Hildenbrand, T.G., and Kucks, R.P., 1988b, Total intensity magnetic anomaly map of Nevada: Nevada Bureau of Mines and Geology Map 93A, scale 1:750,000.

Hintze, L.F., 1980a, Geologic map of Utah: Utah Geological and Mineralogical Survey, scale 1:500,000.

Hintze, L.F., 1980b, Preliminary geologic map of the Sand Pass NW quadrangle, Juab County, Utah: U.S. Geological Survey Miscellaneous Field Studies Map MF-1149, scale 1:24,000.

Hintze, L.F., 2005, Utah's spectacular geology: How it came to be. Provo, Utah, Brigham Young University.

Hintze, L.F., Anderson, R.E., and Embree, G.F., 1994, Geologic map of the Motoqua and Gunlock quadrangles, Washington County, Utah: U.S. Geological Survey Miscellaneous Investigations Series Map I-2427, scale 1:24,000.

Hintze, L.F., and Davis, F.D., 2002a, Geologic map of the Tule Valley 30′ × 60′ quadrangle and parts of the Ely, Fish Springs, and Kern Mountains 30′ × 60′ quadrangles, northwest Millard County, Utah: Utah Geological Survey Map 186, scale 1:100,000, 2 sheets.

Hintze, L.F., and Davis, F.D., 2002b, Geologic map of the Wah Wah Mountains North 30' × 60' quadrangle and part of the Garrison 30' × 60' quadrangle, southwest Millard County and part of Beaver County, Utah: Utah Geological Survey Map 182, scale 1:100,000, 2 sheets.

Hintze, L.F., and Davis, F.D., 2003, Geology of Millard County, Utah: Utah Geological Survey Bulletin 133, 305 p.

Hintze, L.F., and Kowallis, B.J., 2009, Geologic history of Utah. Provo, Utah, Brigham Young University Geology Studies Special Publication 9.

Hintze, L.F., Willis, G.C., Laes, D.Y.M., Sprinkel, D.A., and Brown, K.D., 2000, Digital geologic map of Utah: Utah Geological Survey Map 179DM, scale 1:500,000, 2 sheets.

Hitchborn, A.D., Arbonies, D.G., Peters, S.G., Connors, K.A., Noble, D.C., Larson, L.T., Beebe, J.S., and McKee, E.H., 1996, Geology and gold deposits of the Bald Mountain mining district, White Pine County, Nevada, *in* Coyner, A.R., and Fahey, P.L., eds., Geology and Ore Deposits of the American Cordillera: Geological Society of Nevada Symposium Proceedings, Reno/Sparks, Nevada, April 1995, p. 505–546.

Holmes, R.B., Brothers, K., and Entsminger, J.J., 2011, Water development and diversification: Southern Nevada's past, present, and future water needs: Presentation to the Office of the Nevada State Engineer: Southern Nevada Water Authority, Las Vegas, Nevada.

Hood, J.W., and Rush, F.E., 1965, Water-resources appraisal of the Snake Valley area, Utah and Nevada: Nevada Department of Conservation and Natural Resources Water Resources–Reconnaissance Series Report 34, 40 p.

Hose, R.K., 1977, Structural geology of the Confusion Range, west-central Utah: U.S. Geological Survey Professional Paper 971, 9 p.

Hose, R.K., and Blake, Jr., M.C., 1976, Geology and mineral resources of White Pine County, Nevada Part I, Geology: Nevada Bureau of Mines and Geology Bulletin 85, p. 1–35.

Howard, E.L., 1978, Geologic map of the eastern Great Basin, Nevada and Utah: Terrascan Group, Inc., Lakewood, Colorado, scale 1:250,000.

Howard, K.A., Kistler, R.W., Snoke, A.W., and Willden, R., 1979, Geologic map of the Ruby Mountains, Nevada: U.S. Geological Survey Miscellaneous Investigations Series Map I-1136, scale 1:125,000.

Jachens, R.C., and Moring, B.C., 1990, Maps of the thickness of Cenozoic deposits and the isostatic residual gravity over basement for Nevada: U.S. Geological Survey Open-File Report 90–404, 15 p.

Jackson, T.R., 2010, Evaluation of the hydraulic connection between streams and aquifers at Baker and Snake Creek near Great Basin National Park, Snake Valley, White Pine County, Nevada [M.S. thesis]: University of Nevada, Reno, 236 p.

Jayko, A.S., 1990, Shallow crustal deformation in the Pahranagat area, southern Nevada, *in* Wernicke, B.P., ed., Basin and Range extensional tectonics near the latitude of Las Vegas, Nevada: Boulder, Colorado, Geological Society of America Memoir 176, p. 213–236.

Jayko, A.S., 2007, Geologic map of the Pahranagat Range 30′ × 60′ quadrangle, Lincoln and Nye Counties, Nevada: U.S. Geological Survey Scientific Investigations Map 2904, scale 1: 100,000. [http://pubs.usgs.gov/sim/2007/2904/].

Johnson, J.A., 2007, Hydrology of Muddy River Springs, *in* Coache, R., ed., Regional tour of the carbonate system guidebook: Nevada Water Resources Association, Clark County, Nevada, June 18-20, 2007, p. 3–4.

Johnson, M., 2007a, Geyser Spring complex hydrology and Lake Valley activities, *in* Coache, R., ed., Regional tour of the carbonate system guidebook: Nevada Water Resources Association, Clark County, Nevada, June 18-20, 2007, p. 59–60.

Johnson, M., 2007b, Hydrogeology of Pahranagat shear zone and surrounding area, *in* Coache, R., ed., Regional tour of the carbonate system guidebook: Nevada Water Resources Association, Reno, Nevada, p. 11–12.

Johnson, M., Dixon, G.L., Rowley, P.D., Katzer, T.C., and Winters, M., 2002, Hydrology and ground-water conditions of the Tertiary Muddy Creek Formation in the lower Virgin River basin of southeastern Nevada and adjacent Arizona and Utah, *in* Lund, W.R., ed., Field guide to geologic excursions in southwestern Utah and adjacent areas of Arizona and Nevada: Utah Geological Survey Open-File Report 02–172, p. 284–315.

Jones, A.E., ed., 1996, Geology and gold deposits of eastern Nevada—1996 Spring Field Trip Guidebook: Geological Society of Nevada Special Publication No. 23, Reno, Nevada, May 3–5, 1996, 166 p.

Katzer, T., and Donovan, D.J., 2003, Surface-water resources and basin water budget for Spring Valley, White Pine and Lincoln counties, Nevada: Las Vegas Valley Water District, Las Vegas, Nevada, 71 p.

Keller, G.V., 1987, Rock and mineral properties, *in* Nabighian, M.N., ed., Electromagnetic methods in applied geophysics: Volume 1, Theory. Tulsa, Oklahoma, Society of Exploration Geophysicists, Investigations in Geophysics No. 3, p. 13–51.

Kellogg, H.E., 1963, Paleozoic stratigraphy of the southern Egan Range, Nevada: Geological Society of America Bulletin, Vol. 74, p. 685–708.

Kellogg, H.E., 1964, Cenozoic stratigraphy and structure of the southern Egan Range, Nevada: Geological Society of America Bulletin, Vol. 75, p. 949–968.

Kepper, J.C., 1960, Stratigraphy and structure of the southern half of the Fish Springs Range, Juab County, Utah [M.S. thesis]: University of Washington, Seattle, 92 p.

Kirby, S., and Hurlow, H., 2005, Hydrogeologic setting of the Snake Valley hydrologic basin, Millard County, Utah, and White Pine and Lincoln Counties, Nevada—Implications for possible effects of proposed water wells: Utah Geological Survey Report of Investigation 254, 39 p.

Kistinger, G.M., Prieur, J.P., Rowley, P.D., and Dixon, G.L., 2009, Characterization of streams and springs in the Snake Valley area, Utah and Nevada, *in* Tripp, B.T., Krahulec, K., and Jordan, J.L., eds., Geology and geologic resources and issues of western Utah: Utah Geological Association Publication 38, p. 299-323.

Kleinhampl, F.J., and Ziony, J.I., 1985, Geology of northern Nye County, Nevada: Nevada Bureau of Mines and Geology Bulletin 99A, 172 p.

Knochenmus, L.A., 2007, Hydrology of Snake Valley, *in* Coache, R., ed., Regional tour of the carbonate system guidebook: Nevada Water Resources Association, Clark County, Nevada, June 18-20, 2007, p. 53–54.

Knochenmus, L.A., Laczniak, R.J., Moreo, M.T., Sweetkind, D.S., Wilson, J.W., Thomas, J.M., Justet, L., Hershey, R.L., Earman, S., Lyles, B.F., and Lundmark, K.W., 2007, Potentiometric surface of the carbonate-rock aquifer, White Pine County, Nevada, and adjacent areas in Nevada and Utah, *in* Welch, A.H., Bright, D.J., and Knochenmus, L.A., eds., Water resources of the Basin and Range carbonate-rock aquifer system, White Pine County, Nevada, and adjacent areas in Nevada and Utah: U.S. Geological Survey Scientific Investigations Report 2007-5261, 96 p.

Laczniak, R.J., Cole, J.C., Sawyer, D.A., and Trudeau, D.A., 1996, Summary of hydrogeologic controls on ground-water flow at the Nevada Test Site, Nye County, Nevada: U.S. Geological Survey Water-Resources Investigations Report 96–4109, 59 p.

Langenheim, V.E., Beard, L.S., and Faulds, J.E., 2010, Implications of geophysical analysis on basin geometry and fault offsets in the northern Colorado River extensional corridor and adjoining Lake Mead region, Nevada and Arizona, *in* Umhoefer, P.J., Beard, L.S., and Lamb, M.A., eds., Miocene tectonics of the Lake Mead region, central Basin and Range: Geological Society of America Special Paper 463, p. 39–59.

Langenheim, V.E., Miller, J.J., Page, W.R., and Grow, J.A., 2001, Thickness and geometry of Cenozoic deposits in California Wash area, Nevada, based on gravity and seismic-reflection data: U.S. Geological Survey Open-File Report 01-393, 26 p.

Larson, E.R., and Langenheim, Jr., R.L., 1979, The Mississippian and Pennsylvanian (Carboniferous) systems in the United States—Nevada: U.S. Geological Survey Professional Paper 1110-BB, p. BB1–BB19.

Las Vegas Valley Water District, 2001, Water resources and ground-water modeling in the White River and Meadow Valley flow systems, Clark, Lincoln, Nye and White Pine counties, Nevada: Las Vegas Valley Water District, Las Vegas, Nevada, 297 p.

Layne Geosciences, 2009, Status report audiomagnetotelluric surveys Spring and Snake valleys, Nevada: Layne Geosciences, Fontana, California, 274 p.

Leahy, P.P., and Lyttle, P.T., 1998, The re-emerging and critical role of geologic understanding in hydrology, *in* Brahana, J.V., Eckstein, Y., Ongley, L.K., Schneider, R., and Moore, J.E., eds., Gambling with groundwater—Physical, chemical, and biological aspects of aquifer-stream relations: Proceedings International Association of Hydrogeologists and the American Institute of Hydrologists, Las Vegas, Nevada, September 28-October 2, 1998: The American Institute of Hydrology, p. 19–24.

Lee, J., Gans, P.B., and Miller, E.L., 1999a, Geologic map of the Mormon Jack Pass quadrangle, Nevada: Nevada Bureau of Mines and Geology Field Studies Map 17, scale 1:24,000.

Lee, J., Gans, P.B., and Miller, E.L., 1999b, Geologic map of the Third Butte East quadrangle, Nevada: Nevada Bureau of Mines and Geology Field Studies Map 16, scale 1:24,000.

Lee, J., Miller, E.L., Gans, P.B., and Huggins, C.C., 1999c, Geologic map of the Mount Moriah quadrangle, Nevada: Nevada Bureau of Mines and Geology Field Studies Map 19, scale 1:24,000.

Link, P.K., Christie-Blick, N., Devlin, W.J., Elston, D.P., Horodyski, R.J., Levy, M., Miller, J.M.G., Pearson, R.C., Prave, A., Stewart, J.H., et al., 1993, Middle and Late Proterozoic stratified rocks of the western U.S. Cordillera, Colorado Plateau, and Basin and Range province, *in* Reed, Jr., J.C., ed., Precambrian: Conterminous U.S.: Geological Society of America, The Geology of North America, Vol. C-2, p. 463–595.

Lipman, P.W., Prostka, H.J., and Christiansen, R.L., 1972, Cenozoic volcanism and plate-tectonic evolution of the western United States. I. Early and middle Cenozoic: Royal Society of London Philosophical Transactions A, Vol. 271, No. 1213, p. 217–248.

Longwell, C.R., Pampeyan, E.H., Bowyer, B., and Roberts, R.J., 1965, Geology and mineral deposits of Clark County, Nevada: Nevada Bureau of Mines and Geology Bulletin 62, 218 p.

Loucks, M.D., Tingey, D.G., Best, M.G., Christiansen, E.H., and Hintze, L.F., 1989, Geologic map of the Fortification Range, Lincoln and White Pine Counties, Nevada: U.S. Geological Survey Miscellaneous Investigations Series Map I-1866, scale 1:50,000.

Lumsden, W.W., Walker, C.T., and Francis, R.D., 2002, The Precambrian and Paleozoic stratigraphy of the White Pine, Grant and Schell Creek Ranges in eastern Nevada—The key to interpreting structures formed by extension and attenuation, *in* Ehni, W., and Faulds, J., eds., Detachment and attenuation in eastern Nevada and its application to petroleum exploration: Nevada Petroleum Society 2002 Field Trip Guidebook, p. 33–72.

Lund, K., Beard, L.S., and Perry, Jr., W.J., 1991, Structures of the northern Grant Range and Railroad Valley, Nye County, Nevada: Implications for oil occurrences, *in* Flanigan, Donna M.H., Mike Hansen and T. Edward Flanigan, (eds.), Geology of White River Valley, the Grant Range, Eastern Railroad Valley and Western Egan Range, Nevada: 1991 Fieldtrip Guidebook, Nevada Petroleum Society Inc., Reno, p. 1–6.

LVVWD, see Las Vegas Valley Water District.

Maldonado, F., and Schmidt, D.L., 1991, Geologic map of the southern Sheep Range, Fossil Ridge, and Castle Rock area, Clark County, Nevada: U.S. Geological Survey Miscellaneous Investigations Series Map I-2086, scale 1:24,000.

Maldonado, F., Spengler, R.W., Hanna, W.F., and Dixon, G.L., 1988, Index of granitic rock masses in the State of Nevada: U.S. Geological Survey Bulletin 1831, 81 p.

Mankinen, E.A., 2007, Gravity and magnetic studies of the Spring Valley region, *in* Coache, R., ed., Regional tour of the carbonate system guidebook: Nevada Water Resources Association, Clark County, Nevada, June 18-20, 2007, p. 37–38.

Mankinen, E.A., and McKee, E.H., 2009, Geophysical setting of western Utah and eastern Nevada between latitudes 37°45' and 40°N, *in* Tripp, B.T., Krahulec, K., and Jordan, J.L., eds., Geology and geologic resources and issues of western Utah: Utah Geological Association Publication 38, p. 271–286.

Mankinen, E.A., and McKee, E.H., 2011, Principle facts for gravity stations collected in 2010 from White Pine and Lincoln Counties, east-central Nevada: U.S. Geological Survey Open-File Report 2011-1084, 24 p.

Mankinen, E.A., Roberts, C.W., McKee, E.H., Chuchel, B.A., and Moring, B.C., 2006, Geophysical Data from the Spring and Snake valleys area, Nevada and Utah: U.S. Geological Survey Open-File Report 2006–1160, 36 p.

Mankinen, E.A., Roberts, C.W., McKee, E.H., Chuchel, B.A., and Moring, R.L., 2007, Geophysical data from Spring Valley to Delamar Valley, east-central Nevada: U.S. Geological Survey Open-File Report 2007–1190, 42 p.

Mankinen, Edward A., Chuchel, Bruce A., and Moring, Barry C., 2008, Gravity data from Dry Lake and Delamar Valleys, east-central Nevada: U.S. Geological Survey Open-File Report 2008–1299, 30 p. [http://pubs.usgs.gov/of/2008-1299/].

Maxey, G.B., 1964, Hydrostratigraphic units: Journal of Hydrology, Vol. 2, p. 124–129.

McGrew, A.J., 1993, The origin and evolution of the southern Snake Range decollement, east central Nevada: Tectonics, Vol. 12, No. 1, p. 21–34.

McPhee, D.K., 2007, Audiomagnetotelluric imaging of the Spring Valley region, *in* Coache, R., ed., Regional tour of the carbonate system guidebook: Nevada Water Resources Association, Clark County, Nevada, June 18-20, 2007, p. 39–40.

McPhee, D.K., Chuchel, B.A., and Pellerin, L., 2006b, Audiomagnetotelluric data from Spring, Cave, and Coyote Spring valleys, Nevada: U.S. Geological Survey Open-File Report 2006–1164, 43 p.

McPhee, Darcy K., Chuchel, Bruce A., and Pellerin, Louise., 2007, Audiomagnetotelluric data and two- dimensional models from Spring, Snake, and Three Lakes Valleys, Nevada: U.S. Geological Survey Open-File Report 2007–1181, 47 p. [http://pubs.usgs.gov/of/2007/1181/].

McPhee, D.K., Chuchel, B.A., and Pellerin, L., 2008, Audiomagnetotelluric data and preliminary two-dimensional models from Spring, Dry Lake, and Delamar Valleys, Nevada: U.S. Geological Survey Open-File Report 2008-1301, 59 p.

McPhee, D.K., Pari, K., and Baird, F., 2009, Audiomagnetotelluric investigation of Snake Valley, eastern Nevada and western Utah, *in* Tripp, B.T., Krahulec, K., and Jordan, J.L., eds., Geology and geologic resources and issues of western Utah: Utah Geological Association Publication 38, p. 287–298.

McPhee, D.K., Pellerin, L., Chuchel, B.A., and Dixon, G.L., (2005), Resistivity imaging of Spring Valley, Nevada, using the audiomagnetotelluric method, EOS. Trans. AGU, 86(18), Joint Assembly Supplement, Abstract NS23B-06.

McPhee, D.K., Pellerin, L., Chuchel, B.A., Tilden, J.E., and Dixon, G.L., 2006a, Resistivity imaging in eastern Nevada using the audiomagnetotelluric method for hydrogeologic framework studies, *in* Proceedings of the 19th Annual Symposium on the Application of Geophysics to Engineering and Environmental Problems (SAGEEP), Seattle, Washington, April 2–6, 2006, p. 712–718.

Mifflin, M.D., and Wheat, M.M., 1979, Pluvial lakes and estimated pluvial climates of Nevada: Nevada Bureau of Mines and Geology Bulletin 94, 57 p.

Miller, E.L., and Gans, P.B., 1999, Geologic map of The Cove quadrangle, Nevada and Utah: Nevada Bureau of Mines and Geology Field Studies Map 22, scale 1:24,000.

Miller, E.L., Gans, P.B., and Garing, J., 1983, The Snake Range décollement: An exhumed mid-Tertiary ductile-brittle transition: Tectonics, Vol. 2, No. 3, p. 239–263.

Miller, E.L., Dumitru, T.A., Brown, R.W., and Gans, P.B., 1999, Rapid Miocene slip on the Snake Range—Deep Creek Range fault system, east-central Nevada: Geological Society of America Bulletin, Vol. 111, No. 6, p. 886–905.

Miller, E.L., Gans, P.B., and Grier, S.P., 1994, Geologic map of Windy Peak 7.5' quadrangle, White Pine County, Nevada: U.S. Geological Survey Open-File Report 94–687, scale 1:24,000.

Miller, E.L., Grier, S.P., and Brown, J.L., 1995, Geologic map of the Lehman Caves quadrangle, White Pine County, Nevada: U.S. Geological Survey Geologic Quadrangle Map GQ-1758, scale 1:24,000.

Minor, S.A., and Hudson, M.R., 2006, Regional survey of structural properties and cementation patterns of fault zones in the northern part of the Albuquerque Basin, New Mexico—Implications for ground-water flow: U.S. Geological Survey Professional Paper 1719, 28 p.

Misch, P., 1960, Regional structural reconnaissance in central-northeast Nevada and some adjacent areas—Observations and interpretations, *in* Boettcher, J.W., and Sloan, Jr., W.W., eds., Guidebook to the geology of east central Nevada: Intermountain Association of Petroleum Geologists and Eastern Nevada Geological Society, 11th Annual Field Conference, Salt Lake City, Utah, September 8–10, 1960, p. 17–42.

Moores, E.M., Scott, R.B., and Lumsden, W.W., 1968, Tertiary tectonics of White Pine-Grant Range region, east-central Nevada, and some regional implications: Geological Society of America Bulletin, Vol. 79, No. 12, p. 1703–1726.

Morris, H.T., 1987, Preliminary geologic map of the Delta 2° quadrangle, Tooele, Juab, Millard, and Utah Counties, Utah: U.S. Geological Survey Open-File Report 87–185, scale 1:250,000, 3 sheets.

Myers, T., 2006a, Hydrogeology of Spring Valley and effects of groundwater development proposed by the Southern Nevada Water Authority, White Pine and Lincoln County, Nevada: Western Environmental Law Center Reno, Nevada, 84 p.

Myers, T., 2006b, Review of evidence provided by the Southern Nevada Water Authority and minor modification to groundwater model, White Pine and Lincoln County, Nevada: Western Environmental Law Center Reno, Nevada, 32 p.

Myers, T., 2007a, Review of the baseline characterization report for Clark, Lincoln, and White Pine Counties Groundwater Development Project as prepared by the Southern Nevada Water Authority: Western Environmental Law Center Reno, Nevada, 14 p.

Myers, T., 2007b, Hydrogeology of Cave, Dry Lake and Delamar valleys and effects of groundwater development proposed by the Southern Nevada Water Authority, White Pine and Lincoln County, Nevada: Western Environmental Law Center Reno, Nevada, 102 p.

Myers, T., 2007c, Review and rebuttal of SNWA submissions in support of applications for groundwater from Cave, Dry Lake and Delamar valley [sic]: For submission to the Nevada State Engineer for the Cave Valley, Dry Lake, and Delamar Valleys Hearings: Western Environmental Law Center Reno, Nevada, 24 p.

Nelson, R.B., 1966, Structural development of northernmost Snake Range, Kern Mountains, and Deep Creek Range, Nevada and Utah: American Association of Petroleum Geologists Bulletin, Vol. 50, No. 5, p. 921–951.

Nichols, W.D., 2000, Regional ground-water evapotranspiration and ground-water budgets, Great Basin, Nevada: U.S. Geological Survey Professional Paper 1628, 101 p.

Nolan, T.B., 1935, The Gold Hill mining district, Utah: U.S. Geological Survey Professional Paper 177, 172 p.

Nutt, C.J., 2000, Geologic map of the Alligator Ridge area, including the Buck Mountain East and Mooney Basin Summit quadrangles and parts of the Sunshine Well NE and Long Valley Slough quadrangles, White Pine County, Nevada: U.S. Geological Survey Geologic Investigations Series Map I-2691, scale 1:24,000.

Nutt, C.J., Zimbelman, D.R., Campbell, D.L., Duval, J.S., and Hannigan, B.J., 1990, Chapter C: Mineral resources of the Deep Creek Mountains wilderness study area, Juab and Tooele counties, Utah: U.S. Geological Survey Bulletin 1745-C, 40 p.

Oliveira, M.E., 1975, Geology of the Fish Springs mining district, Fish Springs Range, Utah: Brigham Young University Geology Studies, Vol. 22, Pt. 1, p. 69-104.

Otto, B.R., 2008, Geologic map of the central Butte Range, White Pine County, Nevada: Nevada Bureau of Mines and Geology Map 160, scale 1:48,000.

Oviatt, C.G., 1991, Quaternary geology of Fish Springs Flat, Juab County, Utah: Utah Geological Survey Special Study 77, 16 p.

Page, W.R., 1998, Geologic map of the Arrow Canyon NW quadrangle, Clark County, Nevada: U.S. Geological Survey Geologic Quadrangle Map GQ-1776, scale 1:24,000.

Page, W.R., and Dixon, G.L., 1992, Northern terminus of Mesozoic Dry Lake thrust fault, Arrow Canyon Range, southeastern Nevada [abs]: Geological Society of America Abstracts with Programs, Vol. 24, No. 6, p. 56.

Page, W.R., and Ekren, E.B., 1995, Preliminary geologic map of the Bristol Well quadrangle, Lincoln County, Nevada: U.S. Geological Survey Open-File Report 95–580, scale 1:24,000.

Page, W.R., and Pampeyan, E.H., 1996, Preliminary geologic map of the Paleozoic rocks in the Wildcat Wash SE and Wildcat Wash SW quadrangles, Lincoln and Clark Counties, Nevada: U.S. Geological Survey Open-File Report 96–26, scale 1:24,000, 2 sheets.

Page, W.R., Dixon, G.L., Rowley, P.D., and Brickey, D.W., 2005a, Geologic map of parts of the Colorado, White River, and Death Valley groundwater flow systems, Nevada, Utah, and Arizona: Nevada Bureau of Mines and Geology Map 150, scale 1:250,000.

Page, W.R., Lundstrom, S.C., Harris, A.G., Langenheim, V.E., Workman, J.B., Mahan, S.A., Paces, J.B., Dixon, G.L., Rowley, P.D., Burchfiel, B.C., Bell, J.W., and Smith, E.I., 2005b, Geologic and geophysical maps of the Las Vegas 30' × 60' quadrangle, Clark and Nye Counties, Nevada, and Inyo County, California: U.S. Geological Survey Scientific Investigations Map 2814, scale 1:100,000, 2 sheets.

Page, W.R., Scheirer, D.S., and Langenheim, V.E., 2006, Geologic cross sections of parts of the Colorado, White River, and Death Valley regional ground-water flow systems, Nevada, Utah, and Arizona: U.S. Geological Survey Open-File Report 2006–1040, Denver, CO, 80225.

Palacky, G.J., 1987, Resistivity characteristics of geologic targets, *in* Nabighian, M.N., ed., Electromagnetic methods in applied geophysics: Volume 1, Theory: Society of Exploration Geophysicists, Tulsa, Oklahoma, Investigations in Geophysics No. 3, p. 53-129.

Pampeyan, E.H., 1993, Geologic map of the Meadow Valley Mountains, Lincoln and Clark Counties, Nevada: U.S. Geological Survey Miscellaneous Investigations Series Map I-2173, scale 1:50,000, 2 sheets.

Pari, K.T., and Baird, F.A., 2011, Audiomagnetotellurics investigations in selected basins in White Pine and Lincoln Counties, East-Central Nevada: Southern Nevada Water Authority, Las Vegas, Nevada, Doc. No. RDS-ED-0022, 81 p.

Phelps, G.A., Jewel, E.B., Langenheim, V.E., and Jachens, R.C., 2000, Principal facts for gravity stations in the vicinity of Coyote Spring Valley, Nevada, with initial gravity modeling results: U.S. Geological Survey Open-File Report 00–420, 22 p.

Plume, R.W., and Carlton, S.M., 1988, Hydrogeology of the Great Basin region of Nevada, Utah, and adjacent states: U.S. Geological Survey Hydrologic Investigations Atlas HA-694-A, scale 1:1,000,000.

Ponce, D.A., 1992, Complete Bouguer gravity map of Nevada, Ely sheet: Nevada Bureau of Mines and Geology Map 99, scale 1:250,000.

Ponce, D.A., 1997, Gravity data of Nevada: U.S. Geological Survey Digital Data Series DDS-42, 27 p., CD-ROM.

Ponce, D.A., Morin, R.L., and Robbins, S.L., 1996, Bouguer gravity map of Nevada, Elko sheet: Nevada Bureau of Mines and Geology Map 107, scale 1:250,000.

Poole, F.G., and Sandberg, C.A., 1977, Mississippian paleogeography and tectonics of the western United States, *in* Stewart, J.H., Stevens, C.H., and Fritsche, A.E., eds., Paleozoic paleogeography of the western United States: Society of Economic Paleontologists and Mineralogists, Pacific Section, Pacific Coast Paleogeography Symposium 1, April 22, 1977, p. 67–85.

Poole, F.G., and Sandberg, C.A., 1991, Mississippian paleogeography and conodont biostratigraphy of the western United States, *in* Cooper, J.D., and Stevens, C.H., eds., Paleozoic paleogeography of the western United States—II: Society of Economic Paleontologists and Mineralogists, Pacific Section, Pacific Coast Paleogeography, p. 107–136.

Prudic, D.E., 2006, Response to memorandum by Rowley and Dixon regarding U.S. Geological Survey report titled “Characterization of surface-water resources in the Great Basin National Park area and their susceptibility to ground-water withdrawals in adjacent valleys, White Pine County, Nevada”: U.S. Geological Survey Open-File Report 2006-1342, 15 p.

Prudic, D.E., 2007, Hydrology of Great Basin National Park, *in* Coache, R., ed., Regional tour of the carbonate system guidebook: Nevada Water Resources Association, Clark County, Nevada, June 18-20, 2007, p. 49–50.

Prudic, D.E., and Glancy, P.A., 2009, Geochemical investigation of source water to Cave Springs, Great Basin National Park, White Pine County, Nevada: U.S. Geological Survey Scientific Investigations Report 2009-5073, 28 p.

Puchlik, K., 2009, The crypto zinc-indium-copper-molybdenum skarn deposit, western Juab County, Utah: Utah Geological Association Newsletter, Vol. 41, No. 6, p. 1-2.

Raines, G.L., Connors, K.A., Moyer, L.A., and Miller, R.J., 2003, Spatial digital database for the geologic map of Nevada. Digital database, Version 3.0: U.S. Geological Survey Open-File Report 03–66.

Roberts, R.J., Montgomery, K.M., and Lehner, R.E., 1967, Geology and mineral resources of Eureka County, Nevada: Nevada Bureau of Mines and Geology Bulletin 64, 152 p., scale 1:250,000, 12 sheets.

Robinson, J.P., 1993, Provisional geologic map of the Gold Hill quadrangle, Tooele County, Utah: Utah Geological Survey Map 140, scale 1:24,000, 3 sheets.

Rodgers, D.W., 1987, Thermal and structural evolution of the southern Deep Creek Range, west central Utah and east central Nevada [Ph.D. dissertation]: Stanford University, California, 149 p.

Rowley, P.D., 1998, Cenozoic transverse zones and igneous belts in the Great Basin, western United States: Their tectonic and economic implications, *in* Faulds, J.E., and Stewart, J.H., eds., Accommodation zones and transfer zones: The regional segmentation of the Basin and Range province: Geological Society of America Special Paper 323, p. 195–228.

Rowley, P.D., 2002, Water resources technical report: Hydrogeological assessment of the Gunlock part of the Navajo/Kayenta aquifer and its bearing on the Gunlock well field, Washington County, Utah, *in* Bureau of Land Management and Bureau of Indian Affairs, Environmental assessment for the Santa Clara pipeline, UT 045-98-02, p. D-1–D-32.

Rowley, P.D., and Anderson, R.E., 1996, The syntectonic caldera: A new caldera type bounded by synchronous linear faults [abs.]: Geological Society of America Abstracts with Programs, Vol. 28, No. 7, p. A-449.

Rowley, P.D., and Dixon, G.L., 2001, The Cenozoic evolution of the Great Basin area, U.S.A.—New interpretations based on regional geologic mapping, *in* Erskine, M.C., Faulds, J.E., Bartley, J.M., and Rowley, P.D., eds., The geologic transition, High Plateaus to Great Basin—A symposium and field guide: The Mackin Volume: Utah Geological Association Publication 30 and American Association of Petroleum Geologists Publication GB78, September, 20–22, 2001, p. 169–188.

Rowley, P.D., and Dixon, G.L., 2004, The role of geology in increasing Utah's ground-water resources from faulted terranes–Lessons from the Navajo Sandstone, Utah, and the Death Valley flow system, Nevada-California, *in* Spangler, L.E., ed., Ground water in Utah—Resource, protection, and remediation—Field Symposium: Utah Geological Association, Salt Lake City, Utah, September 24–25, 2004, Publication 31, p. 27–41.

Rowley, P.D., and Dixon, G.L., 2010, Geology and hydrogeology of Anderson Junction Reservoir, Anderson Junction well field, and Cottam well field, Washington County, Utah: Washington County Water Conservancy District, St. George, Utah, WCWCD-03, 22 p., scale 1:500.

Rowley, P.D., and Shroba, R.R., 1991, Geologic map of the Indian Cove quadrangle, Lincoln County, Nevada: U.S. Geological Survey Geologic Quadrangle Map GQ-1701, scale 1:24,000.

Rowley, P.D., Dixon, G.L., Burns, A.G., and Collins, C.A., 2009, Geology and hydrogeology of the Snake Valley area, western Utah and eastern Nevada, *in* Tripp, B.T., Krahulec, K., and Jordan, J.L., eds., Geology and geologic resources and issues of western Utah: Utah Geological Association Publication 38, p. 251–269.

Rowley, P.D., Dixon, G.L., D'Agnese, F.A., O'Brien, G.M., and Brickey, D.W., 2004, Geology and hydrology of the Sand Hollow reservoir and well field area, Washington County, Utah: Washington County Water Conservancy District Report WCWCD-01, 14 p.

Rowley, P.D., Hacker, D.B., Maxwell, D.J., Maxwell, J.D., and Boswell, J.T., 2008, Interim geologic map of the Utah part of the Deer Lodge Canyon, Prohibition Flat, Uvada, and Pine Park quadrangles (east part of the Caliente 30' × 60' quadrangle), Iron and Washington Counties, Utah: Utah Geological Survey Open-File Report 530, scale 1:24,000.

Rowley, P.D., Lipman, P.W., Mehnert, H.H., Lindsey, D.A., and Anderson, J.J., 1978, Blue Ribbon lineament, an east-trending structural zone within the Pioche mineral belt of southwestern Utah and eastern Nevada: U.S. Geological Survey Journal of Research, Vol. 6, No. 2, p. 175–192.

Rowley, P.D., Nealey, L.D., Unruh, D.M., Snee, L.W., Mehnert, H.H., Anderson, R.E., and Grommé, C.S., 1995, Stratigraphy of Miocene ash-flow tuffs in and near the Caliente caldera complex, southeastern Nevada and southwestern Utah, *in* Scott, R.B., and Swadley, W.C., eds., Geologic studies in the Basin and Range–Colorado Plateau transition in southeastern Nevada, southwestern Utah, and northwestern Arizona, 1992: U.S. Geological Survey Bulletin 2056, p. 43–88.

Rowley, P.D., Shroba, R.R., Simonds, F.W., Burke, K.J., Axen, G.J., and Olmore, S.D., 1994, Geologic map of the Chief Mountain quadrangle, Lincoln County, Nevada: U.S. Geological Survey Geologic Quadrangle Map GQ-1731, scale 1:24,000.

Rowley, P.D., Snee, L.W., Anderson, R.E., Nealey, L.D., Unruh, D.M., and Ferris, D.E., 2001, Field trip to the Caliente caldera complex, east-striking transverse zones, and nearby mining districts in Nevada-Utah—Implications for petroleum, ground-water, and mineral resources, *in* Erskine, M.C., Faulds, J.E., Bartley, J.M., and Rowley, P.D., eds., The geologic transition, High Plateaus to Great Basin-A symposium and field guide: The Mackin Volume: Utah Geological Association Publication 30 and American Association of Petroleum Geologists Publication GB78, September 20–22, 2001, p. 401–418.

Rowley, P.D., Williams, V.S., Vice, G.S., Maxwell, D.J., Hacker, D.B., Snee, L.W., and Mackin, J.H., 2006, Interim geologic map of the Cedar City 30' × 60' quadrangle, Iron and Washington Counties, Utah: Utah Geological Survey Open-File Report 476DM, scale 1:100,000.

Rush, F.E., and Kazmi, S.A.T., 1965, Water resources appraisal of Spring Valley, White Pine and Lincoln Counties, Nevada: Nevada Department of Conservation and Natural Resources Ground-Water Resources–Reconnaissance Series Report 33, 36 p.

Sack, D., 1990, Quaternary geologic map of Tule Valley, west-central Utah: Utah Geological and Mineral Survey Map 124, scale 1:100,000.

Saltus, R.W., 1988a, Bouguer gravity anomaly map of Nevada: Nevada Bureau of Mines and Geology Map 94A, scale 1:750,000.

Saltus, R.W., 1988b, Regional, residual, and derivative gravity maps of Nevada: Nevada Bureau of Mines and Geology Map 94B, scale 1:000,000, 4 sheets.

Saltus, R.W., and Jachens, R.C., 1995, Gravity and basin-depth maps of the Basin and Range province, western United States: U.S. Geological Survey Geophysical Investigations Map GP-1012, scale 1:2,500,000.

Sandberg, C.A., Morrow, J.R., and Warme, J.E., 1997, Late Devonian Alamo impact event, global Kellwasser Events, and major eustatic events, eastern Great Basin, Nevada and Utah: Brigham Young University Geology Studies, Vol. 42, Pt. 1, p. 129–160.

Saucier, A.E., 1997, The Antler Thrust System in Northern Nevada, *in* Perry, A.J., and Abbott, E.W., eds., The Roberts Mountains Thrust, Elko and Eureka Counties, Nevada: Nevada Petroleum Society, 1997 Field Trip Guidebook, Reno, Nevada, p. 1–16.

Schalla, R.A., 1998, History of recent exploration activity in Snake Valley, *in* French, Don E., and Schalla, Robert A., (eds.), Hydrocarbon habitat and special geologic problems of the Great Basin: 1998 Field Trip Guidebook, Nevada Petroleum Society p. 84-85.

Schalla, R.A., and E.H. Johnson, (eds.), 1994, Oil fields of the Great Basin: Nevada Petroleum Society, Reno, Nevada, 380 p.

Scheirer, D.S., 2005, Gravity studies of Cave, Dry Lake, and Delamar valleys, east-central Nevada: U.S. Geological Survey Open-File Report 2005–1339, 27 p.

Scheirer, D.S., and Andreasen, A.D., 2008, Results of gravity fieldwork conducted in March 2008 in the Moapa Valley region of Clark County, Nevada: U.S. Geological Survey Open-File Report 2008-1300, 35 p. [http://pubs.usgs.gov/of/2008/1300/].

Scheirer, D.S., Page, W.R., and Miller, J.J., 2006, Geophysical studies based on gravity and seismic data of Tule Desert, Meadow Valley Wash, and California Wash basins, southern Nevada: U.S. Geological Survey Open-File Report 2006-1396, 42 p.

Schellart, W.P., Stegman, D.R., Farrington, R.J., Freeman, J., and Moresi, L., 2010, Cenozoic tectonics of western North America controlled by evolving width of Farallon slab: Science, Vol. 329, No. 5989, p. 316–319.

Schmidt, D.L., 1994, Preliminary geologic map of the Farrier quadrangle, Clark and Lincoln Counties, Nevada: U.S. Geological Survey Open-File Report 94–625, scale 1:24,000.

Schmidt, D.L. and Dixon, G.L., 1995, Geology and aquifer system of the Coyote Spring Valley area, southeastern Nevada: U.S. Geological Survey Open-File Report 95–579, 47 p.

Schmidt, D.L., Page, W.R., and Workman, J.B., 1996, Preliminary geologic map of the Moapa West quadrangle, Clark County, Nevada: U.S. Geological Survey Open-File Report 96–521, scale 1:24,000.

Scott, R.B., and Swadley, W.C., 1992, Preliminary geologic map of the Pahroc Summit Pass quadrangle and part of the Hiko SE quadrangle, Lincoln County, Nevada: U.S. Geological Survey Open-File Report 92–613, scale 1:24,000.

Scott, R.B., and Swadley, W.C., eds., 1995, Geologic studies in the Basin and Range–Colorado Plateau transition in southeastern Nevada, southwestern Utah, and northwestern Arizona, 1992: U.S. Geological Survey Bulletin 2056, 275 p.

Scott, R.B., Grommé, C.S., Best, M.G., Rosenbaum, J.G., and Hudson, M.R., 1995, Stratigraphic relationships of Tertiary volcanic rocks in central Lincoln County, southeastern Nevada, *in* Scott, R.B., and Swadley, W.C., eds., Geologic studies in the Basin and Range–Colorado Plateau transition in southeastern Nevada, southwestern Utah, and northwestern Arizona, 1992: U.S. Geological Survey Bulletin 2056, p. 7–41.

Scott, R.B., Rowley, P.D., Snee, L.W., Anderson, R.E., Harding, A.E., Unruh, D.M., Nealey, L.D., Hudson, M.R., Swadley, WC, and Ferris, D.E., 1996, Synchronous Oligocene and Miocene extension and magmatism in the vicinity of caldera complexes in southeastern Nevada: Colorado Geological Survey Open-File Report 96-4, 36 p.

Scott, R.B., Swadley, WC, and Novak, S.W., 1993, Geologic map of the Delamar Lake quadrangle, Lincoln County, Nevada: U.S. Geological Survey Geologic Quadrangle Map GQ-1730, scale 1:24,000.

Seaber, P.R., 1992, Draft of proposed addition to the 1983 North American code of stratigraphic nomenclature *in* Donovan, D.J., 1996, Hydrostratigraphy and allostratigraphy of the Cenozoic alluvium in the northwestern part of Las Vegas Valley, Clark County, Nevada [M.S. thesis]: University of Nevada, Las Vegas, p. 186-191.

Shipton, Z.K., and Cowie, P.A., 2001, Damage zone and slip-surface evolution over µm to km scales in high-porosity Navajo sandstone, Utah: Journal of Structural Geology, Vol. 23, Issue 12, p. 1825–1844.

Sibson, R.H., 1996, Structural permeability of fluid-driven fault-fracture meshes: Journal of Structural Geology, Vol. 18, Issue 8, p. 1031–1042.

Sibson, R.H., 2000, A brittle failure mode plot defining conditions for high-flux flow: Economic Geology, Vol. 95, No. 1, p. 41–48.

Smith, D.L., Gans, P.B., and Miller, E.L., 1991, Palinspastic restoration of Cenozoic extension in the central and eastern Basin and Range province at latitude 39-40^{o} N, *in* Raines, G.L., Lisle, R.E., Schafer, R.W., and Wilkinson, W.H., eds., Geology and ore deposits of the Great Basin, Geological Society of Nevada, Symposium Proceedings, April 1–5, 1990, Vol. 1, p. 75–86.

Snee, L.W., and Rowley, P.D., 2000, New ^{40}Ar/^{39}Ar dates from the Caliente caldera complex, Nevada-Utah—At least 10 million years of Tertiary volcanism in one of the World's largest caldera complexes: Geological Society of America Abstracts with Programs, Vol. 32, No. 7, p. A–461.

SNWA, see Southern Nevada Water Authority.

Snyder, D.B., Healey, D.L., and Saltus, R.W., 1984, Complete Bouguer gravity map of Nevada: Lund sheet: Nevada Bureau of Mines and Geology Map 80, scale 1:250,000.

Snyder, D.B., Wahl, R.R., and Currey, F.E., 1981, Bouguer gravity map of Nevada: Caliente sheet: Nevada Bureau of Mines and Geology Map 70, scale 1:250,000.

Southern Nevada Water Authority, 2008, Baseline characterization report for Clark, Lincoln, and White Pine Counties Groundwater Development Project: Southern Nevada Water Authority, Las Vegas, Nevada, 1146 p.

Southern Nevada Water Authority, 2011, Southern Nevada Water Authority Clark, Lincoln, and White Pine Counties Groundwater Development Project Conceptual Plan of Development: Southern Nevada Water Authority, Las Vegas, Nevada, 152 p.

Stephens, J.C., 1977, Hydrologic reconnaissance of the Tule Valley drainage basin, Juab and Millard counties, Utah: Utah Department of Natural Resources Technical Publication No. 56, 37 p.

Steven, T.A., Morris, H.T., and Rowley, P.D., 1990, Geologic map of the Richfield 1° × 2° quadrangle, west-central Utah: U.S. Geological Survey Miscellaneous Investigations Series Map I-1901, scale 1:250,000.

Stewart, J.H., 1970, Upper Precambrian and Lower Cambrian strata in the southern Great Basin, California and Nevada: U.S. Geological Survey Professional Paper 620, 206 p.

Stewart, J.H., 1974, Correlation of uppermost Precambrian and lower Cambrian strata from southern to east-central Nevada: U.S. Geological Survey Journal of Research, Vol. 2, p. 609–618.

Stewart, J.H., 1976, Late Precambrian evolution of North America: Plate tectonics implication: Geology, Vol. 4, p. 11–15.

Stewart, J.H., 1980, Geology of Nevada: A discussion to accompany the *geologic map of Nevada*: Nevada Bureau of Mines and Geology Special Publication 4, 136 p.

Stewart, J.H., 1984, Stratigraphic sections of lower Cambrian and upper Proterozoic rocks in Nye, Lander, and Lincoln Counties, Nevada, and Sonora, Mexico: U.S. Geological Survey Open-File Report 84–691, 53 p.

Stewart, J.H., and Carlson, J.E., 1976, Cenozoic rocks of Nevada—Four maps and brief description of distribution, lithology, age, and centers of volcanism: Nevada Bureau of Mines and Geology Map 52, scale 1:1,000,000, 4 sheets.

Stewart, J.H., and Carlson, J.E., 1978, Geologic map of Nevada: U.S. Geological Survey, scale 1:500,000.

Stewart, J.H., Moore, W.J., and Zietz, I., 1977, East-west patterns of Cenozoic igneous rocks, aeromagnetic anomalies, and mineral deposits, Nevada and Utah: Geological Society of America Bulletin, Vol. 88, p. 67–77.

Stewart, J.H., and Poole, F.G., 1974, Lower Paleozoic and uppermost Precambrian Cordilleran miogeocline, Great Basin, western United States, *in* Dickinson, W.R., ed., Tectonics and sedimentation: Society of Economic Paleontologists and Mineralogists Special Publication No. 22, p. 28–57.

Stoeser, D.B., 1993, Tertiary calderas and regional extension of the east-central part of the Tintic-Deep Creek mineral belt, eastern Great Basin, Utah, *in* Scott, Jr., R.W., Detra, P.S., and Berger, B.R., eds., Advances related to United States and International Mineral Resources: Developing frameworks and exploration technologies: U.S. Geological Survey Bulletin 2039, p. 5-23.

Swadley, WC, 1995, Maps showing modern fissures and quaternary faults in the Dry Lake Valley area, Lincoln County, Nevada: U.S. Geological Survey Miscellaneous Investigations Series Map I-2501, scale 1:50,000.

Swadley, W.C., Page, W.R., Scott, R.B., and Pampeyan, E.H., 1994, Geologic map of the Delamar 3 SE quadrangle, Lincoln County, Nevada: U.S. Geological Survey Geologic Quadrangle Map GQ-1754, scale 1:24,000.

Swadley, W.C., and Rowley, P.D., 1994, Geologic map of the Pahroc Spring SE quadrangle, Lincoln County, Nevada: U.S. Geological Survey Geologic Quadrangle Map GQ-1752, scale 1:24,000.

Sweetkind, D.S., 2007b, Geology of Great Basin National Park, *in* Coache, R., ed., Regional tour of the carbonate system guidebook: Nevada Water Resources Association, Clark County, Nevada, June 18-20, 2007, p. 47–48.

Sweetkind, D.S., 2007a, Geology of Snake Range, *in* Coache, R., ed., Regional tour of the carbonate system guidebook: Nevada Water Resources Association, Clark County, Nevada, June 18-20, 2007, p. 43–44.

Sweetkind, D.S., and duBray, E.A., 2008, Compilation of stratigraphic thicknesses for caldera-related tertiary volcanic rocks, east-central Nevada and west-central Utah: U.S. Geological Survey Data Series 271, 40 p.

Sweetkind, D.S., Knochenmus, L.A., Ponce, D.A., Wallace, A.R., Scheirer, D.S., Watt, J.T., and Plume, R.W., 2007b, Hydrogeologic framework, *in* Welch, A.H., Bright, D.J., and Knochenmus, L.A., eds., Water resources of the Basin and Range carbonate-rock aquifer system, White Pine County, Nevada, and adjacent areas in Nevada and Utah: U.S. Geological Survey Scientific Investigations Report 2007–5261, p. 11–36.

Sweetkind, D.S., Knochenmus, L.A., Ponce, D.A., Wallace, A.R., Scheirer, D.S., Watt, J.T., and Plume, R.W., 2007a, Hydrogeologic map and cross sections, White Pine County, Nevada, and adjacent areas in Nevada and Utah, *in* Welch, A.H., Bright, D.J., and Knochenmus, L.A., eds., Water resources of the Basin and Range carbonate-rock aquifer system, White Pine County, Nevada, and adjacent areas in Nevada and Utah: U.S. Geological Survey Scientific Investigations Report 2007–5261, Plate 1, scale 1:500,000.

Taylor, M.E., Poole, F.G., and Cook, H.E., 1991, Summary of Paleozoic stratigraphy in the southern Egan and Schell Creek ranges, east-central Nevada, *in* Flanigan, Donna M.H., Mike Hansen and T. Edward Flanigan, (eds.), Geology of White River Valley, the Grant Range, Eastern Railroad Valley and Western Egan Range, Nevada: 1991 Fieldtrip Guidebook, Nevada Petroleum Society Inc., Reno, p. 29–35.

Taylor, W.J., Bartley, J.M., Martin, M.W., Geissman, J.W., Walker, J.D., Armstrong, P.A., and Fryxell, J.E., 2000, Relations between hinterland and foreland shortening: Sevier orogeny, central North American Cordillera: Tectonics, Vol. 19, No. 6, p. 1124–1143.

Taylor, W.J., Dobbs, S.W., Nelson, S.L., and Armstrong, P.A., 1994, Generation of four-way closure through multiple tectonic events: Structures of the Timpahute Range, southern Nevada, *in* Dobbs, S.W., and W.J. Taylor, eds., Structural and Stratigraphic Investigations and Petroleum Potential of Nevada, with Special Emphasis South of the Railroad Valley Producing Trend: Nevada Petroleum Society Conference Volume II, p. 141–156.

Telford, W.M., Geldart, L.P., and Sheriff, R.E., 1990, Applied geophysics. Second edition: New York, Cambridge University Press.

Thomas, J.M., and Mihevc, T.M., 2011, Evaluation of groundwater origins, flow paths, and ages in east-central and southeastern Nevada: Desert Research Institute, Reno, Nevada, Publication No. 41253, 61 p.

Thomas, J.M., Calhoun, S.C., and Apambire, W.B., 2001, A deuterium mass-balance interpretation of groundwater sources and flows in southeastern Nevada: Desert Research Institute, Las Vegas, Nevada, Publication No. 41169, 46 p.

Tingley, J.V., Pizarro, K.A., Ross, C. and Pearthree, P.A., 2010, A geologic and natural history tour through Nevada and Arizona along U.S. Highway 93, with GPS coordinates: Nevada Bureau of Mines and Geology Special Publication 35 and Arizona Geological Survey Down-to-Earth 19, 175 p.

Tschanz, C.M., and Pampeyan, E.H., 1970, Geology and mineral deposits of Lincoln County, Nevada: Nevada Bureau of Mines and Geology Bulletin 73, 187 p.

UDOGM, see Utah Division of Oil, Gas, and Mining.

UDWR, see Utah Division of Water Rights.

U.S. Geological Survey, 2008, A study of the connection among basin-fill aquifers, carbonate-rock aquifers, and surface-water resources in southern Snake Valley, Nevada: U.S. Geological Survey Fact Sheet 2008-3071, 2 p.

USGS, see U.S. Geological Survey.

Utah Division of Oil, Gas, and Mining, 2006, Online oil and gas information system, well logs, database [Internet], [accessed March 8, 2006], available from http://utstnrogmsg/3.state.ut.us/UTAHRBDMSWeb/Logs.htm.

Utah Division of Oil, Gas, and Mining, 2008, Online oil and gas information system, well logs database [Internet], [accessed on May 4, 2011], available from http://oilgas.ogm.utah.gov.

Utah Division of Water Rights, 2006, Well drilling database [Internet], [accessed March 8, 2006], available from http://nrwrt1.nr.state.ut.us/cgi/bin/wellview.exe.

Vandervoort, D.S., and Schmitt, J.G., 1990, Cretaceous to early Tertiary paleogeography in the hinterland of the Sevier thrust belt, east-central Nevada: Geology, Vol. 18, p. 567–570.

Van Loenen, R.E., 1987, Geologic map of the Mount Grafton wilderness study area, Lincoln and White Pine counties, Nevada: U.S. Geological Survey Miscellaneous Field Studies Map MF-1938, scale 1:50,000.

Vozoff, K., 1991, The magnetotelluric method, *in* Nabighian, M.N., ed., Electromagnetic methods in applied geophysics: Volume 2, Application Parts A and B: Society of Exploration Geophysicists, Tulsa, Oklahoma, Investigations in Geophysics No. 3, p. 641-711.

Walker, C.D., Anders, M.H., and Christie-Blick, N., 2007, Kinematic evidence for downdip movement on the Mormon Peak detachment: Geology, Vol. 35, No. 3, p. 259–262.

Warme, J.E., Morrow, J.R., and Sandberg, C.A., 2008, Devonian carbonate platform of eastern Nevada: Facies, surfaces, cycles, sequences, reefs, and cataclysmic Alamo impact breccia, *in* Duebendorfer, E.M., and Smith, E.I., eds., Field guide to plutons, volcanoes, faults, reefs, dinosaurs, and possible glaciation in selected areas of Arizona, California, and Nevada: Geological Society of America Field Guides, Vol. 11, p. 215–247.

Webring, M., 1985, SAKI: A Fortran program for generalized linear inversion of gravity and magnetic profiles: U.S. Geological Survey Open-File Report 85–122, 108 p.

Welch, A.H., Bright, D.J., and Knochenmus, L.A., eds., 2007, Water resources of the Basin and Range carbonate-rock aquifer system, White Pine County, Nevada, and adjacent areas in Nevada and Utah: U.S. Geological Survey Scientific Investigations Report 2007–5261, 96 p.

Wernicke, B., Walker, J.D., and Beaufait, M.S., 1985, Structural discordance between Neogene detachments and frontal Sevier thrusts, central Mormon Mountains, southern Nevada: Tectonics, Vol. 4, No. 2, p. 213–246.

Whitebread, D.H., 1969, Geologic map of the Wheeler Peak and Garrison quadrangles, Nevada and Utah: U.S. Geological Survey Miscellaneous Geologic Investigations Map I-578, scale 1:48,000.

SE ROA 43324

JA_13204

Williams, N., and Taylor, W.J., 2002, Extensional oblique-slip barrier transfer fault—The Currant Summit fault, east-central Nevada, *in* Ehni, W. and Faulds, J., eds., Detachment and attenuation in eastern Nevada and its application to petroleum exploration: Nevada Petroleum Society 2002 Field Trip Guidebook, p. 149-163.

Williams, V.S., 1996, Preliminary geologic map of the Mesquite quadrangle, Clark and Lincoln Counties, Nevada, and Mohave County Arizona: U.S. Geological Survey Open-File Report 96–676, scale 1:24,000.

Williams, V.S., 1997, Preliminary geologic map of the Flat Top Mesa quadrangle, Clark and Lincoln Counties, Nevada: U.S. Geological Survey unpublished data, scale 1:24:000.

Williams, V.S., Best, M.G., and Keith, J.D., 1997, Geologic map of the Ursine-Panaca Summit-Deer Lodge area, Lincoln County, Nevada, and Iron County, Utah: U.S. Geological Survey Miscellaneous Investigations Series Map I-2479, scale 1:50,000.

Willis, J.B., Best, M.G., Kowallis, B.J., and Best, V.C., 1987, Preliminary geologic map of the northern Wilson Creek Range, Lincoln County, Nevada: U.S. Geological Survey Miscellaneous Field Studies Map MF-1971, scale 1:50,000.

Winograd, I.J., and Thordarson, W., 1968, Structural control of ground-water movement in miogeosynclinal rocks of south-central Nevada, *in* Eckel, E.B., ed., Nevada Test Site: Geological Society of America Memoir 110, p. 35–48.

Winograd, I.J., and Thordarson, W., 1975, Hydrogeologic and hydrochemical framework, south-central Great Basin, Nevada-California, with special reference to the Nevada Test Site: U.S. Geological Survey Professional Paper 712-C, 126 p.

Workman, J.B., Menges, C.M., Page, W.R., Ekren, E.B., Rowley, P.D., and Dixon, G.L., 2002a, Tectonic map of the Death Valley ground-water model area, Nevada and California: U.S. Geological Survey Miscellaneous Field Studies Map MF-2381-B, 58 p., scale 1:250,000.

Workman, J.B., Menges, C.M., Page, W.R., Taylor, E.M., Ekren, E.B., Rowley, P.D., Dixon, G.L., Thompson, R.A., and Wright, L.A., 2002b, Geologic map of the Death Valley ground-water model area, Nevada and California: U.S. Geological Survey Miscellaneous Field Studies MF-2381-A, 26 p., 1:250,000 scale, 2 sheets.

Wright, J.E., and Snoke, A.W., 1993, Tertiary magmatism and mylonitization in the Ruby-East Humboldt metamorphic core complex, northeastern Nevada: U-Pb geochronology and Sr, Nd, and Pb isotope geochemistry: Geological Society of America Bulletin, Vol. 105, No. 7, p. 935–952.

Zonge, K.L., and Hughes, L.J., 1991, Controlled source audio-frequency magnetotellurics, *in* Nabighian, M.N., ed., Electromagnetic methods in applied geophysics: Volume 2, Application Parts A and B: Society of Exploration Geophysicists, Tulsa, Oklahoma, Investigations in Geophysics, No. 3, p. 713-809.

Map Bibliography

The following geologic maps and reports were used in the compilation of the geologic maps and cross sections. Many of these are not cited in the text of the report.

Abbott, J.T., Best, M.G., and Morris, H.T., 1983, Geologic map of the Pine Grove-Blawn Mountain area, Beaver County, Utah: U.S. Geological Survey Miscellaneous Investigations Series Map I-1479, scale 1:24,000.

Ahlborn, R.C., 1977, Mesozoic-Cenozoic structural development of the Kern Mountains, eastern Nevada-western Utah [M.S. thesis]: Brigham Young University Geology Studies, Vol. 24, Pt. 2, p. 117–131.

Anderson, R.E., 2003, Geologic map of the Callville Bay quadrangle, Clark County, Nevada and Mohave County, Arizona: Nevada Bureau of Mines and Geology Map 139, scale 1:24,000.

Anderson, R.E., and Hintze, L.F., 1993, Geologic map of the Dodge Spring quadrangle, Washington County, Utah, and Lincoln County, Nevada: U.S. Geological Survey Geologic Quadrangle Map GQ-1721, scale 1:24,000.

Armstrong, P.A., 1991, Displacement and deformation associated with lateral thrust propagation: An example from the Golden Gate Range, southern Nevada [M.S. thesis]: University of Utah, Salt Lake City, 162 p.

Bartley, J.M., Axen, G.J., Taylor, W.J., and Fryxell, J.E., 1988, Cenozoic tectonics of a transect through eastern Nevada near 38°N latitude, *in* Weide, D.L., and Faber, M.L., eds., This extended land—Geological journeys in the southern Basin and Range—Field trip guidebook: Geological Society of America, Cordilleran section meeting, Las Vegas, Nevada, p. 1–20.

Beard, L.S., Campagna, D.J., and Anderson, R.E., 2010, Geometry and kinematics of the eastern Lake Mead fault system in the Virgin Mountains, Nevada and Arizona, *in* Umhoefer, P.J., Beard, L.S., and Lamb, M.A., eds., Miocene tectonics of the Lake Mead region, central Basin and Range: Geological Society of America Special Paper 463, p. 243–274.

Best, M.G., 1987, Geologic map and sections of the area between Hamlin Valley and Escalante Desert, Iron County, Utah: U.S. Geological Survey Miscellaneous Investigations Series Map I-1774, scale 1:50,000.

Best, M.G., Armstrong, R.L., Graustein, W.C., Embree, G.F., and Ahlborn, R.C., 1974, Mica granites of the Kern Mountains pluton, eastern White Pine County, Nevada: Remobilized basement of the Cordilleran miogeosyncline?: Geological Society of America Bulletin, Vol. 85, p. 1277–1286.

Best, M.G., Christiansen, E.H., and Blank, Jr., R.H., 1989, Oligocene caldera complex and calc-alkaline tuffs and lavas of the Indian Peak volcanic field, Nevada and Utah: Geological Society of America Bulletin, Vol. 101, p. 1076–1090.

Best, M.G., Christiansen, E.H., Deino, A.L., Grommé, C.S., McKee, E.H., and Noble, D.C., 1989, Eocene through Miocene volcanism in the Great Basin of the western United States *in* Chapin, C.E., and Zidek, J., eds., Field excursions to volcanic terranes in the western United States, Volume II: Cascades and Intermountain West: New Mexico Bureau of Mines and Mineral Resources Memoir 47, p. 91–133.

Best, M.G., Grant, S.K., Hintze, L.F., Cleary, J.G., Hutsinpiller, A., and Saunders, D.M., 1987, Geologic map of the Indian Peak (southern Needle Range), Beaver and Iron Counties, Utah: U. S. Geological Survey Miscellaneous Investigations Series Map I-1795, scale 1:50,000.

Best, M.G., Hintze, L.F., Deino, A.L., and Maughan, L.L., 1998, Geologic map of the Fairview Range and Grassy Mountain, Lincoln County, Nevada: Nevada Bureau of Mines and Geology Map 114, scale 1:24,000, 2 sheets.

Best, M.G., Hintze, L.F., and Holmes, R.D., 1987, Geologic map of the southern Mountain Home and northern Indian Peak Ranges (central Needle Range), Beaver County, Utah: U.S. Geological Survey Miscellaneous Investigations Series Map I-1796, scale 1:50,000.

Best, M.G., Morris, H.T., Kopf, R.W., and Keith, J.D., 1987, Geologic map of the southern Pine Valley area, Beaver and Iron Counties, Utah: U.S. Geological Survey Miscellaneous Investigations Series Map I-1794, scale 1:50,000.

Best, M.G., Scott, R.B., Rowley, P.D., Swadley, W.C., Anderson, R.E., Grommé, C.S., Harding, A.E., Deino, A.L., Christiansen, E.H., Tingey, D.G., and Sullivan, K.R., 1993, Oligocene-Miocene caldera complexes, ash-flow sheets, and tectonism in the central and southeastern Great Basin, *in* Lahren, M.M., Texler, Jr., J.H., and Spinosa, C., eds., Crustal evolution of the Great Basin and Sierra Nevada—Field trip guidebook: Geological Society of America, Cordilleran and Rocky Mountain sections meeting, p. 285–311.

Best, M.G., Toth, M.I., Kowallis, J.B., Willis, J.B., and Best, V.C., 1989, Geologic map of the northern White Rock Mountains-Hamlin Valley area, Beaver County, Utah, and Lincoln County, Nevada: U.S. Geological Survey Miscellaneous Investigations Series Map I-1881, scale 1:50,000.

Best, M.G., and Williams, V.S., 1997, Geologic map of the Rose Valley quadrangle, Lincoln County, Nevada: U.S. Geological Survey Geologic Quadrangle Map GQ-1765, scale 1:24,000.

Biek, R.F., 2003, Geologic map of the Hurricane quadrangle, Washington County, Utah: Utah Geological Survey Map 187, scale 1:24,000, 2 sheets.

Biek, R.F., Rowley, P.D., Hacker, D.B., Hayden, J.M., Willis, G.C., Hintze, L.F., Anderson, R.E., and Brown, K.D., 2007, Interim geologic map of the St. George 30' × 60' quadrangle and east part of the Clover Mountains 30' × 60' quadrangle, Washington and Iron Counties, Utah: Utah Geological Survey Open-File Report 478, scale 1:100,000, 2 sheets.

Biek, R.F., Rowley, P.D., Hayden, J.M., Hacker, D.B., Willis, G.C., Hintze, L.F., Anderson, R.E., and Brown, K.D., 2009, Geologic map of the St. George and east part of the Clover Mountains 30' × 60' quadrangles, Washington and Iron Counties, Utah: Utah Geological Survey Map 242, 109 p.

Billingsley, G.H., and Workman, J.B., 2000, Geologic map of the Littlefield 30' × 60' quadrangle, Mohave County, northwestern Arizona: U.S. Geological Survey Geologic Investigations Series Map I-2628, scale 1:100,000.

Black, B.D., Hecker, S., Hylland, M.D., Christenson, G.L., and McDonald, G.N., 2003, Quaternary fault and fold database and map of Utah: Utah Geological Survey Map 193DM, scale 1:500,000. (CD-ROM).

Bohannon, R.G., 1983, Geologic map, tectonic map and structure sections of the Muddy and Northern Black Mountains, Clark County, Nevada: U.S. Geological Survey Miscellaneous Investigations Series Map I-1406, scale 1:62,500.

Bohannon, R.G., 1992, Geologic map of the Weiser Ridge quadrangle, Clark County, Nevada: U.S. Geological Survey Geologic Quadrangle Map GQ-1714, scale 1;24,000.

Brokaw, A.L., Bauer, H.L., and Breitrick, R.A., 1973, Geologic map of the Ruth quadrangle, White Pine County, Nevada: U.S. Geological Survey Geologic Quadrangle Map GQ-1085, scale 1:24,000.

Brokaw, A.L., and Barosh, P.J., 1968, Geologic map and sections of the Riepetown quadrangle, White Pine County, Nevada: U.S. Geological Survey Geologic Quadrangle Map GQ-758, scale 1:24,000.

Brokaw, A.L., and Heidrick, T., 1966, Geologic map and sections of the Giroux Wash quadrangle, White Pine County, Nevada: U.S. Geological Survey Geologic Quadrangle Map GQ-476, scale 1:24,000.

Brokaw, A.L., and Shawe, D.R., 1965, Geologic map and sections of the Ely 3 SW quadrangle, White Pine County, Nevada: U.S. Geological Survey Miscellaneous Geological Investigations Map I-449, scale 1:24,000.

Brown, C.L., and Schmitt, J.G., 1991, Horse Camp Formation: Record of Miocene-Pliocene extensional basin development, northern Grant Range, Nevada, *in* Flanigan, Donna M.H., Mike Hansen and T. Edward Flanigan, (eds.), Geology of White River Valley, the Grant Range, Eastern Railroad Valley and Western Egan Range, Nevada: 1991 Fieldtrip Guidebook, Nevada Petroleum Society Inc., Reno, p. 7–13.

Carpenter, J.A., and Carpenter, D.G., 1994, Fold-Thrust Structure, Synorogenic Rocks, and Structural Analysis of the North Muddy and Muddy Mountains, Clark County Nevada, *in* Dobbs, S.W., and W.J. Taylor, eds., Structural and Stratigraphic Investigations and Petroleum Potential of Nevada, with Special Emphasis South of the Railroad Valley Producing Trend: Nevada Petroleum Society Conference Volume II, p. 65–94.

Carpenter, J.A., Carpenter, D.G., and Dobbs, S.W., 1994, Antler Orogeny: Paleostructural Analysis and Constraints on Plate Tectonic Models with a Global Analogue in Southeast Asia, *in* Dobbs, S.W., and W.J. Taylor, eds., Structural and Stratigraphic Investigations and Petroleum Potential of Nevada, with Special Emphasis South of the Railroad Valley Producing Trend: Nevada Petroleum Society Conference Volume II, p. 187–240.

Castor, S.B., Faulds, J.E., Rowland, S.M., and dePolo, C.M., 2000, Geologic map of the Frenchman Mountain quadrangle, Clark County, Nevada: Nevada Bureau of Mines and Geology Map 127, scale 1:24,000.

Coats, R.R., 1987, Geology of Elko County, Nevada: Nevada Bureau of Mines and Geology Bulletin 101, 112 p.

Cook, K.L., Bankey, V., Mabey, D.R., and DePangher, M., 1989, Complete Bouguer gravity anomaly map of Utah: Utah Geological and Mineral Survey Map 122, scale 1:500,000.

Cornwall, H.R., 1972, Geology and mineral deposits of southern Nye County, Nevada: Nevada Bureau of Mines and Geology Bulletin 77, 49 p.

Crafford, A.E.J., 2007, Geologic Map of Nevada: U.S. Geological Survey Data Series 249, 1 CD-ROM, 46 p., 1 plate.

Dixon, G.L., Hedlund, D.C., and Ekren, E.B., 1972, Geologic map of the Pritchards Station quadrangle, Nye County, Nevada: U.S. Geological Survey Miscellaneous Geologic Investigations Map I-728, scale 1:48,000.

Dixon, G.L., and Katzer, T., 2002, Geology and hydrology of the lower Virgin River Valley in Nevada, Arizona, and Utah: Virgin Valley Water District, Mesquite, Nevada, Report VVWD-01, 126 p.

Donovan, D.J., Dixon, G.L., and Rowley, P.D., 2004, Detailed geologic mapping in the Muddy Springs area, Clark County, Nevada [abs.]: Nevada Water Resources Association Annual Conference, Mesquite, Nevada, February 24–26, 2004, p. 23.

duBray, E.A., and Hurtubise, D.O., 1994, Geologic map of the Seaman Range, Lincoln and Nye counties, Nevada: U.S. Geological Survey Miscellaneous Investigations Series Map I-2282, scale 1:50,000.

Duebendorfer, E.M., 2003, Geologic map of the Government Wash quadrangle, Clark County, Nevada: Nevada Bureau of Mines and Geology Map 140, scale 1:24,000.

Ekren, E.B., Anderson, R.E., Rogers, C.L., and Noble, D.C., 1971, Geology of northern Nellis Air Force Base Bombing and Gunnery Range, Nye County, Nevada: U.S. Geological Survey Professional Paper 651, 91 p.

Ekren, E.B., Bath, G.D., Dixon, G.L., Healey, D.L., and Quinlivan, W.D., 1974, Tertiary history of Little Fish Lake Valley, Nye County, Nevada, and implications as to the origin of the Great Basin: U.S. Geological Survey Journal of Research, Vol. 2, No. 1, p. 105–118.

Ekren, E.B., Bucknam, R.C., Carr, W.J., Dixon, G.L., and Quinlivan, W.D., 1976, East-trending structural lineaments in central Nevada: U.S. Geological Survey Professional Paper 986, 16 p.

Ekren, E.B., and Byers, Jr., F.M., 1985, Geologic map of the Gabbs Mountain, Mount Ferguson, Luning, and Sunrise Flat quadrangles, Mineral and Nye Counties, Nevada: U.S. Geological Survey Miscellaneous Investigations Series Map I-1577, scale 1:48,000.

Ekren, E.B., and Byers, Jr., F.M., 1985, Geologic map of the Win Wan Flat, Kinkaid NW, Kinkaid, and Indian Head Peak quadrangles, Mineral County, Nevada: U.S. Geological Survey Miscellaneous Investigations Series Map I-1578, scale 1:48,000.

Ekren, E.B., Hinrichs, E.N., and Dixon, G.L., 1972, Geologic map of The Wall quadrangle, Nye County, Nevada: U.S. Geological Survey Miscellaneous Geologic Investigations Map I-719, scale 1:48,000.

Ekren, E.B., Hinrichs, E.N., Quinlivan, W.D., and Hoover, D.L., 1973, Geologic map of the Moores Station quadrangle, Nye County, Nevada: U.S. Geological Survey Miscellaneous Geologic Investigations Map I-756, scale 1:48,000.

Ekren, E.B., Orkild, P.P., Sargent, K.A., and Dixon, G.L., 1977, Geologic map of Tertiary rocks, Lincoln County, Nevada: U.S. Geological Survey Miscellaneous Investigations Series Map I-1041, scale 1:250,000.

Ekren, E.B., and Page, W.R., 1995, Preliminary geologic map of the Coyote Spring quadrangle, Lincoln County, Nevada: U.S. Geological Survey Open-File Report 95–550, scale 1:24,000.

Ekren, E.B., Quinlivan, W.D., Snyder, R.P., and Kleinhampl, F.J., 1974, Stratigraphy, structure, and geologic history of the Lunar Lake caldera of northern Nye County, Nevada: U.S. Geological Survey Journal of Research, Vol. 2, No. 5, p. 599–608.

Ekren, E.B., Rogers, C.L., and Dixon, G.L., 1973, Geologic and bouguer gravity map of the Reveille quadrangle, Nye County, Nevada: U.S. Geological Survey Miscellaneous Geologic Investigations Map I-806, scale 1:48,000.

Ekren, E.B., Rowley, P.D., Dixon, G.L., Page, W.R., and Brandt, J.M., in press, Geology of the Quinn Canyon Range and vicinity, Nye and Lincoln Counties, Nevada: Southern Nevada Water Authority, Las Vegas, Nevada.

Elliott, P.E., Beck, D.A., and Prudic, D.E., 2006, Characterization of surface-water resources in the Great Basin National Park area and their susceptibility to ground-water withdrawals in adjacent valleys, White Pine County, Nevada: U.S. Geological Survey Scientific Investigations Report 2006-5099, 156 p. Available at URL:http://pubs.water.usgs.gov/sir2006-5099.

Erskine, M.C., 2001, Structural overlap of passive continental margin stratigraphic packages onto the Colorado Plateau cratonic package in southwestern Utah, *in* Erskine, M.C., Faulds, J.E., Bartley, J.M., and Rowley, P.D., eds., The geologic transition, High Plateaus to Great Basin—A symposium and field guide: The Mackin Volume: Utah Geological Association Publication 30, and American Association of Petroleum Geologists Publication GB78, September 20–22, 2001, p. 365–377.

Fouch, T.D., Lund, K., Schmitt, J.G., Good, S.C., and Hanley, J.H., 1991, Late Cretaceous(?) and Paleogene sedimentary rocks and extensional(?) basins in the region of the Egan and Grant ranges, and White River and Railroad valleys, Nevada: Their relation to Sevier and Laramide contractional basins in the southern Rocky Mountains and Colorado Plateau, *in* Flanigan, Donna M.H., Mike Hansen and T. Edward Flanigan, eds., Geology of White River Valley, the Grant Range, Eastern Railroad Valley and Western Egan Range, Nevada: 1991 Fieldtrip Guidebook, Nevada Petroleum Society Inc., p. 15–28.

Gans, P.B., 2000, The northern White Pine Range, *in* Gans, P.B., and Seedorff, E., eds., Geology and ore deposits 2000: The Great Basin and beyond: Geological Society of Nevada, Symposium Proceedings, May 15–18, 2000, p. 83–95.

Gans, P.B., 2000, The Snake Range metamorphic core complex—Geologic overview of the northern Snake Range, *in* Gans, P.B., and Seedorff, E., eds., Geology and ore deposits 2000: The Great Basin and beyond: Geological Society of Nevada, Symposium Proceedings, May 15–18, 2000, p. 99–117.

Gans, P.B., Mahood, G.A., and Schermer, E., 1989, Synextensional magmatism in the Basin and Range province: A case study from the eastern Great Basin: Geological Society of America Special Paper, Vol. 233, 53 p.

Gans, P.B., Miller, E.L., Huggins, C.C., and Lee, J., 1999, Geologic map of the Little Horse Canyon quadrangle, Nevada and Utah: Nevada Bureau of Mines and Geology Field Studies Map 20, scale 1:24,000.

Gans, P.B., Miller, E.L., and Lee, J., 1999, Geologic map of the Spring Mountain quadrangle, Nevada and Utah: Nevada Bureau of Mines and Geology Field Studies Map 18, scale 1:24,000.

Gans, P.B., Miller, E.L., McCarthy, J., and Ouldcott, M.L., 1985, Tertiary extensional faulting and evolving ductile-brittle transition zones in the northern Snake Range and vicinity: New insights from seismic data: Geology, Vol. 13, p. 189–193.

Guth, P.L., 1980, Geology of the Sheep Range, Clark County, Nevada [Ph.D. dissertation]: Massachusetts Institute of Technology, Cambridge, Massachusetts, 189 p.

Harding, A.E., Scott, R.B., Mehnert, H.H., and Snee, L.W., 1995, Evidence of the Kane Springs Wash caldera in the Meadow Valley Mountains, southeastern Nevada, *in* Scott, R.B., and Swadley, W.C., eds., Geologic studies in the Basin and Range–Colorado Plateau transition in southeastern Nevada, southwestern Utah, and northwestern Arizona, 1992: U.S. Geological Survey Bulletin 2056, p. 135–180.

Hauser, E., Potter, C., Hauge, T., Burgess, S., Burtch, S., Mutschler, J., Allmendinger, R., Brown, L., Kaufman, S., and Oliver, J., 1987, Crustal structure of eastern Nevada from COCORP deep seismic reflection data: Geological Society of America Bulletin, Vol. 99, p. 833–844.

Healey, D.L., Snyder, D.B., Wahl, R.R., and Currey, F.E., 1981, Bouguer gravity map of Nevada: Caliente sheet: Nevada Bureau of Mines and Geology Map 70, scale 1:250,000.

Hildenbrand, T.G., and Kucks, R.P., 1988, Filtered magnetic anomaly maps of Nevada: Nevada Bureau of Mines and Geology Map 93B, scale 1:000,000, 5 sheets.

Hildenbrand, T.G., and Kucks, R.P., 1988, Total intensity magnetic anomaly map of Nevada: Nevada Bureau of Mines and Geology Map 93A, scale 1:750,000.

Hintze, L.F., 1980, Geologic map of Utah: Utah Geological and Mineralogical Survey, scale 1:500,000.

Hintze, L.F., 1988, A field guide to Utah's rocks: Geologic history of Utah: Brigham Young University Geology Studies, Special Publication 7, 202 p.

Hintze, L.F., Anderson, R.E., and Embree, G.F., 1994, Geologic map of the Motoqua and Gunlock quadrangles, Washington County, Utah: U.S. Geological Survey Miscellaneous Investigations Series Map I-2427, scale 1:24,000.

Hintze, L.F., and Axen, G.J., 1995, Geologic map of the Scarecrow Peak quadrangle, Washington County, Utah, and Lincoln County, Nevada: U.S. Geological Survey Geologic Quadrangle Map GQ-1759, scale 1:24,000.

Hintze, L.F., and Axen, G.J., 2001, Geologic map of the Lime Mountain quadrangle, Lincoln County, Nevada: Nevada Bureau of Mines and Geology Map 129, scale 1:24,000.

Hintze, L.F., and Davis, F.D., 2002, Geologic map of the Tule Valley 30′ × 60′ quadrangle and parts of the Ely, Fish Springs, and Kern Mountains 30′ × 60′ quadrangles, northwest Millard County, Utah: Utah Geological Survey Map 186, scale 1:100,000, 2 sheets.

Hintze, L.F., and Davis, F.D., 2002, Geologic map of the Wah Wah Mountains North 30' × 60' quadrangle and part of the Garrison 30' × 60' quadrangle, southwest Millard County and part of Beaver County, Utah: Utah Geological Survey Map 182, scale 1:100,000, 2 sheets.

Hintze, L.F., and Davis, F.D., 2003, Geology of Millard County, Utah: Utah Geological Survey Bulletin 133, 305 p.

Hintze, L.F., Grant, S.K., Weaver, C.L., and Best, M.G., 1994, Geologic map of the Blue Mountain-Lund area, Beaver and Iron Counties, Utah: U.S. Geological Survey Miscellaneous Investigations Map I-2361, scale 1:50,000.

Hintze, L.F., and Hammond, B.J., 1994, Geologic map of the Shivwits quadrangle, Washington County, Utah: Utah Geological Survey Map 153, scale 1:24,000, 2 sheets.

Hintze, L.F., Willis, G.C., Laes, D.Y.M., Sprinkel, D.A., and Brown, K.D., 2000, Digital geologic map of Utah: Utah Geological Survey Map 179DM, scale 1:500,000, 2 sheets.

Hitchborn, A.D., Arbonies, D.G., Peters, S.G., Connors, K.A., Noble, D.C., Larson, L.T., Beebe, J.S., and McKee, E.H., 1996, Geology and gold deposits of the Bald Mountain mining district, White Pine County, Nevada, *in* Coyner, A.R., and Fahey, P.L., eds., Geology and Ore Deposits of the American Cordillera: Geological Society of Nevada Symposium Proceedings, Reno/Sparks, Nevada, April 1995, p. 505–546.

Hose, R.K., 1977, Structural geology of the Confusion Range, west-central Utah: U.S. Geological Survey Professional Paper 971, 9 p.

Hose, R.K., and Blake, Jr., M.C., 1976, Geology and mineral resources of White Pine County, Nevada Part I, Geology: Nevada Bureau of Mines and Geology Bulletin 85, p. 1–35.

Howard, E.L., 1978, Geologic map of the eastern Great Basin, Nevada and Utah: Terrascan Group, Inc., Lakewood, Colorado, scale 1:250,000.

Howard, K.A., Kistler, R.W., Snoke, A.W., and Willden, R., 1979, Geologic map of the Ruby Mountains, Nevada: U.S. Geological Survey Miscellaneous Investigations Series Map I-1136, scale 1:125,000.

Jayko, A.S., 1990, Shallow crustal deformation in the Pahranagat area, southern Nevada, *in* Wernicke, B.P., ed., Basin and Range extensional tectonics near the latitude of Las Vegas, Nevada: Boulder, Colorado, Geological Society of America Memoir 176, p. 213–236.

Jayko, A.S., 2007, Geologic map of the Pahranagat Range 30′ × 60′ quadrangle, Lincoln and Nye Counties, Nevada: U.S. Geological Survey Scientific Investigations Map 2904, scale 1: 100,000. [http://pubs.usgs.gov/sim/2007/2904/].

Keith, J.D., Tingey, D.G., and Best, M.G., 1994, Geologic map of the Rice Mountain quadrangle, Nevada and Utah: Nevada Bureau of Mines and Geology Field Studies Map 7, scale 1:24,000.

Kellogg, H.E., 1963, Paleozoic stratigraphy of the southern Egan Range, Nevada: Geological Society of America Bulletin, Vol. 74, p. 685–708.

Kellogg, H.E., 1964, Cenozoic stratigraphy and structure of the southern Egan Range, Nevada: Geological Society of America Bulletin, Vol. 75, p. 949–968.

Kleinhampl, F.J., and Ziony, J.I., 1985, Geology of northern Nye County, Nevada: Nevada Bureau of Mines and Geology Bulletin 99A, 172 p.

Lee, J., Gans, P.B., and Miller, E.L., 1999, Geologic map of the Mormon Jack Pass quadrangle, Nevada: Nevada Bureau of Mines and Geology Field Studies Map 17, scale 1:24,000.

Lee, J., Gans, P.B., and Miller, E.L., 1999, Geologic map of the Third Butte East quadrangle, Nevada: Nevada Bureau of Mines and Geology Field Studies Map 16, scale 1:24,000.

Lee, J., Miller, E.L., Gans, P.B., and Huggins, C.C., 1999, Geologic map of the Mount Moriah quadrangle, Nevada: Nevada Bureau of Mines and Geology Field Studies Map 19, scale 1:24,000.

Link, P.K., Christie-Blick, N., Devlin, W.J., Elston, D.P., Horodyski, R.J., Levy, M., Miller, J.M.G., Pearson, R.C., Prave, A., Stewart, J.H., et al., 1993, Middle and Late Proterozoic stratified rocks of the western U.S. Cordillera, Colorado Plateau, and Basin and Range province, *in* Reed, Jr., J.C., ed., Precambrian: Conterminous U.S.: Geological Society of America, The Geology of North America, Vol. C-2, p. 463–595.

Longwell, C.R., Pampeyan, E.H., Bowyer, B., and Roberts, R.J., 1965, Geology and mineral deposits of Clark County, Nevada: Nevada Bureau of Mines and Geology Bulletin 62, 218 p.

Loucks, M.D., Tingey, D.G., Best, M.G., Christiansen, E.H., and Hintze, L.F., 1989, Geologic map of the Fortification Range, Lincoln and White Pine Counties, Nevada: U.S. Geological Survey Miscellaneous Investigations Series Map I-1866, scale 1:50,000.

Lund, K., Beard, L.S., and Perry, Jr., W.J., 1991, Structures of the northern Grant Range and Railroad Valley, Nye County, Nevada: Implications for oil occurrences, *in* Flanigan, Donna M.H., Mike Hansen and T. Edward Flanigan, (eds.), Geology of White River Valley, the Grant Range, Eastern Railroad Valley and Western Egan Range, Nevada: 1991 Fieldtrip Guidebook, Nevada Petroleum Society Inc., Reno, p. 1–6.

Maldonado, F., and Schmidt, D.L., 1991, Geologic map of the southern Sheep Range, Fossil Ridge, and Castle Rock area, Clark County, Nevada: U.S. Geological Survey Miscellaneous Investigations Series Map I-2086, scale 1:24,000.

Maldonado, F., Spengler, R.W., Hanna, W.F., and Dixon, G.L., 1988, Index of granitic rock masses in the State of Nevada: U.S. Geological Survey Bulletin 1831, 81 p.

Miller, E.L., and Gans, P.B., 1999, Geologic map of The Cove quadrangle, Nevada and Utah: Nevada Bureau of Mines and Geology Field Studies Map 22, scale 1:24,000.

Miller, E.L., Gans, P.B., and Garing, J., 1983, The Snake Range décollement: An exhumed mid-Tertiary ductile-brittle transition: Tectonics, Vol. 2, No. 3, p. 239–263.

Miller, E.L., Gans, P.B., and Grier, S.P., 1994, Geologic map of Windy Peak 7.5' quadrangle, White Pine County, Nevada: U.S. Geological Survey Open-File Report 94–687, scale 1:24,000.

Miller, E.L., Gans, P.B., Grier, S.P., Huggins, C.C., and Lee, J., 1999, Geologic map of the Old Mans Canyon quadrangle, Nevada: Nevada Bureau of Mines and Geology Field Studies Map 21, scale 1:24,000.

Miller, E.L., Grier, S.P., and Brown, J.L., 1995, Geologic map of the Lehman Caves quadrangle, White Pine County, Nevada: U.S. Geological Survey Geologic Quadrangle Map GQ-1758, scale 1:24,000.

Morris, H.T., 1987, Preliminary geologic map of the Delta 2° quadrangle, Tooele, Juab, Millard, and Utah Counties, Utah: U.S. Geological Survey Open-File Report 87–185, scale 1:250,000, 3 sheets.

Nelson, R.B., 1966, Structural development of northernmost Snake Range, Kern Mountains, and Deep Creek Range, Nevada and Utah: American Association of Petroleum Geologists Bulletin, Vol. 50, No. 5, p. 921–951.

Nolan, T.B., 1935, The Gold Hill mining district, Utah: U.S. Geological Survey Professional Paper 177, 172 p.

Nolan, T.B., Merriam, C.W., and Blake, Jr., M.C., 1974, Geologic map of the Pinto Summit quadrangle, Eureka and White Pine Counties, Nevada: U.S. Geological Survey Miscellaneous Investigations Series Map I-793, scale 1:31,680.

Nolan, T.B., Merriam, C.W., and Brew, D.A., 1971, Geologic map of the Eureka quadrangle, Eureka and White Pine Counties, Nevada: U.S. Geological Survey Miscellaneous Geologic Investigations Map I-612, scale 1:31,680, 2 sheets.

Nutt, C.J., 2000, Geologic map of the Alligator Ridge area, including the Buck Mountain East and Mooney Basin Summit quadrangles and parts of the Sunshine Well NE and Long Valley Slough quadrangles, White Pine County, Nevada: U.S. Geological Survey Geologic Investigations Series Map I-2691, scale 1:24,000.

Nutt, C.J., and Hart, K.S., 2004, Geologic map of the Big Bald Mountain quadrangle and part of the Tognini Spring quadrangle, White Pine County, Nevada: Nevada Bureau of Mines and Geology Map 145, scale 1:24,000.

Nutt, C.J., Zimbelman, D.R., Campbell, D.L., Duval, J.S., and Hannigan, B.J., 1990, Chapter C: Mineral resources of the Deep Creek Mountains wilderness study area, Juab and Tooele counties, Utah: U.S. Geological Survey Bulletin 1745-C, 40 p.

Otto, B.R., 2008, Geologic map of the central Butte Range, White Pine County, Nevada: Nevada Bureau of Mines and Geology Map 160, scale 1:48,000.

Oviatt, C.G., 1991, Quaternary geology of Fish Springs Flat, Juab County, Utah: Utah Geological Survey Special Study 77, 16 p.

Page, W.R., 1992, Preliminary geologic map of the Paleozoic rocks in the Arrow Canyon quadrangle, Clark County, Nevada: U.S. Geological Survey-Open File Report 92–681, scale 1:24,000.

Page, W.R., 1998, Geologic map of the Arrow Canyon NW quadrangle, Clark County, Nevada: U.S. Geological Survey Geologic Quadrangle Map GQ-1776, scale 1:24,000.

Page, W.R., Dixon, G.L., Rowley, P.D., and Brickey, D.W., 2005, Geologic map of parts of the Colorado, White River, and Death Valley groundwater flow systems, Nevada, Utah, and Arizona: Nevada Bureau of Mines and Geology Map 150, scale 1:250,000.

Page, W.R., Lundstrom, S.C., Harris, A.G., Langenheim, V.E., Workman, J.B., Mahan, S.A., Paces, J.B., Dixon, G.L., Rowley, P.D., Burchfiel, B.C., Bell, J.W., and Smith, E.I., 2005, Geologic and geophysical maps of the Las Vegas 30' × 60' quadrangle, Clark and Nye Counties, Nevada, and Inyo County, California: U.S. Geological Survey Scientific Investigations Map 2814, scale 1:100,000, 2 sheets.

Page, W.R., and Pampeyan, E.H., 1996, Preliminary geologic map of the Paleozoic rocks in the Wildcat Wash SE and Wildcat Wash SW quadrangles, Lincoln and Clark Counties, Nevada: U.S. Geological Survey Open-File Report 96–26, scale 1:24,000, 2 sheets.

Page, W.R., Scheirer, D.S., and Langenheim, V.E., 2006, Geologic cross sections of parts of the Colorado, White River, and Death Valley regional ground-water flow systems, Nevada, Utah, and Arizona: U.S. Geological Survey Open-File Report 2006–1040, Denver, CO, 80225.

Page, W.R., Swadley, W.C., and Scott, R.B., 1990, Preliminary geologic map of the Delamar 3 SW quadrangle, Lincoln County, Nevada: U.S. Geological Survey Open-File Report 90–336, scale 1:24,000.

Pampeyan, E.H., 1993, Geologic map of the Meadow Valley Mountains, Lincoln and Clark Counties, Nevada: U.S. Geological Survey Miscellaneous Investigations Series Map I-2173, scale 1:50,000, 2 sheets.

Ponce, D.A., 1992, Complete Bouguer gravity map of Nevada, Ely sheet: Nevada Bureau of Mines and Geology Map 99, scale 1:250,000.

Ponce, D.A., Morin, R.L., and Robbins, S.L., 1996, Bouguer gravity map of Nevada, Elko sheet: Nevada Bureau of Mines and Geology Map 107, scale 1:250,000.

Poole, F.G., and Sandberg, C.A., 1977, Mississippian paleogeography and tectonics of the western United States, *in* Stewart, J.H., Stevens, C.H., and Fritsche, A.E., eds., Paleozoic paleogeography of the western United States: Society of Economic Paleontologists and Mineralogists, Pacific Section, Pacific Coast Paleogeography Symposium 1, April 22, 1977, p. 67–85.

Poole, F.G., and Sandberg, C.A., 1991, Mississippian paleogeography and conodont biostratigraphy of the western United States, *in* Cooper, J.D., and Stevens, C.H., eds., Paleozoic paleogeography of the western United States—II: Society of Economic Paleontologists and Mineralogists, Pacific Section, Pacific Coast Paleogeography, p. 107–136.

Quinlivan, W.D., and Rogers, C.L., 1974, Geologic map of the Tybo quadrangle, Nye County, Nevada: U.S. Geological Survey Miscellaneous Investigations Series Map I-821, scale 1:48,000.

Quinlivan, W.D., Rogers, C.L., and Dodge, Jr., H.W., 1974, Geologic map of the Portuguese Mountain quadrangle, Nye County, Nevada: U.S. Geological Survey Miscellaneous Investigations Series Map I-804, scale 1:48,000.

Raines, G.L., Connors, K.A., Moyer, L.A., and Miller, R.J., 2003, Spatial digital database for the geologic map of Nevada. Digital database, Version 3.0: U.S. Geological Survey Open-File Report 03–66.

Roberts, R.J., Montgomery, K.M., and Lehner, R.E., 1967, Geology and mineral resources of Eureka County, Nevada: Nevada Bureau of Mines and Geology Bulletin 64, 152 p., scale 1:250,000, 12 sheets.

Robinson, J.P., 1993, Provisional geologic map of the Gold Hill quadrangle, Tooele County, Utah: Utah Geological Survey Map 140, scale 1:24,000, 3 sheets.

Rowley, P.D., 1998, Cenozoic transverse zones and igneous belts in the Great Basin, western United States: Their tectonic and economic implications, *in* Faulds, J.E., and Stewart, J.H., eds., Accommodation zones and transfer zones: The regional segmentation of the Basin and Range province: Geological Society of America Special Paper 323, p. 195–228.

Rowley, P.D., Cunningham, C.G., Steven, T.A., Workman, J.B., Anderson, J.J., and Theissen, K.M., 2002, Geologic map of the central Marysvale volcanic field, southwestern Utah: U.S. Geological Survey Geologic Investigations Series Map I-2645-A, scale 1:100,000.

Rowley, P.D., and Dixon, G.L., 2001, The Cenozoic evolution of the Great Basin area, U.S.A.—New interpretations based on regional geologic mapping, *in* Erskine, M.C., Faulds, J.E., Bartley, J.M., and Rowley, P.D., eds., The geologic transition, High Plateaus to Great Basin—A symposium and field guide: The Mackin Volume: Utah Geological Association Publication 30 and American Association of Petroleum Geologists Publication GB78, September, 20–22, 2001, p. 169–188.

Rowley, P.D., Hacker, D.B., Maxwell, D.J., Maxwell, J.D., and Boswell, J.T., 2008, Interim geologic map of the Utah part of the Deer Lodge Canyon, Prohibition Flat, Uvada, and Pine Park quadrangles (east part of the Caliente 30' × 60' quadrangle), Iron and Washington Counties, Utah: Utah Geological Survey Open-File Report 530, scale 1:24,000.

Rowley, P.D., Lipman, P.W., Mehnert, H.H., Lindsey, D.A., and Anderson, J.J., 1978, Blue Ribbon lineament, an east-trending structural zone within the Pioche mineral belt of southwestern Utah and eastern Nevada: U.S. Geological Survey Journal of Research, Vol. 6, No. 2, p. 175–192.

Rowley, P.D., Nealey, L.D., Unruh, D.M., Snee, L.W., Mehnert, H.H., Anderson, R.E., and Grommé, C.S., 1995, Stratigraphy of Miocene ash-flow tuffs in and near the Caliente caldera complex, southeastern Nevada and southwestern Utah, *in* Scott, R.B., and Swadley, W.C., eds., Geologic studies in the Basin and Range–Colorado Plateau transition in southeastern Nevada, southwestern Utah, and northwestern Arizona, 1992: U.S. Geological Survey Bulletin 2056, p. 43–88.

Rowley, P.D., and Shroba, R.R., 1991, Geologic map of the Indian Cove quadrangle, Lincoln County, Nevada: U.S. Geological Survey Geologic Quadrangle Map GQ-1701, scale 1:24,000.

Rowley, P.D., Shroba, R.R., Simonds, F.W., Burke, K.J., Axen, G.J., and Olmore, S.D., 1994, Geologic map of the Chief Mountain quadrangle, Lincoln County, Nevada: U.S. Geological Survey Geologic Quadrangle Map GQ-1731, scale 1:24,000.

Rowley, P.D., Williams, V.S., Vice, G.S., Maxwell, D.J., Hacker, D.B., Snee, L.E., and Mackin, J.H., 2006, Interim geologic map of the Cedar City 30' × 60' quadrangle, Iron and Washington Counties, Utah: Utah Geological Survey Open-File Report 476DM, scale 1:100,000.

Saltus, R.W., 1988, Bouguer gravity anomaly map of Nevada: Nevada Bureau of Mines and Geology Map 94A, scale 1:750,000.

Saltus, R.W., 1988, Regional, residual, and derivative gravity maps of Nevada: Nevada Bureau of Mines and Geology Map 94B, scale 1:000,000, 4 sheets.

Saltus, R.W., and Jachens, R.C., 1995, Gravity and basin-depth maps of the Basin and Range province, western United States: U.S. Geological Survey Geophysical Investigations Map GP-1012, scale 1:2,500,000.

Sargent, K.A., and Roggensack, K., 1984, Map showing outcrops of pre-Quaternary ash-flow tuffs and volcaniclastic rocks, Basin and Range province, Nevada: U.S. Geological Survey Water-Resources Investigations Report 83–4119-E, scale 1:500,000, 2 sheets.

Saucier, A.E., 1997, The Antler Thrust System in Northern Nevada, *in* Perry, A.J., and Abbott, E.W., eds., The Roberts Mountains Thrust, Elko and Eureka Counties, Nevada: Nevada Petroleum Society, 1997 Field Trip Guidebook, Reno, Nevada, p. 1–16.

Scheirer, D.S., 2005, Gravity studies of Cave, Dry Lake, and Delamar valleys, east-central Nevada: U.S. Geological Survey Open-File Report 2005–1339, 27 p.

Schmidt, D.L., 1994, Preliminary geologic map of the Farrier quadrangle, Clark and Lincoln Counties, Nevada: U.S. Geological Survey Open-File Report 94–625, scale 1:24,000.

Schmidt, D.L., Page, W.R., and Workman, J.B., 1996, Preliminary geologic map of the Moapa West quadrangle, Clark County, Nevada: U.S. Geological Survey Open-File Report 96–521, scale 1:24,000.

Scott, R.B., Grommé, C.S., Best, M.G., Rosenbaum, J.G., and Hudson, M.R., 1995, Stratigraphic relationships of Tertiary volcanic rocks in central Lincoln County, southeastern Nevada, *in* Scott, R.B., and Swadley, W.C., eds., Geologic studies in the Basin and Range–Colorado Plateau transition in southeastern Nevada, southwestern Utah, and northwestern Arizona, 1992: U.S. Geological Survey Bulletin 2056, p. 7–41.

Scott, R.B., Harding, A.E., Swadley, W.C., and Pampeyan, E.H., 1991, Preliminary geologic map of the Vigo NW quadrangle, Lincoln County, Nevada: U.S. Geological Survey Open-File Report 91–389, scale 1:24,000.

Scott, R.B., Novak, S.W., and Swadley, W.C., 1990, Preliminary geologic map of the Delamar 3 NE quadrangle, Lincoln County, Nevada: U.S. Geological Survey Open-File Report 90–33, scale 1:24,000.

Scott, R.B., Page, W.R., and Swadley, W.C., 1990, Preliminary geologic map of the Delamar 3 NW quadrangle, Lincoln County, Nevada: U.S. Geological Survey Open-File Report 90–405, scale 1:24,000.

Scott, R.B., Rowley, P.D., Snee, L.W., Anderson, R.E., Harding, A.E., Unruh, D.M., Nealey, L.D., Hudson, M.R., Swadley, WC, and Ferris, D.E., 1996, Synchronous Oligocene and Miocene extension and magmatism in the vicinity of caldera complexes in southeastern Nevada: Colorado Geological Survey Open-File Report 96-4, 36 p.

Scott, R.B., Swadley, W.C., and Novak, S.W., 1993, Geologic map of the Delamar Lake quadrangle, Lincoln County, Nevada: U.S. Geological Survey Geologic Quadrangle Map GQ-1730, scale 1:24,000.

Scott, R.B., Swadley, W.C., Page, W.R., and Novak, S.W., 1991, Preliminary geologic map of the Gregerson Basin quadrangle, Lincoln County, Nevada: U.S. Geological Survey Open-File Report 90–646, scale 1:24,000.

Slate, J.L., Berry, M.E., Rowley, P.D., Fridrich, C.J., Williams, V.S., Morgan, K.S., Workman, J.B., Young, O.D., Dixon, G.L., Williams, V.S., et al., 1999, Digital geologic map of the Nevada Test Site and vicinity, Nye, Lincoln, and Clark Counties, Nevada, and Inyo County, California: U.S. Geological Survey Open-File Report 99–554-A, 53 p.

Smith, D.L., Gans, P.B., and Miller, E.L., 1991, Palinspastic restoration of Cenozoic extension in the central and eastern Basin and Range province at latitude 39-40° N, *in* Raines, G.L., Lisle, R.E., Schafer, R.W., and Wilkinson, W.H., eds., Geology and ore deposits of the Great Basin, Geological Society of Nevada, Symposium Proceedings, April 1–5, 1990, Vol. 1, p. 75–86.

Snyder, D.B., Healey, D.L., and Saltus, R.W., 1984, Complete Bouguer gravity map of Nevada: Lund sheet: Nevada Bureau of Mines and Geology Map 80, scale 1:250,000.

Snyder, R.P., Ekren, E.B., and Dixon, G.L., 1972, Geologic map of the Lunar Crater quadrangle, Nye County, Nevada: U.S. Geological Survey Miscellaneous Geologic Investigations Map I-700, scale 1:48,000.

Steven, T.A., Morris, H.T., and Rowley, P.D., 1990, Geologic map of the Richfield 1° × 2° quadrangle, west-central Utah: U.S. Geological Survey Miscellaneous Investigations Series Map I-1901, scale 1:250,000.

Stewart, J.H., 1980, Geology of Nevada: A discussion to accompany the *geologic map of Nevada*: Nevada Bureau of Mines and Geology Special Publication 4, 136 p.

Stewart, J.H., and Carlson, J.E., 1976, Cenozoic rocks of Nevada—Four maps and brief description of distribution, lithology, age, and centers of volcanism: Nevada Bureau of Mines and Geology Map 52, scale 1:1,000,000, 4 sheets.

Stewart, J.H., and Carlson, J.E., 1978, Geologic map of Nevada: U.S. Geological Survey, scale 1:500,000.

Swadley, W.C., Page, W.R., Scott, R.B., and Pampeyan, E.H., 1994, Geologic map of the Delamar 3 SE quadrangle, Lincoln County, Nevada: U.S. Geological Survey Geologic Quadrangle Map GQ-1754, scale 1:24,000.

Swadley, W.C., and Rowley, P.D., 1994, Geologic map of the Pahroc Spring SE quadrangle, Lincoln County, Nevada: U.S. Geological Survey Geologic Quadrangle Map GQ-1752, scale 1:24,000.

Swadley, W.C., and Scott, R.B., 1991, Preliminary geologic map of the Delamar NW quadrangle, Lincoln County, Nevada: U.S. Geological Survey Open-File Report 90–622, scale 1:24,000.

Sweetkind, D.S., Knochenmus, L.A., Ponce, D.A., Wallace, A.R., Scheirer, D.S., Watt, J.T., and Plume, R.W., 2007, Hydrogeologic framework, *in* Welch, A.H., Bright, D.J., and Knochenmus, L.A., eds., Water resources of the Basin and Range carbonate-rock aquifer system, White Pine County, Nevada, and adjacent areas in Nevada and Utah: U.S. Geological Survey Scientific Investigations Report 2007–5261, p. 11–36.

Sweetkind, D.S., Knochenmus, L.A., Ponce, D.A., Wallace, A.R., Scheirer, D.S., Watt, J.T., and Plume, R.W., 2007, Hydrogeologic map and cross sections, White Pine County, Nevada, and adjacent areas in Nevada and Utah, *in* Welch, A.H., Bright, D.J., and Knochenmus, L.A., eds., Water resources of the Basin and Range carbonate-rock aquifer system, White Pine County, Nevada, and adjacent areas in Nevada and Utah: U.S. Geological Survey Scientific Investigations Report 2007–5261, Plate 1, scale 1:500,000.

Taylor, M.E., Poole, F.G., and Cook, H.E., 1991, Summary of Paleozoic stratigraphy in the southern Egan and Schell Creek ranges, east-central Nevada, *in* Flanigan, Donna M.H., Mike Hansen and T. Edward Flanigan, (eds.), Geology of White River Valley, the Grant Range, Eastern Railroad Valley and Western Egan Range, Nevada: 1991 Fieldtrip Guidebook, Nevada Petroleum Society Inc., Reno, p. 29–35.

Taylor, W.J., Dobbs, S.W., Nelson, S.L., and Armstrong, P.A., 1994, Generation of four-way closure through multiple tectonic events: Structures of the Timpahute Range, southern Nevada, *in* Dobbs, S.W., and W.J. Taylor, eds., Structural and Stratigraphic Investigations and Petroleum Potential of Nevada, with Special Emphasis South of the Railroad Valley Producing Trend: Nevada Petroleum Society Conference Volume II, p. 141–156.

Tschanz, C.M., and Pampeyan, E.H., 1970, Geology and mineral deposits of Lincoln County, Nevada: Nevada Bureau of Mines and Geology Bulletin 73, 187 p.

Van Loenen, R.E., 1987, Geologic map of the Mount Grafton wilderness study area, Lincoln and White Pine counties, Nevada: U.S. Geological Survey Miscellaneous Field Studies Map MF-1938, scale 1:50,000.

Vikre, P.G., 1998, Intrusion-related, polymetallic carbonate replacement deposits in the Eureka district, Eureka County, Nevada: Nevada Bureau of Mines and Geology Bulletin 110, 52 p.

Wernicke, B., Walker, J.D., and Beaufait, M.S., 1985, Structural discordance between Neogene detachments and frontal Sevier thrusts, central Mormon Mountains, southern Nevada: Tectonics, Vol. 4, No. 2, p. 213–246.

Whitebread, D.H., 1969, Geologic map of the Wheeler Peak and Garrison quadrangles, Nevada and Utah: U.S. Geological Survey Miscellaneous Geologic Investigations Map I-578, scale 1:48,000.

Williams, V.S., 1996, Preliminary geologic map of the Mesquite quadrangle, Clark and Lincoln Counties, Nevada and Mohave Counties Arizona: U.S. Geological Survey Open-File Report 96–676, scale 1:24,000.

Williams, V.S., Best, M.G., and Keith, J.D., 1997, Geologic map of the Ursine-Panaca Summit-Deer Lodge area, Lincoln County, Nevada, and Iron County, Utah: U.S. Geological Survey Miscellaneous Investigations Series Map I-2479, scale 1:50,000.

Williams, V.S., Bohannon, R.G., and Hoover, D.L., 1997, Geologic map of the Riverside quadrangle, Clark County, Nevada: U.S. Geological Survey Geologic Quadrangle Map GQ-1770, scale 1:24,000.

Williams, V.S., Schmidt, D.L., and Bohannon, R.G., 1997, Preliminary geologic map of the Moapa East quadrangle, Clark County, Nevada: U.S. Geological Survey Open-File Report 97-449, scale 1:24,000.

Willis, J.B., Best, M.G., Kowallis, B.J., and Best, V.C., 1987, Preliminary geologic map of the northern Wilson Creek Range, Lincoln County, Nevada: U.S. Geological Survey Miscellaneous Field Studies Map MF-1971, scale 1:50,000.

Workman, J.B., Menges, C.M., Page, W.R., Ekren, E.B., Rowley, P.D., and Dixon, G.L., 2002, Tectonic map of the Death Valley ground-water model area, Nevada and California: U.S. Geological Survey Miscellaneous Field Studies Map MF-2381-B, 58 p., scale 1:250,000.

Workman, J.B., Menges, C.M., Page, W.R., Taylor, E.M., Ekren, E.B., Rowley, P.D., Dixon, G.L., Thompson, R.A., and Wright, L.A., 2002, Geologic map of the Death Valley ground-water model area, Nevada and California: U.S. Geological Survey Miscellaneous Field Studies MF-2381-A, 26 p., 1:250,000 scale, 2 sheets.

This Page Left Intentionally Blank

Appendix A

General Photos of the Study Area

View northwest of Jackman Narrows, where the Muddy River cuts into folded and faulted Permian carbonate rocks of the northern part of the North Muddy Mountains. Towns of Glendale and Moapa in the background.

View north in Jackman Narrows showing highly fractured and contorted Permian limestone.

View overlooking Muddy River Springs, the source of the Muddy River northwest of Moapa.

View north of east dipping volcanic rocks underlain by Paleozoic rocks in northern Coyote Springs Valley. US 93 in center of photograph.

View north into southern Delamar Valley. Delamar Lake is light-colored playa in left center of photograph. Maynard Lake strand of the Pahranagat shear zone forms the scarp that is in shadows in the foreground, whereas the Delamar Lake strand passes beneath Delamar Lake and north of the hills on the left side of the photograph. Delamar Mountains in the right background.

View west from the Meadow Valley Mountains across the oblique-slip fault scarp of the Kane Springs fault zone (foreground), then across Kane Springs Valley, toward the Kane Springs Wash caldera complex in the Delamar Mountains.

View north along the northeast-southwest trace of the Maynard Lake Fault zone. Volcanic rocks highly fractured and faulted along fault zone. Maynard Lake (dry) in bottom of photograph.

View north of Rainbow Canyon, where perennial Meadow Valley Wash here cuts through the Caliente caldera complex south of Caliente, Nevada.

View north of Maynard Lake left-lateral fault segment of the Pahranagat Shear Zone. Note slickensides along the central core zone in center of photograph and brecciated volcanic rocks adjacent to this fault.

Brecciated fault debris along the Maynard Lake fault segment.

View west-northwest of Delamar mining district and northern Delamar Valley. Although Nevada's largest gold district from 1895 to 1910, now only a few walls of buildings remain along the main street.

View north of the Dry Lake Quaternary fault scarp (center foreground) on eastern side of Dry Lake Valley.

View east at drill hole 180W902M in Cave Valley near Sidehill Pass. Devonian and Silurian sedimentary rocks in background.

View to the southwest along the trace of the Shingle Pass fault zone in the southern Egan Range. The fault goes from the lower left of the view along the right base of the mountain in the center background.

View to the south looking at springs (to the right of the Nevada Highway 318 in left foreground and right middleground) in southern White River Valley. Seaman Range is in the background.

Plates

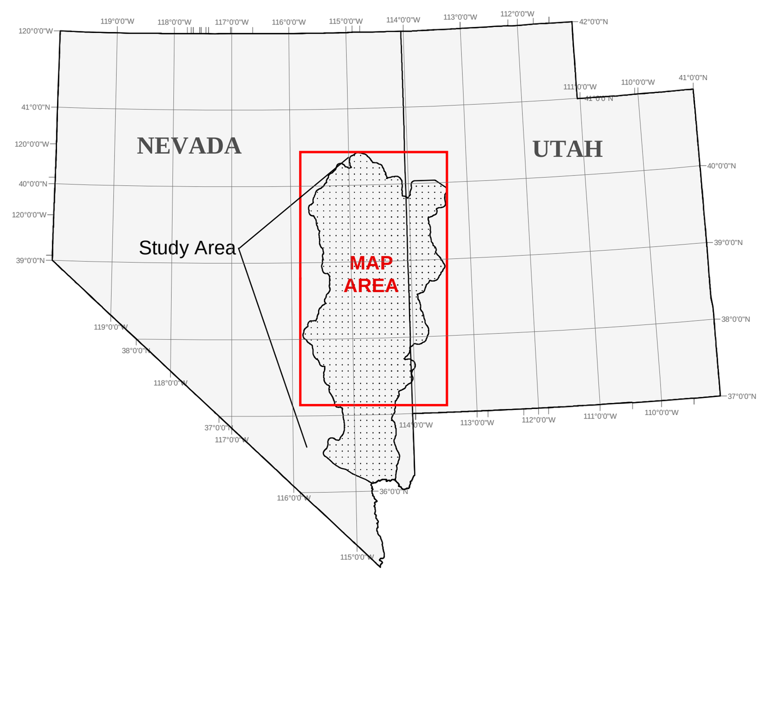

Explanation

Geologic Units

QTa	Quaternary and Tertiary basin-fill deposits
QTb	Quaternary and Tertiary thin basalt flows and cinder cones
Ts4	Tertiary fluvial and lacustrine sediments
Tt4	Tertiary poorly-densely welded ash-flow tuff and interbedded airfall tuff
Ta4	Tertiary andesitic and locally dacitic lava flows, flow breccia, and mudflow breccia
Tr4	Tertiary high-silica rhyolite lava flows and volcanic domes
Tr3	Tertiary low-silica rhyolite lava flows and volcanic domes
Ta3	Tertiary andesitic and locally dacitic lava flows, flow breccia, and mudflow breccia
Ts3	Tertiary mostly fluvial tuffaceous sandstone and bedded airfall tuff
Tt3	Tertiary poorly-densely welded ash-flow tuff and interbedded airfall tuff
Ts2	Tertiary mostly fluvial tuffaceous sandstone and bedded airfall tuff
Ta2	Tertiary andesitic and locally dacitic lava flows, flow breccia, and mudflow breccia
Tr2	Tertiary low-silica rhyolite lava flows and volcanic domes
Tt2	Tertiary poorly-densely welded ash-flow tuff and interbedded airfall tuff
Tt1	Tertiary poorly-densely welded ash-flow tuff and interbedded airfall tuff
Tr1	Tertiary low-silica rhyolite lava flows and volcanic domes
Ta1	Tertiary andesitic and locally dacitic lava flows, flow breccia, and mudflow breccia
Ts1	Tertiary fluvial and lacustrine sediments
Tmb	Tertiary intracaldera megabreccia
Ti	Tertiary intrusive rocks
TKi	Tertiary-Cretaceous intrusive rocks
Ki	Cretaceous intrusive rocks
Ks	Upper and Lower Cretaceous sedimentary rocks, undivided
Ji	Jurassic intrusive rocks
₮s	Triassic sedimentary rocks, undivided
Pp	Upper and Lower Permian Park City Group, undivided
Par	Permian Arcturus Formation and Rib Hill Sandstone
Pa	Permian Arcturus Formation
Pr	Lower Permian Rib Hill Sandstone
PIP	Permian and Pennsylvanian Riepe Spring Limestone and Ely Limestone, undivided
IP	Pennsylvanian Ely Limestone
MDd	Upper Mississippian to Upper Devonian Diamond Peak Formation, Chainman Shale, Joana Limestone, and Pilot Shale, undivided
Md	Upper Mississippian Diamond Peak Formation
Mc	Upper Mississippian Chainman Shale
MD	Lower Mississippian to Upper Devonian Joana Limestone and Pilot Shale, undivided
D€	Devonian to Upper Cambrian sedimentary rocks, undivided
DS	Devonian and Silurian sedimentary rocks, undivided
Du	Devonian carbonate sedimentary rocks, undivided
Dd	Upper and Middle Devonian Devils Gate Formation
Dg	Upper and Middle Devonian Guilmette Formation
Dn	Middle and Lower Devonian Nevada Formation
Ds	Middle and Lower Devonian Simonson and Sevy Dolomites
SOu	Silurian and Upper Ordovician dolomite, undivided
Ol	Middle and Lower Ordovician, mostly Eureka Quartzite and the Pogonip Goup
€c	Cambrian carbonate sedimentary rocks, undivided
€u	Lower Ordovician? And Upper Cambrian limestone and shale, undivided
€m	Upper and Middle Cambrian limestone and shale
€p€s	Middle Cambrian to Late Proterozoic sedimentary rocks
p€	Late to Early Proterozoic metamorphosed and crystalline Precambrian basement rocks
	Open Water

Regional Faults

Normal Fault
Solid where known; Dashed where inferred; dotted where concealed. Bar and ball on downthrown side.

Strike-slip Fault
Solid where known; Dashed where inferred; dotted where concealed. Arrows show direction of movement.

Thrust Fault
Solid where known; Dashed where inferred; dotted where concealed. Sawteeth on upper plate.

Detachment Fault
Solid where known; Dashed where inferred; dotted where concealed. Sawteeth on upper plate.

Quaternary Fault
Solid where known; Dashed where inferred; dotted where concealed. Bar and ball on downthrown side.

Subsidiary Faults

Normal Fault
Solid where known; dashed where inferred; dotted where concealed; dotted and queried where uncertain. Bar and ball on downthrown side.

Strike-slip Fault
Solid where known; dashed where inferred; dotted where concealed; dotted and queried where uncertain Arrows show direction of movement.

Thrust Fault
Solid where known; dashed where inferred; dotted where concealed; dotted and queried where uncertain. Sawteeth on upper plate.

Detachment Fault
Solid where known; dashed where inferred; dotted where concealed; dotted and queried where uncertain. Hollow sawteeth on upper plate.

Quaternary Normal Fault
Solid where known; dashed where inferred; dotted where concealed; dotted and queried where uncertain. Bar and ball on downthrown side.

Caldera Boundary
Solid where known; dashed where inferred; dotted where concealed

Cross Sections (Plates 4 and 5)

Major Road

Transverse Zone
(Zone of possible disruption)

National Park Service

Oil Well Data Used in Cross Sections
Nevada: Nevada Bureau of Mines and Geology
Utah: Utah Division of Oil, Gas and Mining

Wells

Town

Strike and Dip of Beds

Overturned Beds

N
W E
S

SCALE 1:250,000

Projection: UTM Zone 11 NAD83

0 25,000 50,000 75,000 Feet
0 5,000 10,000 15,000 20,000 25,000 Meters
0 5 10 15 20 Miles

SOUTHERN NEVADA WATER AUTHORITY

MAP ID 18286-3211 05/17/2011 JAB/BP

PLATE 1. GEOLOGY OF WHITE PINE AND NORTHERN LINCOLN COUNTIES, NEVADA, AND ADJACENT AREAS, NEVADA AND UTAH

SE ROA 43354

JA_13234

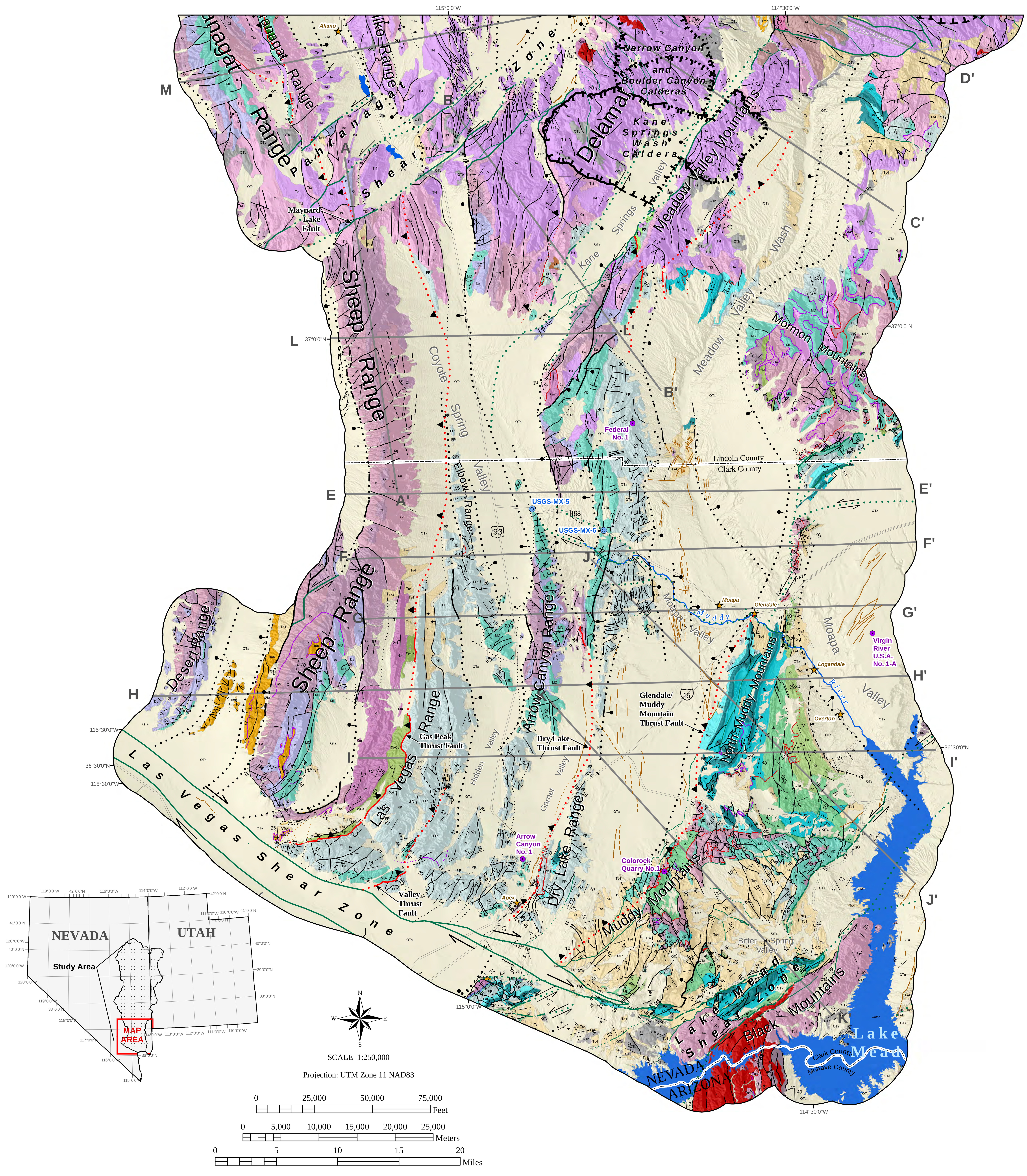

Explanation

Geologic Units

Unit	Description
QTa	Quaternary and Tertiary basin-fill deposits
QTb	Quaternary and Tertiary thin basalt flows and cinder cones
Ts4	Tertiary fluvial and lacustrine sediments
Tt4	Tertiary poorly-to-densely welded ash-flow tuff and interbedded airfall tuff
Ta4	Tertiary andesitic and locally dacitic lava flows, flow breccia, and mudflow breccia
Tr4	Tertiary high-silica rhyolite lava flows and volcanic domes
Ta3	Tertiary andesitic and locally dacitic lava flows, flow breccia, and mudflow breccia
Tt3	Tertiary poorly-densely welded ash-flow tuff and interbedded airfall tuff
Tt2	Tertiary poorly-densely welded ash-flow tuff and interbedded airfall tuff
Ts1	Tertiary fluvial and lacustrine sediments
Tmb	Tertiary megabreccia
Ti	Tertiary intrusive rocks
Ks	Upper and Lower Cretaceous sedimentary rocks, undivided
Js	Jurassic sedimentary rocks, undivided
T̄s	Triassic sedimentary rocks, undivided
Pp	Upper and Lower Permian Park City Group, undivided
Par	Permian Arcturus Formation and Rib Hill Sandstone
PIP	Permian and Pennsylvanian Riepe Spring Limestone and Ely Limestone, undivided
Md	Upper Mississippian Diamond Peak Formation
Mc	Upper Mississippian Chainman Shale
MD	Lower Mississippian to Upper Devonian Joana Limestone and Pilot Shale, undivided
Ds	Middle and Lower Devonian Simonson and Sevy Dolomites
Du	Devonian carbonate sedimentary rocks, undivided
SOu	Silurian and Upper Ordovician dolomite, undivided
Ol	Middle and Lower Ordovician, mostly Eureka Quartzite and the Pogonip Goup
Ꞓc	Cambrian carbonate sedimentary rocks, undivided
Ꞓu	Lower Ordovician? And Upper Cambrian limestone and shale, undivided
Ꞓm	Upper and Middle Cambrian limestone and shale
ꞒpꞒs	Middle Cambrian to Late Proterozoic sedimentary rocks
pꞒ	Late to Early Proterozoic metamorphosed and crystalline Precambrian basement rocks
	Open Water

Regional Faults

Normal Fault
Solid where known; Dashed where inferred; dotted where concealed. Bar and ball on downthrown side.

Strike-slip Fault
Solid where known; Dashed where inferred; dotted where concealed. Arrows show direction of movement.

Thrust Fault
Solid where known; Dashed where inferred; dotted where concealed. Sawteeth on upper plate.

Detachment Fault
Solid where known; Dashed where inferred; dotted where concealed. Sawteeth on upper plate.

Quaternary Normal Fault
Solid where known; Dashed where inferred; dotted where concealed.

Subsidiary Faults

Normal Fault
Solid where known; dashed where inferred; dotted where concealed; dotted and queried where uncertain. Bar and ball on downthrown side.

Strike-slip Fault
Solid where known; dashed where inferred; dotted where concealed; dotted and queried where uncertain. Arrows show direction of movement.

Thrust Fault
Solid where known; dashed where inferred; dotted where concealed; dotted and queried where uncertain. Sawteeth on upper plate.

Detachment Fault
Solid where known; dashed where inferred; dotted where concealed; dotted and queried where uncertain. Hollow sawteeth on upper plate.

Quaternary Normal Fault
Solid where known; dashed where inferred; dotted where concealed; dotted and queried where uncertain. Bar and ball on downthrown side.

Caldera Boundary
Solid where known; dashed where inferred; dotted where concealed

Cross Sections (Plates 4 and 5)

Major Road

Transverse Zone (Zone of possible disruption)

Town

Strike and Dip of Beds

Overturned Beds

Oil Well Data Used in Cross Sections
Nevada: Nevada Bureau of Mines and Geology

Well

SOUTHERN NEVADA WATER AUTHORITY

MAP ID 18287-3211 05/17/2011 BP

PLATE 2. GEOLOGY OF SOUTHERN LINCOLN AND NORTHERN CLARK COUNTIES, NEVADA , AND ADJACENT AREAS, ARIZONA

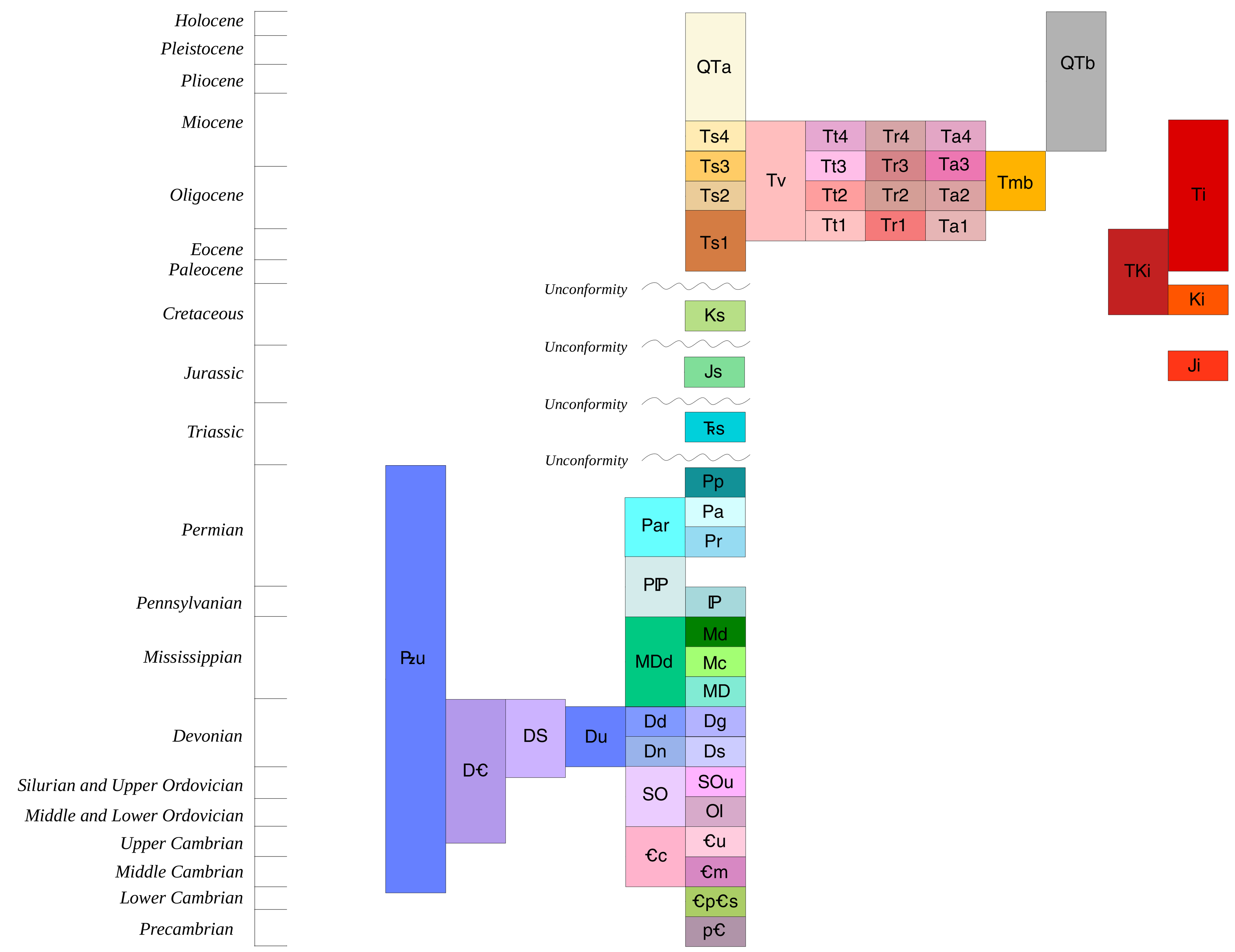

QTa Surficial and basin-fill deposits (Holocene to upper Miocene)—Unconsolidated to moderately consolidated, locally tuffaceous beds of sand, gravel, silt, and minor limestone deposited mostly by streams and small playa lakes. Generally thin but, where unit fills basin-range-fault-bounded basins, may be 0-5000 feet thick and forms the upper valley-fill aquifer. Some basin-fill deposits bear local names, including the Muddy Creek Formation (southern part of Plate 2), Panaca Formation (southern part of Plate 1), Horse Camp Formation (northwestern part of Plate 1), and Salt Lake Formation (northeastern part of Plate 1).

QTb Basalt lava flows (Holocene to lower Miocene)—Resistant, thin, basalt lava flows and cinder cones. The mafic end of the bimodal volcanic sequence that is synchronous with basin-range extensional faulting.

Ts4 Sedimentary rocks, unit 4 (Miocene)—Moderately to well consolidated, mostly fluvial sandstone, conglomerate, and minor lacustrine limestone. Primarily the Horse Spring Formation (11 to 20 Ma), a basal basin-fill sedimentary unit that is locally thick (3000+ feet) in the southern part of Plate 2.

Ts3 Sedimentary rocks, unit 3 (Miocene and Oligocene)—Moderately to well consolidated, thin, mostly fluvial, tuffaceous sandstone and bedded airfall tuff

Ts2 Sedimentary rocks, unit 2 (Oligocene)—Moderately to well consolidated, thin, mostly fluvial, tuffaceous sandstone and conglomerate. Includes the Gilmore Gulch Formation, with an age of about 30 Ma, in the northwestern part of Plate 1.

Ts1 Sedimentary rocks, unit 1 (Oligocene to Upper Cretaceous?)—Moderately to well consolidated, mostly fluvial sandstone, conglomerate, and minor lacustrine limestone. Primarily the Sheep Pass Formation, but in the central part of Plate 1, includes the Paleocene and Upper Cretaceous(?) Grapevine Wash Formation and the Eocene and Paleocene Claron Formation. Includes the Fowkes Formation and White Sage Formation in the northeastern part of Plate 1. Unit in most places underlies all volcanic rocks.

Tv Volcanic rocks (Miocene to Eocene)—Unit shown only in Plates 4, 5, 6, 7, 8, and 9, where it is referred to as the volcanic aquifer. May be several thousand feet thick in many places, and in calderas and near other source vents, may be many thousands of feet thick. On Plates 1 and 2, unit is separated into several rock types based on age, following the mapping strategy of Ekren et al, (1977).

Tt4 Ash-flow tuff and interbedded airfall tuff, unit 4 (Miocene)—Poorly to densely welded, bimodal high-silica rhyolite and locally peralkaline ash-flow tuff and related airfall tuffs. Includes the tuff of Honeycomb Rock (12.0 Ma), Ox Valley Tuff (14.0 Ma), tuff of Etna (14.0 Ma), tuff of Rainbow Canyon (15.6 Ma), tuff of Acklin Canyon (17.1 Ma), and tuff of Dow Mountain (17.4 Ma), derived from the Caliente caldera complex. Includes the Kane Wash Tuff (14.4 to 14.7 Ma), the tuff of Boulder Canyon (15.1 Ma), and the tuff of Narrow Canyon (15.8 Ma), derived from the Kane Springs Wash caldera complex.

Tt3 Ash-flow tuff and interbedded airfall tuff, unit 3 (Miocene and Oligocene)—Poorly to densely welded, calc-alkaline, low-silica rhyolite to dacite ash-flow tuff and related airfall tuffs. Includes the tuff of Teepee Rocks (17.8 Ma), Hiko Tuff (18.3 Ma), Racer Canyon Tuff (18.7 Ma), and both Bauers Tuff Member (22.8 Ma) and Swett Tuff Member (23.7 Ma) of the Condor Canyon Formation, all derived from the Caliente caldera complex. Also includes the Harmony Hills Tuff (22.0 Ma), probably derived from the eastern Bull Valley Mountains; the Leach Canyon Formation (23.8 Ma), probably derived from the Caliente caldera complex; the Bates Mountain Tuff (22.8 Ma), derived from Lander County, Nevada; and the tuff of Saulsbury Wash (21.6 Ma), the Pahranagat Formation (22.6 Ma), the tuff of White Blotch Spring (24 to 25 Ma), the tuff of Kiln Canyon (24.1 to 25.1 Ma), the tuff of Lunar Cuesta (24.6 Ma), the tuff of the Quinn Canyon Range, and the Shingle Pass Tuff (26.4), all derived from the central Nevada caldera complex; and the tuff of Bald Mountain (about 25 Ma), derived from the Bald Mountain caldera in the Groom Range.

Tt2 Ash-flow tuff and interbedded airfall tuff, unit 2 (Oligocene)—Poorly to densely welded, calc-alkaline, low-silica rhyolite to dacite and trachydacite ash-flow tuff and related airfall tuffs. Includes the Isom Formation (about 27 Ma), probably derived from the Indian Peak caldera complex; the outflow Monotony Tuff (27.3 Ma), the intracaldera tuff of Goblin Knobs (27.3 Ma), and the tuff of Hot Creek Canyon (30.0 Ma), all derived from the central Nevada caldera complex; the outflow Windous Butte Formation (31.4 Ma) and intracaldera tuff of Williams Ridge and Morey Peak (31.3 Ma), derived from the Williams Ridge caldera of the central Nevada caldera complex; and the Needles Range Group (29 to 32 Ma), derived from the Indian Peak caldera complex.

Tt1 Ash-flow tuff and interbedded airfall tuff, unit 1 (Oligocene and Eocene)—Poorly to densely welded, calc-alkaline, low-silica rhyolite to dacite and trachydacite ash-flow tuff and related airfall tuffs. Deposited in the northern part of Plate 1. Includes the Pancake Summit Tuff (33.7 Ma), derived from the Broken Back caldera west of Eureka; the Stone Cabin Formation (35.4 Ma), derived from an unknown caldera in or near northern Railroad Valley; and the Kalamazoo Tuff (35 Ma), derived from an unknown source probably in the northern Schell Creek Range or beneath adjacent northern Spring Valley. In Utah, includes the Tunnel Spring Tuff (35.4 Ma).

Tr4 Rhyolite lava flows, unit 4 (Miocene)—High-silica rhyolite lava flows and volcanic domes, mostly in and near the Caliente and Kane Springs Wash caldera complexes.

Tr3 Rhyolite lava flows, unit 3 (Miocene and Oligocene)—Low-silica rhyolite lava flows and volcanic domes, mostly in and near the Indian Peak, Caliente, and central Nevada caldera complexes.

Tr2 Rhyolite lava flows, unit 2 (Oligocene)—Low-silica rhyolite lava flows and volcanic domes, mostly in and near the central Nevada and Indian Peak caldera complexes.

Tr1 Rhyolite lava flows, unit 1 (Oligocene and Eocene)—Low-silica rhyolite lava flows and volcanic domes, exposed in the northern part of Plate 1.

Ta4 Intermediate-composition lava flows, unit 4 (Miocene)—Andesitic and locally dacitic lava flows, flow breccia, and mudflow breccia. Includes andesite of the Hamblin-Cleopatra volcano (11.5 to 14.2 Ma) in the Lake Mead area.

Ta3 Intermediate-composition lava flows, unit 3 (Miocene and Oligocene)—Andesitic and locally dacitic lava flows, flow breccia, and mudflow breccia. Includes andesite between the Racer Canyon Tuff and Condor Canyon Formation in the southeastern part of Plate 2, between the Caliente and Kane Springs Wash caldera complexes, and in and near the Indian Peak and central Nevada caldera complexes.

Ta2 Intermediate-composition lava flows, unit 2 (Oligocene)—Andesitic and locally dacitic lava flows, flow breccia, and mudflow breccia. Includes andesite in and near the Indian Peak caldera complex and in the southern Egan Range.

Ta1 Intermediate-composition lava flows, unit 1 (Oligocene and Eocene)—Andesitic and locally dacitic lava flows, flow breccia, and mudflow breccia. Exposed in the northern part of Plate 1. In the northeastern part of Plate 1 includes thin ash-flow tuffs, notably the Kalamazoo tuff. In Utah, includes the Horn Silver Andesite.

Tmb Megabreccia (Miocene and Oligocene)—Masses of mostly Paleozoic sedimentary rocks and intertongued volcanic breccia deposited within calderas from landsliding of the oversteepened caldera margins following caldera subsidence as a result of rapid eruptions of ash-flow tuff. Includes rocks in the Indian Peak caldera complex, Caliente caldera complex and central Nevada caldera complex. Includes gravity slides west of the Sheep Range and Beaver Dam Mountains.

Ti Intrusive rocks (Miocene to Paleocene)—Mostly silicic, calc-alkaline plutons.

TKi Intrusive rocks (Miocene to Cretaceous)—Mostly silicic, calc-alkaline plutons.

Ki Intrusive rocks (Upper Cretaceous)—Mostly silicic, calc-alkaline plutons that accompanied Sevier deformation.

Ks Sedimentary rocks, undivided (Upper and Lower Cretaceous)—Sevier-age, mostly thin, fluvial synorogenic clastic deposits, including the Baseline Sandstone (Upper and Lower Cretaceous) and Willow Tank Formation (Upper Cretaceous) in the southern part of Plate 2, and the Iron Springs Formation (Upper Cretaceous), Cedar Mountain Formation (Upper Cretaceous), and Dakota Sandstone (Upper Cretaceous) in the southeastern part of Plate 2; and the Newark Canyon Formation (Paleocene? to Lower Cretaceous?) in the northern part of Plate 1.

Ji Intrusive rocks (Jurassic)—Mostly silicic, calc-alkaline plutons that accompanied Sevier deformation.

Js Sedimentary rocks, undivided (Jurassic)—Includes, in the southeastern part of Plate 2, the mostly marine Carmel and underlying Temple Cap formations (Middle Jurassic). Also in the southeastern part of Plate 2, includes the eolian Navajo Sandstone and mostly fluvial Kayenta and Moenave formations, all Lower Jurassic. Mostly clastic units. In the southern part of Plate 2, the Aztec Sandstone is the equivalent of the Navajo. Includes the Dunlop Formation (Lower Jurassic) in the northwestern part of Plate 1.

Ꞧs Sedimentary rocks, undivided (Triassic)—Includes, in the southeastern part of Plate 2, the mostly fluvial Chinle Formation (Upper Triassic) and mostly fluvial Moenkopi Formation (Middle? and Lower Triassic). Includes the Luning Formation (Upper Triassic) in the northwestern part of Plate 1. In the northeastern part of Plate 1, includes the Thaynes Formation (Lower Triassic). The majority of these rocks are clastic.

Pzu Paleozoic sedimentary rocks, undivided—Shown on Plates 4, 5, 8, and 9, where rocks in the hanging wall of the Snake Range decollement are buried by younger rocks.

Pp Park City Group, undivided (Upper and Lower Permian)—From top to base, consists of the Gerster Limestone (Upper Permian), Plympton Formation (Upper and Lower Permian), Kaibab Limestone (Lower Permian), and Toroweap Formation (Lower Permian). These make up the top of the upper carbonate aquifer.

Par Arcturus Formation and Rib Hill Sandstone, undivided (Lower Permian)—Included within the upper carbonate aquifer. Includes the Pequop Formation in Elko County, a redbed unit in the southern part of Plate 2, and the Queantoweap Sandstone in the southeastern part of Plate 2.

Pa Arcturus Formation (Lower Permian)—Predominantly carbonate rocks in the northern part of Plate 1, thickening eastward.

Pr Rib Hill Sandstone (Lower Permian)—Only in the northwestern part of Plate 1.

PꞮP Riepe Spring Limestone and Ely Limestone, undivided (Lower Permian and Pennsylvanian)— Mapped only in the northern part of Plate 1. The Riepe Spring Limestone (Lower Permian) is exposed in the northwestern part of Plate 1. Includes the Brock Canyon Formation (Permian and/or Pennsylvanian) in the northwestern part of Plate 1; the Oquirrh Group (Lower Permian and Pennsylvanian) in the northeastern part of Plate 1; and the Bird Spring Formation (Lower Permian to Upper Mississippian) in Clark County, Nevada and the Pakoon Formation (Lower Permian) in Utah.

ꞮP Ely Limestone (Pennsylvanian)—May include Missippian rocks at its base. Mapped mostly in the central and northern part of Plate 1, thickening eastward. Includes the Wildcat Peak Formation in the northwestern part of Plate 1 and the Callville Limestone in the southern and eastern part of Plate 2.

MDd Diamond Peak Formation, Chainman Shale, Joana Limestone, and Pilot Shale, undivided (Upper Mississippian to Upper Devonian)

Md Diamond Peak Formation (Upper Mississippian)—Only in the northwestern part of Plate 1. This is a clastic unit derived from erosion of the Antler highland, including the Roberts Mountain thrust formed during the Antler deformational event. Includes the Scotty Wash Quartzite in the southwestern part of Plate 2.

Mc Chainman Shale (Upper Mississippian)—A clastic confining unit that has a similar origin to the Diamond Peak Formation. The two make up the upper aquitard in the northern half of Plate 1. Thus for this part of the map area, it separates the upper from the lower carbonate aquifer; in the area of Plate 2, the Chainman is thin and does not constitute a significant regional aquitard.

MD Joana Limestone and Pilot Shale, undivided (Lower Mississippian to Upper Devonian)—The Joana Limestone (Lower Mississippian) and Pilot Shale (Lower Mississippian and Upper Devonian) make up the top of the lower carbonate aquifer in the northern half of Plate 1. Includes local Lower Mississippian units Mercury Limestone and Bristol Pass Limestone. Includes the Rogers Spring Limestone (Lower Mississippian) and Monte Cristo Limestone (Upper and Lower Mississippian) in the southern part of Plate 2; the Eleana Formation (Mississippian and Upper Devonian) in the western part of Plate 2; the Webb Formation (Lower Mississippian) in Elko County ; the Ochre Mountain Limestone and underlying Woodman Formation (Lower Mississippian) in the eastern part of Plate 1; and the West Range Limestone (Upper Devonian) in northern Lincoln County. May include, at the top, thin deposits of the Chainman Shale.

DꞒ Devonian to Upper Cambrian carbonate and clastic rocks, undivided.

DS Devonian and Silurian sedimentary rocks, undivided—Only shown on some cross sections (Plates 4, 5, 8, and 9).

Du Devonian carbonate sedimentary rocks, undivided—Includes the Woodruff Formation (Upper and Middle Devonian) in Elko County; and the Muddy Peak Limestone (Upper and Middle? Devonian) in the southern part of Plate 2.

Dd Devils Gate Formation (Upper and Middle Devonian)—The western equivalent of the Guilmette Formation.

Dg Guilmette Formation (Upper and Middle Devonian)—Mapped throughout, except in the western part of Plate 1. Includes the Sultan Limestone in Clark County.

Dn Nevada Formation (Middle and Lower Devonian)—The western equivalent of the Simonson and Sevy Dolomites. Includes the Cockalorum Wash Formation, also in the western part of Plate 1.

Ds Simonson Dolomite (Middle and Lower Devonian) and Sevy Dolomite, undivided (Lower Devonian)—Mapped in all but the western part of Plate 1.

SO Silurian and Ordovician sedimentary rocks, undivided—Shown on some cross sections (Plates 4, 5, 8, and 9).

SOu Upper part (Silurian and Upper Ordovician)--Includes the Laketown Dolomite (Silurian), Fish Haven Dolomite (Upper Ordovician), Ely Springs Dolomite (Upper Ordovician), and Hanson Creek Formation (Upper Ordovician). Includes the Roberts Mountains Formation and the Lone Mountain Dolomite in the northwestern part of Plate 1.

Ol Lower part (Middle and Lower Ordovician)—Mostly the Eureka Quartzite (Middle Ordovician) and the Pogonip Group (Middle and Lower Ordovician). Includes the Vinini Formation and Valmy Formation in the northwestern part of Plate 1. Includes the Ely Springs Dolomite where it is thin in Clark County. In Utah, includes the Crystal Peak, Watson Ranch, and Fillmore formations and the House Limestone.

Ꞓc Cambrian carbonate sedimentary rocks, undivided—Shown only on some cross sections (Plates 4, 5, 8, and 9).

Ꞓu Upper part (Lower Ordovician? and Upper Cambrian)—Includes the Notch Peak Limestone, Orr Formation, Windfall Formation, Nopah Limestone, Dunderberg Shale, and Corset Spring Shale. In the extreme southwestern part of Plate 2, includes the Emigrant Formation (Upper and Middle Cambrian).

Ꞓm Middle part (Upper and Middle Cambrian)—Mostly the Highland Peak Formation and its southwestern equivalent, the Bonanza King Formation. In Nevada, includes local units known as the Pole Canyon Limestone, Lincoln Peak Formation, Patterson Pass Shale, Hamburg Formation, Secret Canyon Shale, Geddes Limestone, and Eldorado Formation. Includes the Muav Limestone in eastern Clark County. In Utah, includes the Wah Wah Summit, Trippe, Pierson Cove, Eye of Needle, Swasey, Whirlwind, Dome, Chisholm, and Howell formations. This unit is a thick limestone sequence that marks the base of the lower carbonate aquifer.

ꞒpꞒs Lower part (Middle Cambrian to Late Proterozoic)—Chisholm Shale (Middle Cambrian), Lyndon Limestone (Middle Cambrian), Pioche Shale (Middle and Lower Cambrian), Carrara Formation (Middle and Lower Cambrian), Stella Lake Quartzite (Lower Cambrian), Prospect Mountain Quartzite (Lower Cambrian and Late Proterozoic), and Johnnie Formation (Late Proterozoic). The Prospect Mountain, in turn, has been subdivided into the Zabriskie Quartzite (Lower Cambrian), Wood Canyon Formation (Lower Cambrian), and Sterling Quartzite (Lower Cambrian and Late Proterozoic). Locally includes the Reed Dolomite (Lower Cambrian) and underlying Wyman Formation (Lower Cambrian?) in the southwestern part of Plate 2.

pꞒ Metamorphosed and crystalline Precambrian basement rocks (Late to Early Proterozoic)—Throughout most of Plates 1 and 2, consists of metamorphosed quartzite of Late Proterozoic age, namely the McCoy Creek Group and, in Utah, also the underlying Trout Creek Group. Locally, in the southern part of Plate 2, includes crystalline basement rocks.

Open Water

PLATE 3. EXPLANATION OF GEOLOGIC UNITS FOR THE MAPS AND CROSS SECTIONS OF PLATES 1, 2, 4, AND 5.

MAP ID 18288-3211 04/20/2011 BP

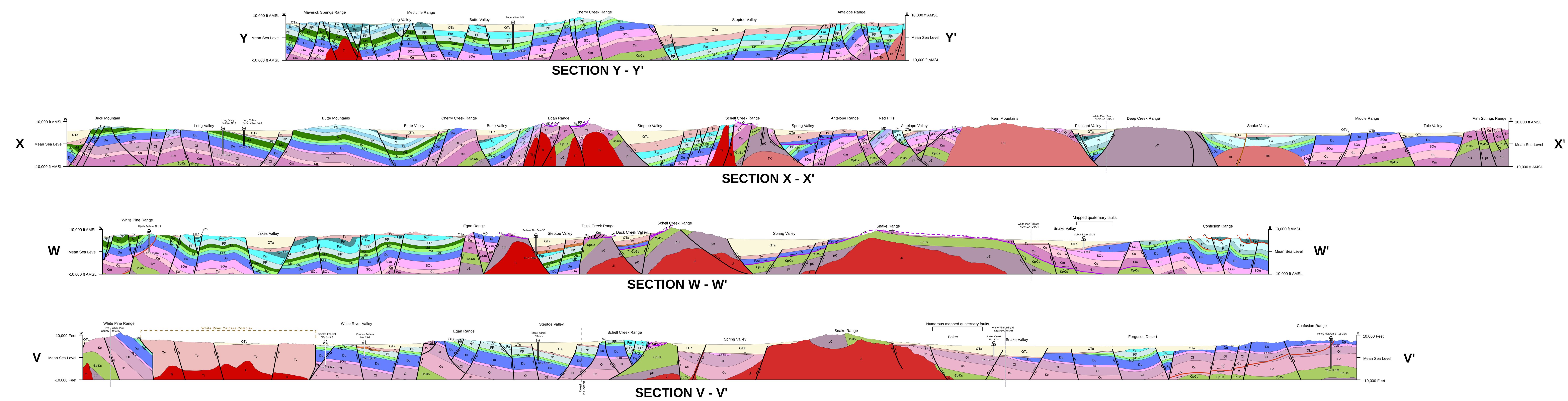

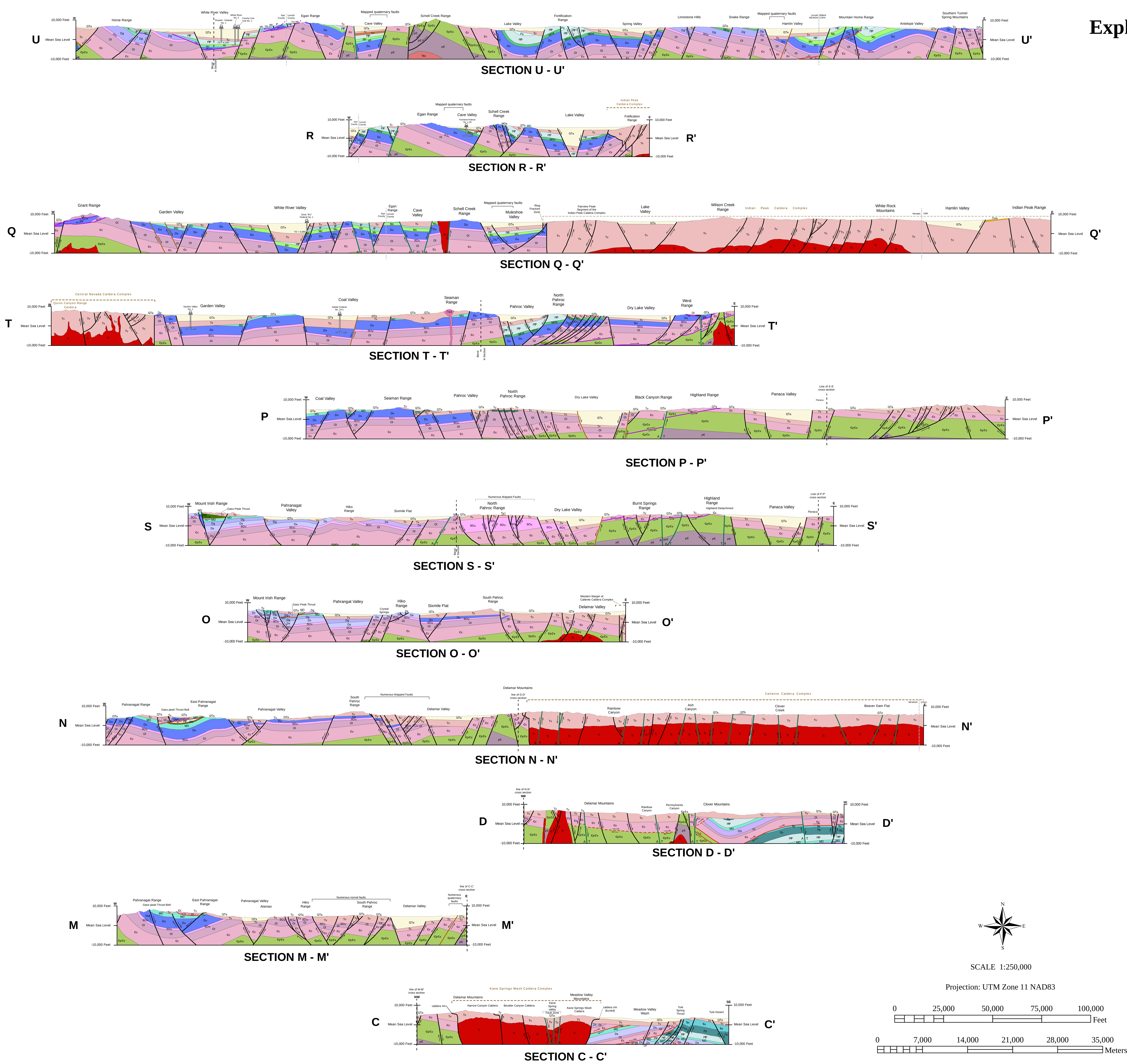

Explanation of Geologic Units

Shown on Cross Section

QTa	Quaternary and Tertiary basin-fill deposits
QTb	Quaternary and Tertiary thin basalt flows and cinder cones
Tv	Tertiary volcanic ash-flows, flows and ash-fall tuffs
Ta3	Tertiary andesitic and locally dacitic lava flows, flow breccia, and mudflow breccia
Ts1	Tertiary fluvial and lacustrine sediments
Tmb	Tertiary intracaldera megabreccia
Ti	Tertiary intrusive rocks
TKi	Tertiary-Cretaceous intrusive rocks
Ki	Cretaceous intrusive rocks
Ks	Upper and Lower Cretaceous sedimentary rocks, undivided
Ji	Jurassic intrusive rocks
Js	Jurassic sedimentary rocks, undivided
₮s	Triassic sedimentary rocks, undivided
Pzu	Paleozoic Rocks, Undifferentiated
Pp	Upper and Lower Permian Park City Group, undivided
Par	Permian Arcturus Formation and Rib Hill Sandstone
Pa	Permian Arcturus Formation
Pr	Lower Permian Rib Hill Sandstone
PIP	Permian and Pennsylvanian Riepe Spring Limestone and Ely Limestone, undivided
IP	Pennsylvanian Ely Limestone
MDd	Upper Mississippian to Upper Devonian Diamond Peak Formation, Chainman Shale, Joana Limestone, and Pilot Shale, undivided
Md	Upper Mississippian Diamond Peak Formation
Mc	Upper Mississippian Chainman Shale
MD	Lower Mississippian to Upper Devonian Joana Limestone and Pilot Shale, undivided
DS	Devonian and Silurian sedimentary rocks, undivided
Du	Devonian carbonate sedimentary rocks, undivided
Dd	Upper and Middle Devonian Devils Gate Formation
Dg	Upper and Middle Devonian Guilmette Formation
Dn	Middle and Lower Devonian Nevada Formation
Ds	Middle and Lower Devonian Simonson and Sevy Dolomites
SOu	Silurian and Upper Ordovician dolomite, undivided
Ol	Middle and Lower Ordovician, mostly Eureka Quartzite and the Pogonip Goup
€c	Cambrian carbonate sedimentary rocks, undivided
€u	Lower Ordovician? And Upper Cambrian limestone and shale, undivided
€m	Upper and Middle Cambrian limestone and shale
€p€s	Middle Cambrian to Late Proterozoic sedimentary rocks
p€	Late to Early Proterozoic metamorphosed and crystalline Precambrian basement rocks

Geologic Structure

Normal Fault
Solid where known; Dashed where inferred; dotted where concealed. Arrows show direction of movement.

Strike-slip Fault
T A
Solid where known; Dashed where inferred; dotted where concealed. Arrows show direction of movement. T= Towards, A = Away.

Thrust Fault
Solid where known; Dashed where inferred; dotted where concealed. Arrows show direction of movement.

Detachment Fault
Solid where known; Dashed where inferred; dotted where concealed. Arrows show direction of movement.

Quaternary Fault
Solid where known; Dashed where inferred; dotted where concealed. Arrows show direction of movement.

Well Name
TD=1,234'
Oil Well Data Used in Cross Sections
TD = Total Depth (Feet)

SOUTHERN NEVADA WATER AUTHORITY

PLATE 4. CROSS SECTIONS SHOWING GEOLOGY OF WHITE PINE AND NORTHERN LINCOLN COUNTIES, NEVADA, AND ADJACENT AREAS, NEVADA AND UTAH

MAP ID 18433-3211 05/25/2011 JAB/BP

Explanation of Geologic Units
Shown on Cross Section

QTa	Quaternary and Tertiary basin-fill deposits
Tv	Tertiary volcanic ash-flows, flows and ash-fall tuffs
Ts4	Tertiary fluvial and lacustrine sediments
Tmb	Tertiary megabreccia
Ti	Tertiary intrusive rocks
Ks	Upper and Lower Cretaceous sedimentary rocks, undivided
Js	Jurassic sedimentary rocks, undivided
T̄s	Triassic sedimentary rocks, undivided
Pp	Upper and Lower Permian Park City Group, undivided
PIP	Permian and Pennsylvanian Riepe Spring Limestone and Ely Limestone, undivided
MD	Lower Mississippian to Upper Devonian Joana Limestone and Pilot Shale, undivided
DЄ	Devonian to Upper Cambrian sedimentary rocks, undivided
DS	Devonian and Silurian sedimentary rocks, undivided
Du	Devonian carbonate sedimentary rocks, undivided
Ds	Middle and Lower Devonian Simonson and Sevy Dolomites
Ol	Middle and Lower Ordovician, mostly Eureka Quartzite and the Pogonip Goup
Єc	Cambrian carbonate sedimentary rocks, undivided
ЄpЄs	Middle Cambrian to Late Proterozoic sedimentary rocks
pЄ	Late to Early Proterozoic metamorphosed and crystalline Precambrian basement rocks

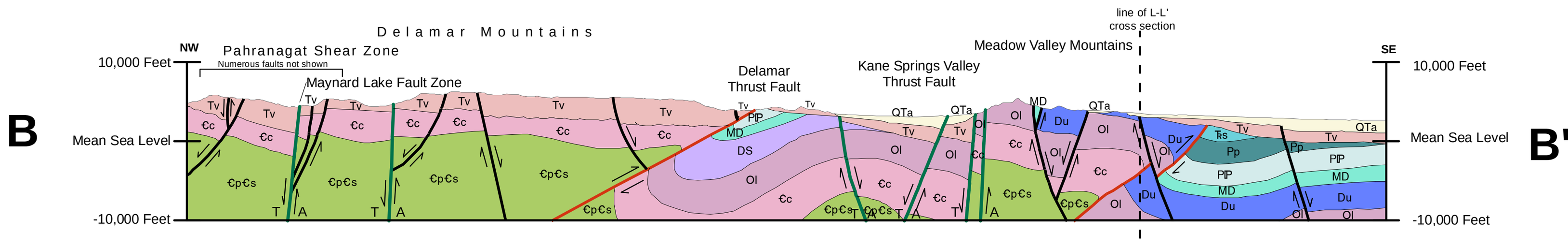

SECTION B - B'

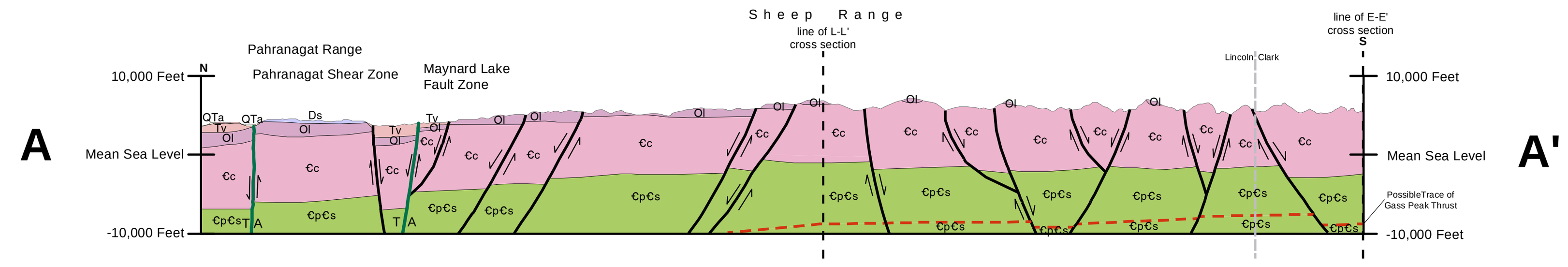

SECTION A - A'

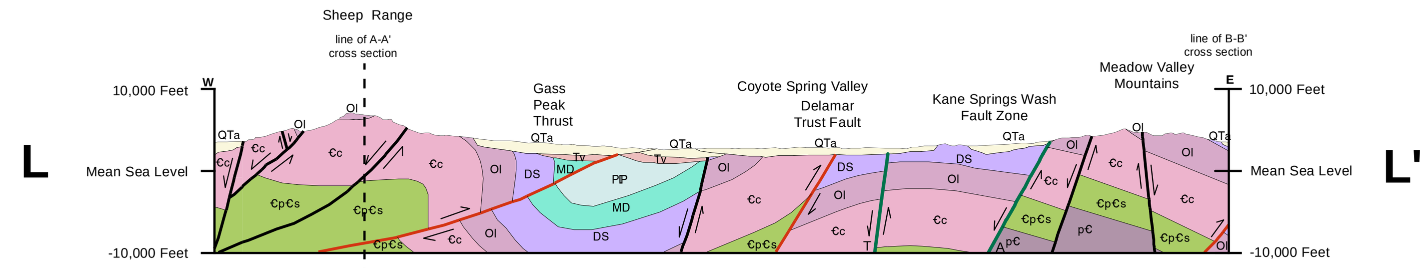

SECTION L - L'

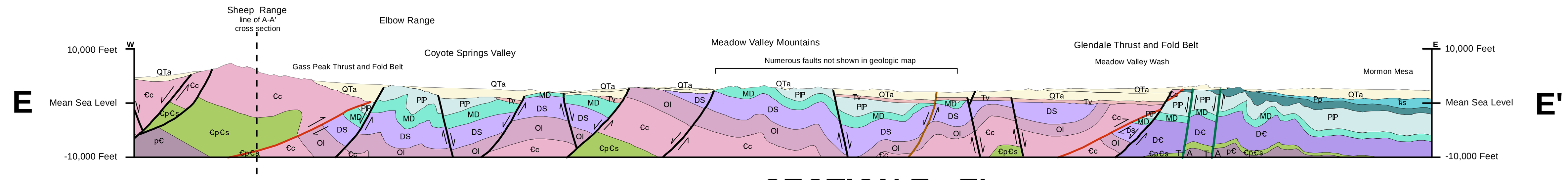

SECTION E - E'

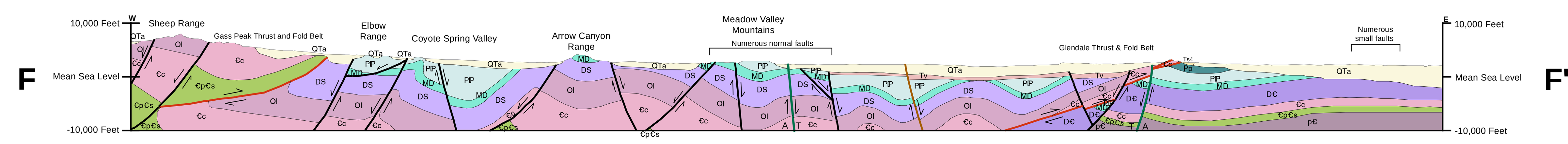

SECTION F - F'

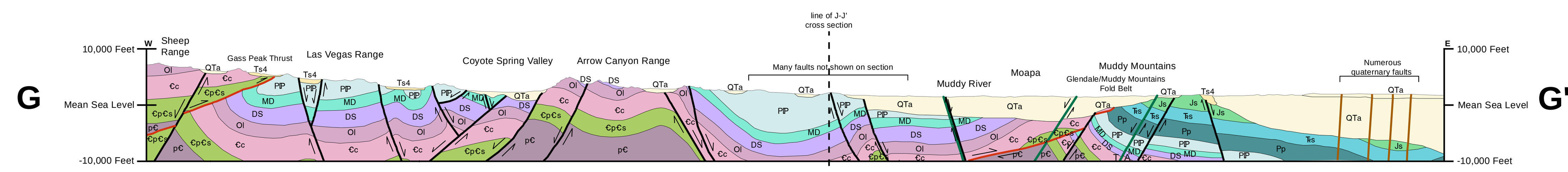

SECTION G - G'

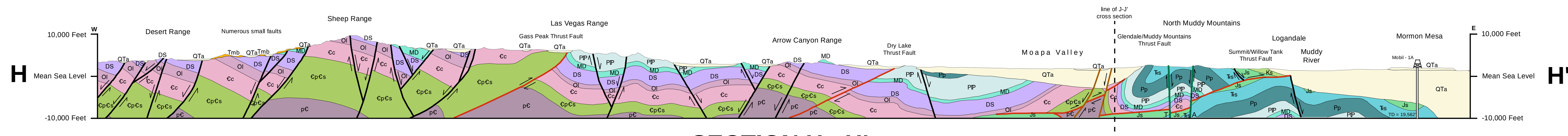

SECTION H - H'

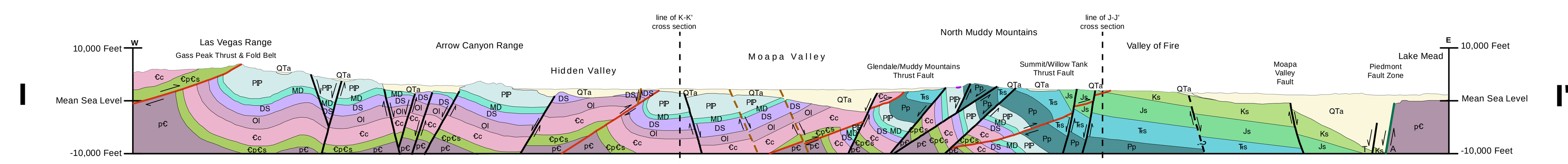

SECTION I - I'

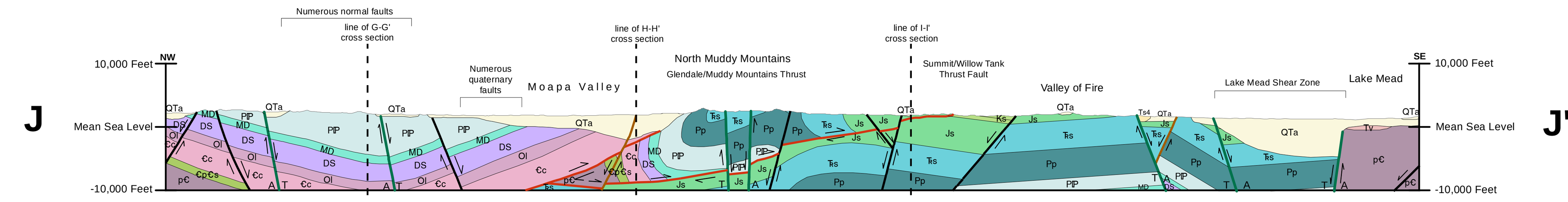

SECTION J - J'

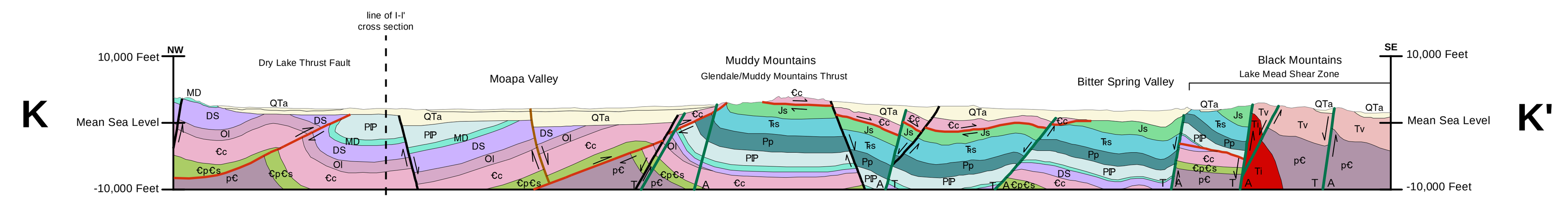

SECTION K - K'

Geologic Structure

Normal Fault
Solid where known; Dashed where inferred; dotted where concealed. Arrows show direction of movement.

Strike-slip Fault
Solid where known; Dashed where inferred; dotted where concealed. Arrows show direction of movement. T= Towards, A = Away.

Thrust Fault
Solid where known; Dashed where inferred; dotted where concealed. Arrows show direction of movement.

Detachment Fault
Solid where known; Dashed where inferred; dotted where concealed.

Quaternary Fault
Solid where known; Dashed where inferred; dotted where concealed. Arrows show direction of movement.

Well Name TD=1,234' — Oil Well Data Used in Cross Sections; TD = Total Depth (Feet)

SCALE 1:250,000
Projection: UTM Zone 11 NAD83
NO VERTICAL EXAGGERATION

0 25,000 50,000 75,000 Feet
0 5,000 10,000 15,000 20,000 25,000 Meters
0 5 10 15 20 Miles

PLATE 5. CROSS SECTIONS SHOWING GEOLOGY OF SOUTHERN LINCOLN AND NORTHERN CLARK COUNTIES, NEVADA

SOUTHERN NEVADA WATER AUTHORITY
MAP ID 18434-3211 05/17/2011 BP

Explanation

Hydrogeologic Units

QTs	Quaternary-Tertiary sediments
QTb	Quaternary-Tertiary basalts
Tv	Tertiary volcanic rocks
Tos	Tertiary older sediments
TJi	Tertiary-Jurassic intrusive rocks
KTRs	Cretaceous-Triassic clastic rocks
PIPc	Permian-Pennsylvanian carbonate rocks
Ms	Mississippian siliciclastic rocks
MOc	Mississippian-Ordovician carbonate rocks
€c	Cambrian carbonate rocks
€p€s	Cambrian-Precambrian siliciclastic rocks
p€m	Precambrian metamorphic rocks
	Open water

Regional Faults

Normal Fault
Solid where known; Dashed where inferred; dotted where concealed. Bar and ball on downthrown side.

Strike-slip Fault
Solid where known; Dashed where inferred; dotted where concealed. Arrows show direction of movement.

Thrust Fault
Solid where known; Dashed where inferred; dotted where concealed. Sawteeth on upper plate.

Detachment Fault
Solid where known; Dashed where inferred; dotted where concealed. Sawteeth on upper plate.

Quaternary Fault
Solid where known; Dashed where inferred; dotted where concealed. Bar and ball on downthrown side.

Subsidiary Faults

Normal Fault
Solid where known; dashed where inferred; dotted where concealed; dotted and queried where uncertain. Bar and ball on downthrown side.

Strike-slip Fault
Solid where known; dashed where inferred; dotted where concealed; dotted and queried where uncertain Arrows show direction of movement.

Thrust Fault
Solid where known; dashed where inferred; dotted where concealed; dotted and queried where uncertain. Sawteeth on upper plate.

Detachment Fault
Solid where known; dashed where inferred; dotted where concealed; dotted and queried where uncertain. Hollow sawteeth on upper plate.

Quaternary Normal Fault
Solid where known; dashed where inferred; dotted where concealed; dotted and queried where uncertain. Bar and ball on downthrown side.

Caldera Boundary
Solid where known; dashed where inferred; dotted where concealed

Cross Sections (Plates 4 and 5)

Major Road

Transverse Zone
(Zone of possible disruption)

National Park Service

Oil Well Data Used in Cross Sections
Nevada: Nevada Bureau of Mines and Geology
Utah: Utah Division of Oil, Gas and Mining

Wells

Town

Strike and Dip of Beds

Overturned Beds

SCALE 1:250,000

Projection: UTM Zone 11 NAD83

0 25,000 50,000 75,000 Feet
0 5,000 10,000 15,000 20,000 25,000 Meters
0 5 10 15 20 Miles

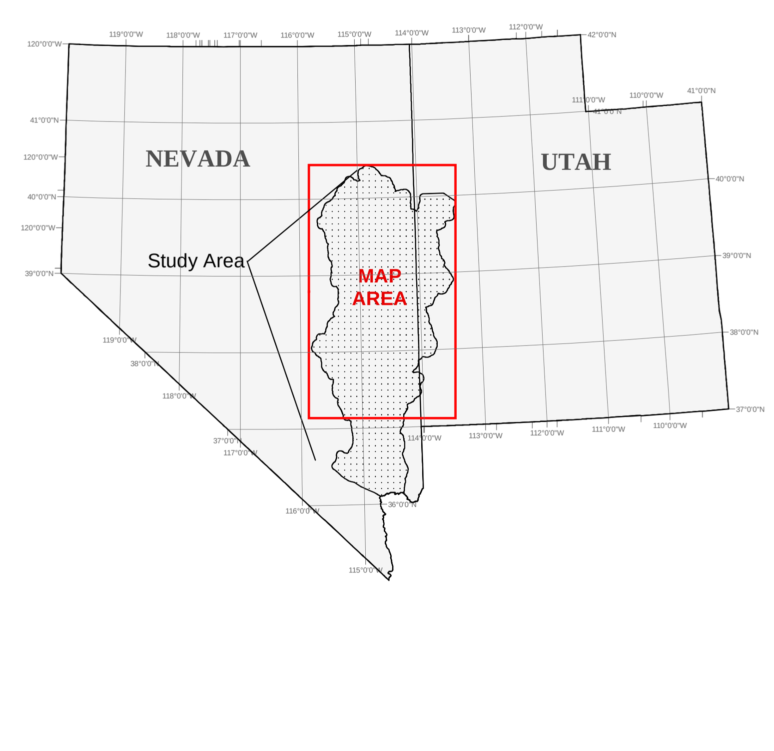

PLATE 6. HYDROGEOLOGY OF WHITE PINE AND NORTHERN LINCOLN COUNTIES, NEVADA, AND ADJACENT AREAS, NEVADA AND UTAH

SOUTHERN NEVADA WATER AUTHORITY
MAP ID 18291-3211 05/17/2011 JAB/BP

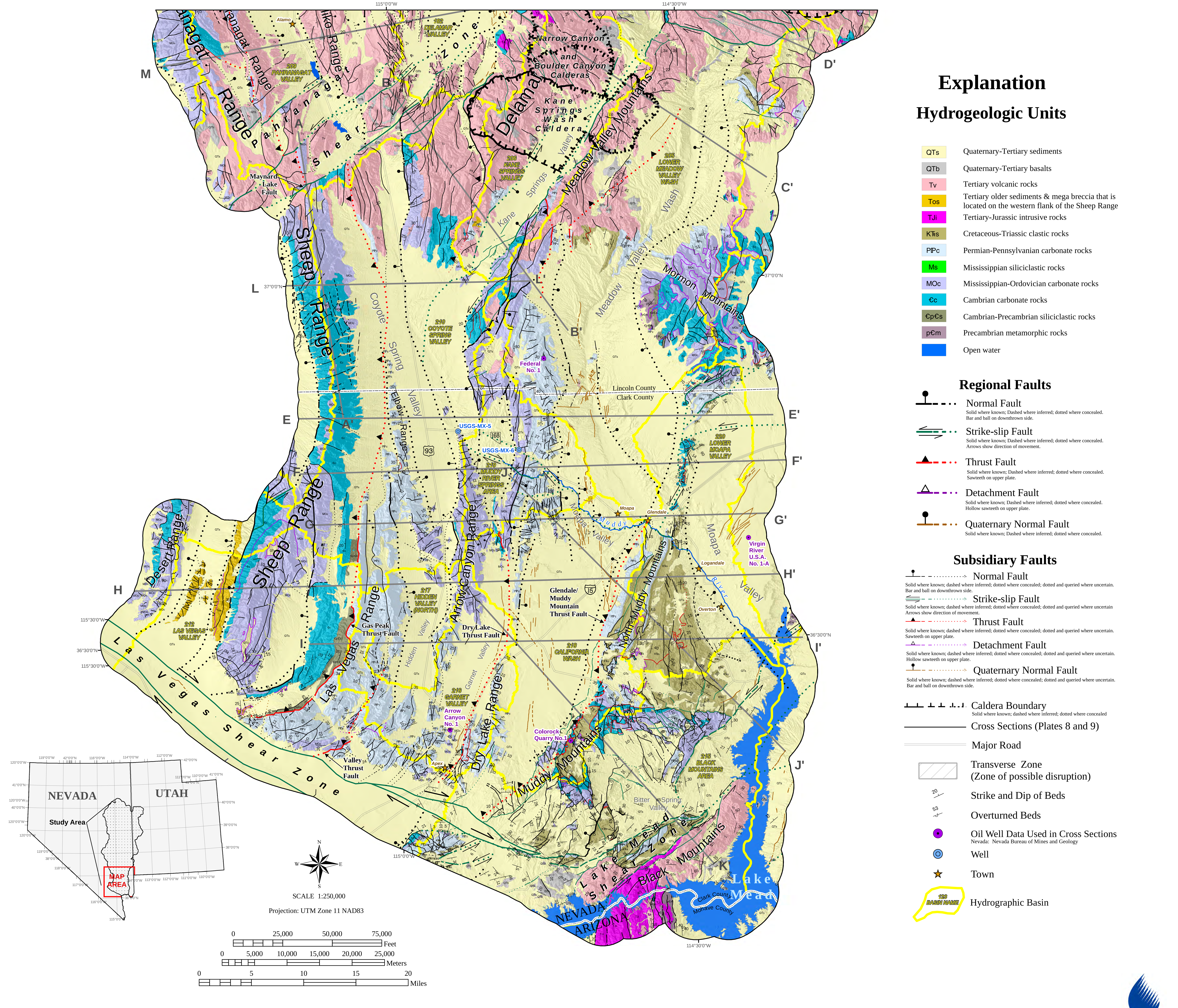

PLATE 7. HYDROGEOLOGY OF SOUTHERN LINCOLN AND NORTHERN CLARK COUNTIES, NEVADA, AND ADJACENT AREAS, ARIZONA

SE ROA 43360

JA_13240

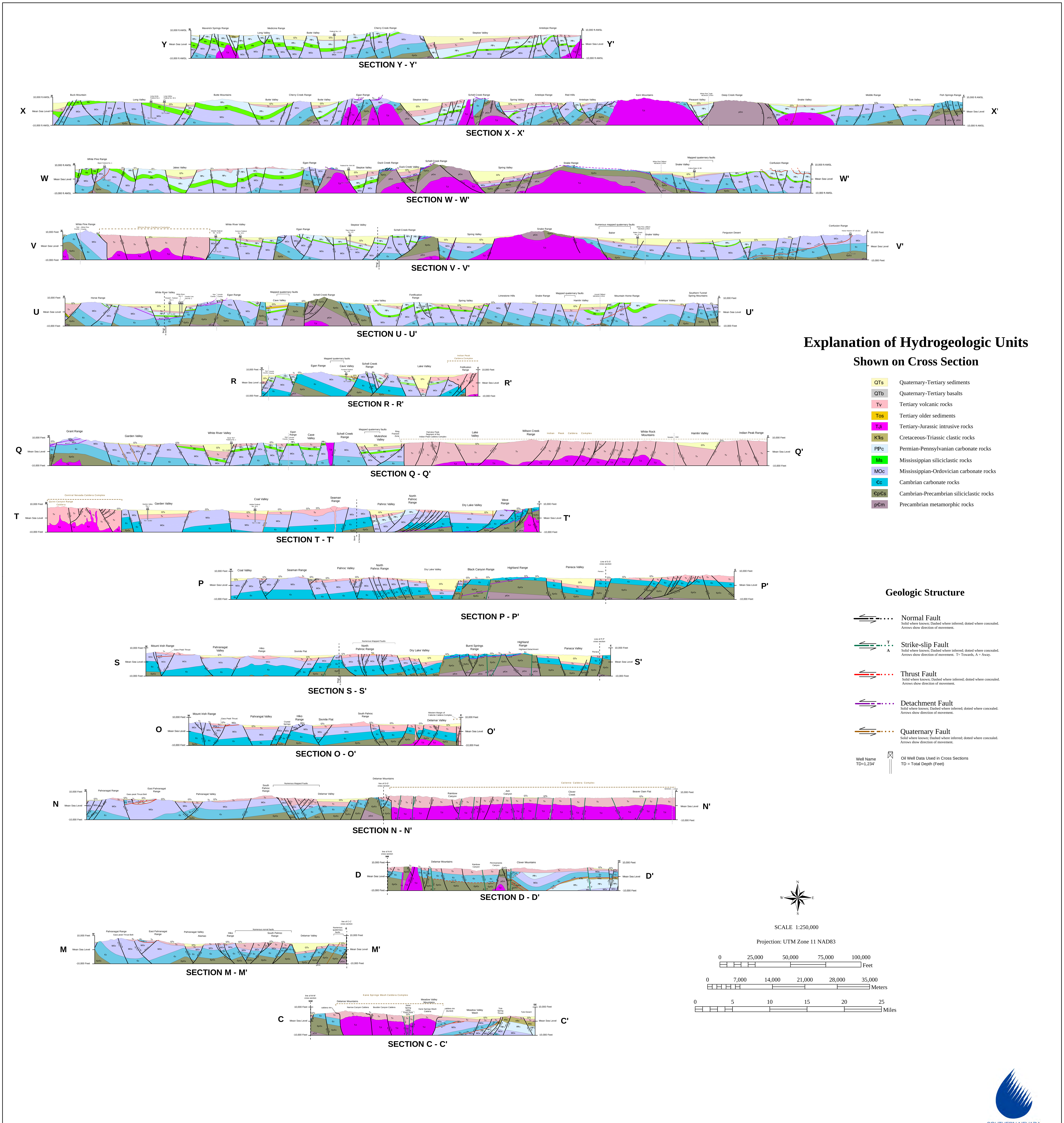

PLATE 8. CROSS SECTIONS SHOWING HYDROGEOLOGY OF WHITE PINE AND NORTHERN LINCOLN COUNTIES, NEVADA, AND ADJACENT AREAS, NEVADA AND UTAH

MAP ID 18435-3211 05/17/2011 BP

Explanation of Hydrogeologic Units
Shown on Cross Section

QTs	Quaternary-Tertiary sediments
Tv	Tertiary volcanic rocks
TJi	Tertiary-Jurassic intrusive rocks
KTRs	Cretaceous-Triassic clastic rocks
PPc	Permian-Pennsylvanian carbonate rocks
MOc	Mississippian-Ordovician carbonate rocks
Cc	Cambrian carbonate rocks
CpCs	Cambrian-Precambrian siliciclastic rocks
pCm	Precambrian metamorphic rocks

Geologic Structure

Normal Fault
Solid where known; Dashed where inferred; dotted where concealed.
Arrows show direction of movement.

Strike-slip Fault
Solid where known; Dashed where inferred; dotted where concealed.
Arrows show direction of movement. T= Towards, A = Away.

Thrust Fault
Solid where known; Dashed where inferred; dotted where concealed.
Arrows show direction of movement.

Detachment Fault
Solid where known; Dashed where inferred; dotted where concealed.

Quaternary Fault
Solid where known; Dashed where inferred; dotted where concealed.
Arrows show direction of movement.

Well Name
TD=1,234'
Oil Well Data Used in Cross Sections
TD = Total Depth (Feet)

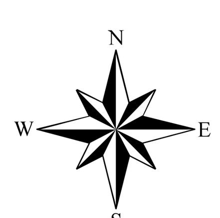

SCALE 1:250,000
Projection: UTM Zone 11 NAD83
NO VERTICAL EXAGGERATION

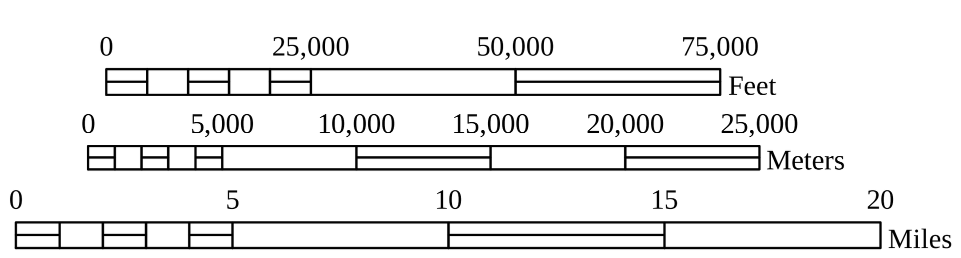

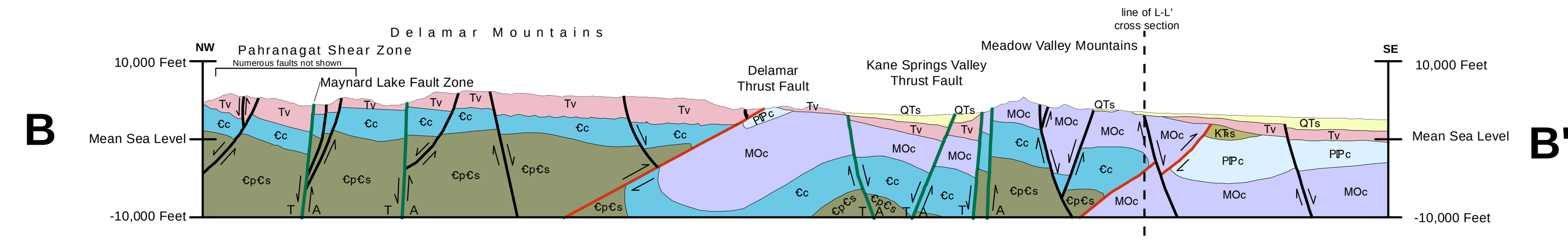

SECTION B - B'

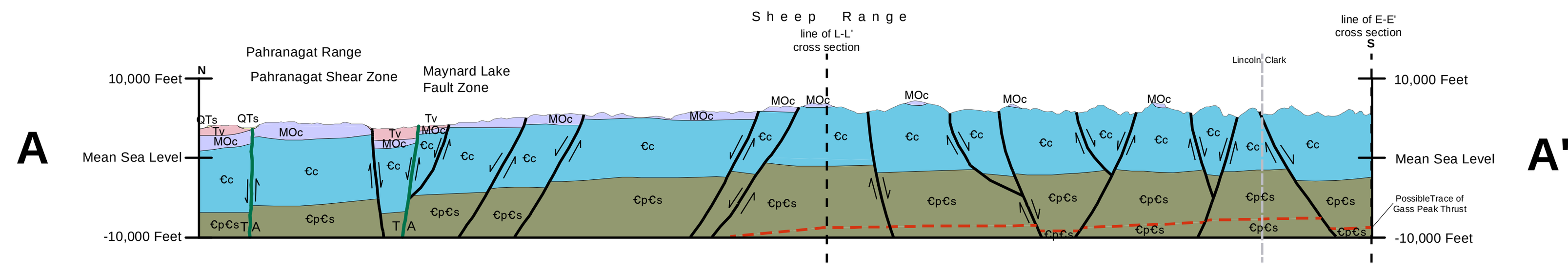

SECTION A - A'

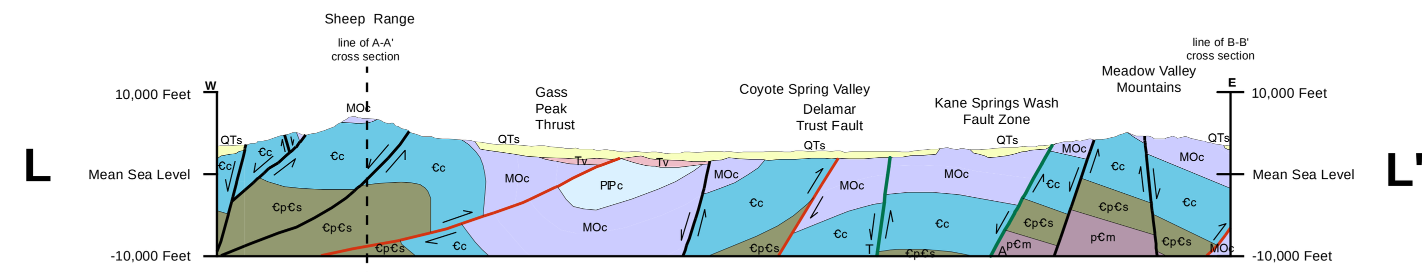

SECTION L - L'

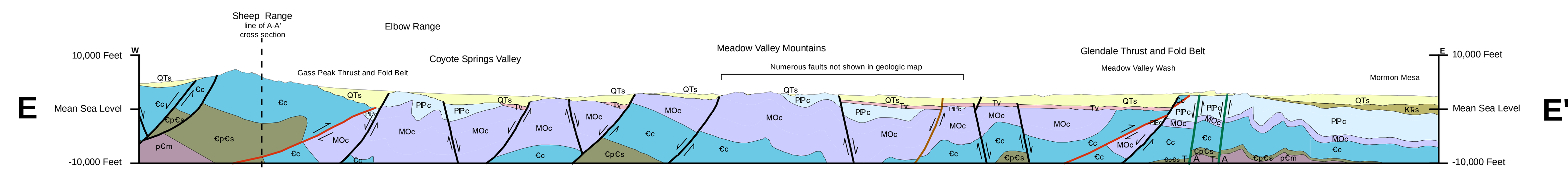

SECTION E - E'

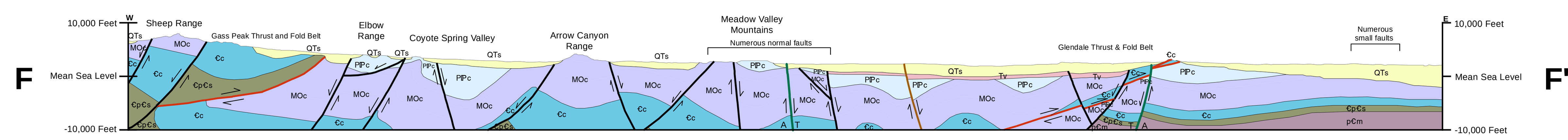

SECTION F - F'

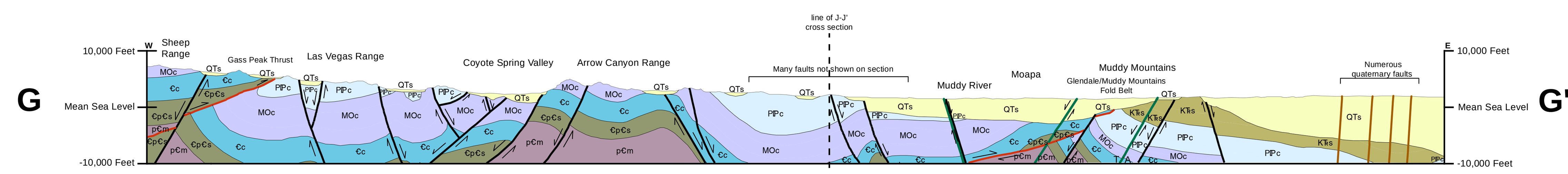

SECTION G - G'

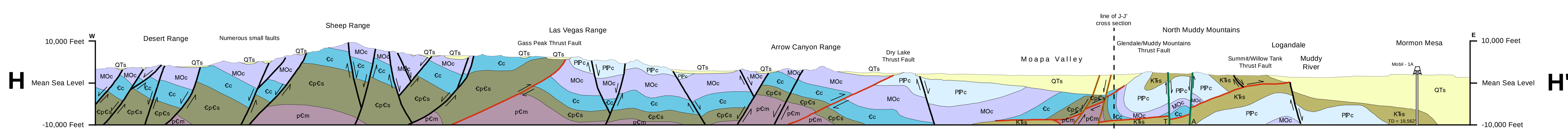

SECTION H - H'

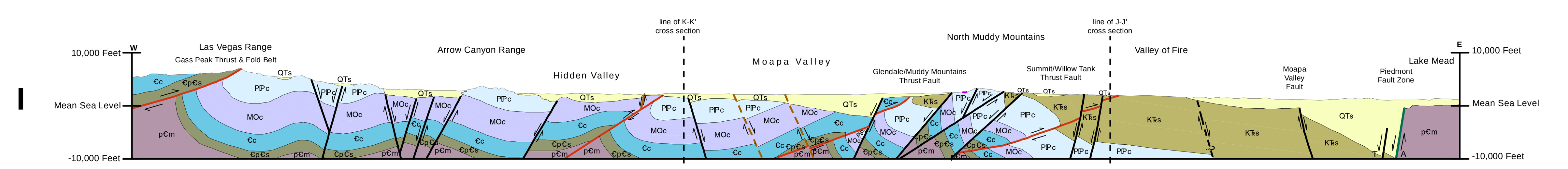

SECTION I - I'

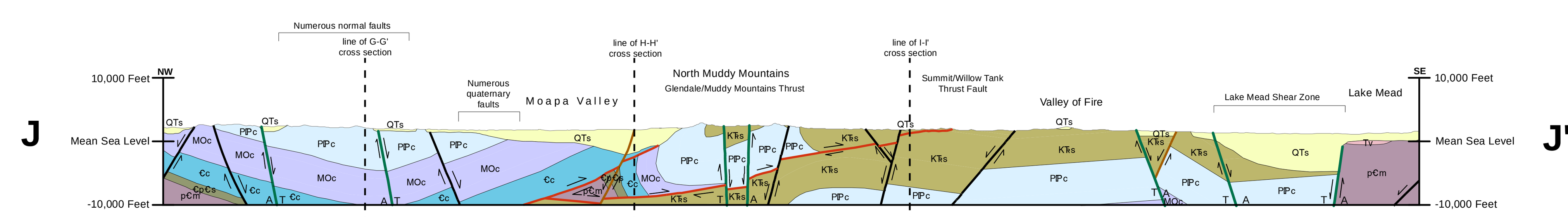

SECTION J - J'

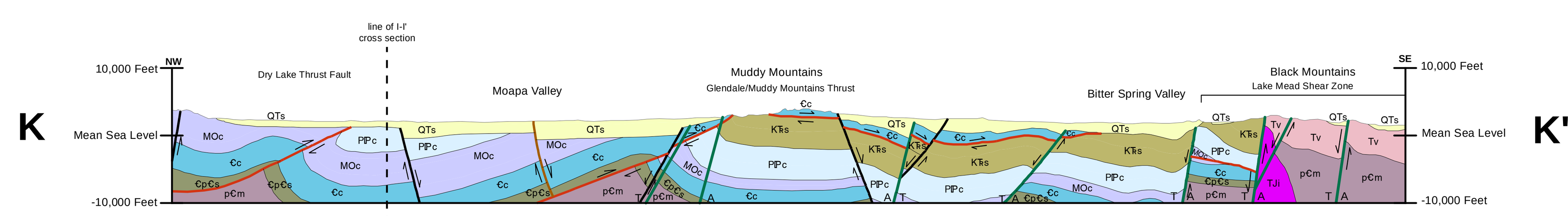

SECTION K - K'

SOUTHERN NEVADA WATER AUTHORITY

PLATE 9. CROSS SECTIONS SHOWING HYDROGEOLOGY OF SOUTHERN LINCOLN AND NORTHERN CLARK COUNTIES, NEVADA

MAP ID 18436-3211 05/17/2011 BP